A COMPARISON BETWEEN THE FLAT DILATOMETER AND THE CONE PENETROMETER TEST WITH THE AID OF ARTIFICIAL NEURAL NETWORKS

by

Marco Holtrigter

A thesis submitted in fulfilment
of the requirements for the degree of

MASTER OF ENGINEERING

in

Civil and Environmental Engineering
The University of Auckland, December 2010

ABSTRACT

The Flat Dilatometer (DMT) has been used for 30 years in Europe and other parts of the world, but has only recently been introduced to New Zealand. This study compares the DMT test with the more established Cone Penetration Test (CPT) at 10 sites in the upper North Island. The purpose of the study was to compare the results and interpretations of the CPT and DMT tests in general terms and also to undertake analysis of the data to investigate possible correlations between the two tests.

The DMT tests were carried out next to the CPT tests with a total of 16 CPT-DMT pairs included in the study. Some of the data was found to be unreliable due to uncertainty of the positioning of some CPT tests that were done previous to the DMT tests. The more reliable data was analysed using the artificial neural network method of general regression neural network (GRNN) and good correlations were obtained between the CPT results and the DMT parameters. However, robust validation of the networks was hindered by the lack of reliable data.

Other correlations between CPT and DMT recently reported in the literature (Robertson 2009b) were tested on the data from this study and found to perform less favourably. Slight adjustments are suggested to these correlations that were shown to give some improvement.

The study shows promising results that suggest possible CPT-DMT correlations. However, further research is needed to validate or improve these correlations. The relative success of the GRNN analysis in this study gives confidence in the technique for use in further research in this area.

DEDICATION

To my beautiful wife, Lynette.

ACKNOWLEDGEMENTS

The author wishes to express special gratitude to Andy O'Sullivan of Hiway Geotechnical for his encouragement of the introduction of the DMT equipment to New Zealand and his continued support in its use. Andrew Holland of AECOM, Hamilton City Council and Hiway Geotechnical are gratefully acknowledged for permitting the use of data for this study. Thanks also to Warren Sillitoe of Ground Investigation Ltd for many hours working on the rig.

In addition, I would like to thank my supervisor, Dr. Hossam Abuel-Naga of The University of Auckland for his support and encouragement.

Finally, I would like to thank my wife, Lynette, for her loving support and understanding.

TABLE OF CONTENTS

LIST OF TABLES

LIST OF FIGURES

1. CHAPTER 1: INTRODUCTION

1.1 GENERAL

The flat dilatometer (DMT) has been used extensively throughout Europe and other parts of the world over the past 30 years, but has only recently been introduced to New Zealand. The test gives a measure of soil parameters such as density, undrained shear strength, modulus values, overconsolidation ratio and coefficient of earth pressure at rest. The test also gives an indication of soil type by way of a material index. The added seismic module provides shear wave velocity, which allows low-strain shear modulus values to be obtained. The test has applications in settlement estimation, liquefaction assessment, predicting slip surfaces and compaction control.

The test is potentially a powerful insitu testing device that may provide useful information on New Zealand soils. The test is particularly sensitive to stress history, prestraining, aging, cementation/bonding and structure. These are factors that are often difficult to measure in the soil, but can greatly affect soil behaviour. Various interpretations and correlations have been established for the test, but these are yet to be validated on local soils.

1.2 PROJECT BACKGROUND

As the device is so new to New Zealand, only limited local field data exists. There is insufficient data to date to allow a comprehensive study comparing soil parameters derived from the DMT with those obtained from reliable laboratory reference tests. However, many DMT tests have been undertaken adjacent to cone penetration tests (CPT). This provides a lot of data as DMT tests are undertaken every 200mm depth and CPT tests provide near continuous results with depth. Given this available data, a comparison between the results of the two side-by-side tests provides an appropriate initial study of the DMT in New Zealand. Recent research by Robertson (2009b) has

compared the results of side-by-side CPT and DMT tests from overseas sites and proposed tentative correlations between the CPT and DMT, subject to further research.

1.3 RESEARCH OBJECTIVES

The purpose of this study is to compare the results of the DMT and CPT tests carried out to date in New Zealand. Given the relatively small database of available test information, it is not intended to develop precise numerical correlations between the two tests or to analyse in detail the tests interpretations. Instead the intention of the study is to provide an initial insight to the comparative results of the two tests. The correlations between the two tests is to be investigated as a continuation of the research by Robertson (2009b) along with the application of artificial neural networks to help develop potential refined correlations. In summary, the objectives of this study are:

1. To subjectively compare the results of the side-by-side CPT and DMT tests.
2. To compare soil parameter interpretations from the CPT and DMT tests by commonly used correlations.
3. To compare the results with the Robertson (2009b) correlations.
4. To analyse the data using artificial neural networks
5. To suggest potential refined CPT-DMT correlations
6. To make suggestions for further research in this area

2. CHAPTER 2: LITERATURE REVIEW

2.1 THE FLAT DILATOMETER (DMT)

2.1.1 Description of the DMT Apparatus

The flat dilatometer (DMT) is an insitu soil testing device developed in Italy circa 1980 (Marchetti 1980). The device is pushed into the ground using a cone penetrometer test (CPT) rig. The updated seismic dilatometer comprises a combination of a mechanical flat dilatometer (DMT) blade and a seismic module located above the DMT blade (Monaco et al. 1997). The combined DMT and seismic module is referred to as the seismic dilatometer (sDMT).

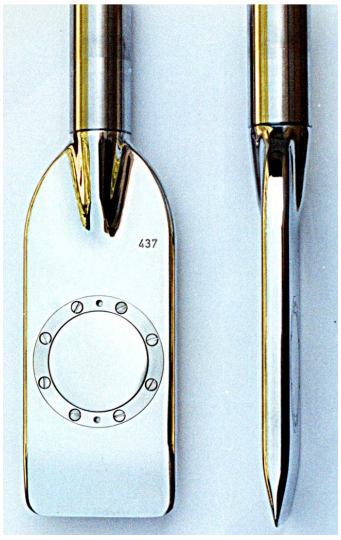

Figure 1. DMT blade

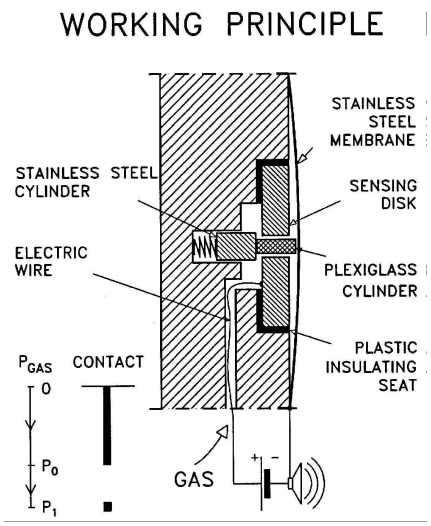

Figure 2. Internal mechanism of DMT blade

The DMT blade is a stainless steel blade approximately 15 mm thick and 96 mm with a 60 mm diameter circular membrane on one side (Figure 1). The blade is connected to a pneumatic-electric tube that transmits both gas pressure through the flexible nylon tube and an electric current through

a single wire that runs through the tube. The tube runs through the penetration rods to connect to a control box at the surface. Nitrogen gas is connected to the control box, which controls and records the pressure delivered to the blade.

The internal mechanism of the blade is illustrated in Figure 2. With the circular membrane pushed flat against the blade, the membrane closes an electrical circuit that runs along the single wire through the tube to the control box. This closed circuit causes a buzzer to activate on the control box. When the membrane is inflated, it 'lifts off' its seating, breaking the circuit and causing the buzzer to deactivate. When the membrane has been inflated by a set displacement of 1.1 mm from the blade, the internal mechanism reconnects the circuit and the buzzer reactivates.

The DMT blade is pushed into the ground using a CPT rig. At 200 mm depth intervals, penetration is stopped and the membrane inflated. When the membrane 'lifts-off', the buzzer goes off, and the pressure required to do so is recorded by the operator from the dial gauge reading on the control box. This is the 'A' reading, which is corrected by membrane calibration to give p_0, the corrected first pressure reading. Inflation of the membrane is continued until the buzzer reactivates, which is when the membrane has inflated by a distance of 1.1 mm. This is the 'B' reading, which corrects to p_1, the corrected second pressure reading. The gas pressure is then released and the test procedure repeated at the next 200 mm depth interval, and so on. The procedure is illustrated in Figure 3. In basic terms, the test gives two values, p_0 and p_1 at each test depth interval.

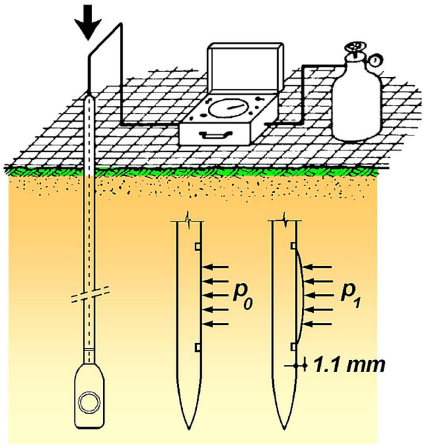

Figure 3. Schematic of DMT test

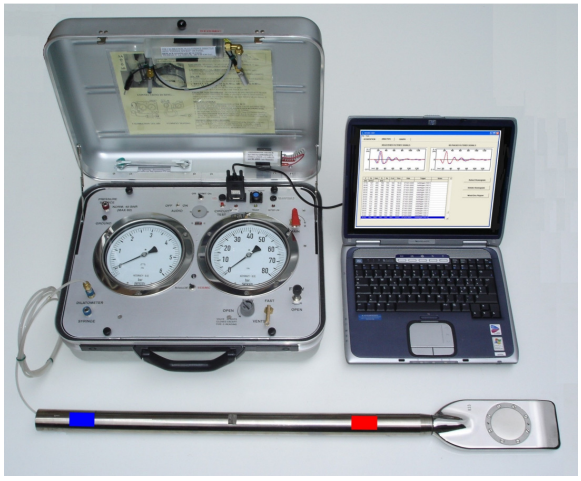

Figure 4. Control box, laptop computer and DMT blade with seismic attachment

The seismic part of the equipment is a separate add-on test carried out in combination with the DMT test. Figure 4 shows the seismic module attached to the DMT blade. The red and blue marks on the photo in Figure 4 represent the geophones, which are 500 mm apart on the module, with the centre point between the two geophones being 500 mm above the centre of the membrane on the DMT blade.

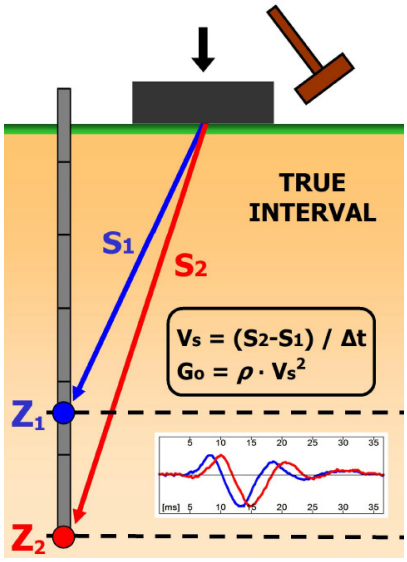

Figure 5. Schematic of seismic test

The seismic test is carried out at 500 mm depth intervals. The test is illustrated schematically in Figure 5. A beam on the ground surface is struck with a hammer to generate a shear wave that propagates through the ground. The shear waves are recorded by the geophones in the seismic module. The geophone signals are sent back up to a computer on the ground surface as seismographs. The seismographs are automatically re-phased by a computer program to obtain a true-interval shear wave velocity.

The sDMT tests presented in this study have been carried out using a Pagani TG63-150 track mounted CPT rig. Most of the CPT tests presented in this study have also been performed with this rig. A photo of the rig is shown in Figure 6.

Figure 7 shows the sDMT set up on the rig, with the DMT blade and seismic module ready for insertion into the ground. The yellow box on the left hand side of the rig is an electrically operated Autoseis Hammer (Mayne and McGillivray 2008), which is designed to optimise shear wave generation and provide consistent energy for each hammer activation. A pressure transducer

seismic box was used with the DMT control box connected to a laptop computer for automatic recording of the DMT and seismic tests using the Marchetti software, Sdmt Elab (Figure 8).

Figure 6. Pagani TG63-150 CPT rig

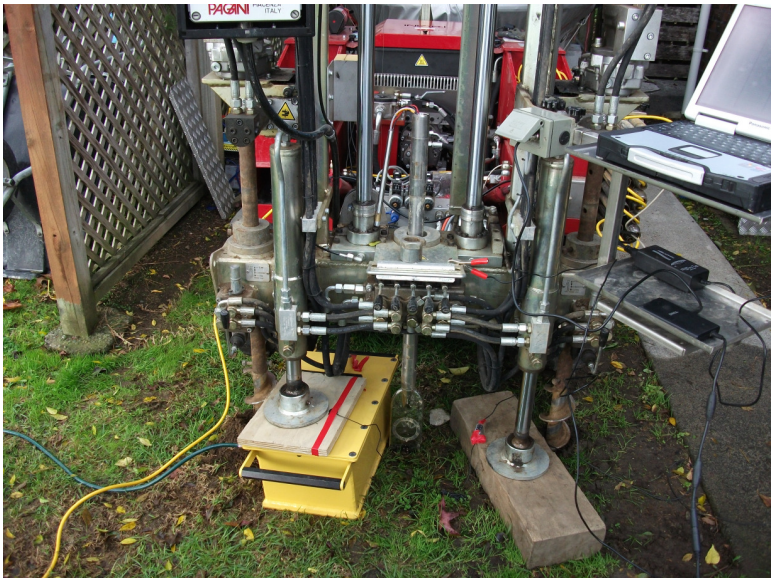

Figure 7. sDMT set up on rig

Figure 8. sDMT Control box and computer

2.1.2 Development of the DMT

The flat dilatometer (DMT) was first developed in the mid 1970's (Marchetti 1975) as a tool to investigate soil modulus values for laterally loaded driven piles. Further experimental work was undertaken to determine other practical applications for the test to obtain empirical correlations with geotechnical parameters (Marchetti 1980) and the equipment was further refined. Since 1980, however, the mechanical DMT equipment has remained relatively unchanged.

The seismic DMT (sDMT) was first developed by Hepton (1988) as a prototype with a single triaxial geophone located just above the standard mechanical DMT blade. A later single horizontal velocity transducer positioned just above the DMT blade was introduced in 1996 (Kates 1996). The sDMT was subsequently improved at Georgia Tech, Atlanta, USA (Martin and Mayne 1997, 1998; Mayne et al. 1999), but only one geophone was still used (Figure 9). The current sDMT was developed in Italy (Monaco et al. 2007) in which the seismic module above the DMT blade has two geophones (Figure 4).

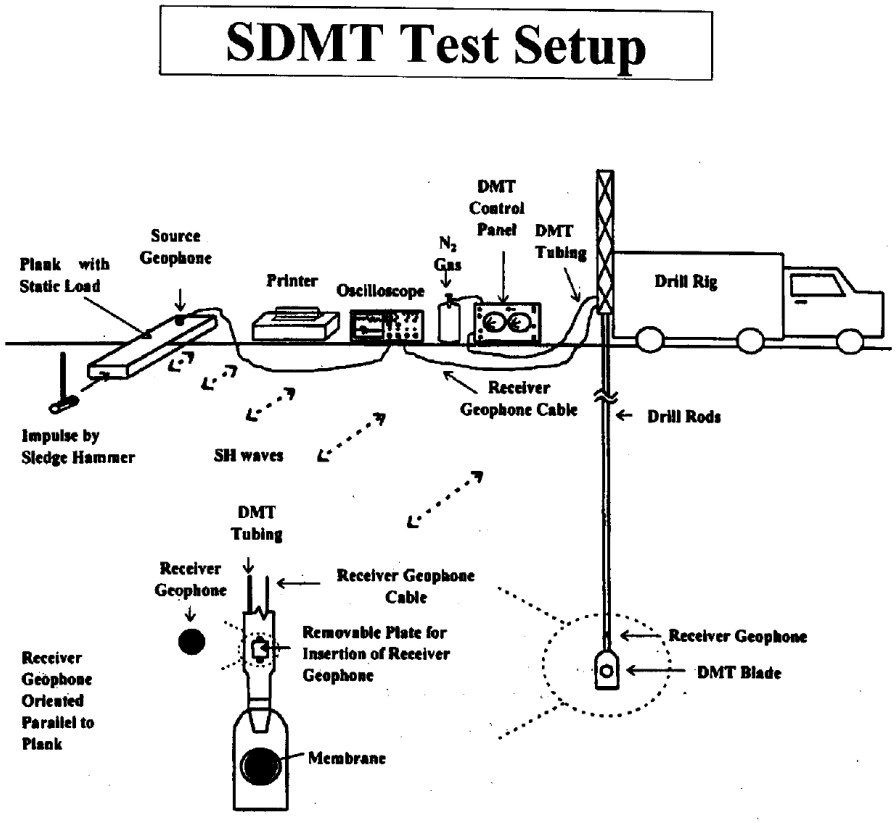

Figure 9: Early sDMT Setup (Mayne and Martin 1998)

2.1.3 Reduction of DMT Data

Two readings are obtained from the DMT; reading 'A' (at 'lift-off') and reading 'B' (at 'expansion' of 1.1 mm). These readings are corrected for membrane stiffness in order to determine pressures p_0 and p_1, as follows:

$$p_0 = A + \Delta A \quad (1)$$

$$p_1 = B - \Delta B \quad (2)$$

,where ΔA = the external pressure which must be applied to the membrane in free air to keep it in contact with its seating on the blade. ΔB = the internal pressure which, in free air, lifts the membrane 1.1 mm from its seating. These are determined by calibration before and after conducting the test.

The difference between the two pressures $(p_1 - p_0)$ can be converted into a modulus of elasticity of the soil using elastic theory. For this problem a solution is available if the space surrounding the dilatometer is taken to be formed by two elastic half spaces in contact along the plane of symmetry of the blade. For an elastic half space, having a Young's modulus, E and Poisson's ratio, ν, the solution is:

$$s_0 = 2D.(p_1 - p_0).(1 - \nu^2)/(\pi.E) \quad (3)$$

For a membrane diameter D = 60 mm and s_0 = 1.1 mm, becomes:

$$E/(1 - \nu^2) = 34.7(p_1 - p_0) \quad (4)$$

The term $E/(1 - \nu^2)$ is defined by Marchetti (1980) as the Dilatometer Modulus, E_D. Two other index values were also defined. The three index parameters are (Marchetti 1980):

Material Index: $$I_D = (p_1 - p_0)/(p_0 - u_0) \quad (5)$$

Horizontal Stress Index: $$K_D = (p_0 - u_0)/\sigma_v' \quad (6)$$

Dilatometer Modulus: $$E_D = 34.7(p_1 - p_0) \quad (7)$$

,where u_0 = the insitu porewater pressure prior to insertion of the DMT blade
σ_v' = insitu effective vertical overburden pressure

2.1.4 Correlations to Soil Parameters (Marchetti 1980)

The original correlations undertaken by Marchetti (1980) considered eight test sites, mostly in Italy. The sites represented variable soil types ranging from sands through to clays, and of variable stress history. The dilatometer index parameters (Eqns 5-7) obtained from these sites were empirically correlated to known soil parameters. These are summarised below.

2.1.4.1 Material Index

It was found that the Material Index, I_D closely relates to grain size fraction, with I_D increasing rapidly as the amount of soil fines decreases, irrespective of soil stress history (Marchetti 1980). Although the Material Index was found to closely relate to grain size, it cannot provide detailed information on grain size distribution. For example similar I_D values were found for 100% silts and for clays containing a small sand fraction (Marchetti 1980). In this way, the value I_D was considered to be a function of the mechanical consequences of the grain size distribution as a whole.

It was suggested that the Material Index can be regarded as a ratio of soil stiffness (as measured by $p_1 - p_0$) and soil strength (as measured by $p_0 - u_0$). The independent parameters of soil stiffness and soil strength provide the wide range of Material Index values reflecting the basic behavioural qualities of different soil types by grain size. Interestingly, no correlation was found between plasticity index (PI) and I_D. Table 1 shows the soil classification system based on I_D.

Table 1: Soil Classification Based on I_D (Marchetti 1980)

Peat or sensitive clays	Clay		Silt			Sand	
	Clay	Silty clay	Clayey silt	Silt	Sandy silt	Silty sand	Sand
(1)	(2)	(3)	(4)	(5)	(6)	(7)	(8)
I_D values	0.10	0.35	0.6	0.9	1.2	1.8	3.3

2.1.4.2 K_o and OCR

The 'lift-off' pressure, p_0 (and therefore K_D) is influenced by the horizontal pressure developed by the insertion of the blade and, therefore, K_D is not a direct measure of the horizontal insitu stress, σ_h. Insitu K_o values were plotted against K_D measured at the test sites, which showed the data to plot well along a single curve (Figure 10). This results in the following relationship:

$$K_o = (K_D/1.5)^{0.47} - 0.6 \qquad (8)$$

It should be noted that this is a purely empirical relationship based on uncemented clays. The correlation was not considered relevant for clays that have experienced aging, thixotropic hardening, cementation, etc. In such soils, K_D probably reflects the additional strength contributed by these factors (Marchetti 1980).

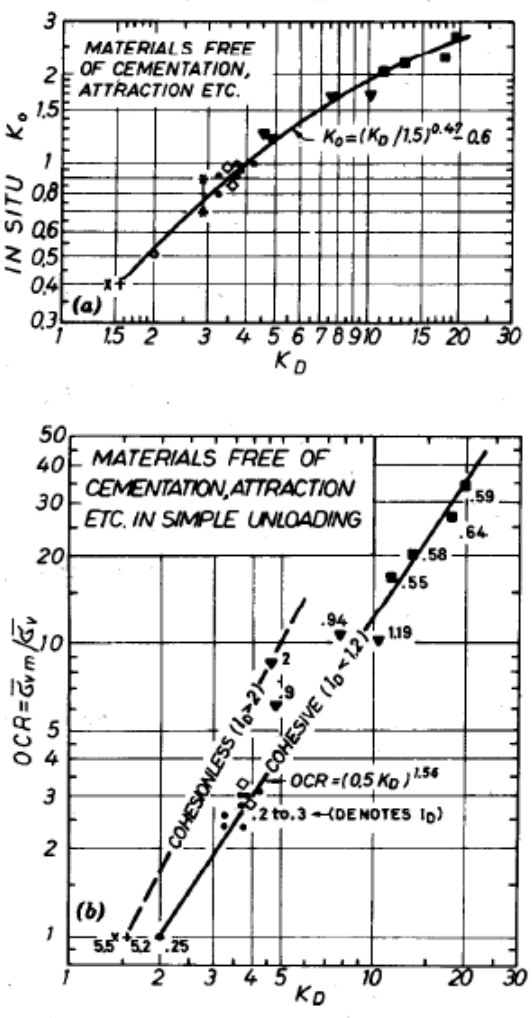

Figure 10: Correlation between (a) K_0 and K_D; (b) OCR and K_D (Marchetti 1980)

In terms of the overconsolidation ratio (OCR), the experimental points were found to fall within a narrow band, which is fairly well defined by the expression:

$$OCR = (0.5K_D)^{1.56} \quad (9)$$

This relationship only applies to clayey soils ($I_D < 1.2$). In cohesionless soils, there appeared to be a different relationship based on limited experimental data.

It was also found that K_D in the range of 1.8 – 2.3 (≈2) represents a clay in a normally consolidated state.

2.1.4.3 Constrained Modulus, M

There was considered to be no unique relationship between constrained modulus ($1/m_v$) and the dilatometer modulus, E_D, as E_D is dependent on a large number of factors. However, the Material Index, I_D and the horizontal stress index, K_D contain information on the soil type and stress history, respectively. By considering I_D and K_D, it was found that a relationship appears to exist between the dilatometer modulus, E_D and vertical drained constrained modulus, M ($=1/m_v$), as:

$$M = R_M E_D \quad (10)$$

,where R_M = a dimensionless non-constant factor dependant on I_D and K_D

From the experimental data (Figure 11), the following formulae for R_M were derived:

If $I_D \leq 0.6$ $\quad R_M = 0.14 + 2.36 \log K_D$;

If $I_D \geq 3.0$ $\quad R_M = 0.5 + 2 \log K_D$;

If $0.6 < I_D < 3.0$ $\quad R_M = R_{M,0} + (2.5 - R_{M,0}) \log K_D$, where $R_{M,0} = 0.14 + 0.15 (I_D - 0.6)$;

If $I_D > 10$ $\quad R_M = 0.32 + 2.18 \log K_D$;

If $R_M < 0.85$, then set $R_M = 0.85$ (11)

If was noted that the scatter in the correlation was considerable but it was considered that at least some of the scatter is probably due to the uncertainty of the M values used as reference. However, it was considered that the margin of uncertainty in obtaining the correlation of data (Figure 11) is probably acceptable given the reliability of alternative methods and the accuracy normally expected for M.

The reference values of M used for establishing the correlation are local tangent values, therefore the correlated M values from E_D are also local tangent modulus values. This means that the M value is applicable in settlement analysis provided that the increase in stress increment is small. If stresses exceed pre-consolidation stresses (and on to virgin consolidation), the estimated M values from the dilatometer may be too small.

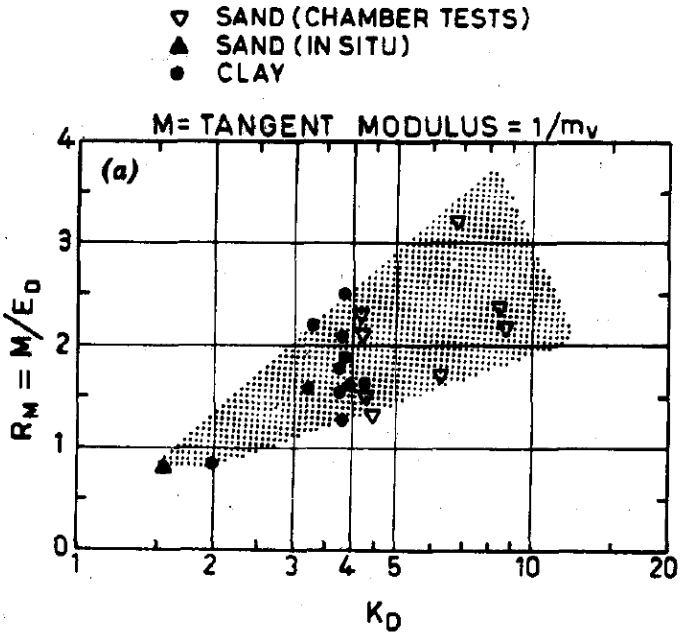

Figure 11: R_M vs. K_D from Experimental Data (Marchetti 1980)

2.1.4.4 Undrained Shear Strength, c_u

The estimation of undrained shear strength from the dilatometer test is based on the relationship:

$$(c_u/\sigma_v')_{OC} = (c_u/\sigma_v')_{NC}. \, OCR^m \qquad (12)$$

This relationship assumes the ratio c_u/σ_v' in the normally consolidated (NC) state can be factored up to provide an overconsolidated ratio of c_u/σ_v' by the overconsolidation ratio (OCR) to the power of a factor m, which is approximately 0.8, according to Ladd et al. (1977). By equating Eqns. 9 and 12, the relationship becomes:

$$(c_u/\sigma_v')_{OC} = (c_u/\sigma_v')_{NC}.(0.5\ K_D)^{1.25} \qquad (13)$$

The experimental data (Marchetti 1980) of c_u/σ_v' against K_D are plotted on Figure 12 (for cohesive soils, $I_D \leq 1.2$). The dashed line on Figure 12 represents a value of $(c_u/\sigma_v')_{NC} = 0.22$ as suggested by the literature (Mesri 1975), which presents a reasonable fit to the data. This then gives:

$$c_u = 0.22\ \sigma_v'\ (0.5\ K_D)^{1.25} \qquad (14)$$

The dashed line gives a lower strength than the average of the experimental data and should therefore represent a fairly conservative estimate of the insitu c_u. It was noted that there is indication (Marchetti 1979) that the correlation represented in Figure 12 (and Eqn 14) applies even if the clay is apparently overconsolidated for reasons other than removal of overburden (e.g. aging, thixotropic hardening, cementation, etc). This would imply that a high K_D corresponds to a high c_u/σ_v' no matter what the origin of K_D.

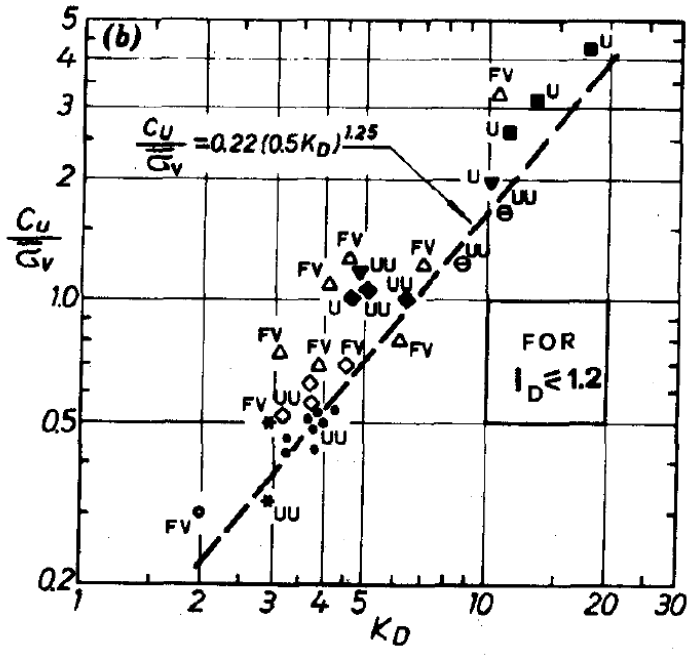

Figure 12: Correlation between c_u/σ_v' and K_D (Marchetti 1980)

2.1.4.5 Summary of Marchetti Correlations

The empirical correlations by Marchetti (1980) form the basis for the current reduction data commonly used for interpreting the flat dilatometer. Table 2 below gives a summary these correlations (Totani et al. 2001). The table includes a correlation for friction angle (ϕ) in sand (not discussed above), which represents a 'lower bound' estimate of ϕ based on K_D (Marchetti 1997). This applies only to sands ($I_D > 1.8$).

A chart for determining the soil type and unit weight from I_D and E_D was developed by Marchetti and Crapps (1981), which is given in Figure 13. This chart is considered to be a good average for 'normal' soils. However, the intention of the chart is not an accurate estimation of unit weight, but more a method of approximating the insitu effective vertical stress (σ_v') required for other reduction formulae.

Table 2: Marchetti DMT Interpretation Formulae (Totani et al. 2001)

SYMBOL	DESCRIPTION	BASIC DMT REDUCTION FORMULAE	
p_0	Corrected First Reading	$p_0 = 1.05\ (A - Z_M + \Delta A) - 0.05\ (B - Z_M - \Delta B)$	Z_M = Gage reading when vented to atm. If ΔA & ΔB are measured with the same gage used for current readings A & B, set $Z_M = 0$ (Z_M is compensated)
p_1	Corrected Second Reading	$p_1 = B - Z_M - \Delta B$	
I_D	Material Index	$I_D = (p_1 - p_0) / (p_0 - u_0)$	u_0 = pre-insertion pore pressure
K_D	Horizontal Stress Index	$K_D = (p_0 - u_0) / \sigma'_{v0}$	σ'_{v0} = pre-insertion overburden stress
E_D	Dilatometer Modulus	$E_D = 34.7\ (p_1 - p_0)$	E_D is NOT a Young's modulus E. E_D should be used only AFTER combining it with K_D (Stress History). First obtain $M_{DMT} = R_M E_D$, then e.g. $E \approx 0.8\ M_{DMT}$
K_0	Coeff. Earth Pressure in Situ	$K_{0,DMT} = (K_D / 1.5)^{0.47} - 0.6$	for $I_D < 1.2$
OCR	Overconsolidation Ratio	$OCR_{DMT} = (0.5\ K_D)^{1.56}$	for $I_D < 1.2$
c_u	Undrained Shear Strength	$c_{u,DMT} = 0.22\ \sigma'_{v0}\ (0.5\ K_D)^{1.25}$	for $I_D < 1.2$
Φ	Friction Angle	$\Phi_{safe,DMT} = 28° + 14.6°\ \log K_D - 2.1°\ \log^2 K_D$	for $I_D > 1.8$
c_h	Coefficient of Consolidation	$c_{h,DMTA} \approx 7\ cm^2 / t_{flex}$	t_{flex} from A-log t DMT-A decay curve
k_h	Coefficient of Permeability	$k_h = c_h\ \gamma_w / M_h$ ($M_h \approx K_0\ M_{DMT}$)	
γ	Unit Weight and Description	(see chart in Fig. 16)	
M	Vertical Drained Constrained Modulus	$M_{DMT} = R_M E_D$ if $I_D \le 0.6$: $R_M = 0.14 + 2.36 \log K_D$ if $I_D \ge 3$: $R_M = 0.5 + 2 \log K_D$ if $0.6 < I_D < 3$: $R_M = R_{M,0} + (2.5 - R_{M,0}) \log K_D$ with $R_{M,0} = 0.14 + 0.15\ (I_D - 0.6)$ if $K_D > 10$: $R_M = 0.32 + 2.18 \log K_D$ if $R_M < 0.85$: set $R_M = 0.85$	
u_0	Equilibrium Pore Pressure	$u_0 = p_2 = C - Z_M + \Delta A$	In free-draining soils

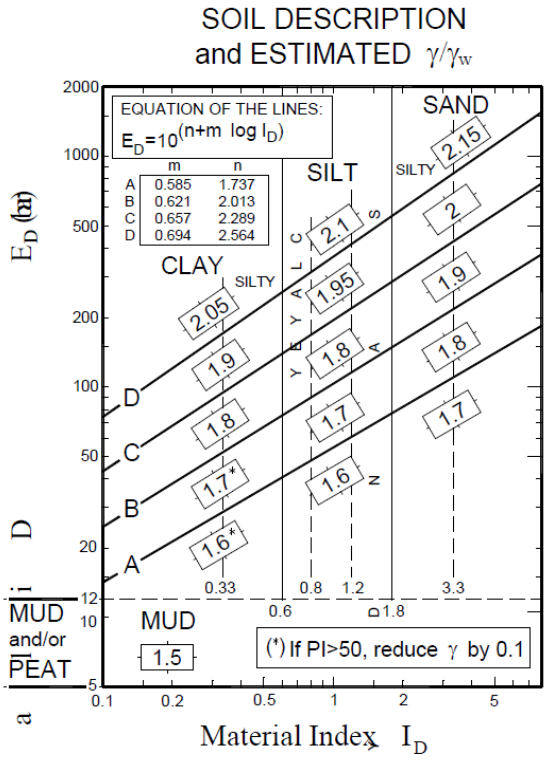

Figure 13: Chart for Estimating Soil Type and Unit Weight (Marchetti and Crapps 1981)

2.1.5 Verification of Marchetti Correlations

Since the initial work by Marchetti (1980), much research has been done to compare and verify (or otherwise) the Marchetti correlations (Table 2). That research is summarised below for the various soil parameters considered.

2.1.5.1 Material Index

There appears to be little research done on comparing the dilatometer material index, I_D to other soil classification tests or descriptions. Nor is there much available literature comparing measured soil unit weights with those assessed by the dilatometer. The Building Research Establishment (BRE) in the UK, however, undertook a comparison of the DMT to known soil properties are various test sites throughout the UK (Powell & Uglow 1988). As part of that work, the dilatometer modulus, E_D

and the material index, I_D of the soil types tested were plotted on the Marchetti classification chart (Figure 14). Some of these soils were correctly identified by the chart (silty clays and clayey silts), but others, which were >60% clay, appeared to be incorrectly plotted close to the clay/silt border on the chart. It was suggested that this may be due to the very high degree of overconsolidation and relative age of those soils affecting the material index value.

The comparison with unit weights also gave mixed success with the assessed weights generally underestimated the measured values (Figure 15). However, the assessed unit weights provided a good comparison to measured values for some soil types and showed the trend of variation in unit weight, albeit overemphasising that variation.

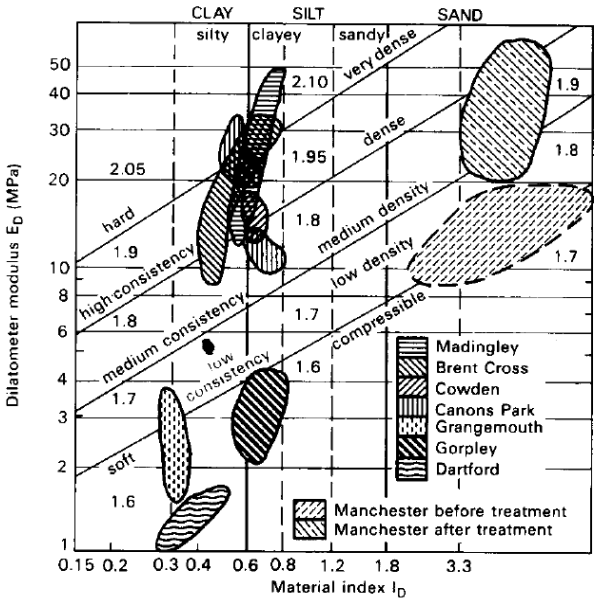

Figure 14: Soil Classification Chart (Powell & Uglow 1988)

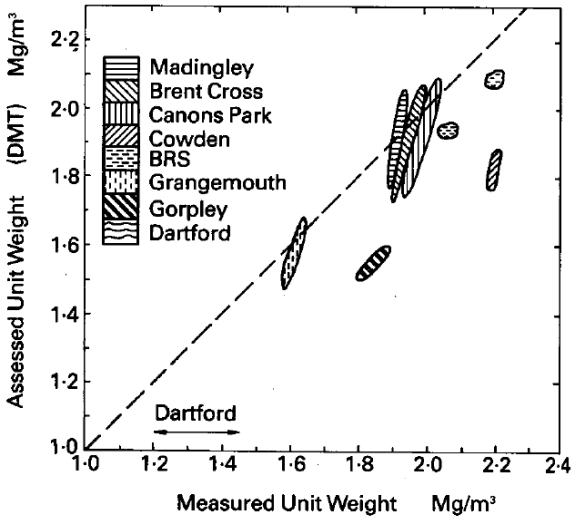

Figure 15: Comparison of Measures and assessed Unit Weights (Powell & Uglow 1988)

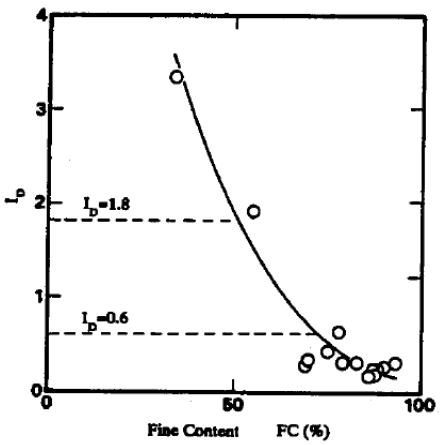

Figure 16: Fines Content vs. Material Index, I_D (Iwasaki et al. 1991)

Research by Iwasaki t al. (1991) on soft alluvial clays in Japan showed a reasonable relationship between fines content and the dilatometer material index, I_D (Figure 16). The 50% fines content point corresponds to an I_D of 1.8, which is the boundary between silt and sand.

2.1.5.2 K_0 and OCR

The research undertaken by Powell and Uglow (1988) considered the overconsolidation ratio (OCR) and K_0 values of various UK soils plotted against the dilatometer horizontal stress index (K_D) and compared them to the Marchetti correlations (Table 2). The resulting plots are shown on Figure 17 and Figure 18.

The results show tended to show that the more heavily overconsolidated clays tended to plot above the Marchetti correlation curves in both the K_0 and OCR plots with the softer and younger clays tending to plot below the correlation line. The plots however, do show the same general trend as the correlation and it was suggested that site specific correlations could be developed. For the 'young' clays, the following correlations were suggested:

$$K_0 = 0.34\ K_D^{0.55} \quad (15)$$

And

$$OCR = 0.24\ K_D^{1.32} \quad (16)$$

For the older and heavily overconsolidated clays, OCR estimation is difficult from oedometer tests, due to the very high preconsolidation pressures and so relationships based on these are difficult to establish.

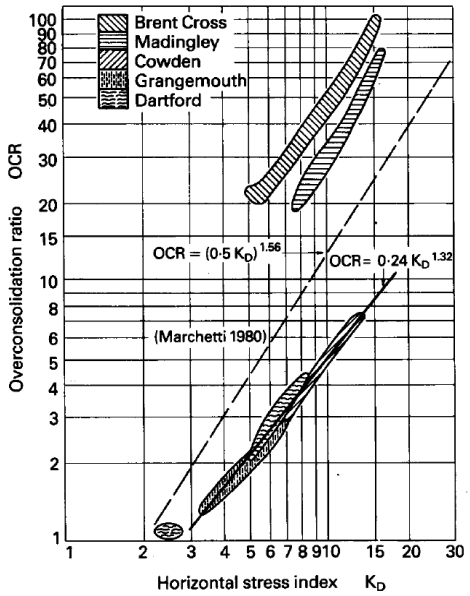

Figure 17: OCR vs. K_D (Powell & Uglow 1988)

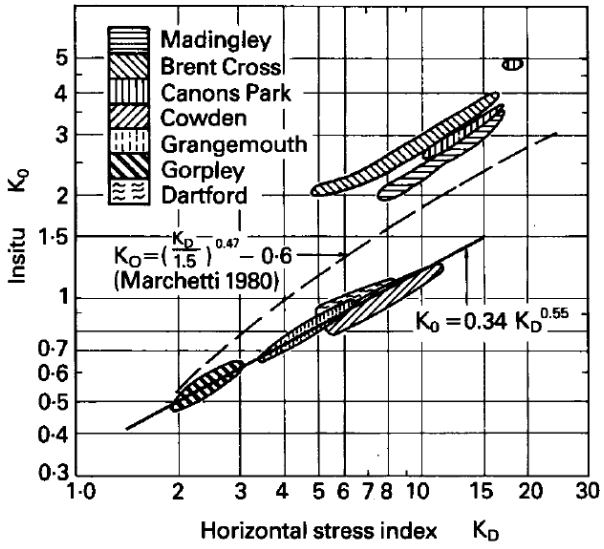

Figure 18: K_0 vs. K_D (Powell & Uglow)

Marchetti et al. in the Report to the ISSMGE Technical Committee 16 (TC16 2001) suggested that the research by Powell & Uglow (1988) indicates that:

- The original correlation line is intermediate between the UK data points
- The data points relative to each UK site were in a remarkably narrow band parallel to the original correlation line
- The narrowness of the data points band for each site is a confirmation of the remarkable resemblance of the OCR and K_D profiles, and the parallelism of the data points for each site to the original line is confirmation of its slope.

The research by Iwasaki et al. (1991) on soft alluvial clays in Japan showed good comparison between the dilatometer and other tests for estimation of K_0 (Figure 19). The dilatometer results fall generally midway between the other test results and are in close agreement with the self-boring pressuremeter and triaxial test results.

Wong et al. (1993) also showed good comparison between DMT and self-boring pressuremeter assessed K_0 values, also on soft alluvial soils (Figure 20).

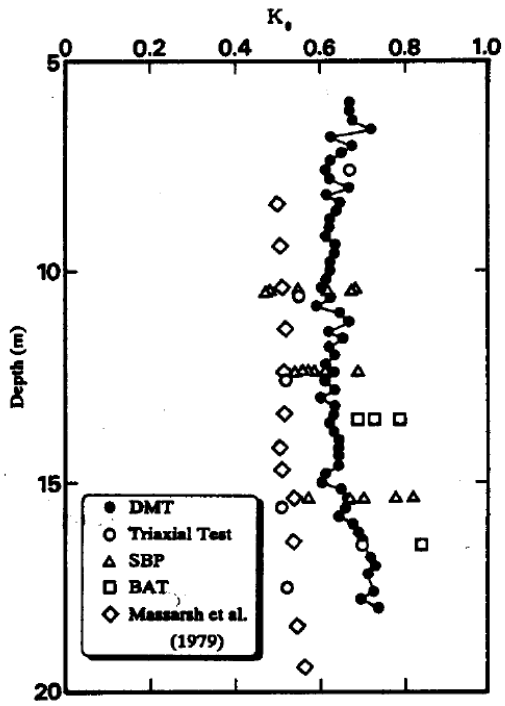

Figure 19: K_0 obtained from various tests vs. depth (Iwasaki 1991)

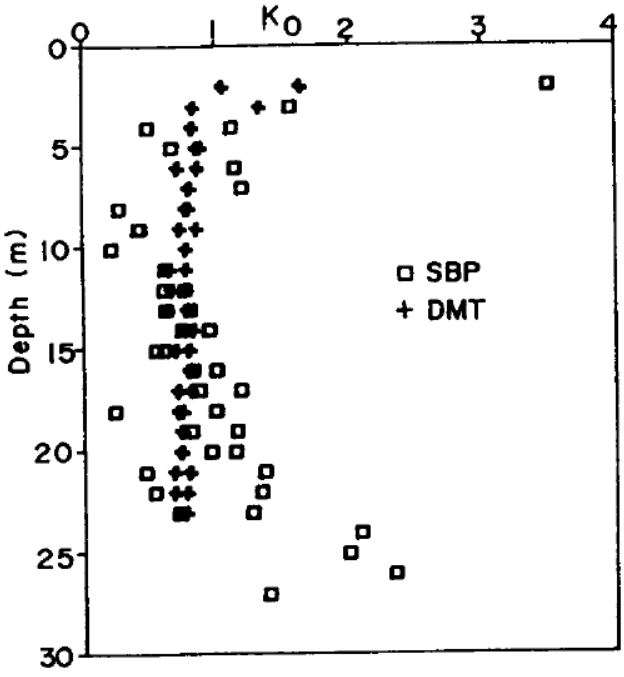

Figure 20: Comparison of K_0 values from SBP and DMT (Wong et al. 1993)

Close comparison to K_0 values between DMT tests and self-boring pressuremeter tests were also found by Aversa (1997) based on research carried out at Bothkennar, UK (Nash et al. 1992) and at Fucino, Italy (Burghignoli et al. 1991), shown in Figure 21.

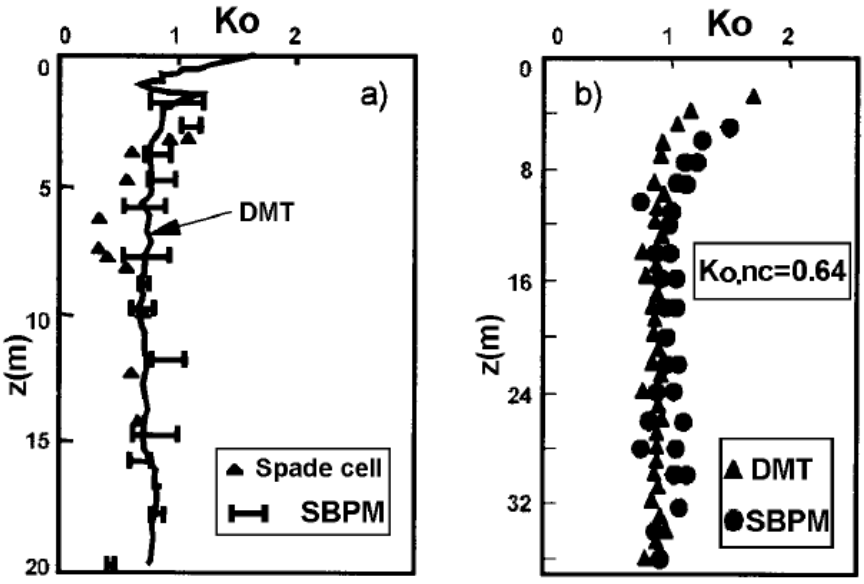

Figure 21: K_0 from DMT vs. K_0 from other methods (Aversa 1997)
a) Bothkennar (Nash et al. 1992) and, b) Fucino (Burghignoli et al. 1991)

The original Marchetti (1980) overconsolidation correlation with K_D (Eqn 9) was compared to a comprehensive collection of data by Kamei and Iwasaki (1995). The plot of data is shown on Figure 22. From this plot, they suggested an alternative relationship as:

$$OCR = (0.47.K_D)^{1.43} \quad (17)$$

This is remarkably similar to the original Marchetti (1980) equation: $OCR = (0.5.K_D)^{1.56}$ (Eqn 9), as illustrated on the plot on Figure 22.

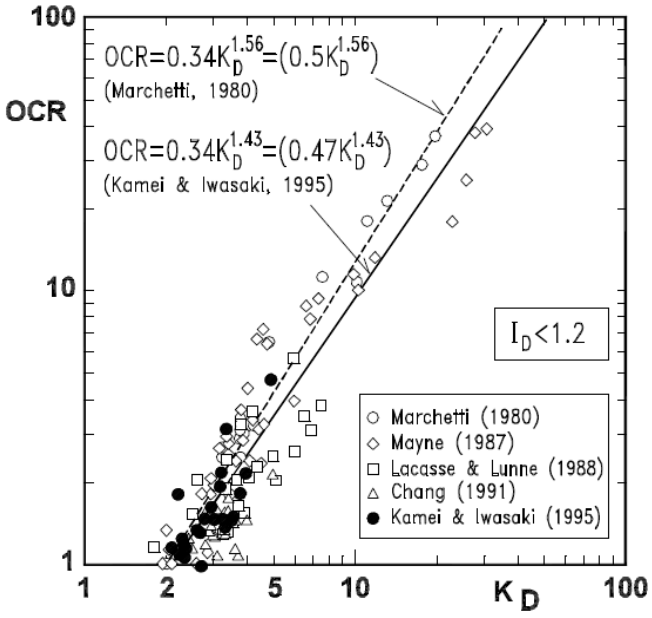

Figure 22: Correlation of K_D and OCR for Cohesive Soils all over the World (Kamei & Iwasaki 1995)

The K_D – OCR relationship was also confirmed by Finno (1993) considering the three dimensional strain path method (Baligh 1985) and anisotropic bounding space model (Figure 23).

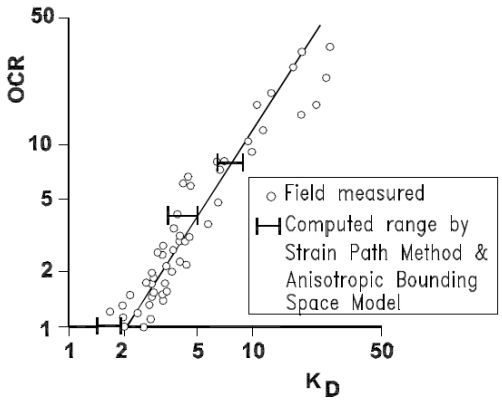

Figure 23: Theoretical K_D vs. OCR (Finno 1993)

2.1.5.3 Constrained Modulus, M

Powell and Uglow (1988) compared the dilatometer modulus, E_D with high quality oedometer tests from various UK test site. The resulting plot is shown on Figure 24. The results indicate a linear relationship between E_D and M, but at different gradients for different soil types. This suggests that a relationship does exist between M and E_D, as the Marchetti (1980) correlation suggests ($M = R_M.E_D$) (Eqn 10). However, the factor, R_M, is not a unique proportionality constant, but is dependent on both the material index, I_D, and the horizontal stress index, K_D (Eqn 11). It is not known what the I_D and K_D values are for the data used by Powell and Uglow (1988) so the full Marchetti correlation is not tested.

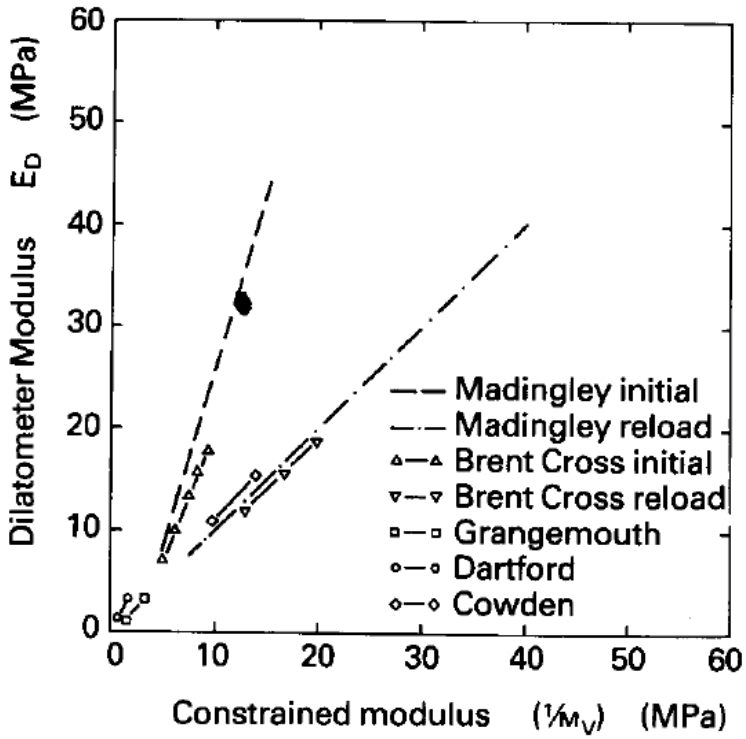

Figure 24: Constrained Modulus vs. DMT Modulus (Powell & Uglow)

Constrained modulus values obtained from high quality oedometer tests (where $M_{oed} = 1/m_v$) were compared to constrained modulus values estimated from the dilatometer using the Marchetti (1980) correlation (Eqns. 10 and 11) by Lacasse (1986) and also by Iwasaki (1991). These studies were both undertaken on soft clays. The results of those comparisons are shown on Figure 25, which generally show good correlation.

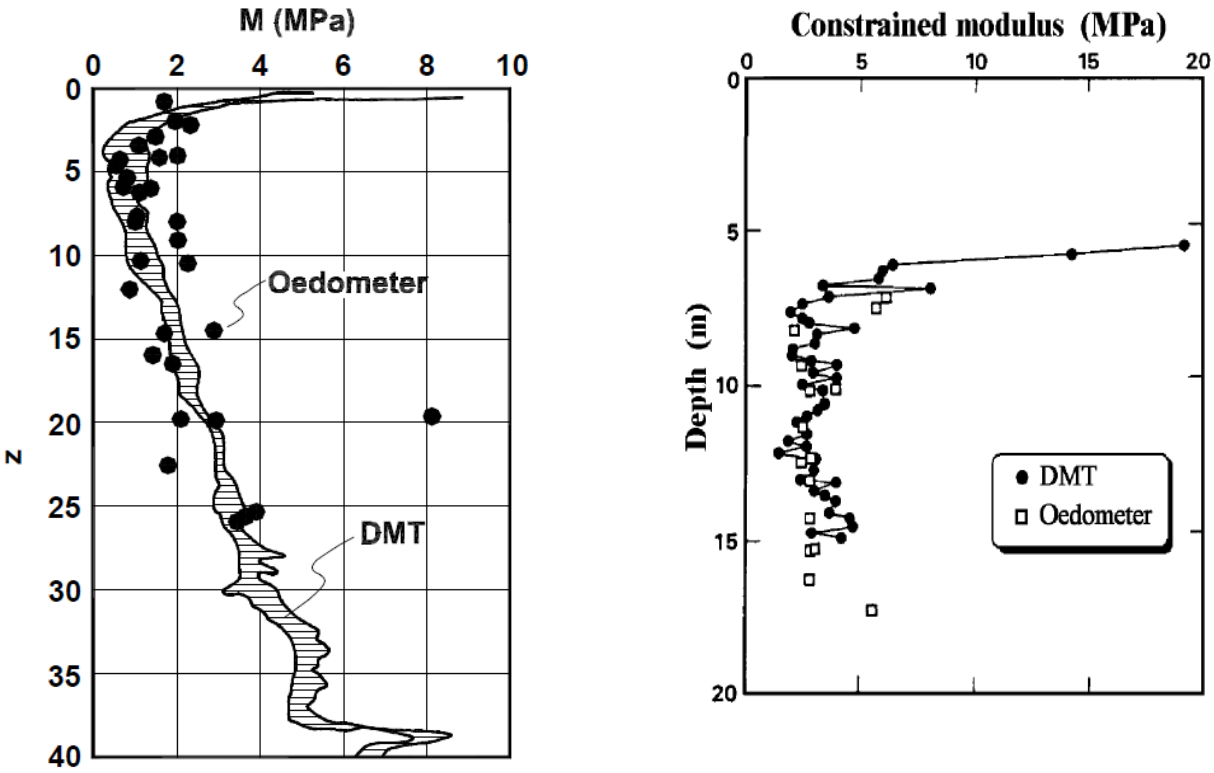

a)Onsoy Clay, Norway (Lacasse 1986) **b) Komatsugawa, Japan (Iwasaki et al.)**

Figure 25: Comparison between M determined from DMT and from Oedometer Tests

Failmezger et al. (1999) compared the constrained modulus by oedometer and DMT on both alluvial soils and residual soils in Virginia, USA. The results showed good correlation (Figure 26).

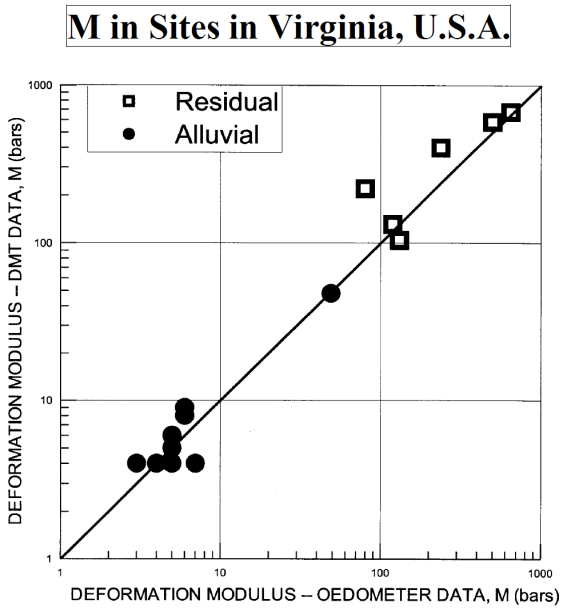

Figure 26: Oedometer vs. DMT Modulus Values (Failmezger et al. 1999)

2.1.5.4 Undrained Shear Strength, c_u

The research undertaken by Powell & Uglow (1998) on various UK soils showed good correlation of horizontal stress index, K_D, and the ratio of shear strength over effective overburden stress (Figure 27). The Marchetti (1980) correlation formula for c_u (Eqn 14) plotted on the graph in Figure 27 shows a straight line through the centre of the data points, suggesting a good correlation.

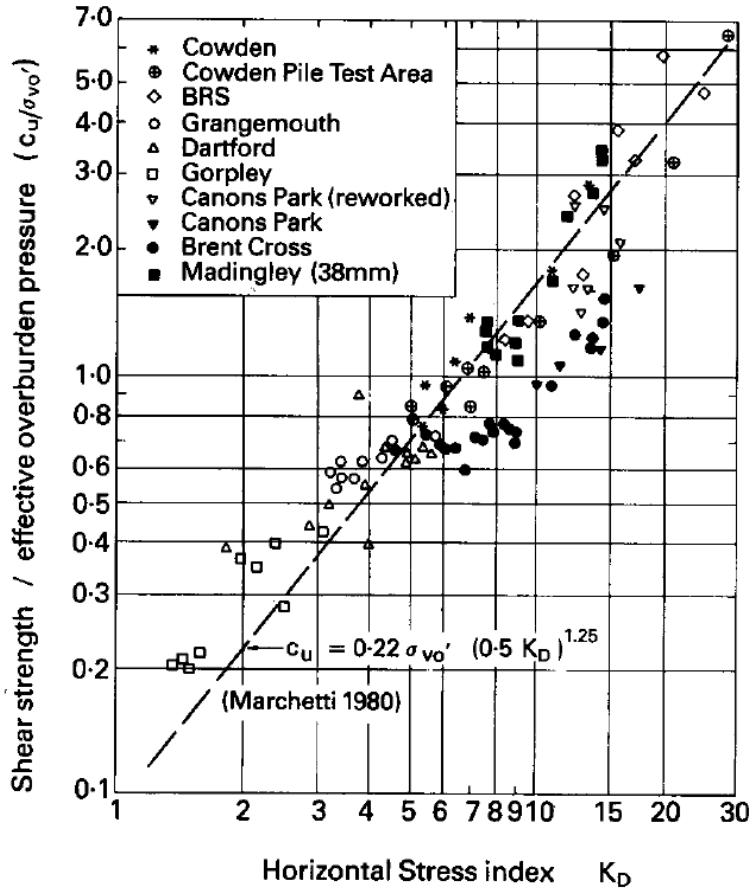

Figure 27: Shear Strength/effective Overburden Stress vs. K_D (Powell & Uglow 1988)

Much research has been carried comparing c_u assessed from DMT (Eqn 14) and those obtained from other laboratory and in-situ tests on a variety of clay soils in different parts of the world. The results of some of this research are illustrated below in graphical form vs. depth in Figure 28. The results generally show the DMT assessed c_u values to fall in between the values obtained by other methods.

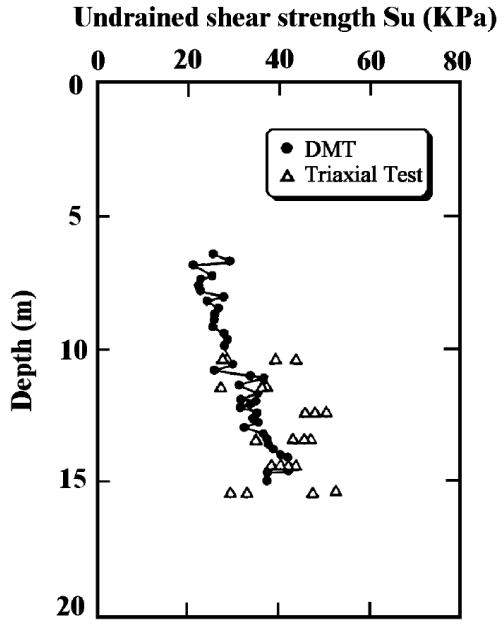

a) Compared to Triaxial Tests on Tokyo Bay Clay (Iwasaki et al. 1991)

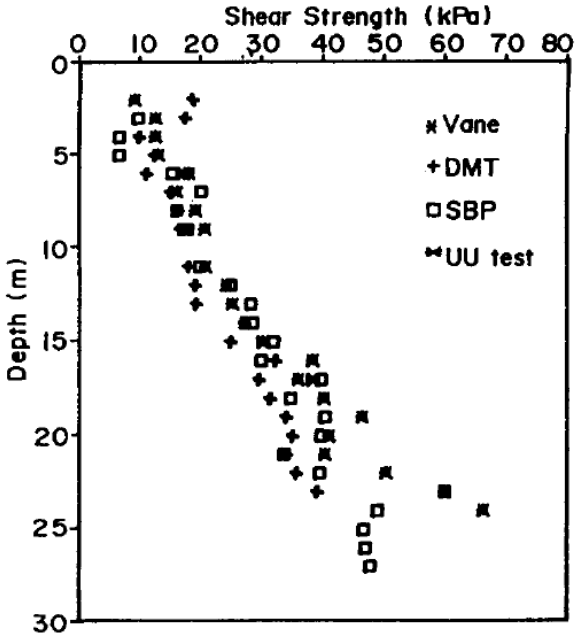

b) Compared to Vane, SBP and UU Tests in Malaysian Alluvial Clay (Wong et al. 1993)

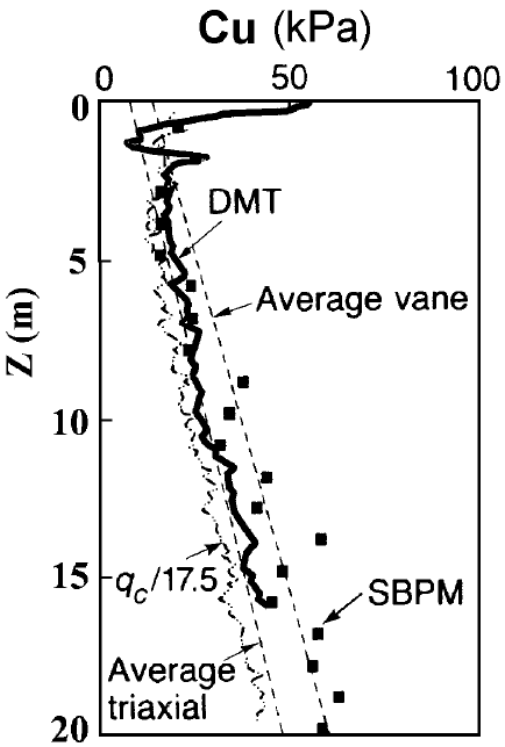

c) Compared to SBP, CPT, Vane and Triaxial Tests at Bothkennar, UK (Nash et al. 1995)

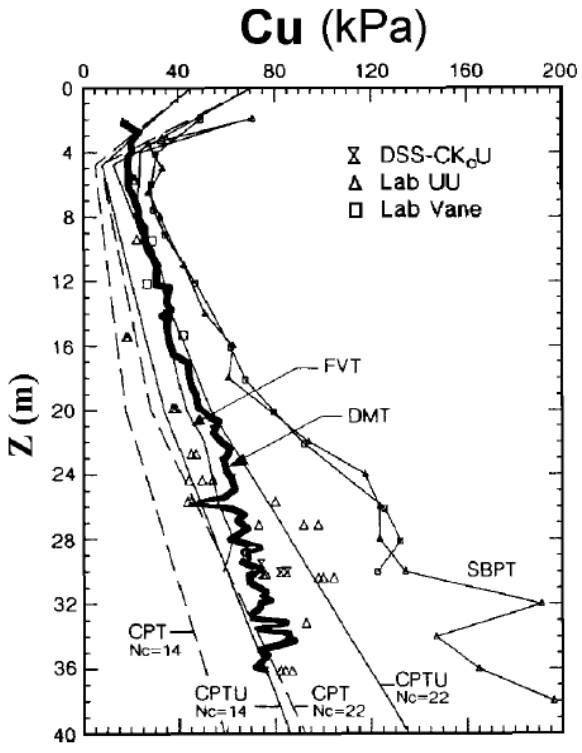

d) Compared to SBP, CPT, Vane and Triaxial Tests at Fucino, Italy (Burghignoli et al. 1991)

Figure 28: Comparison of Cu from DMT and from other Tests

2.1.5.5 Discussion on Marchetti (1980) Correlations

The original Marchetti (1980) interpretations were based on empirical correlations at 11 test sites, mostly in Italy. Despite the limited data and the empirical nature of the relationships, it is surprising that these original correlations, in many cases, show such good agreement with a wide range of soil types throughout the world. However, the wealth of research information on cross-comparisons between other reference tests has shown local variations and the development of new or improved relationships (e.g. Powell & Uglow 1988, Lacasse & Lunne 1988 and Lunne et al. 1992).

Mayne and Martin (1998) undertook a comprehensive review of the available comparative studies on DMT correlations. Table 5 in Appendix A gives a summary of some of the comparative studies completed and reported in the literature at that time. In this table the studies are organised according to individual soil parameters with brief comments and derived relationships listed for each study, along with the literature reference. Full details of each of the relationships are not discussed as this is beyond the scope and intent of this thesis, but the table is indicative of the wealth of research that has been undertaken in this area.

The complexities of the blade penetration, disturbance effects, membrane inflation and deflation, uncertainty in boundary and drainage conditions, rate effects, and other factors preclude a rigorous and exact method of interpretation for any soil parameter. Instead the correlation to soil parameters is heavily dependent on empirical relationships and, as such, variations can be expected in different soil types and geological units.

The computer program that accompanies the DMT uses only the standard Marchetti relationships (Table 2) without the ability to easily amend the correlations for local conditions. The use of this information should, therefore, be taken with some caution and with appreciation that the correlations may not be completely applicable for the particular soil type being tested. However, the Marchetti correlations (Table 2) provide a useful first approximation to soil parameters, which can be obtained in a quick and inexpensive manner. The results of the test (in the absence of other reference tests) may be adequate depending on the nature of the project concerned. However, the test should ideally be undertaken in conjunction with other reliable insitu or laboratory tests to confirm the correlations or develop new relationships, particularly in new soil types and for projects where the accuracy of the soil properties is crucial for design.

2.1.6 Shear Wave Testing using sDMT

The addition of a seismic module located above the mechanical DMT blade creates the 'seismic dilatometer' (sDMT). The two tests (DMT and Seismic) are separate tests that are undertaken together in the same sounding. The DMT tests are typically carried out every 200mm and the seismic test every 500mm depth. The addition of the seismic module allows shear wave velocity (V_S) to be obtained. The seismic module is equipped with two geophones spaced at 500mm vertical distance. The 'true-interval' test configuration avoids possible inaccuracy in the determination of the 'zero time' at the hammer impact, sometimes observed in 'pseudo-interval' one-receiver configurations. Furthermore, the two seismograms recorded by the two geophones at a given depth correspond to the same hammer blow and not to different blows in sequence, which are not necessarily identical. Hence the accuracy and repeatability of V_S measurements are considerably improved with observed V_S repeatability typically 1-2% (Marchetti 2008).

Figure 29 shows an example of seismographs obtained by sDMT tests at various depths at the research site at Fucino, Italy (Marchetti 2008). The two seismographs (relating to the two geophones) for each hammer blow are plotted together (left hand side of Figure 29) and then re-phased to bring the seismographs together (right hand side of Figure 29). Thus the delay time (Δt) in the arrival of the impulse from the first to the second geophone can be determined. This allows the shear wave velocity to be calculated simply as:

$$V_S = (S_2 - S_1)/\Delta t \qquad (18)$$

Where, $(S_2 - S_1)$ = different in distance between the source and the two geophones

The small-strain shear modulus (G_0) is determined from the relationship:

$$G_0 = \rho(V_S)^2 \qquad (19)$$

,where, $\rho = \gamma_T/g_a$, γ_T = total soil unit weight, g_a = gravitational acceleration (9.81)

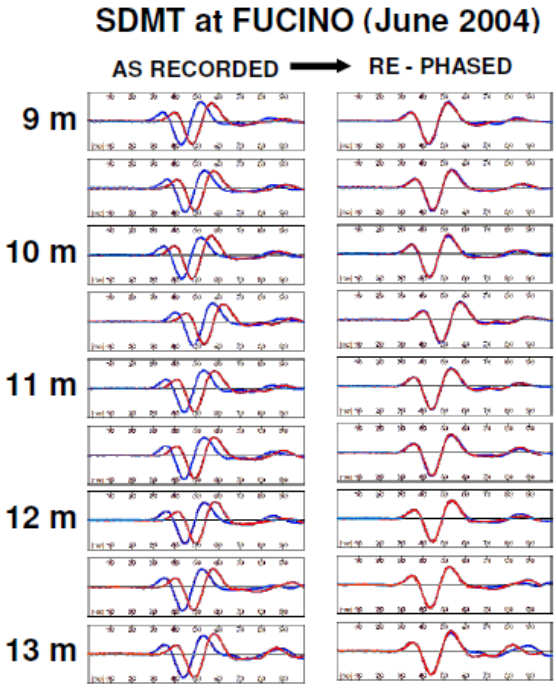

Figure 29: Example of Seismograms Obtained by SDMT at the Site of Fucino, Italy (Marchetti 2008)

V_S measurements by sDMT have been validated by comparison to those obtained by other methods at various research sites (Marchetti 2008). Figure 30 shows V_S comparisons at the research site of Fucino, Italy. This shows the sDMT derived V_S values (2004) to be in good agreement with those obtained by seismic CPT, Cross-hole and SASW in previous investigations (AGI 1991). Similar favourable comparisons are reported by various authors, for example, by Hepton (1988), McGillivray and Mayne (2004) and Mlynarek et al. (2006).

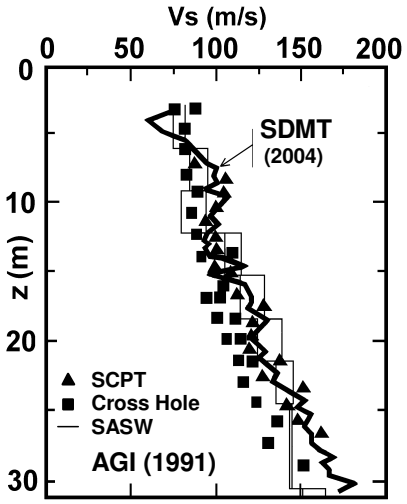

Figure 30: Comparison of V_S obtained by sDMT and by other methods at Fucino (Marchetti 2008)

The seismic test in combination with the DMT test allow both small strain modulus values (G_0) and larger strain ('working strain') modulus (M_{DMT}) to be determined from the sounding.

Research by Marchetti (2008) shows that the ratio of G_0/M_{DMT} is highly dependent on (at least) both soil type (represented by I_D) and stress history (represented by K_D). Plots of G_0/M_{DMT} vs. K_D for the three soil types (clay, silt and sand) from experimental sDMT data are given in Figure 31. These show a general trend represented by the following equations:

$$G_0/M_{DMT} = 26.177\ K_D^{-1.0066} \quad \text{for } I_D < 0.6 \qquad (20)$$

$$G_0/M_{DMT} = 15.686\ K_D^{-0.921} \quad \text{for } 0.6 < I_D < 1.8 \qquad (21)$$

$$G_0/M_{DMT} = 26.177\ K_D^{-1.0066} \quad \text{for } I_D > 1.8 \qquad (22)$$

It is suggested that if points fall significantly above the lines represented by Eqns 20 to 22 in Figure 31 (i.e. G_0 and K_D are high in relation to M_{DMT}) this may then represent bonding in the soil material.

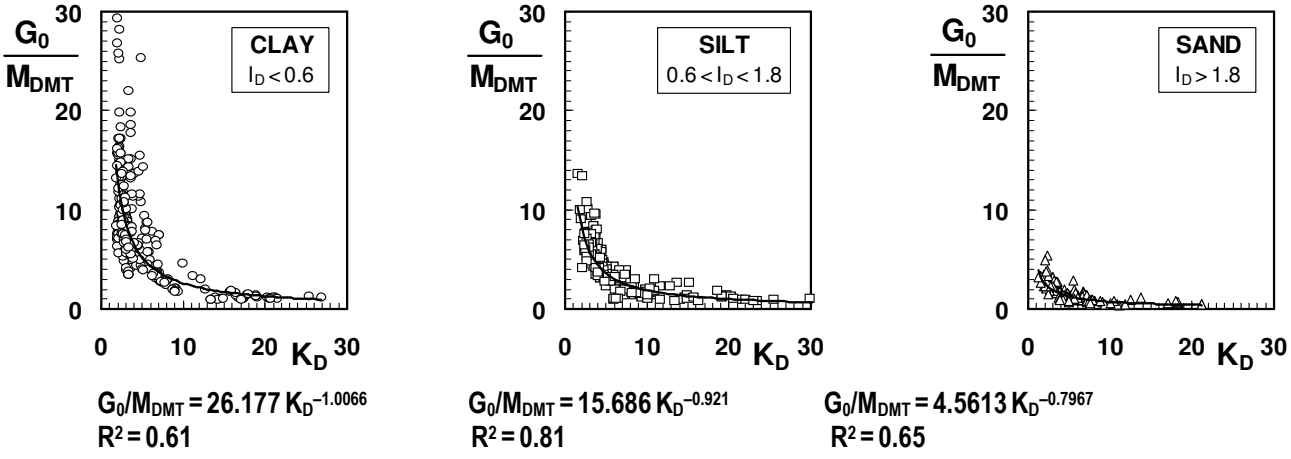

Figure 31: Ratio G_0/M_{DMT} vs. K_D for Clay, Silt and Sand (Marchetti 2008)

The working strain shear modulus, G_{DMT} can be determined from elastic theory as follows:

$$G = M/[2(1-\nu)/(1-2\nu)] \qquad (23)$$

Assuming an 'average' value of $\nu = 0.2$, Eqn 23 then becomes:

$$G_{DMT} = M_{DMT}/2.67 \quad (24)$$

The ratio of G_{DMT}/G_0 (modulus decay ratio) can then be determined. Plots of G_{DMT}/G_0 are shown on Figure 32. These show a general trend represented by the following equations:

$$G_{DMT}/G_0 = -0.0002K_D^2 + 0.022K_D - 0.0173 \quad \text{for } I_D < 0.6 \quad (25)$$

$$G_{DMT}/G_0 = 0.0241K_D^{0.919} \quad \text{for } 0.6 < I_D < 1.8 \quad (26)$$

$$G_{DMT}/G_0 = 0.0826K_D^{0.7961} \quad \text{for } I_D > 1.8 \quad (27)$$

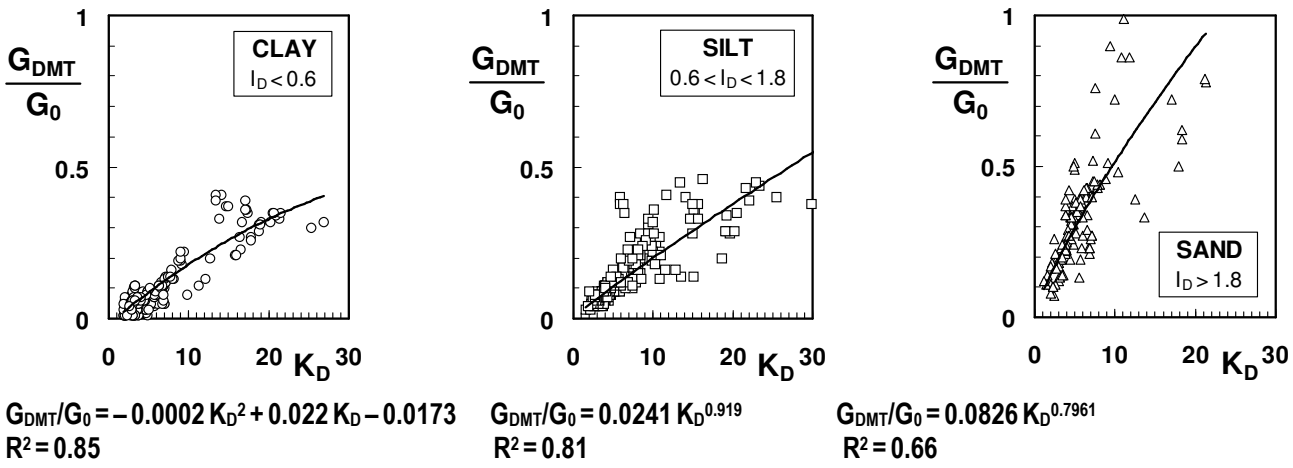

Figure 32: Decay ratio G_{DMT}/G_0 vs. K_D for clay, silt and sand (Marchetti 2008)

The decay ratio (G_{DMT}/G_0) could be used to derive a G-γ curve by the tentative method suggested by Marchetti (2008). This method involves determining G_{DMT}/G_0 from the relationships described above and plotting on 'reference typical-shape' laboratory curves at an appropriate strain value.

Mayne (2001) suggests the DMT moduli represents an intermediate strain level of $\gamma \approx 0.05–0.1\%$. Plotting G_{DMT}/G_0 at this strain level will help select the most appropriate standard curve for use in further analysis. A similar approach is described by Mayne et al. (1999).

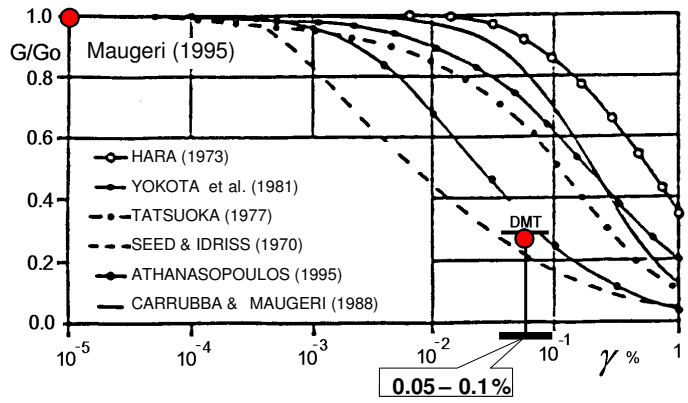

Figure 33: Example of G_0 and G/G_0 from sDMT plotted with Reference Typical-Shape Laboratory Curves (Marchetti 2008)

The shear wave velocity can also be used to assess liquefaction potential of sandy soils (Andrus and Stokoe 2000). The horizontal stress index, K_D, obtained from the DMT test in the same sounding can be used to provide an alternative method for assessing liquefaction (Monaro et al. 2005). Thus two totally independent evaluations of liquefaction potential can be made from the sDMT results.

2.2 CONE PENETRATION TEST (CPT)

2.2.1 Development of the CPT

The cone penetration test (CPT) was first developed in the Netherlands in the 1930's as a mechanical test using a 35mm dia. cone attached to a steel inner rod inside a 35mm dia. gas pipe (Figure 34). The test was performed by pushing the inner rod with cone through the outer 'casing' pipe a distance of 150mm and measuring the force required to do so. The casing was then pushed down to the cone and then both the casing and the inner rods were pushed down together until the next test depth. Improvements to the system were made by Vermeiden (1948) by adding a conical part just above the cone to prevent soil from entering the gap between the casing and the rods (Figure 35). Begemann (1953) significantly improved the Dutch cone test by adding an 'adhesion jacket' behind the cone (Figure 36). Both the Vermeiden type cone and the Begemann cone are still regularly used today in some parts of the world.

In 1965 an electric cone was developed by Fugro (de Ruiter 1971), the size and shape of which forms the basis for all modern day CPT cones. The main improvements relative to the mechanical cone penetrometers were:

- Elimination of incorrect readings due to friction between inner and outer rods and weight of inner rods.
- Continuous testing with continuous rate of penetration without the need for alternate movements of different parts of the penetrometer and no undesirable soil movements influencing the cone resistance.
- Simpler and more reliable electrical measurement of cone resistance and sleeve friction.

Cone penetrometers that could also measure pore water pressure (piezocone) were introduced in the 1970's (Janbu and Senneset 1974). The pore water pressure was measured through a porous filter located in the probe. Numerous variations of the piezocone were developed with the porous filter in different locations, half-way up the cone (u_1 position); just behind the cone (u_2 position) and; above the friction sleeve (u_3 position). Gradually the practice has changed so that the recommended (and most common) position is just behind the cone, i.e. the u_2 position (ISSMFE 1989; Figure 37).

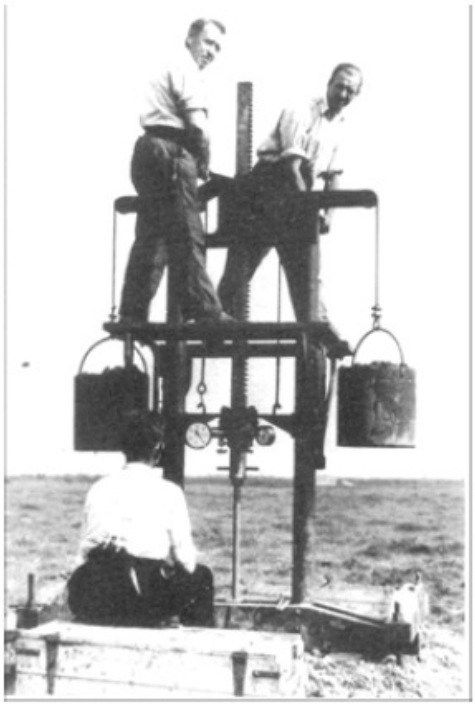

a) CPT 'rig' of 1930's-1940's era

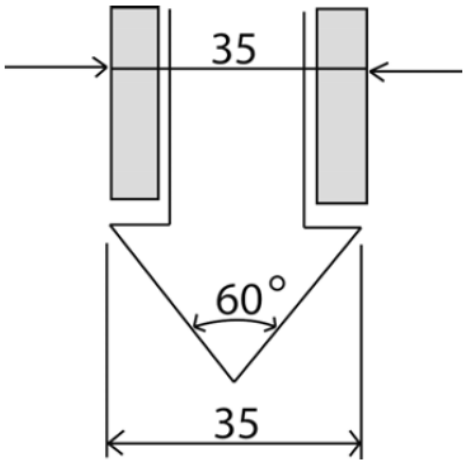

b) Original Dutch Cone

Figure 34: Early Dutch Mechanical Cone System used in the 1940's (after Delft Geotechnics)

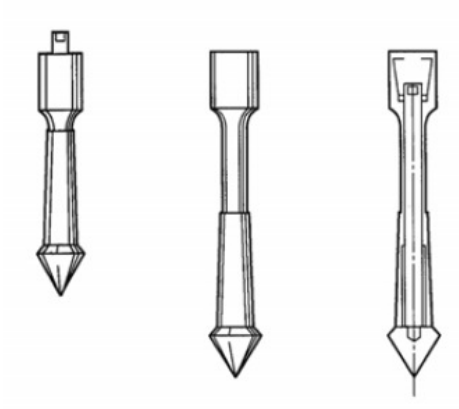

Figure 35: 'Vermeiden' Type Cone

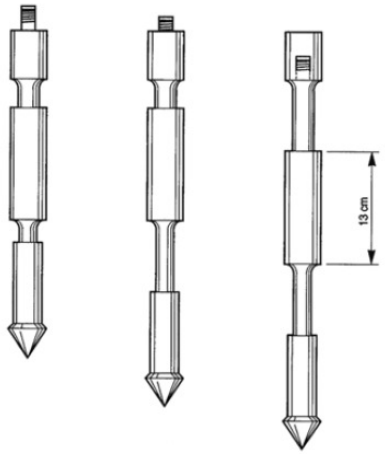

Figure 36: "Begemann' Type Cone

Different size piezocones are available (Figure 37) but the most common size is 10 cm^2, which is the 'standard' size, although the larger 15 cm^2 cone is sometimes used in harder ground (Robertson and Cabal 2010).

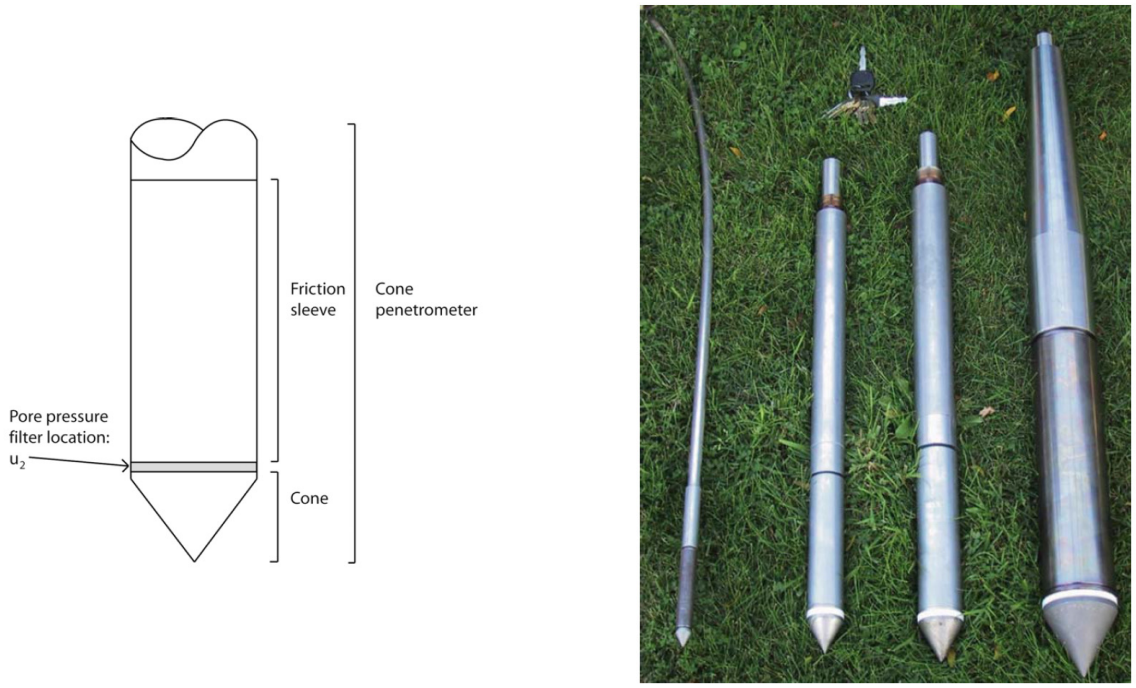

a) Schematic diagram of a piezocone **b) variety of piezocones (2, 10, 15 & 40 cm^2)**

Figure 37: Electric Piezocones with Porewater Pressure Filter in the u_2 Position

2.2.2 CPT Test Procedure and Basic Results

The CPT probe is pushed into the ground at a constant rate of 20 mm/s ± 5 mm/s (ISSMFE 1989). The sensors in the cone produce continuous analogue data of cone resistance (q_c), sleeve friction (f_s) and pore water pressure (u_2) that is converted to digital form at intervals of between 20 mm and 200 mm, depending on the equipment and test standard used.

Due to the inner geometry of the cone the ambient water pressure acts on the shoulder behind the cone and on the ends of the friction sleeve. This effect is often referred to as the unequal end area effect (Campanella et al., 1982). Figure 38 illustrates the key features for water pressure acting behind the cone and on the end areas of the friction sleeve (Lunne et al. 1997). In soft clays and silts and in over water work, the measured q_c must be corrected for pore water pressures acting on the cone geometry, thus obtaining the corrected cone resistance, q_t:

$$q_t = q_c + u_2 (1 - a) \qquad (28)$$

,where 'a' is the net area ratio determined from laboratory calibration with a typical value between 0.70 and 0.85.

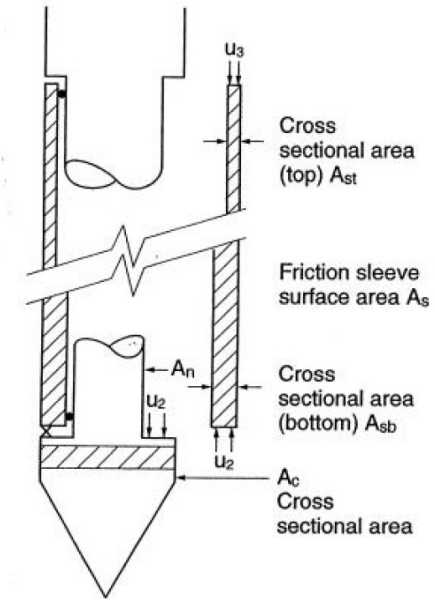

Figure 38: Unequal end area effects on cone tip and friction sleeve

The basic test results are usually plotted as graphs of q_c (or q_t), f_s, u_2 and R_f against depth, where R_f is the friction ratio ($=f_s/q_t$).

2.2.3 CPT Interpretation

2.2.3.1 Soil Behaviour Type Index

The CPT can be used as a soil profiling tool for identifying soil type. Typically, the cone resistance, (q_t) is high in sands and low in clays, and the friction ratio (R_f) is low in sands and high in clays. The CPT cannot be expected to provide accurate predictions of soil type based on physical characteristics, such as, grain size distribution but provide a guide to the mechanical characteristics (strength and stiffness) of the soil, or the 'soil behavior type' (SBT). CPT data provides a repeatable index of the aggregate behavior of the in-situ soil in the immediate area of the probe. Hence, prediction of soil type based on CPT is referred to as Soil Behavior Type (SBT) (Robertson & Cabal 2010).

A soil classification chart was developed by Robertson et al. (1986). This was further adapted by Robertson (1990) using the following normalised CPT parameters to identify soil behaviour type.

$$Q_t = (q_t - \sigma_{vo})/\sigma_{vo}' \quad (29)$$

$$F_r = [f_s/(q_t - \sigma_{vo})] \quad (30)$$

$$B_q = (u_2 - u_o)/(q_t - \sigma_{vo}) \quad (31)$$

,where σ_{vo} = pre-insertion in-situ total vertical stress, σ_{vo}' = pre-insertion in-situ effective vertical stress, u_o = pre-insertion in-situ equilibrium pore water pressure

The normalised soil behaviour type chart developed by Robertson (1990) is shown in Figure 39. Robertson (1990) also suggested another chart based on pore pressure ratio (B_q) to eliminate potential errors with sleeve friction measurements, but recommended that the $Q_t - F_r$ chart was generally more reliable.

Jefferies and Davies (1993) identified that a SBT index, I_c, could represent the SBT zones in the $Q_t - F_r$ chart. Robertson and Wride (1998) modified the definition of Ic to apply to the $Q_t - F_r$ chart, as defined by:

$$I_c = [(3.47 - \log Q_t)^2 + (\log F_r + 1.22)^2]^{0.5} \quad (32)$$

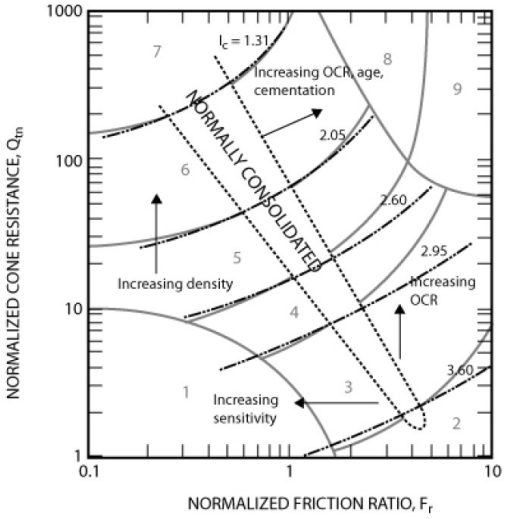

Zone	*Soil Behavior Type*	I_c
1	*Sensitive, fine grained*	N/A
2	*Organic soils – clay*	> 3.6
3	*Clays – silty clay to clay*	2.95 – 3.6
4	*Silt mixtures – clayey silt to silty clay*	2.60 – 2.95
5	*Sand mixtures – silty sand to sandy silt*	2.05 – 2.6
6	*Sands – clean sand to silty sand*	1.31 – 2.05
7	*Gravelly sand to dense sand*	< 1.31
8	*Very stiff sand to clayey sand**	N/A
9	*Very stiff, fine grained**	N/A

** Heavily overconsolidated or cemented*

Figure 39: Normalised SBT Chart for CPT (Robertson 1990)

2.2.3.2 Undrained Shear Strength

Various theoretical and empirical correlations have been reported in the literature (Lunne, et al. 1997). The basis for all theoretical relationships are fundamentally in line with classical bearing capacity theory (Terzaghi 1943), such that:

$$q_c = N_c.c_u + \sigma_{vo} \quad (33)$$

,where c_u = undrained shear strength; N_c = bearing capacity (cone) factor

For CPTu tests, this can be re-arranged to give:

$$c_u = (q_t - \sigma_{vo})/N_{kt} \quad (34)$$

,where N_{kt} = cone factor relating to corrected total cone resistance

Teh (1987) developed a theoretical solution for N_{kt} based on strain path theory (Baligh 1985) as shown on Figure 40. This figure shows that the penetration resistance is affected by the undrained shear strength (s_u), in-situ stress (σ'_{vo}, K_0), rigidity index (I_r) and cone roughness coefficient (α).

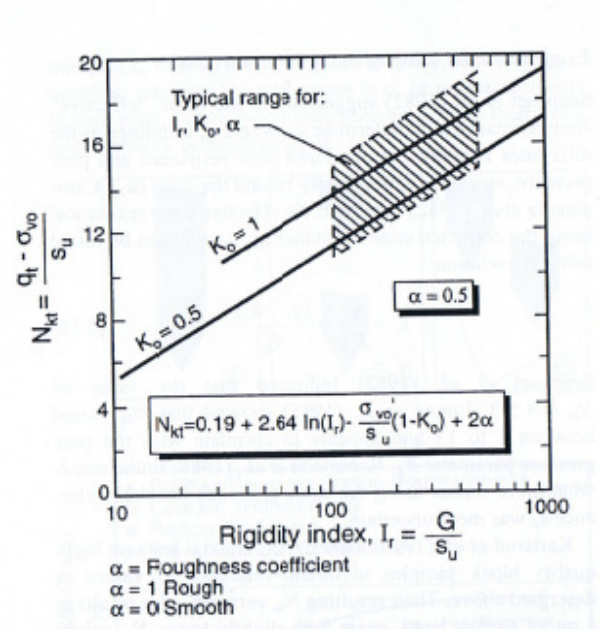

Figure 40: Theoretical Solution for Nkt (Teh, 1987)

Cone penetration is a complex mechanism dependant on many factors. As such, theoretical solutions do not provide a complete answer as assumptions need to be made to account for the various factors. Hence empirical correlations are generally preferred, but the theoretical solutions provide a basic framework for empirical relationships.

From numerous empirical correlations with field and laboratory tests, N_{kt} typically varies from 10 to 18, with an average of approximately 14 (Robertson and Cabal 2010).

Aas et al. (1986) showed that N_{kt} tends to increase with increasing plasticity and decrease with increasing soil sensitivity (Figure 41).

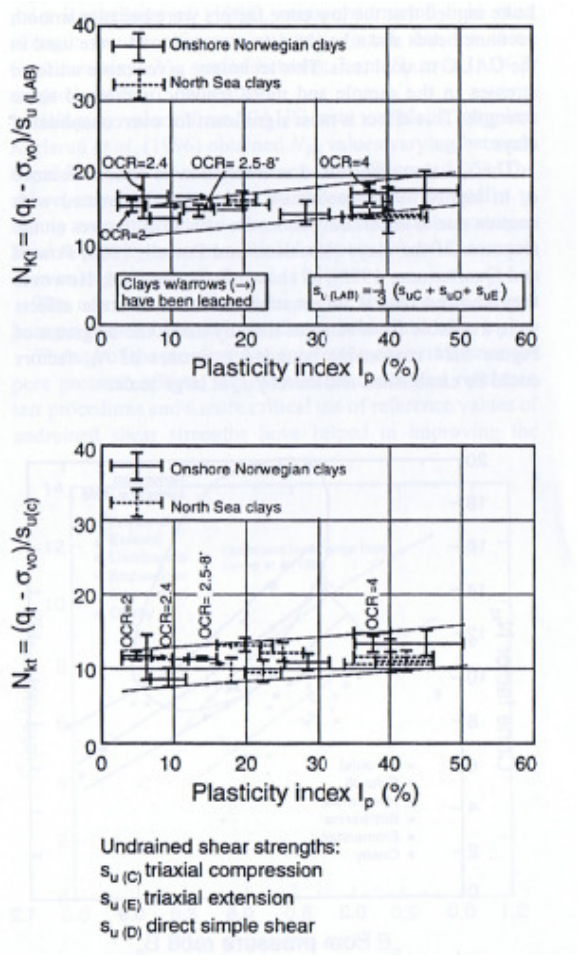

Figure 41: Computed Cone Factor, Nkt vs. Ip (Aas et al. 1986)

Lunne et al. (1997) showed that N_{kt} varies with pore pressure ration. B_q, where N_{kt} decreases as B_q increases. When $B_q \approx 1.0$, N_{kt} can be as low as 6.

In very soft clays, where there may be some uncertainty with the accuracy in q_t, estimates of c_u can be made from the excess porewater pressure as follows (Lunne et al. 1997):

$$c_u = \Delta u / N_{\Delta u} \qquad (35)$$

,where Δu = excess pore pressure = $u_2 - u_0$; $N_{\Delta u}$ = excess pore pressure cone factor

Based on cavity expansion, $N_{\Delta u}$ is theoretically shown to vary between 2 and 20. Lunne at al. (1985) found $N_{\Delta u}$ to correlate well with B_q (Eqn 36) and $N_{\Delta u}$ was found to vary between 4 and 10.

$$N_{\Delta u} = B_q N_{kt} \qquad (36)$$

2.2.3.3 K_o and OCR

For overconsolidated clays, the following general relationship exists:

$$(c_u/\sigma_v')_{OC} = (c_u/\sigma_v')_{NC}. OCR^m \quad (37)$$

This relationship assumes the undrained shear strength ratio c_u/σ_v' in the normally consolidated (NC) state can be factored up to provide an overconsolidated ratio of c_u/σ_v' by the overconsolidation ratio (OCR) to the power of a factor m, which is approximately 0.8, according to Ladd et al. (1977).

Critical state soil mechanics presents a relationship between $(c_u/\sigma_v')_{NC}$ for normally consolidated clays under different loading directions and effective stress friction angle, ϕ'. For normally consolidated clays (Robertson & Cabal 2010):

$$(c_u/\sigma_v')_{NC} = 0.22 \quad (38)$$

,in direct simply shear ($\phi' = 26^o$)

From Eqn 33:

$$(c_u/s'_{vo}) = [(q_t - s_{vo})/N_{kt}]/s'_{vo} = Q_t/N_{kt} \quad (39)$$

Combining Eqns. 37, 38 and 39, gives (Robertson 2009):

$$OCR = 0.25\ (Q_t)^{1.25} \quad (40)$$

Kulhawy and Mayne (1990) suggested a simpler method:

$$OCR = kQ_t \quad (41)$$

for $Q_t < 20$, where k = 0.2 to 0.5, average 0.3

OCR (and K_0) can also be estimated using the correlation by Anderson et al. (Figure 42).

Kulhawy and Mayne (1990) suggested a much simpler approach, using:

$$K_0 = 0.1\ Q_t \qquad (42)$$

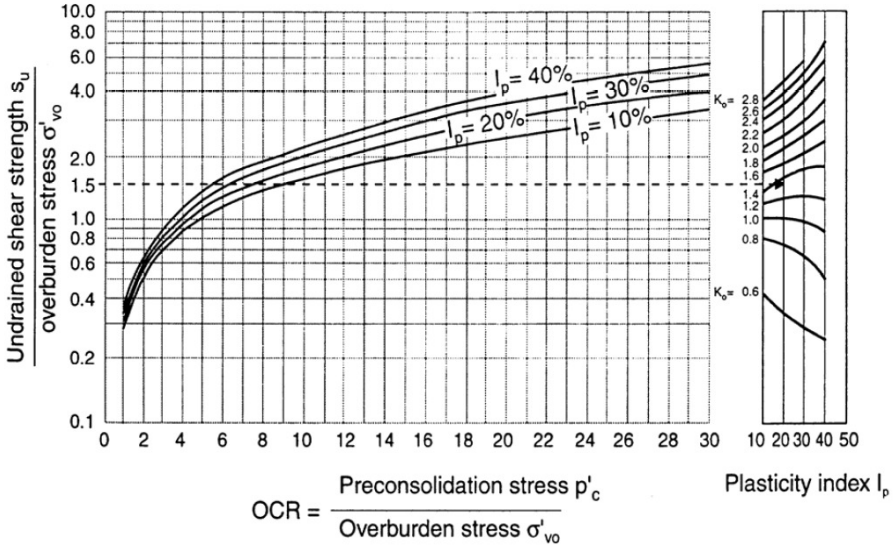

Figure 42: OCR and K_0 from s_u/σ_{vo}' and I_p (Anderson et al. 1979)

2.2.3.4 Constrained Modulus

Constrained modulus, M can be estimated from CPT results using the following empirical relationship (Senneset et al. 1982, 1989):

$$M = \alpha_M(q_t - \sigma_{vo}) \qquad (43)$$

,where α_M = empirically derived dimensionless factor

According to Senneset (1989), α_M varies between 4 and 8. Sangrelat (1972) suggested that α_M varies with plasticity and natural moisture content for a wide range of fine grained soils and organic soils. Meigh (1987) suggested that α_M lies in the range 2 – 8, whereas Mayne (2001) suggested a general value of 8 and Kulhawy and Mayne (1990) a value of 8.25. Robertson (2009a) suggested that α_M varies with Q_t and I_c, such that:

When $I_c > 2.2$, use:

$\alpha_M = Q_t$, when $Q_t < 14$

$\alpha_M = 14$, when $Q_t > 14$

When $I_c < 2.2$, use:

$\alpha_M = 0.0188[10^{(0.55Ic + 1.68)}]$

Lunne et al. (1997) warned that total stress undrained measurements from the CPT are difficult to correlate to drained parameters without the addition of pore pressure measurements. The prediction of consolidation deformation based on cone resistance may be in error by as much as ± 100%.

2.2.3.5 Small Strain Shear Modulus

The small shear strain modulus, G_0 , can be determined from CPT using the following equation (Robertson 2009):

$$G_0 = \alpha_G(q_t - \sigma_{vo}) \quad (44)$$

,where, α_G = shear modulus factor

The shear modulus factor, α_G can be estimated from the SBT index, I_c as follows (Robertson 2009):

$$\alpha_G = 0.0188[10^{(0.55Ic + 1.68)}] \quad (45)$$

Hence:

$$G_0 = 0.0188[10^{(0.55Ic + 1.68)}](q_t - \sigma_{vo}) \quad (46)$$

Robertson (2009) notes that this relationship may be less reliable for use in fine grained soils (I_c>2.6) due to the influence of soil sensitivity on f_s, and hence F_r.

2.3 COMPARISON OF CPT AND DMT

2.3.1 Insertion Effects

During the initial work by Marchetti (1980) consideration was given to the insertion effects of the DMT blade. It was considered that the displacement effects by the blade insertion (approx. 15 mm thick) are much lower than that of the conical tip of a CPT (36 mm). Figure 43 illustrates the comparative strains caused by insertion of wedges and cone (Baligh 1975 and Baligh and Scott 1975). During penetration there is a concentration of shear strain near the edges of the blade so that the soil facing the membrane undergoes comparatively lower shear strain (Marchetti 1979).

The soil at the face of the membrane has been prestained during penetration and, although the shear strains in this area are comparatively low, soil stiffness is sensitive to prestrains. Correction factors are therefore required to evaluate the modulus of the original (undisturbed) soil. Marchetti (1980) makes the point that, in sensitive soils, alterations to soil properties due to penetration are generally large and undefinable, so that the original soil properties cannot be traced back. However, Marchetti (1980) does not undertake any further analysis of such insertion effects, but bases his correlations to soil parameters empirically from experimental data.

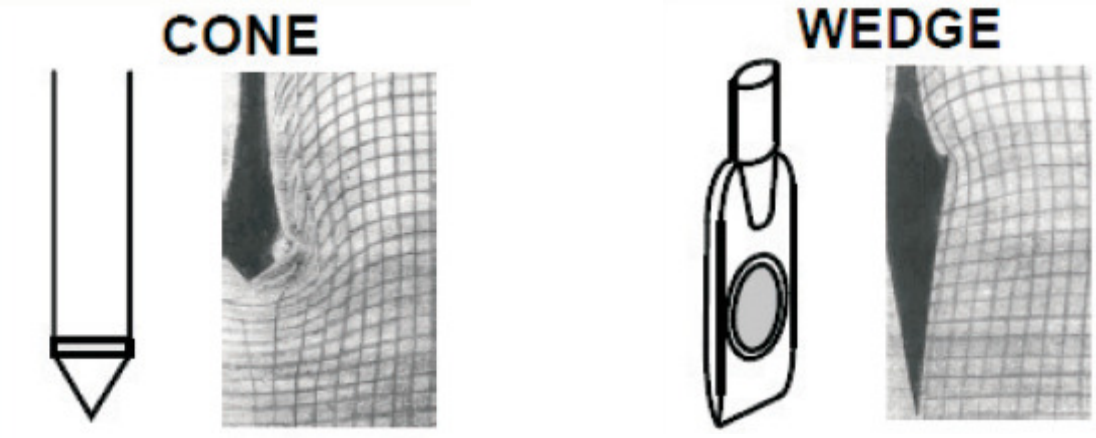

Figure 43: Soil Deformation due to Wedge Penetration compared to Cone Penetration (Baligh and Scott 1975)

Hughes and Robertson (1985) analysed the horizontal stresses against the CPT sleeve in sands. They showed that at the level of the conical tip, σ_h reaches very high values, while behind the tip, σ_h undergoes a large stress reduction. Thus a zone of high residual stress is created some distance from the sleeve, as a sort of arching phenomenon. However, the 'plane' tip of the DMT probe should reduce arching and improve the possibility of sensing σ_h. Also the stress reduction after the wedge is likewise considerably smaller due to the streamlined shape in the transition zone.

More detailed analytical studies of insertion effects have been undertaken by Finno (1993) considering the three dimensional strain path method (Baligh 1985). Cavity expansion analysis has been considered by Yu et al. (1993). Yu (2004) considered and compared the theoretical analysis of the blade insertion by both the strain path and the cavity expansion methods in clays as well as the discrete element method in sands. The conclusions were that the flat cavity expansion method and the strain path method prove to be useful theoretical frameworks for modelling the installation of the dilatometer. It was considered that three dimensional finite element methods would be required to model the expansion of the dilatometer.

Lehane et al. (2004) compared field measurements of DMT tests in sand to numerical analyses of the inserted blade and expanded membrane. In this study, the DMT test was conducted in test pits that were backfilled with sand. The results were compared between tests where the blade was pushed into the backfilled sand and tests where the sand was backfilled around the blade. Numerical analyses were also carried out to model both the insertion effects and the membrane expansion. It was concluded that the E_D value measured following insertion into sand is about 2.5 to 3 times higher than that measured in the backfilled sand. A similar effect was obtained from the numerical analysis.

Ahmadi and Robertson (2005) illustrated by numerical analysis how the cone resistance is affected by the soil ahead and behind the cone. They found that the cone can sense a soil interface up to 15 cone diameters (i.e. 540mm for a standard 36mm cone) ahead and behind the cone. This means that in the transition zone between, say, a sand and a clay, the cone may give misleading results as it will be influenced by both the sand and the clay. Robertson (1990a) suggests that these transition zones may be identified by rapid changes in the soil behaviour type index, I_c, when plotted in depth profile. He suggests that where these transition zones are identified, they should be removed from the data.

2.3.2 CPT – DMT Correlations

There are very few published studies that comprehensively compare CPT and DMT tests. An early study by Campanella and Robertson (1991) considered a specially developed research dilatometer based on the standard Marchetti DMT. The research dilatometer was identical to the standard DMT except that it was able to measure porewater pressure, deflection of the centre of the membrane and penetration force by way of a load cell located just above the blade. The penetration stress, q_D, of the blade installation was compared to the CPT cone resistance, q_c in sands and the following relationship was found:

$$q_D = 1.1\ q_c \qquad (47)$$

,where q_D = trust force/cross-sectional area at the end of the blade.

The 10% increase in the DMT penetration stress over the cone resistance was considered to be due to frictional stresses on the sides of the blade. Figure 44 shows plots of the DMT lift-off and expansion pressures (p_0 and p_1) and the DMT horizontal stress index, K_D against penetration resistance, q_D (normalised for the K_D plot). These plots show an approximate linear relationship between penetration resistance and the values of p_0, p_1 and K_D. By combining the equations obtained from these linear relationships with Eqn 47, the following correlations with CPT q_c were obtained:

$$E_D = 2.63\ q_c \qquad (48)$$

$$q_c/\sigma'_{vo} = 33\ K_D \qquad (49)$$

TC16 2001 suggests the following broad cross relationships based on various experimental studies:

$$M_{DMT}/q_c = 5 - 10 \quad \text{in NC sands} \qquad (50)$$

$$M_{DMT}/q_c = 12 - 24 \quad \text{in OC sands} \qquad (51)$$

The increasing ratio of M/q_c with overconsolidation is a reflection of the DMT's sensitivity to compaction.

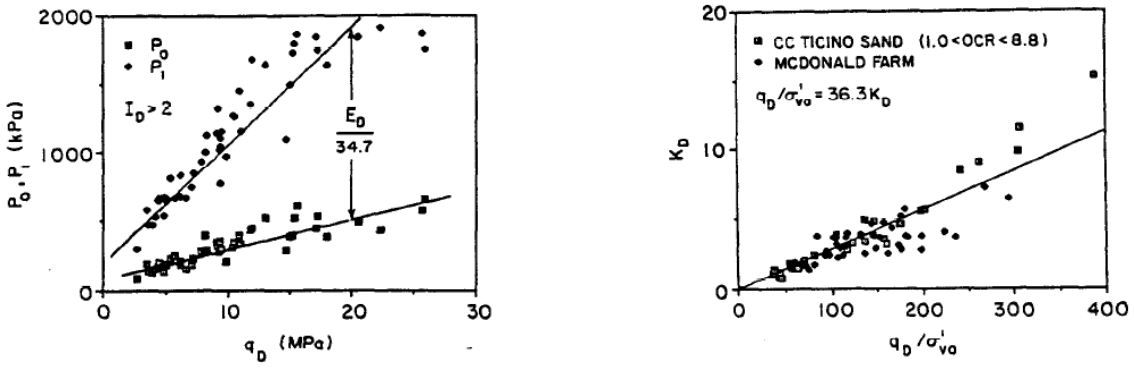

(a) **(b)**

Figure 44: Plots of (a) P_0 & P_1 and (b) K_D vs. DMT Penetration Resistance, q_D (Campanella and Robertson 1991)

TC16 2001 suggests the following broad cross relationships based on various experimental studies:

$$M_{DMT}/q_c = 5 - 10 \qquad \text{in NC sands} \qquad (50)$$

$$M_{DMT}/q_c = 12 - 24 \qquad \text{in OC sands} \qquad (51)$$

The increasing ratio of M/q_c with overconsolidation is a reflection of the DMT's sensitivity to compaction.

Mayne and Liao (2004) compared CPT and DMT tests in Piedmont residual soils that comprise silty fine sands and fine sandy silts. Figure 45 shows the relationship obtained in this material between the DMT modulus and the CPT cone resistance. This suggests a linear relationship of:

$$E_D = 5\ q_t \qquad (52)$$

The DMT material index, I_D, relates to the grain size of the soil, as does the CPT friction ratio, F_r (normalised friction ratio). Thus a relationship may exist between these two values. Figure 45 shows a general trend between I_D and F_r, such that:

$$I_D = 2.0 - 0.14\ F_r \qquad (53)$$

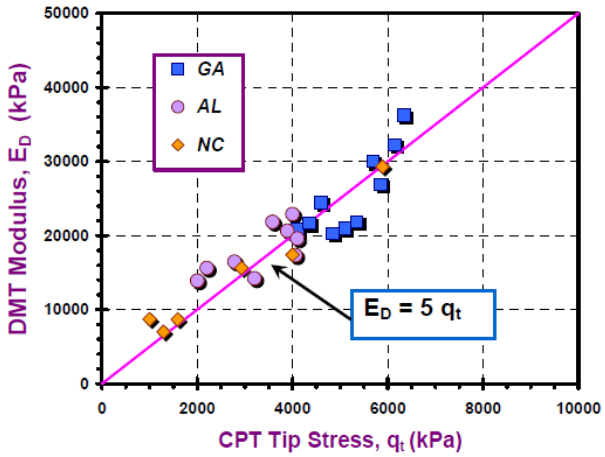

Figure 45: Relationships between DMT E_D and CPT q_t in Piedmont Residual Soil (Mayne and Liao 2004)

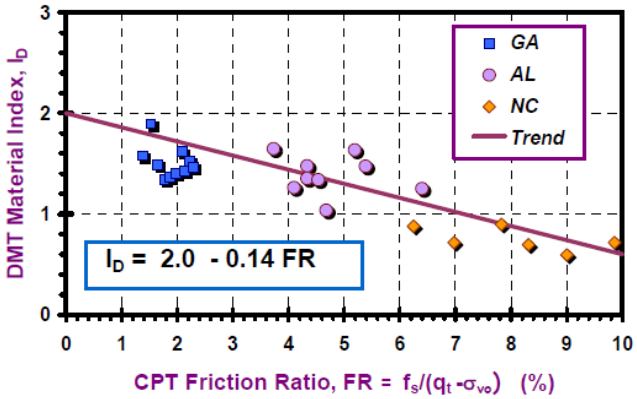

Figure 46: Relationships between DMT I_D and CPT F_r in Piedmont Residual Soil (Mayne and Liao 2004)

The third DMT index value, the horizontal stress index (K_D), can be obtained from the first two indices as follows:

$$K_D = (p_0 - u_o)/\sigma'_{v0} = E_D/(34.7\ I_D\ \sigma'_{v0}) \qquad (54)$$

By combining Eqns 52, 53 and 54:

$$K_D = q_t/[(13.88 - 0.97\ F_r)\ \sigma'_{v0}] \qquad (55)$$

Thus, all three DMT indices can be obtained from conversion of CPT data by way of Eqns 52, 53 and 55. This approach of converting CPT data to DMT indices was validated by Mayne and Liao (2004) by using the DMT indices converted from CPT to obtain M values by the usual Marchetti data reduction equation (Eqn 10) and comparing to the M values obtained from the direct

application of the actual DMT obtained values. Figure 47 shows a plot of the direct DMT derived M values in comparison to those obtained by the conversion of CPT data. This indicates a reasonable comparison, thus suggesting that the CPT conversion approach has some validity.

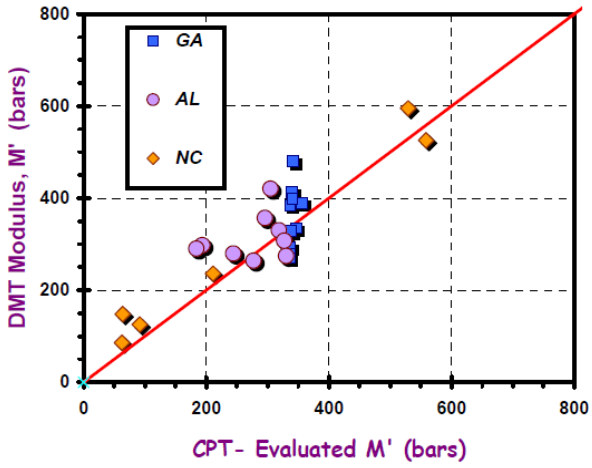

Figure 47: Validation Check on CPT-DMT Conversion for Piedmont Residual Soil (Mayne and Liao 2004)

Mayne and Bachus (1989) investigated the relationship between DMT and CPTu readings and found that the initial contact pressure, p_0, was closely related to the peak penetration porewater pressure obtained in the CPTu test for clays. Figure 48 shows the results of their study with a general trend of:

$$p_0 \approx u_{max} \tag{56}$$

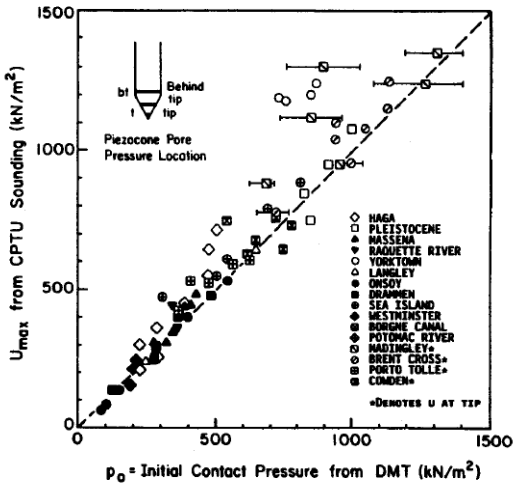

Figure 48: Trend between CPTu Porewater Pressures and DMT p_0 (Mayne and Bachus 1989)

Mayne (2006) considered interrelationships of DMT and CPTu readings in soft clays. Three sites were considered; Amherst, MA; Evanston, IL and; Bothkennar, UK. All three sites comprised lightly overconsolidated intact clays with 1 < OCR < 2. Figure 49 shows of plot of p_0 vs. u_2, which shows a similar trend to that found by Mayne and Bachus (1989) with $p_0 \approx u_2$ for all three sites.

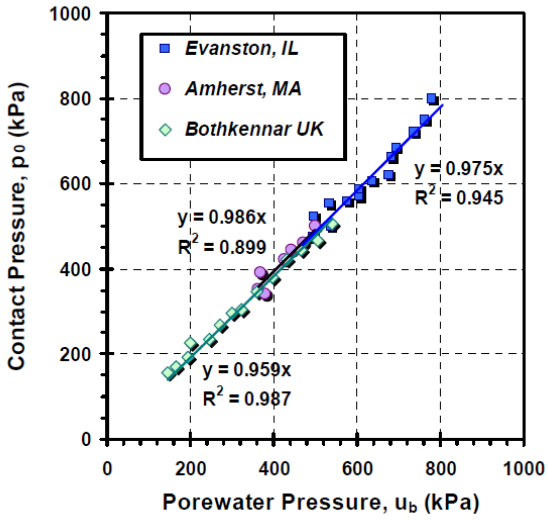

Figure 49: Relationship between DMT p_0 and CPT u_2 (Mayne 2006)

Robertson (2009b) undertook a literature review of published records of documented sites where adjacent CPT and DMT results are available. Table 3 shows a summary of published information on a wide range of soils. The range of different soil types provided an opportunity to consider the correlations between the DMT material index, I_D, and the CPT soil behaviour type index, I_c. Figure 50 shows a plot of the I_D vs. I_C values. Although there is a large amount of scatter with this plot, there is a general trend suggesting:

$$I_c = 2.5 - 1.5 \log I_D \qquad (57)$$

or

$$I_D = 10^{(1.67-0.67Ic)} \qquad (58)$$

Robertson (2009b) found that the relationship in Eqn 53 proposed by Mayne and Liao (2004) for the Piedmont residuum was not supported by the published data (Table 3) over a wider range of soils.

Table 3: Published Records from Adjacent DMT-CPT Profiles (Robertson 2009)

No.	Site	Soil	Reference	Depth range (m)	DMT range I_D	DMT range K_D	DMT range E_D/σ'_v	CPT range Q_{t1}	CPT range F_r (%)	CPT range I_c
1a	McDonald's Farm, BC, Canada	Deltaic sand	Campanella and Robertson 1991	5–12	3.0–8.0	2–6	200–600	40–120	0.3–0.6	1.6–1.9
1b	McDonald's Farm, BC, Canada	Soft silty clay	Campanella and Robertson 1991	17–30	0.2–0.3	2–3	14–30	2–4	1.5–2.5	3.3–3.6
2[a]	Bothkennar, U.K.	Soft clay	Mayne 2006	3–15	0.3–0.4	2–3	15–35	4.5–6	1.0–2.0	2.9–3.2
3[a]	Amherst, MA, U.S.A.	Soft varved sensitive clay	Mayne 2006	6–10	0.2–0.3	3.5–5	20–40	4–6	1.0–2.5	3.1–3.3
4[a]	Ford Center, IL, U.S.A.	Soft glacial clay	Mayne 2006	7–16	0.1–0.3	3–5	10–40	4–6	1.5–3.0	3.1–3.3
5a	Venice Lagoon, Italy	Medium dense sand	Marchetti et al. 2006	4–5	4.0–6.0	3–6	400–600	80–100	0.4–0.6	1.6–1.8
5b	Venice Lagoon, Italy	Soft clayey silt	Marchetti et al. 2006	29–30	0.3–0.5	2–3	20–50	5–7	2.0–3.0	3.0–3.3
6	Zelezny Mine, Poland	Loose silty sand–tailing	Mlynarek et al. 2006	5–20	2.0–4.0	1.2–2.5	130–200	40–80	0.5–0.9	1.8–2.1
7	Hydraulic Fill, Brazil	Loose silt and fine sand–fill	Penna 2006	4–8	0.2–0.3	2–3	14–30	5–8	1.5–3.0	2.9–3.3
8[a]	Baton Rouge, LA, U.S.A.	Stiff fissured clay	Mayne 2006	10–30	0.5–0.8	4–10	80–175	10–20	2.5–3.0	2.8–3.0
9[a]	Georgia Piedmont, U.S.A.	Stiff silty sand to sandy silt—residual soil	Mayne and Liao 2004	4–12	1.2–1.8	2.7–5.0	110–300	25–55	1.4–2.2	2.3–2.5
10[a]	Alabama Piedmont, U.S.A.	Stiff silty sand, sandy silt—residual soil	Mayne and Liao 2004	2–10	1.1–1.6	4–5	150–250	35–45	4.0–5.0	2.5–2.7
11[a]	North Carolina Piedmont, U.S.A.	Stiff silty sand to clayey silt—residual soil	Mayne and Liao 2004	2–12	0.7–0.9	3–6	70–180	12–30	7.0–9.0	2.9–3.2
12[a]	Cooper Marl, SC, U.S.A.	Stiff cemented silt	Meng et al. 2006	20–30	0.2–0.4	6–10	40–140	15–20	0.9–1.2	2.5–2.7
13[a]	Tainan, Taiwan	Silty sand	C. H. Juang and D.-H. Lee, personal communication, 2008	6–12	1.5–2.5	4–8	300–500	80–150	0.9–1.0	1.7–2.2
14[a]	Tainan, Taiwan	Silty clay	C. H. Juang and D.-H. Lee, personal communication, 2008	4–8	0.3–0.6	2–4	30–50	8–12	2–3	2.9–3.1
15	Cowden, U.K.	Very stiff clay	Powell and Uglow 1988	4–10	0.5–0.7	5–10	100–150	20–60	1.5–2.5	2.5–2.7
16	Brent Cross, U.K.	Very stiff clay	Powell and Uglow 1988	2–10	0.4–0.8	5–15	100–200	20–45	2.0–3.5	2.6–2.8
17	Madingley, U.K.	Very stiff clay	Powell and Uglow 1988	2–12	0.5–0.8	8–16	100–300	30–50	3.5–6.0	2.6–2.9
18	Pisa Clay	Soft sensitive clay	M. Jamiolkowski, personal communication, 2008	12–20	0.2–0.3	3–4	30–50	5–7	0.4–1.0	2.9–3.1
19	Univ of Central Florida, U.S.A.	Sand to silty sand	Anderson et al. 2007	3–5	2.0–5.0	4–8	300–800	80–150	0.4–1.0	1.5–1.8

[a]Sites where digital data for both CPT and DMT were available.

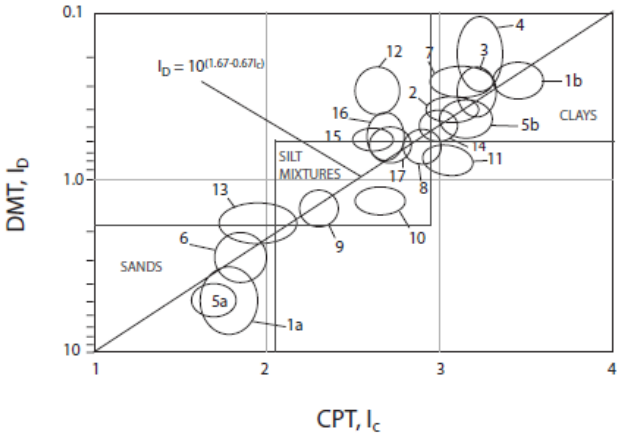

Figure 50: DMT I_D vs. CPT I_c (Robertson 2009b)

Robertson (2009b) surmised that there would likely be a relationship between DMT K_D and CPT Q_t given that both parameters are strongly influenced by OCR with only a small influence from soil sensitivity in fine grained clay-like soils. The relationship proposed by Marchetti (1980) between OCR and K_D is given by Eqn 59:

$$OCR = (0.5\ K_D)^{1.56} \tag{59}$$

Kulhawy and Mayne (1990) proposed a simplistic relationship between Q_t and OCR shown in Eqn 60, whilst a slightly modified correlation is given by Eqn 61.

$$OCR = 0.24\ Q_t^{1.25} \tag{60}$$

$$OCR = 0.3\ Q_t \quad (61)$$

By combining these relationships between OCR and Q_t (Eqns 60 and 61) with the relationships between OCR and K_D (Eqn 59), the following two alternative correlations between Q_t and K_D can be derived:

$$K_D = 0.88\ Q_t^{0.64} \quad (62)$$

And

$$K_D = 0.8\ Q_t^{0.80} \quad (63)$$

Mayne and Bachus (1989) and Mayne (2006) showed that the DMT p_0 is related to the excess porewater pressure around the DMT probe, which is similar to the excess pore water pressure behind the CPT cone at u_2. Schneider et al. (2008) developed a series of relationships between $\Delta u_2/\sigma'_{v0}$ and Q_t for insensitive clays based on critical state soil mechanics and cavity expansion theory, which are in the form:

$$\Delta u_2/\sigma'_{v0} = \beta(Q_t)^{0.95} + 1.05 \quad (64)$$

,where β varies between $0.2 < \beta < 0.5$, with an average value of 0.3

Assuming that the lift-off pressure p_0 is equal to the excess porewater pressure from the CPT, u_2, then:

$$K_D = (u_2 - u_0)/\sigma'_{v0} = \Delta u_2/\sigma'_{v0} = 0.3(Q_t)^{0.95} + 1.05 \quad (65)$$

Hence, it is expected that K_D should show similar values as the CPT $\Delta u_2/\sigma'_{v0}$ in soft clays. Schneider et al. (2008) also developed a relationship for sensitive clays:

$$(K_D =)\ \Delta u_2/\sigma'_{v0} = 0.67(Q_t)^{0.91} + 1.1 \quad (66)$$

Robertson (2009b) plotted the published records of K_D against Q_t (Figure 51) along with the derived correlations between K_D and Q_t given in Eqns 62, 63, 65 and 66. From this plot, it was considered

that Eqn 65 provided the best fit over the full range of data. The relationship represented by Eqn 66 for sensitive clays plots close to the sites 1b, 3 and 4, where the clays are somewhat sensitive.

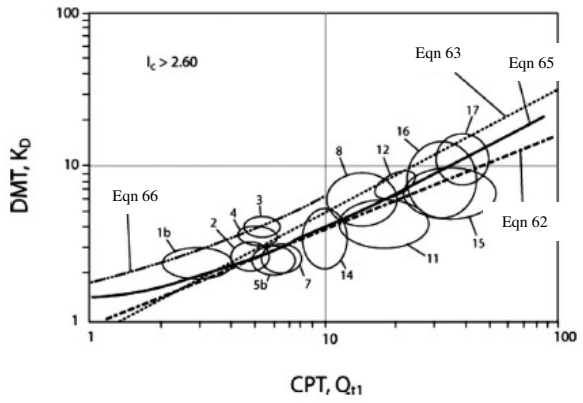

Figure 51: Comparison of CPT Q_t and DMT K_D in fine-grained soils (I_c > 2.60) (Robertson 2010)

Robertson (2000b) did not develop any relationships between K_D and Q_t for sand-like soils, but considered that there may be a possibility that, in coarse grained soils, K_D varies with both Q_t and F_r.

Mayne and Liao (2004) suggested the relationship given in Eqn 67 for Piedmont residual soils:

$$E_D = 5\ q_t \tag{67}$$

Based on the data on which this relationship was derived, Robertson (2009b) considered that the data fits equally well in terms of net cone resistance, hence:

$$E_D = 5(q_t - \sigma_{v0}) \tag{68}$$

With the normalised form being:

$$E_D/\sigma'_{v0} = 5\ Q_t \tag{69}$$

Figure 52 presents a summary of the published records for all soils. This shows that Eqn 69 provides a reasonable fit to the data.

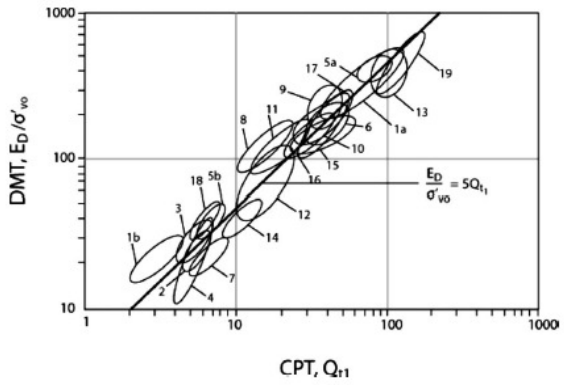

Figure 52: Comparison of CPT Q_t and DMT E_D/σ'_{v0} (Robertson 2009b)

Since E_D/σ'_{v0} is also a function of I_D and K_D (Eqn 54), it follows that:

$$34.7I_DK_D = 5Q_t \tag{70}$$

Hence:

$$K_D = 0.144\ Q_t/I_D \tag{71}$$

Using the correlation between I_D and I_C (Eqn 58), this becomes:

$$K_D = 0.144\ Q_t/[10^{(1.67-0.67Ic)}] \tag{72}$$

Robertson (2010) suggested that this relationship (Eqn 72) may represent a framework for future refinements as more comparison data becomes available. In the meantime, the relationship represented but Eqn 65 is considered the most appropriate. The proposed correlations are then:

$$I_D = 10^{(1.67-0.67Ic)} \tag{73}$$

$$K_D = 0.3(Q_t)^{0.95} + 1.05 \qquad \text{,when } I_c > 2.60 \tag{74}$$

$$E_D/\sigma'_{v0} = 5\ Q_t \tag{75}$$

The suggested correlations by Robertson (2009b) for K_D and I_D are plotted on the normalised CPT SBT Q_t – F_r chart in Figure 53. The contours of K_D shown on Figure 53 indicate a possible transition zone in the region of $1.2>I_D>0.60$, which represents silt-mixture soils that may be influenced by possible drainage during the pause between penetration and testing.

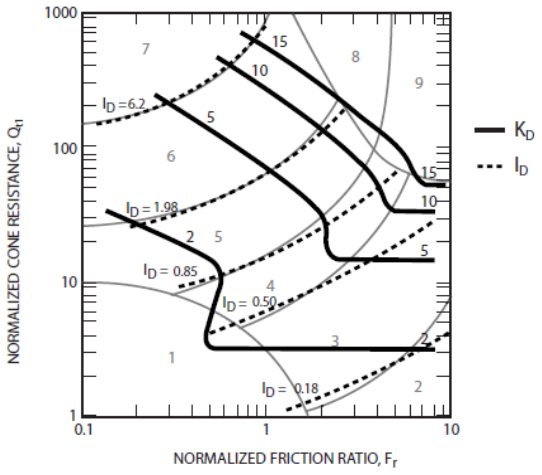

Figure 53: Proposed Contours of DMT KD and ID on the CPT Normalised SBT Qt-Fr Chart (Robertson 2009b)

Robertson (2009b) considered a site at Moss Landing, California, where two CPT tests and one DMT test were carried out in close proximity (1m apart). The directly measured DMT index values (I_D, K_D and E_D) were compared to those predicted by Eqns 73 to 75 from the CPT data. A comparison between the measured and predicted DMT parameters is illustrated on Figure 54. In general, the comparison between measured DMT parameters and those predicted by the CPT using the proposed correlations show reasonable trends.

Robertson (2009b) concluded that the proposed correlations are approximate and will likely be influenced by variations in in-situ stress state, soil density, stress history, age, cementation and soil sensitivity. It was suggested that the correlations may provide further insight into future correlations for the DMT with other geotechnical parameters given the more extensive theoretical background and larger database provided by the CPT, with further research.

Recent studies comparing DMT and CPT tests in soft organic soils and alluvial soils (Bihs et al. 2010, Mlynarek et al. 2010 and Aykin et al. 2010) showed generally good correlations between the two tests. Mlynarek et al. (2010) found that the DMT soil type classification system (Marchetti and Crapps 1981) seemed to provide a reliable system for identifying organic soils.

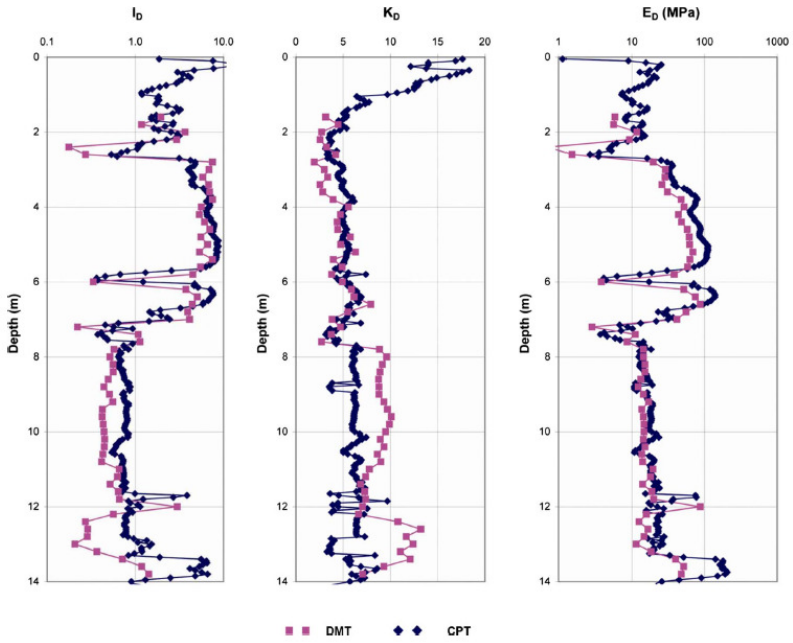

Figure 54: Comparison Between measured DMT parameters and those predicted using CPT (Robertson 2009b)

McNulty and Harney (2010) compared effective friction angle derived from 47 CPT (CPT and SCPT) and 13 DMT (DMT and sDMT) tests on clayey and silty sands. The CPT derived fiction angle, ϕ', compared well with laboratory measurements and DMT results below the water table. Above the water table, CPT derived ϕ' values were significantly higher than laboratory measurements. The DMT derived ϕ' values general compared well with other data sources, except in the looser layers.

Marchetti (2010) considered the sensitivity of both the CPT and DMT to stress history and aging in sand. Two cases where CPT and DMT tests in calibration chambers were reported, which showed the DMT to be considerably more sensitive to the simulated prestressing and aging than the CPT. A full scale embankment study was also reported where a 6.7m high embankment was constructed, the ground allowed to consolidate and then the embankment removed. CPT and DMT tests were conducted before and after embankment construction and then again after complete removal of the embankment. The results indicate much greater sensitivity in the DMT results (K_D and M_{DMT}) than in the CPT. This suggests that the DMT K_D is a better parameter than CPT q_t for assessing the behaviour of sands to liquefaction, which is affected by stress history and aging. This also suggests that correlations between CPT and DMT derived parameters may not be valid in some soils.

2.4 ARTIFICIAL NEURAL NETWORKS

2.4.1 General

Artificial neural network technology uses mathematical algorithms to create patterns to match an existing data of set output and input values so that predictions of outputs can be made for new sets of input data. They operate in a similar way to that of the biological neural functioning in the brain. Just as humans apply knowledge gained from past experience to new problems or situations, a neural network takes previously solved examples to build a system of 'neurons' that makes new decisions, classifications and forecasts.

Neural networks take a set of known solved data and learn the pattern between the input and output information for a selected set of the data. This is called 'training' and the data to which the training is applied is called to 'training set'. Once a pattern is obtained in this way, the network is applied to the untrained part of the solved data. This is called 'testing' with the data so tested called the 'test set'. The network can also be applied to the combined training and test sets. The outputs obtained by the neural network are compared to the actual output values. Results should be evaluated by consideration of the correlation coefficient and also in terms of the percentage of correct answers that result from the model.

Neural networks excel at problem diagnosis, decision making, prediction, and other classifying problems where pattern recognition is important and precise computational answers are not required. This makes neural networks ideal for the comparison of geotechnical parameters, where there may not be exact solutions, but patterns between the data can be more helpful.

There are many different types of artificial neural network systems. Figure 55 illustrates a simple network structure. The basic building block of the neural network technology is the simulated 'neuron', depicted as the circles in Figure 55. The network processes a number of inputs from the outside world to produce an output. The neurons are connected by 'weights' (depicted as lines in Figure 55) which are applied to values passed from one neuron to the next.

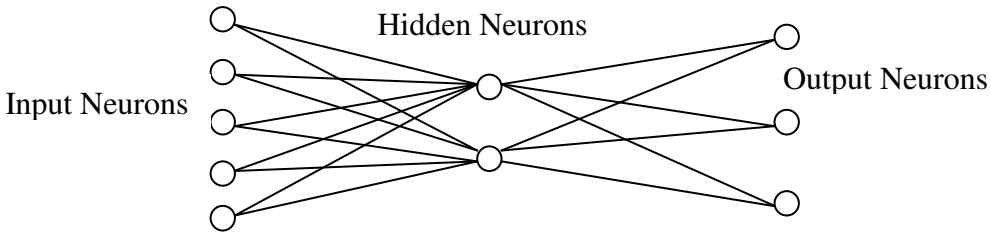

Figure 55: Neuron Network Structure

A group of neurons is called a 'slab'. Neurons are also produced into 'layers' by their connection to the outside world. For example, if a neuron receives data from the outside the network, it is considered to be in the input layer. If a neuron contains the network's predictions or classifications, it is in the output layer. Neurons in between the input and output layers are in the hidden layer(s). A layer may contain one or more slabs of neurons.

Input values in the first layer are weighted and passed to the second (hidden) layer. Neurons in the hidden layer 'fire' or produce outputs that are based upon the sum of weighted values passed to them. The hidden layer passes values to the output layer in the same fashion, and the output layer produces the desired results. The network 'learns' by adjusting the interconnection weights between layers. The answers the network is producing are repeatedly compared with the correct answers and each time the connecting weights are adjusted slightly in the direction of the correct answers. Eventually, if the problem can be learned, a stable set of weights adaptively evolves and will produce good answers. The real power of neural networks is evident when the trained network is able to produce good results for data which the network has not 'seen' before.

For this study a type of artificial neural network called 'General Regression Neural Network' (GRNN) has been used. This network system is discussed in more detail below.

2.4.2 General Regression Neural Network (GRNN)

The general regression neural network algorithm was developed by Specht (1991). It is a four layer, single pass model with a parallel structure. The architecture of GRNN is illustrated in Figure 56.

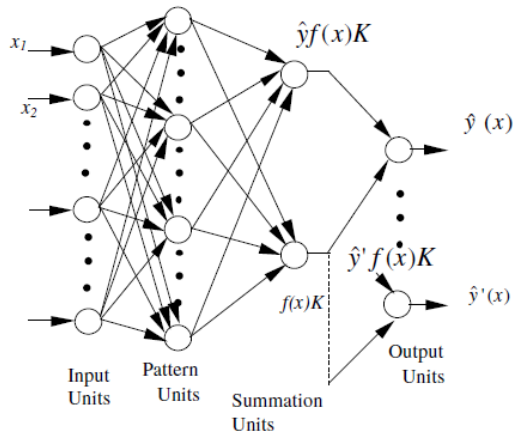

Figure 56: Schematic diagram of GRNN architecture

The GRNN is composed of four layers; input layer, pattern layer, summation layer, and output layer. The total number of parameters equal the number of input units in the first layer. The input variables (x_1, x_2, etc) are scaled from their numeric range into the numeric range that the neural network can deal with efficiently. In this study a tanh scaling factor was used which uses a hyperbolic tangent function (tanh) to scale the data between -1 and 1. The scaled values then pass to all the neurons on the second layer (pattern layer). Each pattern neuron is dedicated to one training pattern and its output measures the distance of the input from the stored patterns. The square of the differences are fed into a nonlinear activation function. The output from the pattern units are passed to the summation units. Each pattern layer unit is linked to the two neurons in the summation layer (the S-summation neuron and the D-summation neuron). Here, the sum of the weighted outputs of the pattern layer is calculated by the S-summation and the unweighted outputs of the pattern neurons is computed by the D-summation. The linkage weight between the S-summation neuron and the *i*th neuron in the pattern layer is y*i*; the target output value corresponding to the *i*th input pattern. The linkage weight for D-summation is unity. The output layer just divides the output of each S-summation neuron by the output of each D-summation neuron, supplying the predicted value to an unknown input vector x as:

$$\hat{y}_i(x) = \frac{\sum_{i=1}^{n} y_i \exp[-D(x, x_i)]}{\sum_{i=1}^{n} \exp[-D(x, x_i)]} \tag{76}$$

The number of training patterns is indicated by n and the Gaussian D function in Eqn 76 is explained as:

$$D(x, x_i) = \sum_{j=1}^{p} \left(\frac{x_j - x_{ij}}{\zeta} \right)^2 \tag{77}$$

Where p shows the number of input elements. The x*j* and x*ij* values represent the *j*th elements of x and x*i*, respectively. The value ζ is the spread factor or smoothing factor. In this study, the smoothing factor was determined using a genetic algorithm. If the spread becomes larger, the function approximation will be smoother. If the spread is too large, then a lot of neurons will be required to fit a fast changing function. Too small a spread means many neurons will be needed to fit a smooth function, and the network may not generalise well. The genetic algorithm uses a 'fitness' measure to determine which of the individuals in the population survive and reproduce (Goldberg 1989). The measure of fitness for the GRNN is the mean squared error of the outputs for the entire data set. The genetic algorithm seeks to minimise this squared error.

2.4.3 The use of ANN in Geotechnical Engineering

The ground is a natural product consisting of variable soil and rock materials which are created in a variety of different complex geological processes. This creates a material, whose properties and behaviour is difficult to predict and is influenced by many factors. Conventional geomechanics attempts to predict soil and rock behaviour by applying theories and creating models that must make assumptions about the numerous factors affecting that behaviour. ANNs only consider the numeric data only without concern about any theoretical justification between the particular variables. This allows the relationships between the variables to be fully utilised in order to determine the underlying pattern that defines the ground model. This makes ANNs ideally suited to geotechnical

problems as solutions may be found that conventional models may not be able to predict because of the unknown influence and interaction of the various factors that may be involved.

Consequently, artificial neural networks (ANN) have been used successfully for many geotechnical applications. Shahin, et al. (2001) provides a summary of ANN applications to various geotechnical problems provided in the literature. Reference is made to over 70 studies involving the application of ANNs to problems involving pile capacity, settlement of foundations, soil properties and behaviour, liquefaction, site characteristics, earth retaining structures, slope stability and tunnels. The most successful applications appear to be predicting driven pile capacity, liquefaction and soil properties and behaviour (Shahin et al. 2001). For example, Abu-Kiefa (1998) successfully utilised the GRNN method to predict the capacity of driven piles in cohesionless soils. Goh (1995) used ANN to model the correlation between relative density and CPT cone resistance. ANN was also used by Goh (1994) to model the complex relationship between seismic and soil parameters in order to investigate liquefaction potential. There are many other examples described by Shanin et al. (2001). In many of the cases, the ANNs performed better than conventional methods.

Abuel-Naga (2001) used the ANN architectures of GRNN and GMDH to model the correlation between dynamic cone penetration test (dynamic probe) and the standard penetration test (SPT) in cohesionless soils.

Conventional methods generally rely on assuming the structure of the model in advance. This requires assumptions to be made on the relationships between the variables involved based on known theory. ANNs however work only with the data and the model is developed by training on input and output values to determine the pattern of the model. Furthermore the model can be improved at a later date by adding new data and re-training the network. The model is not inhibited by any preconceived theory. The downside of this is that the underlying mathematical relationships behind the ANN model is not known and can not be validated theoretically. Shanin et al. (2001) concludes that despite the limitations of ANNs, they have a number of significant benefits that make them a powerful and practical tool for solving many geotechnical problems.

From review of the literature the ANN method does not appear to have been used specifically for determining correlations between CPT and DMT. However, there are many examples of the successful use of the technique in similar problems. Consequently ANN is considered to be a suitable method of analysis for this study.

3. CHAPTER 3: METHODOLOGY

3.1 METHODOLOGY

3.1.1 In-situ Testing

Dilatometer (DMT) and CPT tests were carried out next to each other at various sites. The DMT and CPT tests were carried out using a Pagani TG63-150 push rig (see Figure 6). In some cases the DMT tests were carried out close to previous CPT tests done by others.

The CPT tests were carried out in accordance with ASTM standard D5778-07. The DMT tests were carried out in accordance with ASTM D6635-01(2007) and TC16 (2001). The CPT tests were all piezocone tests (CPTu) using 10cm^2 cone with the porewater pressure element at the u_2 position. The DMT tests were carried out with the seismic module to measure shear wave velocities (sDMT). An electric Autoseis hammer (Mayne and McGillivray 2008) was used to generate the shear waves.

The standard Marchetti data reduction computer program (Sdmt Elab) that accompanies the DMT was used to acquire the data obtained from the sDMT tests. The CPT field data was uploaded using the Pagani TGSW03 software.

In accordance with standard practice, DMT tests were generally carried out at 200mm depth intervals with the seismic tests carried out every 500mm. Continuous data with depth is obtained from the CPTu testing, which is processed at 10mm intervals by the software program (TGSW03). Where CPT tests were carried out previously by others, similar data acquisition software producing data at 10 mm intervals were used.

3.1.2 Interpretation of Results

The standard Marchetti Sdmt Elab software was used to reduce the sDMT data to create plots of material Index (I_D). constrained modulus (M), undrained shear strength (c_u), horizontal stress index (K_D) and shear wave velocity (V_s). The software also interprets and tabulates data and correlations for p_0, p_1, unit soil weight (γ), effective overburden pressure (σ'_{vo}), insitu porewater pressure (u_o), I_D, K_D, E_D, at-rest earth pressure (K_0), overconsolidation ratio (OCR), angle of friction of sands (ϕ'), undrained shear strength of clays (c_u),V_s, small strain shear modulus (G_0) and a soil description based on I_D. The interpretations to index values and soil parameters are based on the Marchetti (1980) correlations (see Table 2).

The data from the CPT tests were input into the computer program CPeT-IT (by Geologismiki Geotechnical Software). This software has been developed in association with Professor Robertson using the correlations by Robertson (2009a) and Robertson and Cabal (2010), which have been described in Section 2.2.3 of this Thesis. The software presents the basic CPT data, normalised data and interpretation of soil parameters in various graphical forms as well as in comprehensive tabular formats. Of relevance to this study are the basic parameters, q_t, f_s, u_2, q_t, u_0, q'_{vo}, the normalised parameters, Q_t and F_r, and the soil behaviour type index, I_c. Also the interpreted soil parameters c_u, M, G_0, OCR and ϕ'.

The tabulated data from the interpretation software were collated into an excel spreadsheet. Side-by-side or overlaid Graphs were then generated in order to compare the results and interpretations between the CPT and DMT data. The Robertson (2009b) correlations (Eqns 72 to 75) were also overlaid on the graphs of I_D, K_D and E_D for comparison purposes.

3.1.3 Analysis

The data was reduced by averaging the CPT results over 200mm depth increments (moving average). The basic test results (q_c, f_s, u_2, and q_t), the normalised parameters (Q_t, F_r) and I_c were all averaged in this manner. The DMT data was not reduced as it is already at 200mm depth increments. The CPT data in between the DMT data points were then removed so that the data set

includes only points where both the CPT and DMT data exists at the same depths (i.e. 200mm depth increments).

The results in graphical form were examined and the results between the CPT and DMT data compared. From that examination, the data that was considered the most reliable was selected for more detailed analysis.

The selected reduced data was analysed using the general regression neural network algorithm (GRNN) to investigate possible correlation from the CPT data to the DMT data. The computer program, NeuroShell 2 by Ward Systems Group Inc. was used to run the GRNN in this study. The results were presented in a tabular format with the best error results shown graphically to assist in the selection of the successful network. The successful network was applied to the whole of the data (including the data rejected in the data reduction process) to investigate the correlations with the 'unseen' data.

The GRNN results do not provide an equation or known mathematical formula that represents the successful network algorithm. In this respect it is a 'black box'. So, despite the apparent success of the GRNN, its equations are hidden. The actual formulas are expected to be highly complex and not easily validated theoretically. To provide added value, the results of the GRNN were also compared to the Robertson (2009b) correlations to compare and co-validate the successful GRNN and Robertson correlations. An attempt was made to refine the Robertson correlations in line with the GRNN results on theoretically reasonable input parameters.

3.2 DESCRIPTION OF TEST SITES

3.2.1 Location of Sites

The in-situ testing was carried out at ten sites of different geology within the upper half of the North Island of New Zealand. The locations of the test sites are shown in Figure 57. The sites are project sites rather than specific research sites.

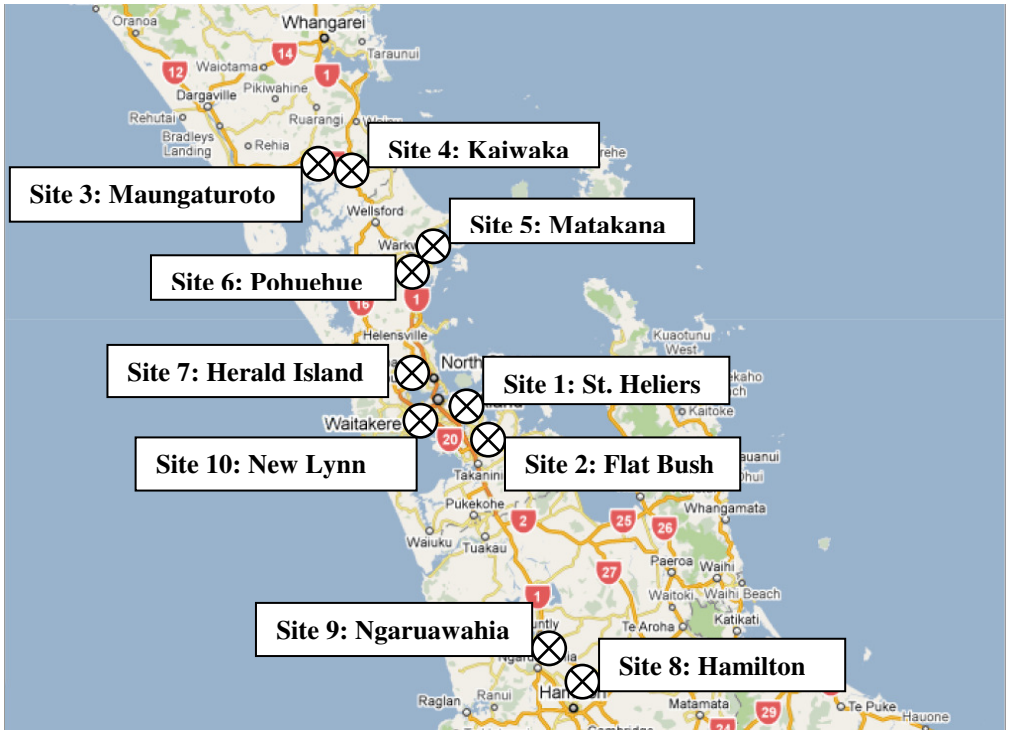

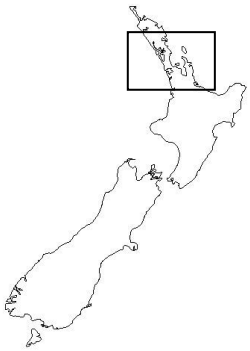

Figure 57: Location of Test Sites

3.2.2 In-situ Testing

Table 4 gives a summary of the tests carried out at each test site. At least one DMT test and one CPT test were carried out close to each other at each test site. At two sites (Hamilton and Ngaruawahia), four pairs of CPT and DMT were carried out. In total there are 16 CPT and DMT pairs. In Table 4 the test sites have been number 1 to 10, with each pair denoted by a letter (a, b, c, etc) for each site.

Table 4: Summary of Test Sites

Site	Location	CPT/DMT Pair Number	Depth* of sounding (m)	Depth to water table (m)	Geology	Soil Type(s)
1.	St. Heliers	a.	8.0	1.5	Alluvium	Silty clay, organic clay
2.	Flat Bush	a.	10.2	4.0	Alluvium	Silty clay, clayey silt
3.	Maungaturoto	a.	4.3	1.0	Alluvium	Silty clay, clay
4	Kaiwaka	a.	7.4	5.0	Residual Soil	Layered silty clay, clayey silt, sandy lenses
5.	Matakana	a.	8.0	1.0	Residual Soil	Silty clay, clayey silt
6.	Pohuehue	a.	6.6	2.0	Residual Soil	Layered silty clay, clayey silt
7.	Herald Island	a.	9.0	3.4	Residual Soil	Layered clayey silt, silty clay, silt, sandy lenses
8.	Hamilton	a. b. c.** d.**	19.0 15.6 17.2 16.0	1.75 6.7 4.8 2.3	Volcanic Soil	a. Layered silty sand/sand, clay lenses b. Clayey silt, clay, sandy silt c. Layered silty clay, clayey silt, silty sand d. Layered clayey silt, silt, silty sand
9.	Ngaruawahia	a.** b.** c.** d.**	6.0 15.0 10.4 14.4	2.0 2.0 2.0 3.0	Volcanic Soil	a. Layered sand, silty sand, silt, clayey lenses b. Layered silty sand, silt, clayey lenses c. Silt, sandy silt, silty sand d. Layered silt, sandy silt, sand
10.	New Lynn	a.**	15.0	1.7	Alluvium	Silty clay and clayey silt

*Depth relates to the depth of the DMT test (corresponding CPT test may be deeper at some sites)
**CPT carried out by others previous to DMT test

Some of the CPT results are from CPT tests carried out by others some time previous to the DMT tests. The digital information from these CPT tests (other than for New Lynn) have been supplied. Digital data was not available for the New Lynn site, but the data was manually estimated from the hard copy plot.

In most cases, the DMT test was carried out within 3m horizontal distance of the CPT test. However, where the CPTs were carried out previously by others, the exact location of those CPTs were not known and so the distance between the DMT and the CPT is not known. It is likely that these tests will be within approximately 10m of each other, but they could also be further apart. The CPT at Herald Island was carried out approximately 6 months prior to the DMT test. These are approximately 2m apart.

The elevation of the ground surface (relating to depth = 0) of the CPTs and DMTs are not known. It has been assumed that the depth = 0 point of each pair of soundings is at the same elevation, although this may not be the case. It is expected that the elevation difference between pairs of soundings are within 200mm, but that difference may be greater in some instances.

3.2.3 Ground Conditions

In some cases, boreholes have been drilled next to, or close to the DMT and CPT pairs. The logs from these boreholes have been examined to confirm likely soil types and geology as well as to estimate the depth to the groundwater table. This information and the material index parameters (I_D and I_C) of the DMT and CPT tests have been used to provide a general description of the soil type and geology in Table 4. The water table depth indicated in Table 4 has been estimated from nearby borehole/piezometer information. Where borehole or piezometer information does not exist, a reasonable guess of the likely water table depth has been made.

The borehole information, where available, has not been included for simplicity reasons. The borehole information has only been used as a guide to estimate geology and water table information in general terms. This study is specifically limited to the comparison between DMT and CPT tests. The comparison with borehole information is considered outside the scope of this study and so the borehole information has been excluded. Although the comparison between soil descriptions given on borehole logs and the material indices (I_D and I_C) would be interesting, borehole logs are not available in all cases and the boreholes are, in some cases, some distance away from the DMT/CPTs. It would also be of value to compare of soil parameters determined from laboratory testing of borehole samples to those determined by correlation from DMT/CPTs. However this laboratory testing information is extremely sparse and of limited value in this study. Consequently, any borehole information or laboratory testing has been excluded and the study focused only on the direct comparison between DMT and CPT tests and their respective interpretations.

The geology given in Table 4 is generalised and may not be strictly correct geologically. For example, the soils at the sites in Hamilton and Ngaruawahia (sites 8 and 9) are derived primarily from volcanic ash and ignimbrite (pumiceous materials from the Taupo eruptions), however, much of these soils have been redeposited as alluvial soils (Puketoka Formation) or may be layered

alluvium, ash, and ignimbrite. For simplicity, the geology for these sites has been referred to as 'Volcanic soils' as this relates best to the origin of the material. Similarly some of the sites described as 'alluvium' may include volcanic derived soils or run into residual soils at depth. Consequently, the geological descriptions in Table 4 provide a general guide rather than an exact geological classification. No attempt has been made in this study to investigate the results in reduced groups based on geological origin. There is possibly geologically specific correlations, but the size of the available data base and the difficulty in classifying the data in appropriate geological units makes such comparisons too specific for this study. Instead the study has been restricted to general comparisons across all the various geological origins presented.

4. CHAPTER 4: RESULTS

4.1 RESULTS AND INTERPRETATIONS

4.1.1 Presentation of Data

The CPT test measures data continuously and records information at 10mm depth intervals. Consequently, the CPT test creates a huge amount of data. In the 16 CPT tests presented in this study, there are over 20,000 groups of data at 10mm depth increments. It is not feasible to present the complete data in tabular form, as this would take up hundreds of pages. Instead the data has been presented in graphical format and attached in Appendix B. Here the various parameters are plotted against depth in a series of graphs with the DMT and CPT data plotted side-by-side or overlain on the same graphs. A set of graphs has been produced for each test site. As an example, Figure 58 and Figure 59 show the format of the data presentation from one of the test sites.

For each test site, two pages of data are presented. The first page (represented by Figure 58) shows the basic results with the top row of graphs showing the basic raw data of q_c, f_s and u_2 from the CPT, and p_0, p_1 and V_s from the DMT. Note that the shear velocity, V_s, is obtained from the seismic module added to the DMT (sDMT). The CPT data is shown in blue and the DMT data in red. The lower row of graphs in the results page gives the normalised CPT cone resistance, Q_t, the normalised friction ratio, F_r, and the soil behaviour type index, I_c from the CPT. Alongside that is the DMT material index, I_D, the horizontal stress index, K_D and the dilatometer modulus, E_D. Again the CPT information is in blue with the DMT alongside in red.

The second page (Figure 59) presents common interpretations of the basic data to estimates of soil parameters. The soil parameters considered are undrained shear strength, c_u, constrained modulus, M, small strain shear modulus, G_0, overconsolidation ratio, OCR and angle of internal friction, ϕ'. These parameters have been interpreted using the computer software CPeT-IT for the CPT data and the standard Marchetti dilatometer software, Sdmt Elab for the DMT. The derivation of these correlations is discussed in previous sections. These are commonly used correlations, primarily based on Robertson (2009a) and Marchetti (1980).

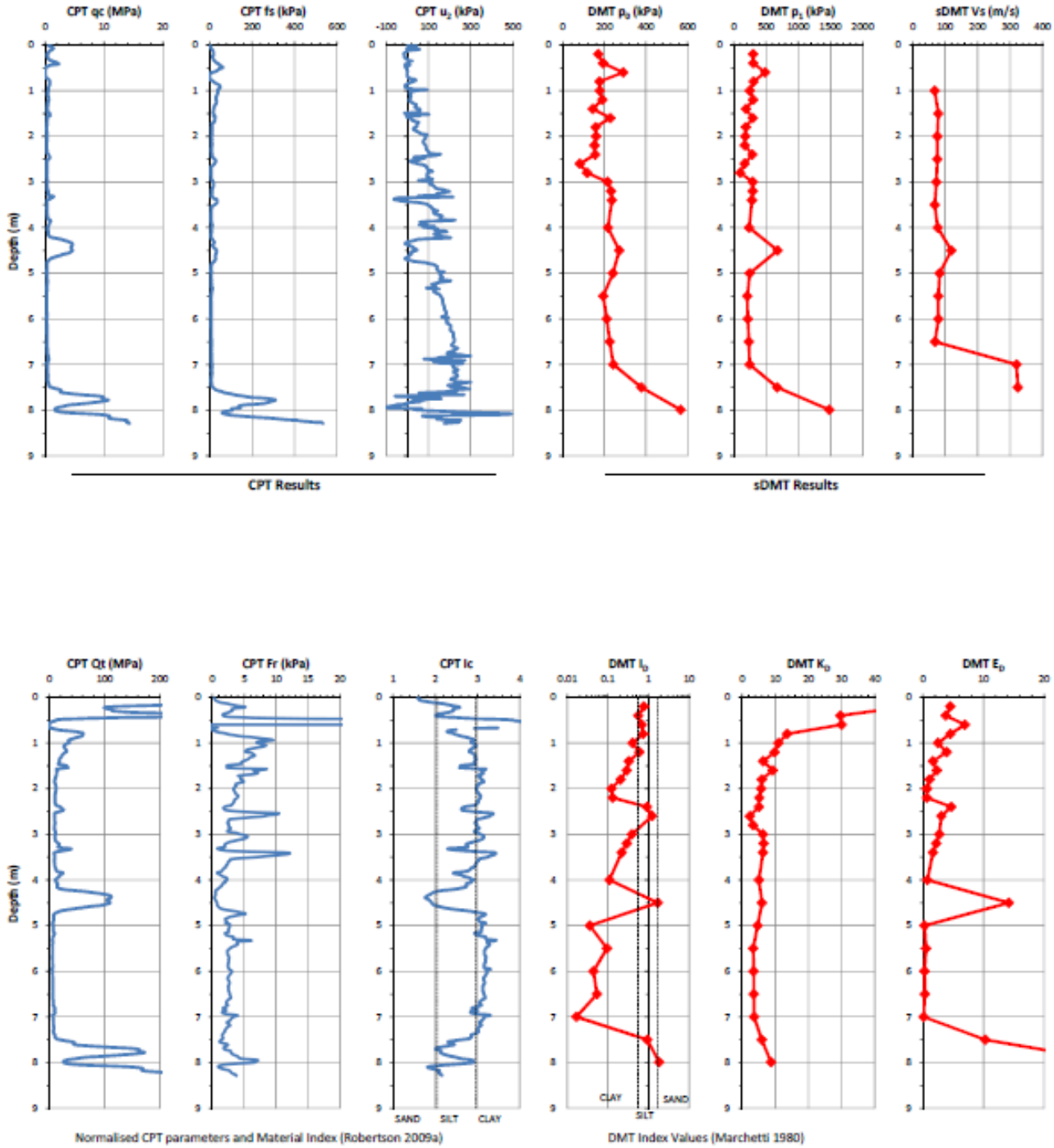

Figure 58: Example of Data Presentation (CPT-DMT Results)

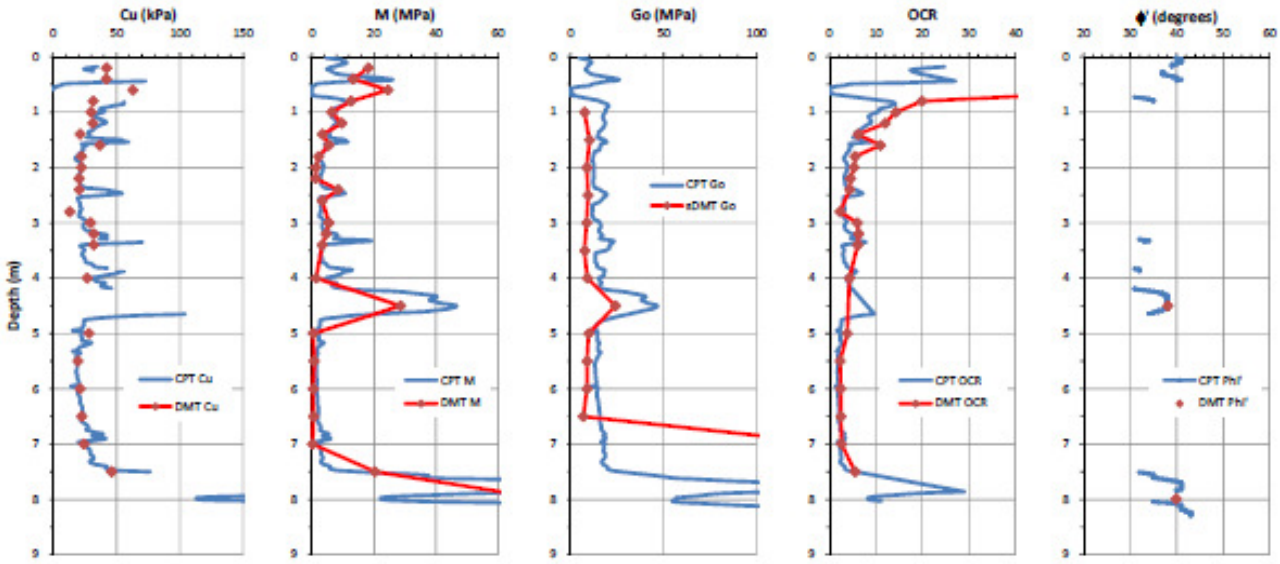

DMT correlations based on Marchetti (1980) and TC16 (2001) using Marchetti Elab software
CPT corelations based on Robertson (2009a) and Kulhawy & Mayne (1990) using CPeT-IT software

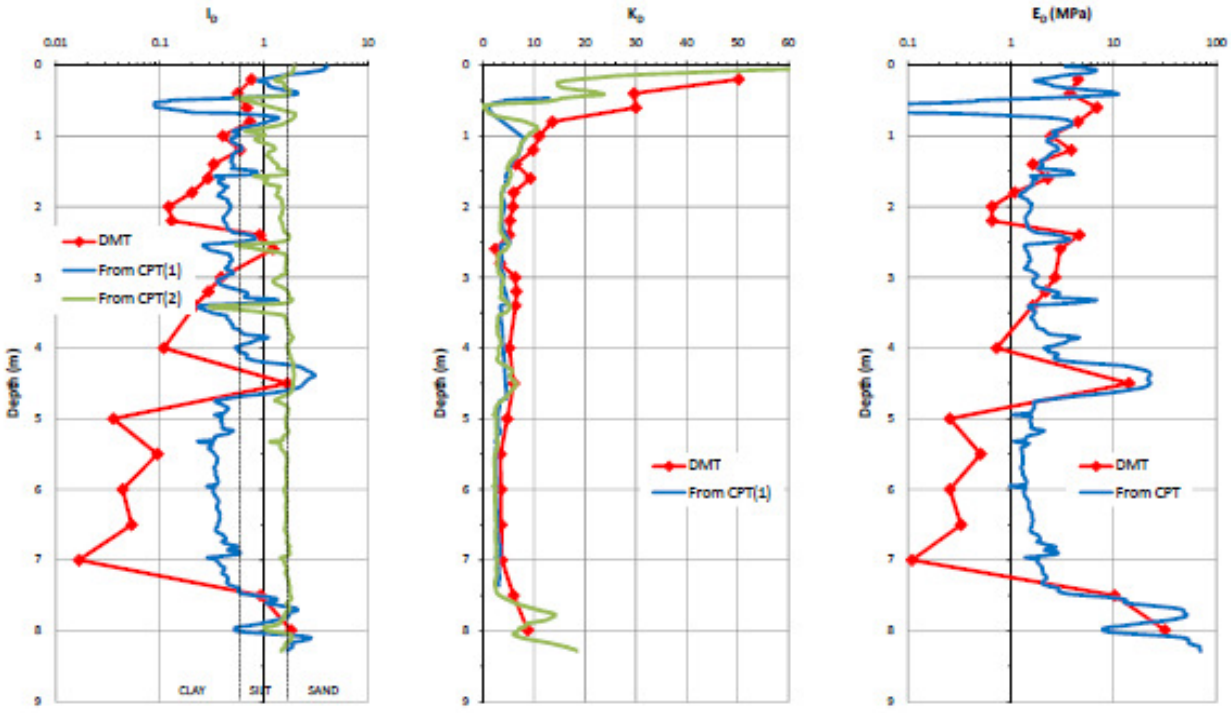

CPT(1): $I_D = 10^{(1.67-0.67Ic)}$ (Robertson 2009b)
CPT(2): I_D = 2.0-0.14F, (Mayne & Liao 2004)

CPT(1): $K_D = 0.3(Qt)^{0.95} + 1.05$, for Ic>2.95
CPT(2): $K_D = 0.144Qt/[10^{(1.67-0.67Ic)}]$
(Robertson 2009b)

CPT: $E_D = 5\ Qt\ \sigma'_{vo}$
(Robertson 2009b)

Figure 59: Example of Data Presentation (Interpretations)

The soil parameters obtained by correlation from the DMT are shown in red, whilst those from the CPT are shown in Blue.

The lower row of graphs on the interpretations page are the DMT index values (I_D, K_D and E_D shown in red) along with the Robertson (2009b) CPT-DMT correlations overlain in green and blue. These correlations have been discussed in previous sections. In summary, they are:

$$I_D = 10^{(1.67-0.67Ic)} \quad (78)$$

$$I_D = 2.0 - 0.14\ F_r \qquad \text{(Mayne and Liao 2004)} \quad (79)$$

$$K_D = 0.144\ Q_t/[10^{(1.67-0.67Ic)}] \quad (80)$$

$$K_D = 0.3(Q_t)^{0.95} + 1.05 \qquad \text{,when } I_c > 2.60 \quad (81)$$

$$E_D/\sigma'_{v0} = 5\ Q_t \quad (82)$$

To be consistent with convention and with Robertson (2009b), the DMT indices I_D and E_D have been plotted on a logarithmic scale, whereas K_D is plotted on a natural scale.

The data has been presented in the way described above so that a visual comparison of the graphical results can be made. The visual examination of the graphical data is discussed for each of the test sites in the following sections. The purposes of such visual examination are:

(a) To obtain an initial 'feel' for the data
(b) To compare the soil types predicted by the CPT and DMT (by I_c and I_D)
(c) To compare the estimates of soil parameters derived from the two tests
(d) To compare the Robertson (2009b) correlations with the DMT results
(e) To select reliable data for further analysis

It should be noted that the visual examination of the data is not intended to be a rigorous analysis, particularly for the derived soil parameters (i.e. c_u, M, etc). Analysis of the derived soil parameters would necessitate reliable independent reference tests (e.g. laboratory tests). It is not the purpose of

this study to consider the correlations with soil parameters, but they have been included to help provide a comparison of the capabilities and responses of the two tests. Bearing in mind that this is the first time DMT and CPT tests have been compared in New Zealand soils, it is of interest to examine and compare the derived soil parameters. This all leads to a better understanding of how the DMT (and CPT) tests behave.

A comparison between DMT p_0 and the excess porewater pressure, u_2, measured by the CPT are compared separately following the individual observations of other parameters for each site.

4.1.2 St. Heliers

The CPT shows low q_c values with a layer of higher values at around 4m depth and harder ground below about 7.5m-8m. The Q_t and F_r plots show occasional spikes in the upper 4m and these spikes are also represented in the soil behaviour type index (I_c) plot with the graph hovering around the silt/clay boundary (at $I_c = 2.95$). At around 4.5m, the I_c plot spikes distinctly into the sand region ($I_c < 2.05$), after which it returns to a distinctive clay layer. At around 7.5m it goes into the silt region, zigzagging between the sand boundary and the clay boundary. The CPT thus suggests soft silty clay over the upper 4m with the soil layered with variable silt and clay content, a sand layer at around 4.5m followed by soft clay down to a competent stratum below about 7.5m (probably sandstone).

The DMT material index (I_D) plot is less spiky than the I_c plot. It shows similar soil type in that silty clay and clay is shown in the upper 4m or so, but the plot distinctly moves well into the clay region ($I_D < 0.6$) and with a silty/sandy layer around 2.5m returning back to the clay zone at about 3m depth, before showing a silty sand layer at about 4.5m, below which, the plot goes well into the clay layer and is described by the DMT software as 'mud and/or peat'. The plot goes into the silt zone at about 7.5m, tending towards the sand boundary. In general it would appear that the CPT I_c and DMT I_D are in agreement with respect to the general soil profile. Although the shapes of the plots vary, their interpretation of the soil types matches reasonably well. The biggest difference is the apparent more layered and variable silt/clay mixture indicated by the CPT in the upper 4m or so. It should be noted, however, that the DMT I_D plot is on a log scale, which may distort the shape of the plot, by exaggerating the lower values. This may explain to some extent the apparent differences in the shapes of the two plots.

Observation of the derived soil parameters, shows that the undrained shear strength (c_u) and the constrained modulus (M) derived from both the CPT and DMT compare very well, the only significant variation being a higher M value predicted by the CPT in the sand layer at 4.5m. The small strain shear modulus (G_0) as predicted by the CPT also compares reasonably well with that measured by the sDMT. The G_0 from the sDMT has been obtained from the shear wave velocity measured directly from the seismic module of the test equipment and so would be considered to be more accurate. Considering that the G_0 from the CPT has been estimated from q_t and I_c, the results are very similar to the sDMT results, although they are consistently higher than the measured sDMT results, except near the bottom of the sounding where the sDMT G_0 spikes early.

The overconsolidation ratio (OCR) has also been very similarly predicted by both tests. The results show overconsolidation (probably by desiccation) at the surface and the two tests do vary in their predictions over this upper layer. However, from about 1.5m and below, the two tests provide a very similar prediction of OCR. The results suggest that the soil is lightly overconsolidated between about 1.5m and 4m and approximately normally consolidated from about 5m to 7m. This is mirrored by the K_D plot, which shows K_D approaching 2 between these depths (suggesting normally consolidated).

Where the tests indicate sandy soil, the friction angles predicted by both tests compare well.

The plot of I_D with the Robertson (2009b) correlations superimposed, show a generally poor direct correlation between I_D and I_C, although the general soil type interpretations are similar. The log scale may be exaggerating the difference, however. The Mayne and Liao (2004) correlation with F_r does not compare well at all.

Apart for some deviation in the upper 1m, the Robertson (2009b) correlations with K_D compare very well to the measured DMT K_D values, albeit slightly lower that the measured values. The Robertson (2009b) correlation for E_D, however, does not compare as favourably to the measured values, although they do follow the same general trend. The log scale, again, may be distorting the difference somewhat.

In summary, the estimated soil types from I_D and I_C compared reasonably well and the derived soil parameters from each tests compared favourably. The estimated K_D values from the Robertson

(2009b) correlations compared well, but the correlations for I_D and E_D were not as favourable, although the general trends were followed.

4.1.3 Flat Bush

The I_c and I_D plots indicate silt in the upper two metres and then follow the silt/clay boundary down to about 6.5m depth. The two tests agree reasonably well over this depth range (to 6.5m). Below 6.5m, the DMT I_D indicates sandy silt and sand becoming more silty below about 9m, whereas the CPT I_c indicates silt soil below 6.5m becoming slightly more sandy with depth.

There is a small blip in the q_c and f_s plots at around 2.5m depth, which is mirrored in the DMT p_0 and p_1 plot also. Both tests indicate a harder layer (likely sandstone) at around 10m depth. The predicted undrained shear strength corresponds well in both tests in the upper 6.5m, after which the CPT suggests a very stiff clayey soil, whereas the DMT is interpreting the soil to be sandy ($\phi' \approx 35^o$). The constrained modulus, M, estimated by the DMT is higher than that of the CPT in the upper 3m and is lower than the CPT predictions below about 7.5m depth. However, between about 3m and 7.5m, the two tests show similar estimates of M. The measured G_0 by the sDMT compares very well with that predicted by the CPT in the upper 7m. Below 7m, the CPT predicts generally higher G_0 values than measured by the sDMT. The OCR predicted by both tests compares favourably in the zone between 3m and 7m, but the DMT estimates higher OCR in the upper 3m (due to desiccation).

With respect to the Robertson (2009b) correlations, the estimated I_D from CPT follows more-or-less the same trend as the DMT measured I_D over the upper 7m or so. Below 7m, however, the CPT estimated I_D does not match well being on the clayey side of the silt range, whereas the DMT I_D indicates sandy soils. The Mayne and Liao (2004) correlation with Fr does not compare well, but comes closer to the measured I_D values in places below 7m depth.

The two Robertson (2009b) correlations to K_D compare very well between themselves, but are lower than the DMT K_D values to about 7m depth, after which they become slightly larger than the measured K_D values. However, the estimated K_D values do follow the same shape and fit reasonably well with the measured values, particularly between 4m and 7m depth.

The E_D values estimated from CPT by the Robertson (2009b) correlation generally follow the same profile of the measured DMT E_D values, but are lower. The two curves come closer together below about 8m depth, but the individual depth values compare relatively poorly in general.

In general, the derived soil parameters (c_u, M, G_0 and OCR) from both tests compare reasonably well, except below about 7m depth. This may be due to a different geological unit being encountered. Below this depth the DMT and CPT have interpreted different soil types. The Robertson (2009b) correlation for K_D plotted reasonably closely to the DMT K_D curve, however the correlations for I_D and E_D were less favourable.

4.1.4 Maungaturoto

The I_c and I_D plots show similar results, with the graphs falling mostly on the clay side of the silt/clay boundary with more clayey material between about 1.5m and 2.5m depth. At the base of the soundings, both material indices go strongly to the sand side. This represents a hard layer at the base of soft clay deposits. The undrained shear strengths vary with the CPT generally predicting slightly higher values, but the two curves follow the same general trend and the comparison is reasonable. The constrained modulus, G_0 and OCR show similar comparisons between the two tests. The undrained shear strength is generally between 20kPa and 50kPa suggesting a soft to firm soil consistency and a c_u-depth profile that would extrapolate to the origin of the graph. This would suggest a possible normally consolidated state, but the OCR estimated from both tests is generally greater than 5. The soils do become softer below about 3.7m depth where c_u, M and OCR all reduce and the OCR reduces to about 2 to 3. However, the OCR does appear high considering the nature oft the other derived soil parameters.

The tests appear to be out-of-phase with the DMT results needing to shift up approximately 300mm. However, the end depth on the hard stratum is the same in both tests. The variation could be explained to some extent by variations in the ground conditions between the soundings.

The Robertson (2009b) correlation to I_D shows the same trends as the measured DMT I_D, with the plots falling into the same soil categories. The numeric values vary, but the numbers do look more closely related below about 2.5m depth. Very similar shaped plots to those of the I_D graph are shown on the E_D graph with similar variations. It appears that the DMT has picked up a soft layer at

around 2.2m depth that has not been picked up by the CPT. The estimated K_D values from both correlations provided by Robertson (2009b) show reasonable agreement with the trend of the measured K_D plot, but with generally slightly higher estimated values.

In summary, the CPT and DMT derived soil parameters and Robertson (2009b) correlations showed similar trends on the graphical plots but the numerical values at the depths points are significantly different in places.

4.1.5 Kaiwaka

The material index plots of the two tests do not relate well at this site. The DMT I_D plot is highly variable with the I_D values zigzagging across the sit zone from clay to silt. This suggests that the soil is a variable layered material of alternating silty clays and silty sands. Apart from the upper 2m, this is not reflected in the CPT I_c plot that shows a more-or-less consistent clayey silt soil between 2m and 5m depth. Above 2m and below 5m, the I_c plot is variable, but the variations do not appear to correspond to those of the I_D plot.

The estimates of undrained shear strength vary greatly between the two tests but are more closely in alignment between about 2m and 4m depth. But above and below this depth range, the CPT estimated c_u values are approximately twice those of the DMT predictions. A similar relationship exists for the estimates of constrained modulus, with the two estimates agreeing reasonably well between 2m and 4m, but the CPT M values are higher above and below. The CPT estimated G_0 and measured DMT G_0 show reasonable agreement, except through the zone 3m to 5m, where the DMT G_0 values are higher. The OCR predicted by the CPT shows reasonable agreement with that predicted by the DMT between about 2.5m and 4m, but again tends to be higher above and below.

The Robertson (2009b) and Mayne and Liao (2004) correlations to I_D compare extremely poorly to the DMT I_D. The Robertson (2009b) predicted curve plots along the clay/silt boundary, whilst the Mayne and Liao (2004) plots along the silt/sand boundary and the measured DMT I_D curve zigzags in between the two predictions. The Robertson (2009b) correlation for E_D also compares poorly to the DMT E_D. Although the two curves follow the same general trend, the values at the individual depth points vary greatly. The K_D plot, however, generally shows a better comparison between the Robertson (2009b) correlation and the DMT K_D, particularly below 3m depth.

In summary, the DMT and CPT tests, interpretations and correlations generally compare poorly to the extent that they could be measuring completing different soil. The only exception is that the Robertson (2009b) correlation with K_D appears to fit reasonably well with the measured DMT K_D values.

4.1.6 Matakana

The I_D and I_C plots show similar responses and predictions of soil type. They both show silty soil in the upper metre followed by clay along the silt/clay boundary with hard sand/silt at the base (probably sandstone). The undrained shear strength, constrained modulus and G_0 predictions from both tests are reasonably close, except below about 6m depth where there is some variation with the CPT derived values tending to plot higher. The OCR predictions are less compatible, although they do follow the same general trend.
The Robertson (2009b) correlations plot relatively well for I_D but less so for K_D and I_D, although the general trend is followed between the predicted and measured values and the correlations become better below about 6m depth.

In general, the correlations and derived soil parameters compare reasonably well between the CPT and DMT at this site, but the trends show closer approximation than the numeric values.

4.1.7 Pohuehue

The I_D and I_c plots compare well with both index values giving approximately the same soil type interpretations, except the DMT is indicating a silt soil at around 4m depth (as opposed to the clay from the I_c) and a sandier material at around 5.5m to 6m, whereas the CPT indicates silt.

The soil parameters c_u, M and G_0 estimated from the CPT and DMT tests showed reasonable comparison, except at around 3.5m to 4m depth where there is a distinct variation in the estimates for cu and M. The G_0 estimates compare remarkably well, although they vary below about 5m depth. The OCR estimates from the two tests are slightly different and more so in the approximate

depth range of 3.5m to 4m depth. The DMT estimated OCR is higher than the OCR estimated from CPT.

The Robertson (2009b) correlations for I_D, K_D and E_D are reasonably good, except in the zone of approximately 3.5m to 4m. The Mayne and Liao (2004) correlation with I_D does not match well.

In general the relative estimated soil parameters and correlations are reasonably good between the two tests at this site. There is a consistent variation across the parameters at around 3.5m to 4m depth, which is likely to be due to natural variation between the two soundings at this depth.

4.1.8 Herald Island

The plots of I_c and I_D are relatively compatible with the curves plotting mostly along the silt/clay boundary. However, the I_D curve spikes into silty and sandy soils at around 4.2m and again at about 5m, which do not appear to be picked up by the CPT I_c. Another sand layer identified by I_D at 7m is picked up by the CPT I_c, but, whereas the I_D is clearly within the sand zone, the I_c remains in the silt zone (sandy silt rather than sand).

The estimated c_u values from both tests compares very well on the graphical plot, except at the upper 2m where the values estimated by the CPT are significantly higher. This may be a result of changing moisture content (and suction) in the soil due to summer desiccation and winter wetting. The CPT test was carried out in summer and the DMT in winter. The constrained modulus predicted by the DMT is higher than CPT estimated values, particularly in the upper 3m. The G_0 values are closely approximated by the two tests, but the measured DMT values are lower in the upper 2m and higher below about 6m in relation to the CPT derived values. The OCR estimated from DMT is higher than that estimated by the CPT, but the relationship is fairly close and the same trend is followed.

The Robertson (2009b) correlation to DMT I_D is fairly good at this site, except at around 4.2m and 5m, where the CPT did not recognise sand layers. The Mayne and Liao (2004) correlation from F_r compares very poorly (no correlation) with the I_D plot. Both the DMT K_D and E_D curves plot higher than those estimated from CPT using the Robertson (2009b) correlations, but the same general trend is followed.

At this site, the undrained shear strength values derived from both tests compared very well. For the remaining soil parameters and correlations, the DMT data tended to plot slightly higher than the CPT information, although the same trends were followed.

4.1.9 Hamilton

4.1.9.1 Pair 8a

At this location (Pair 8a) the raw data (q_c, f_s, u_2, p_0 and p_1) show very spiky curves suggesting significant variability with depth. The I_c and I_D curves, however, appear to mirror each other very well with the soil mostly sand or near the sand/silt interface with distinct clay lenses picked up by both indices.

The estimated soil parameters M, G_0 and ϕ' compare well between the two tests. The Robertson (2009b) correlations of I_D, K_D and E_D compare well at this location.

4.1.9.2 Pair 8d

The I_D and I_c plots show similar general trends with silt over the upper 4m, followed by clay and sandy silt below 14m. However, the I_D plot shows greater variability in the clay layer (4m to 14m) with silty soils identified between 10.5m and 12m, which is not seen in the I_c plot.

The estimated undrained shear strength from the two tests compare reasonably well, except around 3m and 5m where the DMT estimated values are higher and below 10m, where the DMT parameters are lower. The M values derived form the two tests compare well, except over the upper 4m, where the DMT derived values are higher. The derived G_0 values compare well below 8m, but vary greatly above 8m depth. The measured DMT values are significantly higher than the CPT derived values in this zone. The OCR estimates are higher from the DMT than the CPT, although the two are fairly similar below about 6m depth (where they appear to show a normally consolidated state).

The Robertson (2009b) correlations with I_D, K_D and E_D compare well to the DMT values in places and poorly in others. The I_D correlation fits reasonably well, except between about 10m and 14m, where the DMT has identified silt and the CPT clay. The Mayne and Liao (2004) correlation fits poorly except below 10m, where it seems to correlate well. The K_D correlations are reasonable below about 6m depth. The E_D correlation is relatively close to the measured DMT values at this location, except at between about 7m and 10m depth.

4.1.9.3 Pair 8c

Here the CPT and DMT parameters, correlations and interpretations compare poorly. It is possible that the distance between the CPT and DMT was large enough that the there is significant natural variation in the ground conditions between the two soundings. The CPT was done by others previous to the DMT test and so the exact position of the CPT is not known.

4.1.9.4 Pair 8d

The I_c plot here indicates silt soil to about 8.5m depth, after which the soil is shown to be clay down to 14m. The I_D plot, however, shows silt tending to the sand side over the same depth range of the clay (8.5m to 14m). The undrained shear strengths estimated by the DMT is approximately half that estimated by the CPT. The M values are shown to be fairly close over the depth range 5m to 14m, but the measured sDMT G_0 values are significantly higher than the CPT derived values, although they follow the same trend. The OCR derived from the DMT reduces rapidly down to a normally consolidated state below about 5m depth, whereas the OCR derived from the CPT remains slightly higher.

The Robertson (2009b) correlation with DMT E_D is reasonably good at this location, although the correlations for I_D and K_D are less favourable here.

4.1.10 Ngaruawahia

4.1.10.1 Pair 9a

At this location the I_D and I_c plots compare quite well with both tests indicating sand close to the silt boundary with spikes indicating occasional clayey layers. The estimated M values from the two tests compare reasonably well considering the varied layered nature of the ground. The estimated G_0 values from the CPT test, however, are significantly higher than those measured using the sDMT.

The Robertson (2009b) correlations for I_D, K_D and E_D from CPT compare reasonably well with the DMT values. However, the same intensity of the spikes in the DMT data is not matched by the CPT correlations. There is also an apparent lag or out-of-phase element of the plots, which is probably due to natural variations in the layer thicknesses and elevations and the relative ground elevations at each of the soundings may also affect this out-of-phase feature. However, the lag is not consistent and so it is not possible to simply shift the data up or down. Rather the positioning of the spikes due to the layers is variable.

4.1.10.2 Pair 9b

Here the CPT and DMT parameters, correlations and interpretations compare poorly. It is possible that the distance between the CPT and DMT was large enough that the there is significant natural variation in the ground conditions between the two soundings. The CPT was done by others previous to the DMT test and so the exact position of the CPT is not known.

4.1.10.3 Pair 9c

At this location the I_D and I_c plots both show predominantly silt soils (on the sand side) down to about 5m, after which the I_c plot moves into the sand zone, but the I_D stays within the silt boundary,

albeit slightly closer to the sand boundary. Below 8m, the DMT I_D shows variable layers of silt and sand, which is not identified by the I_c.

The raw CPT q_c plot shows the cone resistance to increase from about 5m to about 7m, reaching approximately q_c = 20 MPa, which continues until the end of the sounding. The porewater pressure, u_2, becomes negative below about 8m depth. This would suggest a dense sand, which creates a suction due to dilation as the cone penetrates the ground. However, over at the same depth (8m) the DMT p_0 and p_1 show a dramatic reduction, which is not consistent with a dense sand. The measured shear modulus, however, from the sDMT shows increasing values with depth, consistent with a dense sand and also consistent with the estimated G_0 from the CPT. There appears to be some inconsistency in the DMT data between 8m and 10m, which is affecting the correlations with CPT. By ignoring the DMT over this depth range, the Robertson (2009b) correlation for E_D compares reasonably well with the DMT E_D. The Correlations with I_D and K_D are, however, less favourable. The inconsistency of the DMT results here makes this set of data unreliable.

4.1.10.4 Pair 9d

Here the CPT and DMT parameters, correlations and interpretations compare poorly. It is possible that the distance between the CPT and DMT was large enough that the there is significant natural variation in the ground conditions between the two soundings. The CPT was done by others previous to the DMT test and so the exact position of the CPT is not known.

4.1.11 New Lynn

The I_c and I_D plots compare relatively well with mostly clay soils being identified with a silty layer at about 7m depth. At the same depth, the raw CPT q_c shows a large spike (up to about 20 MPa), which is not picked up as increased strength in the DMT p_0 or p_1. Consequently, this spike is carried through to the interpretations of the CPT, but not in those from the DMT. It is possible that there is a natural variation in the soil between the soundings such that that layer does not exist at the DMT location or is less significant. The CPT was done some time previous to the DMT and the exact location of the CPT is not known, hence such natural variation is possible.

By ignoring the effects of that spike at 7m depth, the correlations and interpretations from the CPT are not particularly good, although, in places, comparisons between the estimates of c_u, M and G_0 are reasonable between the two tests. The Robertson (2009b) correlations with I_D, K_D and E_D show the same general trends as the DMT plots, but are off-set somewhat, particularly below 7m depth.

Digital data was not available for the CPT at this location, so the data has been manually extracted from the hard copy CPT plot. Considering this and that the exact location of the CPT in relation to the DMT is not known, this data set would be considered unreliable.

4.2 COMPARISON BETWEEN CPT u_2 AND DMT p_0

Mayne and Bachus (1989) and Mayne (2006) found that the DMT lift-off pressure, p_0, approximates to the porewater pressure measured behind the CPT cone, u_2 in soft clay soils on the assumption that the excess porewater generation due to inserting the cone and the DMT blade are the same. The data in this study includes some soft clays so it is of interest to investigate the possible relationship between these parameters.

The p_0 and corresponding u_2 data have been plotted against depth for each data pair. The resulting graphs are given in Appendix C. The plots from sites containing soft clays (taken as cu < 50 kPa) have been reproduced in Figure 60.

From Figure 60 and from the other plots in Appendix C, there is no apparent relationship between u_2 and p_0 with the data in this study. The plots in Figure 60 show some places where u_2 is close to p_0, particularly in the upper 5m of the Kaiwaka site (c), the central zone of the Matakana Site (d), around 4m deep in the Maungaturoto site (b) and in the 5m to 7m zone of the St. Heliers site (a). These are generally the softest zones of these soundings. The relationship therefore is only expected to be of relevance in very soft mud like soils. Much of the data in this study comprises silt mixture soils, usually variable alternating layers of sandy silts and clayey silts. These soils are unlikely to act in a completely undrained manner (nor completed drained manner) and so some degree of drainage (to an indeterminate extent) is likely to occur in response to the insertion of the cone or DMT blade such that full excess porewater pressures are unlikely to be generated. Consequently, correlations of the data in this study using the CPT u_2 values are likely to be ineffective.

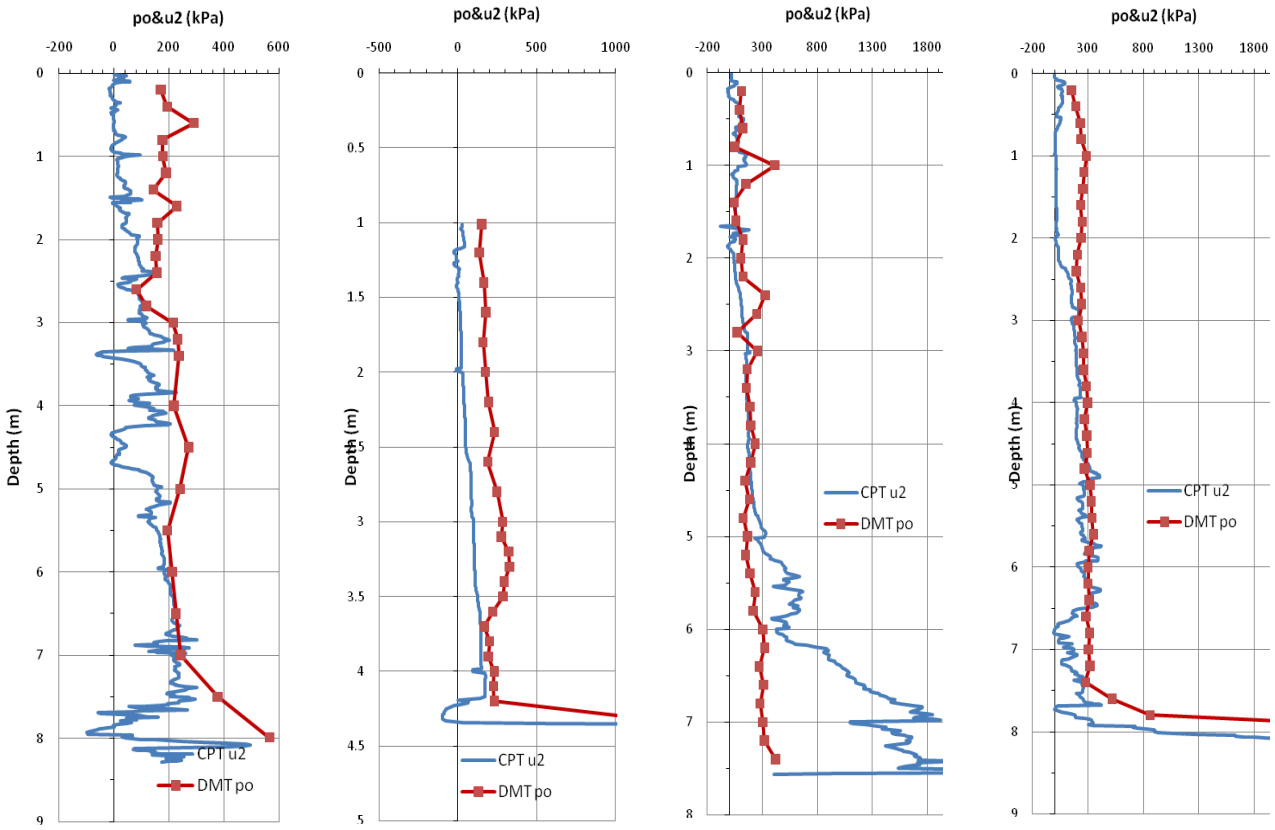

(a) St. Heliers **(b) Maungaturoto** **(c) Kaiwaka** **(d) Matakana**

Figure 60: Plots of u_2 and p_0 vs. Depth

4.3 GENERAL COMMENTS ON RESULTS

The data in this study comprises sites with a wide range of soil types. However, as discussed above, the bulk of the soils are layered silt mixtures, i.e. a variable mixture of silty sands, sandy silts, clayey silts or silty clays. This is typical of much of the North Island soils. Robertson (2009a) has suggested that soils within the transition zone between layers of different soil types should be ignored due to the influence of the soil ahead and behind the cone (which can be as much as 15 times the cone diameter ≈ 500mm or so). So in layered soils where interbedded layers of sandy and clayey soils of 500mm or so layer thickness occur, the cone results may be constantly affected by the influence of the soils in vertically adjacent layers. Furthermore the drainage characteristics of these soils are such that the soils below and around the cone are at constantly changing degrees of drainage as the cone is pushed through the various silty layers. In much of these soils, the soil is neither in a completely undrained state nor in a completely undrained state during the CPT test, but

some where indeterminately in between. Similarly the drainage around the DMT, both during plate insertion and testing, may be in an indeterminate state. Furthermore the degree of drainage occurring during the CPT test may be different to that during the DMT test in the same soil. Both the DMT test and the CPT test assume that clay soils will be in a completely undrained state and sands will be in a completely drained state during the test. Partial drainage may affect the results and interpretations of the tests.

As a further complication with the data is the variability of the soils between the CPT and DMT locations. The soils in this study are generally highly variable and, even if very close together, the ground conditions may vary between the two test locations. Also the elevation of the ground surface at each test may be different. Considering that the CPT measures at 10mm depth intervals, the variation in the data comparisons due to subsoil variations and/or ground elevations can be substantial in a variable layered soil. Some of the graphical data in this study shows possible lags in the spikes between the CPT and adjacent DMT results, which may be the result of ground surface elevation differences or natural ground variability.

There is also variation simply in the nature of the tests themselves. The CPT is a large plastic strain vertical penetration test, whilst the DMT is a smaller strain modulus test in the horizontal direction. A direct theoretical solution between the two tests is not immediately apparent. So it would be expected that the tests may not necessarily be exactly compatible.

Despite the inherent difficulties in comparing the CPT and DMT in this study, the results discussed in detail above do show reasonable comparisons between the results and interpretations of the two types of test. The main subjective observations of the test comparisons are:

(a) The material indices of CPT I_c and DMT I_D generally show similar soil types, although spikes indicating thin layers of differing soil type are often identified by one and not the other.
(b) The soil parameters of c_u, M, G_0, OCR and ϕ' derived from the CPT using CPeT-IT software (based on Robertson 2009a) and those derived from DMT using the Marchetti software (based on Marchetti 1980 and TC2001) generally show reasonable agreement.
(c) Values of c_u appear to compare very well between the tests (using N_{kt} = 14 for the cone factor).

(d) The modulus values of M and G_0 also generally show reasonable agreement. Values of G_0 are remarkably similar considering that the G_0 from the CPT is primarily derived from the cone resistance, whereas the G_0 from the DMT in this study have been obtained by direct measurement of shear wave velocity.

(e) In almost all cases the OCR estimated from the DMT is higher than that estimated from the CPT, although they show similar results in general.

(f) The Robertson (2009b) correlation between CPT I_c and DMT I_D generally does not correlate well with the data in this study. Although the Ic derived I_D and the DMT I_D usually indicate similar soil types, they do not compare well numerically.

(g) The Mayne and Liao (2004) correlation between CPT F_r and I_D does not correlate well with any of the data.

(h) The Robertson (2009b) correlation of I_c and Q_t with DMT K_D generally plots close to the DMT K_D curve, but the CPT derived values are often too low in the upper few metres. This is probably because the K_D is derived from the CPT relationship with OCR (see (e), above).

(i) The Robertson (2009b) correlation with E_D usually plots to show a similar trend, but is mostly significantly off the mark numerically.

(j) Some of the data pairs do not correlate at all. These seem to be mostly sites where the CPT was done some time previous to the DMT and the exact location of the CPT is not known. In these cases, there may be natural variation in the ground due to a possible larger distance between the soundings. Consequently some of the data can be considered unreliable.

Based on the knowledge of the sounding locations and observation of the test results, the most reliable data is considered to be at the sites of: St. Heliers, Flat Bush, Matakana, Herald Island, Hamilton (8a) and Ngaruawahia (9a). These six sites represent a wide range of soil types, geology and geographical locations. Two of the sites are in Alluvial Soils (St. Heliers and Flat Bush), two in Residual Soils (Matakana and Herald Island) and two in Volcanic Soils (Hamilton and Ngaruawahia). These sites are considered suitable for further analysis, whereas the others may be considered with some uncertainty.

Figure 61 shows a comparison between the estimated soil parameters derived from the CPT and those derived from the DMT considering only the data from the six ‘reliable’ sites.

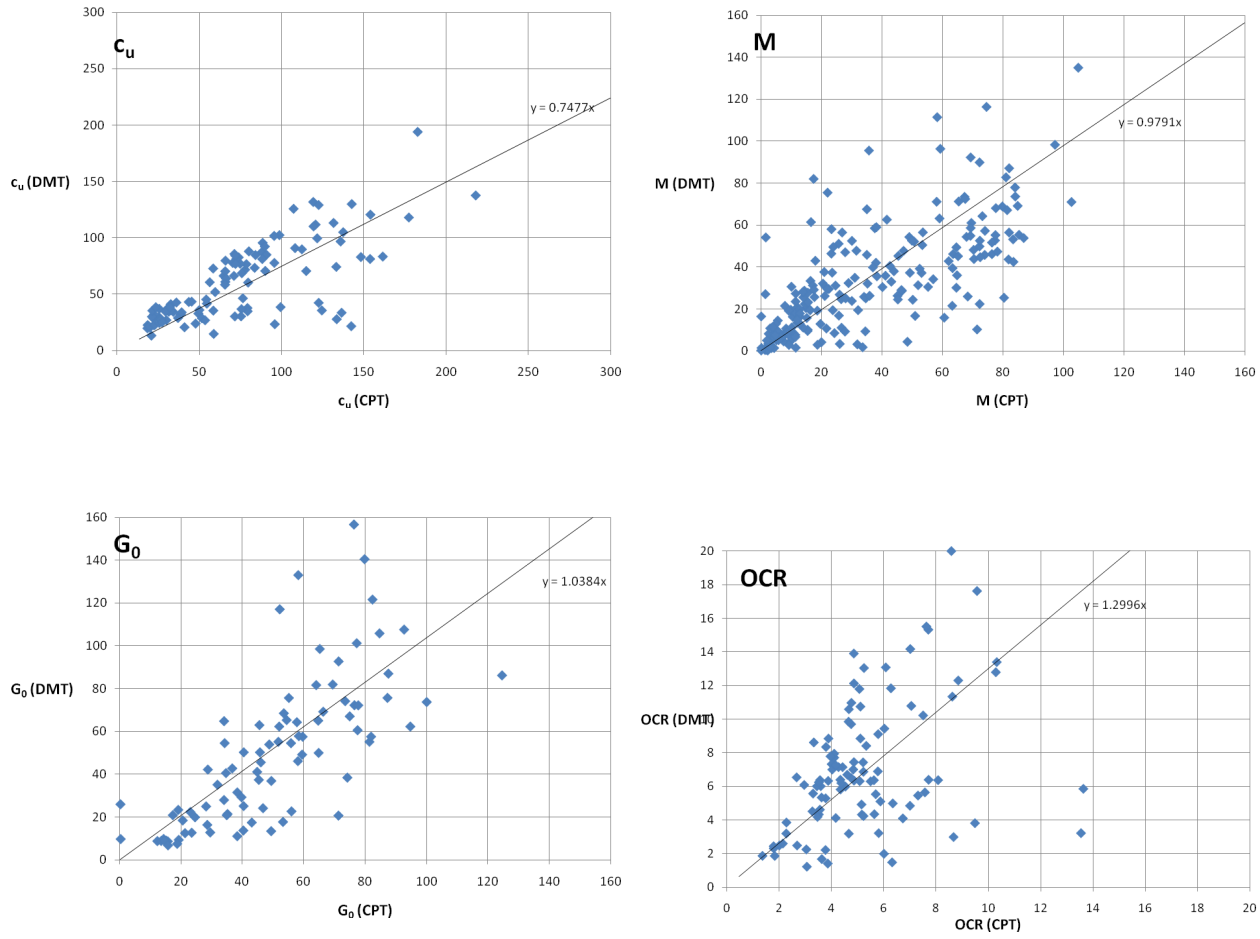

Figure 61: Comparison of Derived Soil Parameters from CPT and sDMT

From Figure 61 it can be seen there is some spread in the graphs, but there is a reasonable relationship between the parameters derived from each test. The linear regression with the data in the graphs indicates the following general equations along with their linear correlation coefficients:

$$c_u \text{ (DMT)} \approx 0.75\ c_u \text{ (CPT)} \qquad (r = 0.740) \qquad (83)$$

,with CPT $N_{kt} = 14$

$$M \text{ (DMT)} \approx M \text{ (CPT)} \qquad (r = 0.722) \qquad (84)$$

$$G_0 \text{ (DMT)} \approx G_0 \text{ (CPT)} \qquad (r = 0.624) \qquad (85)$$

$$OCR \text{ (DMT)} \approx 1.3\ OCR \text{ (CPT)} \qquad (r = 0.740) \qquad (86)$$

It is interesting that the modulus values (M and G_0) derived from the CPT compare so well with the sDMT, considering that the DMT measures modulus directly. The seismic module (sDMT) measures G_0 from shear wave velocity and is considered to be an accurate measure of small strain shear modulus, so it is interesting that the CPT, which derives G_0 from cone resistance, appears to correlate so well with the measured values.

The c_u and OCR relationships (Eqn 83 and 86) vary between the CPT and DMT estimations by the approximate same factor (i.e. $1.3 \approx {}^{1}/_{0.75}$). This is most likely because c_u and OCR are interrelated in the same manner in both the CPT and DMT correlations.

The above approximate relationships have been obtained from a relatively small database. It is likely that these relationships will vary with material type, geology, aging, particle bonding and so on. Further research will be required to better establish these relationships. This research is best undertaken with reliable independent tests of the particular soil parameters (such as laboratory testing) as a reference.

5. CHAPTER 5: ANALYSIS

5.1 AVERAGED DATA

Due to the huge volume of data that is obtained from the CPT tests, the spreadsheet of the full data involved in this study comprises over 20,000 rows. This full set of data is too large to present in this thesis as it would involve hundreds of sheets of paper. However, the full data is not of use when comparing CPT (at 10mm depth intervals) with DMT results (at 200mm intervals). To equate the two different depth intervals, the CPT data was averaged out over 200mm intervals (100mm above and below the depth point in question) as a running average down each of CPT results. All of the rows of data in between the DMT results were then deleted so that the only data that remained related to the DMT test depths with the corresponding CPT data averaged over a 200mm depth zone. This reduced the data from over 20,000 rows to approximately 870 rows. The spreadsheet containing this averaged data is given in Appendix D.

5.2 GRNN ANALYSIS

5.2.1 General

As discussed previously, some of the data in the averaged data set (Appendix D) contains information from sites that are considered to be unreliable. The inherent problems between the test methods and the quality of the data exclude a rigorous statistical analysis to determine an exact solution. Instead, it is the intention here to investigate the possibility of obtaining a reasonable correlation between the CPT and DMT using the artificial neuron network method of GRNN, which has been described in detail in Section 2.4.2. The best opportunity to achieve a suitable outcome is to use the most reliable data that is available. Consequently, the data at the six selected sites of St. Heliers, Flat Bush, Matakana, Herald Island, Hamilton (8a) and Ngaruawahia (9a) is used in the analysis. However, the complete set of data is run first to determine initial compatibility followed by the selected data.

The computer program, NeuroShell 2 was used to run the GRNN in this study. The program allows automatic termination of training once 20 generations have passed with no improvement beyond 1% error. At termination of the training, the smoothing factor adjustment values are provided for each input parameter. This provides an indication as to which input parameters are of relevance in the analysis and which can be omitted. The GRNN was run over many combinations of different input parameters, starting with all of the CPT parameters being considered. The criteria for the success of the trained network was based on the correlation coefficient, r, in conjunction with the percentage of estimated values that are closest to the actual data when run when the trained network is applied to the test set, the combined test set and the training set. The test set was randomly chosen from 20% of the applied data. The chosen network has then applied to the entire data (including those excluded in the training/testing set) for validation.

The input parameters considered are the CPT parameters of q_c, f_s, u_2, q_t, σ_{vo}, u_0, σ'_{vo}, Q_t, F_r and I_c. Various combinations of these input parameters have been considered, including using all of these parameters together, even though some parameters are simply a combination of the others (all arising from q_c, f_s, u_2, u_0, σ_{vo}). The network, however, is not concerned over the theoretical connection between any of the input parameters, nor any theoretical connection between the input parameters and the output parameters. It merely processes numbers and the optimum network arrangement may consist of a set of input parameters that seem illogical. However, the input parameters used in this analysis have been chosen bearing in mind possible theoretical connections.

The output parameters are the DMT parameters, p_0, p_1, I_D, K_D and E_D. A number of network arrangements were run for differing input parameters to one output parameter. Only one output parameter at a time was considered.

5.2.2 GRNN Results

5.2.2.1 Presentation of Results

76 runs using different combinations of input and output parameters were carried out. The results of these runs are given in Table 7 in Appendix E. The table shows the input parameters used for each

run and the smoothing factor adjustments resulting for each of the chosen input parameters at the end of the run. The table shows which output parameter was considered for each run. The trained network of each run was applied to the data used, which is referred to as the combined set (combination of training set and test set). For selected runs, the trained networks were also applied to the training and test sets to compare the performance of the network on the selected data. The set to which the trained network was applied and the corresponding correlation coefficient (r) and the percentages of the predicted data that are within certain percentages of the actual data (<5%, 5-10%, 10-20%, 20-30%, >30%) were listed for each run (see Table 7). The network was refined by selecting runs that show the best coefficient of correlation in combination with the best percentages within actual data and adjusting the input parameters by examining the smoothing factor adjustments of the input parameters. Low values of smoothing factor adjustment indicates that the corresponding input parameter has less relevance in the network and omitting that parameter in subsequent runs may improve the network.

The first 24 runs shown on Table 7 were undertaken considering all of the averaged data. These are numbered 1 to 24 and are described as 'ALL DATA-XX', where the XX denotes the particular output parameter being considered (i.e. p_0, p_1, I_D, K_D or E_D). Runs 25 to 75 were undertaken considering the selected data (which is the data for the six 'reliable' sites, described above). These are described as 'SELECT-XX'. For some runs, the correlation coefficient and the percentages with actual data were summarised in graphical form to help assist with the selection of the successful network. These graphs are presented after Table 7 in Appendix E.

The results of the GRNN analysis on both the complete data (All Data) and on the selected data (Selected Data) are discussed below.

5.2.2.2 All Data

Figure 62 show the results of the GRNN analysis on all the data. These have been determined using the full set of input parameters (q_c, f_s, u_2, q_t, σ_{vo}, u_0, σ'_{vo}, Q_t, F_r and I_c). Consideration to alternative combinations of input parameters have been made in subsequent runs, but these showed no improvement on correlation coefficient or percentages within actual data (see Table 7).

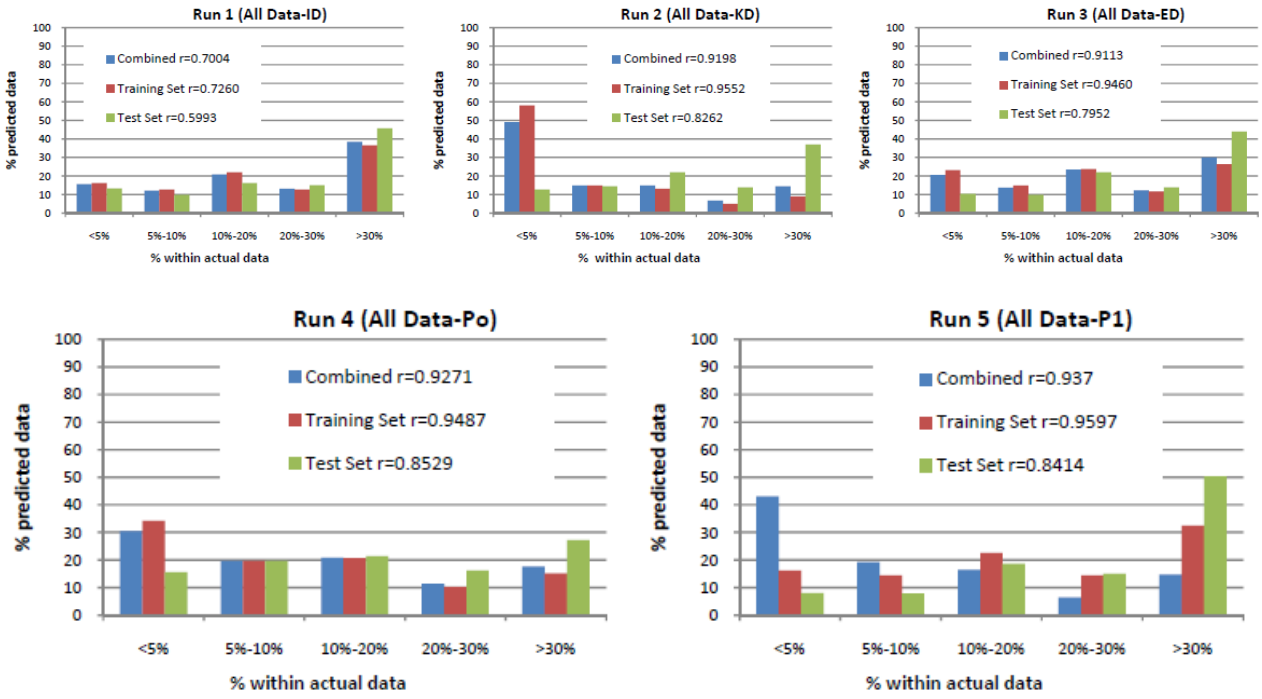

Figure 62: Results of GRNN on All Data to I_D, K_D and E_D, p_0 and p_1

The graphs in Figure 62 show the percentages of the predicted data that falls within specific ranges of the actual data with the network applied to the training set, test set and the combination of test and training sets. The correlation coefficient, r, is also shown for each network application.

From these graphs it can be seen that the correlations are fairly poor. The worst correlation is that to I_D (Run1), which shows around 40% of the predicted data to be more than 30% from the actual values and r values of 0.700, 0.726 and 0.599 for the combined, training and test sets, respectively. The correlation with E_D (Run 3) is also poor with a similar trend of larger proportions of predicted data away from the actual data.

The best correlation at first glance is that to K_D, (Run 2), which shows around 50% of the predicted data within 5% of the actual data for both the training set and combined set. However, with application to the test set, the pattern reverses such that approximately 40% of the predicted data is more than 30% from the actual data. The correlation coefficient falls from 0.955 in the training set to 0.826 in the test set.

The correlations with p_0 and p_1 (Runs 4 and 5) are also poor. Interestingly, the network application to the combined set in Run 5 (for p_1) shows better results than those for both the test set and training set. This would indicate that the network is struggling to find a reliable correlation with this data.

The poor results are likely to be, in part, due to the quality of the data, which includes potentially unreliable information, as has been discussed previously.

5.2.2.3 Selected Data

The GRNN analysis has been applied to the selected data, which includes the information for the selected six test sites only (St. Heliers, Flat Bush, Matakana, Herald Island, Hamilton 8a and Ngaruawahia 9a), which are considered to represent more reliable data.

Figure 63 shows the results of the GRNN analysis for the best correlations that were obtained for over 50 various combinations of input parameters (see Table 7 in Appendix E).

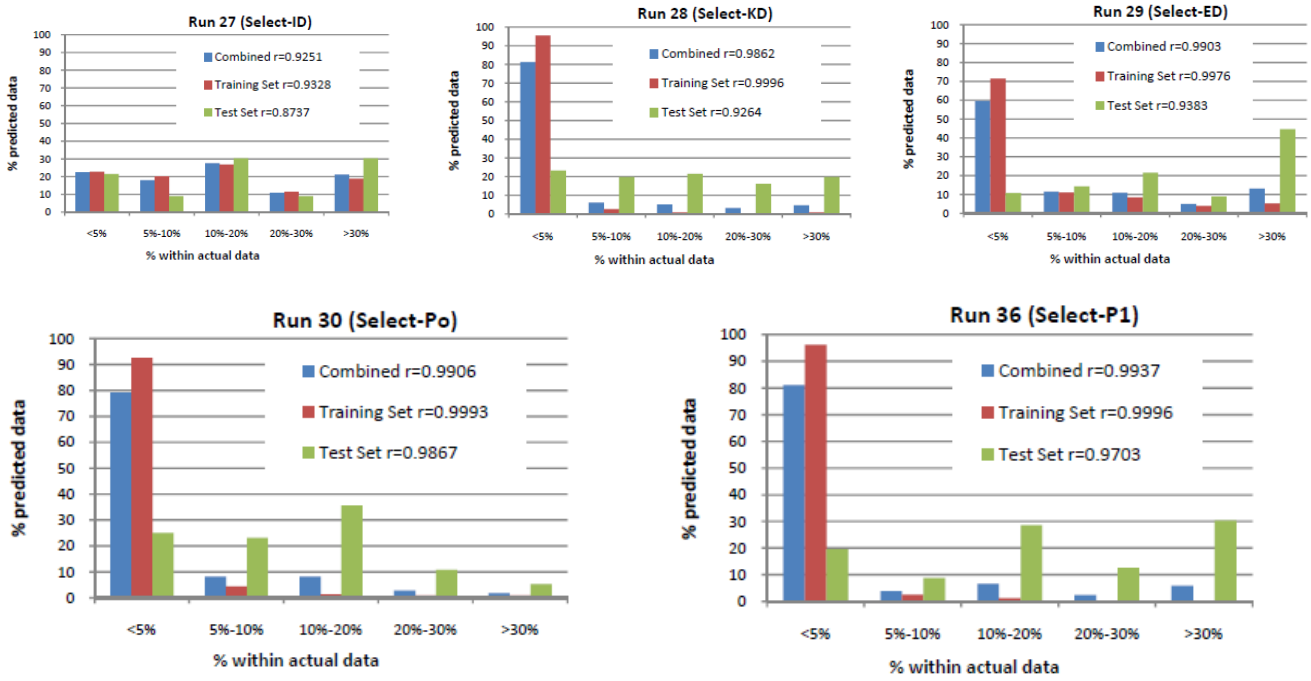

Figure 63: Results of GRNN on Selected Data to I_D, K_D and E_D, p_0 and p_1

The runs that provided the best correlations for I_D, K_D and E_D (Runs 27, 28 and 29), as shown in Figure 63, have been undertaken using the full set of input parameters (q_c, f_s, u_2, q_t, σ_{vo}, u_0, σ'_{vo}, Q_t, F_r and I_c). Consideration to alternative combinations of input parameters have been made in subsequent runs, but these showed no significant improvement on correlation coefficient or percentages within actual data (see Table 7).

The best correlation is the one for K_D (Run 28) with over 80% of the predicted data from the combined and training sets within 5% of the actual values and r values of 0.9862 and 0.9996 for the combined and training sets, respectively. However, for the test set, the correlation coefficient drops to 0.9264 and the predicted data is spread further from the actual data (≈ 20% of the predicted data more than 30% from the actual).

The correlation with E_D (Run 29) is poorer than that of K_D with around 60% and 70% of the predicted data within 5% of the actual data for the combined and training sets, respectively. Application of the test set shows a bigger spread of data away from the actual values with greater than 40% of the predicted values greater than 30% from the actual. However, the correlation coefficients of 0.9903, 0.9976 and 0.9383 for the combined, training and test sets are reasonable.

The correlation with I_D (Run 27) is perhaps the worst, but still significantly better with the selected data than with the complete data (Run 1, in Figure 62). The r values, however, are reasonable (0.9251, 0.9328 and 0.8414) and, although there is significant spread of data, more than 50% of the predicted data is within 20% of the actual values, which is fair considering the difficulty in obtaining a correlation with this parameter.

The results of the GRNN analysis for the p_0 correlations (Run 30 in Figure 63) has been run with the input parameters q_c, f_s, u_2, σ_{vo} and u_0, whereas that for p_1 (Run 36) was run with the normalised parameters Q_t, F_r and I_c in conjunction with σ'_{vo}. These were found to provide the optimum results. The network provided relatively good correlations for these parameters with around 80% of the predicted data from the combined set and over 90% of the predicted data from the training set within 5% of the actual values. However, as with the other correlations, the application of the network to the test set showed less favourable results, although for the p_0 correlation, 80% of the predicted values are within 20% of the actual data and the r value is a reasonable 0.9867. For the p_1 correlation, the predicted data is slightly more spread with approximately 60% within 20% of actual values and about 30% of the predicted data greater than 30% from actual.

5.2.2.4 Validation of GRNN Networks

The surviving GRNN arrangements (Runs 27, 28, 29, 30 and 36) from the selected data analysis described above have been applied to the entire data (averaged data given in Appendix D) as a form of validation of the networks. The results are shown on Figure 64.

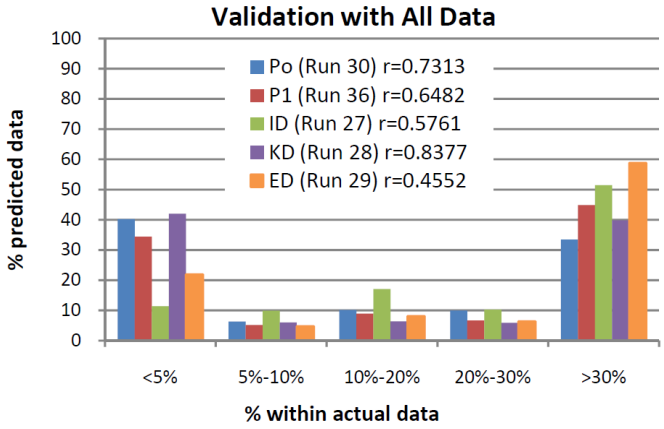

Figure 64: Results of GRNN Validation with All Data

This shows that the chosen networks generally correlate poorly with the overall data and so can not present validation of these correlations to this data. The K_D correlation (Run 28) shows the best result with a correlation coefficient, r = 0.8377 and approximately 40% of the predicted data within 5% of actual values. However, there is still 40% of the predicted data that is greater than 30% from the actual. Similar large spreads also exits for the other correlations. The worst correlations appear to be for I_D and E_D (Runs 27 and 29) with these showing r = 0.5761 and 0.4552, respectively. More than 50% of the predicted data resulting from these networks were more than 30% from actual values.

This appears to demonstrate that the chosen networks are not applicable in the wider sense, however, this process is not considered to be an appropriate 'validation' as much of the data is suspected to be unreliable. However, this 'validation' process does help highlight the relative difficulty or ability in establishing correlations between CPT and DMT parameters. It is apparent from the GRNN analyses that the correlations to K_D appear to be strongest, whilst those for E_D and, particularly, I_D are the most challenging. Despite the inability to satisfactorily validate the surviving network arrangements, the correlations do appear to be fair in relation to the analysed (Selected)

data, of which there is a reasonable level of confidence. A relative validation of the networks would be to compare these correlations graphically to the measured DMT data for each of the selected test sites.

5.2.3 Graphical Comparison of GRNN and DMT Results

5.2.3.1 Graphical Presentation

The correlations obtained from the GRNN analyses have been plotted along with the measured DMT values and the Robertson (2009b) correlations for each of the six selected test sites. Graphs of p_0, p_1, I_D, K_D and E_D vs depth have been plotted. The graphs for I_D and E_D have been plotted on a natural scale, as opposed to the conventional logarithmic scale to allow better visual comparison of the data.

The GRNN correlations for p_0 and p_1 are plotted with the measured p_0 and p_1 values from the DMT. As p_0 and p_1 are the raw data from the DMT, the GRNN derived p_0 and p_1 values can also be used to calculate I_D, K_D and E_D values using the Marchetti (1980) formula. These I_D, K_D and E_D values so calculated from the GRNN derived p_0 & p_1 values are plotted along with the I_D, K_D and E_D values derived directly from the respective GRNN network arrangement. These are plotted along with the measured DMT values and the Robertson (2009b) correlations. Thus, the I_D, K_D and E_D graphs have four superimposed plots, being:

1. The actual DMT values (denoted as 'DMT' on the graphs)
2. The values calculated from the p_0 and p_1 values derived from GRNN (denoted as 'GRNN p_0 & p_1')
3. The values derived directly form the respective GRNN network (denoted 'GRNN (Rxx)', where xx refers to the Run number of the GRNN network used)
4. The values derived from the Robertson (2009b) correlations (denoted 'Robertson')

The graphs of p_0, p_1 and I_D are presented side-by-side as one figure and the plots of K_D and E_D together in a separate figure for each test site and the results discussed.

5.2.3.2 St. Heliers

Graphs of p_0, p_1 and I_D for the data at the St. Heliers site are presented in Figure 65 along with the various correlations by GRNN and Robertson (2009b). Those for K_D and E_D are given in Figure 66.

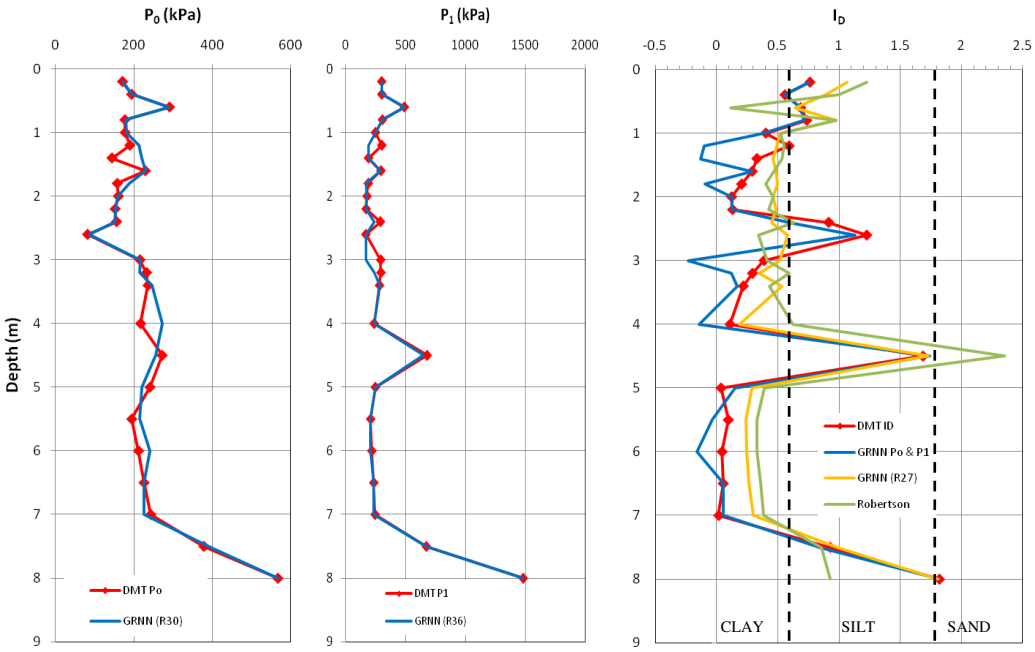

Figure 65: GRNN derived p_0, p_1 and I_D values compared to DMT values and Robertson (2009b) correlations for St. Heliers

The GRNN derived p_0 and p_1 values plot very closely to the measured DMT values, suggesting a good correlation. However, when those derived values are used to calculate I_D, an irregular plot is generated, which compares poorly in places to the measured DMT I_D values and they also produce some negative values (see the blue line in the I_D plot in Figure 65). The I_D values derived directly from GRNN (Run 27) show a fair comparison to the DMT values over the lower half of the sounding, but less so in the upper half. The GRNN (R27) correlation, however, appears to be a closer match to the Robertson (2009b) correlation. None of the correlations for I_D, however, are ideal.

In the K_D plot in Figure 66, both the GRNN (R28) derived values and those calculated from the GRNN derived p_0 and p_1 values compare very well to the DMT values. The Robertson (2009b) correlation is close, but shows lower values.

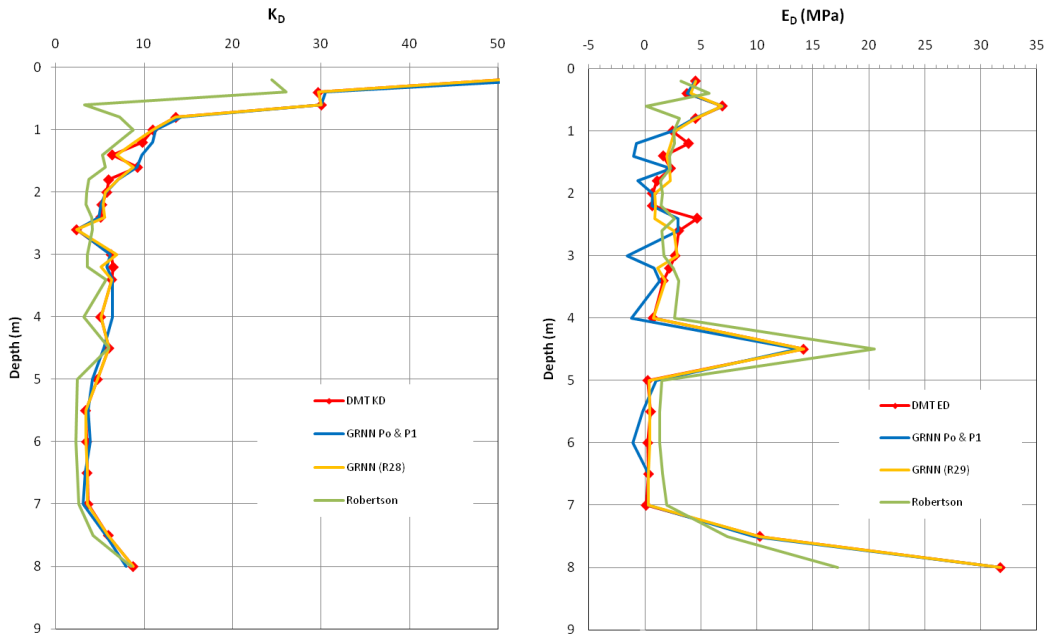

Figure 66: GRNN derived K_D and E_D values compared to DMT values and Robertson (2009b) correlations for St. Heliers

The E_D values calculated form the GRNN derived p_0 and p_1 produce an irregular curve that, similar to that in the I_D plot, shows negative values in places. The GRNN (R29) curve appears to correlate very well with the DMT results. The Robertson (2009b) also fits reasonably well to the GRNN (R29) curve and the DMT results over the upper half, but shows slightly larger values over the lower half.

5.2.3.3 Flat Bush

Graphs of p_0, p_1 and I_D for the data at the Flat Bush site are presented in Figure 67 along with the various correlations by GRNN and Robertson (2009b). Those for K_D and E_D are given in Figure 68.

The GRNN correlations for p_0 and p_1 appear to compare very well with the measured DMT values, except for occasional minor spikes. In the I_D plot, the calculated I_D from the GRNN derived p_0 and p_1 values generally follows the DMT values, except for some erratic spikes and a negative value in one place. The I_D values derived directly from the GRNN (R27) network appears to correlate very well but doesn't pick up all the spikes in the DMT plot. The Robertson correlation does not fit particularly well, especially at the lower half of the graph where it doesn't recognise the sandy material.

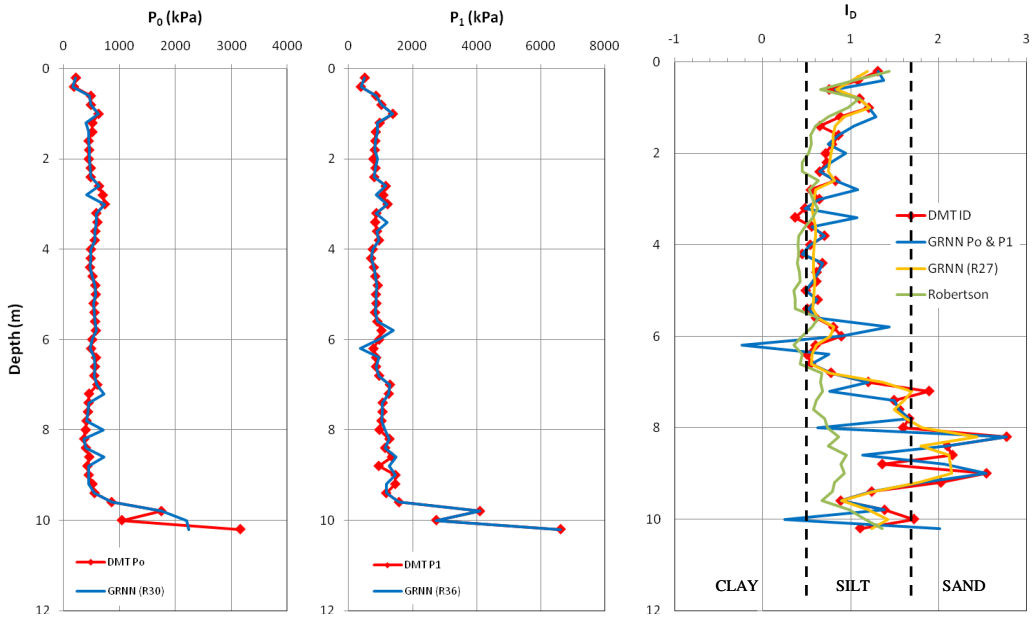

Figure 67: GRNN derived p_0, p_1 and I_D values compared to DMT values and Robertson (2009b) correlations for Flat Bush

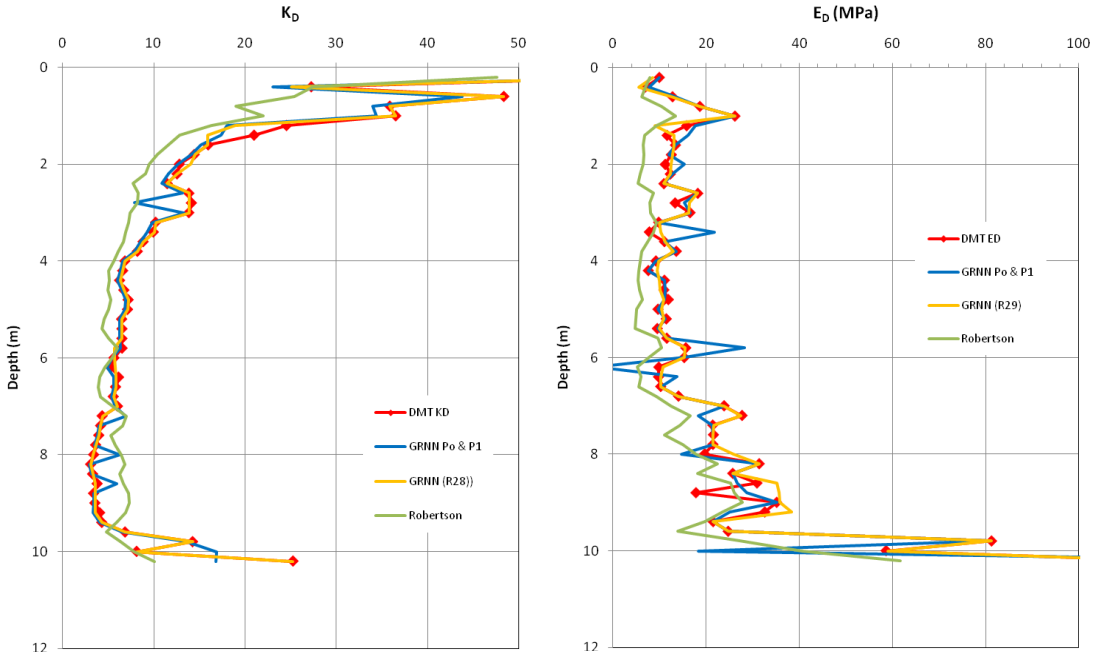

Figure 68: GRNN derived K_D and E_D values compared to DMT values and Robertson (2009b) correlations for Flat Bush

The GRNN networks Run 28 and Run 29 provide good correlation to the DMT K_D and E_D values respectively in Figure 68. The blue lines, which have been calculated from the GRNN derived p_0 and p_1 values, compare well with the DMT values in both the K_D and E_D plots, except for

occasional erratic spikes and one negative number of E_D. The Robertson correlations tend to follow the same general trends as the DMT, but is offset somewhat.

5.2.3.4 Matakana

Graphs of p_0, p_1 and I_D for the data at the Matakana site are presented in Figure 69 along with the various correlations by GRNN and Robertson (2009b). Those for K_D and E_D are given in Figure 70.

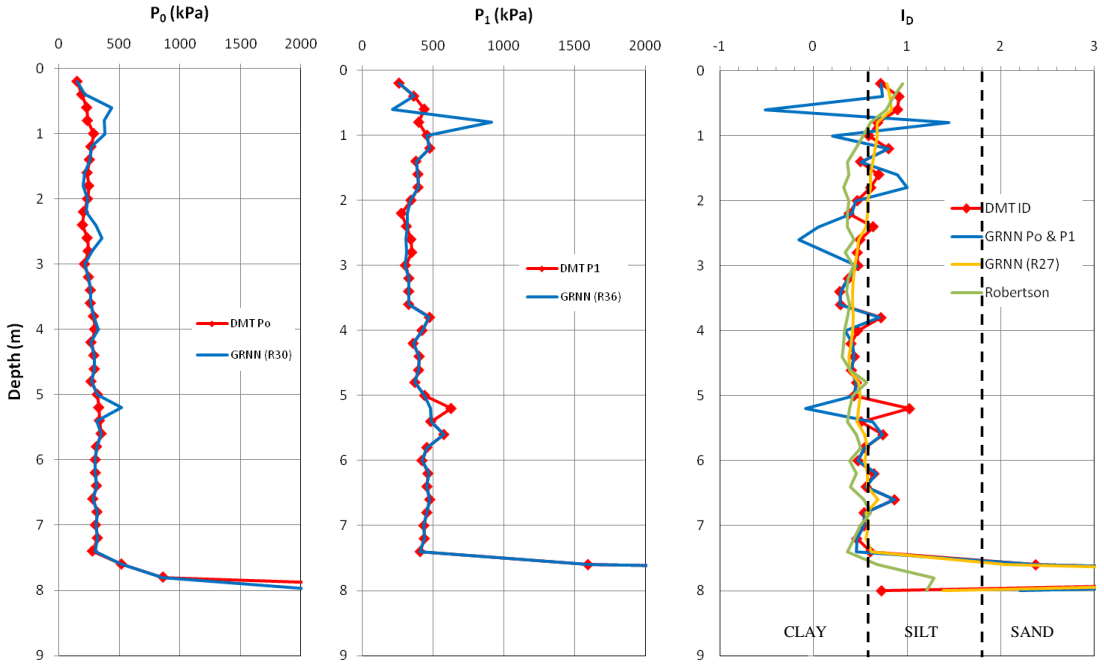

Figure 69: GRNN derived p_0, p_1 and I_D values compared to DMT values and Robertson (2009b) correlations for Matakana

The p_0 and p_1 derived from the GRNN correlations (R30 and R36) show good comparison with the measured values, except for some minor spikes that are added or missed. The I_D values calculated from the GRNN derived p_0 and p_1 values again follow the DMT plot except for occasional erratic spikes that, in some cases, oppose the spike direction of the DMT values and, in some places, are negative numbers. The GRNN (R27) correlation follows the DMT curve well but misses out spikes, creating a kind of 'average' curve, which is quite similar to the Robertson (2009b) correlation. The Robertson correlation falls short of identifying the sand layer shown by the DMT at the bottom of the holes, but the other GRNN based correlations do pick this up following the DMT curve exactly.

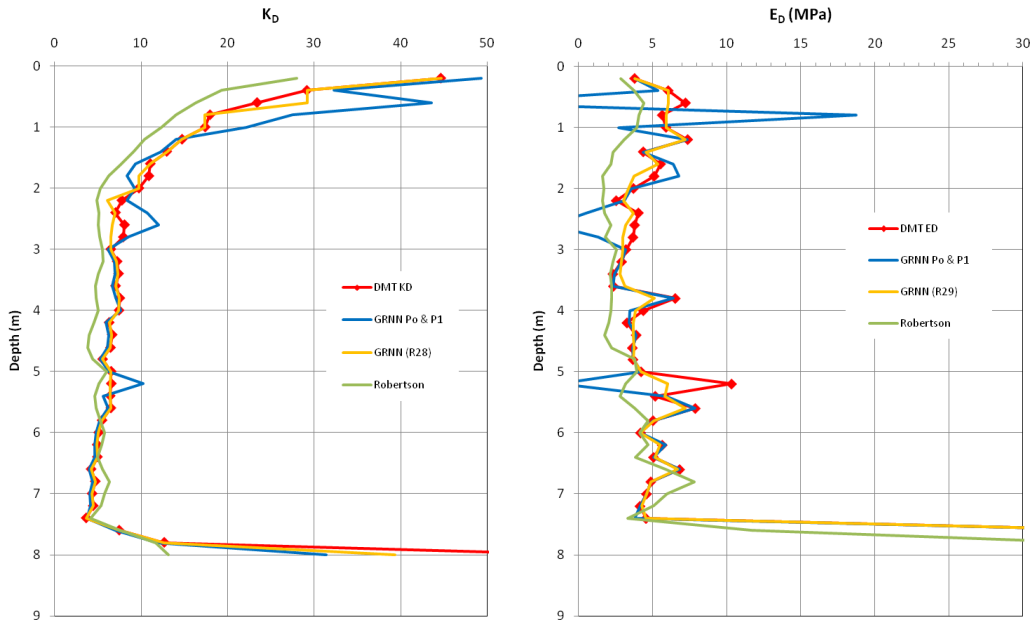

Figure 70: GRNN derived K_D and E_D values compared to DMT values and Robertson (2009b) correlations for Matakana

The GRNN derived correlations (R28 and R29) in Figure 70 show very good agreement with the DMT curves with some minor deviation, although some of the peaks in comparison to the DMT K_D curve are not fully expressed. The K_D and E_D values calculated from the GRNN derived p_0 and p_1 values once again show erratic peaks, particularly in the E_D plot, and some negative E_D values are shown.

The Robertson (2009b) correlations for K_D and E_D show general agreement in trend, but their curves generally fall short of the other plots.

5.2.3.5 Herald Island

Graphs of p_0, p_1 and I_D for the data at the Herald Island site are presented in Figure 71 along with the various correlations by GRNN and Robertson (2009b). Those for K_D and E_D are given in Figure 72.

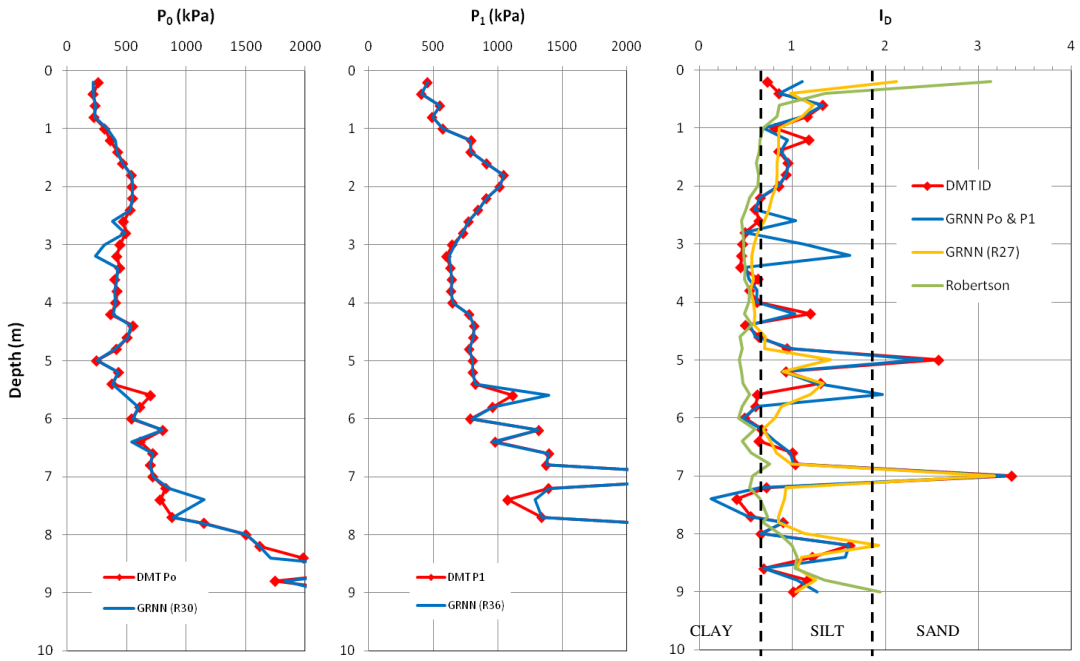

Figure 71: GRNN derived p_0, p_1 and I_D values compared to DMT values and Robertson (2009b) correlations for Herald Island

The p_0 and p_1 values calculated from the GRNN Run 30 and 36 again should good comparison with the measured DMT values with slight deviations and occasional missed and added spikes. The I_D values calculated from these derived p_0 and p_1 values compare well with the DMT I_D plot but there are a few additional spikes provided by the predicted curve. The GRNN (27) curve is less favourable although it fits reasonably well. The Robertson (2009b) derived I_D does not compare particularly well.

The GRNN (R28) correlation for K_D shown on Figure 72 compares very well with the DMT K_D values. The K_D values calculated from the GRNN derived p_0 and p_1 values fall slightly short of the DMT curve, although the same general trend is followed. On the E_D plot, both the GRNN (R29) correlation and the calculated values from GRNN p_0 and p_1 show good agreement with the DMT E_D values, although those calculated from GRNN derived p_0 and p_1 show occasional spikes that deviate significantly from the actual values.

The Robertson (2009b) correlations for both K_D and E_D do not match particularly well here.

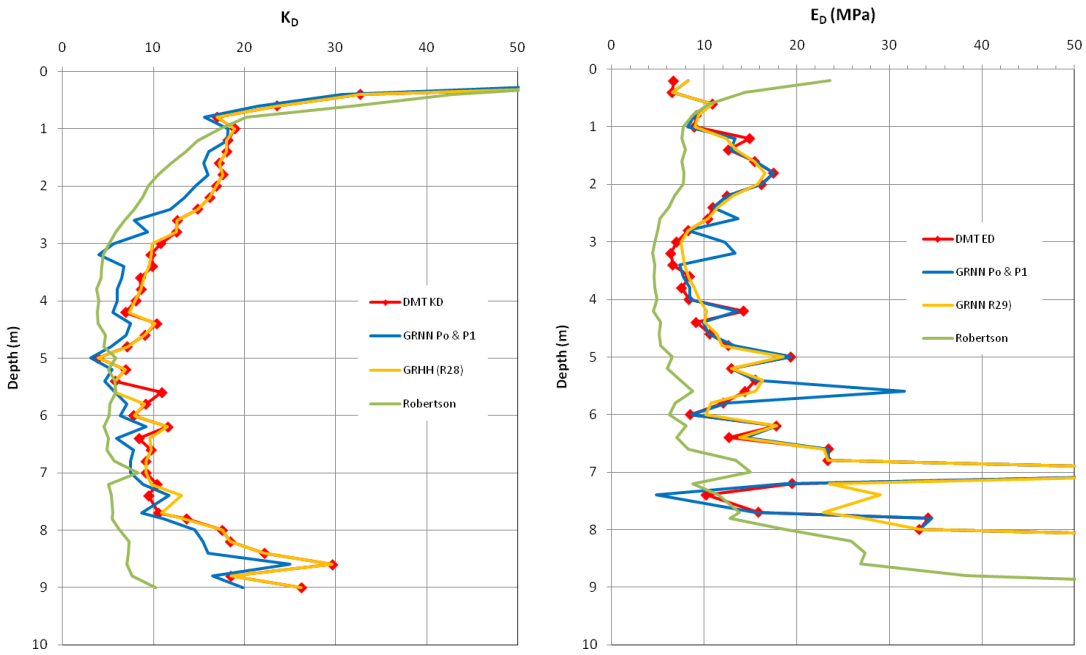

Figure 72: GRNN derived K_D and E_D values compared to DMT values and Robertson (2009b) correlations for Herald Island

5.2.3.6 Hamilton (8a)

Graphs of p_0, p_1 and I_D for the data at the Hamilton 8a site are presented in Figure 73 along with the various correlations by GRNN and Robertson (2009b). Those for K_D and E_D are given in Figure 74.

The GRNN (R30 and R36) correlations for p_0 and p_1 fit the measured DMT values remarkably well considering the spiky variability of the curve. The translation of the GRNN derived p_0 and p_1 values into I_D also compares well with the DMT I_D values, although there is the odd erratic spike. The GRNN (R27) correlation provides a reasonable fit to the DMT values, but tends to miss some peaks creating a smoothed 'averaging' plot through the DMT I_D curve. The Robertson (2009b) I_D curve tends to follow the DMT curve quite well, except tends to overestimate the I_D values in the sand and is off at the bottom of the sounding. All correlations, however, work reasonably well in identifying the soil type and boundaries between the soil types.

The GRNN derived correlations for K_D (on Figure 74) both compare well with the DMT curve, particularly the GRNN (R28) curve, which follows the DMT curve almost exactly. The calculated

K_D from the GRNN derived p_0 and p_1 values also correlates very well, except for occasional spikes. The Robertson (2009b) correlation for K_D also plots comparatively well.

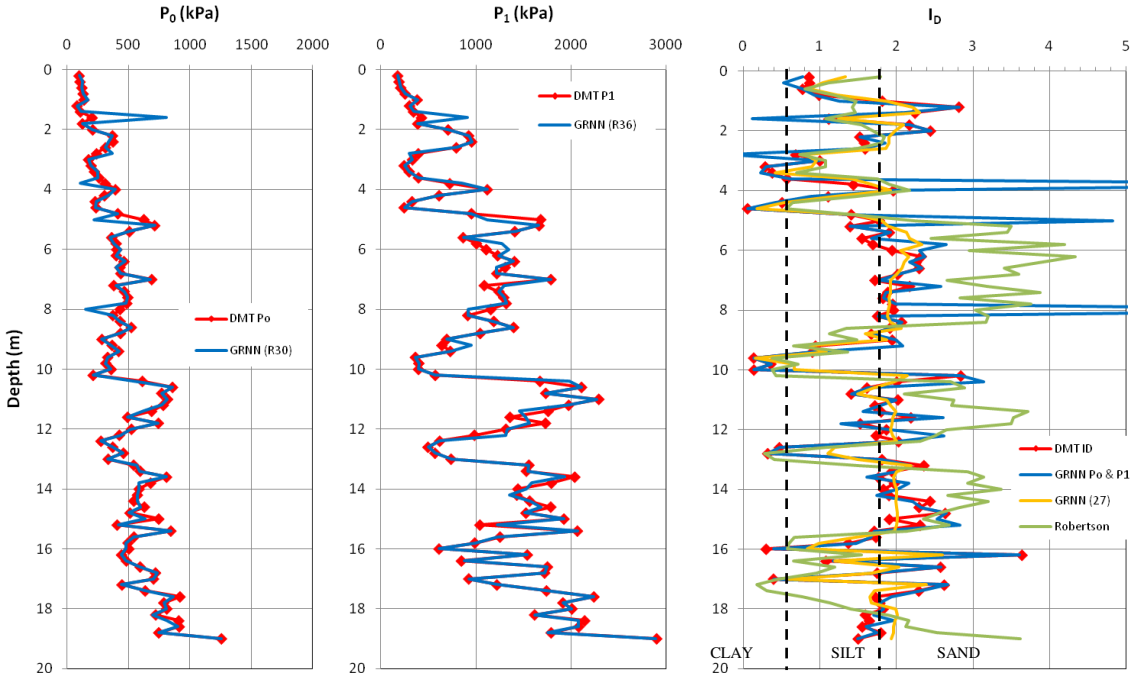

Figure 73: GRNN derived p_0, p_1 and I_D values compared to DMT values and Robertson (2009b) correlations for Hamilton (8a)

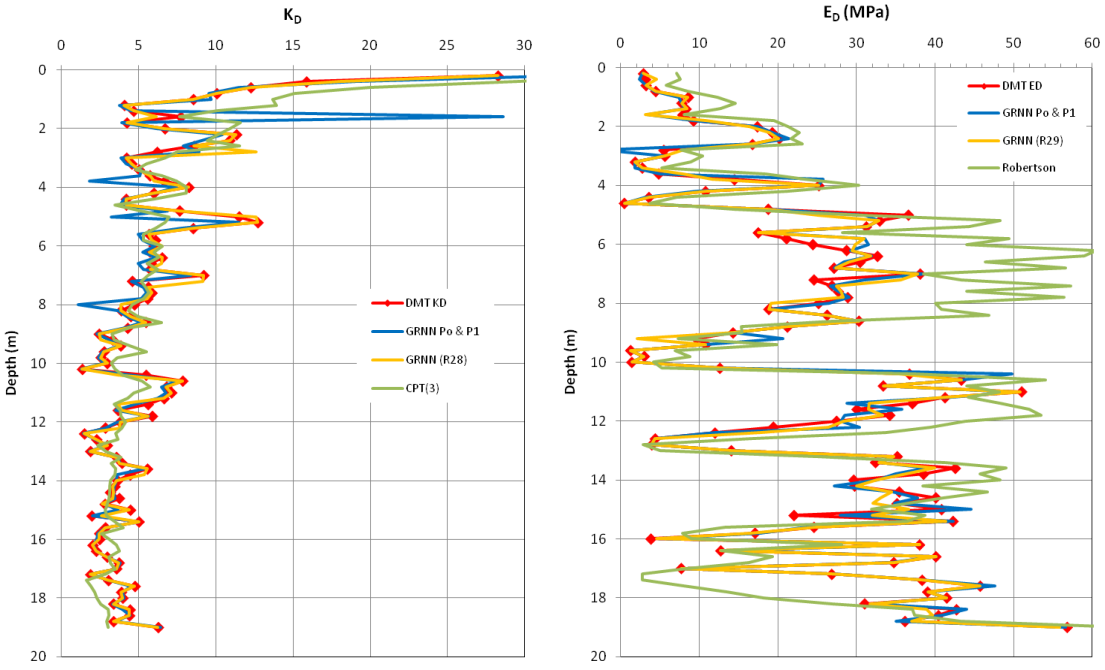

Figure 74: GRNN derived K_D and E_D values compared to DMT values and Robertson (2009b) correlations for Hamilton (8a)

The GRNN derived correlations for E_D also compare very well with the actual DMT data. The Robertson correlation, though significantly overestimates E_D values in the central part of the sounding.

5.2.3.7 Ngaruawahia (9a)

Graphs of p_0, p_1 and I_D for the data at the Ngaruawahia 9a site are presented in Figure 75 along with the various correlations by GRNN and Robertson (2009b). Those for K_D and E_D are given in Figure 76.

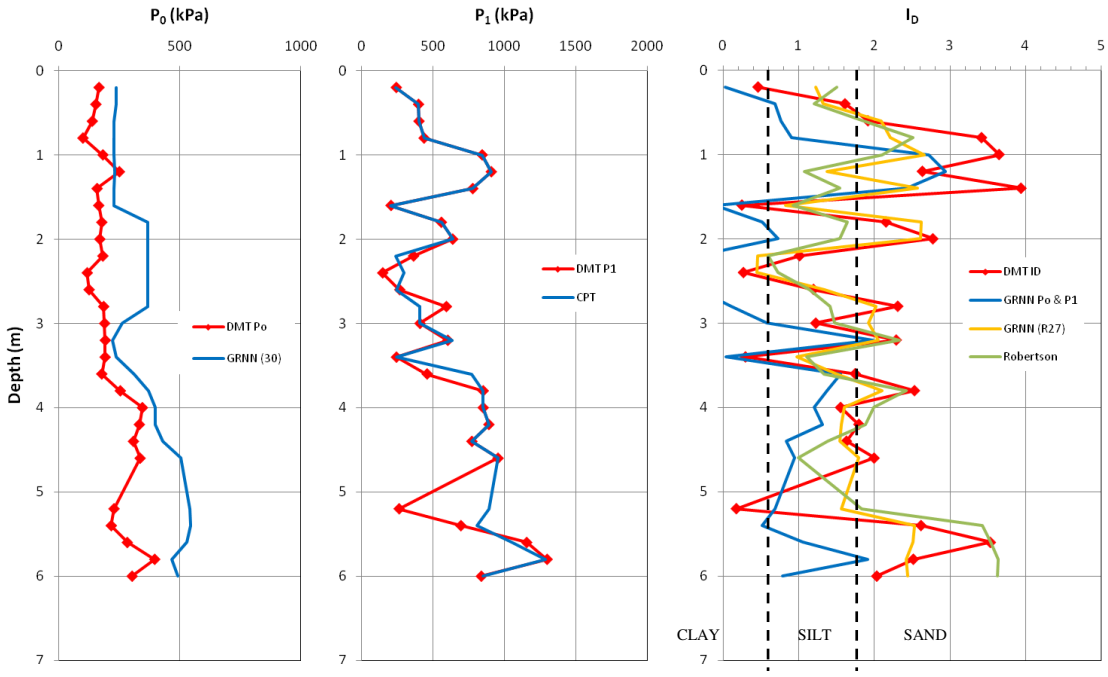

Figure 75: GRNN derived p_0, p_1 and I_D values compared to DMT values and Robertson (2009b) correlations for Ngaruawahia (9a)

The GRNN (R30) correlation for p_0 does not correlate very well at all with the measured DMT values at this site. The GRNN (R36) correlation for p_1, however, seems to fit the actual data quite well, except at around 5m depth, where a spike in the DMT data is missed. On the I_D plot, the values calculated from the GRNN derived p_0 and p_1 values does not compare well with the DMT data and some negative values are obtained. This is most probably because of the error in the derived p_0 values. The GRNN (R27) correlation compares reasonably well in places, but misses or

underestimates the DMT peaks in other places. The Robertson (2009b) correlation with I_D is somewhat similar to the GRNN (R27) curve.

The GRNN (R28) curve on the K_D plot on Figure 76 shows a good comparison with the DMT values, except at around 5m depth where its peaks away from the DMT plot. The Robertson correlation also matches reasonably well here. The K_D calculated from the GRNN derived p_0 and p_1 values, however, did not compare well (due to the error in the p_0 estimation).

On the E_D plot, the GRNN (R29) correlation matches fairly well, except again around 5m depth, where it fails to match a peak in the DMT plot. The calculated E_D from GRNN derived p_0 and p_1 values again does not compare well due to error in the initial p_0 estimation. The Robertson (2009b) correlation also does not fit well with the DMT data here.

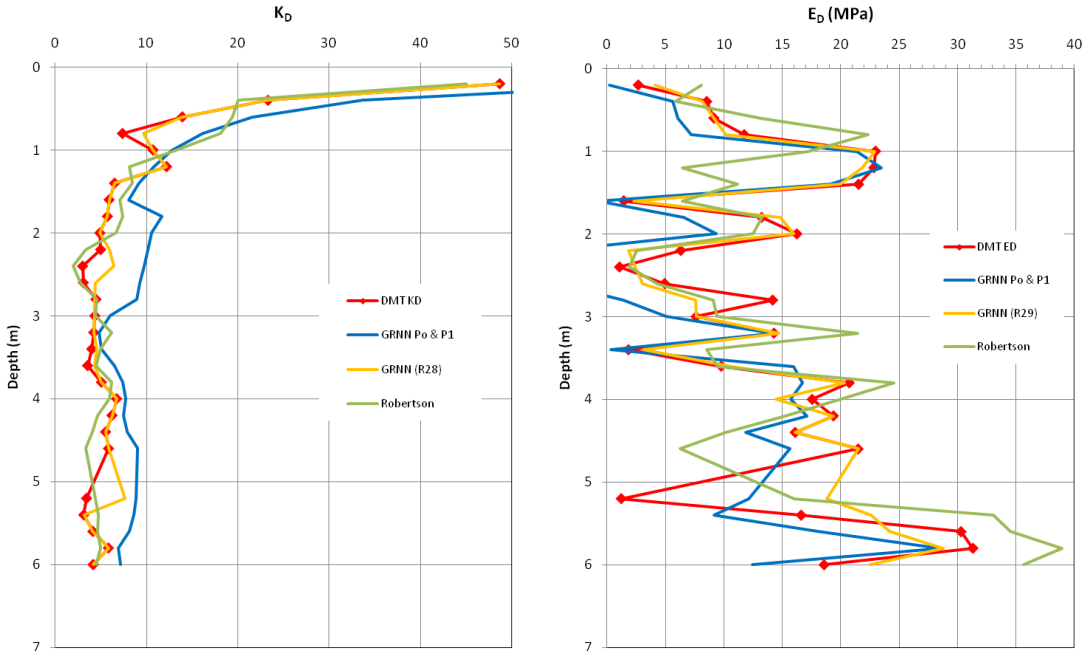

Figure 76: GRNN derived K_D and E_D values compared to DMT values and Robertson (2009b) correlations for Ngaruawahia (9a)

5.2.4 General Comments on GRNN and Robertson Correlations

In general the GRNN correlations compared very well to the actual DMT data. However, the network has been trained to this data, which is a relatively small data pool of the six selected sites. Further analysis with additional reliable data from other sites would need to be undertaken in order to validate these network correlations over a wider range of data. The reliability of the data in this study (outside the selected six sites) is questionable and has inhibited validation of the trained networks in this study. However the apparent success of the GRNN correlations (at least over the six selected sites) suggests that this may provide a good mechanism for developing more robust correlations with further research.

The GRNN correlations with DMT p_0 and p_1, were generally very good with the derived p_0 and p_1 plots matching almost exactly the measured DMT profile on the depth plots. The exception was at the Ngaruawahia site, where the derived p_0 values varied significantly from the measured DMT values. Other than that site, the correlations appear to be very good, with only occasional minor discrepancies, mostly the addition or omission of minor peaks in the graphs. This is encouraging, however, when the DMT test is carried out in the field, the p_1 value is always larger than the p_0 value, but in soft clays, these values can be very close together. The DMT index values of I_D and E_D are directly proportional to the difference between the p_0 and p_1 values ($p_1 - p_0$) and so are sensitive to these values, particularly when they are close together (i.e. when $p_1 - p_0$ is small) as in the case of soft clays. Small errors in the p_0 and p_1 can lead to larger errors, or even negative numbers, in the I_D and E_D values. This was observed in many of the results, where occasional negative values and erratic peaks in the I_D and E_D plots occurred.

In the interpretation of the DMT results, the p_0 and p_1 values are first converted to the index values of I_D, K_D and E_D and then those index values are used in the various correlations to soil parameters. The p_0 and p_1 values are not used directly in any of the correlations, so correlating CPT parameters to the raw DMT data of p_0 and p_1 only introduces another step in the interpretation process, which can introduce significant error even with apparent good correlation. Thus correlations to p_0 and p_1 should be avoided and correlations should instead concentrate directly on the index values (I_D, K_D and E_D). Consequently, the I_D, K_D and E_D values calculated from the GRNN derived p_0 and p_1 in this study are not discussed further.

The DMT material index, I_D, was found to be the most difficult of the three index parameters to correlate to. The GRNN analysis was the least successful with this parameter. However, the resulting correlation was reasonable when observed on the I_D plots, comparing relatively well with the actual DMT values, although the predicted values tended to 'smooth out' the DMT profile by missing occasional peaks. The Robertson (2009b) correlation to I_D shows variable success, but generally correlates poorly. It is somewhat surprising that this parameter is so difficult to correlate to, after all, both the material indices (CPT I_c and DMT I_D) are able to identify similar soil types. This has been shown in the observations of the data in this study, where the I_c and I_D values when plotted side-by-side generally confirmed the same soil types and boundary elevations. It would be expected, therefore, that a simple relationship between I_c and I_D would exist, as postulated by Robertson (2009b). This, however, does not seem to be the case on the evidence of the data in this study. Even the plot of I_D vs. I_c presented by Robertson (2009b) (Figure 50) shows significant scatter, particularly with consideration to the logarithmic scale of I_D axis. In this respect, the numeric values of the predicted I_D can vary significantly from actual DMT values.

I_D, K_D and E_D are all derived from only two parameters (p_0 and p_1). Thus any one of these index values can be derived from the manipulation of the other two. Robertson (2009b) uses this manipulation to derive a relationship between K_D, Q_t and I_D from the proposed relationship between E_D and Q_t ($E_D/\sigma'_{vo} = 5\ Q_t$), thus arriving at $K_D = 0.144\ Q_t/I_D$. The simple relationship between I_c and I_D is then inserted to arrive at $K_D = 0.144\ Q_t/[10^{(1.67-0.67Ic)}]$, which is suggested as a possible correlation over a wider range of soil types. Thus the simple relationship between I_c and I_D ($I_D = 10^{(1.67-0.67Ic)}$) becomes the link allowing a derivation of K_D from E_D. For this to be satisfactory both correlations for I_D and E_D need to be reliable, otherwise the inherent error will be transferred. It would seem that the I_c to I_D relationship is not reliable and so this approach may not be appropriate.

The I_D value is not used directly in any of the DMT correlations but is used as a guide for determining which correlations are applicable as some apply only to sands, some only to clays and some have varying equations depending on the range in which the I_D value sits. The actual numeric value of I_D is not as important as the range into which it falls, i.e. whether or not is it above or below a certain boundary value. Slight inaccuracy in determining these boundary values is unlikely to greatly affect the interpretations subsequently made in the DMT correlations. In this respect, the GRNN correlation to I_D is considered adequate. The Robertson (2009b) simplistic correlation in many cases provides a reasonable estimate of I_D for these purposes, but is not entirely satisfactory. In any case, it is considered inappropriate to back correlate to obtain K_D or E_D values through the

application of the Robertson (2009b) simplistic I_c to I_D relationship. Rather it is best to correlate directly to K_D and E_D without relying on the link with I_D.

The direct GRNN correlations for K_D and E_D were found to match the actual DMT data very well. These correlations were significantly better than the Robertson (2009b) correlations; however, in many instances the Robertson correlations provided a reasonable estimate of the actual DMT values. The Robertson (2009b) correlations for these parameters are primarily based on the relationship $E_D/\sigma'_{vo} = 5\ Q_t$, and the K_D is simply derived from this E_D using I_D from I_c to relationship, as discussed above. Thus the estimated K_D values are related to the estimated E_D values and this is apparent in some of the plots where the K_D plots assume a similar lag behind or ahead of the actual DMT data.

Figure 77 gives comparative plots of predicted values against actual DMT values for I_D, K_D and E_D for the GRNN and Robertson (2009b) correlations with their respective correlation coefficients. From these plots, it can be seen that the GRNN correlations compare very well with correlation coefficients of 0.9251, 0.9862 and 0.6140 for the I_D, K_D and E_D correlations respectively. The spread in the Robertson's correlations for I_D and E_D are quite wide and this is reflected in the correlation coefficients of 0.5518 and 0.6140, respectively. The Robertson correlation for K_D, however, shows slighter better results with a correlation coefficient, r=0.8241. The strength of the K_D relationship is probably because it strongly reflects the OCR of the soils, which is generally estimated well by both the CPT and DMT.

One of the problems with the artificial neural network (ANN) approach is that the actual equations that describe the correlations are not known. These are likely to be complex mathematical relationships trained to the numeric values of the input and output values of the particular data set without regard to the theoretical correctness of such relationships. In this study, the networks have trained on a relatively small selected database, however, that database does cover a range of different sites, soils and geologies and so is not overly specific. Once more data is available to provide a larger (and reliable) database, the GRNN correlations can be further assessed, validated and refined. Further research on a larger database would also allow the opportunity to develop more theoretically sound relationships in parallel with the ANN approach.

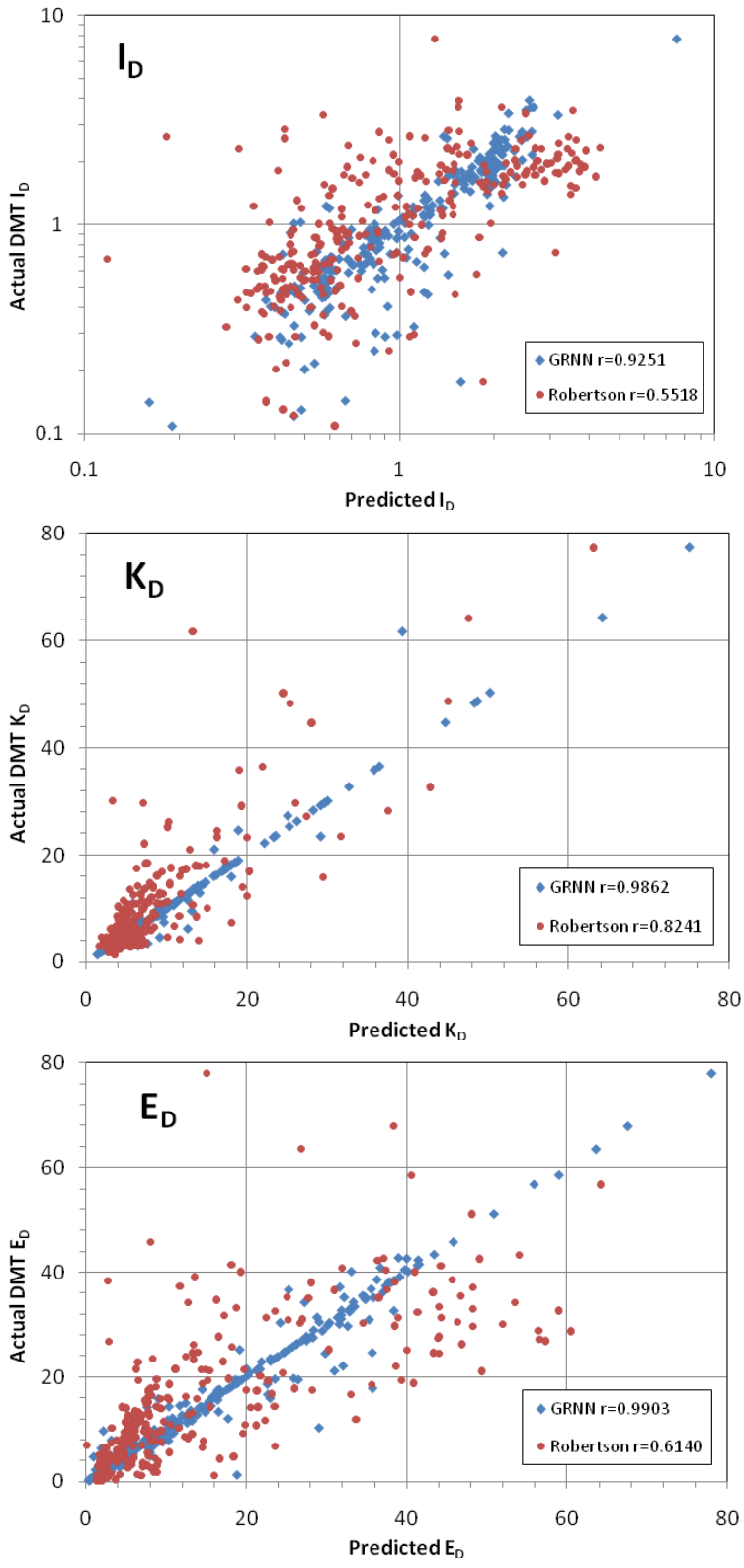

Figure 77: Comparative plots of GRNN and Robertson (2009b) correlations with I_D, K_D and E_D

5.3 SUGGESTED ADJUSTMENTS TO THE ROBERTSON CORRELATIONS

5.3.1 Material Index, I_D

This parameter has proven to be difficult to correlate to. As far as the standard Marchetti (1980) correlations to soil parameters are concerned, the I_D factor serves only to provide a guide as to what formula to use in the interpretation rather than its numeric value being used in the formula itself. As such the important function of correlating to I_D from the CPT results is to provide an estimate of I_D that falls within the range that is suitable for that soil type. In this respect, the current simple correlation (Eqn 87) from I_c proposed by Robertson (2009b) may be adequate.

$$I_D = 10^{(1.67-0.67Ic)} \qquad (87)$$

This correlation, however, is based on a simple straight line relationship on the I_c-logI_D plot running from I_c = 1, I_D = 10 to I_c = 4, I_D =0.1, which are considered to be the full practical range of the indices values, as shown on Figure 78. This seems reasonable, but the line misses the key boundary crossing points between sand, silt and clay, which are I_c = 2.05, I_D = 1.8 and I_c = 2.95, I_D = 0.6.

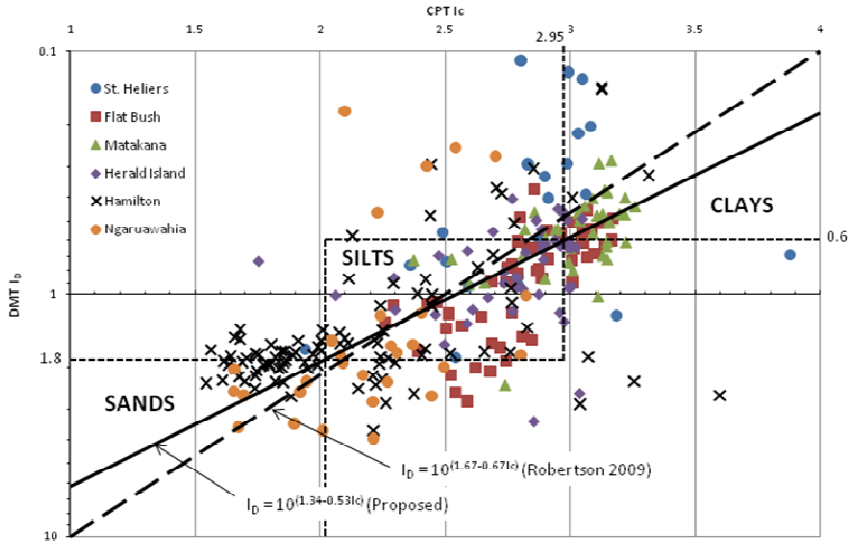

Figure 78: DMT I_D vs CPT Ic for the Selected Data Set

It is therefore proposed to skew the line so that these intercepts are picked up in the line representing the relationship. In this way there is possibly better chance of correctly identifying the appropriate

soil type when close to the sand/silt and silt/clay boundaries. In doing so, the line is also skewed slightly more in favour of the data (for this study at least) as can be seen in Figure 78, which shows the data from the selected data set.

The proposed line creates a slightly different equation:

$$I_D = 10^{(1.34-0.53Ic)} \quad (88)$$

This is proposed relationship is plotted below on the I_D graph for the Flat Bush site along with the Robertson (2009b) correlation.

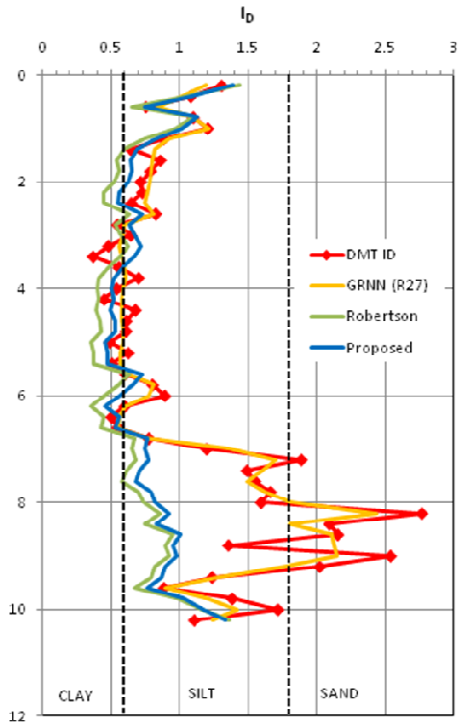

Figure 79: Proposed ID Correlation

Although this proposed equation appears to show very little difference to the previous Robertson (2009b) correlation, on closer inspection of the clay/silt boundary (I_D = 0.6) in Figure 79 it can be seen that the proposed correlation identifies the soil types relative to this boundary slightly better. The suggested new correlation also plots a little closer to the GRNN correlation, although it still correlates poorly at the lower part of the sounding, where the DMT has identified sand, but the CPT has not.

5.3.2 Dilatometer Modulus, E_D

As discussed above, the Robertson (2009b) correlations are based primarily on the following relationship between E_D and Q_t:

$$E_D/\sigma'_{vo} = \alpha\, Q_t, \qquad (89)$$

$$,where\ 2 < \alpha < 10$$

Robertson (2009b) has used $\alpha = 5$, which was considered a reasonable average. However, the α factor can vary from 2 to 10, which represents a huge variation in the possible E_D correlations. Figure 80 shows a plot of E_D/σ'_{vo} for the data from the current study. From this it can be seen that there is much spread in this data but most of the data plots above the $\alpha = 5$ line. A reasonable estimate from this data would be approximately $\alpha = 8$.

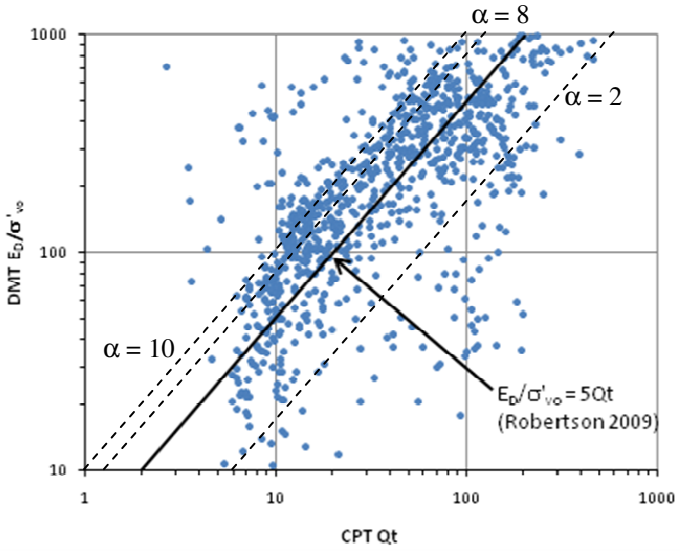

Figure 80: Plot of E_D/σ'_{vo} vs. CPT Q_t

Eqn 89 then becomes:

$$E_D/\sigma'_{vo} = 8\, Q_t, \qquad (90)$$

Using the Flat Bush site as an example, Eqn 89 has been applied to the data and the result is shown on the E_D plot in Figure 81 along with the originally proposed $E_D / \sigma'_{vo} = 5\ Q_t$ Robertson correlation and the GRNN correlation.

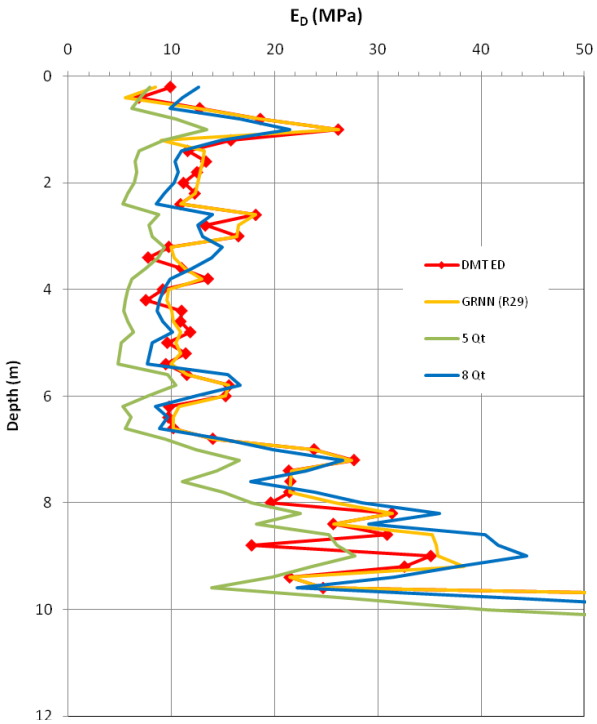

Figure 81: Adjusted Robertson Correlation for E_D

The adjusted correlation to $\alpha = 8$ provides a better match with the DMT data and also plots quite closely to the GRNN correlation. So it would appear that a relationship in the form of Eqn 89 provides reasonable correlation. However, the value of α needs to be carefully considered as the range of potential variation can create significant error in the estimation of E_D. Robertson (2009b) suggests that α is likely to vary with age and stress history. It is likely to vary with respect to soil type, relative density or plasticity and it may be related to the rigidity index of the soil. Further research on additional reliable data will be required to investigate the nature of this correlation.

5.3.3 Horizontal Stress Index, K_D

The Robertson (2009b) correlation for K_D uses the E_D correlation, $E_D = \alpha Q_t \sigma'_{vo}$ (Eqn 89) with $\alpha = 5$ and then converts to K_D with use of the I_D correlated from I_c to give:

$$K_D = 0.144 Q_t / [10^{(1.67-0.67Ic)}] \quad (91)$$

The denominator term being the correlation, $I_D = 10^{(1.67-0.67Ic)}$ (Eqn 87). It is suggested that Eqn 91 be adjusted for the proposed new I_D correlation given in Eqn 88 and that the α term remain variable for user selection. Thus:

$$K_D = 0.0288\ \alpha\ Q_t / [10^{(1.34-0.53Ic)}] \quad (92)$$

,where $2 < \alpha < 10$, on average $\alpha = 5$

By application of Eqn 92 (using α =8), the resulting K_D plot (for the Flat Bush site) is shown on Figure 82 in black.

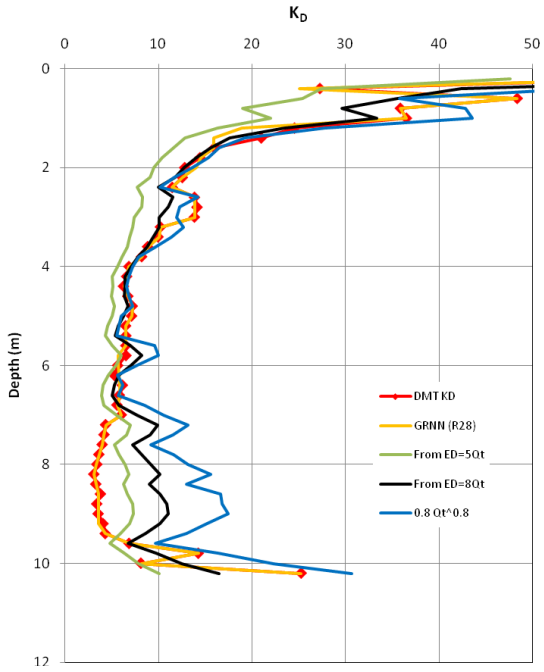

Figure 82: Adjusted Correlations for K_D

An alternative equation for K_D was also presented by Robertson (2009b) as:

$$K_D = 0.8\ (Qt)^{0.8} \quad (93)$$

This relationship has also been plotted on Figure 82 (blue line) for comparison purposes. The original Robertson (2009b) curve ($\alpha = 5$) is shown in green. Dismissing the lower part of the curve, the plots represented by Eqn 92 (with $\alpha = 8$) and Eqn 93 show good agreement with the measured DMT values. They also match well to the GRNN correlation (except for the lower end of the sounding).

5.3.4 Summary

The following equations are suggested as tentative refinements of the Robertson (2009b) correlations:

$$I_D = 10^{(1.34-0.53Ic)} \quad (94)$$

$$K_D = 0.0288\ \alpha\ Q_t/[10^{(1.34-0.53Ic)}] \quad (95)$$

,where $2 < \alpha < 10$*, on average* $\alpha = 5$

or,

$$K_D = 0.8\ (Q_t)^{0.8} \quad (96)$$

$$E_D/\sigma'_{vo} = \alpha\ Q_t, \quad (97)$$

,where $2 < \alpha < 10$*, on average* $\alpha = 5$

These are not considered to provide exact solutions and further research is required to confirm or develop these correlations further. In general, the GRNN analysis provided better correlations than these, which suggests that further research using GRNN is warranted.

6. CHAPTER 6: CONCLUSION

6.1 CONCLUSIONS

The estimated soil parameters of c_u, M, G_0, OCR and ϕ' derived from the DMT test using the standard Marchetti (1980) and TC2001 correlations generally compared well with those derived from the CPT using commonly used correlations (Robertson 2009a).

No obvious relationship was observed between the DMT lift off pressure, p_0 and the porewater pressure developed behind the cone, u_2 as has been found by other researchers (e.g. Mayne and Bachus 1989). This may be due to the layered silty soils in this study, which may not have behaved in a fully undrained manner during testing.

Some of the data pairs did not compare well at all. These seem to be sites where the CPT test was done by others previous to the DMT test and the exact location of the CPT test was not known and the actual distance between the two tests may have been large enough to result in natural variation in the ground between the test locations. Consequently the full data set was reduced to a smaller selected set of 6 pairs of more reliable data for analysis. In general, the test sites in this study comprised mostly variable layered soils which make the development of correlations more difficult.

The artificial neural network method of general regression neural network (GRNN) produced generally good correlations between the CPT data and the DMT data using the selected data set (of 6 sites). The GRNN correlations to the raw DMT data, p_0 and p_1, were statistically the strongest (r= 0.9906 and 0.9937). However, the correlation to the raw data was found to be erroneous because minor errors in the p_0 and p_1 values can result in large errors and/or negative numbers in the subsequent conversion to the index parameter, I_D, K_D and E_D. Consequently, it is recommended that correlations be made directly to the index parameters to avoid the possibility of this compounded error.

The material index I_D was the most difficult to correlate to. However, the GRNN correlation provided a reasonable correlation (r = 0.9521) which compared well when plotted against the actual DMT I_D values, although some peaks in the plot were smoothed out by the correlation.

The GRNN correlations for K_D and E_D were found to provide very good comparison to actual values with correlation coefficients of r = 0.9862 and r = 0.9903, respectively.

The Robertson (2009b) correlations generally performed relatively poorly, particularly for I_D (r = 0.518). The Robertson (2009) correlation for K_D was the strongest with r = 0.8241, but with E_D the correlation coefficient using Robertson's correlation was poor, r = 0.6140. The relatively stronger K_D correlation is probably due to the DMT K_D's link with OCR, which is estimated well by both the CPT and DMT.

The Robertson (2009b) correlations, however, may be improved slightly by use of the following proposed equations, which include a slight adjustment to the Robertson correlations:

$$I_D = 10^{(1.34-0.53Ic)} \quad (94)$$

$$K_D = 0.0288\ \alpha\ Q_t/[10^{(1.34-0.53Ic)}] \quad (95)$$

,where 2 < α < 10, on average α = 5

or,

$$K_D = 0.8\ (Q_t)^{0.8} \quad (96)$$

$$E_D/\sigma'_{vo} = \alpha\ Q_t, \quad (97)$$

,where 2 < α < 10, on average α = 5

At this stage, these equations have not shown particularly good correlations, and so are not recommended for general use in practice. However they may serve as a basis for further research. Successful correlations using the above equations (Eqns 94, 95 and 97) are dependant on the appropriate choice of the factor, α. Further research is required to determine suitable guidelines for the choice of this parameter.

6.2 SUGGESTIONS FOR FUTURE RESEARCH

This study, particularly with the relative success of the GRNN analyses, has highlighted the possibility of determining a reliable correlation between CPT and DMT. Additional reliable data, preferably from sites with more homogeneous soil, will need to be obtained to allow further research in this area. This additional data could be used to validate (and improve) the GRNN correlations already developed from this study. In any case GRNN analysis is recommended for future research. Future research could also be undertaken to further refine the Robertson (2009b) correlations or develop new correlations in conjunction with the GRNN analysis. The effect of the correlation on differing geological units should also be investigated. Further research on the comparative abilities of the two tests in estimating common soil parameters would also be of interest.

APPENDIX A: TABLE 5: SUMMARY OF STUDIES ON DMT CORRELATIONS

Table 5: Summary of Some Comparative Studies on DMT Correlations (after Mayne & Martin 1998)

PARAMETER	*RELATIONSHIP*	*NOTES*	*REFERENCE*
Soil Type, Classification, and Consistency	Soil type = $f(I_D)$ where I_D = material index	Clay: $I_D < 0.6$ Silt: $0.6 < I_D < 1.8$ Sand: $I_D > 1.8$	Marchetti (1980)
	Soil type & consistency = $f(E_D, I_D)$	For clays, silts, and sands.	Marchetti & Crapps (1981)
	Soil type & consistency = $f(E_D, I_D)$	Modified for clays, silts, and sands.	Schmertmann (1986a)
	Field study	Data from three OC clay sites in U.K.	Powell & Uglow (1986)
	Field study	Evaluation of Marchetti & Crapps classification chart	Lacasse & Lunne (1988)
	Soil type = $f(I_D, p_2)$	Based on field data from 7 North American sites.	Lutenegger (1988)
	Field study	Data summary for 8 clays and 1 sand from U.K.	Powell & Uglow (1988a)
	Liquidity index, LI: $LI = 1.17 - 0.02\ E_D$	Correlation for fat clay at Poleg site, Israel	Blechman & Feferbaum (1997)
Total Unit Weight (γ_T)	$\gamma_T = f(I_D, E_D)$	General chart for clays, silts, and sands	Marchetti & Crapps (1981)
	$\rho \approx 1.12(E_D/\sigma_a)^{+0.1}(I_D)^{-0.05}$ where $\rho = (\gamma_T/\gamma_w)$ and σ_a = atmospheric pressure	Approximate diagram for clays, silts, and sands.	Schmertmann (1986a)
	Field and lab Study	Reported data from 3 OC clay sites in U.K.	Powell & Uglow (1986)
	Field and lab Study	DMT underpredicted γ_T in soft Norwegian clays	Lacasse & Lunne (1988)
	Field and lab Study	DMT overpredicted γ_T in heavily OC clays in U.K.	Powell & Uglow (1988b)
	Field and lab Study	DMT underpredicted γ_T in 3 soft-firm Korean clays	Kim (1991)
Stress History: Effective Vertical Preconsolidation Stress (σ_p' or σ_{vmax}')	$\sigma_p'=(p_0-u_0)/\delta$	$1<\delta<3$. Based on 23 NC to OC clays	Mayne (1987)
	$\sigma_p'=(p_0-u_0)/\delta$	Review of correlations for clays in SOA Report	Lutenegger (1988)
	$\sigma_p'=(p_0-u_0)/\delta$	Data from 22 intact and 7 fissured clays	Mayne & Bachus (1989)
	$\sigma_p'=0.509(p_0-u_0)$	Average statistical trend from 24 intact clays	Kulhawy & Mayne (1990)
	$\sigma_p'=0.61(p_0-u_0)$	Statistical analysis of data on intact clays	Pool (1994)
	$\sigma_p'=1.1(p_0-u_0)/\delta$	Analytical model: $\delta=4/3(\phi'/100)\ln(I_r)$ where I_r = rigidity index.	Mayne (1995)
Stress History: Overconsolidation Ratio $OCR = (\sigma_p'/\sigma_{vo}')$	$OCR=(0.5K_D)^{1.56}$	Cohesive soils, $I_D<1.2$	Marchetti (1979, 1980)
	$OCR=(0.67K_D)^{1.91}$	Cohesionless soils, $I_D>1.2$	Marchetti (1980)
	$OCR = (0.372K_D)^{1.40}$	Based on 14 tests on highly OC cohesive Florida soils	Davidson & Boghrat (1983)

Table 5, cont.

PARAMETER	*RELATIONSHIP*	*NOTES*	*REFERENCE*
	Field study $OCR = f(K_D)$	Comparison with oedometer tests on three UK clay sites	Powell & Uglow (1986)
	$OCR=f(K_D)$	Based on 23 soft to firm to hard clays.	Mayne (1987)
	$OCR=0.24(K_D)^{1.32}$	Modification for young clays from U.K.	Powell & Uglow (1988a,b)
	$OCR=0.225(K_D)^{m}$	For $I_D<1.2$ and $OCR>1.25$: exponent $1.35 < m < 1.67$.	Lacasse & Lunne (1988)
	Field & lab study where $OCR_{DMT} = g \cdot OCR_{oedometer}$	OC cemented clays in Italy: Taranto: g = 0.85 Augusta g = 1.32	Jamiolkowski et al. (1988)
	Field and lab Study	DMT overpredicts in crust of soft clays in Nebraska	Saye & Lutenegger (1988)
	Evaluating foundation settlements in sands	Separates modulus into OC and NC components	Leonards & Frost (1988)
	$OCR = 2 \cdot [\frac{2 \cdot K_D}{M_c \cdot \ln(I_R)}]^{1/\Lambda}$	Analytical method for clays, where frictional parameter $M_c \approx \phi'/25^\circ$, rigidity index $= I_{r\ =\ G/S_u}$, and $\Lambda \approx 0.8$.	Mayne and Bachus (1989)
	$OCR=10^{0.16 \cdot (K_D - 2.5)}$	Calibrated for sensitive and organic Swedish clays	Larsson & Erikson (1989)
	$OCR=(\beta_o K_D)^{1.56}$	Insensitive clays: $\beta_o=0.50$ sensitive clays: $\beta_o=0.35$ fissured clays: $\beta_o=0.75$ clay tills: $\beta_o=0.27$	Kulhawy & Mayne (1990)
	$OCR=(0.5K_D)^{\lambda}$	Singapore marine clay: $\lambda = 0.84$	Chang (1991a)
	Review of data from ten clays in Northern Europe: $OCR = m_o K_D^{1.17}$	Young clays: $m_o = 0.27$ "Middle aged": $m_o = 0.5$ Old clays: $m_o = 2.7$	Lunne et al. (1992)
	Numerical simulation of DMT in Boston Blue Clay	MIT E-3 constitutive soil model & strain path analysis	Whittle & Aubeny (1993)
	Field and lab study	DMT overpredicted OCR in Malaysian alluvial clays	Wong et al. (1993)
	$OCR=1.65(0.5K_D)^{1.13}$	Compared data from alluvial clays in Taiwan	Su et al. (1993)
	$OCR = f(K_o, K_D, \phi', \lambda, e, \nu)$	Parametric numerical strain path method for clays	Finno (1993)
	$K_D = (1-\sin\phi')OCR^{\sin\phi'} + 4/3\ (S_u/\sigma_{vo}')[\ln(I_r)+1] + [1-(\cos\phi'/2)OCR^{\Lambda}]$	OCR for clays found by iteration from critical-state & cavity expansion model	Pool (1994)
	$OCR = 0.34\ K_D^{1.43}$	Calibration for several soft clay sites in Japan	Kamei & Iwasaki (1995)
	Analytical model for DMT in clays	Cavity expansion and Modified Cam-clay	Smith & Houlsby (1995)
	Field & lab comparision for soft clay in NE Brazil	OCR agrees with relation by Lunne et al. (1992)	Coutinho & Oliveira (1997)

Table 5, cont.

PARAMETER	*RELATIONSHIP*	*NOTES*	*REFERENCE*
	Field & lab comparison for fat Israeli clay	OCR agrees with original Marchetti (1980) relation	Blechman & Feferbaum (1997)
	$OCR = 2\cdot[\frac{\sqrt{3}\cdot(p_o-\sigma_{vo})}{1.57\cdot\sigma_{vo}'M_c\cdot(lnI_R+1)}]^{1/l}$	Cavity expansion and Cam clay model (see Mayne & Bachus, 1989 for terms)	Chang et al. (1997)
	Field & lab comparison for soft clay in Rio de Janeiro, Brazil	OCR agreed with relation by Lacasse & Lunne (1998)	Mello Vieira et al. (1997)
Horizontal Stress State $K_o = \sigma_{ho}'/\sigma_{vo}'$ = lateral at-rest coefficient, where σ_{ho}' = in-situ effective lateral stress	$K_o = (K_D/1.5)^{0.47} - 0.6$	Based on 8 uncemented Italian clays and 2 sands	Marchetti (1979, 1980)
	Field and lab study comparison of DMT in Norway	Comparison with hydraulic fracturing and lab estimates	Lacasse & Lunne (1983)
	Theoretical $K_o=f(\phi',K_D)$ for penetration in sands	Solution from wedge plasticity theory	Marchetti (1985)
	Experimental $K_o=f(\phi',K_D)$ from lab and field calibration	Chamber tests on Ticino sand; Field data at Po River	Jamiolkowski, et al., (1985)
	$K_o = f(K_D, q_c, \sigma_{vo}')$ in clean quartzitic sands	Requires paired data from DMT and CPT soundings	Marchetti (1985)
	Field comparision studies in Norwegian clays	K_o from pressuremeter and hydraulic fracture tests	Aas, et al. (1986)
	$K_o = 0.376 + \frac{K_D}{10.5} - \frac{(q_c/\sigma_{vo}')}{217}$	Based on unaged, quartzitic, uncemented sands in calibration chamber tests	Baldi, et al. (1986)
	Field study in North American clay	Comparison of DMT and Iowa stepped blade (ISB)	Lutenegger & Timian (1986)
	Field study in Canadian clay	Comparison of DMT and push-in spade cells	Chan & Morgenstern (1986)
	Field study in OC clays in U.K.	Compared DMT & prebored pressuremeter (PMT)	Powell & Uglow (1986)
	Field study in hydraulic fill sands in cofferdam	Comparison of DMT and self-boring pressuremeter	Clough & Goeke (1986)
	Amplification Factor: $K_D/K_o = a\exp(m\psi)$, where ψ = state parameter	Calibration chamber tests on Ticino and Hokksund sands: a = 1.35; m = -8.08	Jamiolkowski et al. (1988)
	$K_o = 0.34(K_D)^{0.55}$ for British clays	Modified expression for young clays	Powell & Uglow (1988)
	$K_o = 0.34K_D^m$ for Norwegian clays	For $K_D<10$, the exponent ranges $0.44 < m < 0.64$.	Lacasse & Lunne (1988)
	$P_{CH}'=f(p_o,u_0)$ = effective lateral preconsolidation stress	Four clays tested in horizontal oedometer tests	Lutenegger (1988)
	$K_o = K_N/2.27$, where $K_N = (p_{of}'+a')/(\sigma_{vo}'+a')$	Attraction = a'; final value from A-dissipation = p_{of}'	Roque et al. (1988)

Table 5, cont.

PARAMETER	*RELATIONSHIP*	*NOTES*	*REFERENCE*
	$K_o = 10^{[0.055 \cdot (K_D - 3.5)]} - 0.4$	Correlation for sensitive organic clays in Sweden	Larsson & Eskilson (1989)
	$K_o = (1 - \sin\varphi')\left[\frac{2K_D}{\sin\phi'(\ln I_R + 1)}\right]^{\sin\phi'/\Lambda}$	Analytical solution where ϕ' = friction angle, I_r = rigidity index, and $\Lambda \approx 0.8$.	Mayne & Kulhawy (1990)
	Experimental trends from ten clays in Northern Europe: $K_o = m_k \cdot K_D^{0.54}$	Young clays: $m_k = 0.34$ Old clays: $m_k = 0.68$	Lunne et al. (1990)
	Statistical study: $K_o = 0.27K_D$	Variety of clays tested by self-boring PMT	Mayne & Kulhawy (1990)
	Field study of two clays in North America	Comparison of data from SBPMT and DMT	Benoit et al. (1990)
	Field study of New York marine clay	DMT blade at different orientations with reference values from SBPMT	Huang & Haefele (1990)
	Field study of different devices in British Columbian clay	Compared DMT, total stress cells, and lateral stress cone	Sully & Campanella (1990)
	Summary trends: $K_o = (K_D/\beta_k)^{0.47} - 0.6$	Insensitive clays: $\beta_k = 1.5$ Sensitive clays: $\beta_k = 2.0$ Glacial till: $\beta_k = 3.0$ Fissured clays: $\beta_k = 0.9$	Kulhawy & Mayne (1990)
	Amplification factor for North Carolina Cape Fear sand:: $K_D/K_o = a \exp(m\psi)$	Laboratory calibration chamber tests: $a = 2.74$; $m = -2.31$	Lawter & Borden (1990)
	Field study of DMT in glacial till, Iowa	Compared K_o with spade cells, full-displacement PMT, & hydraulic fracturing	Lutenegger (1990)
	Field study in Singapore clay	Compare different field test interpretations	Chang (1991b)
	Field study in cemented Fucino clay, Italy	Good agreement between DMT and SBPMT	Burghigholi et al. (1991)
	Field study of DMT in Japanese alluvial clay	DMT values intermediate between SBPMT & HF tests	Iwasaki et al. (1991)
	Laboratory calibration chamber tests	Correlations for NC Cape Fear sand	Borden (1991)
	Field study of DMT in Malaysian alluvial clay	DMT underpredicts in comparison with SBPMT	Wong et al. (1993)
	Field study in two soft clays in New England	DMT in agreement with SBPMT tests	Benoît & Lutenegger (1993)
	Analytical model for clays	Hybrid cavity expansion & Cam-clay concepts	Pool (1994)
	Field experimental study in sensitive Québec clay	SBPMT, DMT, and HF confirmed $\beta_k = 2$ for K_0 trend	Hamouche et al. (1995)
	Field study in three Norwegian soils	Comparisons of dilatometer and Iowa stepped blade	Masood & Kibria (1994)

Table 5, cont.

PARAMETER	*RELATIONSHIP*	*NOTES*	*REFERENCE*
	Analytical model for clays	Cavity expansion and modified Cam-clay approach	Smith & Houlsby (1995)
	Laboratory experiments in clay	Calibration chamber tests on prestressed clays	Smith & Houlsby (1995)
	Field studies in Brazilian soft clay near Rio	DMT agrees with lab correlation; slightly higher than hydraulic fracture tests	Mello Vieira et al. (1997)
Undrained Shear Strength (s_u)	$s_u=0.22(0.5K_D)^{1.25}\ \sigma_{vo}'$	Insensitive Italian clays and silts with $I_D<1.2$	Marchetti (1979, 1980)
	Experimental field study of two Norwegian clays	Sites tested by vane shear, SBPMT, & lab triaxial	Lacasse & Lunne (1983)
	Field DMT tests in Canadian clays	General applications on project sites	Fabius (1984)
	Field study at four clay sites in British Columbia	Compared DMT strengths with field vane data	Grieg et al. (198)
	Field studies in three marine clays in New York & Ontario	Comparison of DMT strengths with lab UU data	Lutenegger & Timian (1986)
	Field studies at three British clay sites	Comparison of plate load and triaxial data with DMT	Powell & Uglow (1986)
	Field studies in Singapore clays	Comparison of vane and lab tests with DMT results	Chang (1987)
	Bearing capacity evaluation: $s_u=(p_1 - \sigma_{ho})/N_c$ where $\sigma_{ho}=K_o\sigma_{vo}'+u_o$	For Norwegian soils: Brittle clay and silt: $N_c=5$ Medium clay: $N_c=7$ Insensitive plastic clay:$N_c=9$	Roque et al. (1988)
	$s_u=0.20(0.5K_D)^{1.25}\ \sigma_{vo}'$	Norwegian clays calibrated to triaxial compression	Lacasse & Lunne (1988)
	$s_u=0.19(0.5K_D)^{1.25}\ \sigma_{vo}'$	Norwegian clays with field vane comparisons	Lacasse & Lunne (1988)
	$s_u=0.14(0.5K_D)^{1.25}\ \sigma_{vo}'$	Norwegian clays compared with simple shear data	Lacasse & Lunne (1988)
	Experimental data: $(p_o-u_o)/s_u > 3$	Uncorrected vane shear strengths from 7 U.S. clays	Lutenegger (1988)
	Field studies in Britain	Soft clays, clay tills, and fissured OC clays	Powell & Uglow (1988a, b)
	Swedish clay data: $s_u = (p_1-u_o)/F$	Inorganic clays: F = 10.3 Organic clays: F = 9.0	Larsson & Eskilson (1989)
	Field studies in Brazilian clays	Comparison of DMT with field vane strengths	Bogossian et al. (1989)
	Cavity expansion theory: $s_u/\sigma_{vo}' = K_D/8$	Derived for undrained loading, assuming $P_L = p_o$	Schmertmann (1989)
	Field studies in Singapore clays	Comparison of some laboratory and field tests	Chang (1991b)
	Field studies in Japanese alluvial clays	Evaluation of DMT in comparison with vane	Iwasaki et al. (1991)

Table 5, cont.

PARAMETER	*RELATIONSHIP*	*NOTES*	*REFERENCE*
	Experimental trend: $s_u = (p_o-u_o)/10$	Approximate expression for clays	Schmertmann (1991)
	Field and lab study in Malaysian alluvial clay	Compares DMTs with lab UU, field SBPMT, and VST	Wong et al. (1993)
	$s_u=0.41(0.5K_D)^{0.59}\ \sigma_{vo}'$	Calibrated with field vane tests in Taiwan clay	Su et al. (1993)
	$s_u=0.27(0.5K_D)^{1.49}\ \sigma_{vo}'$	Referenced to laboratory UC tests on Taiwan clay	Su et al. (1993)
	$s_u=0.22(0.5K_D)^{1.25}\ \sigma_{vo}'$	Referenced to UU triaxial tests on Taiwan clay	Su et al. (1993)
	$s_u=(p_o-\sigma_{ho})/N_{po}$	Finite element analysis: $N_{po} = 1.57\cdot\ln(G/s_u) - 1.75$	Yu et al. (1993)
	$s_u=f(\phi', \Lambda, p_0, p_1, \sigma_{vo}')$	Combined cavity expansion and modified Cam-clay	Pool (1994)
	$s_u = 0.018\ E_D$	Calibration with UU and UC tests on Japanese clays	Kamei & Iwasaki (1995)
	Field & lab study in soft Recife clay of NE Brazil	DMT estimates compare well with lab UU and CIUC	Coutinho & Oliveira (1997)
	Field & lab study of alluvial clays of Portugal	DMT compared with FV, CIU, and CK_oUC tests	Cruz, et al. (1997)
	Field study in Sarapui soft clay near Rio, Brazil	DMT (1980) correlation lower than FV results	Mello Vieira et al. (1997)
Drained Strength: Effective Stress Friction Angle of Sands (ϕ')	Empirical relationship: $\phi'=f(I_D,\sigma_{vo}',E_D)$	Clean quartz sands	Marchetti & Crapps (1981)
	Bearing capacity theory: $\phi' = f(\sigma_{vo}',K_o,q_D)$	Derived for sands using blade resistance (q_D)	Schmertmann (1982)
	Field comparative studies on hydraulic sand fill	DMT, drive samples, CPT, and PMT in cofferdam	Clough & Goeke (1986)
	Field study for sands in Norway	Comparison of DMT with drained triaxial tests.	Lacasse & Lunne (1988)
	$\phi' \approx 37.3\left(\frac{K_D-0.8}{K_o+0.8}\right)^{0.082}$	Based on limit plasticity theory and experimental field results for McDonalds sand	Campanella & Robertson (1991)
	$\phi' \approx 28^\circ + 14.6\cdot\log K_D - \frac{(\log K_D)^2}{0.476}$	Sands: Lower bound to wedge plasticity theory for all K_o values and assumed K_D - qc/σ_{vo}' relation	Marchetti (1997)

Table 5, cont.

PARAMETER	*RELATIONSHIP*	*NOTES*	*REFERENCE*
	$\phi' = 31^\circ + \frac{1}{\frac{0.236}{K_D}+0.066}$	Sands: Wedge plasticity theory solution for passive case solution (K_p)	approximation to solution in Marchetti (1997)
Modulus Constrained Modulus, $M = 1/m_v$	General: $M=R_M \cdot E_D$ $R_M=0.14+2.36 \cdot \log K_D$ $R_M=0.5+2\log \cdot K_D$ $R_M=R_{mo}+(2.5 - R_{mo}) \cdot \log K_D$ $R_M=0.32+2.18 \cdot \log K_D$ where $R_{mo}=0.14+0.14 \cdot (I_D-0.6)$	Modulus ratio, $R_M > 0.85$; For $I_D < 0.6$ For $I_D > 3.0$ For $3 > I_D > 0.6$ For $K_D > 10$	Marchetti (1979, 1980)
	Field and laboratory studies for several sites	Comparison of oedometer tests and DMT estimates	Schmertmann (1981)
	Field and lab studies for two Norwegian clays	Compared oedometer results with DMT data	Lacasse & Lunne (1983)
	Field studies for several sites and projects	DMT compared with backcalculated values from measured settlements	Schmertmann (1986b)
	Laboratory series in fixed-walled chambers	Compacted saturated soils from North Carolina.	Borden et al. (1986)
	Laboratory study	Calibration chamber tests on clean sands	Baldi et al. (1986)
	Field and lab study	Data from 3 soft saturated clays in NY and Ontario.	Lutenegger & Timian (1986)
	Field and lab study	Data from Singapore clays	Chang (1986)
	Field study	Natural sands and densified sands in Norway	Lacasse & Lunne (1986)
	Field and lab studies on three British clays	Compared oedometer moduli with DMT estimates	Powell & Uglow (1986)
	Field and lab study	Data from 3 clays and one sand in Norway	Lacasse & Lunne (1988)
	Laboratory studies on reconstituted sands	Calibration chamber tests on quartz sands	Jamiolkowski et al. (1988)
	Field and lab studies in U.K.	Oedometer tests from five clays from UK	Powell & Uglow (1988b)
	Field and lab study	Consolidation test data from Singapore clays	Chang (1991b)
	U.S. Piedmont residual silts & sands: $R_M = E'/E_D = 1$	Backcalculated E' from foundation settlements	Mayne & Frost (1988)
	Field and lab study	Oedometer data from alluvial cohesive soils in Japan	Iwasaki et al. (1991)
	Laboratory study	Calibration chamber tests on reconstituted sand	Borden (1991)
	$R_M=0.50+\log K_D$ $R_M=M/E_D$	Soft marine clays with $I_D<0.6$ from Taiwan	Su et al. (1993)

Table 5, cont.

PARAMETER	*RELATIONSHIP*	*NOTES*	*REFERENCE*
	Field study on sands	Load tests of shallow footings in sands	Skiles & Townsend (1994)
Modulus: Equivalent Elastic or Young's Modulus, E	$E_D = E/(1-\nu^2)$ where ν = Poisson's ratio	Dilatometer modulus derived from elastic theory	Marchetti (1975, 1979, 1980).
	Initial elastic modulus: $E_i = 1.4\ E_D$	Highly overconsolidated clays in Florida	Davidson & Boghrat (1983)
	Elastic Modulus at 25% ultimate: $E_{25} = E_D$	NC sands in Western Canada	Campanella et al. (1985)
	$E_i = 0.142\ E_D^{1.298}$	Partially saturated compacted fill soil	Borden et al. (1985)
	$E_{25} = 0.85\ E_D$	Based on triaxial data from NC sands from Italy	Baldi et al. (1986)
	$E_{25} = 3.5\ E_D$	Based on triaxial data from OC sands from Italy	Baldi et al. (1986)
	$E_{25} = R_{25}\ E_D$ with $0.7 < R_{25} < 3.5$	Calibrated for clean compacted quartz sands	Leonards & Frost (1987)
	$E'/E_D = 1.05$	Calibration chamber tests on NC clean silica sands	Bellotti et al. (1989)
	$E'/E_D = 3.66$	Calibration chamber tests on OC clean silica sands	Bellotti et al. (1989)
	$E_i = 10\ E_D$	Undrained loading of clay soils in British Columbia	Robertson et al. (1989)
	$E_i = 2\ E_D$	Sand fill in British Columbia	Robertson et al. (1989)
	$E_{25} = E_D$	Secant modulus at 25% of full strength mobilization	Schmertmann (1988b)
	$E_i = f(E_D, I_D)$	Based on UU triaxial tests on cohesive soils	Lutenegger (1988)
	$E_{25} = E_D$	Based on calibration chamber tests in sand	Baldi et al. (1989)
	$E_{50} = E_D$	Clays from Singapore and Malaysia	Chang (1991a)
	Field studies in sands and clays in Canada	Special research dilatometer with instrumented membrane	Campanella & Robertson (1991)
	Field study	DMT compared with PMT and UU moduli in Malaysia	Wong et al. (1993)
	$E_i = 1.13 + 0.14 E_D$	Data from alluvial cohesive soils from Taiwan	Su et al. (1993)
	Sands and clays: $E' = 0.83\ M_{DMT}$	Drained elastic modulus related to DMT-estimated constrained modulus	Marchetti (1997)
Modulus: $G_{max} = G_o$ = small-strain shear modulus	$R_G = G_{max}/E_D$ $0.7 < R_G < 2.2$	Based on field DMT and cross-hole shear tests on Po River sand	Jamiolkowski et al. (1988)
	$R_G = G_{max}/E_D$ $0.59 < R_G < 2.72$	Based on DMT chamber series and resonant-column tests on NC Ticino sand	Baldi et al. (1986)

Table 5, cont.

PARAMETER	*RELATIONSHIP*	*NOTES*	*REFERENCE*
	$R_G=G_{max}/E_D$ $0.7<R_G<2.2$	Based on crosshole tests on Po River sand.	Bellotti et al. (1986)
	Laboratory study on reconstituted sands	Chamber tests of sands with value of G_{max} estimated	Motan & Khan (1988)
	Sands to clays: $G_{max}/E_D = f(K_o)$	K_o evaluated from from DMT correlations	Hryciw & Woods (1988)
	$G_{max}/E_D = f(D_r)$	Field data from Po River Sand, Italy	Jamiolkowski et al. (1988)
	$G_{max} = f(E_D, \sigma_{vo}', p_0, u_0)$	Calibration chamber and field tests in sands	Baldi et al. (1989)
	$G_0 = 1.17E_D$	Field data from NC silty sand in British Columbia	Sully & Campanella (1989)
	$G_{max}=AFK_o^{0.25}(\sigma_{vo}'\sigma_a)^{0.5}$ where $A = 530/(\sigma_{vo}'/\sigma_a)^{0.25}$ and $F = f(\gamma_{dry})$	Nine sites of different soil types. DMT used to estimate K_o, γ_{dry}, and σ_{vo}'	Hryciw (1990)
	Ratio: $R_g = G_0/E_D$ with $4 < R_g < 25$	Greek clays tested by crosshole tests	Kalteziotis et al. (1991)
	$G_o = a_g K_D \sigma_{vo}'$	Clay soils where parameter $80 < a_g < 160$	Lunne et al. (1992)
	$G_o/E_D = f(D_R)$	Data compiled from 4 quartzitic sands	Lunne et al. (1992)
	$G_{sc} = 7.5E_D$ where G_{sc} = seismic cone	Based on two soft clay sites in Japan and one in U.K.	Tanaka et al. (1994)
	$G_0 = (2.96\text{-}0.02\ D_r)\cdot E_D$	For NC Toyoura sand in calibration chamber tests	Bellotti et al. (1994)
	$G_0/E_D = 16.7\text{-}16.3\log(p_{oN}/10)$ where $p_{oN} = p_o/\sqrt{\sigma_{vo}'}$ in kPa	For residual SM/SC soils from granite in Portugal	Cruz, et al. (1997)
In-Situ Shear Wave Velocity (V_s)	$V_s = 3.7\ (p_0)^{0.63}$ Note: V_s in m/s and p_o in kPa	Based on crosshole tests on clays from Greece	Kalteziotis et al. (1991)
	$V_s = 3.0(p_1)^{0.63}$ Note: V_s in m/s and p_1 in kPa	Based on crosshole tests on clays from Greece	Kalteziotis et al. (1991)
	Field study with seismic flat dilatometer in varved clay at Amherst, Massachusetts	Above correlations underestimate V_s in desiccated crust	Martin & Mayne (1997)
Hydrostatic Pore Water Pressure, (u_o)	$u_o = p_2$ where p_2 = closing pressure	Clean sands	Campanella et al. (1985)
	$u_o = p_2$	Clean sands	Schmertmann (1986)
Penetration Pore Water Pressure, (u_p)	Penetration pore pressure: $u_p \approx p_2$	Research DMT in soft clay in British Columbia	Campanella et al. (1985)
	$\Delta u/p_o = f(I_D)$	piezoblade tests in silty clays to sandy silts, Florida	Boghrat (1987)
	$p_2 = u_p$	soft clay in Florida	Schmertmann (1988)
	$p_2 = u_p$	piezoblade tests in intact clays in U.S.	Lutenegger (1988c)
	$u_p \approx p_o$	Trend from 7 intact clays tested by piezocone & DMT	Mayne (1987)

Table 5, cont.

PARAMETER	*RELATIONSHIP*	*NOTES*	*REFERENCE*
	$u_p = p_2$	Data from piezocone & piezoblade in 4 intact clays.	Lutenegger & Kabir (1988)
	$\Delta u = (u_p - u_o) \approx (p_0 - u_0)$	Comparison of piezocone & DMT soundings in 16 clays	Mayne & Bachus (1989)
	$u_p \neq p_2$	Research DMT in stiff OC clay in Western Canada	Campanella & Robertson (1991)
Coefficient of consolidation (c_h)	$p_2/u_o = f(I_D)$	Clays to silts to sands	Schmertmann (1986)
	Dissipation of p_o pressures with time	Italian clays	Marchetti et al. (1986)
	Utilizes p_2 dissipation curve	Comparison of DMT and backcalculated values	Schmertmann (1988)
	Dissipation of p_o, p_1, and p_2.with time	Soft clay, fissured clay, and weathered clay in U.K.	Powell & Uglow (1988)
	Field study of p_2 and u_p dissipations with time in clays	Comparison with piezocone & piezoblade dissipations.	Lutenegger & Kabir (1988)
	Two soft clays in Canada: $c_h = f(p_2, u_o)$	Dissipation tests for p_o, p_1, and p_2.with time	Robertson et al. (1988)
	$c_{h(OC)} = \frac{7cm^2}{t_{flex}}$	Uses p_o-log(t) dissipation curves from 7 Italian clays; t_{flex} = time corresponding to contraflexure point in "backward S" time curve.	Marchetti & Totani (1989)
	Measured p_2 dissipation in soft Japanese alluvial clays	Compares with laboratory data in Tokyo Bay	Iwasaki et al. (1991)
	Measured p_2 dissipation in soft Korean marine clays	DMT results compared with piezocone data	Kim, et al. (1997)
Hydraulic Conductivity (k_h)	$k_h = \frac{c_h \gamma_w}{M_h}$	Horizontal permeability related to c_h and horizontal constrained modulus from: $M_h = K_o \cdot M_{DMT}$	Schmertmann & Crapps (1988)
Limit Pressure (P_L)	$P_L = f(p_1)$	Soft clays in British Columbia	Campanella & Robertson (1983)
	$P_L = (p_1)/f_p$	Empirical Factor f_p = 1.2 in OC Gault clay = 1.4 in OC London clay	Powell & Uglow (1986)
	$P_L = p_0$	NC clays in North America with OCR < 2.5	Lutenegger (1988)
	$1.11 < P_1/P_L < 1.76$	Soft, stiff, and fissured clays from U.K.	Clarke & Wroth (1988)
	Field study of $(P_L - \sigma_{ho})$ versus $(p_1 - p_o)$	Comparison of PMT and DMT data from 11 clays	Lunne et al. (1990)
	$P_L = 10.6 + p_0$ Note: Pressures in kPa	Valid for clays in Greece with $p_0 < 1000$kPa	Kalteziotis (1991)
	$P_L = 0.72(p_1)^{1.013}$ Note: Pressures in kPa	Valid for clays in Greece with $p_1 < 1000$kPa	Kalteziotis (1991)

Table 5, cont.

PARAMETER	*RELATIONSHIP*	*NOTES*	*REFERENCE*
	$P_L = 0.85\ p_0$	Reference data from SBPMT in Malaysian clays	Wong et al. (1993)
Fill Compaction Control	Field study in Norway	Compaction control of a sand and silt fill	Lacasse & Lunne (1986)
	Field study in North Carolina	Compacted saturated soils	Borden et al. (1986)
Blade Thrust Resistance, q_D	Field studies in Florida	Project sites in silty and clean sands	Schmertmann (1982, 1983)
	Clean sands: $q_D=1.1q_c$	Based on natural sands at McDonald's Farm, B.C.	Campanella & Robertson (1991)
	Clean sands: $q_D=1.14q_c$	Reconstituted sands in calibration chamber tests	Bellotti et al. (1994)
Relative Density, D_R	$D_R=f(K_D)$	NC uncemented sands from uncorrected chamber tests	Robertson & Campanella (1986)
	$D_R \approx 100[\frac{(K_D-1)}{7}]^{0.5}$	Based on NC sands from 3 chamber series and 2 natural sands	Reyna & Chameau (1991)
State Parameter for Sands, ψ	Calibration tests on sands: $K_D/K_o=1.73e^{(-6.07\psi)}$	Tests on Cape Fear, Hokksund, & Ticino sands	Borden (1991)
	Ottawa sand: $\psi = f(e_o,K_D,\sigma_{oct})$	Calibration chamber tests with blade "perfectly-placed"	Konrad (1989)
	Toyoura sand: $K_D/K_o=1.05e^{(-3.07\psi)}$	Calibration chamber tests on reconstituted sand	Bellotti et al. (1994)
Estimating Liquefaction Potential	If $K_D < 1.3$, High risk If $K_D > 1.7$, low risk.	Applicable for natural submerged sands	Marchetti (1982)
	Liquefaction = f(cyclic stress ratio, K_D)	Clean unaged uncemented quartzitic sands	Robertson & Campanella (1986a)
	If cyclic stress ratio, $\tau_{cyc}/\sigma_{vo}' > 0.027\ K_D^{1.5}$, then liquefaction likely.	Based on natural sands response in California	Reyna & Chameau (1991)
Pile Skin Friction or Side Resistance, f_s	σ_{hc} evaluated from p_o-dissipation test	Data from Italian clays	Marchetti et al. (1986)
	$\sigma_{ho} = p_o$ after full dissipation	DMT used as a push in spade cell in stiff OC clays	Powell & Uglow (1986)
	$f_s = f(s_u, E_D)$	Cohesive soils	Robertson et al. (1989)
	$f_s = f(s_u, E_D)$	Instrumented piles in clay	Marchetti et al. (1991)
	$f_s = f(\sigma_{hc}',I_D)$	$\sigma_{hc} = p_o$ after full dissipation; Data from OC clays at Haga, Norway and Canons Park, UK	Gabr et al. (1991)
	$f_s/\sigma_{vo}' = f(I_D)$	Backfigured from load tests on driven piles at 7 clay sites	Lunne et al. (1992)
	σ_{hc} for driven pipe piles after p_o equilibrium	Dissipation tests in Italian clays	Totani et al. (1994)

Table 5, cont.

Coefficient of Subgrade Reaction, k_{sh}	$k_{sh} = [p_{0(7)} - p_{0(0)}]/d$ where d = blade thickness	Laboratory tests on laterally-loaded piles in sands	Motan & Gabr (1984)
	$k_{so} = (p_0 - \sigma_{ho})/t$ where t = half-blade thickness	Laterally-loaded piles in sands in calibration chamber test series	Gabr & Borden (1988)
	$k_{sv} = f(K_o, K_D, d, B, \sigma_{vo}')$	Vertical subgrade modulus for mat foundations	Schmertmann (1989)
	Evaluation of nonlinear p-y curves	Laterally-loaded driven piles in clay	Marchetti et al. (1991)
Slope Investigations	$K_D < 2$ indicates possible slip surface	Landslide involving OC fissured clays	Marchetti et al. (1993)
	Site investigation of laterals stress state beneath slopes	K_o reference from total stress cells in Swedish sites	Rankka (1990)
	Detection of landslide surface where $K_D \approx 2$	Case studies involving overconsolidated clays	Marchetti (1997) and Totani et al. (1997)

APPENDIX B: CPT AND DMT RESULTS – GRAPHICAL FORMAT

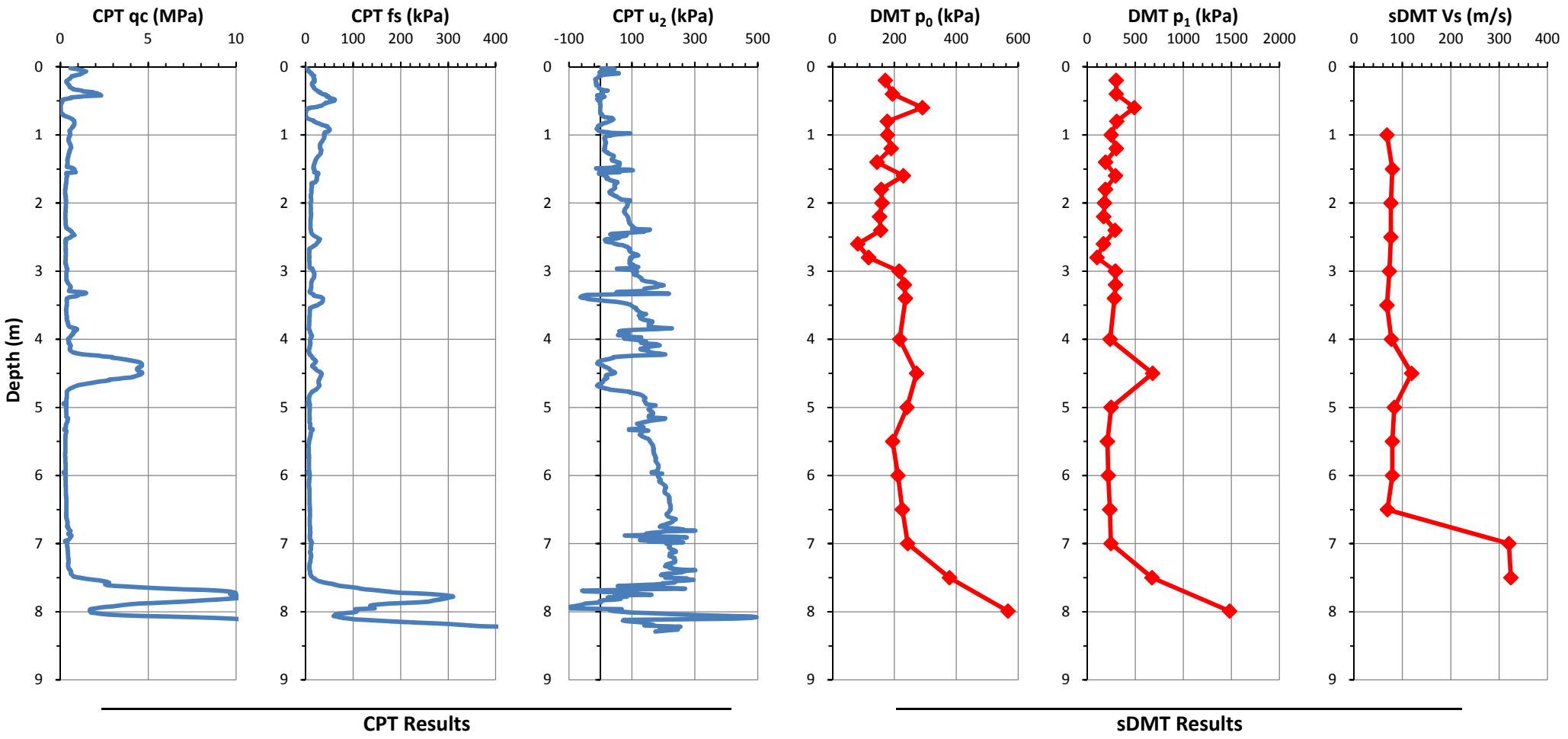

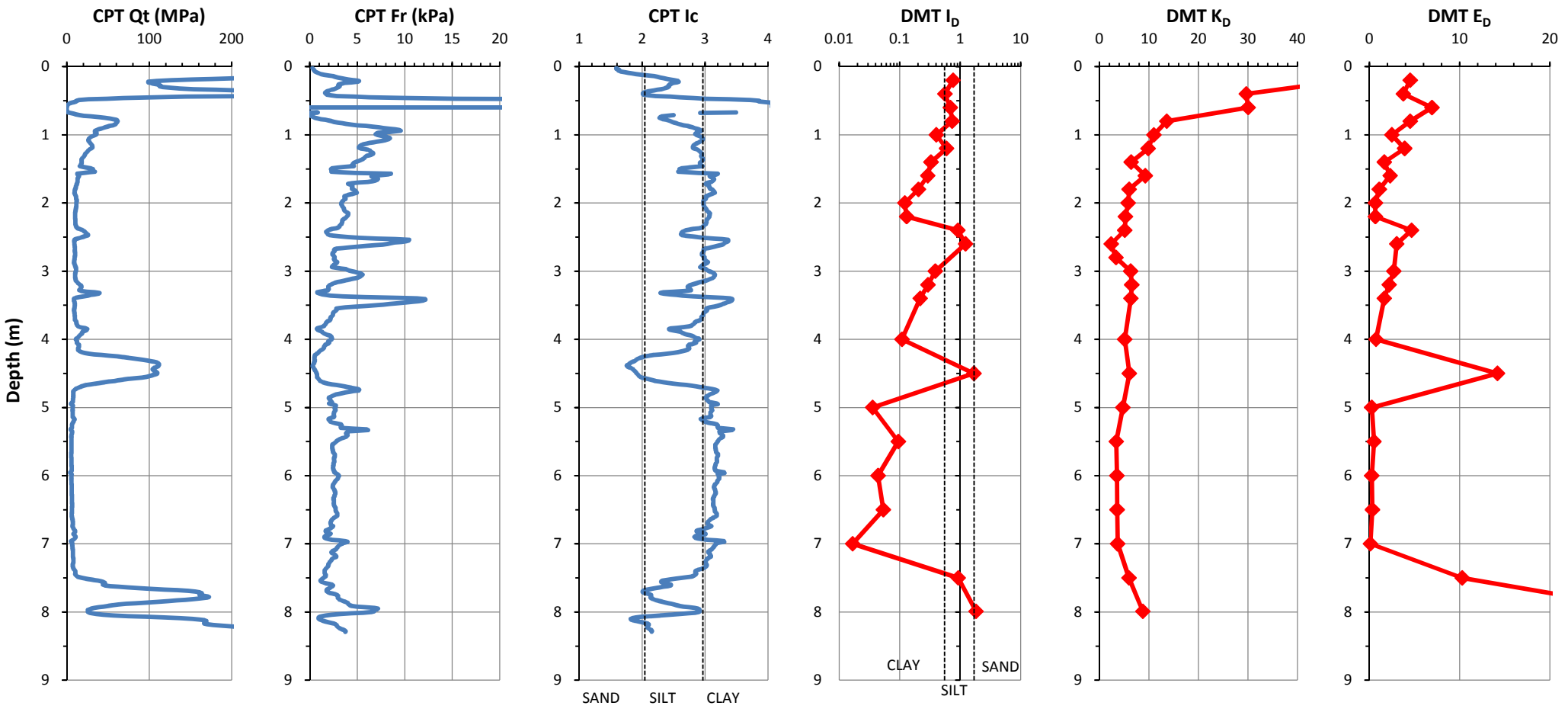

Normalised CPT parameters and Material Index (Robertson 2009a)

DMT Index Values (Marchetti 1980)

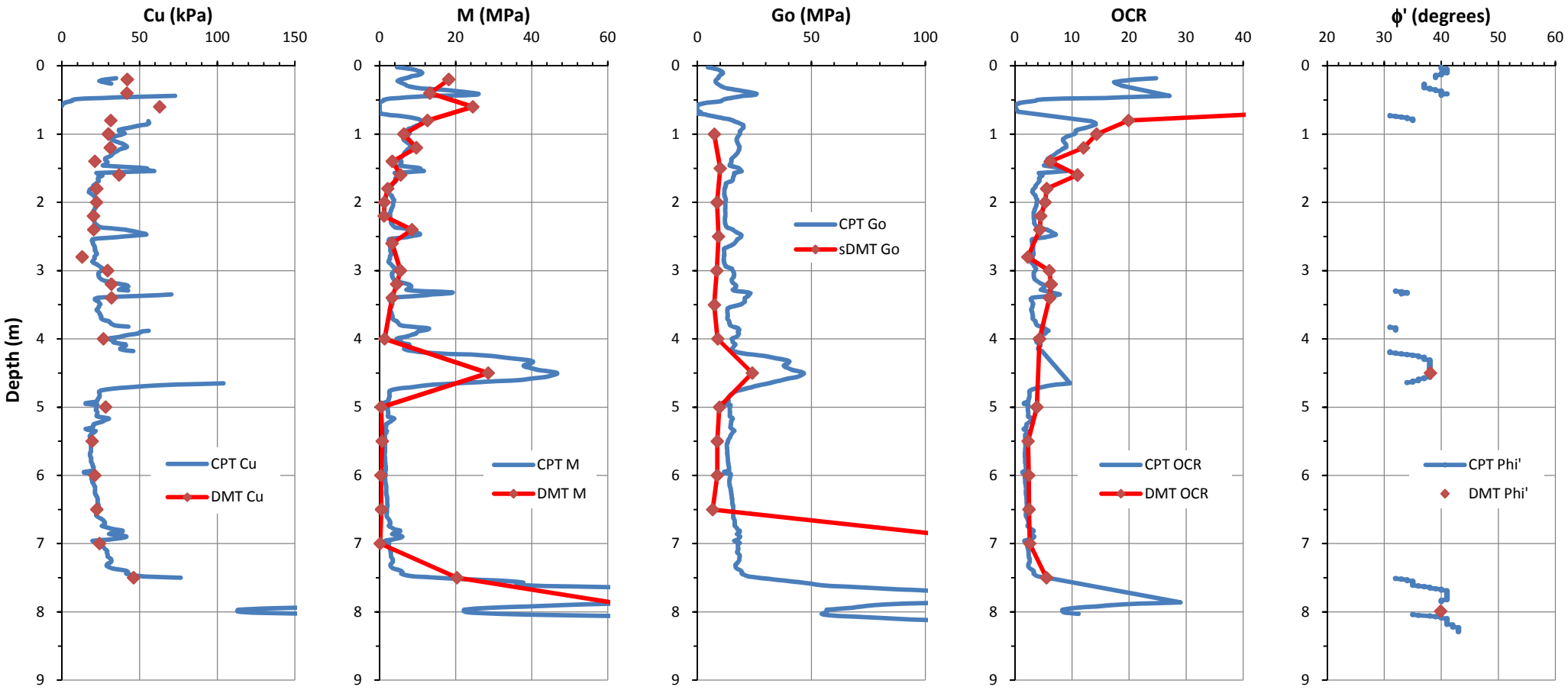

DMT correlations based on Marchetti (1980) and TC16 (2001) using Marchetti Elab software
CPT corelations based on Robertson (2009a) and Kulhawy & Mayne (1990) using CPeT-IT software

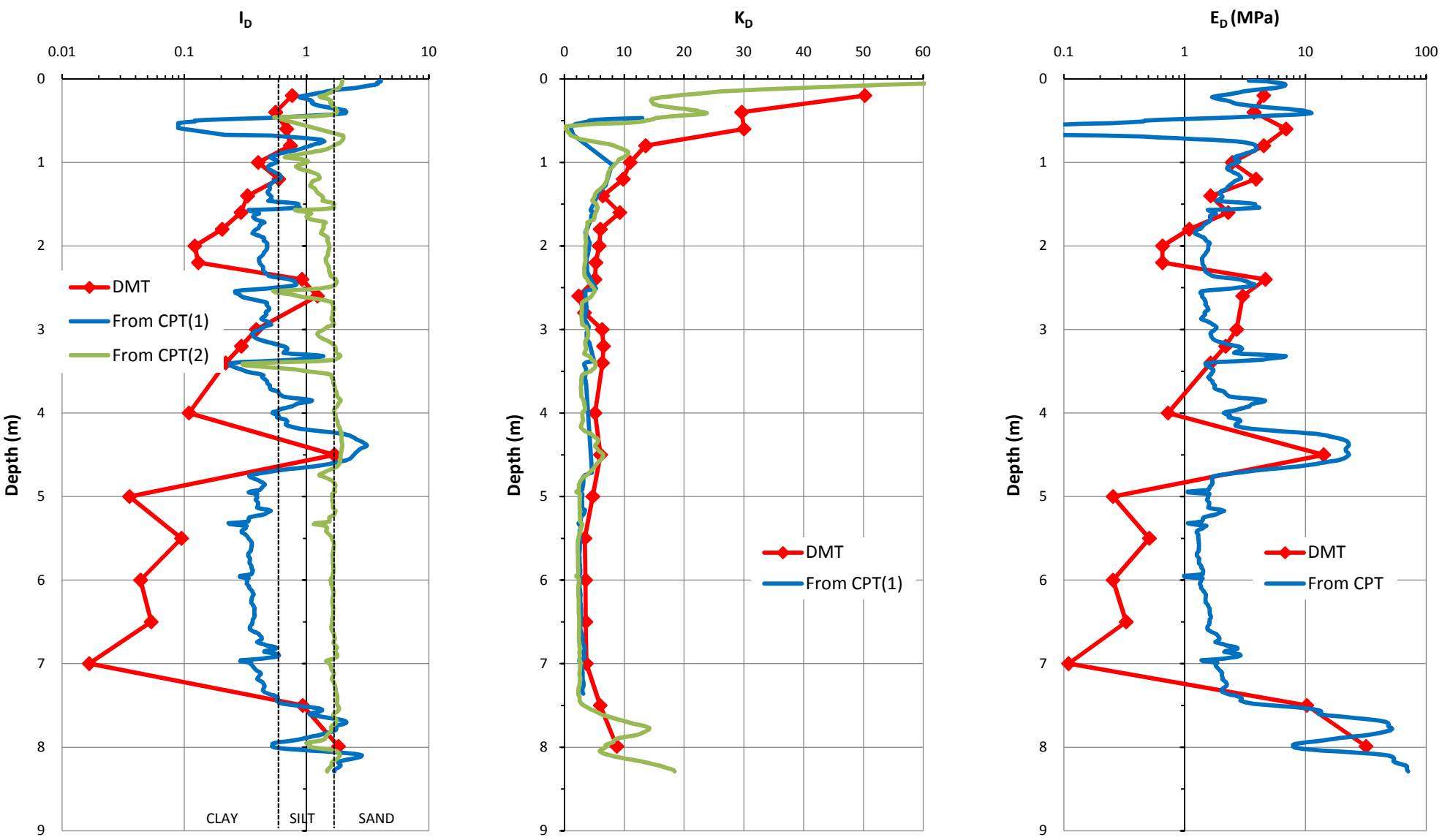

CPT(1): $I_D = 10^{(1.67-0.67Ic)}$ (Robertson 2009b)
CPT(2): $I_D = 2.0-0.14F_r$ (Mayne & Liao 2004)

CPT(1): $K_D = 0.3(Qt)^{0.95} + 1.05$, for Ic>2.95
CPT(2): $K_D = 0.144Qt/[10^{(1.67-0.67Ic)}]$
(Robertson 2009b)

CPT: $E_D = 5\ Qt\ \sigma'_{vo}$
(Robertson 2009b)

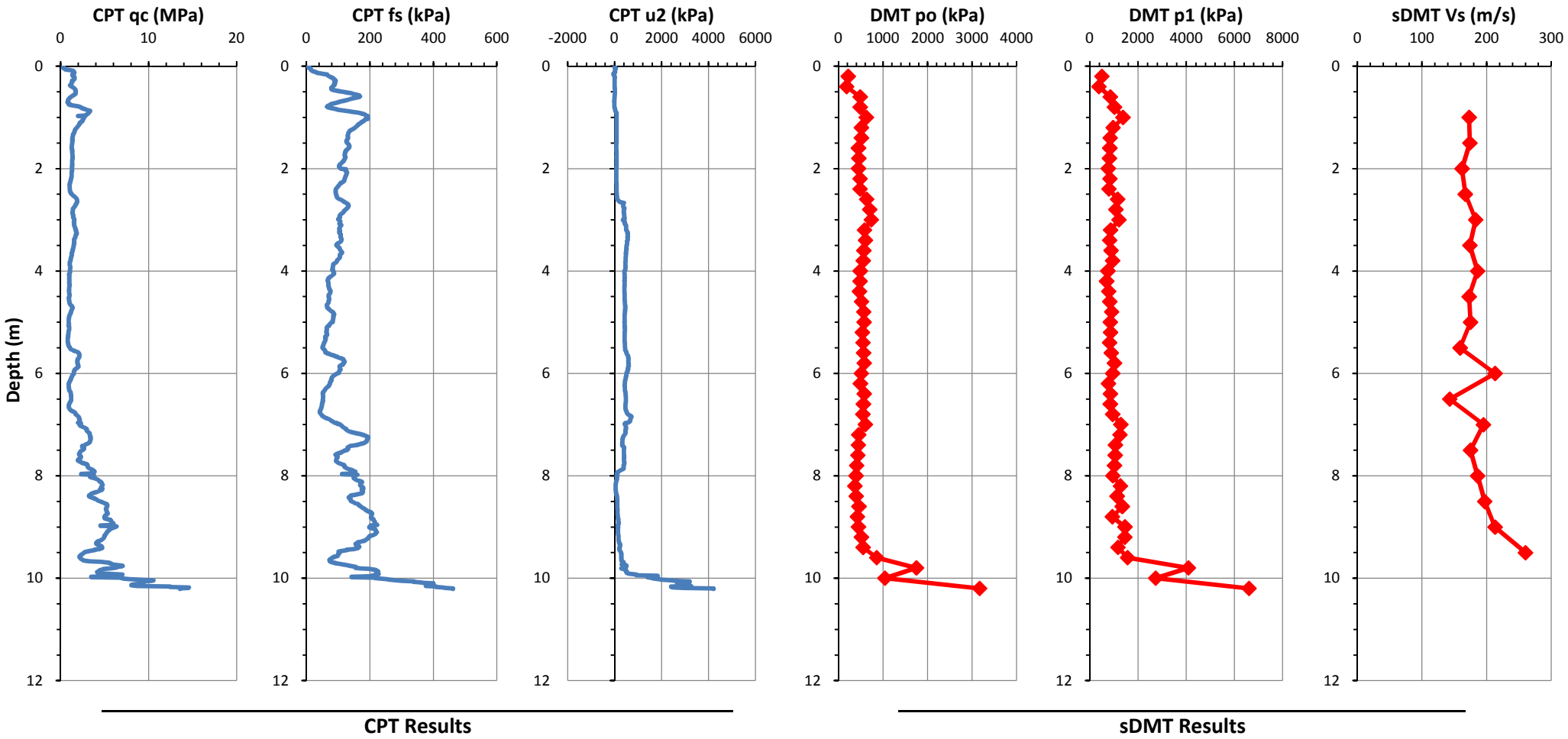

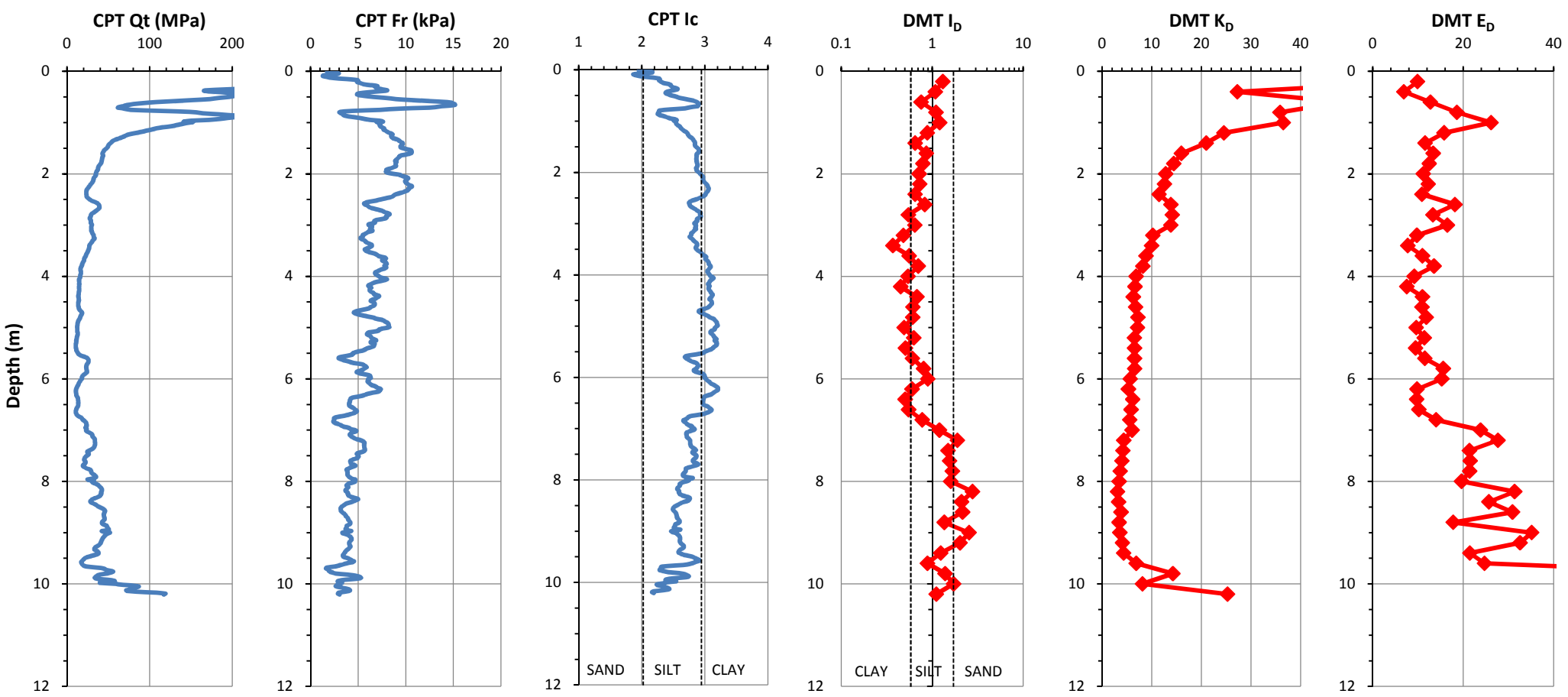

Normalised CPT parameters and Material Index (Robertson 2009a)

DMT Index Values (Marchetti 1980)

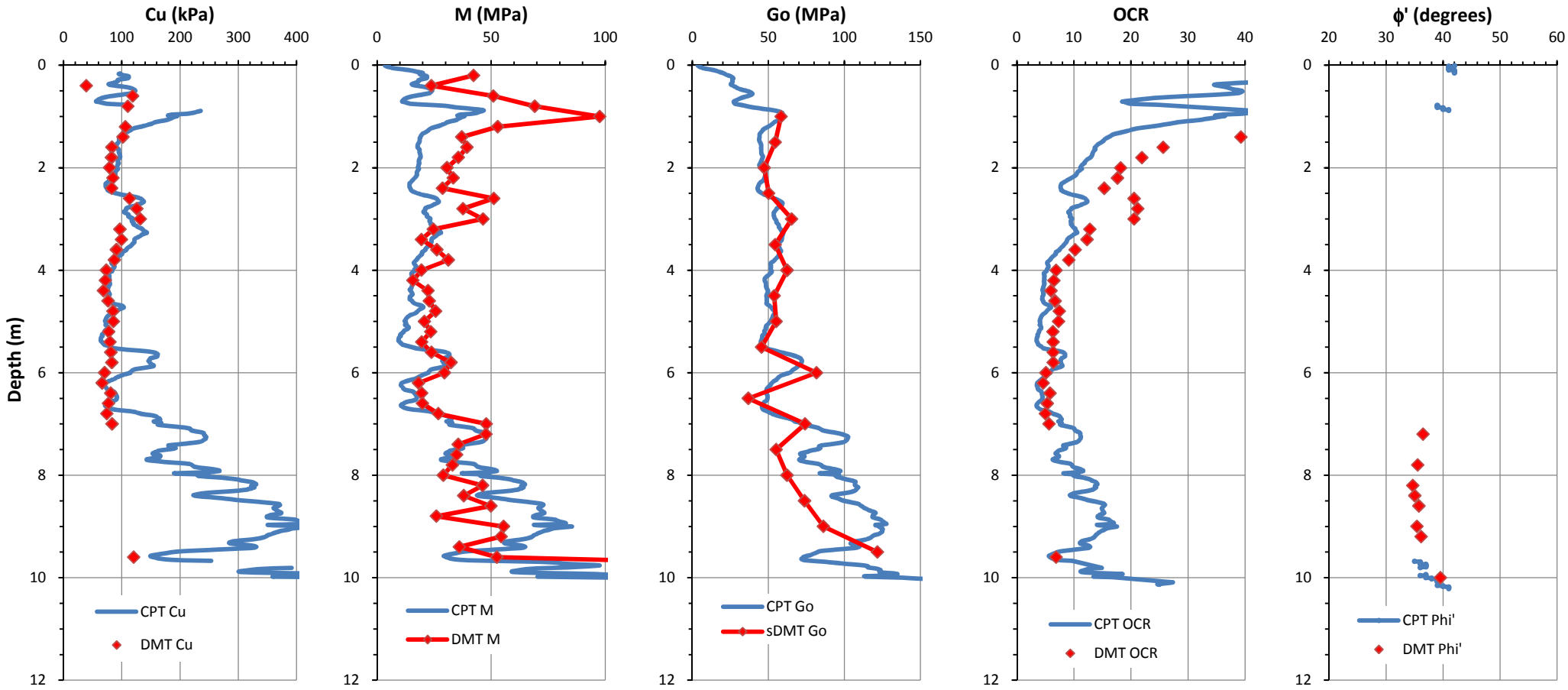

DMT correlations based on Marchetti (1980) and TC16 (2001) using Marchetti Elab software
CPT corelations based on Robertson (2009a) and Kulhawy & Mayne (1990) using CPeT-IT software

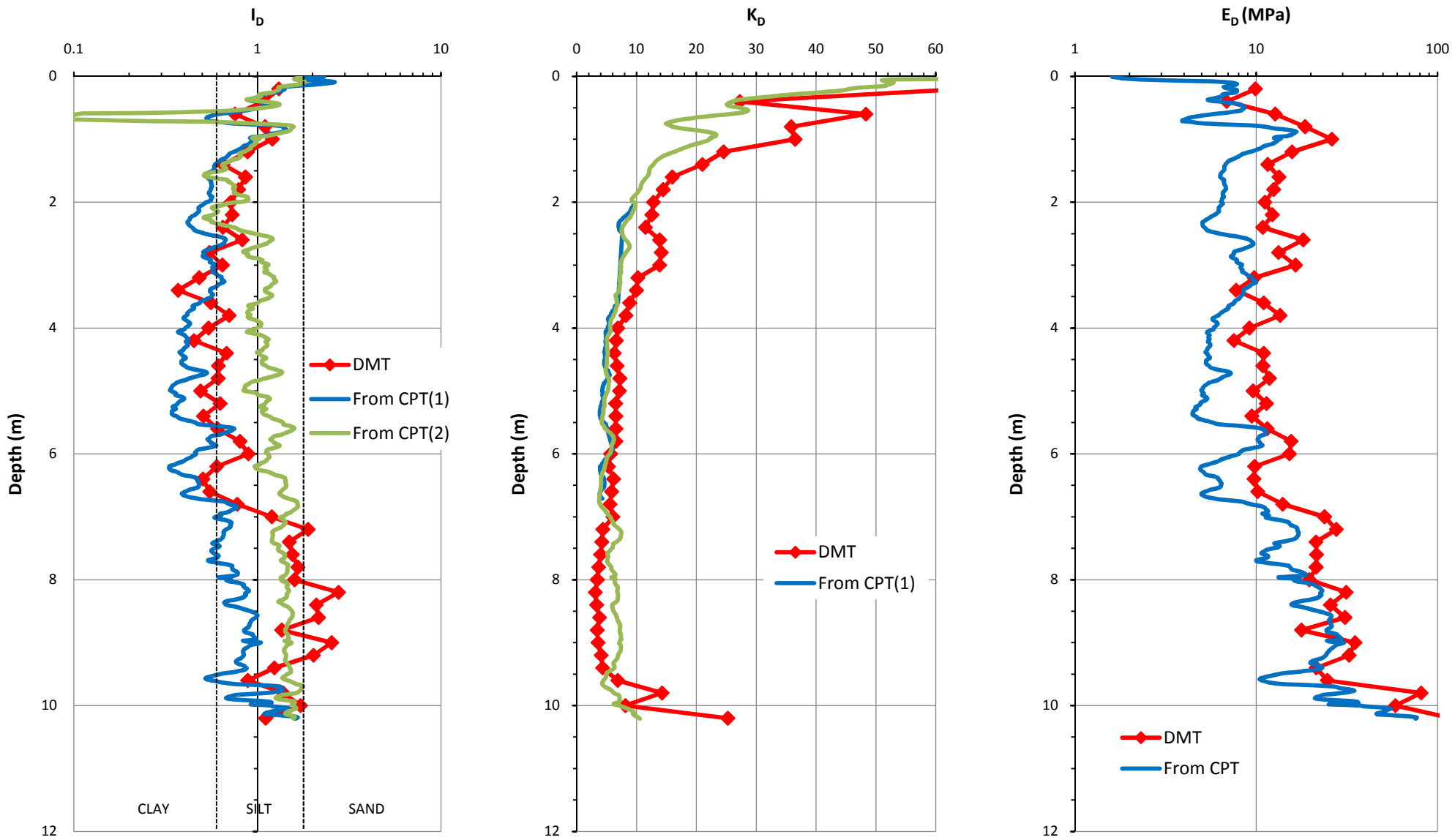

CPT(1): $I_D = 10^{(1.67-0.67Ic)}$ (Robertson 2009b)
CPT(2): $I_D = 2.0-0.14F_r$ (Mayne & Liao 2004)

CPT(1): $K_D = 0.3(Qt)^{0.95} + 1.05$, for Ic>2.95
CPT(2): $K_D = 0.144Qt/[10^{(1.67-0.67Ic)}]$
(Robertson 2009b)

CPT: $E_D = 5\ Qt\ \sigma'_{vo}$
(Robertson 2009b)

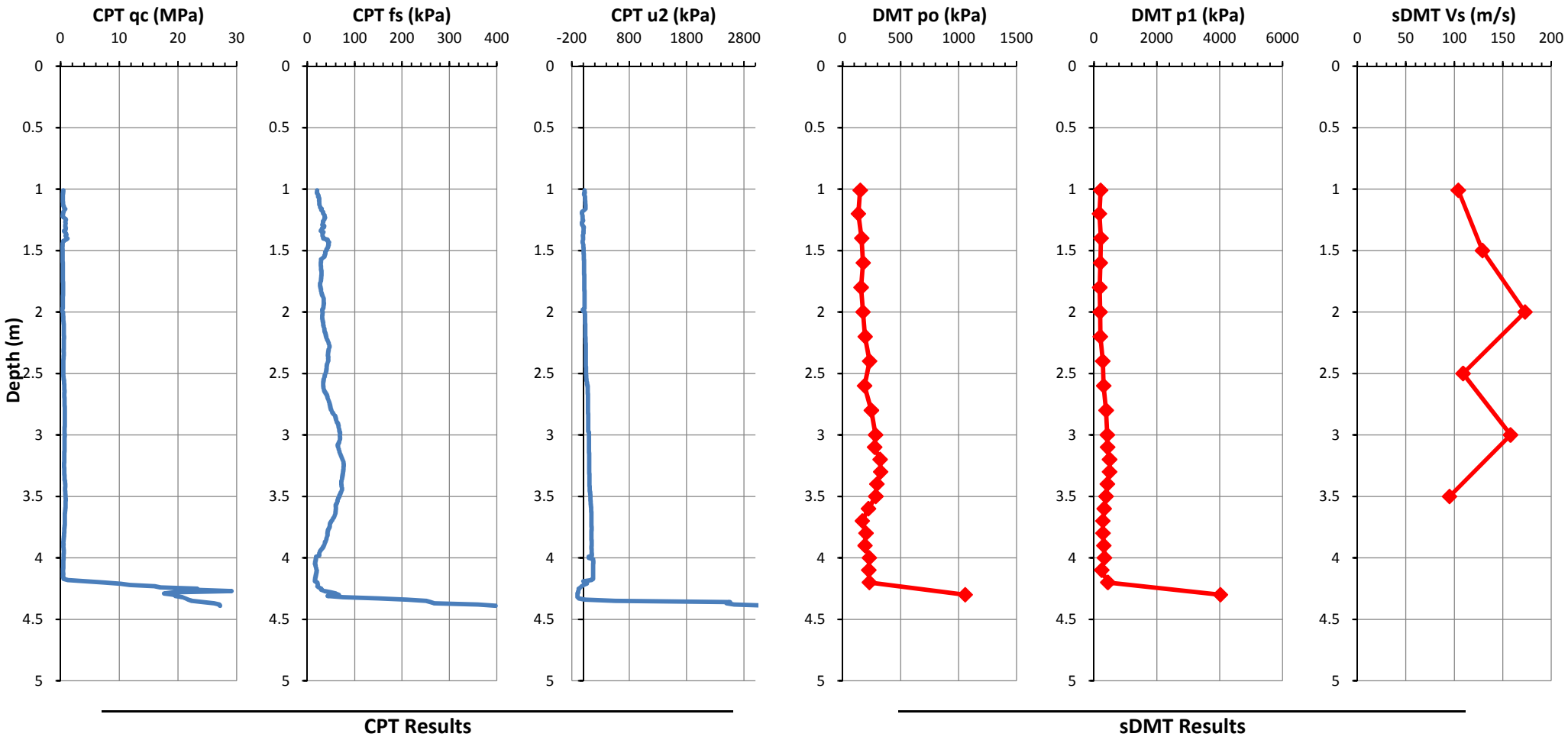
CPT qc (MPa)
0 10 20 30
CPT fs (kPa)
0 100 200 300 400
CPT u2 (kPa)
-200 800 1800 2800
DMT po (kPa)
0 500 1000 1500
DMT p1 (kPa)
0 2000 4000 6000
sDMT Vs (m/s)
0 50 100 150 200
Depth (m)
0 0.5 1 1.5 2 2.5 3 3.5 4 4.5 5
CPT Results
sDMT Results

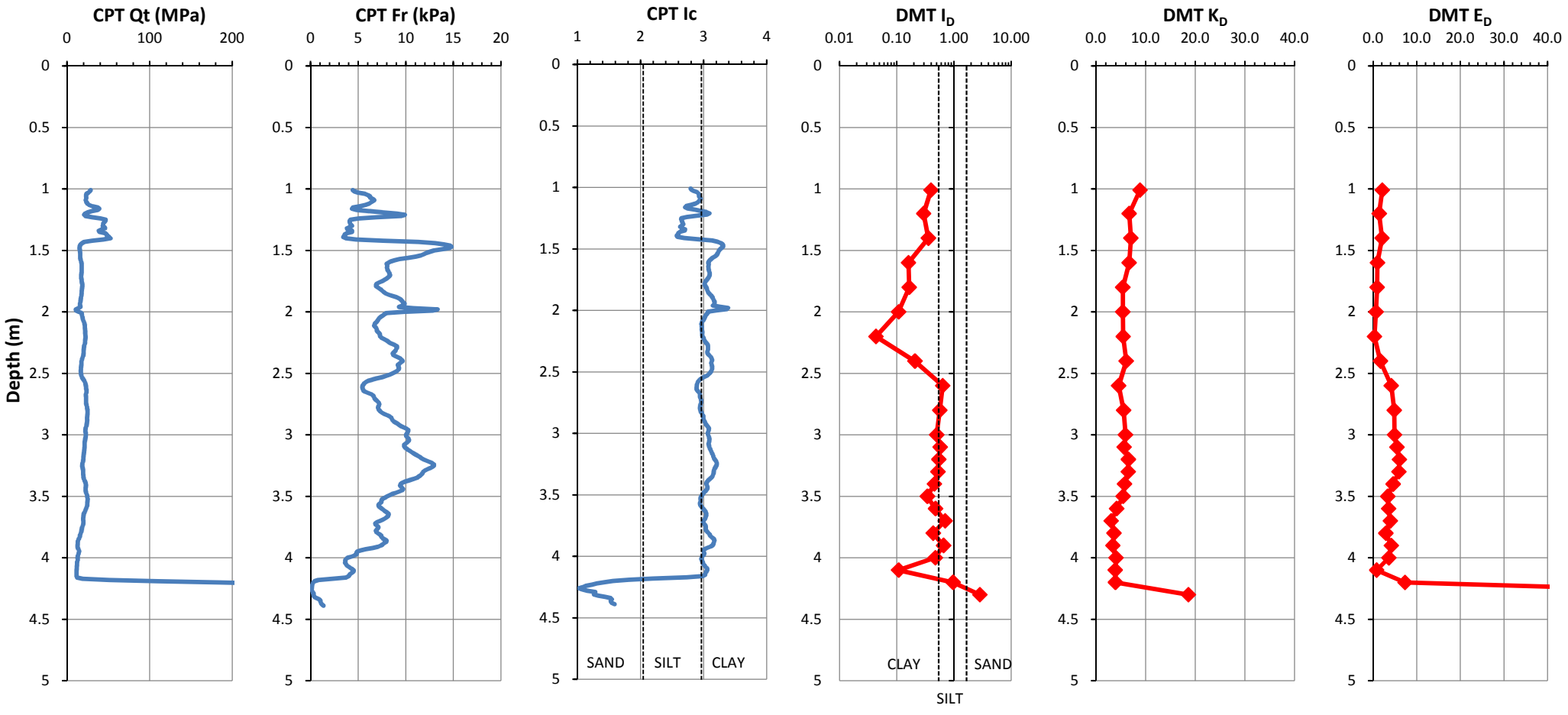
CPT Qt (MPa)
0 100 200
CPT Fr (kPa)
0 5 10 15 20
CPT Ic
1 2 3 4
DMT I_D
0.01 0.10 1.00 10.00
DMT K_D
0.0 10.0 20.0 30.0 40.0
DMT E_D
0.0 10.0 20.0 30.0 40.0
Depth (m)
0 0.5 1 1.5 2 2.5 3 3.5 4 4.5 5
SAND
SILT
CLAY
CLAY
SILT
SAND
Normalised CPT parameters and Material Index (Robertson 2009a)
DMT Index Values (Marchetti 1980)

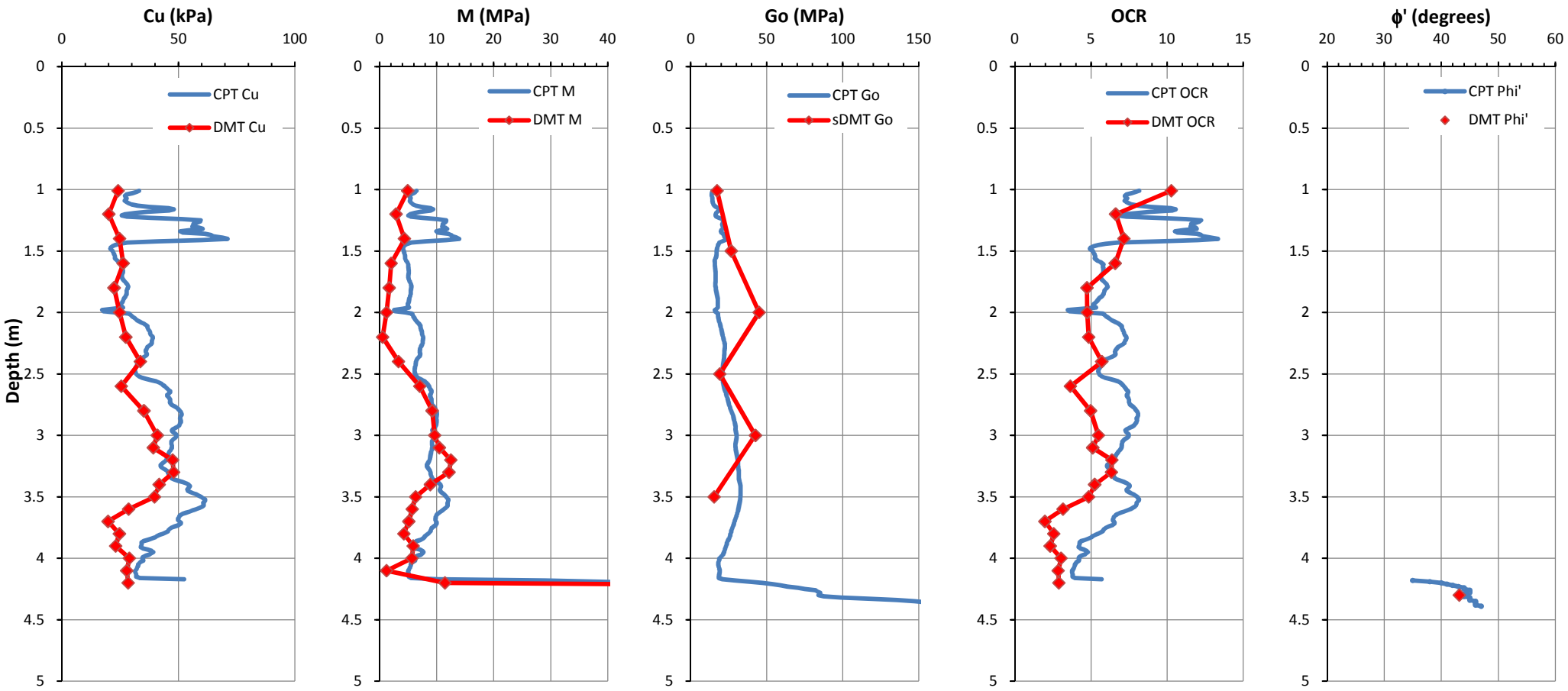

DMT correlations based on Marchetti (1980) and TC16 (2001) using Marchetti Elab software
CPT corelations based on Robertson (2009a) and Kulhawy & Mayne (1990) using CPeT-IT software

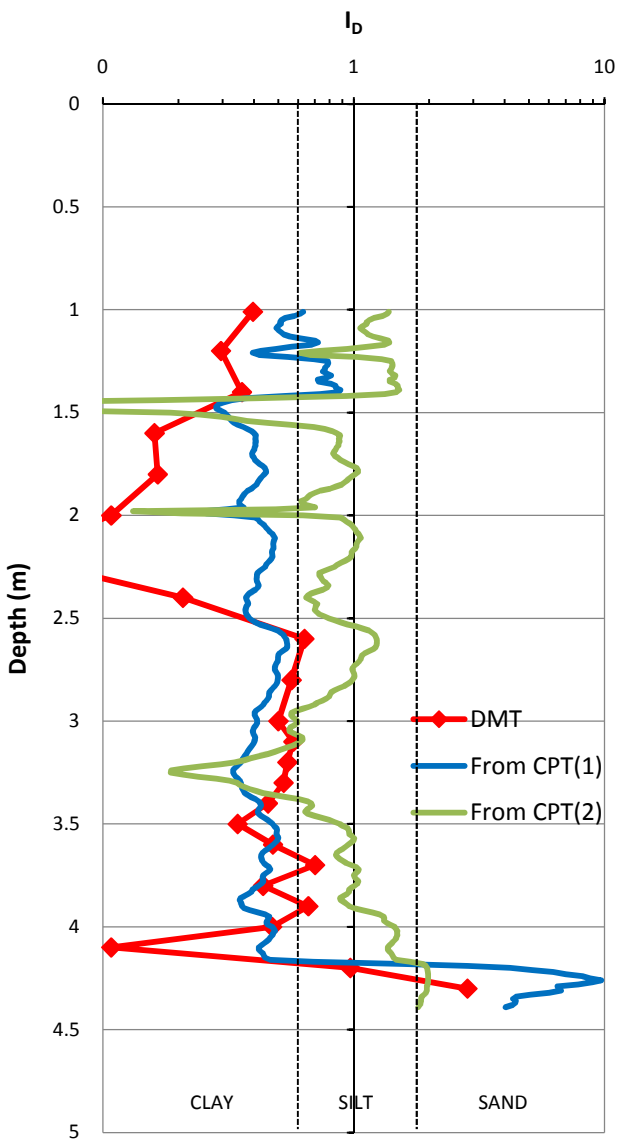

CPT(1): $I_D = 10^{(1.67-0.67Ic)}$ (Robertson 2009b)
CPT(2): $I_D = 2.0-0.14F_r$ (Mayne & Liao 2004)

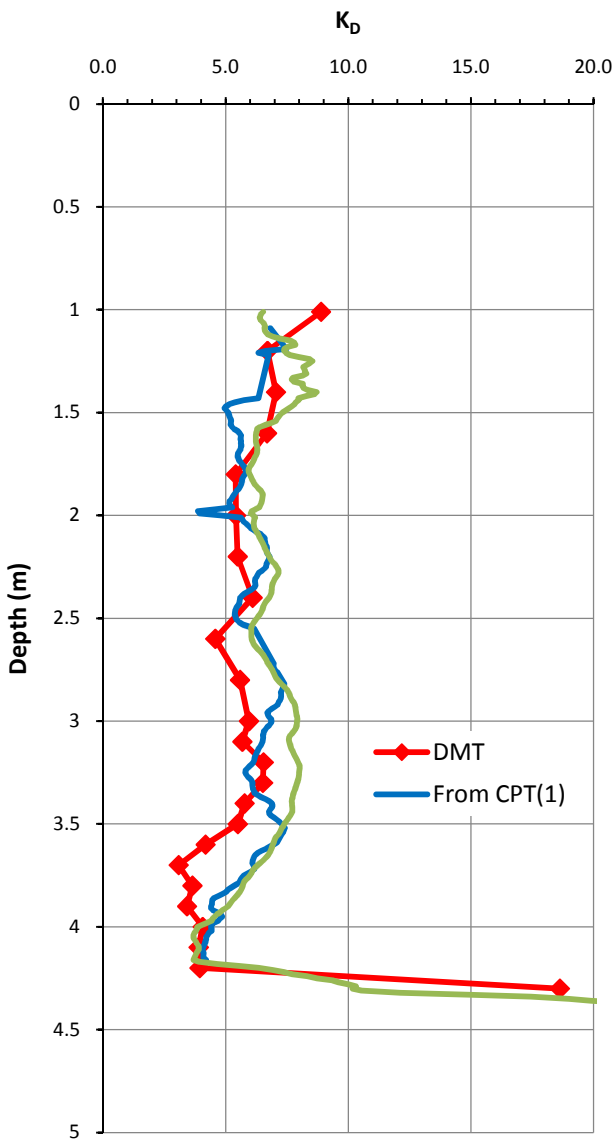

CPT(1): $K_D = 0.3(Qt)^{0.95} + 1.05$, for Ic>2.95
CPT(2): $K_D = 0.144Qt/[10^{(1.67-0.67Ic)}]$
(Robertson 2009b)

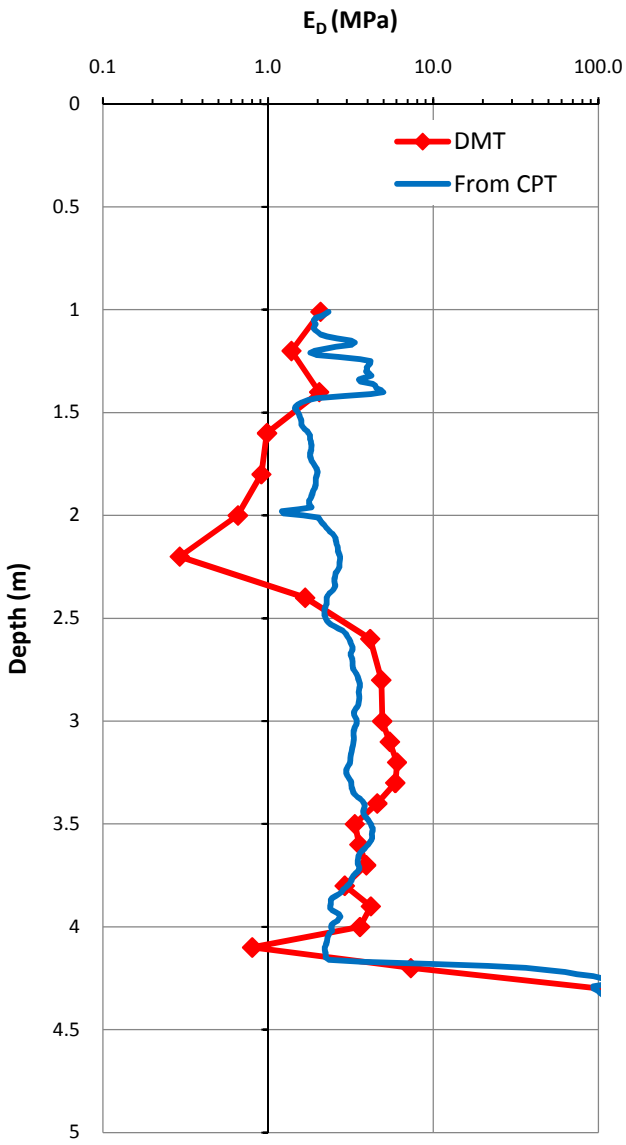

CPT: $E_D = 5\ Qt\ \sigma'_{vo}$
(Robertson 2009b)

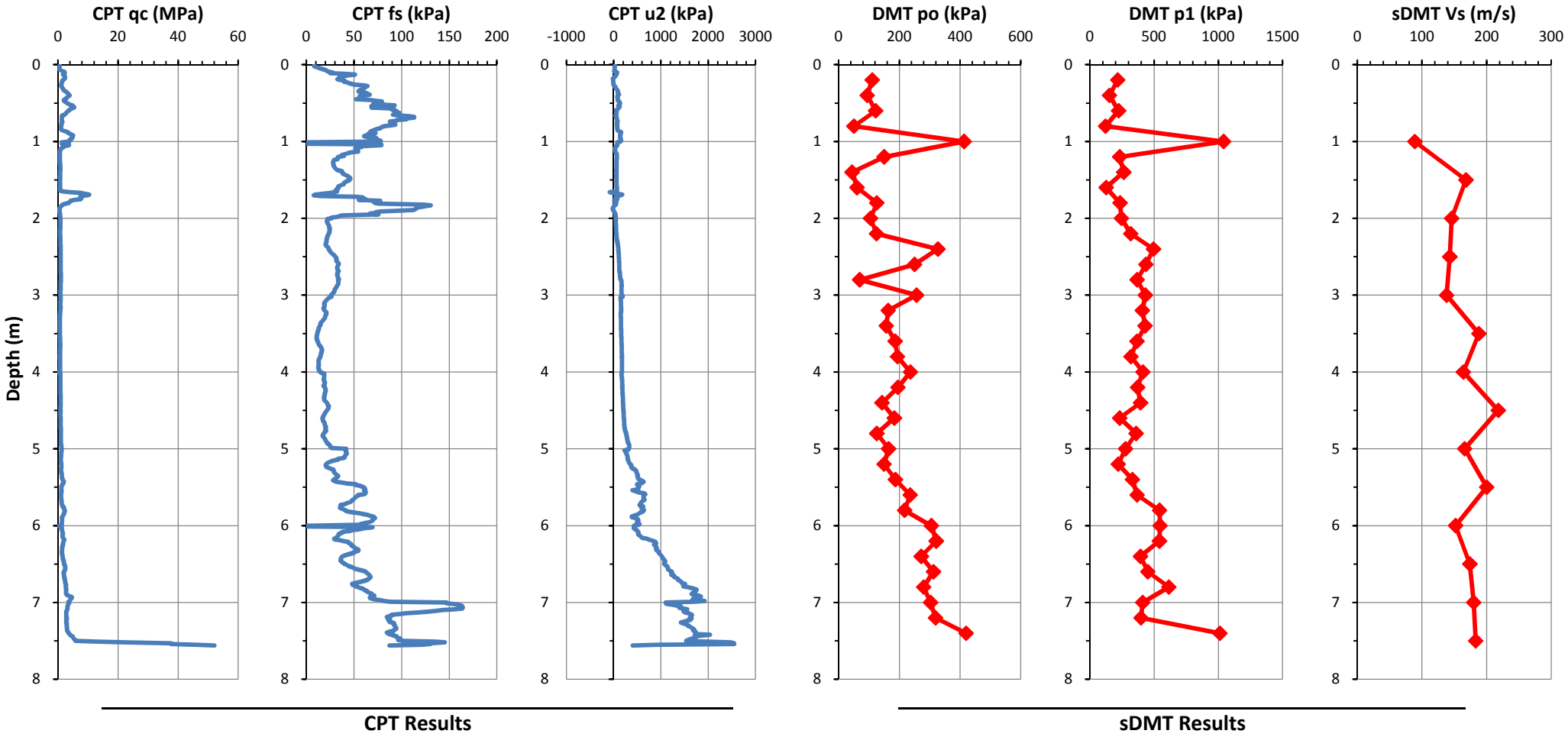
CPT qc (MPa)
CPT fs (kPa)
CPT u2 (kPa)
DMT po (kPa)
DMT p1 (kPa)
sDMT Vs (m/s)
Depth (m)
CPT Results
sDMT Results

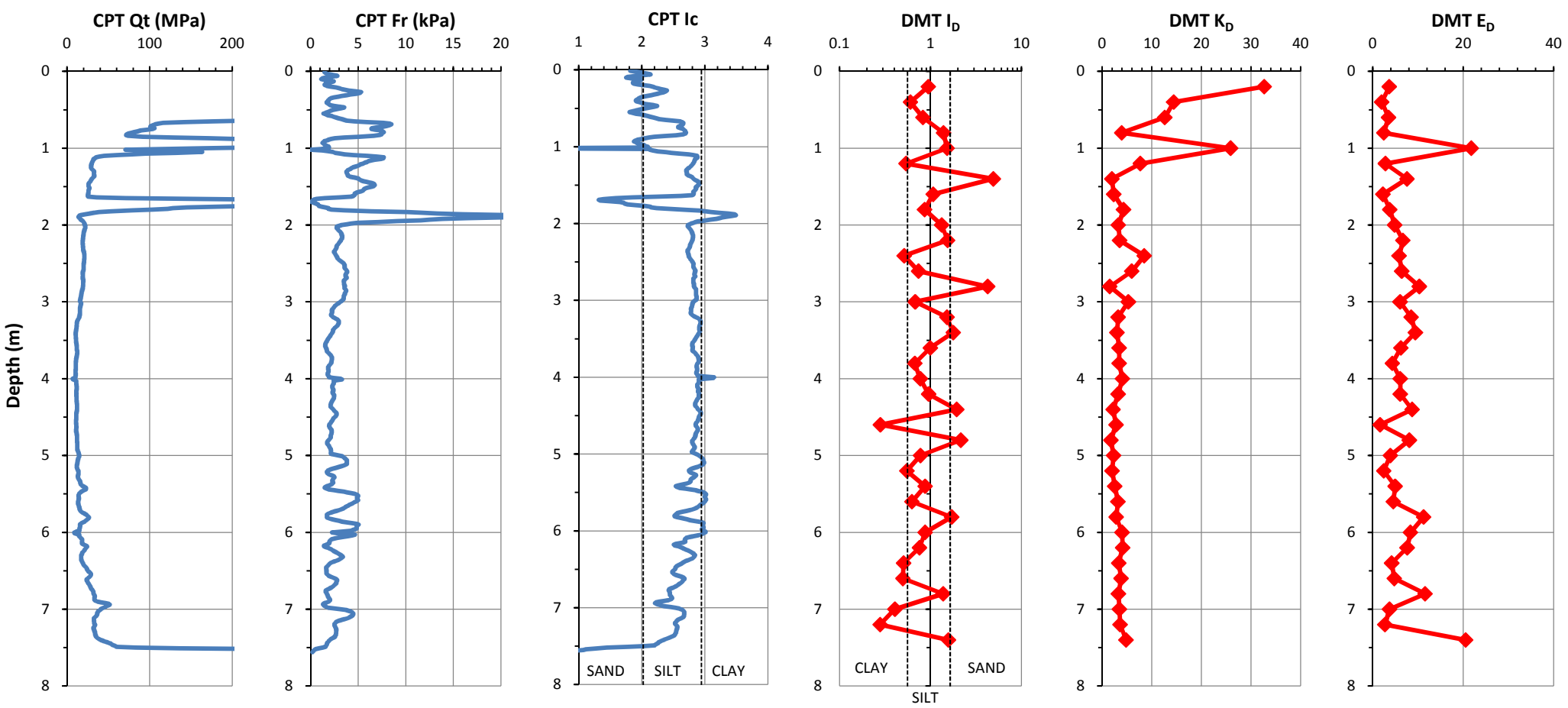
CPT Qt (MPa)
CPT Fr (kPa)
CPT Ic
DMT I_D
DMT K_D
DMT E_D
Depth (m)
SAND
SILT
CLAY
CLAY
SILT
SAND
Normalised CPT parameters and Material Index (Robertson 2009a)
DMT Index Values (Marchetti 1980)

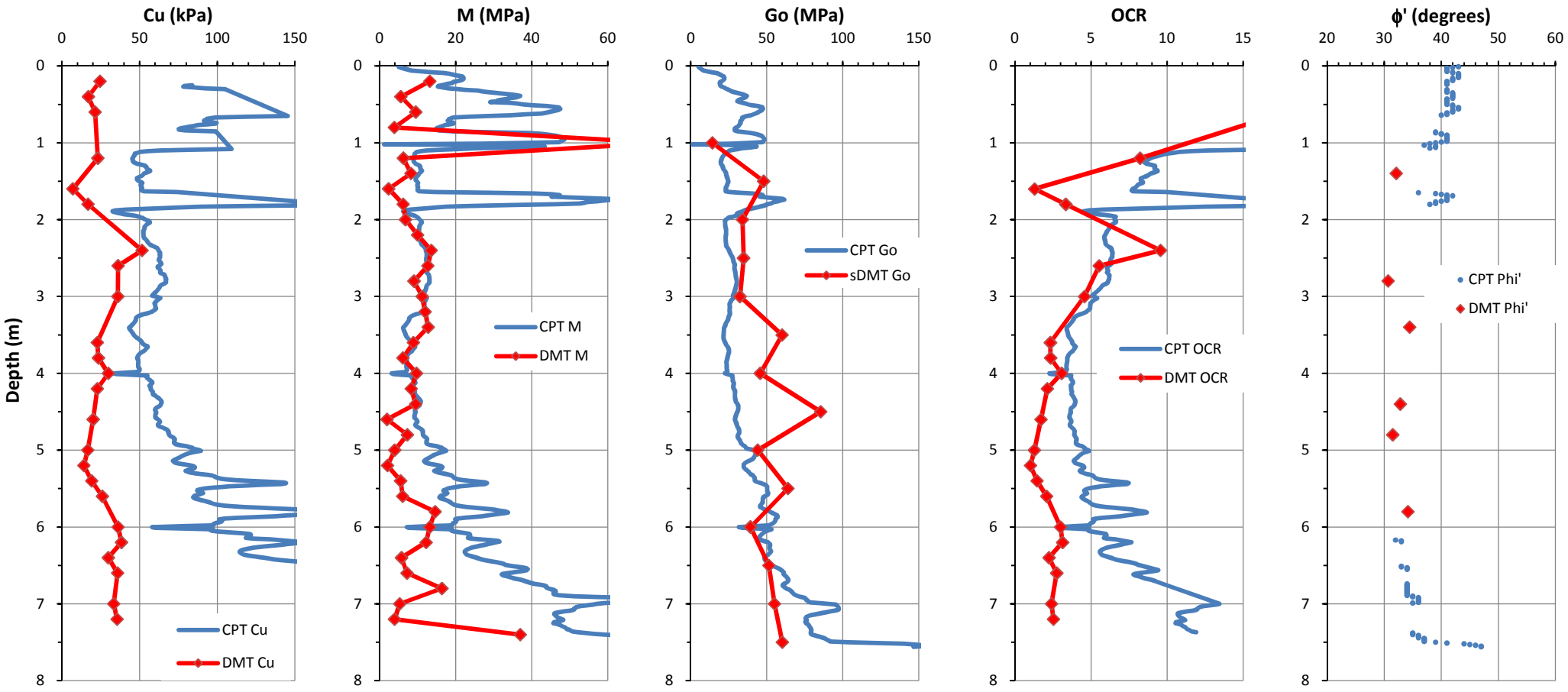

DMT correlations based on Marchetti (1980) and TC16 (2001) using Marchetti Elab software

CPT corelations based on Robertson (2009a) and Kulhawy & Mayne (1990) using CPeT-IT software

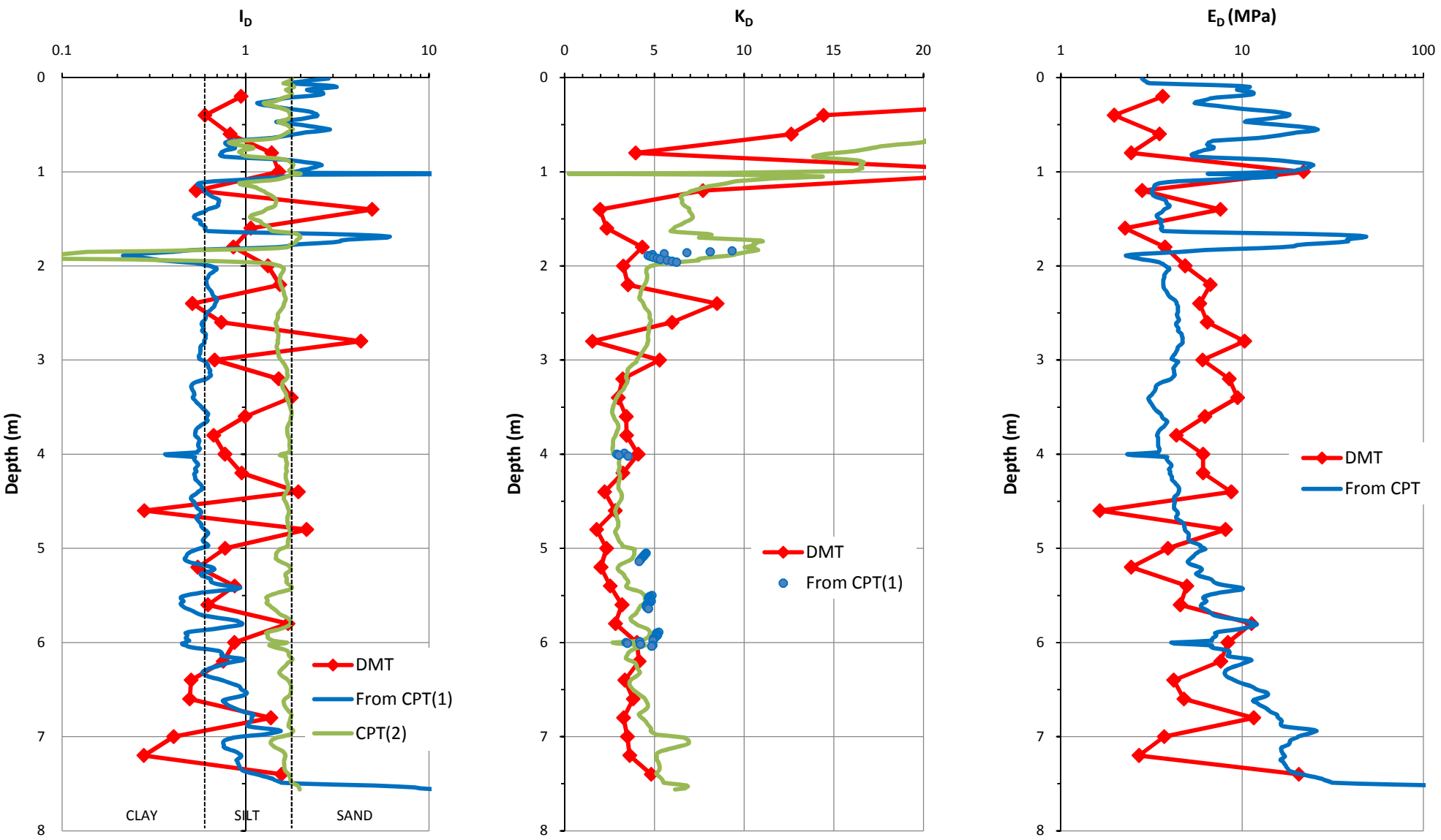

CPT(1): $I_D = 10^{(1.67-0.67Ic)}$ (Robertson 2009b)

CPT(2): $I_D = 2.0-0.14F_r$ (Mayne & Liao 2004)

CPT(1): $K_D = 0.3(Qt)^{0.95} + 1.05$, for Ic>2.95

CPT(2): $K_D = 0.144Qt/[10^{(1.67-0.67Ic)}]$

(Robertson 2009b)

CPT: $E_D = 5\ Qt\ \sigma'_{vo}$

(Robertson 2009b)

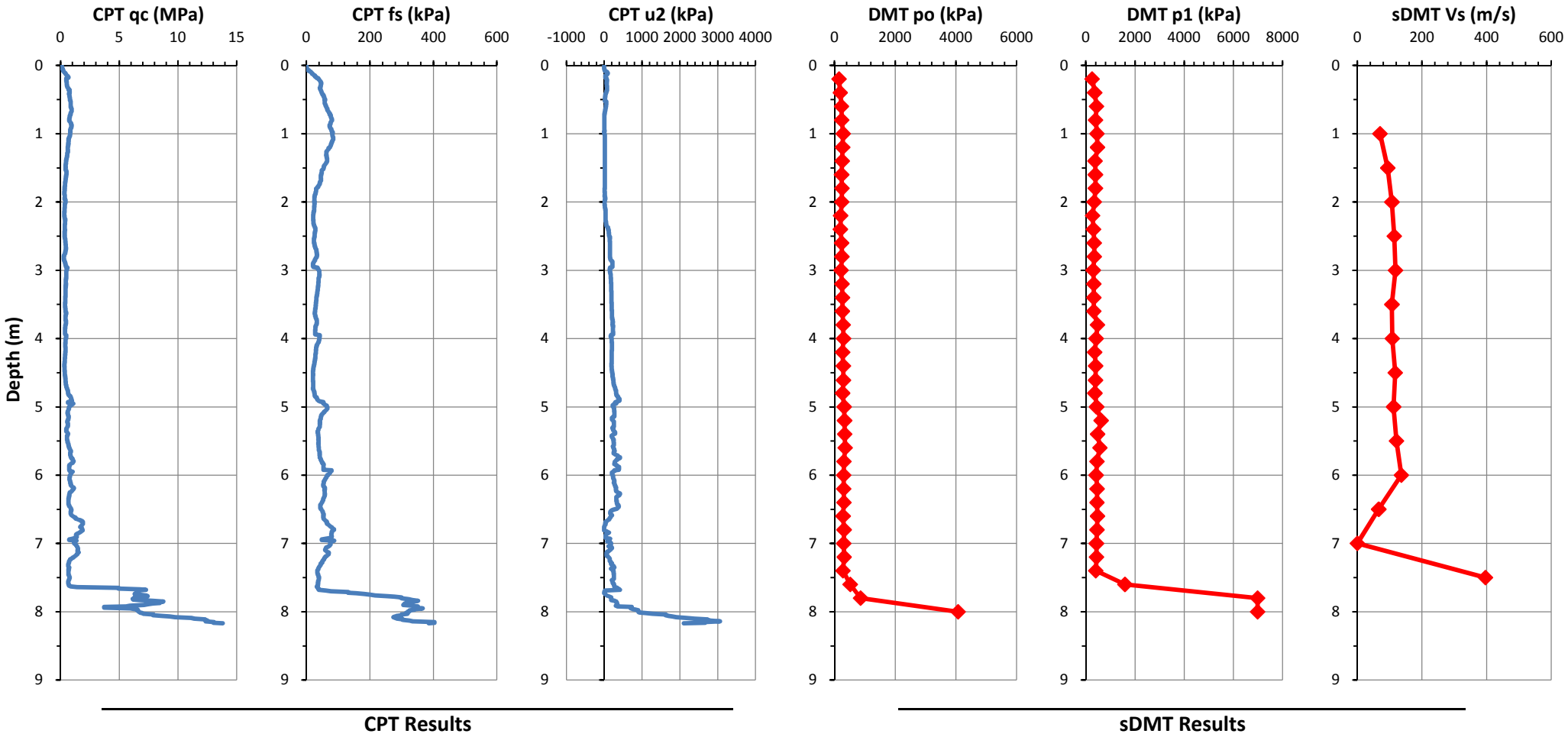
CPT qc (MPa)
CPT fs (kPa)
CPT u2 (kPa)
DMT po (kPa)
DMT p1 (kPa)
sDMT Vs (m/s)
Depth (m)
CPT Results
sDMT Results

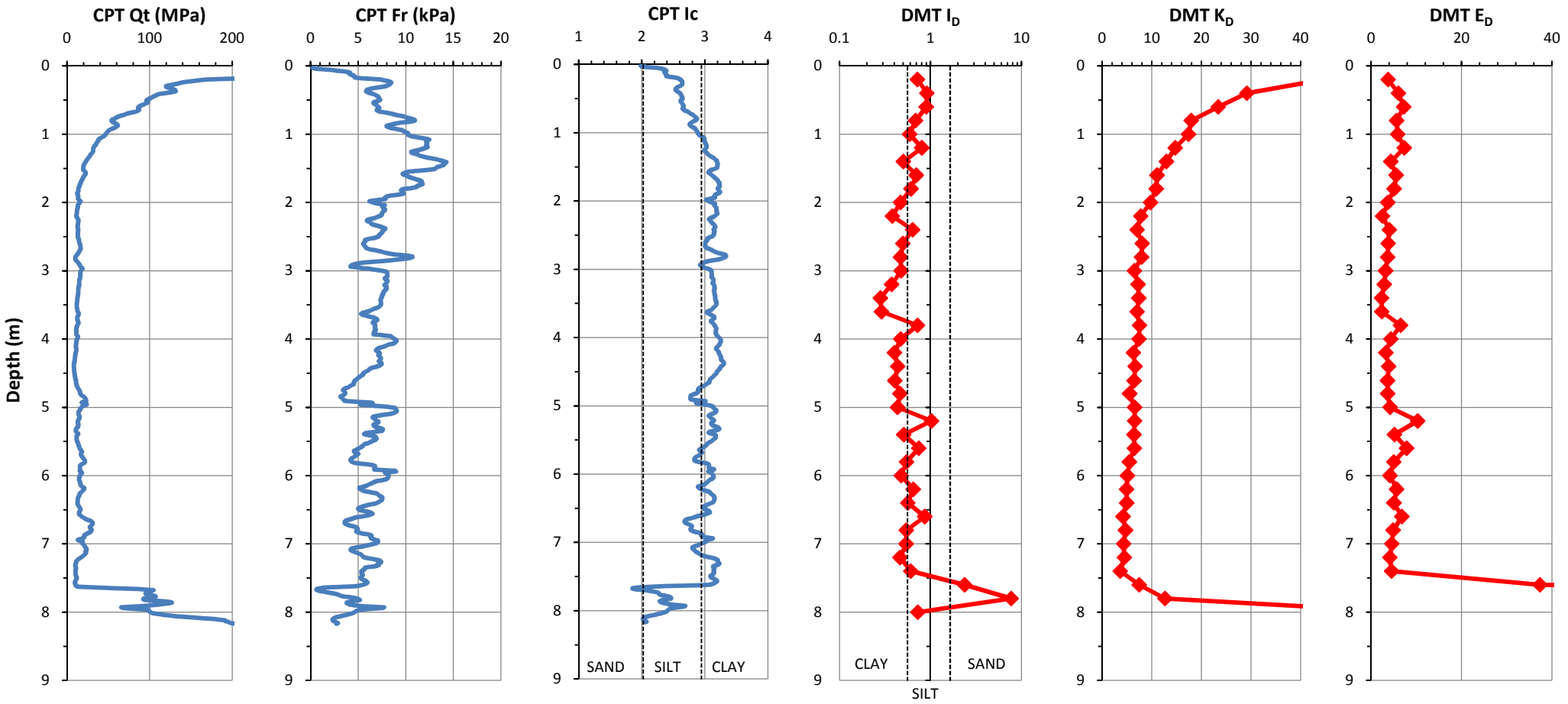
CPT Qt (MPa)
CPT Fr (kPa)
CPT Ic
DMT I_D
DMT K_D
DMT E_D
Depth (m)
SAND
SILT
CLAY
CLAY
SILT
SAND
Normalised CPT parameters and Material Index (Robertson 2009)
DMT Index Values (Marchetti 1980)

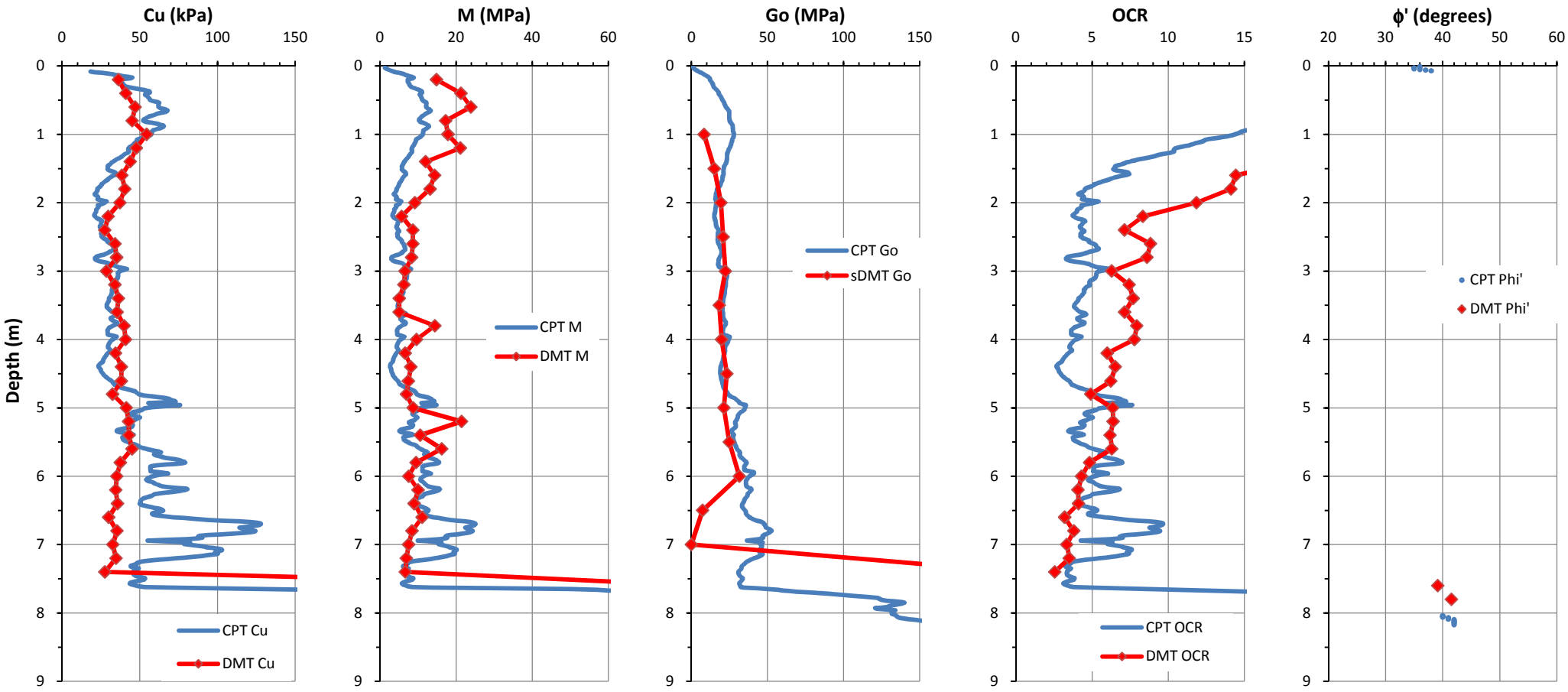

DMT correlations based on Marchetti (1980) and TC16 (2001) using Marchetti Elab software

CPT corelations based on Robertson (2009a) and Kulhawy & Mayne (1990) using CPeT-IT software

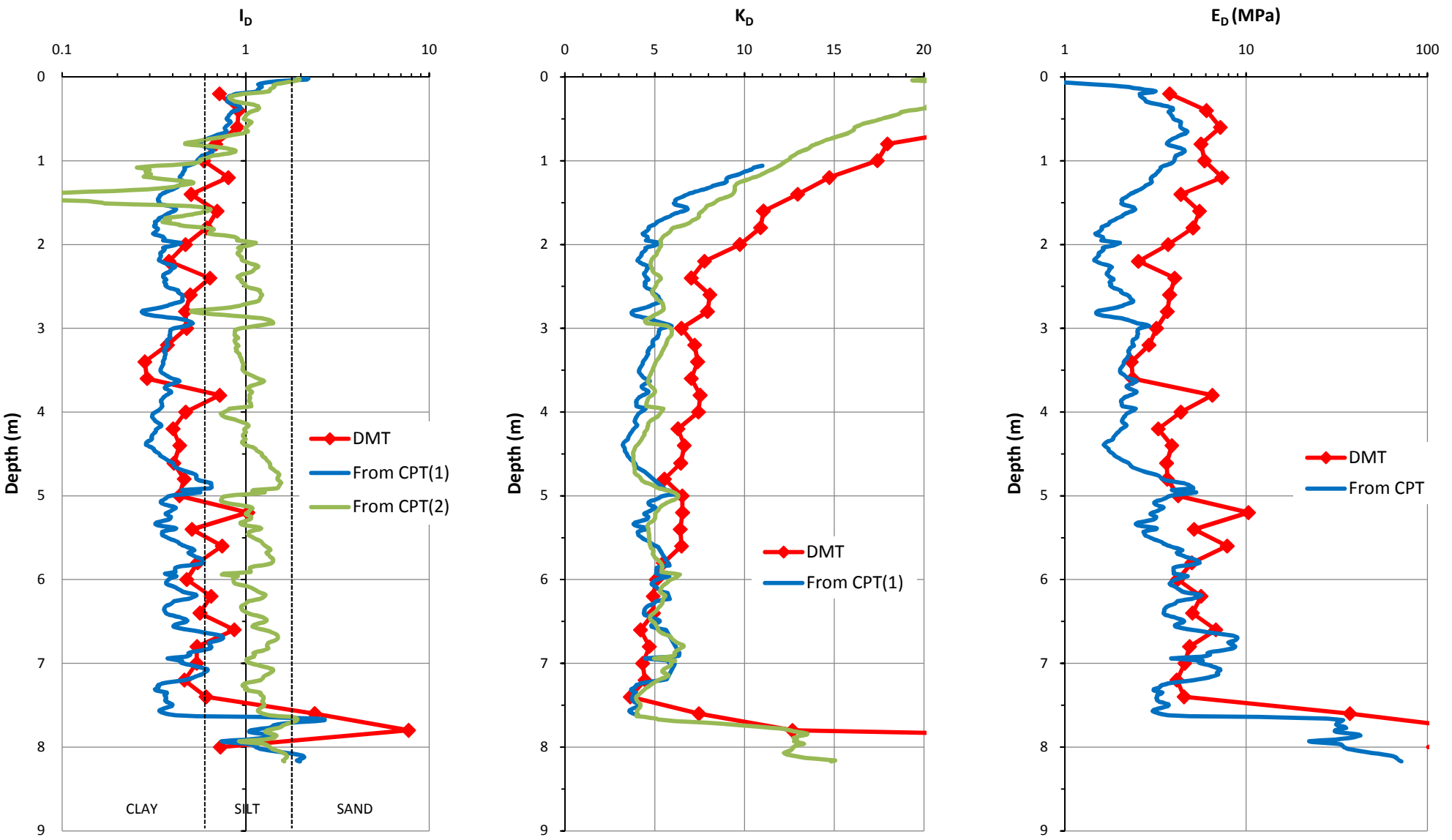

CPT(1): $I_D = 10^{(1.67-0.67Ic)}$ (Robertson 2009b)

CPT(2): $I_D = 2.0-0.14F_r$ (Mayne & Liao 2004)

CPT(1): $K_D = 0.3(Qt)^{0.95} + 1.05$, for Ic>2.95

CPT(2): $K_D = 0.144Qt/[10^{(1.67-0.67Ic)}]$

(Robertson 2009b)

CPT: $E_D = 5\ Qt\ \sigma'_{vo}$

(Robertson 2009b)

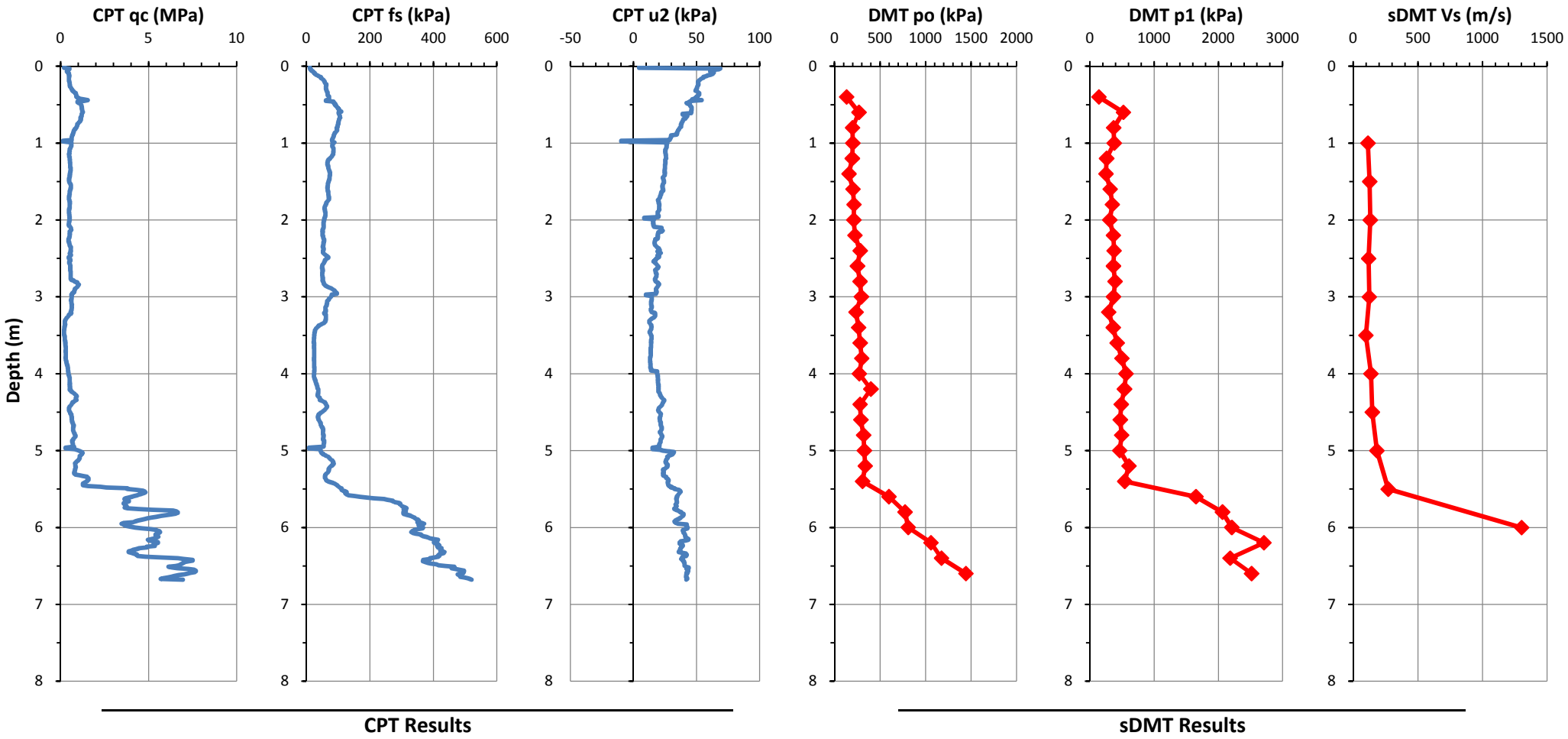

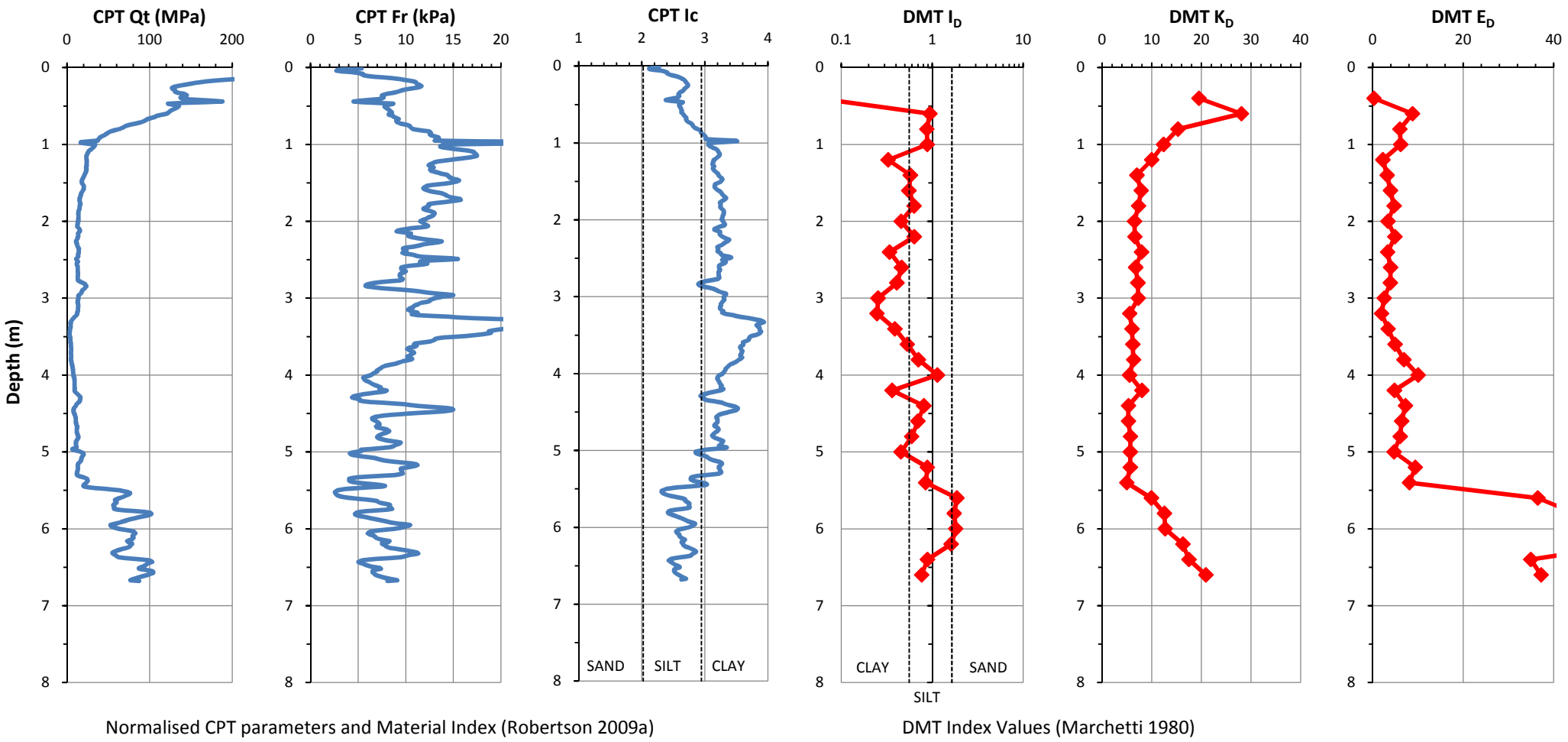

Normalised CPT parameters and Material Index (Robertson 2009a)

DMT Index Values (Marchetti 1980)

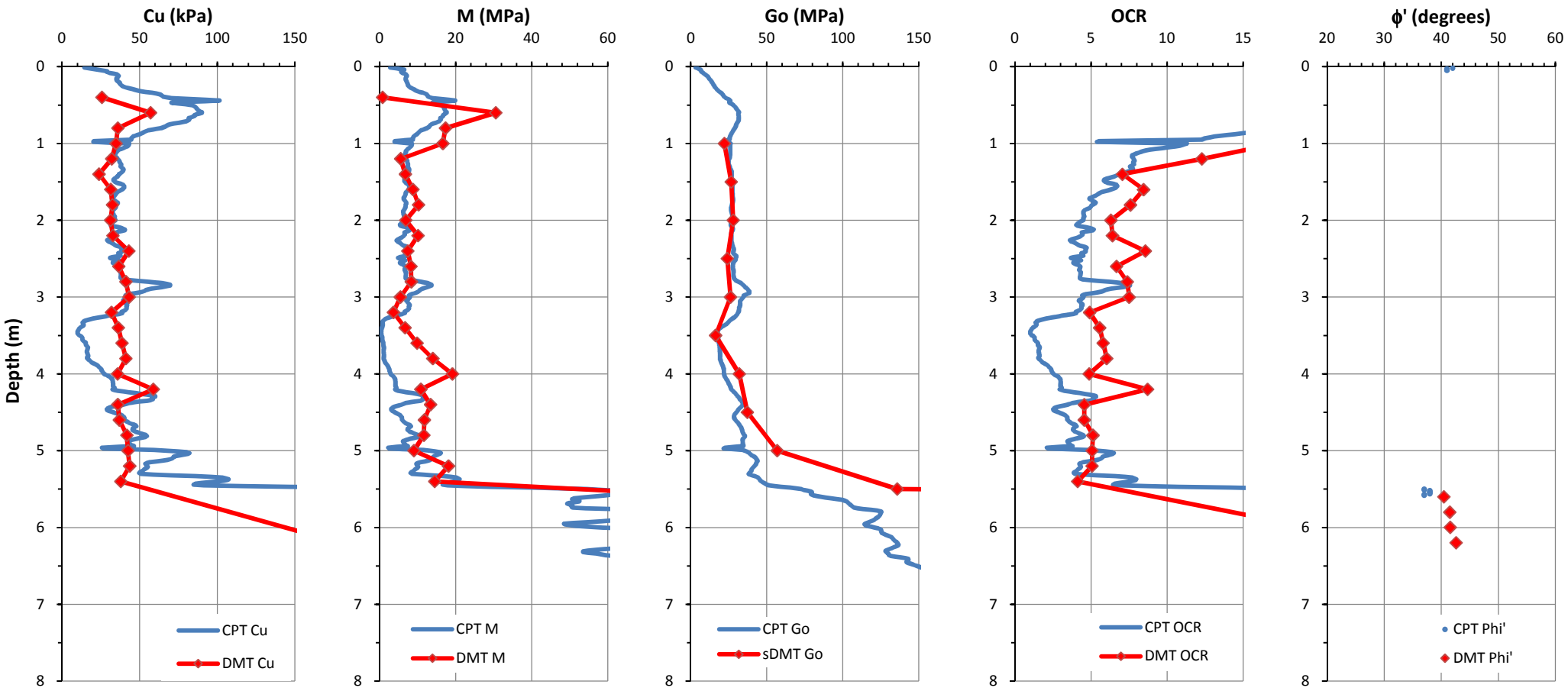

DMT correlations based on Marchetti (1980) and TC16 (2001) using Marchetti Elab software
CPT corelations based on Robertson (2009a) and Kulhawy & Mayne (1990) using CPeT-IT software

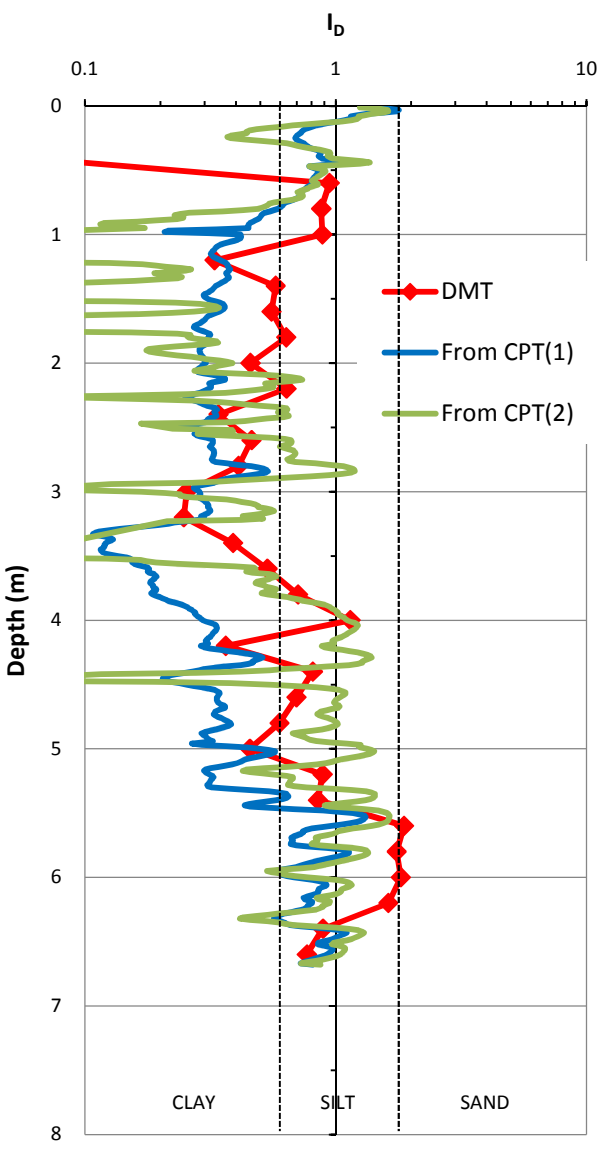

CPT(1): $I_D = 10^{(1.67-0.67Ic)}$ (Robertson 2009b)
CPT(2): $I_D = 2.0-0.14F_r$ (Mayne & Liao 2004)

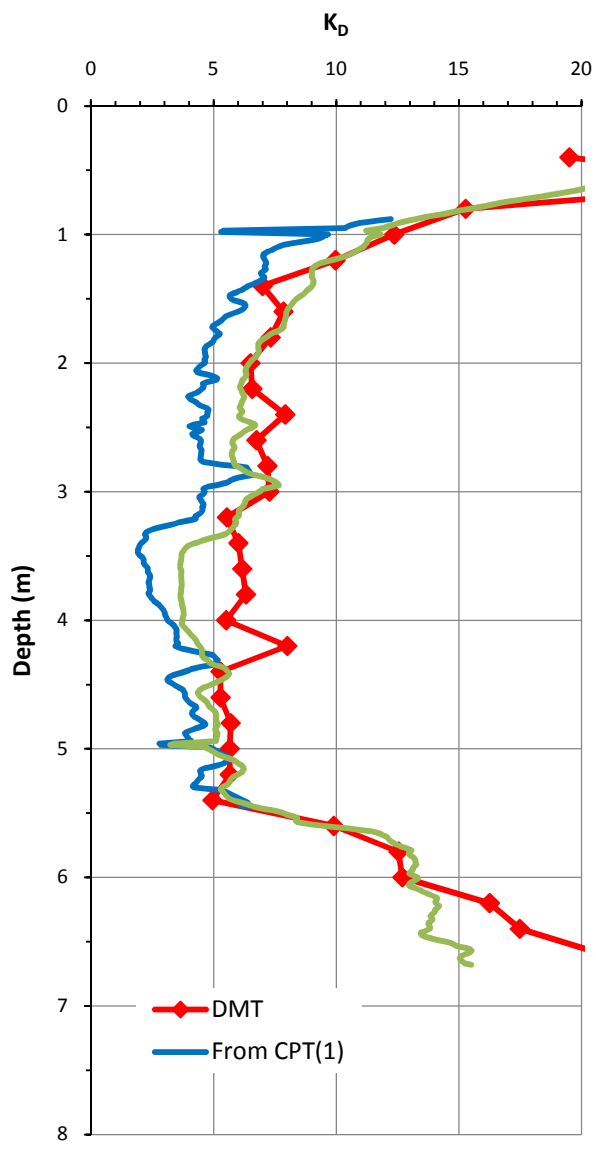

CPT(1): $K_D = 0.3(Qt)^{0.95} + 1.05$, for Ic>2.95
CPT(2): $K_D = 0.144Qt/[10^{(1.67-0.67Ic)}]$
(Robertson 2009b)

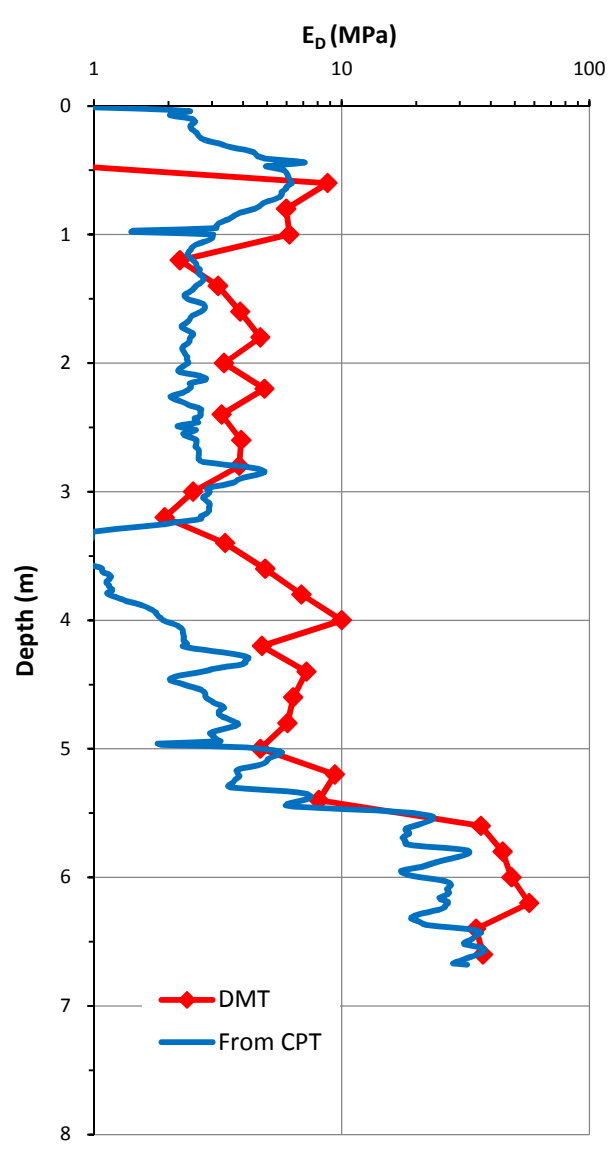

CPT: $E_D = 5\ Qt\ \sigma'_{vo}$
(Robertson 2009b)

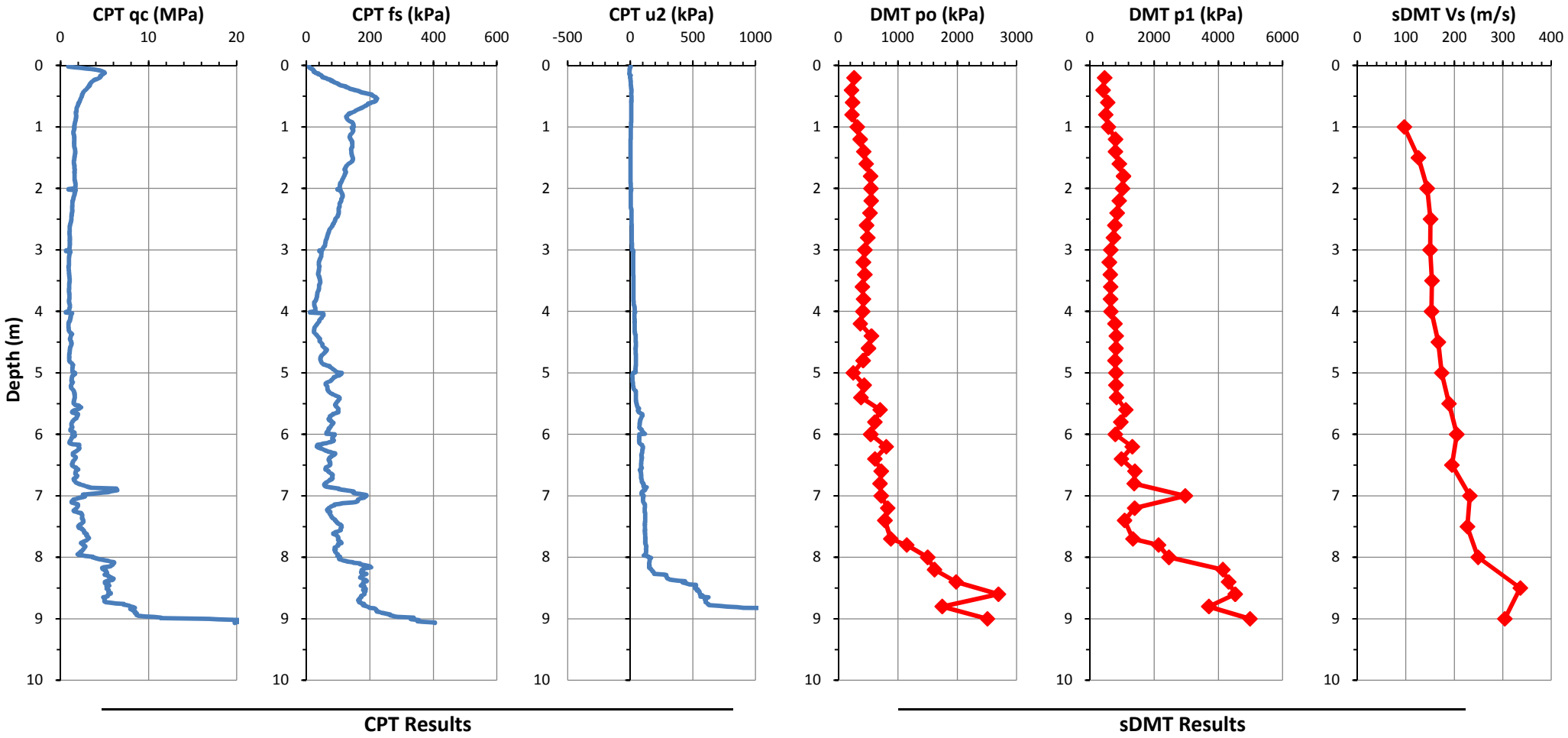
CPT qc (MPa)
CPT fs (kPa)
CPT u2 (kPa)
DMT po (kPa)
DMT p1 (kPa)
sDMT Vs (m/s)
Depth (m)
CPT Results
sDMT Results

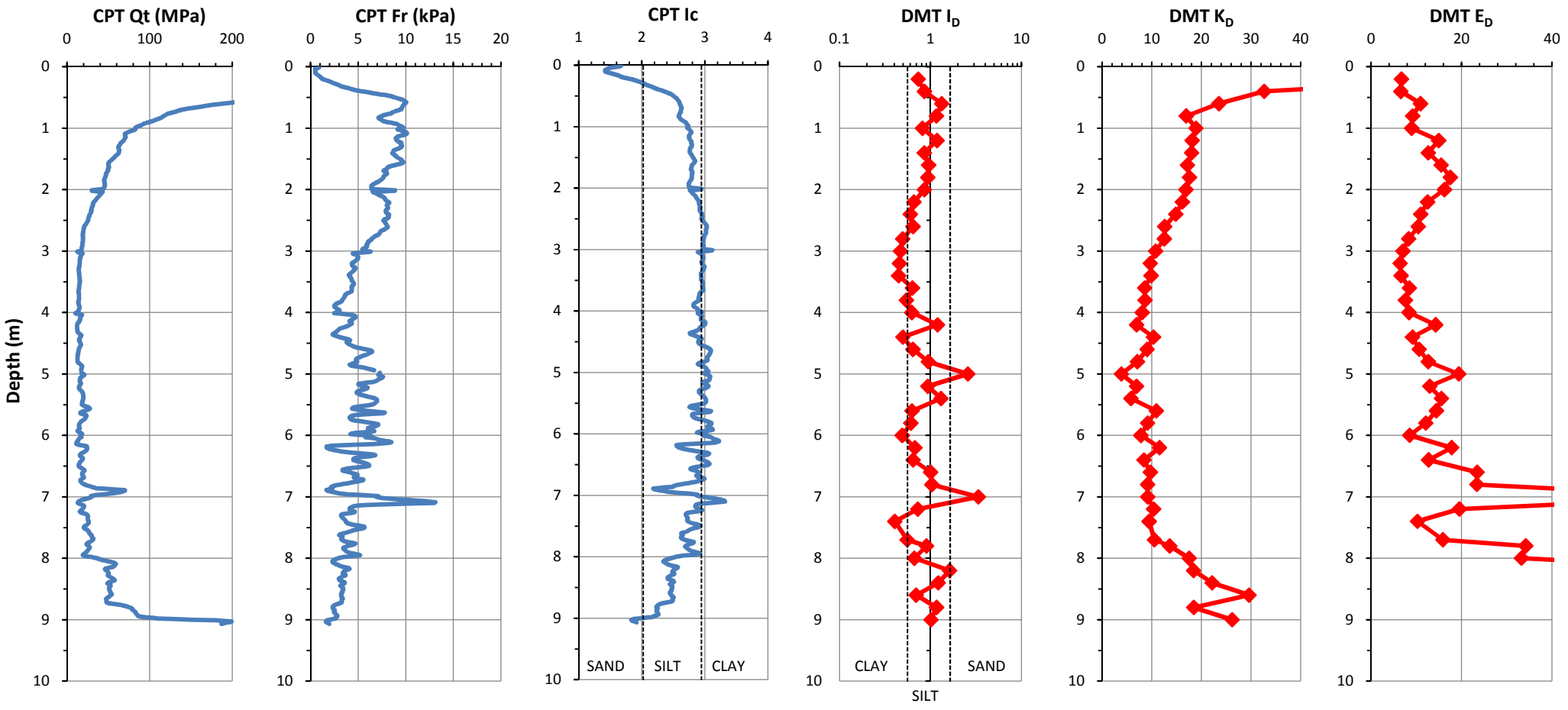
CPT Qt (MPa)
CPT Fr (kPa)
CPT Ic
DMT I_D
DMT K_D
DMT E_D
Depth (m)
SAND
SILT
CLAY
CLAY
SILT
SAND
Normalised CPT parameters and Material Index (Robertson 2009a)
DMT Index Values (Marchetti 1980)

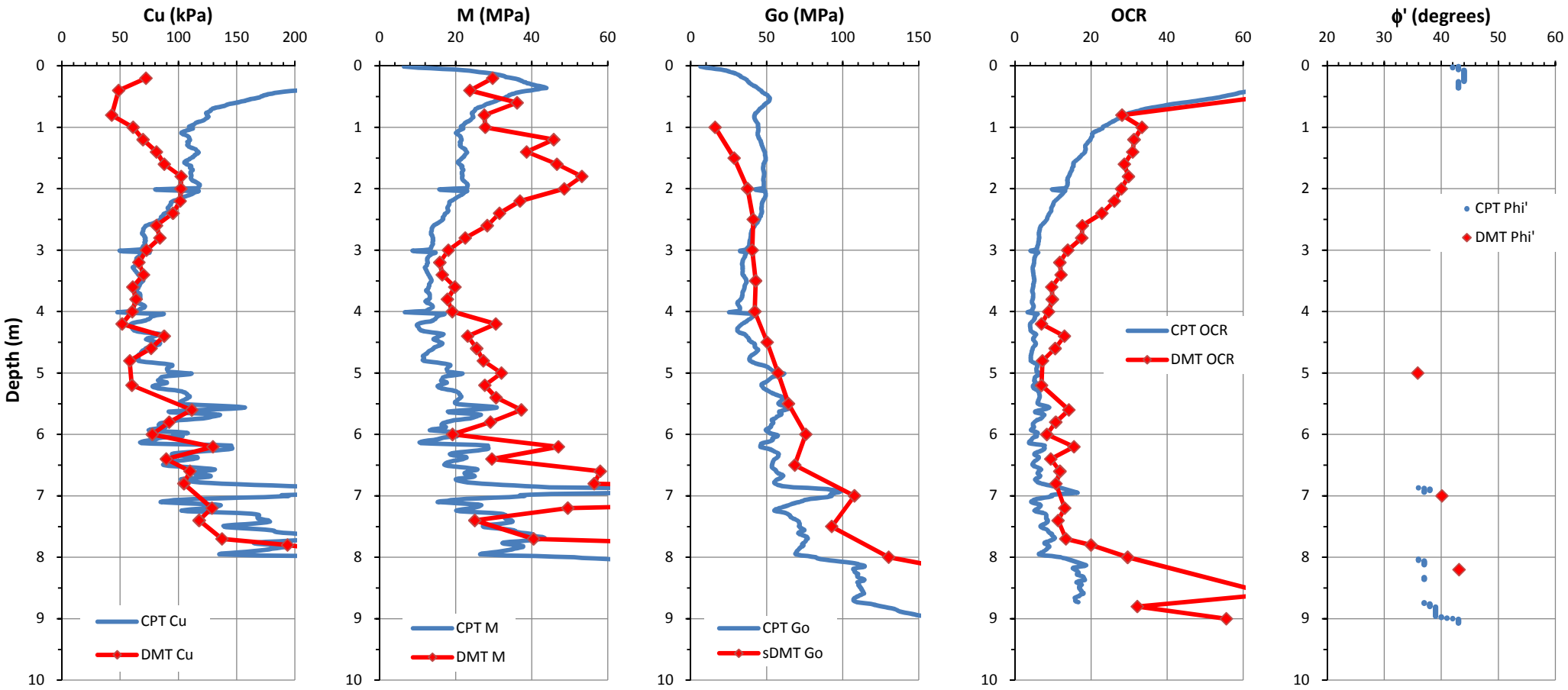

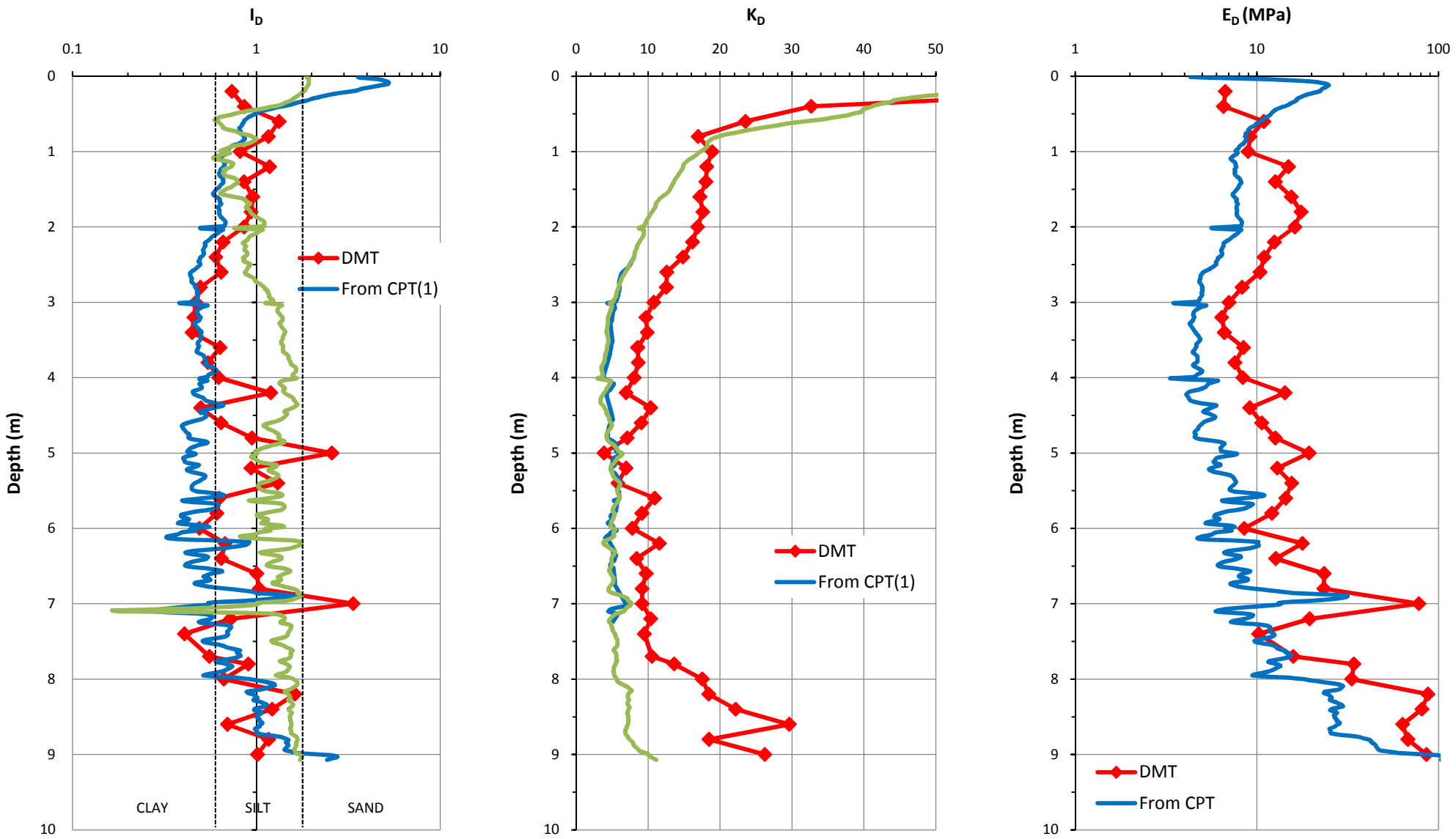

CPT(1): $I_D = 10^{(1.67-0.67Ic)}$ (Robertson 2009b)
CPT(2): $I_D = 2.0-0.14F_r$ (Mayne & Liao 2004)

CPT(1): $K_D = 0.3(Qt)^{0.95} + 1.05$, for Ic>2.95
CPT(2): $K_D = 0.144Qt/[10^{(1.67-0.67Ic)}]$
(Robertson 2009b)

CPT: $E_D = 5\ Qt\ \sigma'_{vo}$
(Robertson 2009b)

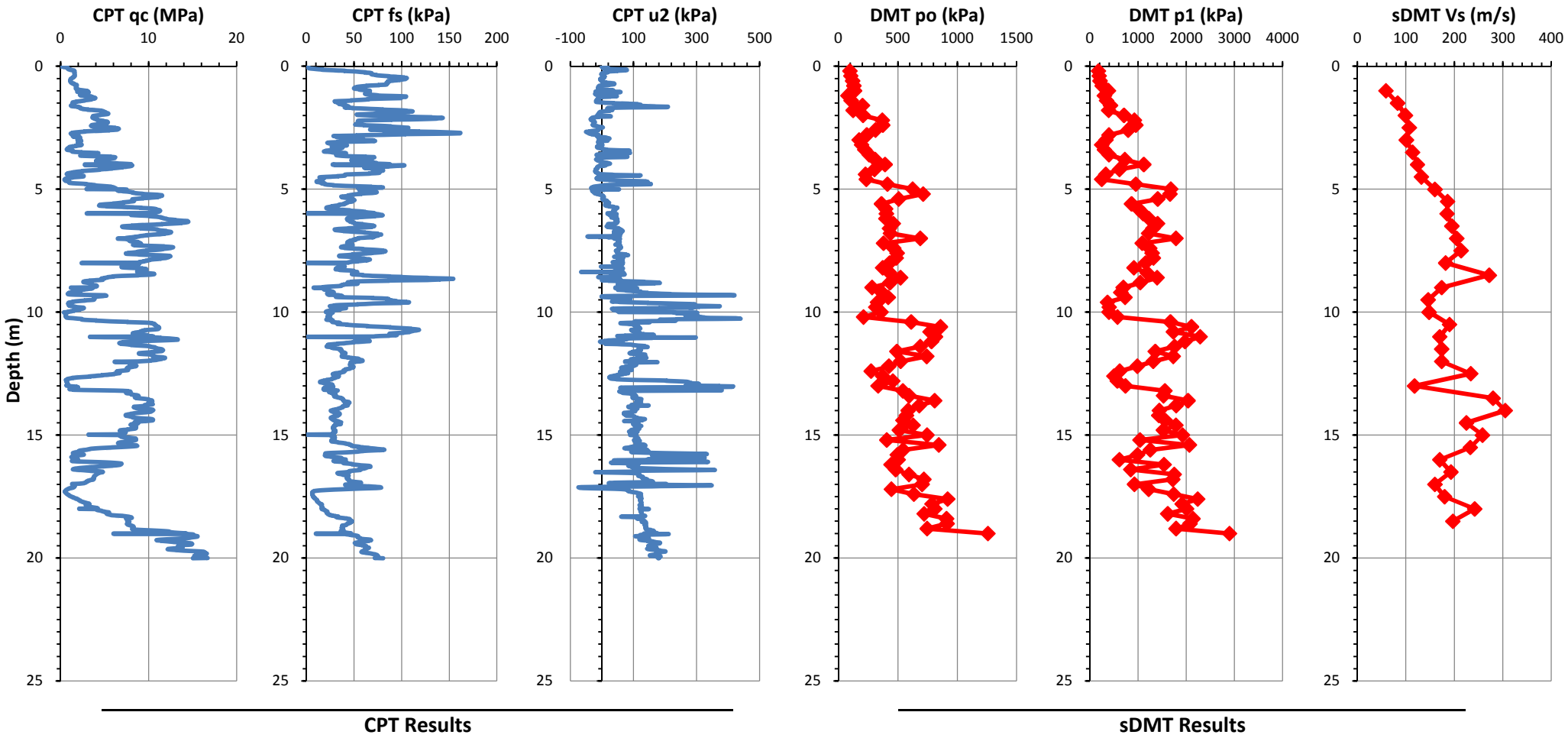
CPT qc (MPa)
0
10
20
CPT fs (kPa)
0
50
100
150
200
CPT u2 (kPa)
-100
100
300
500
DMT po (kPa)
0
500
1000
1500
DMT p1 (kPa)
0
1000
2000
3000
4000
sDMT Vs (m/s)
0
100
200
300
400
Depth (m)
0
5
10
15
20
25
CPT Results
sDMT Results

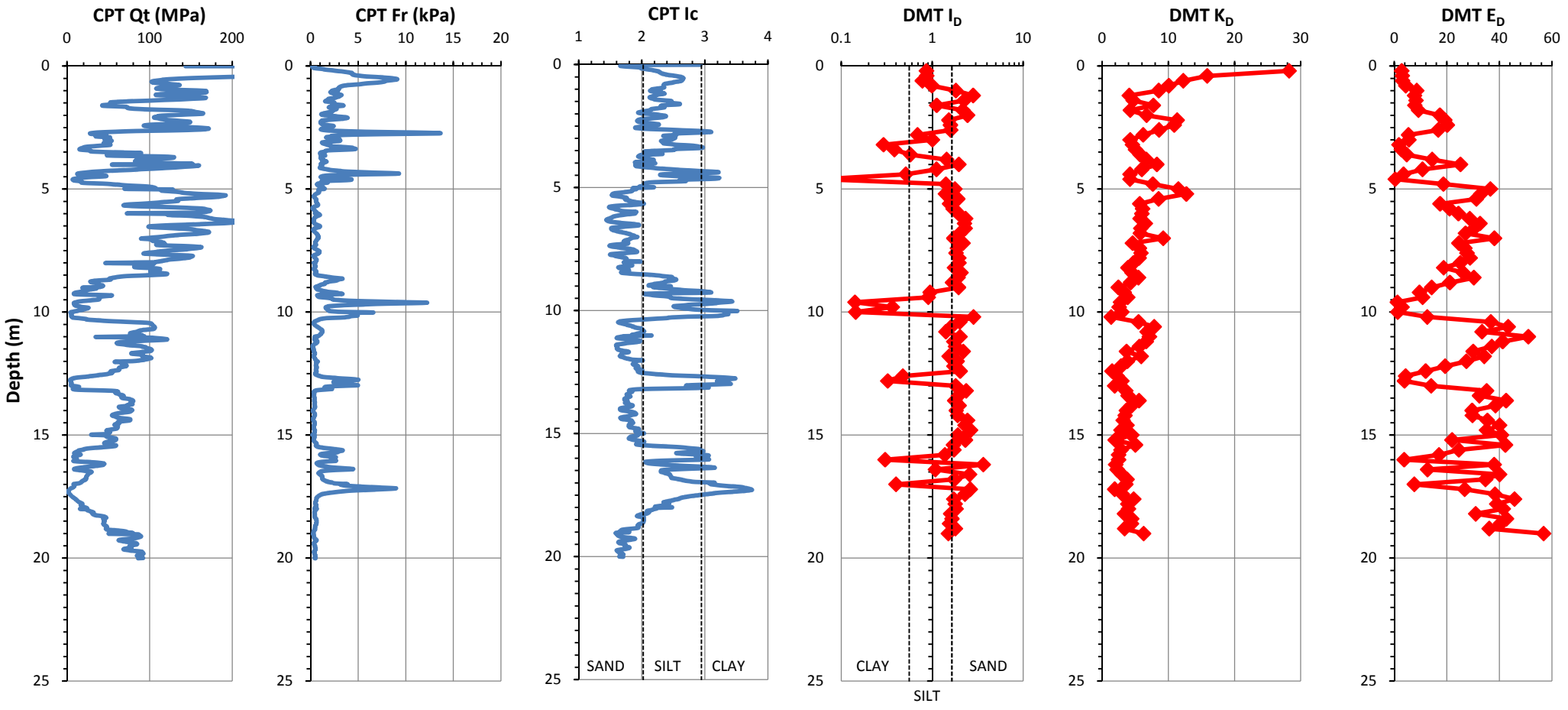
CPT Qt (MPa)
0
100
200
CPT Fr (kPa)
0
5
10
15
20
CPT Ic
1
2
3
4
DMT I_D
0.1
1
10
DMT K_D
0
10
20
30
DMT E_D
0
20
40
60
Depth (m)
0
5
10
15
20
25
SAND
SILT
CLAY
CLAY
SILT
SAND
Normalised CPT parameters and Material Index (Robertson 2009a)
DMT Index Values (Marchetti 1980)

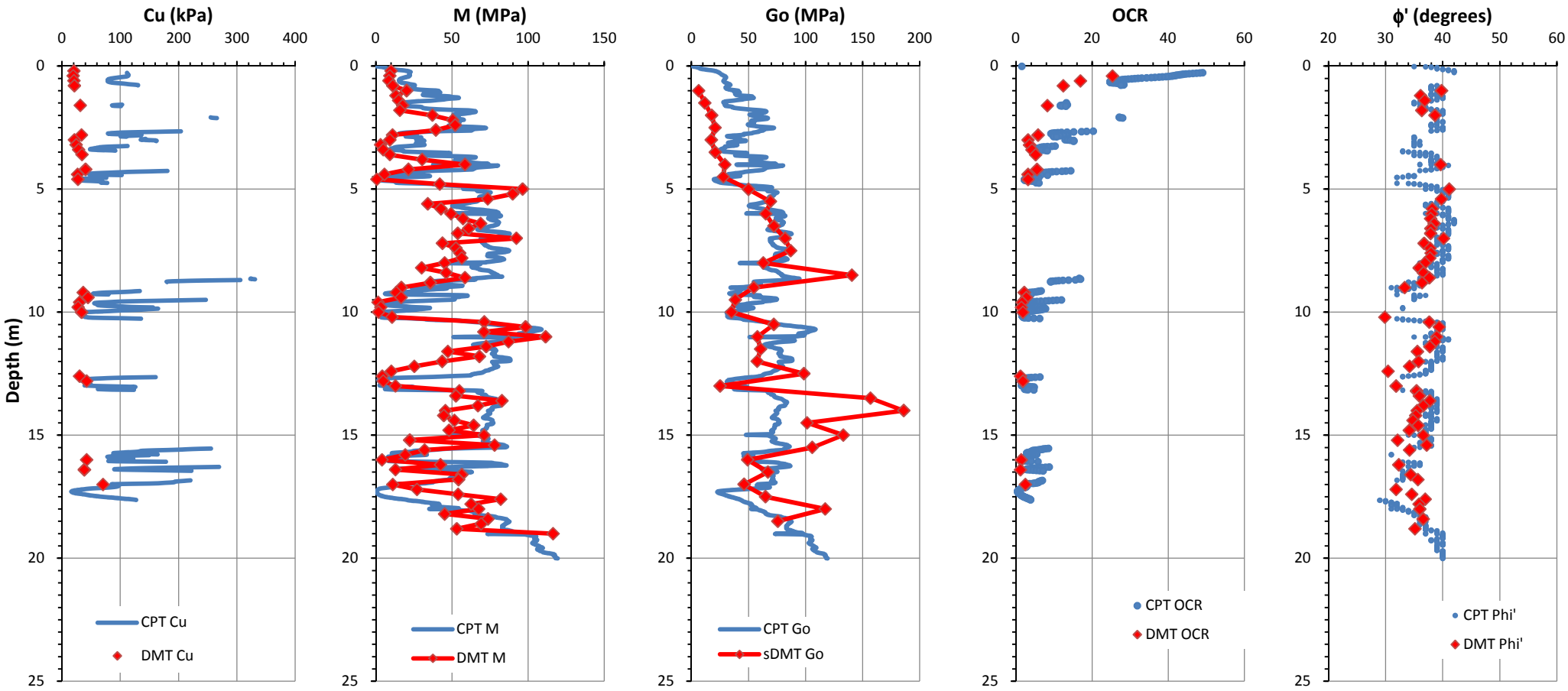

DMT correlations based on Marchetti (1980) and TC16 (2001) using Marchetti Elab software

CPT corelations based on Robertson (2009a) and Kulhawy & Mayne (1990) using CPeT-IT software

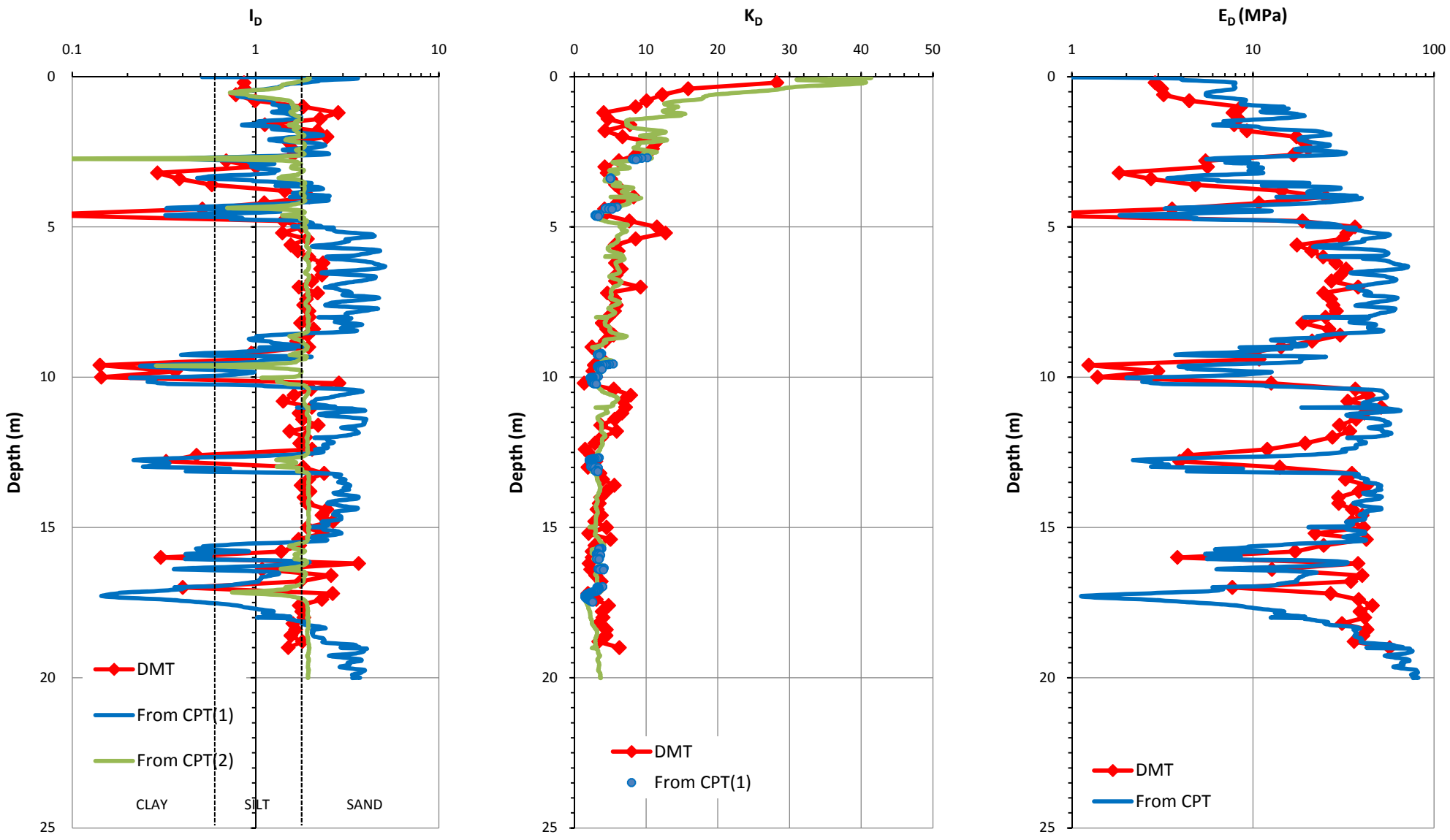

CPT(1): $I_D = 10^{(1.67-0.67Ic)}$ (Robertson 2009b)

CPT(2): $I_D = 2.0-0.14F_r$ (Mayne & Liao 2004)

CPT(1): $K_D = 0.3(Qt)^{0.95} + 1.05$, for Ic>2.95

CPT(2): $K_D = 0.144Qt/[10^{(1.67-0.67Ic)}]$

(Robertson 2009b)

CPT: $E_D = 5\ Qt\ \sigma'_{vo}$

(Robertson 2009b)

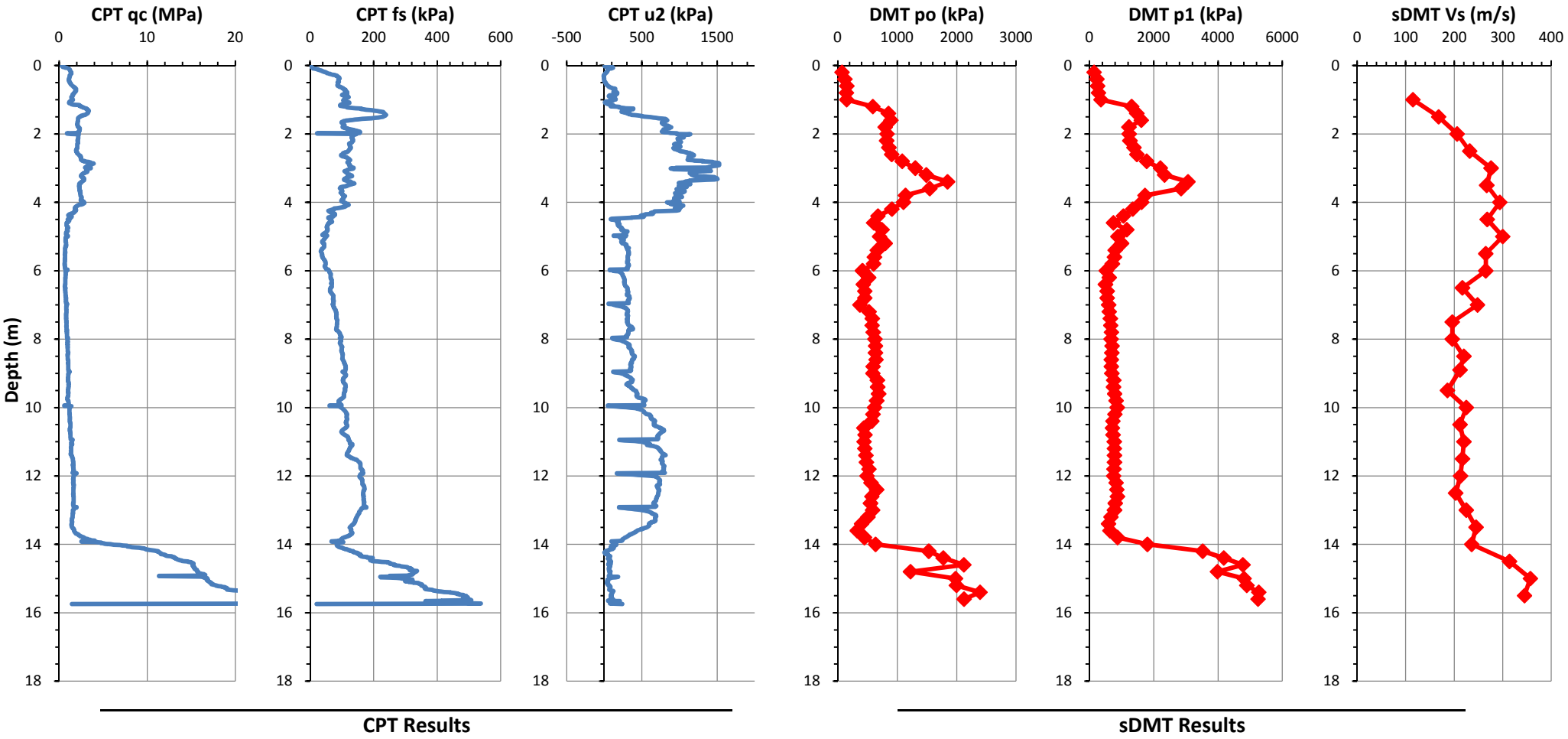
CPT qc (MPa)
CPT fs (kPa)
CPT u2 (kPa)
DMT po (kPa)
DMT p1 (kPa)
sDMT Vs (m/s)
Depth (m)
CPT Results
sDMT Results

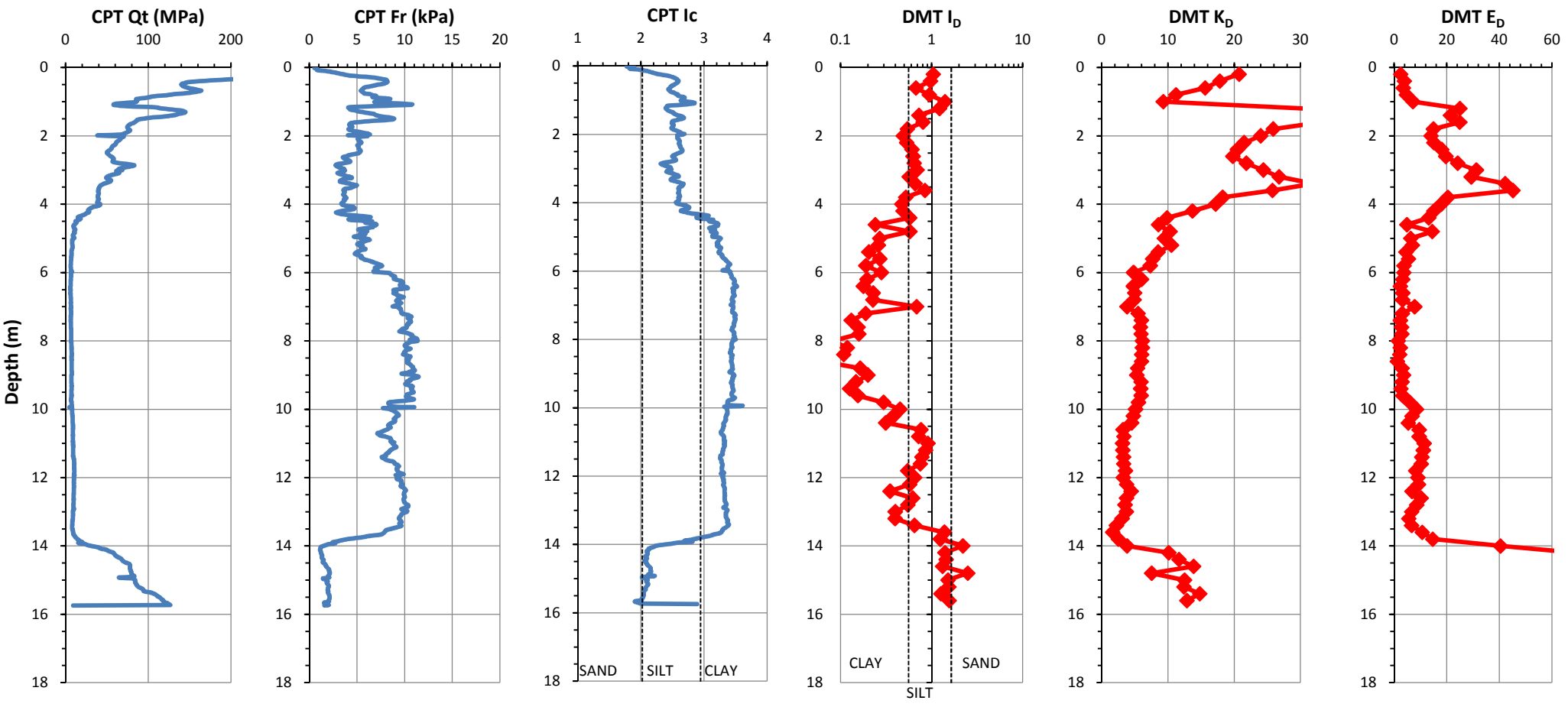
CPT Qt (MPa)
CPT Fr (kPa)
CPT Ic
DMT I_D
DMT K_D
DMT E_D
Depth (m)
SAND
SILT
CLAY
CLAY
SILT
SAND
Normalised CPT parameters and Material Index (Robertson 2009a)
DMT Index Values (Marchetti 1980)

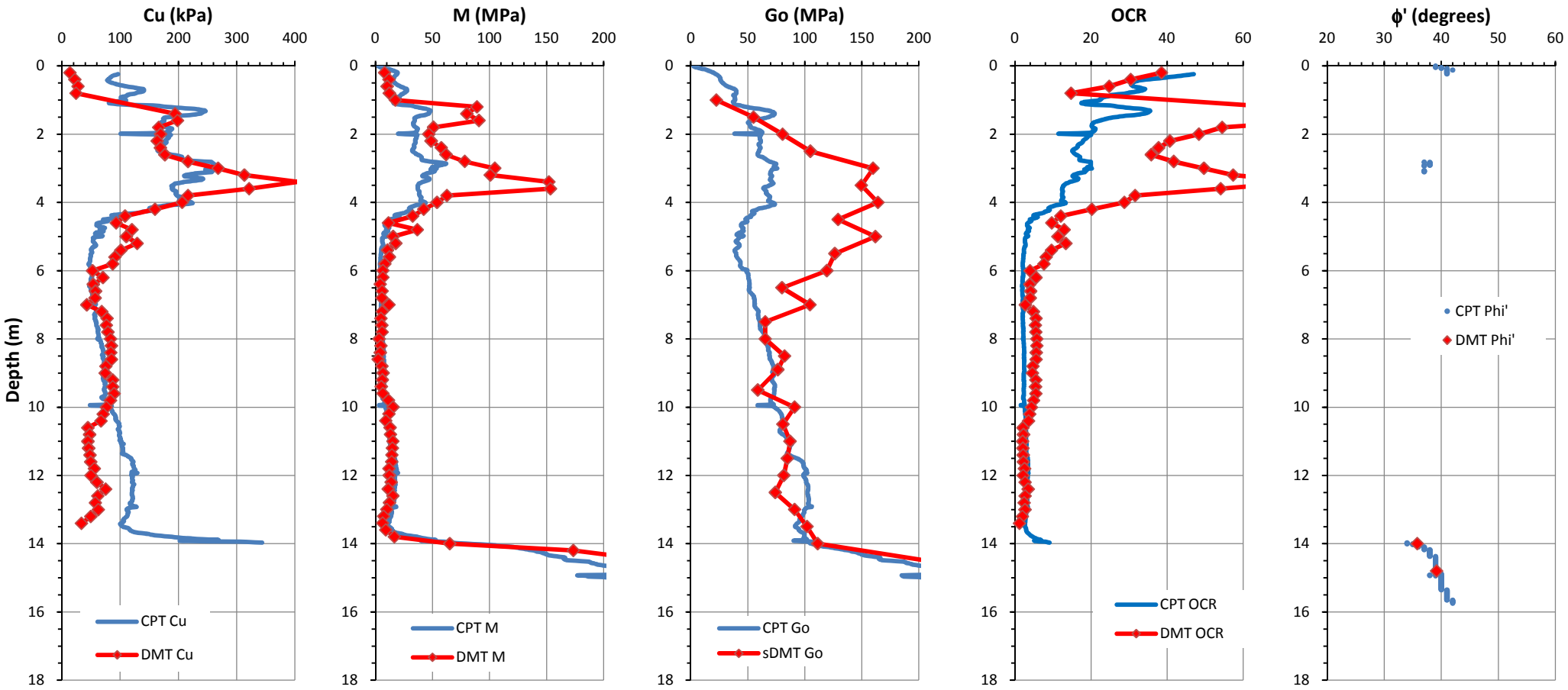

DMT correlations based on Marchetti (1980) and TC16 (2001) using Marchetti Elab software

CPT corelations based on Robertson (2009a) and Kulhawy & Mayne (1990) using CPeT-IT software

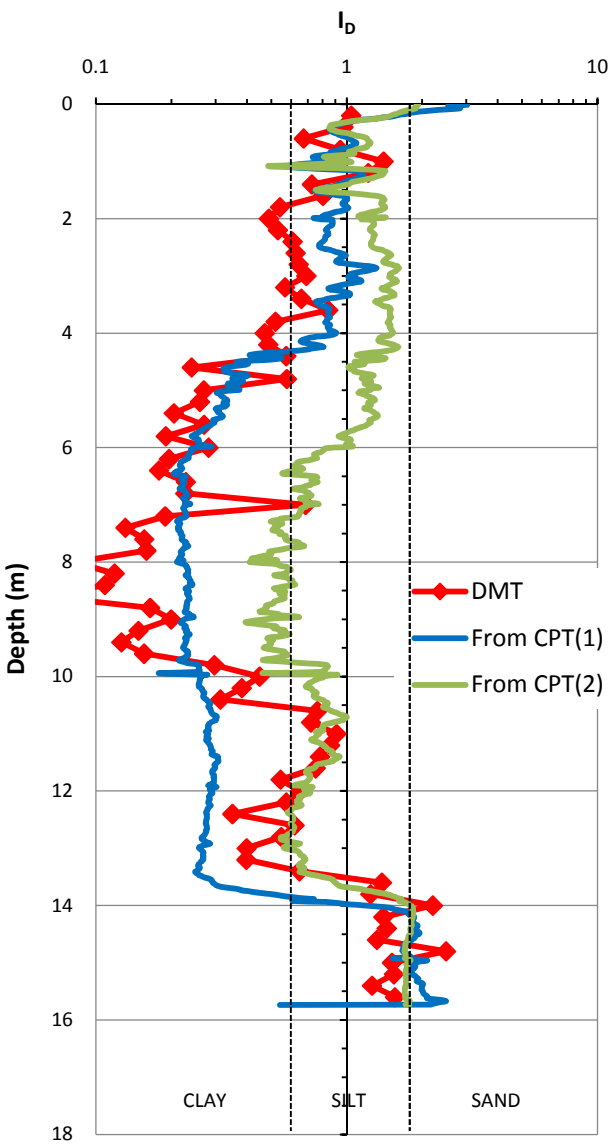

CPT(1): $I_D = 10^{(1.67-0.67Ic)}$ (Robertson 2009b)

CPT(2): $I_D = 2.0-0.14F_r$ (Mayne & Liao 2004)

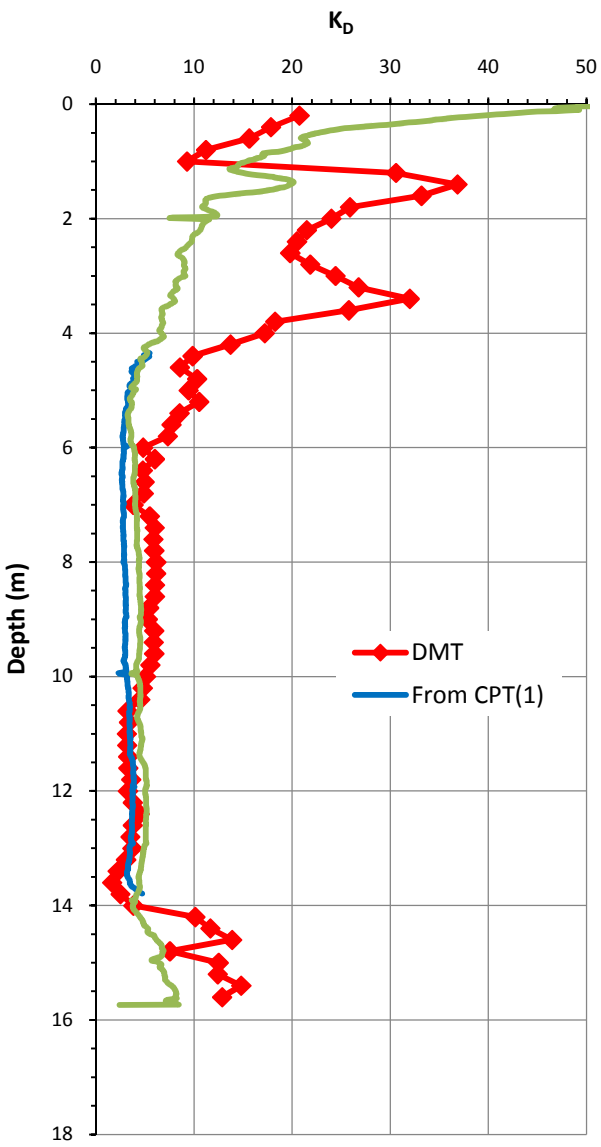

CPT(1): $K_D = 0.3(Qt)^{0.95} + 1.05$, for Ic>2.95

CPT(2): $K_D = 0.144Qt/[10^{(1.67-0.67Ic)}]$

(Robertson 2009b)

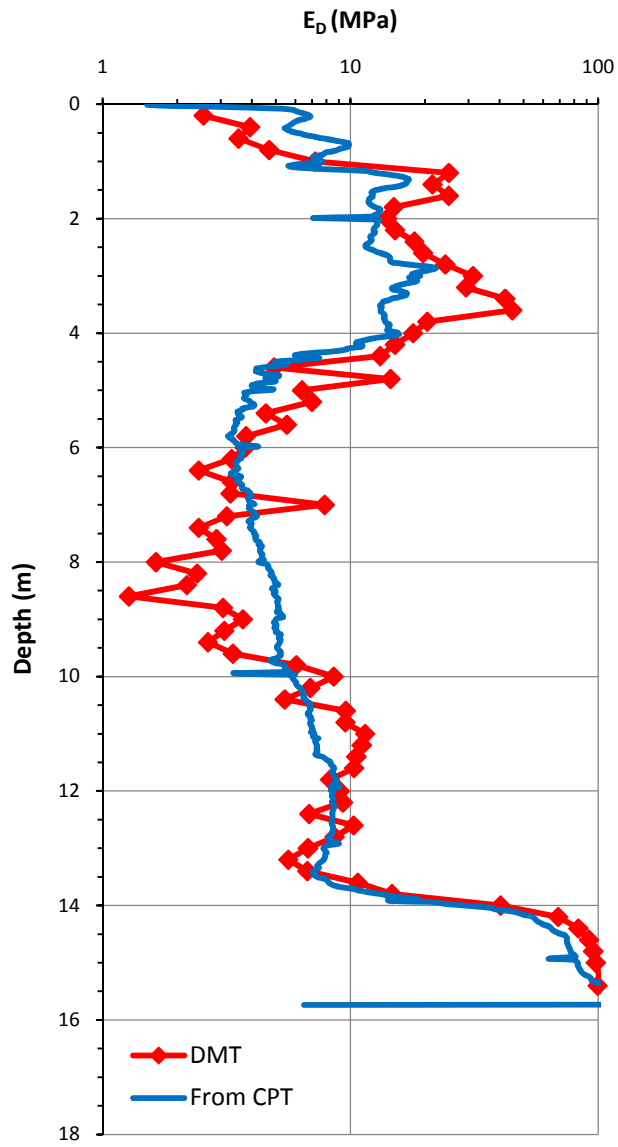

CPT: $E_D = 5\ Qt\ \sigma'_{vo}$

(Robertson 2009b)

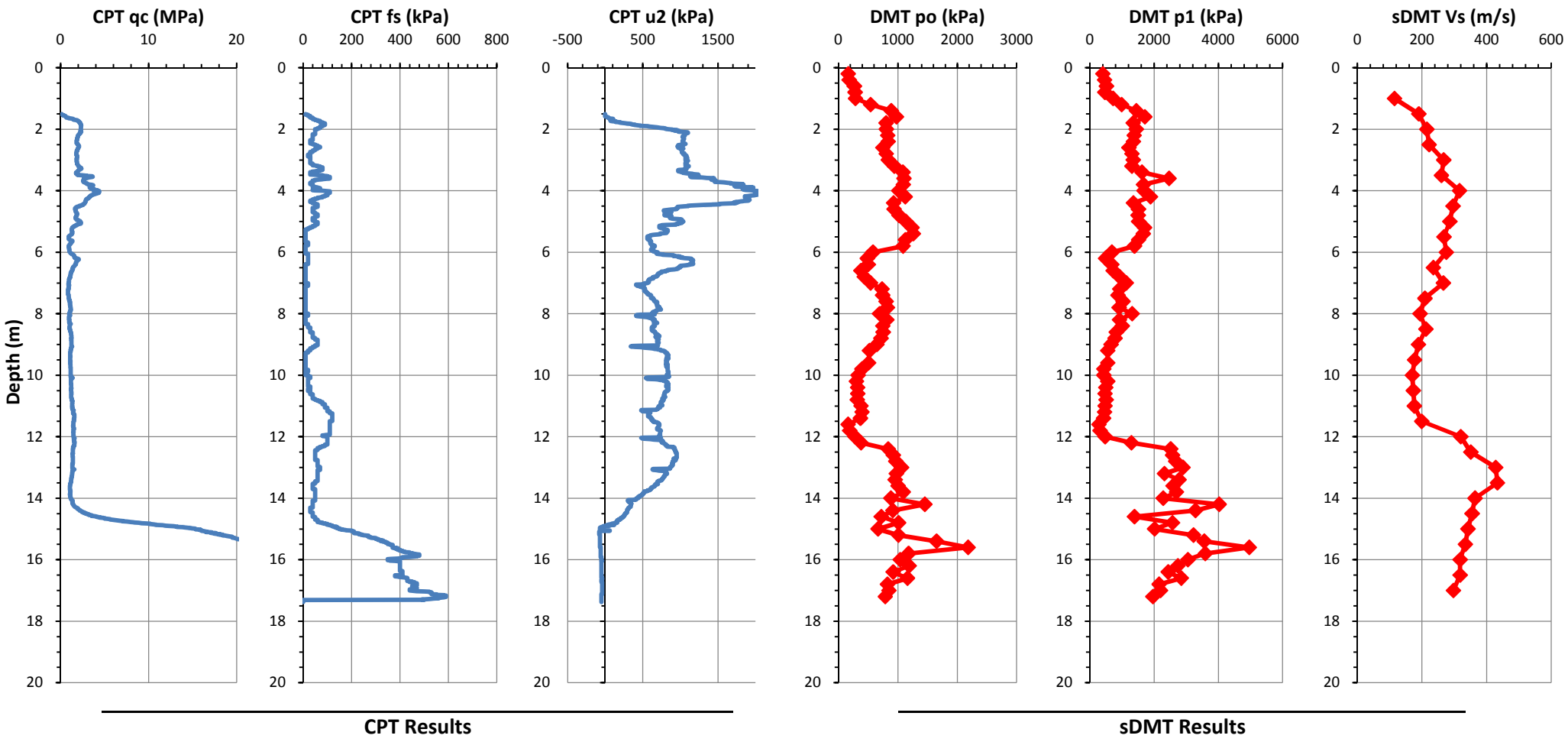
CPT qc (MPa)
CPT fs (kPa)
CPT u2 (kPa)
DMT po (kPa)
DMT p1 (kPa)
sDMT Vs (m/s)
Depth (m)
CPT Results
sDMT Results

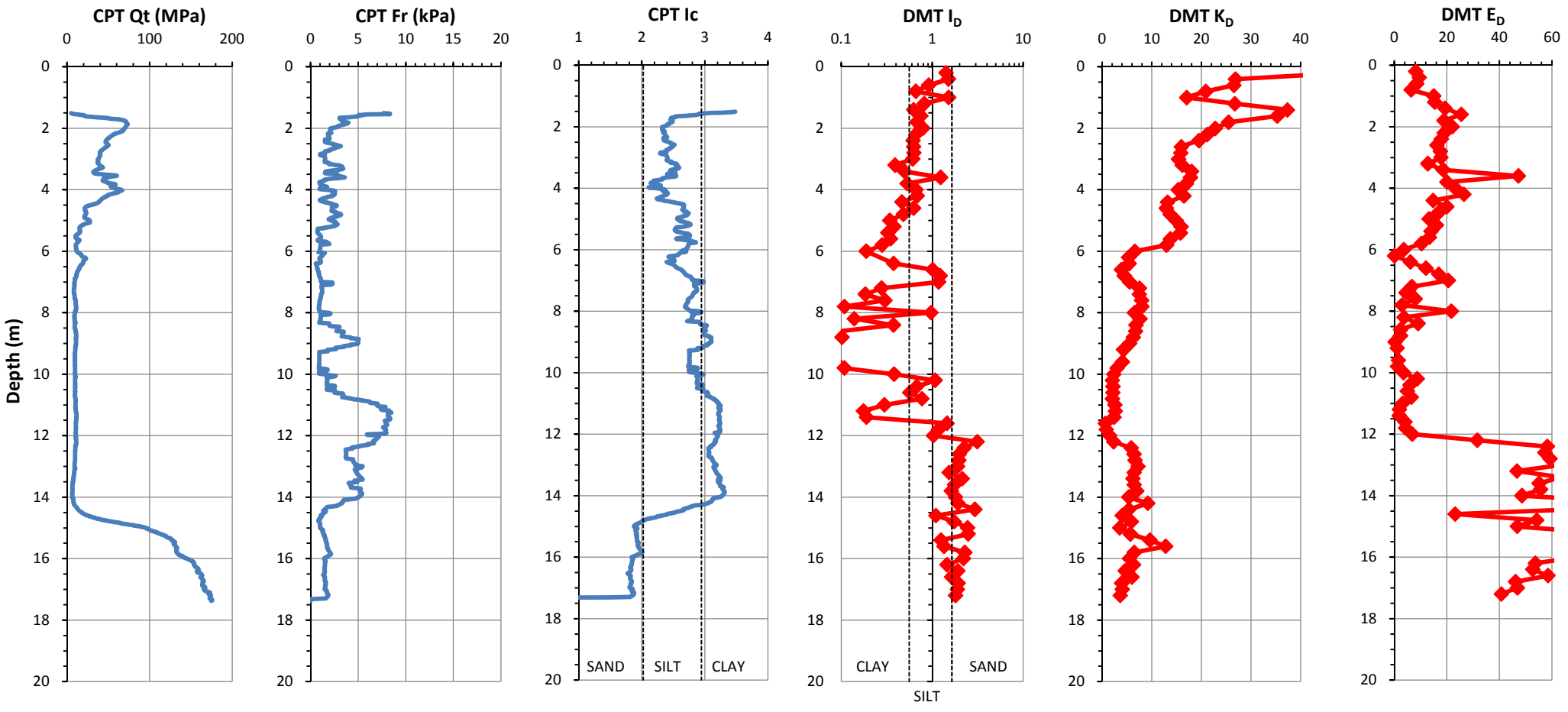
CPT Qt (MPa)
CPT Fr (kPa)
CPT Ic
DMT I_D
DMT K_D
DMT E_D
Depth (m)
SAND
SILT
CLAY
CLAY
SILT
SAND
Normalised CPT parameters and Material Index (Robertson 2009a)
DMT Index Values (Marchetti 1980)

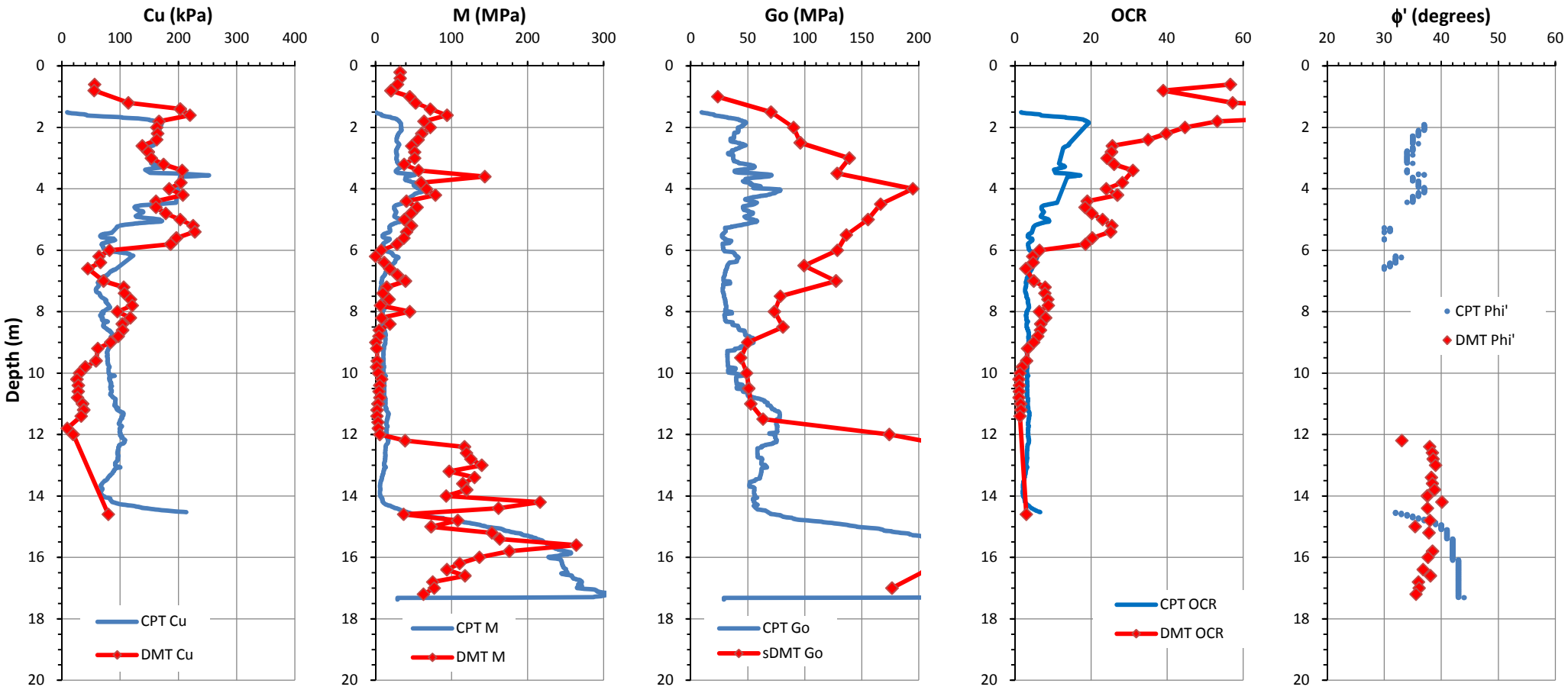

DMT correlations based on Marchetti (1980) and TC16 (2001) using Marchetti Elab software
CPT corelations based on Robertson (2009a) and Kulhawy & Mayne (1990) using CPeT-IT software

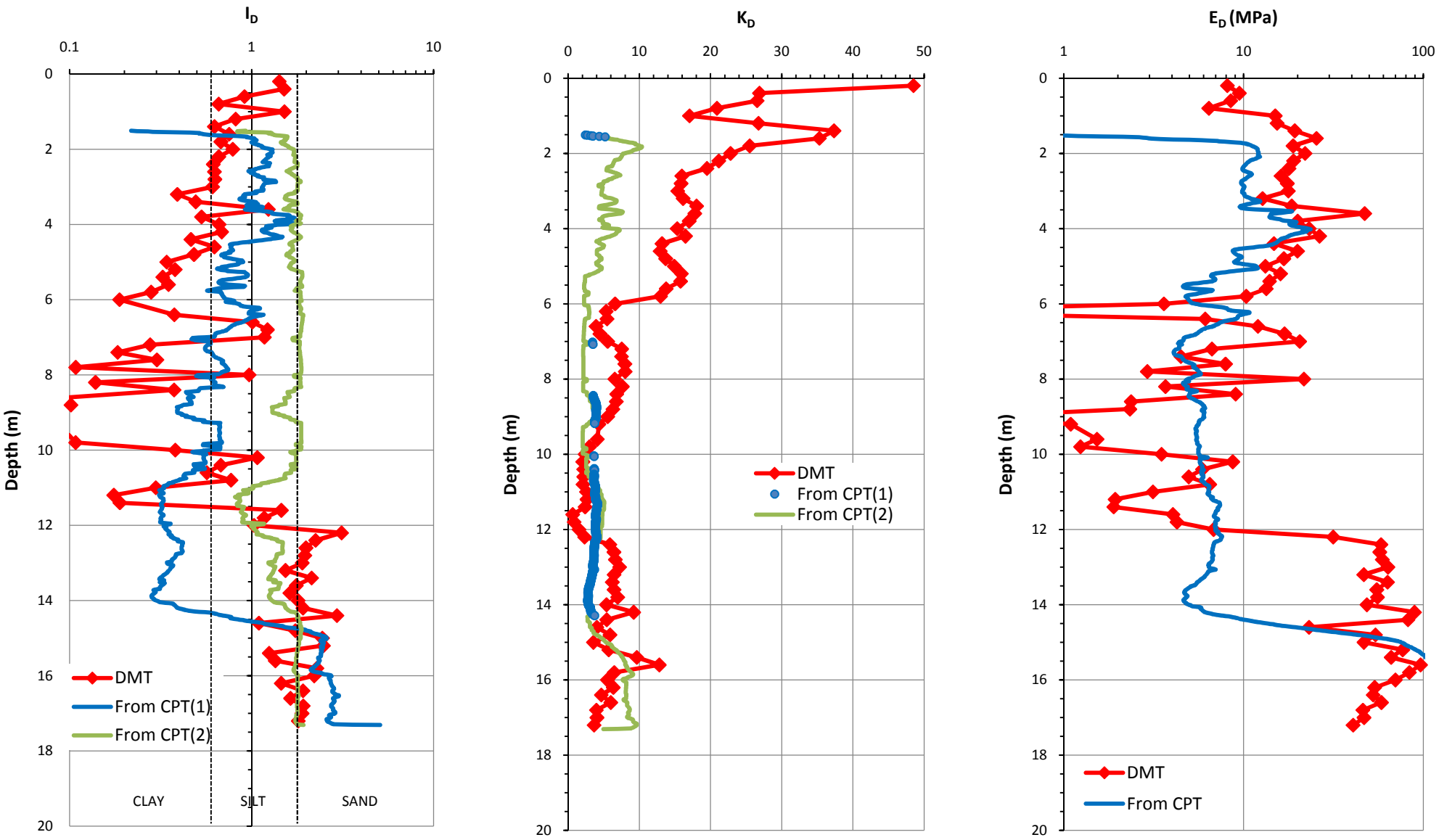

CPT(1): $I_D = 10^{(1.67-0.67Ic)}$ (Robertson 2009b)
CPT(2): $I_D = 2.0-0.14F_r$ (Mayne & Liao 2004)

CPT(1): $K_D = 0.3(Qt)^{0.95} + 1.05$, for Ic>2.95
CPT(2): $K_D = 0.144Qt/[10^{(1.67-0.67Ic)}]$
(Robertson 2009b)

CPT: $E_D = 5\ Qt\ \sigma'_{vo}$
(Robertson 2009b)

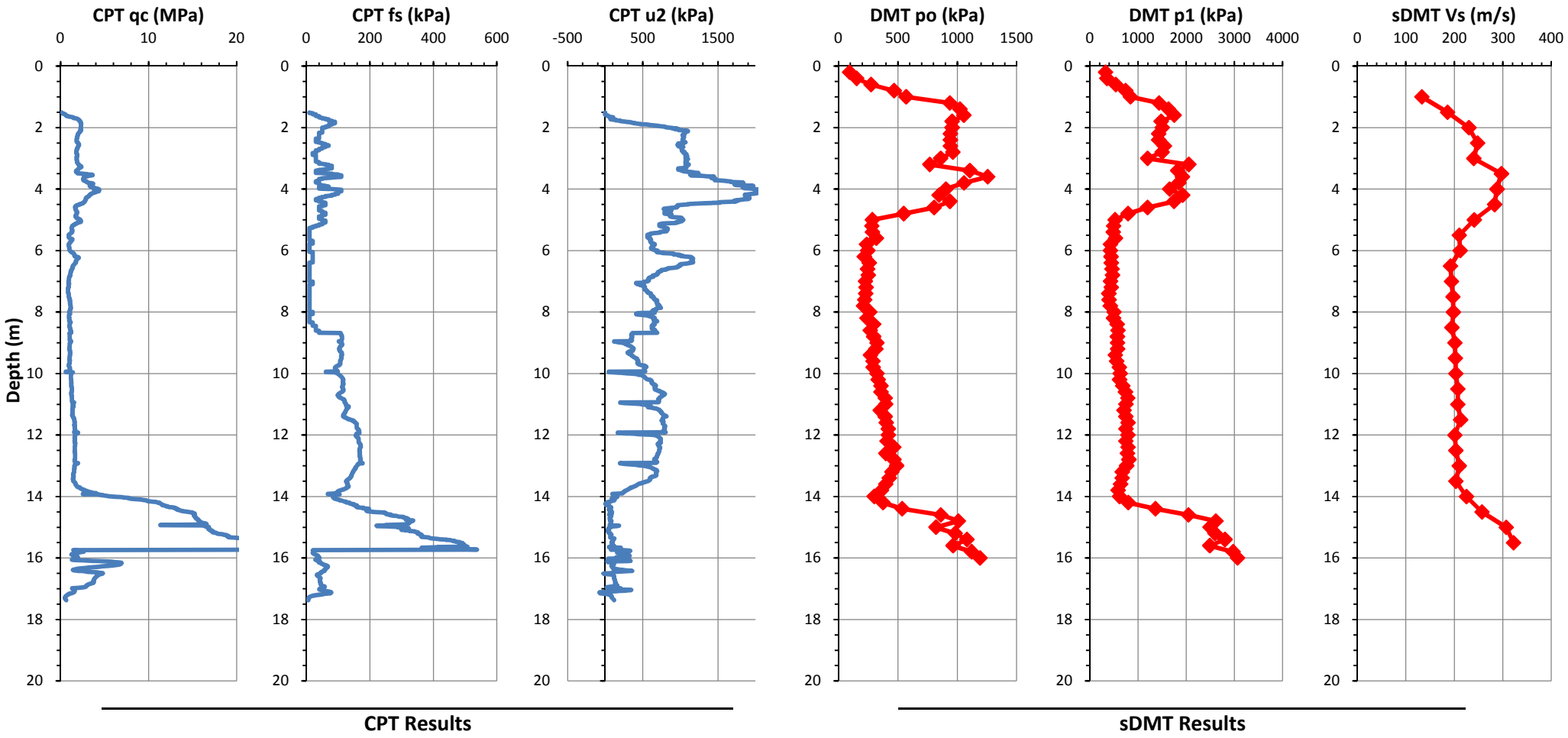

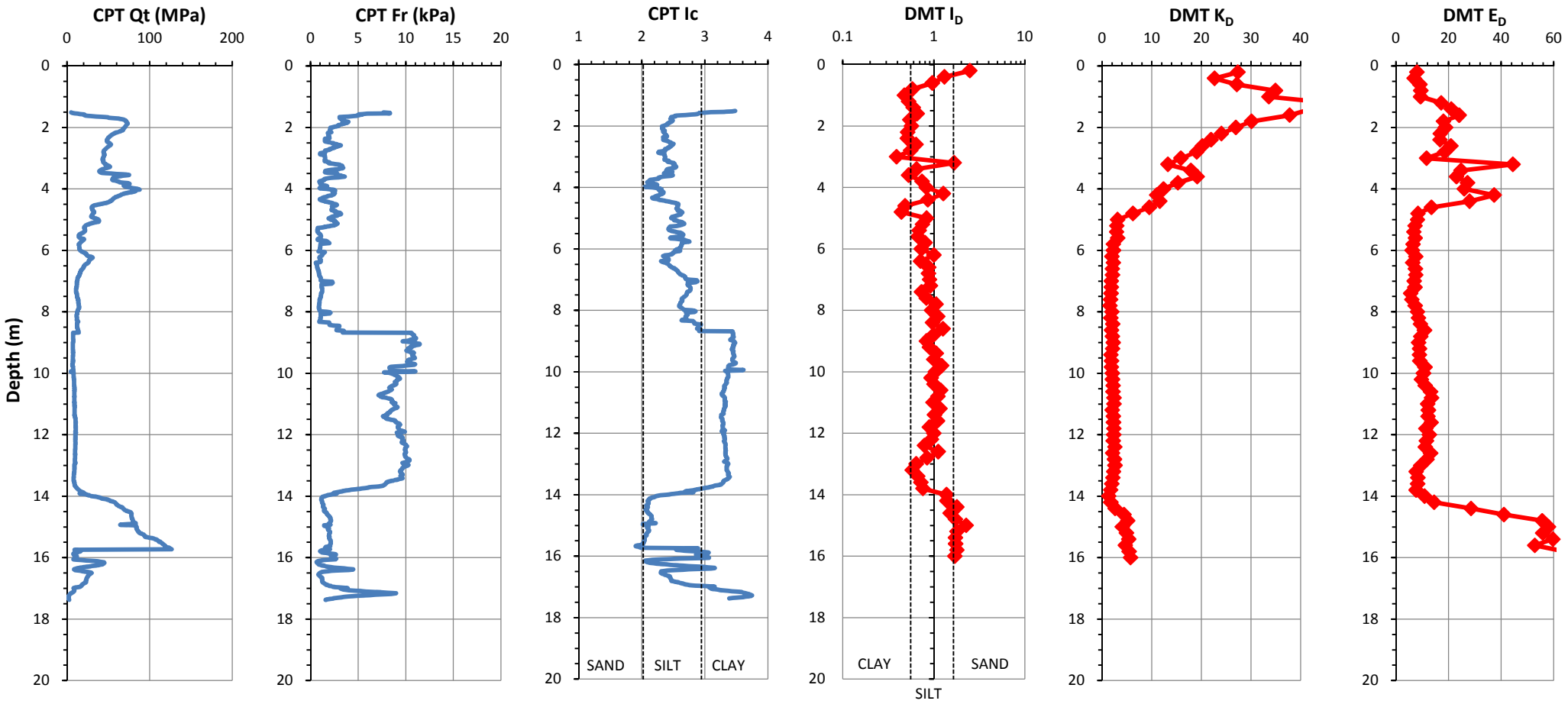

Normalised CPT parameters and Material Index (Robertson 2009a)

DMT Index Values (Marchetti 1980)

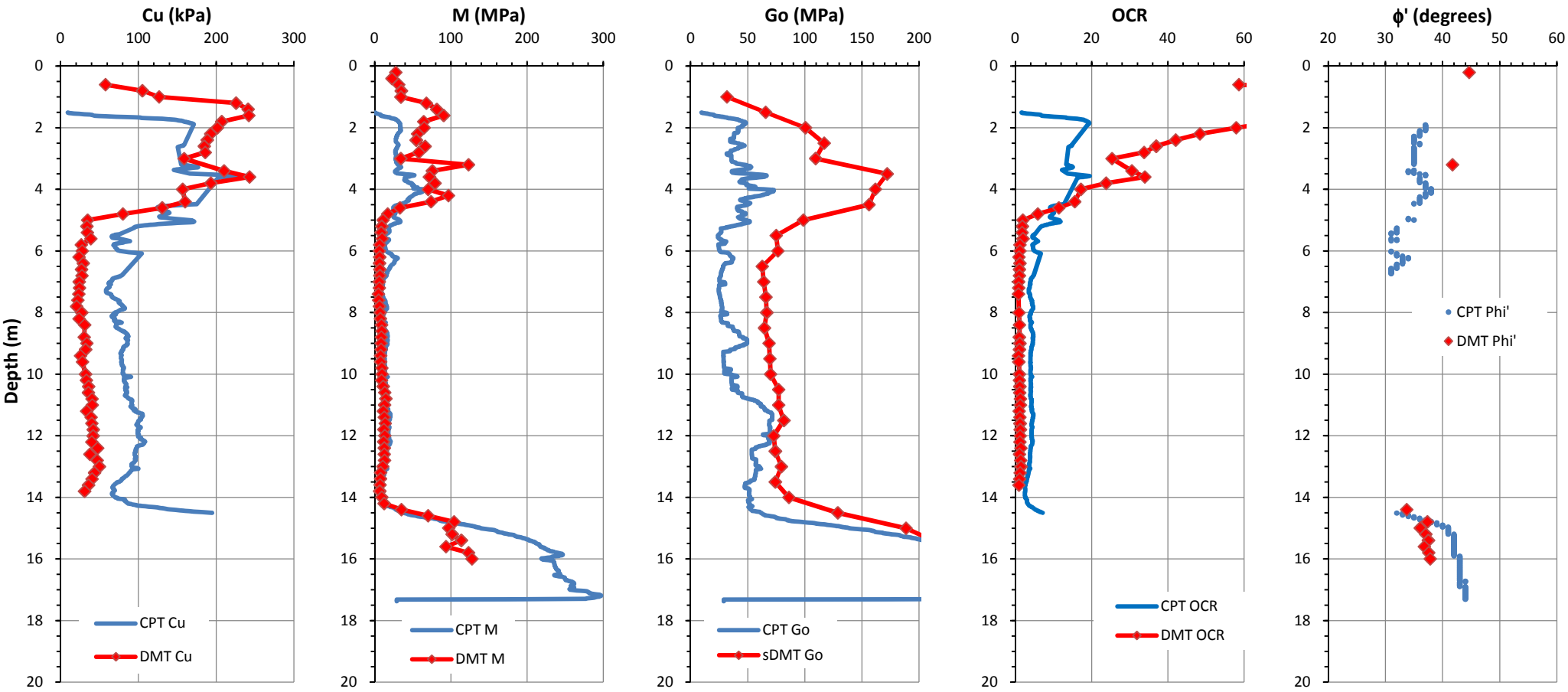

DMT correlations based on Marchetti (1980) and TC16 (2001) using Marchetti Elab software

CPT corelations based on Robertson (2009a) and Kulhawy & Mayne (1990) using CPeT-IT software

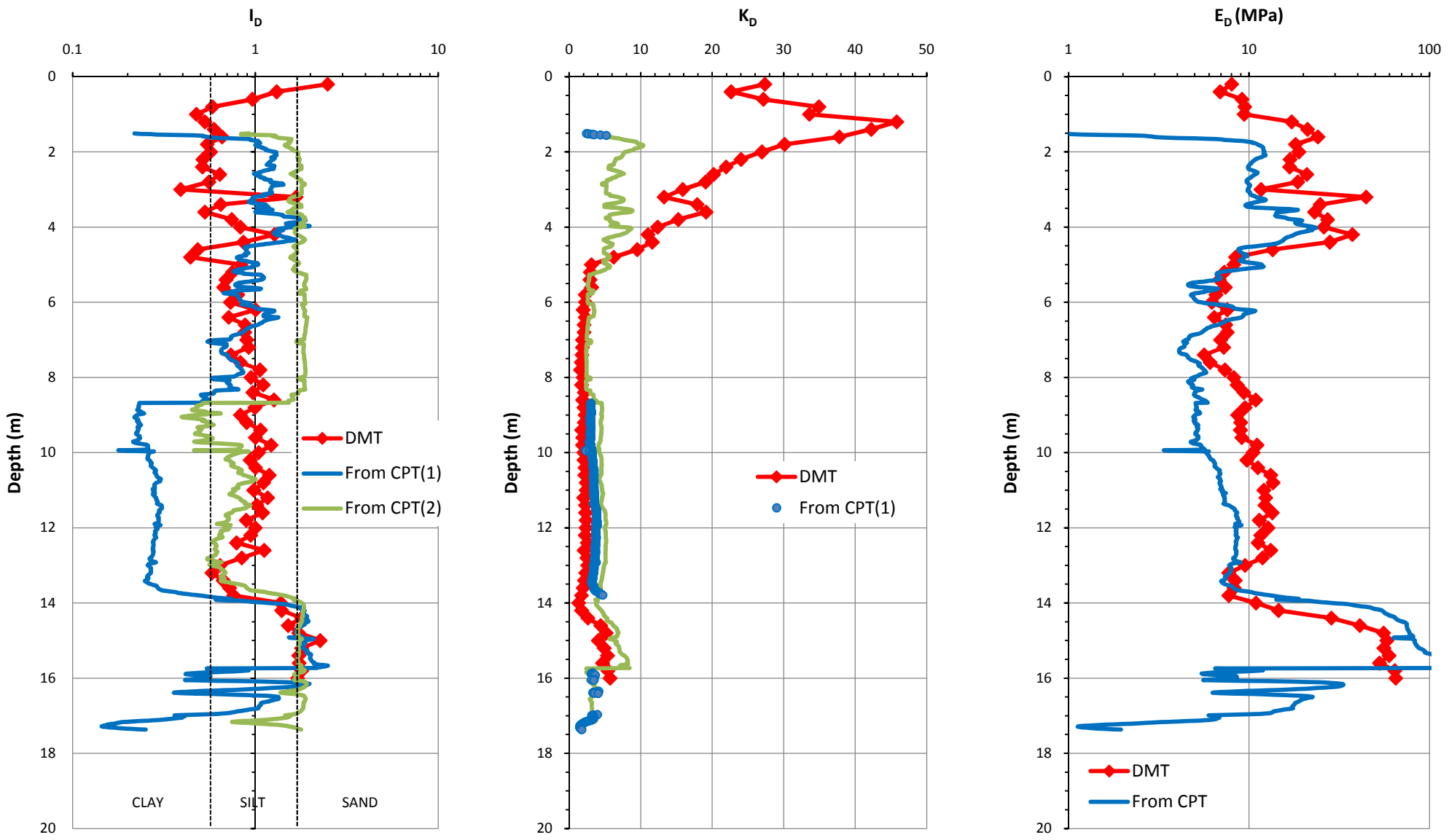

CPT(1): $I_D = 10^{(1.67-0.67Ic)}$ (Robertson 2009a)

CPT(2): $I_D = 2.0-0.14F_r$ (Mayne & Liao 2004)

CPT(1): $K_D = 0.3(Qt)^{0.95} + 1.05$, for Ic>2.95

CPT(2): $K_D = 0.144Qt/[10^{(1.67-0.67Ic)}]$ (Robertson 2009a)

CPT: $E_D = 5\ Qt\ \sigma'_{vo}$ (Robertson 2009a)

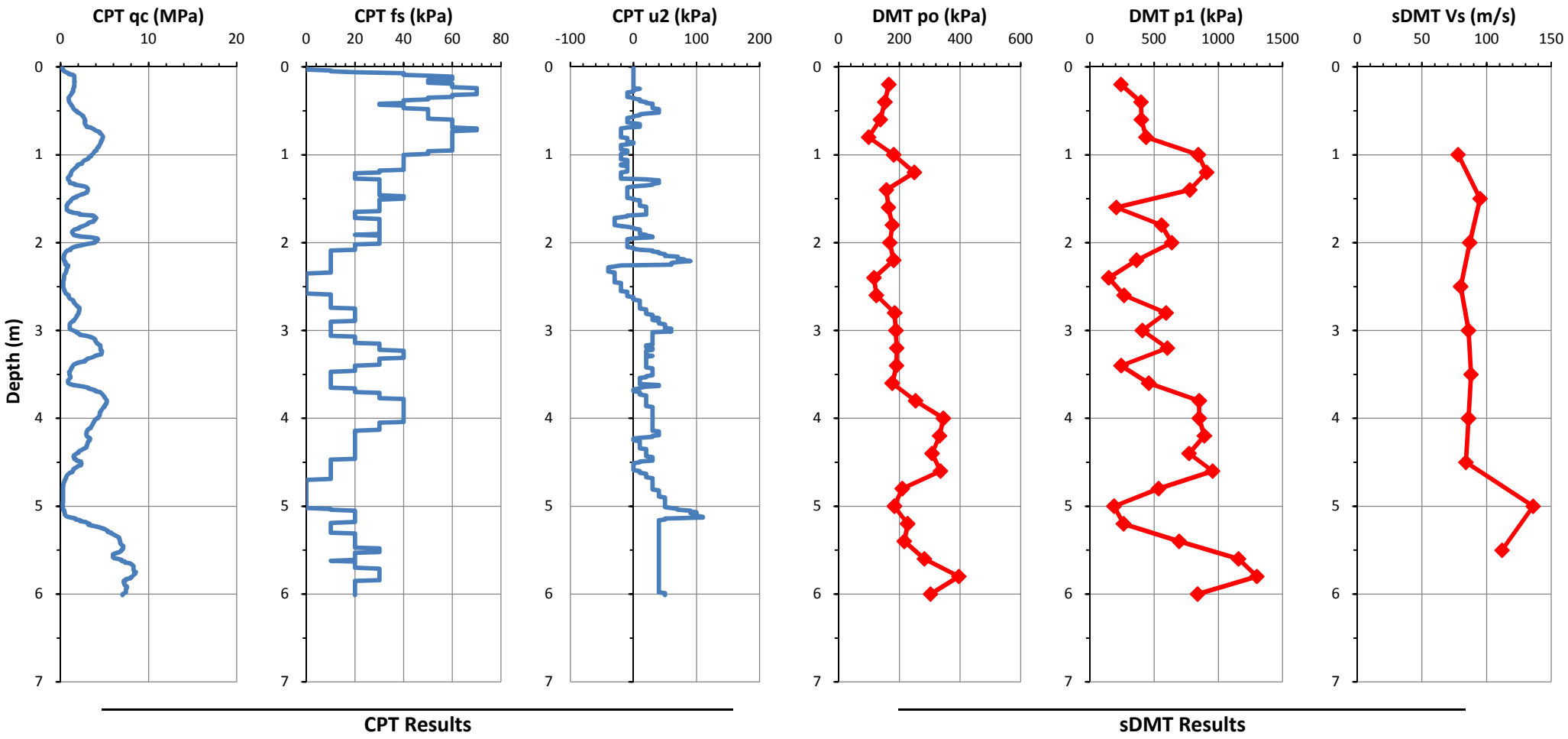

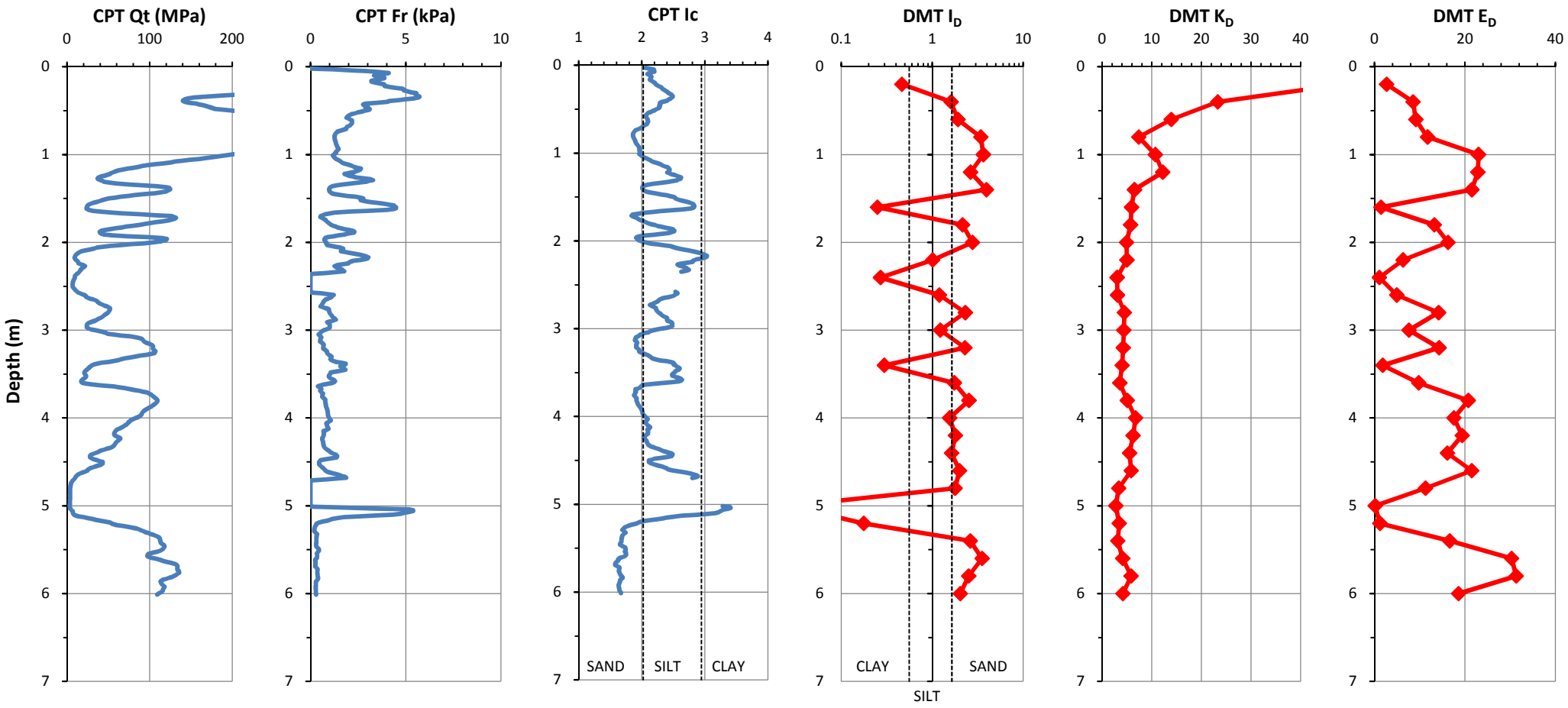

Normalised CPT parameters and Material Index (Robertson 2009a)

DMT Index Values (Marchetti 1980)

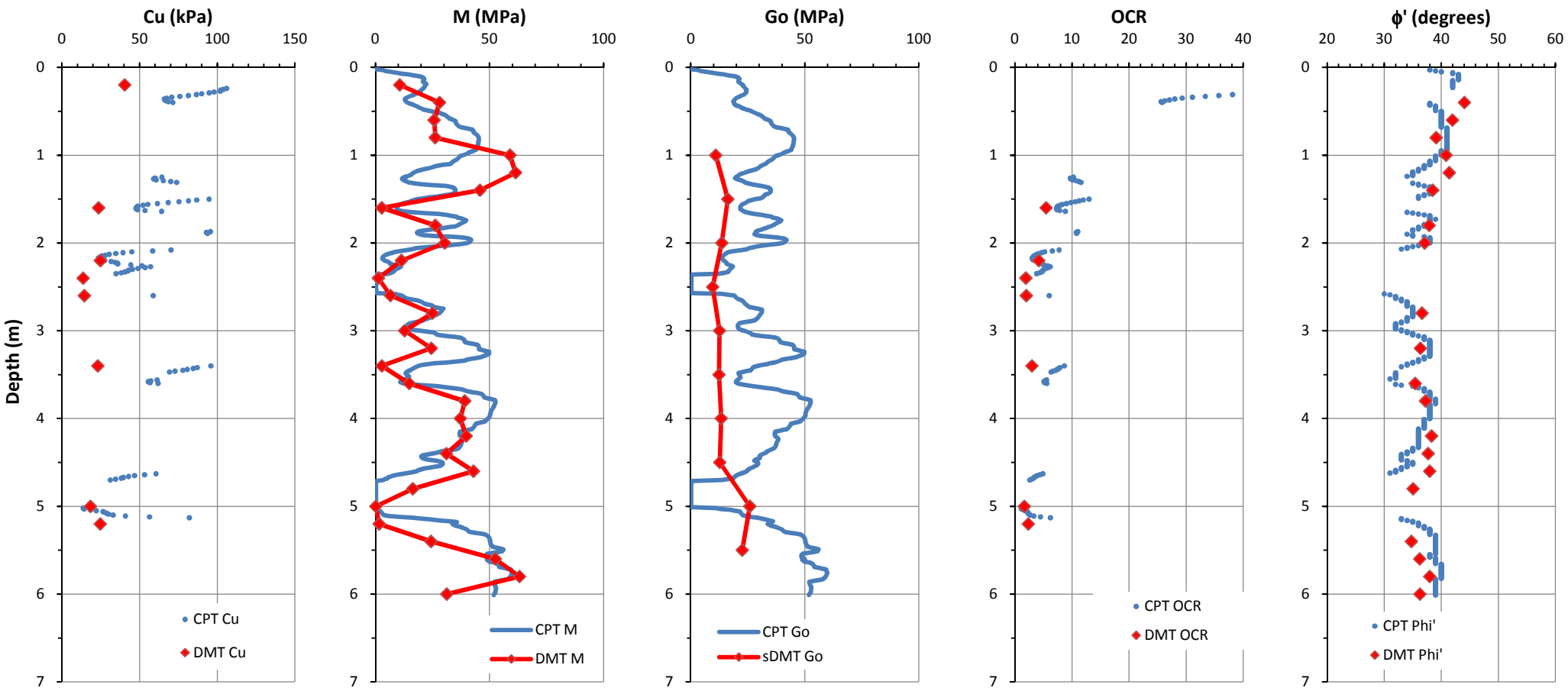

DMT correlations based on Marchetti (1980) and TC16 (2001) using Marchetti Elab software

CPT corelations based on Robertson (2009a) and Kulhawy & Mayne (1990) using CPeT-IT software

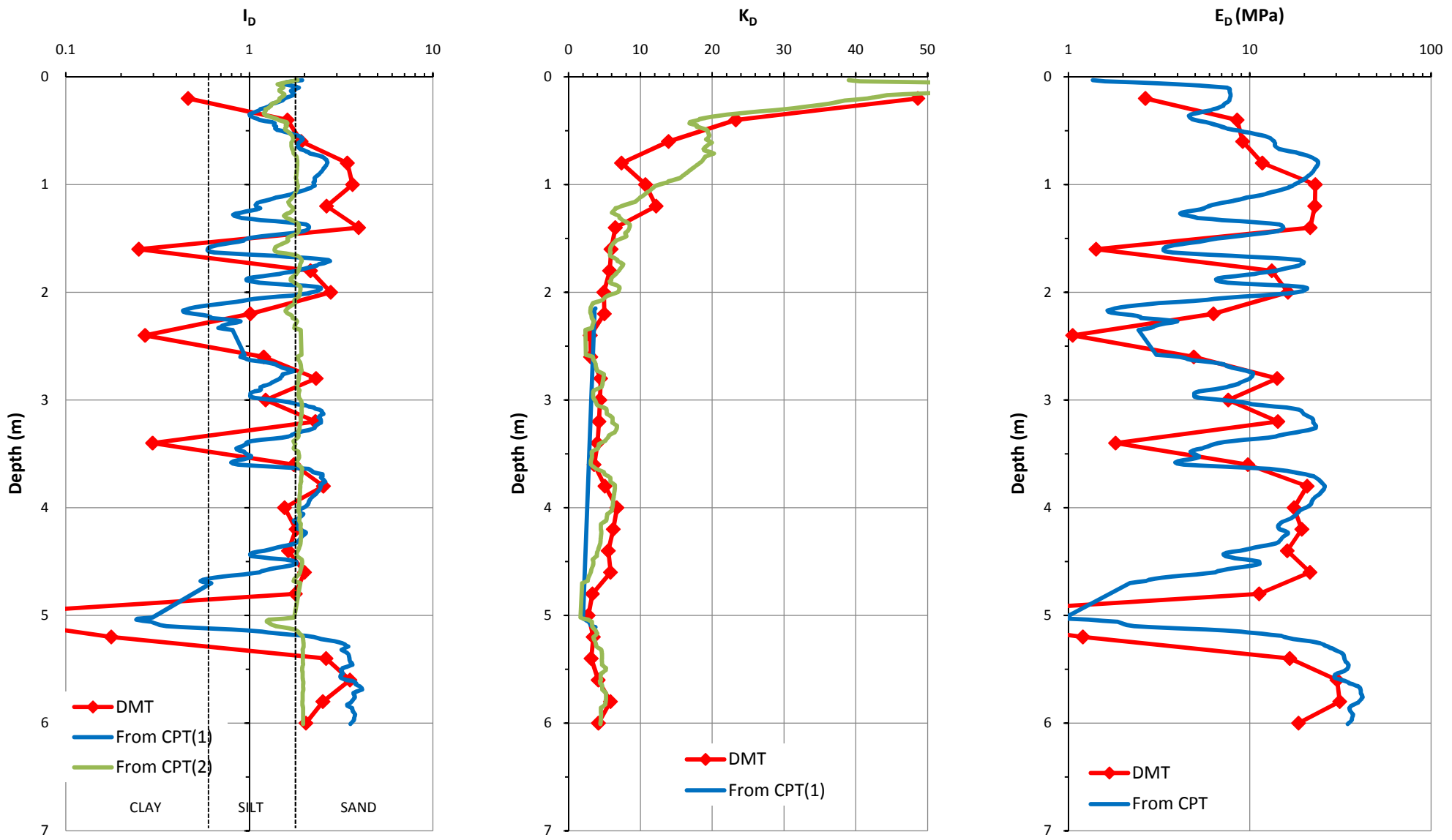

CPT(1): $I_D = 10^{(1.67-0.67Ic)}$ (Robertson 2009a)

CPT(2): $I_D = 2.0-0.14F_r$ (Mayne & Liao 2004)

CPT(1): $K_D = 0.3(Qt)^{0.95} + 1.05$, for Ic>2.95

CPT(2): KD = $0.144Qt/[10^{(1.67-0.67Ic)}]$

(Robertson 2009a)

CPT: $E_D = 5\ Qt\ \sigma'_{vo}$

(Robertson 2009a)

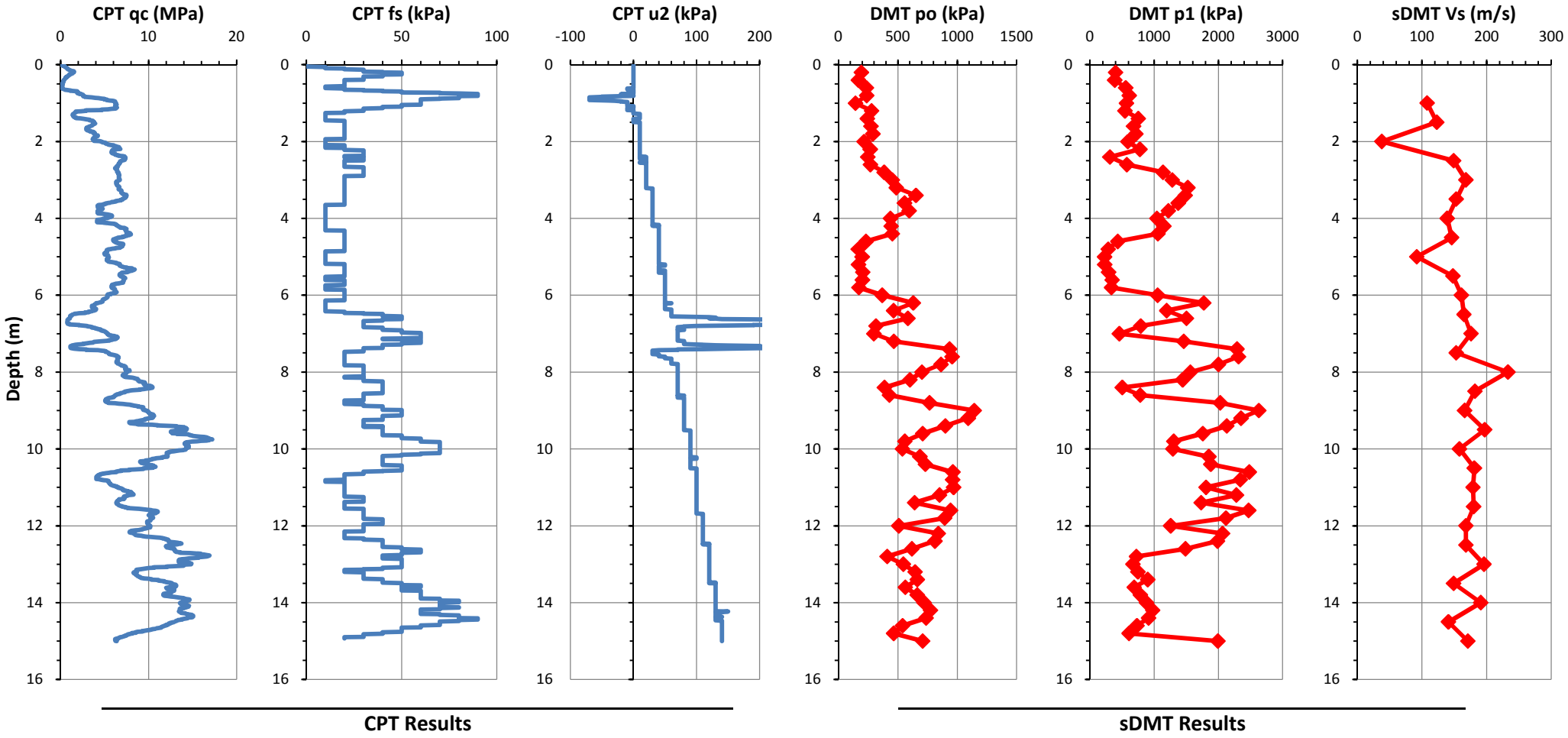

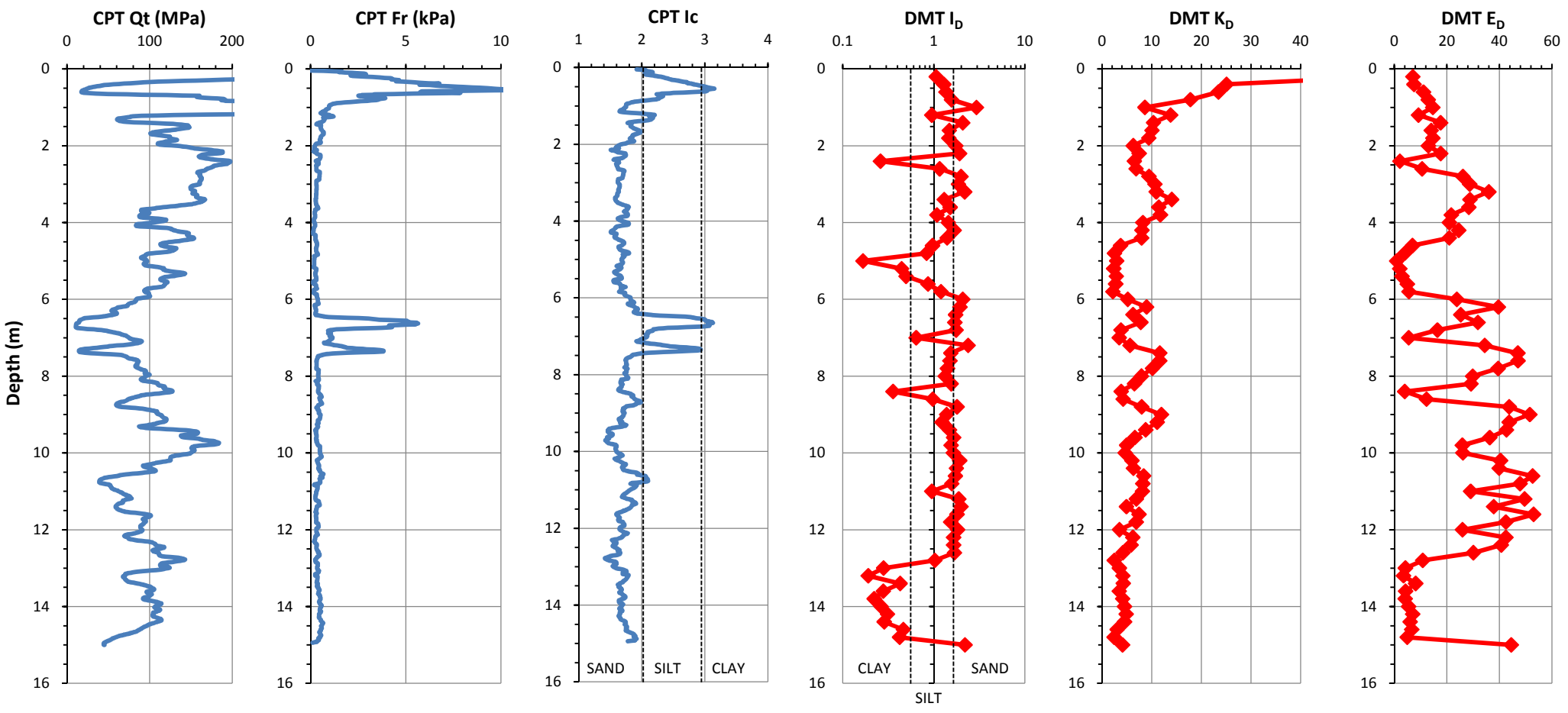

Normalised CPT parameters and Material Index (Robertson 2009a)

DMT Index Values (Marchetti 1980)

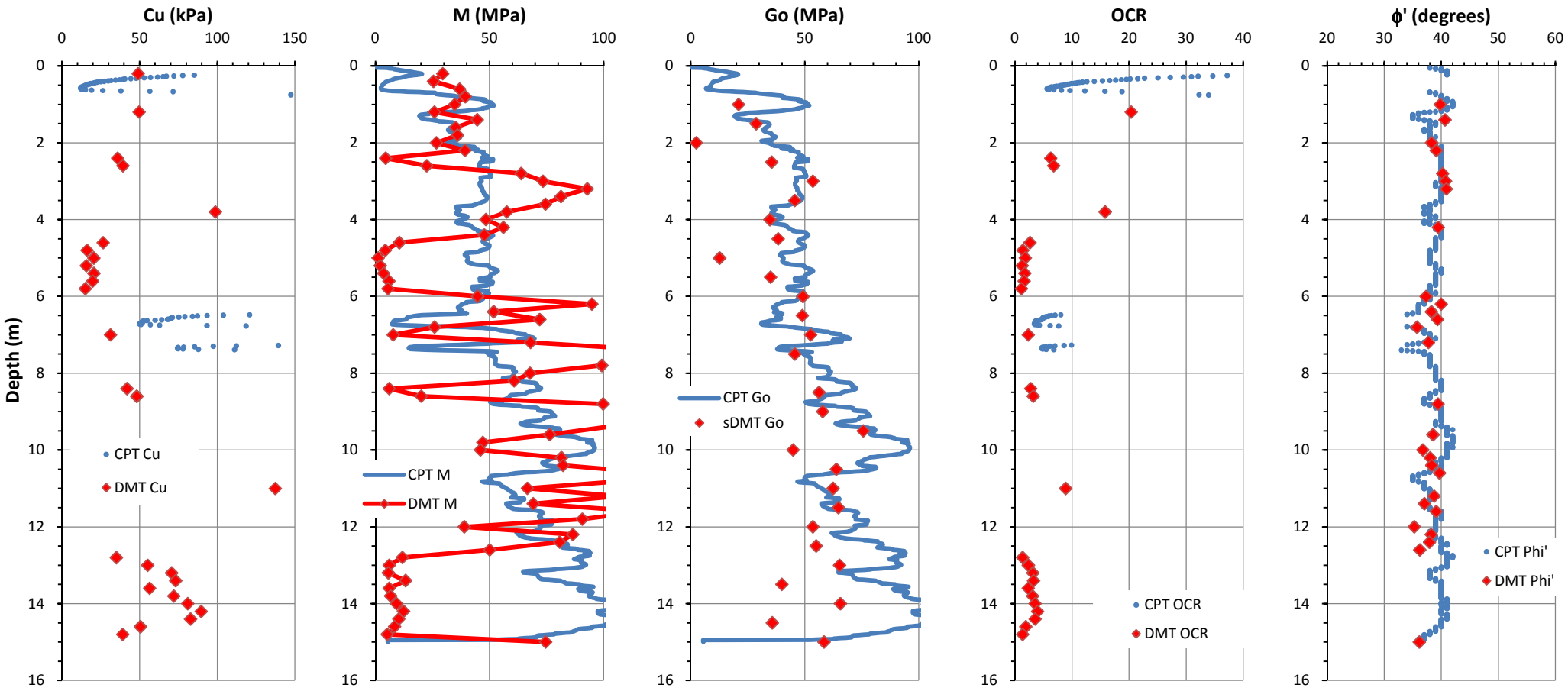

DMT correlations based on Marchetti (1980) and TC16 (2001) using Marchetti Elab software

CPT corelations based on Robertson (2009a) and Kulhawy & Mayne (1990) using CPeT-IT software

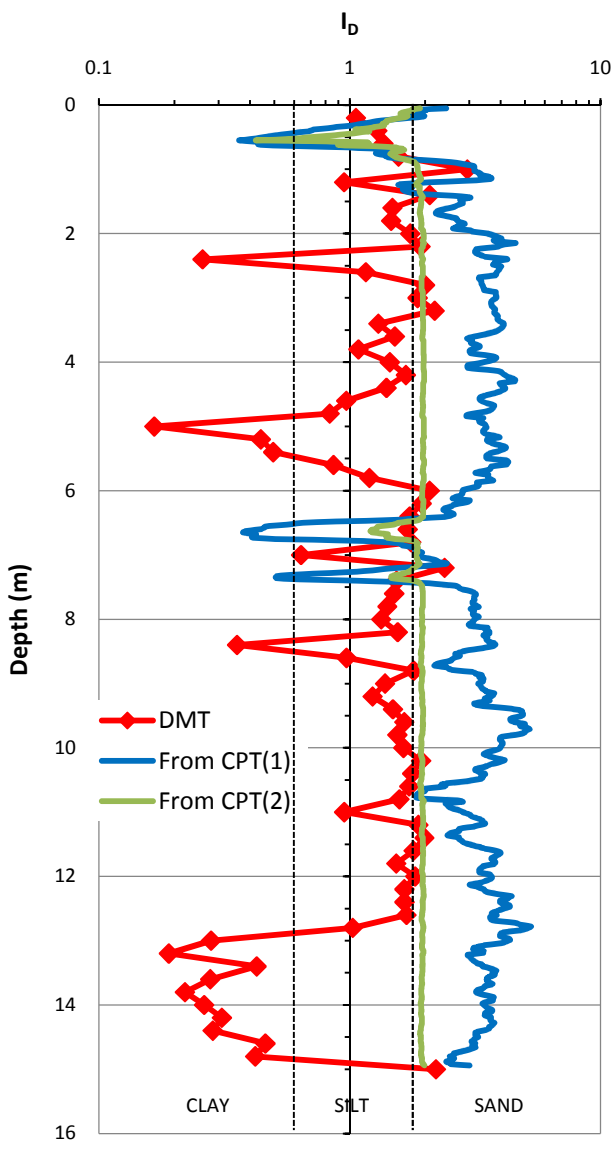

CPT(1): $I_D = 10^{(1.67-0.67Ic)}$ (Robertson 2009b)

CPT(2): $I_D = 2.0-0.14F_r$ (Mayne & Liao 2004)

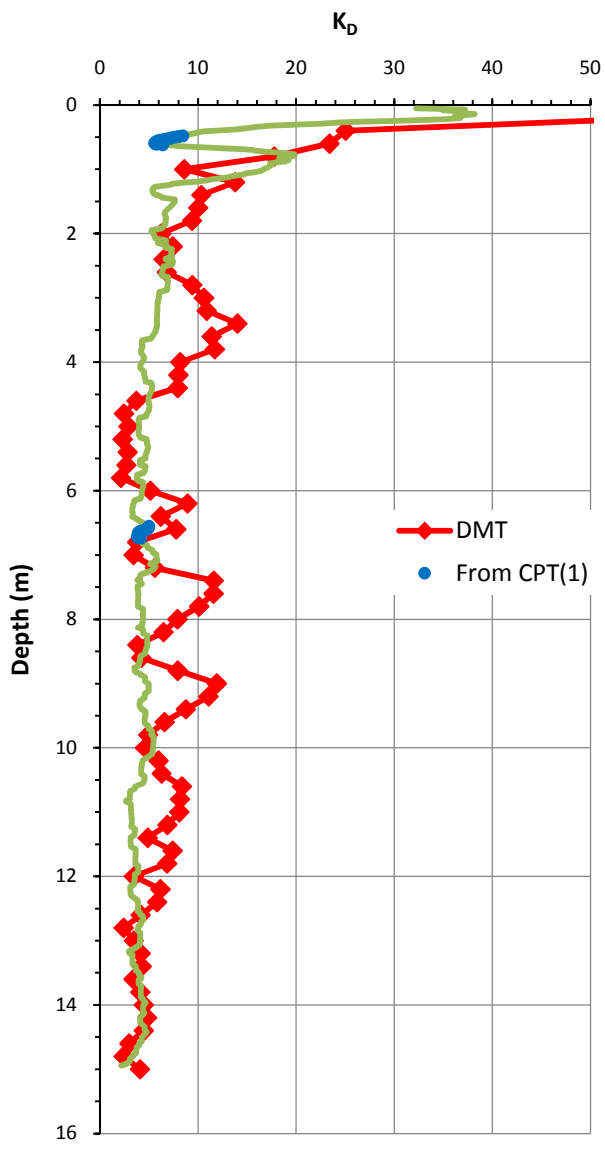

CPT(1): $K_D = 0.3(Qt)^{0.95} + 1.05$, for Ic>2.95

CPT(2): $KD = 0.144Qt/[10^{(1.67-0.67Ic)}]$

(Robertson 2009b)

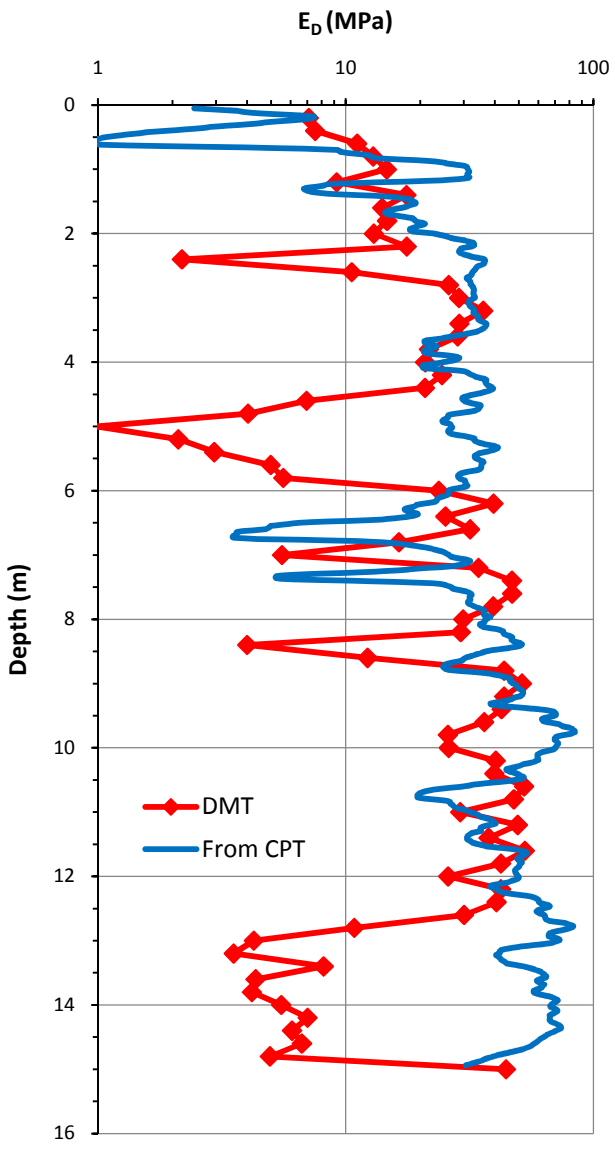

CPT: $E_D = 5\ Qt\ \sigma'_{vo}$

(Robertson 2009b)

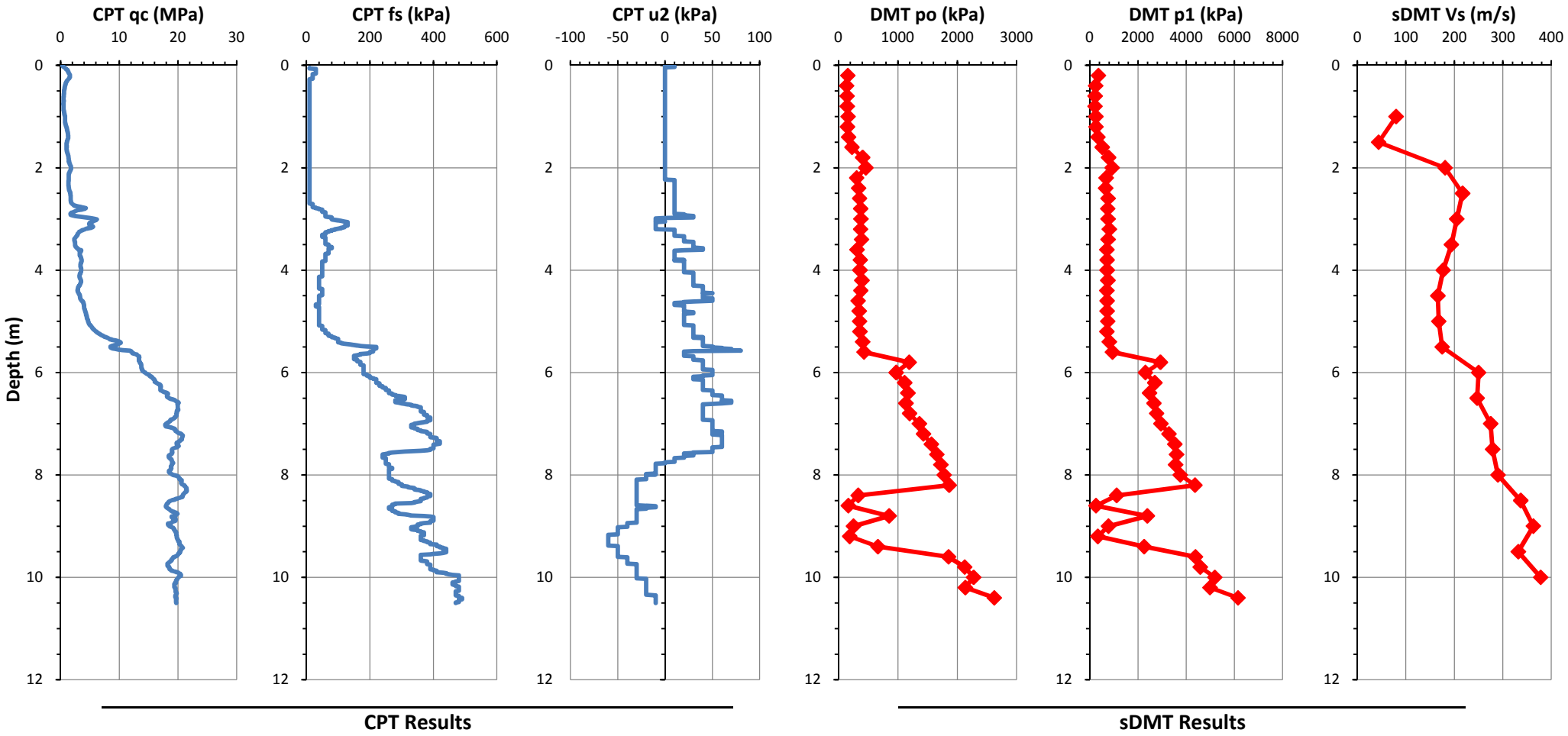
CPT qc (MPa)
CPT fs (kPa)
CPT u2 (kPa)
DMT po (kPa)
DMT p1 (kPa)
sDMT Vs (m/s)
Depth (m)
CPT Results
sDMT Results

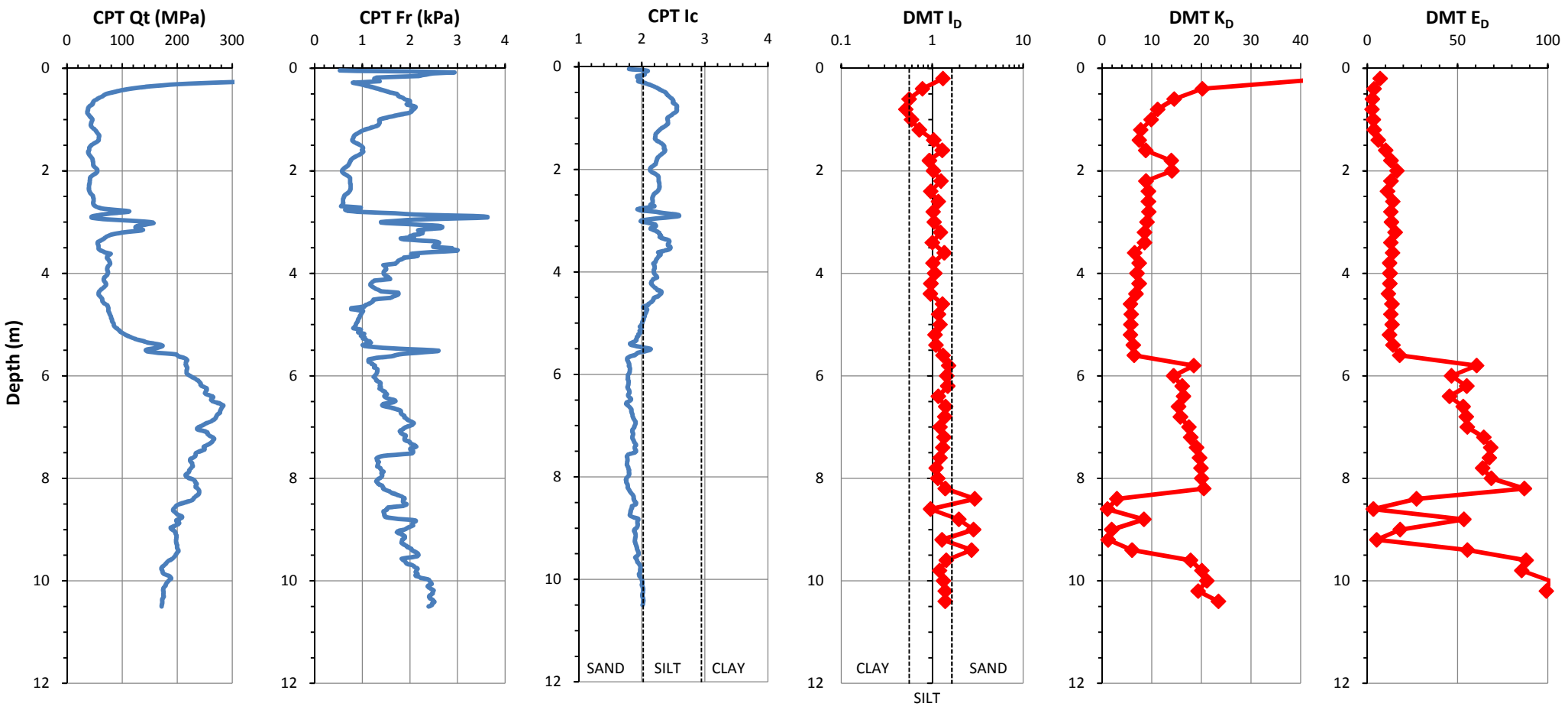
CPT Qt (MPa)
CPT Fr (kPa)
CPT Ic
DMT I_D
DMT K_D
DMT E_D
Depth (m)
SAND
SILT
CLAY
CLAY
SILT
SAND
Normalised CPT parameters and Material Index (Robertson 2009a)
DMT Index Values (Marchetti 1980)

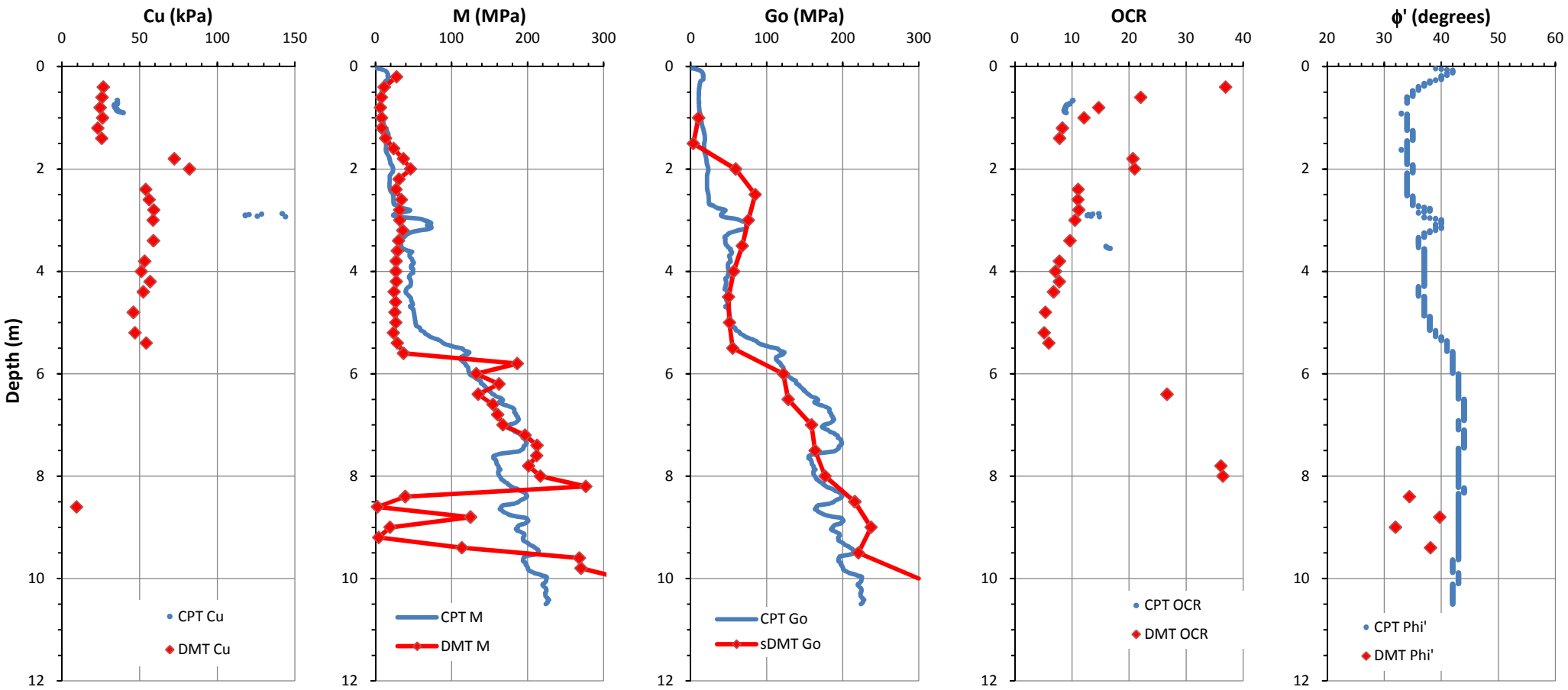

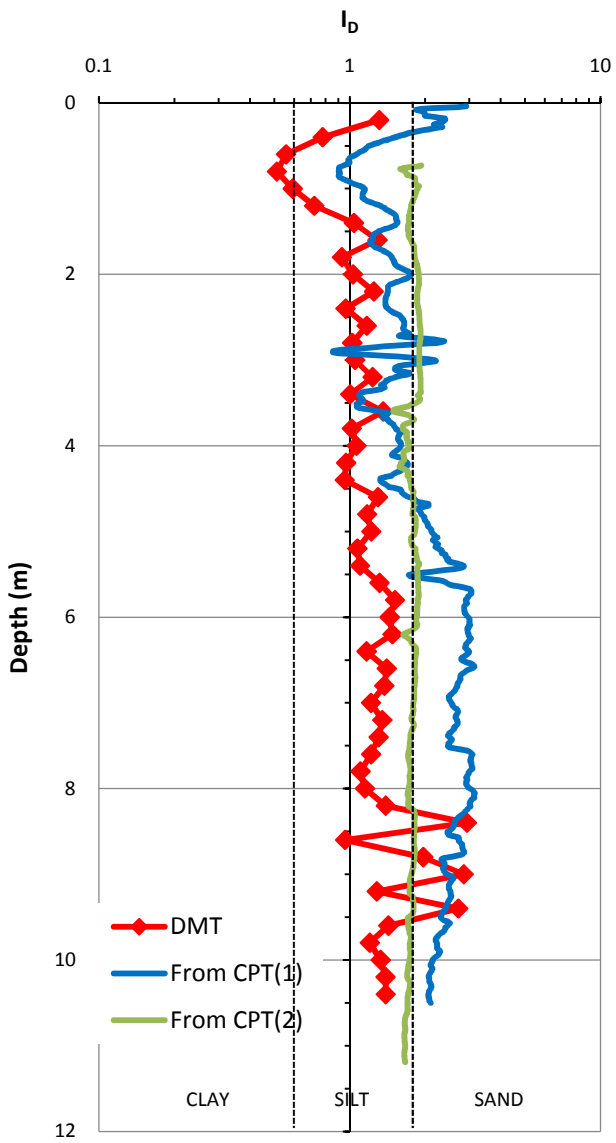

CPT(1): $I_D = 10^{(1.67-0.67Ic)}$ (Robertson 2009b)
CPT(2): $I_D = 2.0-0.14F_r$ (Mayne & Liao 2004)

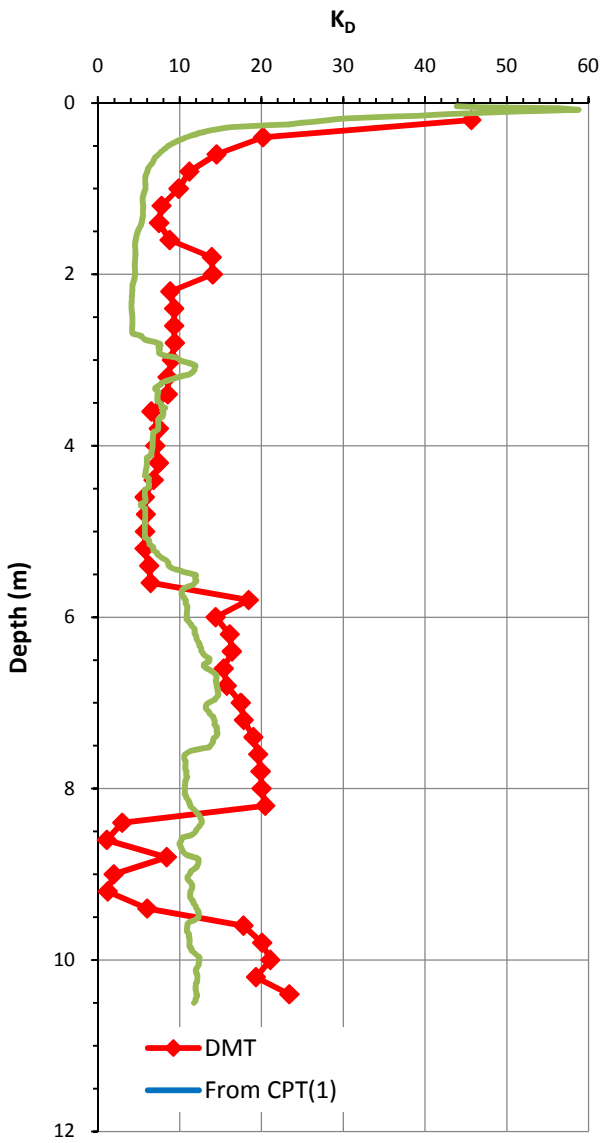

CPT(1): $K_D = 0.3(Qt)^{0.95} + 1.05$, for Ic>2.95
CPT(2): $KD = 0.144Qt/[10^{(1.67-0.67Ic)}]$
(Robertson 2009b)

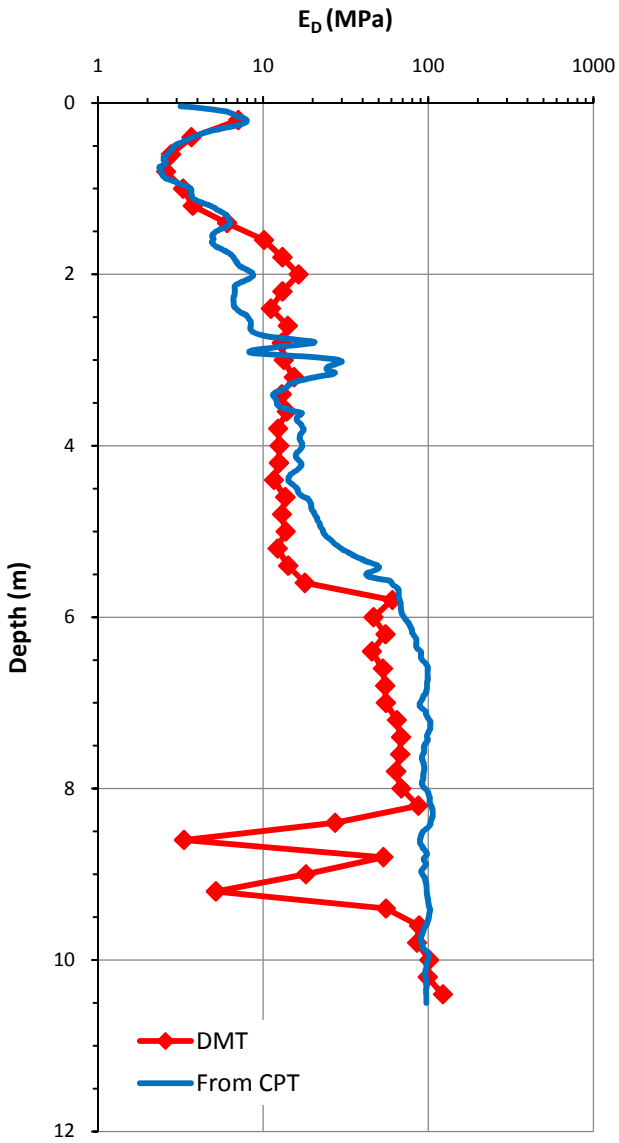

CPT: $E_D = 5\ Qt\ \sigma'_{vo}$
(Robertson 2009b)

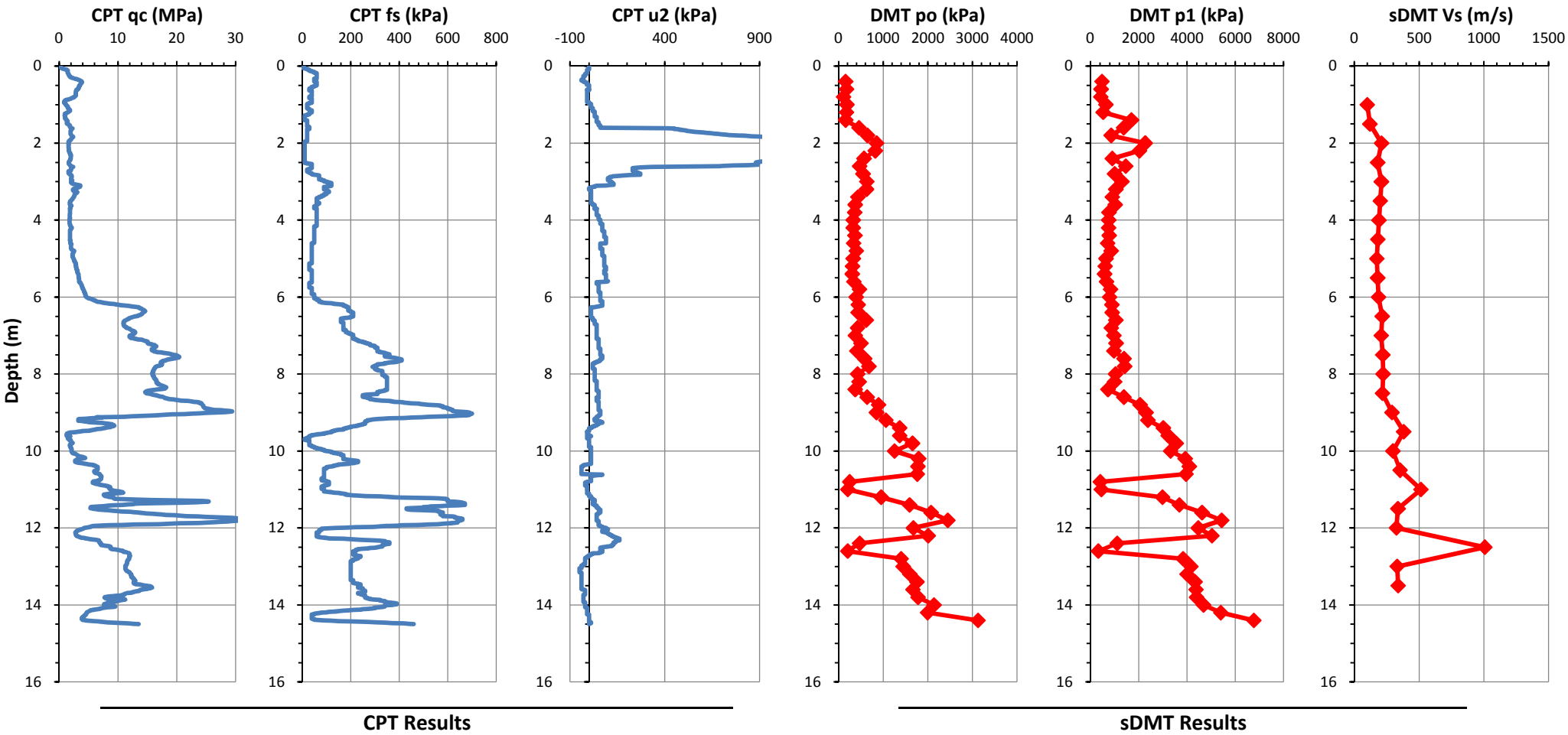
CPT qc (MPa)
CPT fs (kPa)
CPT u2 (kPa)
DMT po (kPa)
DMT p1 (kPa)
sDMT Vs (m/s)
Depth (m)
CPT Results
sDMT Results

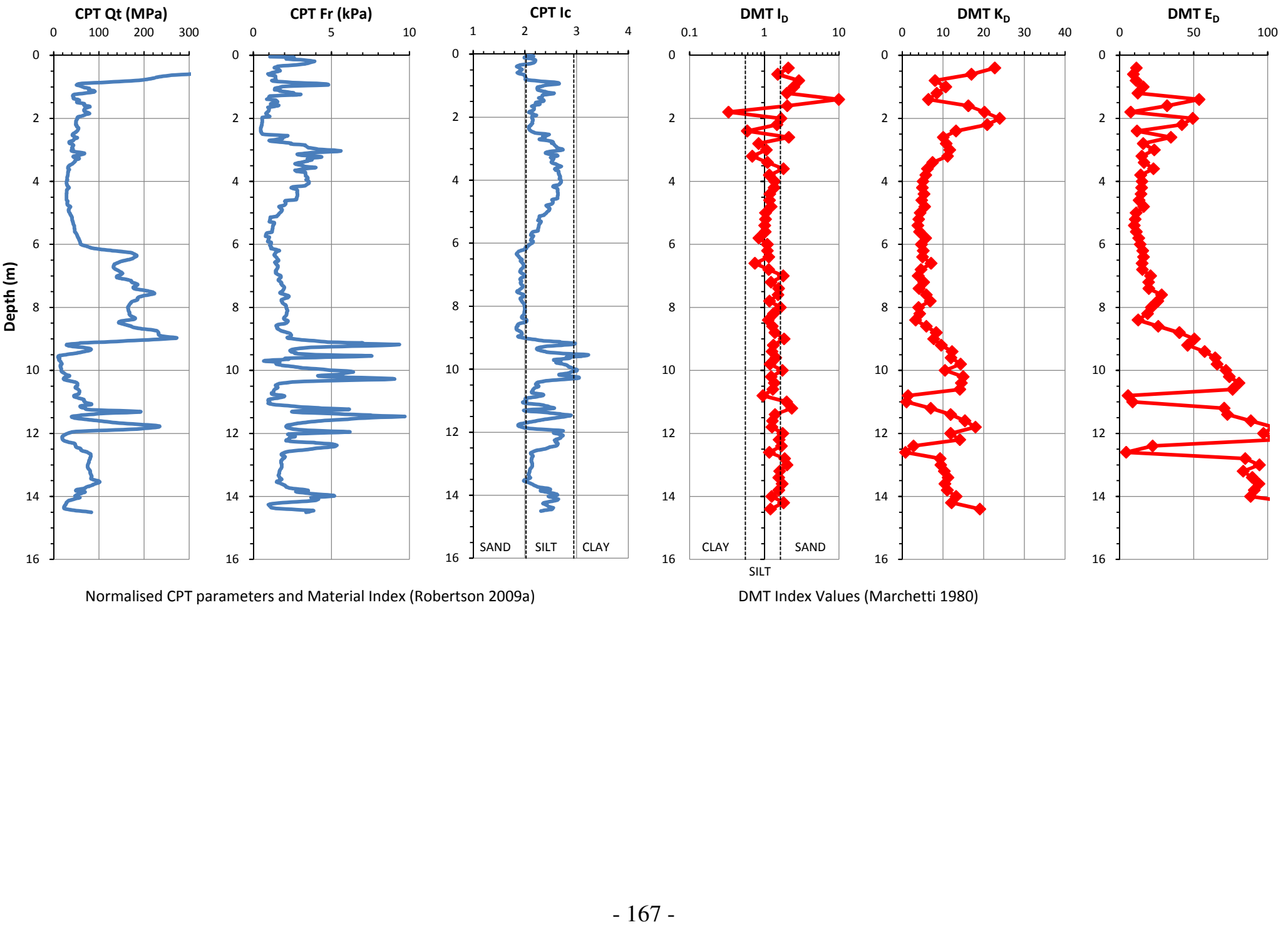
CPT Qt (MPa)
CPT Fr (kPa)
CPT Ic
DMT I_D
DMT K_D
DMT E_D
Depth (m)
SAND
SILT
CLAY
CLAY
SILT
SAND
Normalised CPT parameters and Material Index (Robertson 2009a)
DMT Index Values (Marchetti 1980)

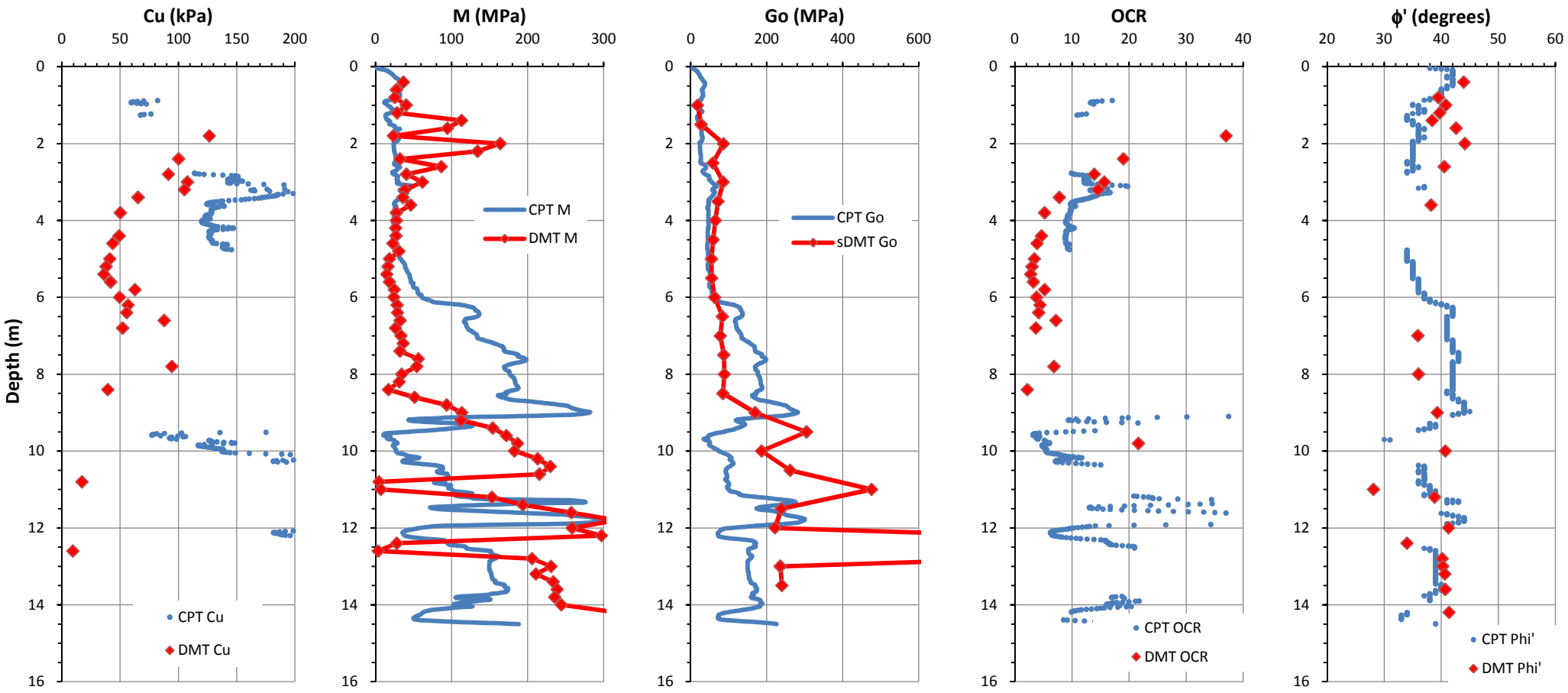

DMT correlations based on Marchetti (1980) and TC16 (2001) using Marchetti Elab software
CPT corelations based on Robertson (2009) and Kulhawy & Mayne (1990) using CPeT-IT software

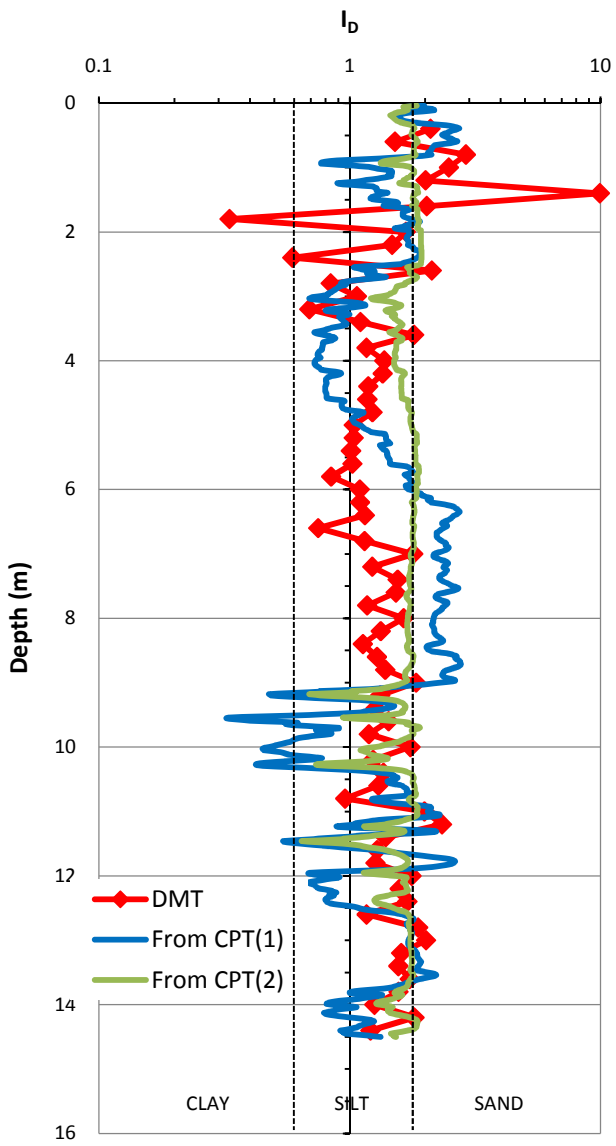

CPT(1): $I_D = 10^{(1.67-0.67Ic)}$ (Robertson 2009b)
CPT(2): $I_D = 2.0-0.14F_r$ (Mayne & Liao 2004)

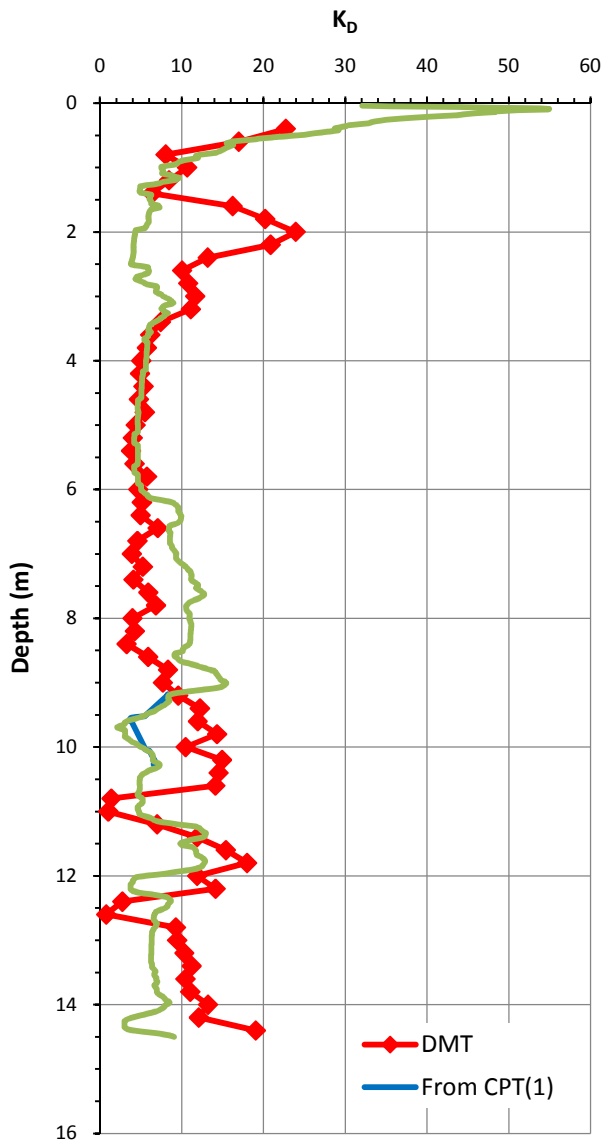

CPT(1): $K_D = 0.3(Qt)^{0.95} + 1.05$, for Ic>2.95
CPT(2): $KD = 0.144Qt/[10^{(1.67-0.67Ic)}]$
(Robertson 2009b)

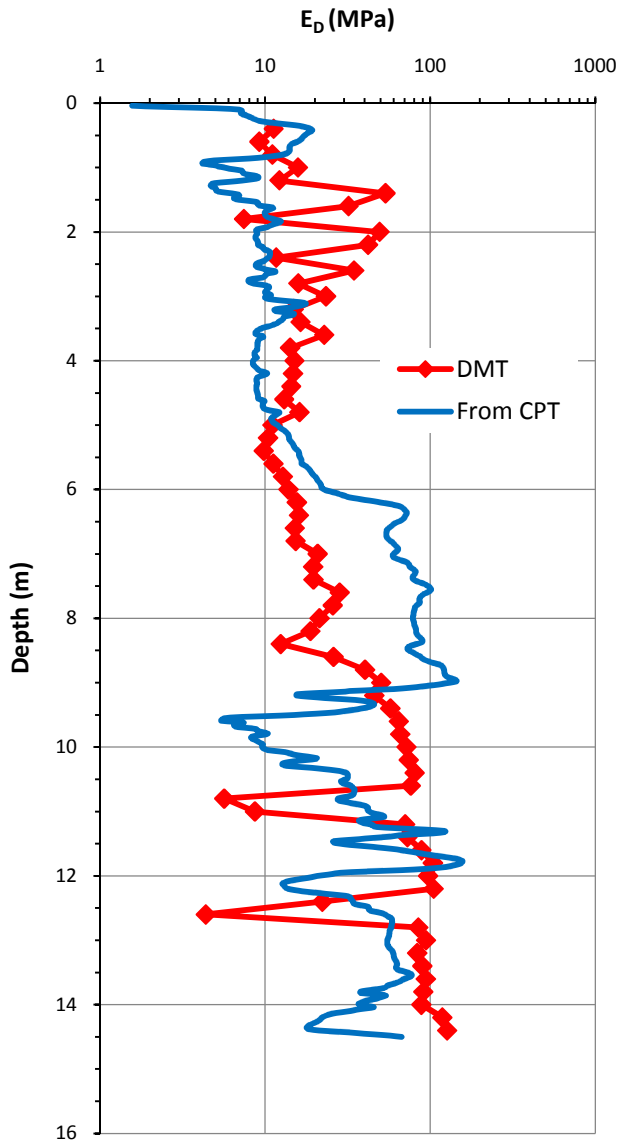

CPT: $E_D = 5\ Qt\ \sigma'_{vo}$
(Robertson 2009b)

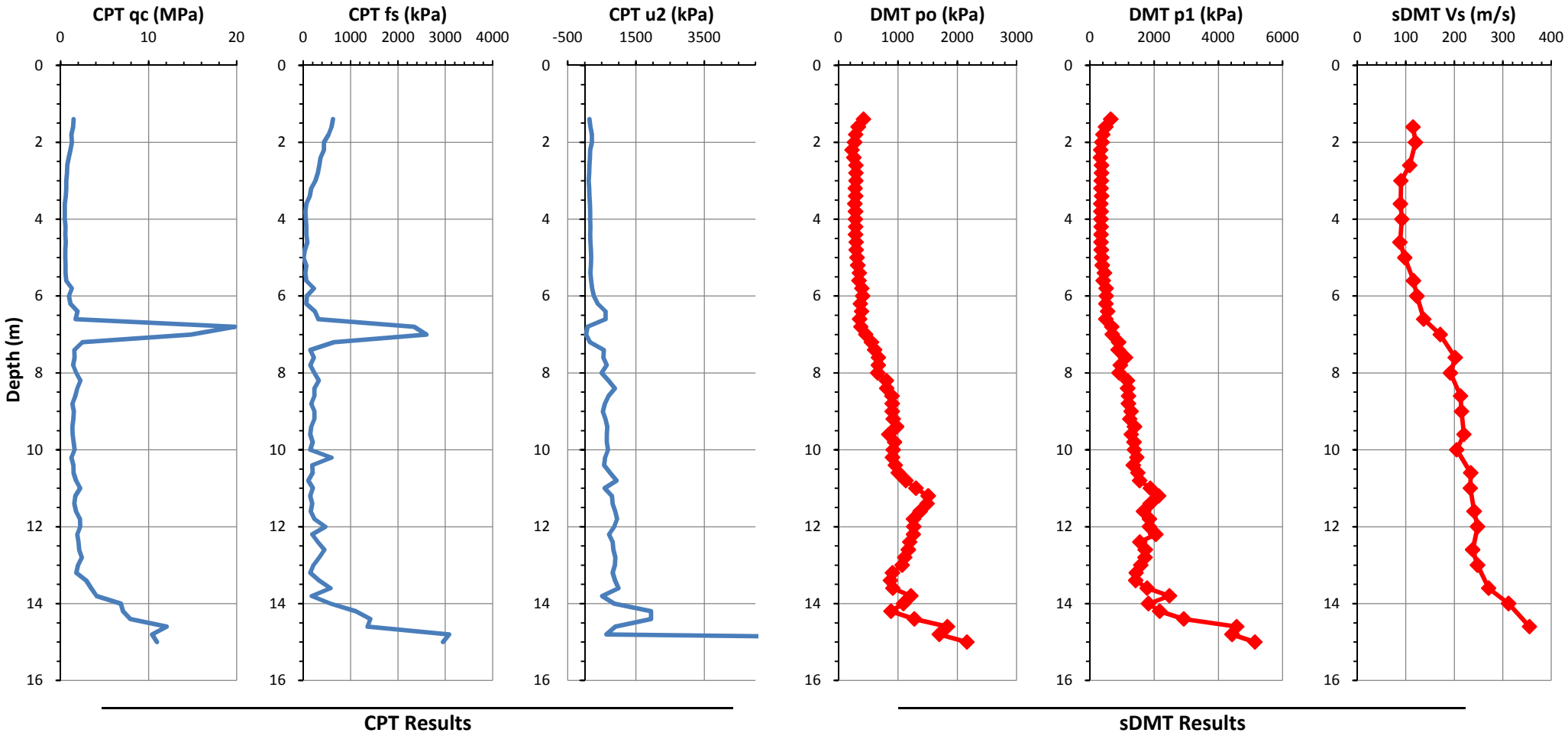

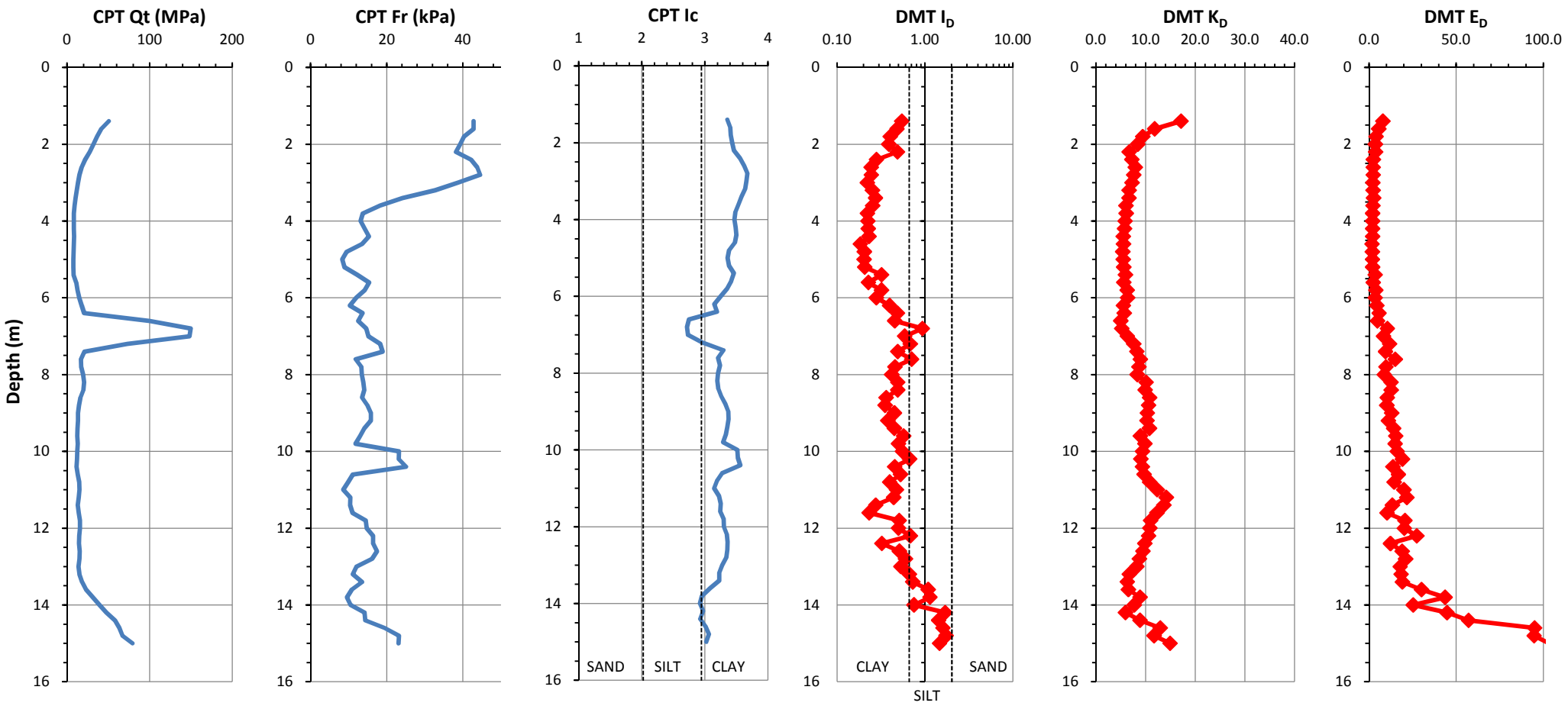

Normalised CPT parameters and Material Index (Robertson 2009a)

DMT Index Values (Marchetti 1980)

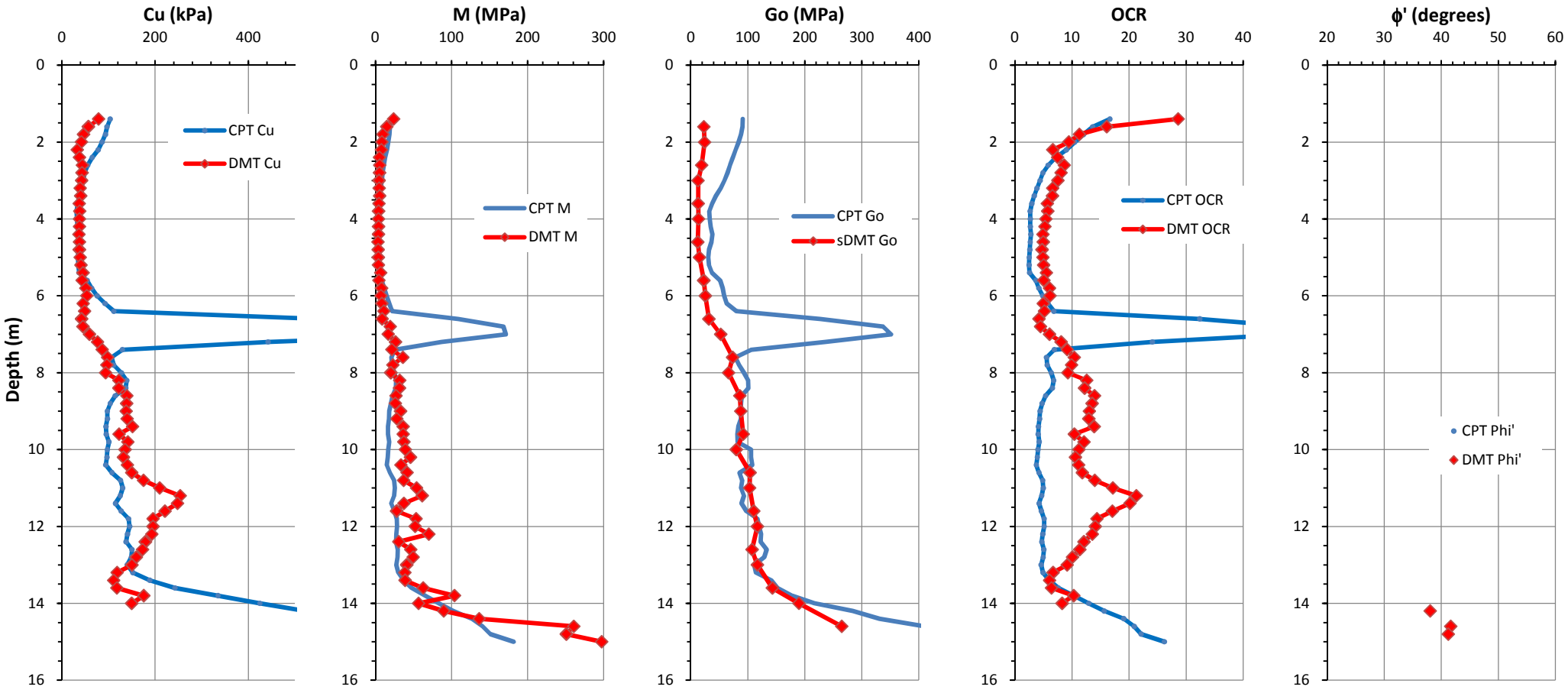

DMT correlations based on Marchetti (1980) and TC16 (2001) using Marchetti Elab software
CPT corelations based on Robertson (2009a) and Kulhawy & Mayne (1990) using CPeT-IT software

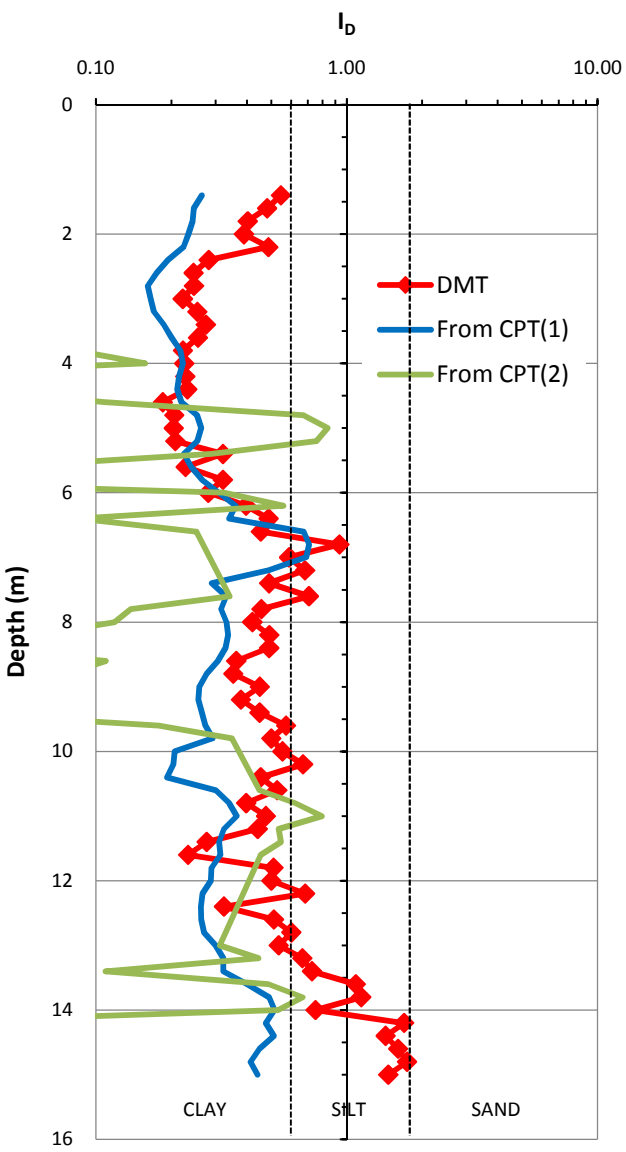

CPT(1): $I_D = 10^{(1.67-0.67Ic)}$ (Robertson 2009b)
CPT(2): $I_D = 2.0-0.14F_r$ (Mayne & Liao 2004)

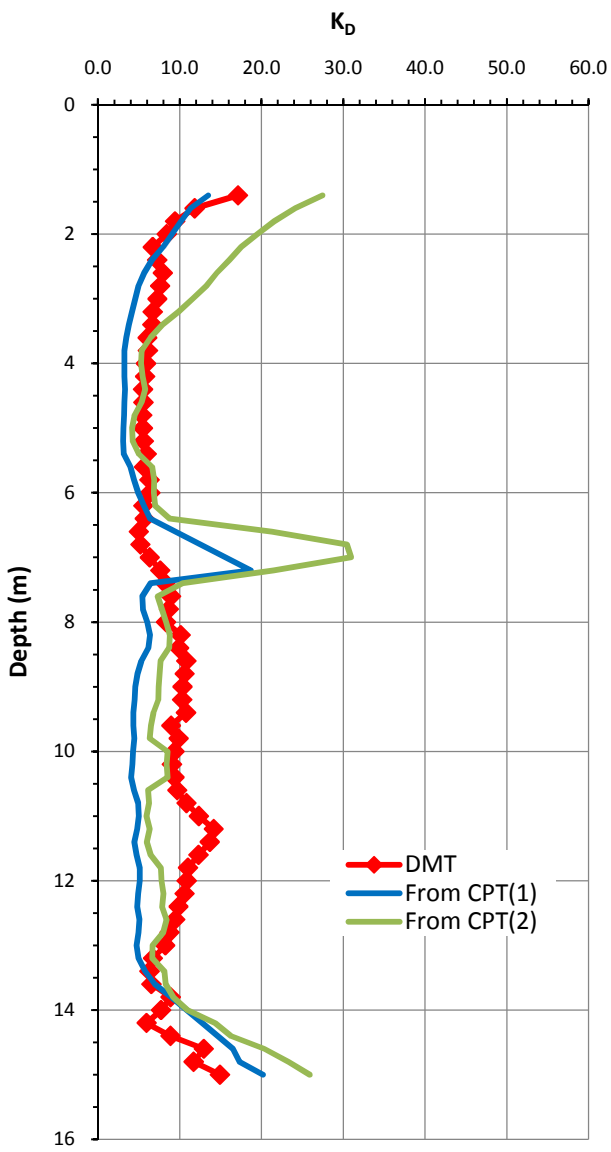

CPT(1): $K_D = 0.3(Qt)^{0.95} + 1.05$, for Ic>2.95
CPT(2): KD = $0.144Qt/[10^{(1.67-0.67Ic)}]$
(Robertson 2009b)

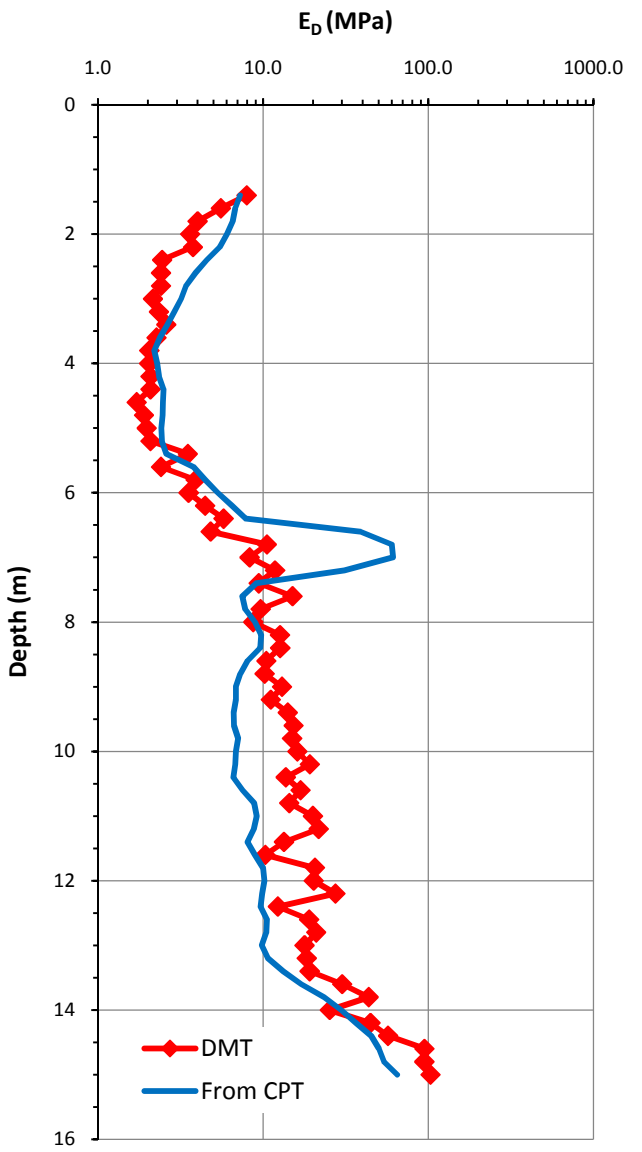

CPT: $E_D = 5\ Qt\ \sigma'_{vo}$
(Robertson 2009b)

APPENDIX C: PLOTS OF u_2 AND p_0 AGAINST DEPTH

CPT u_2 COMPARED TO DMT p_0

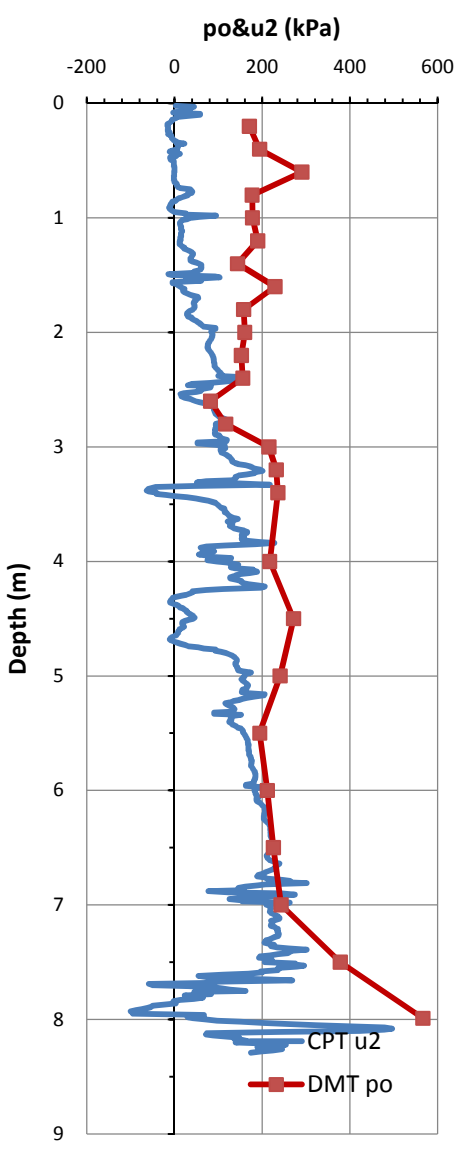

St. Heliers 1a

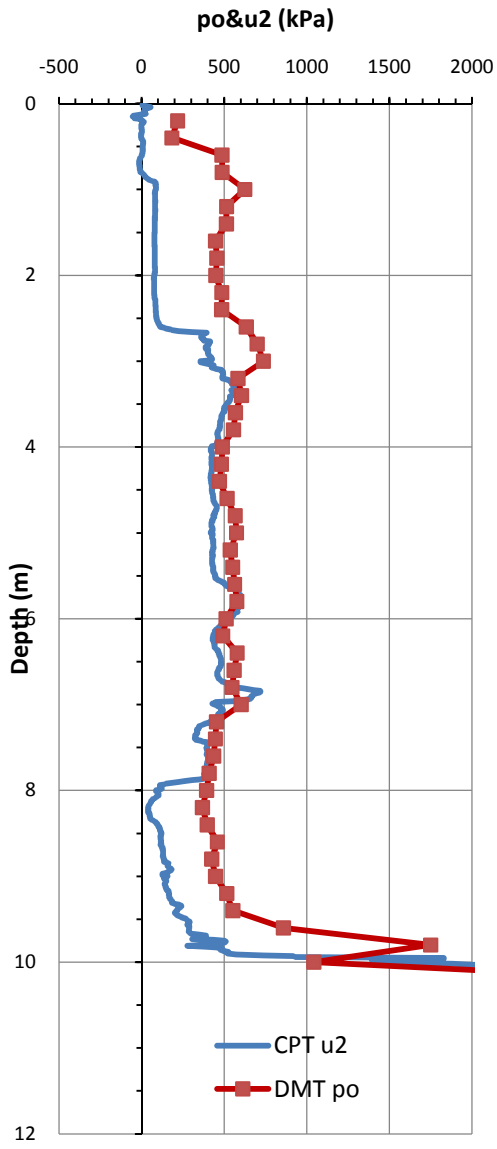

Flat Bush 2a

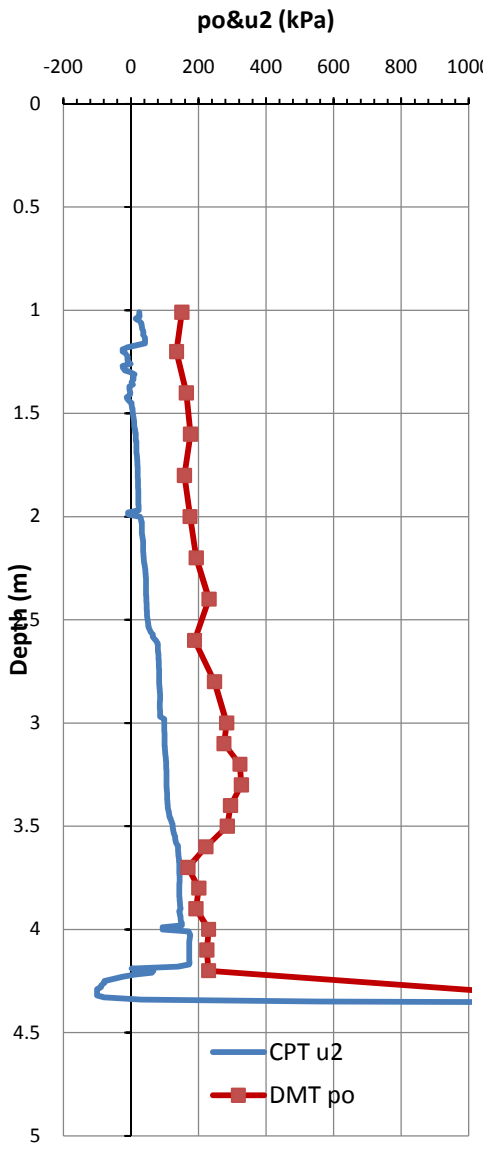

Maungaturoto 3a

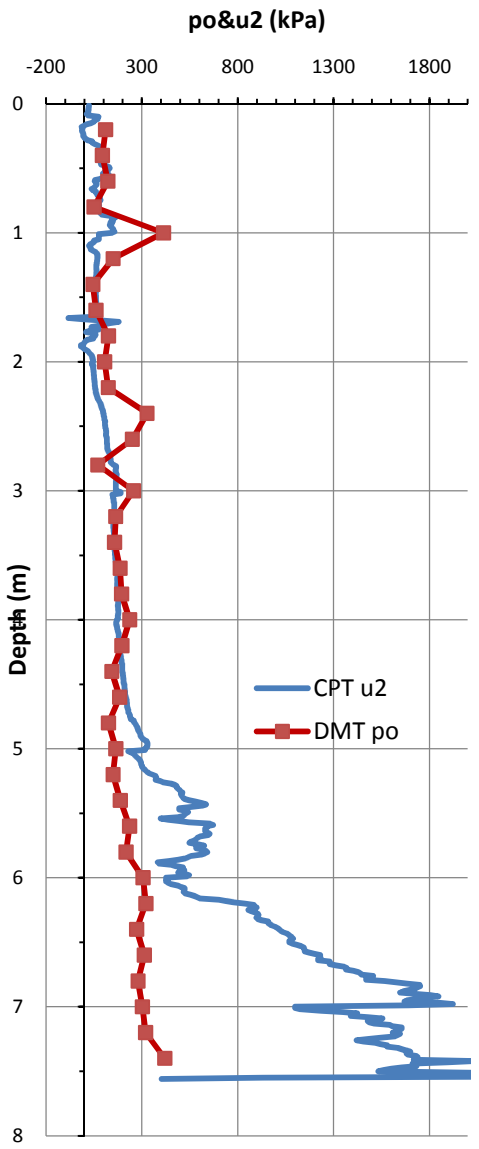

Kaiwaka 4a

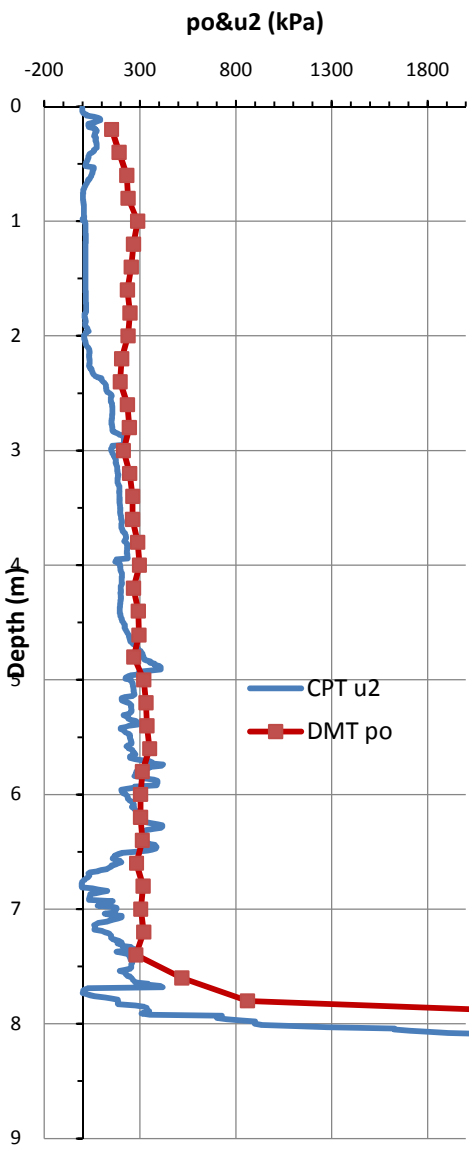

Matakana 5a

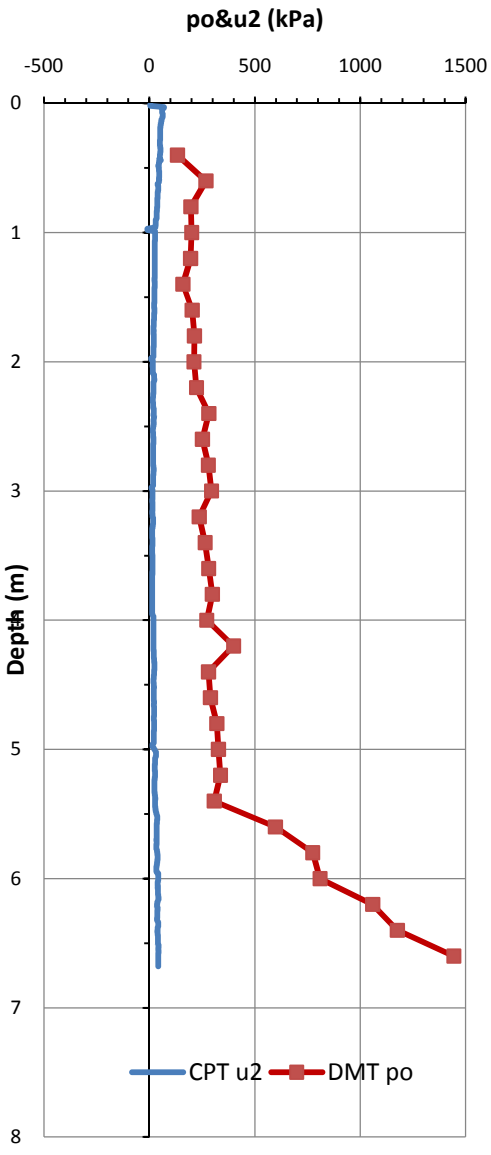

Pohuehue 6a

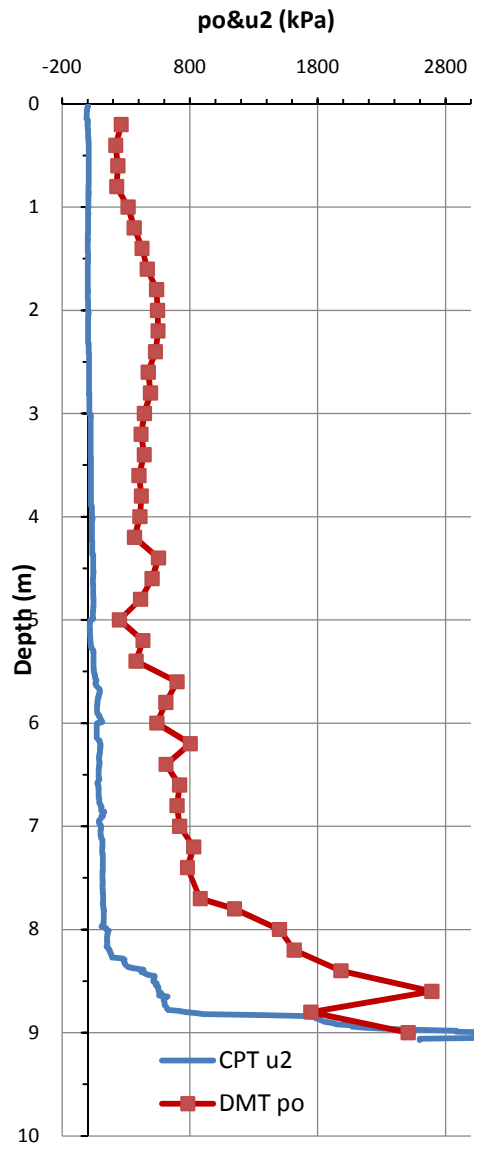

Herald Island 7a

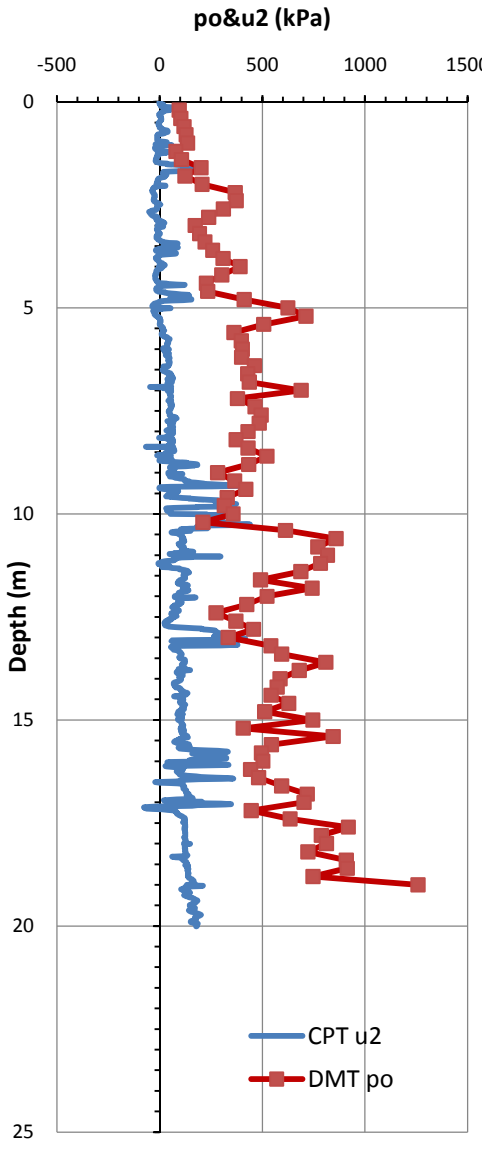

Hamilton 8a

CPT u_2 COMPARED TO DMT p_0

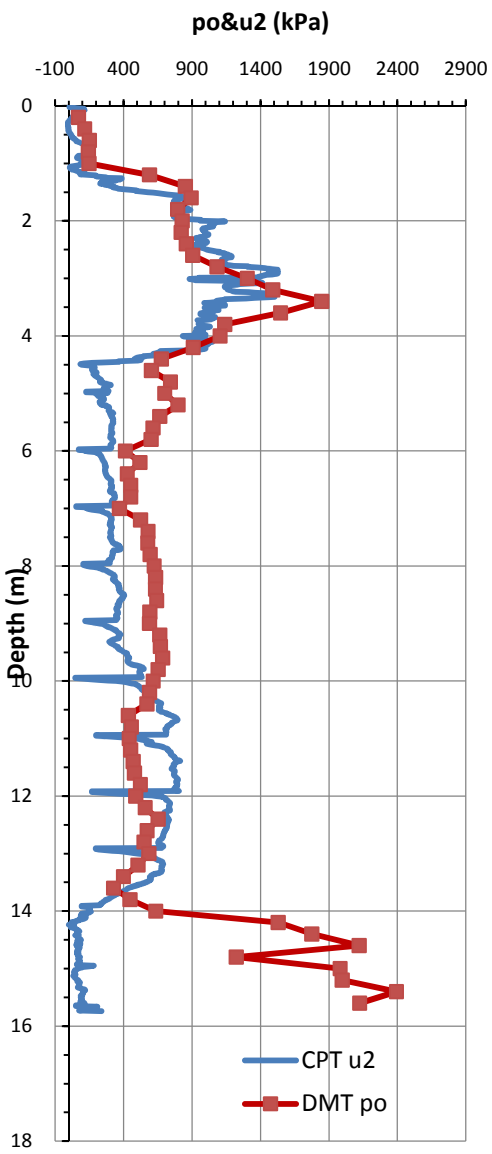

Hamilton 8b

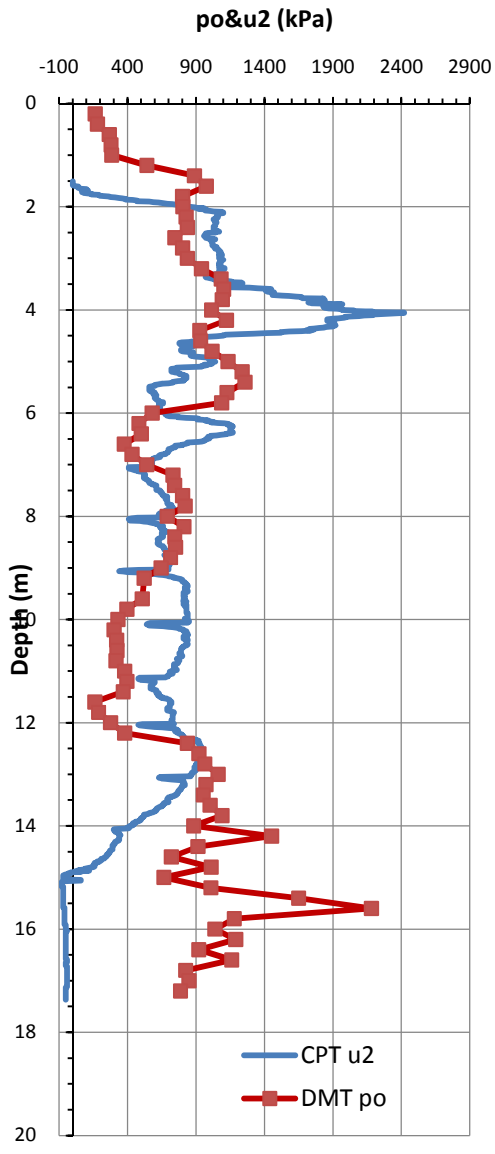

Hamilton 8c

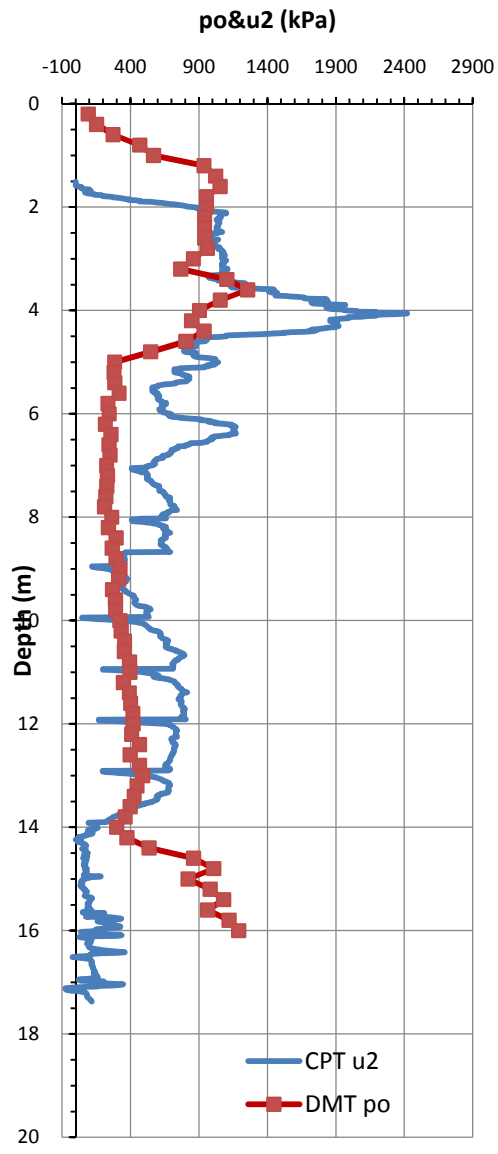

Hamilton 8d

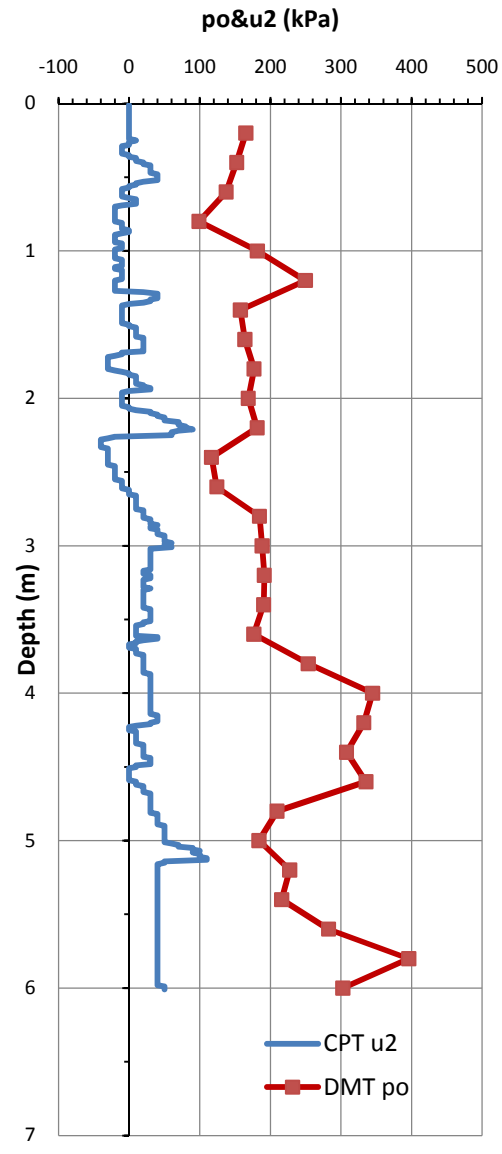

Ngaruawahia a

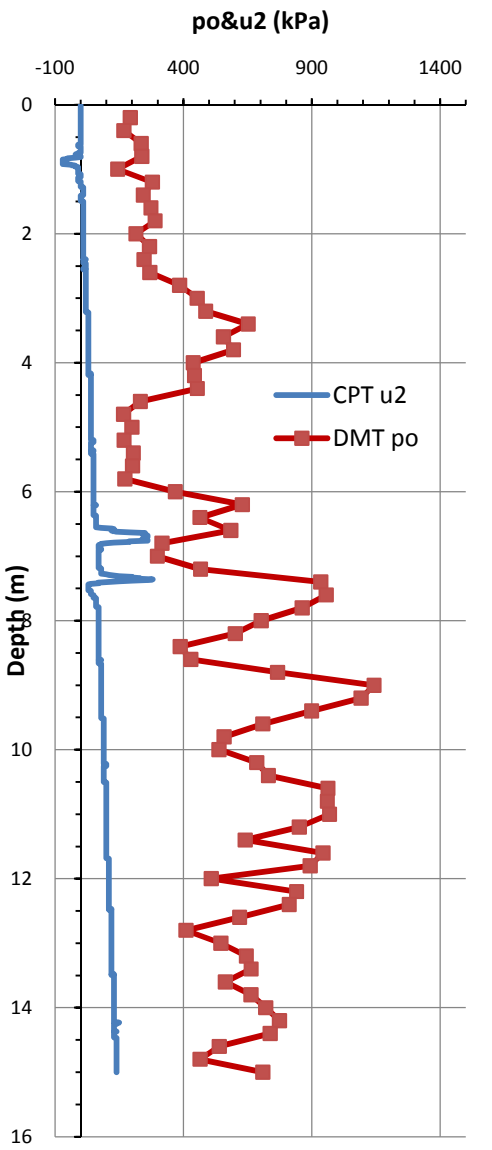

Ngaruawahia 9b

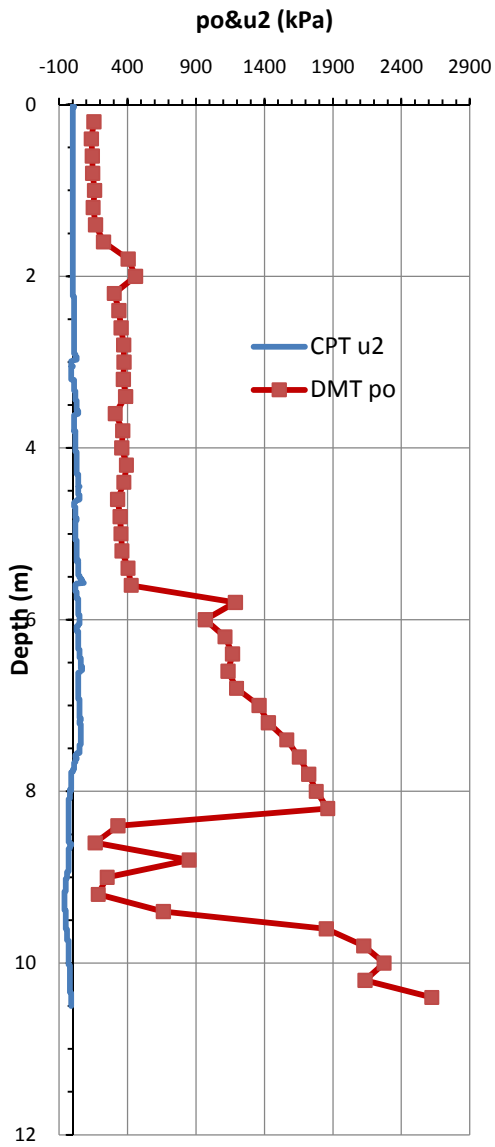

Ngaruawahia 9c

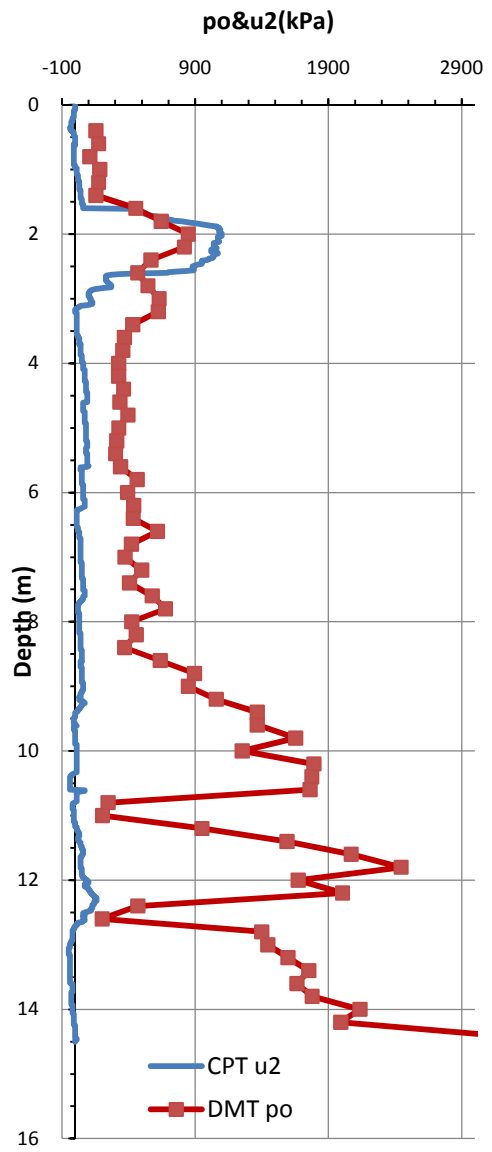

Ngaruawahia 9d

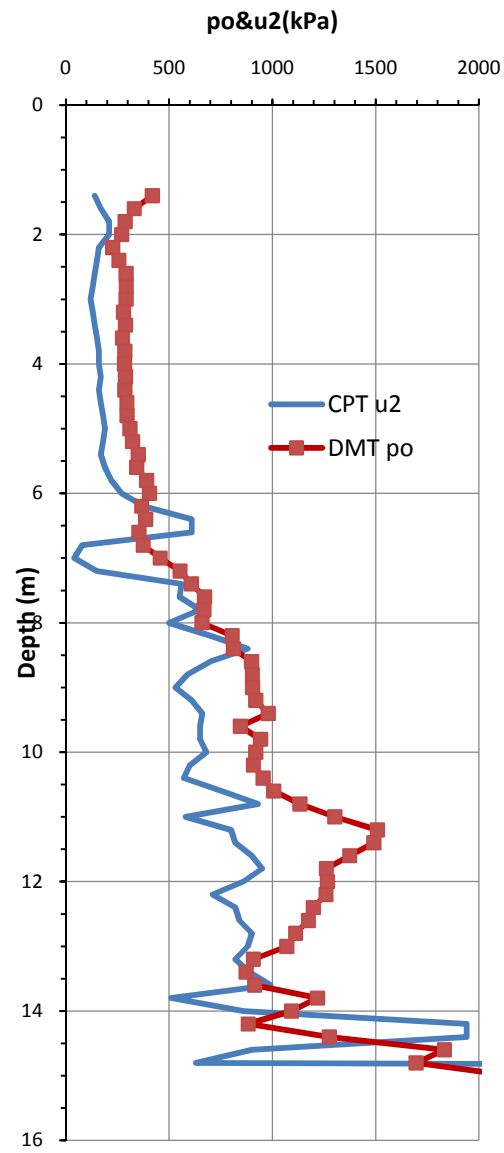

New Lynn 10a

APPENDIX D: AVERAGED CPT AND DMT RESULTS – TABULAR FORMAT

Table 6: CPT and DMT Data

				CPT DATA										DMT DATA				
Site	Pair No.	Soil Type	Depth (m)	q_c (MPa) (ave)	f_s (kPa) (ave)	u_2 (kPa) (ave)	q_t (ave)	σ_{vo} (kPa)	u_0 (kPa)	σ'_{vo} (kPa)	Q_t (ave)	F_r (Ave)	I_c (Ave)	p_o (kPa)	p_1 (kPa)	I_D	K_D	E_D (MPa)
St. Heliers	1a	Alluvium	0.2	0.5485	15.9885	-8.1665	0.54829	3.09891	0	3.0989	208.028	3.26863	2.3606	171	301	0.76	50.2	4.5
St. Heliers	1a	Alluvium	0.4	1.1235	38.6915	1.5845	1.12267	6.356	0	6.356	181.335	10.3809	2.49124	194	302	0.56	29.6	3.8
St. Heliers	1a	Alluvium	0.6	0.0355	18.265	-0.7335	0.03519	9.64184	0	9.6418	2.67295	858.042	3.87846	291	490	0.69	30.0	6.9
St. Heliers	1a	Alluvium	0.8	0.6405	20.924	12.827	0.64537	12.5896	0	12.59	49.3045	2.94142	2.50661	177	307	0.74	13.6	4.5
St. Heliers	1a	Alluvium	1	0.518	41.0235	17.975	0.52642	15.9958	0	15.996	31.9987	8.03645	2.91332	178	249	0.40	11.0	2.5
St. Heliers	1a	Alluvium	1.2	0.535	31.0305	18.083	0.54209	19.3552	0	19.355	27.0177	5.98192	2.87706	190	302	0.59	9.8	3.9
St. Heliers	1a	Alluvium	1.4	0.4515	19.963	42.132	0.47002	22.6485	0	22.649	19.6204	4.67432	2.89661	144	191	0.33	6.4	1.6
St. Heliers	1a	Alluvium	1.6	0.4625	22.284	33.5575	0.47572	25.8803	0.981	24.899	18.1366	5.73401	2.98582	229	295	0.29	9.3	2.3
St. Heliers	1a	Alluvium	1.8	0.285	11.9805	40.4465	0.30238	29.0423	2.943	26.099	10.4683	4.43495	3.08099	158	189	0.20	6.0	1.1
St. Heliers	1a	Alluvium	2	0.308	10.833	78.273	0.34051	32.1073	4.905	27.202	11.3252	3.51521	2.99317	160	179	0.12	5.8	0.7
St. Heliers	1a	Alluvium	2.2	0.285	10.5875	84.6725	0.32092	35.1677	6.867	28.301	10.0854	3.7108	3.04667	152	171	0.13	5.2	0.7
St. Heliers	1a	Alluvium	2.4	0.5255	12.6175	97.2895	0.56505	38.2223	8.829	29.393	17.8423	2.54064	2.79149	156	290	0.92	5.1	4.7
St. Heliers	1a	Alluvium	2.6	0.319	19.637	57.804	0.34441	41.4507	10.79	30.66	9.88366	6.57729	3.18479	82	169	1.23	2.4	3.0
St. Heliers	1a	Alluvium	2.8	0.299	7.6655	99.547	0.34098	44.4839	12.75	31.731	9.33767	2.59094	2.98735	117	102		3.3	
St. Heliers	1a	Alluvium	3	0.3445	14.3785	106.445	0.38921	47.513	14.72	32.798	10.4059	4.2138	3.06081	215	293	0.39	6.3	2.7
St. Heliers	1a	Alluvium	3.2	0.4865	11.783	153.155	0.558	50.6674	16.68	33.99	14.8835	2.52289	2.8296	232	295	0.29	6.5	2.2
St. Heliers	1a	Alluvium	3.4	0.6515	26.842	28.7085	0.65606	53.8524	18.64	35.213	17.1853	6.95449	3.03223	236	283	0.22	6.3	1.6
St. Heliers	1a	Alluvium	4	0.548	10.2865	117.268	0.59647	63.1399	24.53	38.615	13.8103	1.95517	2.80103	217	238	0.11	5.1	0.7
St. Heliers	1a	Alluvium	4.5	4.1615	27.67	26.2055	4.17044	71.2113	29.43	41.781	98.1265	0.69189	1.93916	272	680	1.69	6.0	14.2
St. Heliers	1a	Alluvium	5	0.313	7.613	156.725	0.37881	79.2212	34.34	44.886	6.6663	2.52566	3.10605	241	248	0.04	4.7	0.3
St. Heliers	1a	Alluvium	5.5	0.281	7.492	155.149	0.34613	86.7967	39.24	47.557	5.44932	2.89778	3.20648	194	209	0.09	3.4	0.5
St. Heliers	1a	Alluvium	6	0.281	7.347	183.385	0.35806	94.1816	44.15	50.037	5.26862	2.78142	3.21439	212	219	0.04	3.5	0.3
St. Heliers	1a	Alluvium	6.5	0.3295	8.7205	218.465	0.42144	101.687	49.05	52.637	6.07091	2.729	3.15602	226	235	0.05	3.6	0.3
St. Heliers	1a	Alluvium	7	0.4085	10.736	209.092	0.49663	109.322	53.96	55.367	6.99297	2.87784	3.11667	243	246	0.02	3.7	0.1
St. Heliers	1a	Alluvium	7.5	1.5015	22.9185	230.911	1.59946	117.028	58.86	58.168	25.3635	1.5484	2.59364	378	674	0.93	6.0	10.3
St. Heliers	1a	Alluvium	8	3.5065	98.403	156.911	3.58707	126.561	63.77	62.796	54.8499	4.26037	2.54166	566	1482	1.82	8.8	31.8
Flat Bush	2a	Alluvium	0.2	1.462	69.6395	-7.052	1.45786	3.33098	0	3.331	473.79	4.82853	2.25877	218	504	1.31	64.2	9.9
Flat Bush	2a	Alluvium	0.4	1.406	87.6265	3.236	1.40668	6.97594	0	6.9759	198.534	6.41646	2.46593	184	382	1.08	27.3	6.9
Flat Bush	2a	Alluvium	0.6	1.21	141.847	-2.438	1.20948	10.7001	0	10.7	115.443	12.4753	2.76672	486	854	0.76	48.3	12.8
Flat Bush	2a	Alluvium	0.8	2.1625	93.3725	9.1275	2.16544	14.3607	0	14.361	144.897	5.23789	2.43142	487	1024	1.10	35.8	18.6
Flat Bush	2a	Alluvium	1	2.6585	183.329	83.3045	2.69422	18.1767	0	18.177	147.816	6.91652	2.51254	625	1379	1.21	36.5	26.2
Flat Bush	2a	Alluvium	1.2	1.8345	150.911	81.8985	1.8684	22.0214	0	22.021	84.2027	8.21501	2.68443	514	969	0.88	24.5	15.8
Flat Bush	2a	Alluvium	1.4	1.364	129.314	79.949	1.39808	25.7817	0	25.782	53.201	9.43424	2.82608	514	848	0.65	21.0	11.6
Flat Bush	2a	Alluvium	1.6	1.2945	129.472	78.454	1.32746	29.5225	0	29.523	43.8628	9.98509	2.88656	448	833	0.86	16.0	13.4
Flat Bush	2a	Alluvium	1.8	1.3345	118.546	79.749	1.36849	33.2516	0	33.252	40.0988	8.87307	2.87324	456	816	0.79	14.4	12.5
Flat Bush	2a	Alluvium	2	1.291	115.084	77.8205	1.32318	36.9537	0	36.954	34.7569	8.96387	2.91052	450	772	0.72	12.8	11.2
Flat Bush	2a	Alluvium	2.2	1.1685	118.726	77.7	1.2008	40.6796	0	40.68	28.5183	10.2443	3.00695	485	839	0.73	12.6	12.3
Flat Bush	2a	Alluvium	2.4	1.076	95.371	86.313	1.11342	44.3575	0	44.357	24.0295	8.97904	3.01388	484	798	0.65	11.5	10.9
Flat Bush	2a	Alluvium	2.6	1.7255	109.089	184.952	1.80148	48.0273	0	48.027	36.3715	6.23902	2.79021	633	1157	0.83	13.9	18.2
Flat Bush	2a	Alluvium	2.8	1.451	122.293	391.862	1.61695	51.781	0	51.781	30.2235	7.81932	2.90671	700	1083	0.55	14.1	13.3
Flat Bush	2a	Alluvium	3	1.51	104.603	415.491	1.68401	55.4942	0	55.494	29.2911	6.43172	2.85669	737	1213	0.65	13.9	16.5
Flat Bush	2a	Alluvium	3.2	1.7115	105.619	518.319	1.92841	59.2078	0	59.208	31.5024	5.66839	2.79794	584	865	0.48	10.2	9.8
Flat Bush	2a	Alluvium	3.4	1.5705	104.965	542.713	1.79904	62.9313	0	62.931	27.5716	6.04942	2.85524	604	828	0.37	10.0	7.8
Flat Bush	2a	Alluvium	3.6	1.355	105.93	493.401	1.56208	66.6328	0	66.633	22.4353	7.11474	2.96388	568	885	0.56	8.9	11.0
Flat Bush	2a	Alluvium	3.8	1.107	95.378	467.313	1.30377	70.3288	0	70.329	17.5321	7.72514	3.06643	556	947	0.70	8.2	13.6
Flat Bush	2a	Alluvium	4	1.045	83.561	437.538	1.22877	73.9684	0	73.968	15.6572	7.25146	3.08308	488	753	0.54	6.9	9.2
Flat Bush	2a	Alluvium	4.2	1.001	69.536	424.365	1.17889	77.5769	1.962	75.615	14.5559	6.31878	3.06666	484	701	0.45	6.6	7.5
Flat Bush	2a	Alluvium	4.4	0.984	72.566	422	1.1611	81.1671	3.924	77.243	13.9722	6.72416	3.09775	471	788	0.68	6.3	11.0
Flat Bush	2a	Alluvium	4.6	1.0505	68.38	437.337	1.23499	84.7584	5.886	78.872	14.5679	6.01819	3.0516	518	832	0.61	6.7	10.9
Flat Bush	2a	Alluvium	4.8	1.164	79.1875	437.908	1.34727	88.3559	7.848	80.508	15.6374	6.40806	3.04448	567	908	0.61	7.2	11.8
Flat Bush	2a	Alluvium	5	0.9335	77.4555	427.829	1.11335	91.9859	9.81	82.176	12.4225	7.59044	3.16991	575	852	0.49	7.1	9.6
Flat Bush	2a	Alluvium	5.2	0.9035	62.8765	431.028	1.08421	95.5609	11.77	83.789	11.7963	6.37545	3.1388	536	865	0.63	6.5	11.4
Flat Bush	2a	Alluvium	5.4	0.8745	55.686	433.277	1.05731	99.1035	13.73	85.37	11.2144	5.87002	3.13099	551	824	0.51	6.5	9.5
Flat Bush	2a	Alluvium	5.6	1.8245	72.3475	514.241	2.03886	102.648	15.7	86.952	22.2318	3.77998	2.78902	563	895	0.61	6.5	11.5
Flat Bush	2a	Alluvium	5.8	1.9445	112.964	587.917	2.19126	106.368	17.66	88.71	23.4904	5.42003	2.86791	577	1026	0.80	6.6	15.6
Flat Bush	2a	Alluvium	6	1.4375	94.543	516.479	1.65534	110.092	19.62	90.472	17.0827	6.12079	3.00793	512	952	0.89	5.7	15.3
Flat Bush	2a	Alluvium	6.2	0.988	72.054	440.192	1.17341	113.723	21.58	92.141	11.4992	6.81568	3.1663	492	774	0.60	5.3	9.8
Flat Bush	2a	Alluvium	6.4	1.1315	53.475	464.894	1.32675	117.279	23.54	93.735	12.8932	4.45984	3.00934	579	859	0.51	6.2	9.7
Flat Bush	2a	Alluvium	6.6	1.028	49.041	468.175	1.22534	120.805	25.51	95.299	11.5886	4.46236	3.04774	560	854	0.55	5.8	10.2
Flat Bush	2a	Alluvium	6.8	1.7495	50.584	596.955	1.99933	124.306	27.47	96.838	19.3354	2.73909	2.74699	548	952	0.78	5.6	14.0
Flat Bush	2a	Alluvium	7	2.396	103.2	517.857	2.61377	127.95	29.43	98.52	25.205	4.14609	2.76785	602	1289	1.20	6.0	23.8
Flat Bush	2a	Alluvium	7.2	3.284	170.738	407.079	3.45438	131.758	31.39	100.37	33.0818	5.11919	2.74199	454	1252	1.89	4.4	27.7
Flat Bush	2a	Alluvium	7.4	2.8625	155.814	357.923	3.01064	135.65	33.35	102.3	28.1089	5.39206	2.81134	447	1063	1.49	4.2	21.4
Flat Bush	2a	Alluvium	7.6	2.177	99.8305	399.538	2.34818	139.415	35.32	104.1	21.2114	4.52497	2.84793	435	1056	1.55	4.0	21.5
Flat Bush	2a	Alluvium	7.8	2.9815	117.899	374.185	3.13894	143.144	37.28	105.87	28.263	3.95982	2.71939	409	1026	1.66	3.7	21.4
Flat Bush	2a	Alluvium	8	3.66	149.376	108.566	3.7051	146.968	39.24	107.73	33.0012	4.23558	2.68692	394	960	1.60	3.4	19.6
Flat Bush	2a	Alluvium	8.2	4.6295	174.574	47.4525	4.64647	150.849	41.2	109.65	40.9844	3.88501	2.58982	368	1272	2.77	3.1	31.4
Flat Bush	2a	Alluvium	8.4	3.754	149.303	92.041	3.79782	154.734	43.16	111.57	32.632	4.14229	2.68021	397	1137	2.09	3.3	25.7
Flat Bush	2a	Alluvium	8.6	5.1595	172.41	119.716	5.20695	158.597	45.13	113.47	44.466	3.41139	2.52264	459	1349	2.15	3.8	30.9
Flat Bush	2a	Alluvium	8.8	5.308	207.19	141.778	5.36878	162.535	47.09	115.45	45.0712	3.98646	2.56665	425	937	1.36	3.4	17.8
Flat Bush	2a	Alluvium	9	5.655	213.476	149.547	5.71609	166.496	49.05	117.45	47.2388	3.86067	2.541	448	1460	2.54	3.6	35.1
Flat Bush	2a	Alluvium	9.2	4.8185	196.263	164.014	4.88788	170.455	51.01	119.44	39.4925	4.15887	2.62112	515	1454	2.02	4.1	32.6
Flat Bush	2a	Alluvium	9.4	4.03	143.501	223.949	4.12277	174.352	52.97	121.38	32.5337	3.63641	2.64601	553	1171	1.24	4.3	21.5
Flat Bush	2a	Alluvium	9.6	2.83	86.14	300.009	2.95729	178.113	54.94	123.18	22.5325	3.39821	2.74579	858	1570	0.89	6.9	24.7
Flat Bush	2a	Alluvium	9.8	5.436	172.794	446.337	5.63448	181.888	56.9	124.99	43.6329	3.39772	2.50326	1749	4092	1.38	14.3	81.3
Flat Bush	2a	Alluvium	10	7.532	257.564	1914.79	8.3252	185.842	58.86	126.98	64.0002	3.19112	2.39223	1043	2732	1.72	8.1	58.6
Flat Bush	2a	Alluvium	10.2	11.2073	412.048	3035.12	12.482	189.974	60.82	129.15	95.4603	3.45768	2.2926	3166	6607	1.11	25.2	119.4
Maungaturoto	3a	Alluvium	1.2	0.615	32.082	3.753	0.61649	19.4741	1.962	17.512	33.8763	5.81226	2.81291	135	175	0.30	6.7	1.4
Maungaturoto	3a	Alluvium	1.4	0.6465	37.857	1.025	0.64635	22.8607	3.924	18.937	33.1148	8.01612	2.90035	164	223	0.36	7.1	2.0
Maungaturoto	3a	Alluvium	1.6	0.3645	31.5545	13.107	0.37	26.219	5.886	20.333	16.8643	9.2833	3.12968	177	205	0.16	6.7	1.0
Maungaturoto	3a	Alluvium	1.8	0.403	29.9035	20.5145	0.41161	29.52	7.848	21.672	17.6009	7.8458	3.06804	159	185	0.17	5.4	0.9
Maungaturoto	3a	Alluvium	2	0.4115	33.1275	24.601	0.42184	32.8456	9.81	23.036	16.8224	8.86263	3.11918	175	194	0.11	5.4	0.7
Maungaturoto	3a	Alluvium	2.2	0.5485	40.8035	39.2315	0.56481	36.209	11.77	24.437	21.598	7.72085	3.00065	194	202	0.04	5.5	0.3
Maungaturoto	3a	Alluvium	2.4	0.4875	42.5165	46.121	0.50704	39.6328	13.73	25.899	18.0408	9.10607	3.10714	232	280	0.21	6.1	1.7
Maungaturoto	3a	Alluvium	2.6	0.604	36.6835	69.9155	0.63336	43.0173	15.7	27.321	21.5469	6.29282	2.94656	188	308	0.64	4.6	4.2
Maungaturoto	3a	Alluvium	2.8	0.7045	53.2095	84.4635	0.73997	46.4512	17.66	28.793	24.0408	7.65771	2.96697	247	387	0.56	5.6	4.8
Maungaturoto	3a	Alluvium	3	0.6845	67.2455	94.6415	0.72425	49.9789	19.62	30.359	22.189	9.97758	3.07166	283	425	0.50	5.9	4.9
Maungaturoto	3a	Alluvium	3.1	0.6625	68.56	100.806	0.70467	51.7488	20.6	31.148	20.944	10.5183	3.10524	276	433	0.57	5.7	5.5
Maungaturoto	3a	Alluvium	3.2	0.636	73.2115	103.762	0.67958	53.5221	21.58	31.94	19.5824	11.7197	3.15895	323	497	0.54	6.5	6.0

Table 6: CPT and DMT Data

				CPT DATA										DMT DATA				
Site	Pair No.	Soil Type	Depth (m)	q_c (MPa) (ave)	f_s (kPa) (ave)	u_2 (kPa) (ave)	q_t (ave)	σ_{vo} (kPa)	u_0 (kPa)	σ'_{vo} (kPa)	Q_t (ave)	F_r (Ave)	I_c (Ave)	p_o (kPa)	p_1 (kPa)	I_D	K_D	E_D (MPa)
Maungaturoto	3a	Alluvium	3.3	0.659	74.9095	106.336	0.70383	55.3041	22.56	32.741	19.766	11.6308	3.15364	327	497	0.53	6.5	5.9
Maungaturoto	3a	Alluvium	3.4	0.744	72.292	111.739	0.79111	57.0855	23.54	33.542	21.8348	9.93912	3.07413	295	427	0.45	5.8	4.6
Maungaturoto	3a	Alluvium	3.5	0.8215	66.8125	123.469	0.87302	58.8681	24.53	34.343	23.6704	8.24834	2.99227	285	382	0.34	5.5	3.4
Maungaturoto	3a	Alluvium	3.6	0.788	59.7545	136.213	0.84537	60.6387	25.51	35.133	22.3367	7.63323	2.98908	222	325	0.48	4.2	3.6
Maungaturoto	3a	Alluvium	3.7	0.6955	51.514	142.73	0.75545	62.3931	26.49	35.906	19.299	7.41518	3.02386	169	282	0.70	3.1	3.9
Maungaturoto	3a	Alluvium	3.8	0.5935	42.668	144.18	0.65353	64.1199	27.47	36.652	16.0925	7.2868	3.07915	201	285	0.43	3.6	2.9
Maungaturoto	3a	Alluvium	3.9	0.5195	32.914	140.463	0.57936	65.8199	28.45	37.371	13.7352	6.41052	3.08438	192	313	0.66	3.4	4.2
Maungaturoto	3a	Alluvium	4	0.4885	22.254	154.867	0.55357	67.4728	29.43	38.043	12.7753	4.56114	3.01621	230	334	0.47	4.1	3.6
Maungaturoto	3a	Alluvium	4.1	1.039	18.098	157.614	1.15047	69.0799	30.41	38.669	27.7063	3.3889	2.8234	225	248	0.11	3.9	0.8
Maungaturoto	3a	Alluvium	4.2	10.152	27.2155	44.1685	10.1752	70.7123	31.39	39.32	254.198	1.52862	1.92306	230	441	0.97	3.9	7.3
Maungaturoto	3a	Alluvium	4.3	20.9026	125.153	564.249	21.0848	72.5239	32.37	40.151	521.753	0.52898	1.33048	1057	4019	2.84	18.6	102.8
Kaiwaka	4a	Redisula Soil	0.2	1.659	44.1745	15.01	1.67149	3.34705	0	3.3471	569.143	2.96093	2.10246	111	216	0.95	32.6	3.6
Kaiwaka	4a	Redisula Soil	0.4	2.6725	62.653	92.196	2.71594	6.91165	0	6.9117	391.773	2.44329	2.06178	94	151	0.60	14.4	2.0
Kaiwaka	4a	Redisula Soil	0.6	3.186	91.481	76.8495	3.20966	10.5899	0	10.59	313.767	3.80801	2.18345	122	223	0.82	12.6	3.5
Kaiwaka	4a	Redisula Soil	0.8	1.6595	81.6445	91.2435	1.70501	14.2715	0	14.271	115.438	5.89284	2.51741	51	121	1.39	4.0	2.4
Kaiwaka	4a	Redisula Soil	1	3.1295	56.2435	101.006	3.16177	17.9235	0	17.923	179.259	2.09598	2.03045	413	1041	1.52	25.9	21.8
Kaiwaka	4a	Redisula Soil	1.2	0.665	37.0545	58.819	0.69231	21.4247	0	21.425	31.2617	5.52512	2.81113	150	231	0.54	7.7	2.8
Kaiwaka	4a	Redisula Soil	1.4	0.7335	37.4335	59.9265	0.75901	24.7877	0	24.788	29.611	5.15365	2.80508	45	263	4.90	2.0	7.6
Kaiwaka	4a	Redisula Soil	1.6	2.614	31.3925	64.068	2.60416	28.2117	0	28.212	88.1572	3.6229	2.46339	61	126	1.07	2.3	2.3
Kaiwaka	4a	Redisula Soil	1.8	3.462	86.631	29.913	3.51205	31.7417	0	31.742	112.307	8.02132	2.4993	126	234	0.86	4.3	3.8
Kaiwaka	4a	Redisula Soil	2	0.7295	37.237	40.1115	0.74511	35.3091	0	35.309	20.0208	5.80867	2.90149	105	245	1.33	3.3	4.8
Kaiwaka	4a	Redisula Soil	2.2	0.76	22.931	58.557	0.78461	38.6126	0	38.613	19.283	3.07748	2.79404	125	317	1.54	3.5	6.7
Kaiwaka	4a	Redisula Soil	2.4	0.8585	24.2225	97.7695	0.89938	41.903	0	41.903	20.413	2.81904	2.75328	327	495	0.51	8.5	5.8
Kaiwaka	4a	Redisula Soil	2.6	0.8775	32.5955	116.852	0.9271	45.2728	0	45.273	19.4479	3.69483	2.83273	250	435	0.74	6.0	6.4
Kaiwaka	4a	Redisula Soil	2.8	0.9015	32.894	151.885	0.96493	48.6707	0	48.671	18.806	3.59186	2.83489	70	367	4.25	1.5	10.3
Kaiwaka	4a	Redisula Soil	3	0.8325	25.489	161.612	0.90038	52.0495	0	52.05	16.2779	3.00669	2.83321	257	431	0.68	5.3	6.0
Kaiwaka	4a	Redisula Soil	3.2	0.762	19.4425	154.65	0.82696	55.3323	0	55.332	13.9479	2.54858	2.84607	163	408	1.52	3.2	8.5
Kaiwaka	4a	Redisula Soil	3.4	0.6265	14.2135	156.2	0.69227	58.5691	0	58.569	10.809	2.24175	2.90033	157	429	1.78	3.0	9.4
Kaiwaka	4a	Redisula Soil	3.6	0.714	12.5105	167.06	0.78383	61.7079	0	61.708	11.6791	1.72818	2.81774	186	366	0.99	3.4	6.2
Kaiwaka	4a	Redisula Soil	3.8	0.6855	14.329	173.695	0.75862	64.9055	0	64.905	10.6788	2.06351	2.88622	194	319	0.67	3.4	4.3
Kaiwaka	4a	Redisula Soil	4	0.693	15.691	172.878	0.76578	68.0722	0	68.072	10.2291	2.27789	2.92436	237	412	0.77	4.1	6.1
Kaiwaka	4a	Redisula Soil	4.2	0.806	19.2795	184.01	0.88328	71.3276	0	71.328	11.3691	2.37414	2.89518	196	371	0.95	3.2	6.1
Kaiwaka	4a	Redisula Soil	4.4	0.863	20.9305	199.973	0.94682	74.6024	0	74.602	11.6811	2.4036	2.88762	143	394	1.94	2.2	8.7
Kaiwaka	4a	Redisula Soil	4.6	0.849	18.588	217.195	0.94055	77.8897	0	77.89	11.0623	2.15844	2.88203	184	231	0.28	2.8	1.6
Kaiwaka	4a	Redisula Soil	4.8	0.9485	19.2825	262.211	1.05832	81.1658	0	81.166	12.0235	1.97703	2.83202	126	359	2.15	1.8	8.1
Kaiwaka	4a	Redisula Soil	5	1.087	33.468	295.849	1.21108	84.4813	0	84.481	13.3605	2.96673	2.88604	165	277	0.77	2.3	3.9
Kaiwaka	4a	Redisula Soil	5.4	1.4255	37.8425	534.654	1.64814	91.2892	3.924	87.365	17.8059	2.50768	2.74246	187	330	0.87	2.5	5.0
Kaiwaka	4a	Redisula Soil	5.6	1.1015	55.0905	581.273	1.34644	94.8245	5.886	88.938	14.065	4.41547	2.97612	236	367	0.62	3.2	4.6
Kaiwaka	4a	Redisula Soil	5.8	1.7705	48.8965	549.004	2.0013	98.3264	7.848	90.478	21.0194	2.70166	2.70165	218	542	1.71	2.8	11.3
Kaiwaka	4a	Redisula Soil	6	1.2485	51.6155	489.458	1.45374	101.892	9.81	92.082	14.6712	3.81297	2.92192	306	546	0.87	4.0	8.3
Kaiwaka	4a	Redisula Soil	6.2	1.6565	40.2285	764.767	1.97718	105.367	11.77	93.595	19.9893	2.18957	2.66964	322	541	0.76	4.2	7.6
Kaiwaka	4a	Redisula Soil	6.4	1.5895	42.46	1012.4	2.01702	108.899	13.73	95.165	20.0295	2.31	2.68088	272	393	0.51	3.4	4.2
Kaiwaka	4a	Redisula Soil	6.6	2.162	58.3925	1214.21	2.67117	112.435	15.7	96.739	26.4395	2.2989	2.58511	312	450	0.50	3.8	4.8
Kaiwaka	4a	Redisula Soil	6.8	2.603	58.7575	1579.19	3.2747	116.052	17.66	98.394	32.0769	1.86475	2.46598	280	614	1.38	3.3	11.6
Kaiwaka	4a	Redisula Soil	7	3.6425	119.318	1530.57	4.27301	119.736	19.62	100.12	41.4837	3.02613	2.4881	303	410	0.41	3.5	3.7
Kaiwaka	4a	Redisula Soil	7.2	2.815	95.525	1565.85	3.47541	123.545	21.58	101.96	32.8578	2.8575	2.5706	319	397	0.28	3.6	2.7
Kaiwaka	4a	Redisula Soil	7.4	4.037	92.8295	1699.18	4.86701	127.278	23.54	103.73	45.6131	2.0798	2.37767	420	1012	1.57	4.8	20.5
Matakana	5a	Residual Soil	0.2	0.5165	35.6725	62.745	0.542	3.08135	0	3.0814	185.54	6.57985	2.52345	152	261	0.72	44.6	3.8
Matakana	5a	Residual Soil	0.4	0.735	49.7155	47.897	0.75489	6.51745	0	6.5175	114.881	6.65104	2.59339	191	365	0.91	29.2	6.0
Matakana	5a	Residual Soil	0.6	0.8805	63.297	36.484	0.89548	10.0292	0	10.029	88.1429	7.14595	2.65602	231	439	0.90	23.4	7.2
Matakana	5a	Residual Soil	0.8	0.826	76.388	4.9405	0.82777	13.5985	0	13.598	59.6016	9.4648	2.81166	237	400	0.69	18.0	5.6
Matakana	5a	Residual Soil	1	0.7885	81.157	10.9135	0.79325	17.1845	0	17.184	45.8732	10.5508	2.89947	288	458	0.59	17.4	5.9
Matakana	5a	Residual Soil	1.2	0.626	71.4935	16.1875	0.63297	20.7631	1.962	18.801	32.552	11.6606	3.01068	266	478	0.80	14.7	7.4
Matakana	5a	Residual Soil	1.4	0.483	61.302	15.7435	0.48961	24.2767	3.924	20.353	22.879	13.2441	3.1542	254	380	0.50	13.0	4.4
Matakana	5a	Residual Soil	1.6	0.4585	47.2385	16.18	0.4653	27.7315	5.886	21.846	20.018	10.8544	3.12912	234	394	0.70	11.1	5.5
Matakana	5a	Residual Soil	1.8	0.3515	33.8295	15.9905	0.35821	31.1188	7.848	23.271	14.055	10.2913	3.22137	248	395	0.61	10.9	5.1
Matakana	5a	Residual Soil	2	0.368	25.047	17.64	0.37543	34.3975	9.81	24.588	13.8557	7.38847	3.12812	238	345	0.47	9.7	3.7
Matakana	5a	Residual Soil	2.2	0.3425	22.106	37.011	0.35805	37.6433	11.77	25.871	12.3579	6.94977	3.14699	205	278	0.38	7.8	2.6
Matakana	5a	Residual Soil	2.4	0.3535	25.95	100.363	0.39584	40.8919	13.73	27.158	13.0506	7.30837	3.14378	196	313	0.64	7.0	4.0
Matakana	5a	Residual Soil	2.6	0.414	25.6975	152.52	0.47734	44.1665	15.7	28.47	15.1797	5.9485	3.03594	235	344	0.50	8.1	3.8
Matakana	5a	Residual Soil	2.8	0.34	29.3025	169.652	0.41209	47.4854	17.66	29.827	12.2148	8.24773	3.19667	244	350	0.47	7.9	3.7
Matakana	5a	Residual Soil	3	0.4915	34.6775	175.318	0.56496	50.7837	19.62	31.164	16.4781	6.74203	3.04	214	306	0.48	6.5	3.2
Matakana	5a	Residual Soil	3.2	0.4465	37.0755	182.251	0.52292	54.179	21.58	32.597	14.3695	7.91264	3.13641	246	330	0.37	7.2	2.9
Matakana	5a	Residual Soil	3.4	0.4035	31.9115	193.229	0.48463	57.5396	23.54	33.996	12.5558	7.47001	3.16337	262	329	0.28	7.4	2.3
Matakana	5a	Residual Soil	3.6	0.422	28.0135	201.84	0.50696	60.8585	25.51	35.353	12.5999	6.32544	3.11371	261	329	0.29	7.0	2.4
Matakana	5a	Residual Soil	3.8	0.4155	30.2395	227.819	0.511	64.189	27.47	36.721	12.1643	6.76803	3.14625	288	476	0.72	7.5	6.5
Matakana	5a	Residual Soil	4	0.4235	36.3975	202.503	0.50837	67.5281	29.43	38.098	11.5624	8.23551	3.21729	297	423	0.47	7.4	4.4
Matakana	5a	Residual Soil	4.2	0.393	29.298	201.089	0.47762	70.8795	31.39	39.487	10.2958	7.21391	3.21882	267	361	0.40	6.3	3.3
Matakana	5a	Residual Soil	4.4	0.34	23.2885	198.821	0.42354	74.1697	33.35	40.816	8.55227	6.68076	3.25828	291	403	0.44	6.6	3.9
Matakana	5a	Residual Soil	4.61	0.426	20.977	242.141	0.52803	77.5692	35.41	42.155	10.6663	4.7034	3.08989	294	399	0.41	6.5	3.6
Matakana	5a	Residual Soil	4.8	0.7035	26.3335	333.357	0.84379	80.6793	37.28	43.401	17.5344	3.47488	2.85566	267	373	0.46	5.5	3.7
Matakana	5a	Residual Soil	5	0.7545	57.032	274.175	0.86933	84.1237	39.24	44.884	17.5053	7.51088	3.05697	319	441	0.44	6.5	4.2
Matakana	5a	Residual Soil	5.2	0.6245	43.808	243.556	0.72551	87.6079	41.2	46.406	13.7401	6.87545	3.11024	331	628	1.03	6.6	10.3
Matakana	5a	Residual Soil	5.4	0.548	37.2585	241.435	0.65035	91.0201	43.16	47.856	11.6747	6.71169	3.15617	336	485	0.51	6.4	5.2
Matakana	5a	Residual Soil	5.6	0.75	39.31	256.518	0.85858	94.428	45.13	49.302	15.4714	5.20408	2.99328	350	577	0.74	6.5	7.9
Matakana	5a	Residual Soil	5.8	0.897	48.479	339.032	1.0387	97.8886	47.09	50.801	18.5154	5.26902	2.93778	312	457	0.55	5.5	5.0
Matakana	5a	Residual Soil	6	0.817	64.6885	255.448	0.92424	101.427	49.05	52.377	15.7026	7.85492	3.1056	302	423	0.48	5.1	4.2
Matakana	5a	Residual Soil	6.2	0.905	56.333	325.733	1.04126	104.954	51.01	53.942	17.3492	6.09609	3.0006	302	465	0.65	4.9	5.6
Matakana	5a	Residual Soil	6.4	0.7315	48.937	338.233	0.87392	108.467	52.97	55.493	13.7766	6.48202	3.08989	312	458	0.56	4.9	5.1
Matakana	5a	Residual Soil	6.6	1.2345	55.2755	141.372	1.29397	111.953	54.94	57.017	20.6674	4.99083	2.89762	282	478	0.87	4.2	6.8
Matakana	5a	Residual Soil	6.8	1.663	78.1585	33.7205	1.6768	115.557	56.9	58.659	26.62	5.09569	2.81731	316	457	0.54	4.7	4.9
Matakana	5a	Residual Soil	7	1.254	68.5345	141.679	1.31377	119.169	58.86	60.309	19.7739	5.89047	2.94877	304	436	0.54	4.3	4.6
Matakana	5a	Residual Soil	7.2	1.0795	58.6045	122.688	1.13081	122.756	60.82	61.934	16.3011	6.08685	3.03126	319	439	0.46	4.5	4.2
Matakana	5a	Residual Soil	7.4	0.6915	37.87	240.943	0.79284	126.214	62.78	63.43	10.5005	5.70083	3.14591	279	410	0.61	3.6	4.6
Matakana	5a	Residual Soil	7.6	2.381	40.0655	247.317	2.48383	129.625	64.75	64.879	36.0479	3.84078	2.73764	518	1594	2.38	7.5	37.3
Matakana	5a	Residual Soil	7.8	7.082	268.579	180.575	7.13915	133.381	66.71	66.673	104.921	3.81757	2.32886	861	6980	7.71	12.7	212.3
Matakana	5a	Residual Soil	8	7.2175	317.225	1180.43	7.7506	137.459	68.67	68.789	110.337	4.58627	2.37164	4069	6980	0.73	61.6	101.0
Pohuehue	6a	Residual Soil	0.4	0.981	72.0155	48.614	1.00159	6.82318	0	6.8232	143.521	7.45304	2.5736	133	140	0.06	19.5	0.3
Pohuehue	6a	Residual Soil	0.6	1.1935	102.289	43.475	1.21075	10.4638	0	10.464	115.071	8.52426	2.64885	268	521	0.94	28.1	8.8

Table 6: CPT and DMT Data

				CPT DATA										DMT DATA				
Site	Pair No.	Soil Type	Depth (m)	q_c (MPa) (ave)	f_s (kPa) (ave)	u_2 (kPa) (ave)	q_t (ave)	σ_{vo} (kPa)	u_0 (kPa)	σ'_{vo} (kPa)	Q_t (ave)	F_r (Ave)	I_c (Ave)	p_o (kPa)	p_1 (kPa)	I_D	K_D	E_D (MPa)
Pohuehue	6a	Residual Soil	0.8	0.864	95.704	36.2225	0.88005	14.1311	0	14.131	61.9553	11.2633	2.85743	197	369	0.88	15.3	6.0
Pohuehue	6a	Residual Soil	1	0.548	83.654	23.4145	0.55767	17.7221	0	17.722	30.4594	16.3299	3.13833	201	378	0.88	12.4	6.2
Pohuehue	6a	Residual Soil	1.2	0.5165	74.48	25.398	0.52733	21.2876	0	21.288	23.6875	14.7982	3.17603	195	259	0.33	10.0	2.2
Pohuehue	6a	Residual Soil	1.4	0.527	71.987	24.34	0.53739	24.8161	0	24.816	20.6628	14.1033	3.20338	159	250	0.58	7.0	3.2
Pohuehue	6a	Residual Soil	1.6	0.5355	68.063	22.6705	0.54469	28.343	0	28.343	18.2108	13.2607	3.22054	203	315	0.55	7.8	3.9
Pohuehue	6a	Residual Soil	1.8	0.499	62.412	20.1045	0.50778	31.8589	0	31.859	14.9136	13.1375	3.27679	214	349	0.63	7.3	4.7
Pohuehue	6a	Residual Soil	2	0.4985	56.121	16.506	0.50527	35.3393	0	35.339	13.3693	11.969	3.28239	211	308	0.46	6.5	3.4
Pohuehue	6a	Residual Soil	2.2	0.5095	52.791	19.408	0.51782	38.7999	1.962	36.838	13.0036	11.1635	3.26951	223	364	0.64	6.6	4.9
Pohuehue	6a	Residual Soil	2.4	0.541	56.435	19.288	0.5501	42.2631	3.924	38.339	13.2347	11.2098	3.26333	282	376	0.34	7.9	3.3
Pohuehue	6a	Residual Soil	2.6	0.546	52.6735	17.939	0.55237	45.7442	5.886	39.858	12.6941	10.4478	3.2565	252	365	0.46	6.7	3.9
Pohuehue	6a	Residual Soil	2.8	0.779	57.5615	18.374	0.78672	49.2049	7.848	41.357	17.7761	8.10558	3.07978	280	391	0.41	7.2	3.9
Pohuehue	6a	Residual Soil	3	0.6575	76.9835	14.902	0.66343	52.7762	9.81	42.966	14.2135	12.607	3.28034	295	367	0.25	7.3	2.5
Pohuehue	6a	Residual Soil	3.2	0.524	60.535	15.0915	0.5305	56.295	11.77	44.523	10.6665	14.0315	3.39883	236	292	0.25	5.5	1.9
Pohuehue	6a	Residual Soil	3.4	0.222	37.0795	13.4425	0.22799	59.7185	13.73	45.985	3.65979	21.5704	3.86735	264	362	0.39	6.0	3.4
Pohuehue	6a	Residual Soil	3.6	0.2665	23.867	13.942	0.27219	62.9459	15.7	47.25	4.42071	11.525	3.63094	281	423	0.53	6.2	4.9
Pohuehue	6a	Residual Soil	3.8	0.3155	24.148	13.307	0.32126	66.1813	17.66	48.523	5.24728	9.60868	3.52387	299	497	0.71	6.3	6.9
Pohuehue	6a	Residual Soil	4	0.461	25.108	17.468	0.46817	69.4404	19.62	49.82	7.99026	6.35449	3.26932	272	561	1.14	5.5	10.0
Pohuehue	6a	Residual Soil	4.2	0.636	35.01	20.2045	0.64399	72.7627	21.58	51.181	11.1315	6.41216	3.16332	399	537	0.36	8.0	4.8
Pohuehue	6a	Residual Soil	4.4	0.642	54.951	21.954	0.65189	76.2051	23.54	52.661	10.9461	10.438	3.29692	280	488	0.81	5.3	7.2
Pohuehue	6a	Residual Soil	4.6	0.656	41.861	21.355	0.6648	79.6477	25.51	54.142	10.7911	7.18784	3.2019	289	473	0.70	5.3	6.4
Pohuehue	6a	Residual Soil	4.8	0.7445	53.1835	21.8265	0.75383	83.1149	27.47	55.647	12.046	7.99078	3.19575	320	494	0.60	5.7	6.0
Pohuehue	6a	Residual Soil	5	0.915	49.9975	24.113	0.92446	86.5682	29.43	57.138	14.6233	6.22864	3.07344	328	463	0.45	5.7	4.7
Pohuehue	6a	Residual Soil	5.2	0.859	75.698	25.2895	0.87112	90.1396	31.39	58.748	13.294	9.7303	3.22251	337	608	0.89	5.7	9.4
Pohuehue	6a	Residual Soil	5.4	1.7285	78.541	27.428	1.74838	93.7032	33.35	60.349	27.321	5.20263	2.8296	308	541	0.85	5.0	8.1
Pohuehue	6a	Residual Soil	5.6	4.1165	195.341	35.053	4.12287	97.4673	35.32	62.151	64.7598	5.0663	2.53236	598	1650	1.87	9.9	36.5
Pohuehue	6a	Residual Soil	5.8	5.196	318.536	36.049	5.20696	101.472	37.28	64.194	79.4025	6.5205	2.58341	775	2064	1.75	12.5	44.7
Pohuehue	6a	Residual Soil	6	4.6375	352.836	39.085	4.65926	105.532	39.24	66.292	68.5507	8.01541	2.68688	809	2209	1.82	12.7	48.6
Pohuehue	6a	Residual Soil	6.2	5.0765	406.731	39.058	5.0884	109.618	41.2	68.416	72.7663	8.27049	2.68269	1059	2709	1.62	16.3	57.2
Pohuehue	6a	Residual Soil	6.4	5.82	404.473	39.613	5.83198	113.723	43.16	70.559	80.8411	7.60356	2.62084	1176	2183	0.89	17.5	34.9
Pohuehue	6a	Residual Soil	6.6	6.80722	487.577	42.3817	6.80928	117.867	45.13	72.741	92.0995	7.34311	2.58245	1444	2517	0.77	20.9	37.2
Herald Island	7a	Residual Soil	0.2	4.2225	62.272	-0.3915	4.22017	3.42812	0	3.4281	1374.24	1.57452	1.75208	263	456	0.74	77.3	6.7
Herald Island	7a	Residual Soil	0.4	2.821	157.472	7.542	2.824	7.18106	0	7.1811	403.01	5.80732	2.29509	220	409	0.86	32.7	6.6
Herald Island	7a	Residual Soil	0.6	2.09	201.857	8.557	2.09359	11.0663	0	11.066	190.126	9.68674	2.58763	237	552	1.33	23.5	10.9
Herald Island	7a	Residual Soil	0.8	1.757	138.085	7.4215	1.75995	14.8866	0	14.887	117.246	7.91468	2.60996	227	492	1.16	17.0	9.2
Herald Island	7a	Residual Soil	1	1.5555	145.972	5.3925	1.5586	18.6555	0	18.655	82.5857	9.49063	2.7342	317	575	0.82	18.9	9.0
Herald Island	7a	Residual Soil	1.2	1.535	140.893	3.11	1.53631	22.4255	0	22.425	67.3569	9.31303	2.76943	364	795	1.18	18.2	14.9
Herald Island	7a	Residual Soil	1.4	1.619	142.828	2.2115	1.6196	26.1996	0	26.2	60.6858	8.97006	2.77895	426	790	0.86	18.0	12.6
Herald Island	7a	Residual Soil	1.6	1.553	133.266	1.839	1.55344	29.9733	0	29.973	50.7114	8.76373	2.81133	467	913	0.96	17.2	15.5
Herald Island	7a	Residual Soil	1.8	1.5945	117.727	1.967	1.59583	33.7133	0	33.713	46.24	7.53804	2.78832	540	1045	0.94	17.6	17.5
Herald Island	7a	Residual Soil	2	1.5845	106.618	4.4405	1.58586	37.4286	0	37.429	41.3324	6.95999	2.79295	547	1014	0.86	16.9	16.2
Herald Island	7a	Residual Soil	2.2	1.4045	108.798	3.461	1.40613	41.1374	0	41.137	33.1729	7.97903	2.88962	551	911	0.66	16.2	12.5
Herald Island	7a	Residual Soil	2.4	1.2805	99.3215	9.272	1.28422	44.8249	0	44.825	27.6258	8.01532	2.93944	531	847	0.60	14.8	11.0
Herald Island	7a	Residual Soil	2.6	1.0855	81.168	10.7145	1.09017	48.4755	0	48.476	21.4878	7.78787	3.00589	474	774	0.64	12.6	10.4
Herald Island	7a	Residual Soil	2.8	1.0375	64.086	11.957	1.04269	52.0568	0	52.057	18.9995	6.47624	2.9874	493	732	0.50	12.5	8.3
Herald Island	7a	Residual Soil	3	0.9865	50.213	18.4275	0.99424	55.5895	0	55.589	16.8679	5.3722	2.9732	444	647	0.47	10.8	7.0
Herald Island	7a	Residual Soil	3.2	0.9375	41.027	22.921	0.9473	59.0551	0	59.055	15.0262	4.62058	2.96825	418	603	0.46	9.7	6.4
Herald Island	7a	Residual Soil	3.4	0.977	39.5115	24.3945	0.98691	62.4906	0	62.491	14.8302	4.27722	2.95152	443	634	0.45	9.9	6.6
Herald Island	7a	Residual Soil	3.6	0.9775	39.6455	26.135	0.98864	65.9447	1.962	63.983	14.4144	4.29334	2.96208	401	645	0.63	8.6	8.5
Herald Island	7a	Residual Soil	3.8	0.992	29.5475	26.524	1.00333	69.3606	3.924	65.437	14.2655	3.16684	2.88585	421	639	0.54	8.6	7.6
Herald Island	7a	Residual Soil	4	1.0455	35.5325	34.373	1.05975	72.7114	5.886	66.825	14.7548	3.51156	2.90013	408	650	0.62	8.1	8.4
Herald Island	7a	Residual Soil	4.2	0.957	33.9485	34.743	0.97193	76.1671	7.848	68.319	13.1115	3.76445	2.95896	367	779	1.20	6.9	14.3
Herald Island	7a	Residual Soil	4.4	1.127	34.1485	41.035	1.1449	79.5278	9.81	69.718	15.2679	3.21095	2.86472	554	818	0.50	10.4	9.1
Herald Island	7a	Residual Soil	4.6	1.099	55.505	43.4185	1.11607	83.0175	11.77	71.246	14.498	5.42931	3.02316	504	811	0.64	9.1	10.6
Herald Island	7a	Residual Soil	4.8	1.125	50.7495	44.7055	1.14377	86.5247	13.73	72.791	14.502	4.82473	2.9955	415	779	0.95	7.1	12.6
Herald Island	7a	Residual Soil	5	1.387	92.489	28.1579	1.40605	90.1533	15.7	74.457	17.6478	7.06167	3.03785	248	807	2.57	3.9	19.4
Herald Island	7a	Residual Soil	5.2	1.2915	67.441	24.9735	1.30267	93.7836	17.66	76.126	15.8674	5.61542	3.00436	433	807	0.93	6.9	13.0
Herald Island	7a	Residual Soil	5.4	1.558	92.9055	46.0115	1.57783	97.4047	19.62	77.785	19.0228	6.27665	2.97667	379	827	1.31	5.8	15.6
Herald Island	7a	Residual Soil	5.6	1.8285	93.122	69.8525	1.85597	101.099	21.58	79.517	22.0628	5.46949	2.89054	700	1116	0.63	10.9	14.4
Herald Island	7a	Residual Soil	5.8	1.4405	76.582	78.88	1.47369	104.749	23.54	81.205	16.8631	5.76397	2.99219	611	960	0.61	9.1	12.1
Herald Island	7a	Residual Soil	6	1.326	76.6235	83.8375	1.36084	108.357	25.51	82.851	15.1087	6.22475	3.04874	542	788	0.49	7.8	8.5
Herald Island	7a	Residual Soil	6.2	1.6945	55.6055	90.2475	1.73222	111.942	27.47	84.474	19.1557	3.9814	2.82271	804	1317	0.68	11.6	17.8
Herald Island	7a	Residual Soil	6.4	1.48	77.075	89.312	1.5197	115.55	29.43	86.12	16.3011	5.5397	2.99141	614	980	0.64	8.4	12.7
Herald Island	7a	Residual Soil	6.6	1.7445	71.7215	85.442	1.77789	119.157	31.39	87.765	18.8849	4.35963	2.87527	720	1396	1.01	9.7	23.5
Herald Island	7a	Residual Soil	6.8	2.774	73.7835	103.464	2.81984	122.789	33.35	89.435	30.0585	3.34478	2.6714	700	1374	1.04	9.2	23.4
Herald Island	7a	Residual Soil	7	3.0835	164.435	100.79	3.12512	126.569	35.32	91.253	32.9461	7.35129	2.85495	720	2967	3.36	9.2	78.0
Herald Island	7a	Residual Soil	7.2	1.843	81.328	115.356	1.89211	130.32	37.28	93.042	18.9201	4.80492	2.89425	829	1392	0.73	10.4	19.5
Herald Island	7a	Residual Soil	7.4	2.393	92.406	118.074	2.44309	133.975	39.24	94.735	24.3683	4.05607	2.76867	781	1076	0.41	9.5	10.2
Herald Island	7a	Residual Soil	7.7	2.8465	99.162	120.349	2.89589	139.571	42.18	97.388	28.299	3.64557	2.69167	881	1339	0.56	10.5	15.9
Herald Island	7a	Residual Soil	7.8	2.64	97.703	123.903	2.6937	141.442	43.16	98.278	25.9632	3.84822	2.73566	1149	2135	0.90	13.6	34.2
Herald Island	7a	Residual Soil	8	3.839	111.684	142.024	3.89865	145.16	45.13	100.03	37.4269	3.3298	2.58937	1501	2460	0.67	17.5	33.3
Herald Island	7a	Residual Soil	8.2	5.2455	182.047	184.382	5.32294	149.04	47.09	101.95	50.7331	3.53519	2.49707	1617	4136	1.62	18.4	87.4
Herald Island	7a	Residual Soil	8.4	5.4655	179.213	412.609	5.63767	152.962	49.05	103.91	52.7659	3.27699	2.46091	1982	4317	1.22	22.2	81.0
Herald Island	7a	Residual Soil	8.6	5.2945	177.08	566.787	5.53268	156.887	51.01	105.88	50.761	3.2948	2.47414	2693	4522	0.70	29.6	63.5
Herald Island	7a	Residual Soil	8.8	7.3755	197.077	1107.36	7.84556	160.808	52.97	107.83	71.1644	2.60959	2.29973	1746	3701	1.17	18.5	67.8
Herald Island	7a	Residual Soil	9	14.2488	319.388	2774.45	15.4094	164.851	54.94	109.92	138.61	2.25252	2.06051	2508	4981	1.01	26.2	85.8
Hamilton	8a	Volcanic Soil	0.2	1.39	42.4065	33.5105	1.40389	3.04677	0	3.0468	466.592	2.8384	2.11476	96	179	0.86	28.2	2.9
Hamilton	8a	Volcanic Soil	0.4	1.488	86.87	3.7155	1.48956	6.64792	0	6.6479	228.182	5.99612	2.42242	104	194	0.87	15.9	3.1
Hamilton	8a	Volcanic Soil	0.6	1.1635	90.8575	5.003	1.16711	10.3164	0	10.316	111.811	7.90746	2.63129	119	211	0.78	12.3	3.2
Hamilton	8a	Volcanic Soil	0.8	1.7305	64.9735	4.088	1.73071	13.9518	0	13.952	122.782	3.81768	2.38894	129	257	0.99	10.1	4.4
Hamilton	8a	Volcanic Soil	1	2.503	61.865	3.3815	2.50107	17.5246	0	17.525	140.073	2.5498	2.24058	136	384	1.82	8.5	8.6
Hamilton	8a	Volcanic Soil	1.2	2.972	83.637	0.1365	2.97475	21.1614	0	21.161	137.921	2.84847	2.26294	79	303	2.82	4.1	7.8
Hamilton	8a	Volcanic Soil	1.4	2.5365	48.0165	-10.551	2.53273	24.8552	0	24.855	102.179	1.94851	2.2467	107	346	2.25	4.7	8.3
Hamilton	8a	Volcanic Soil	1.6	1.6055	40.3475	116.914	1.6546	28.3081	0	28.308	57.0369	2.57382	2.44771	202	429	1.12	7.7	7.9
Hamilton	8a	Volcanic Soil	1.8	3.9535	89.5655	13.669	3.96024	31.8977	0.491	31.407	124.47	2.33678	2.20971	123	390	2.17	4.2	9.3
Hamilton	8a	Volcanic Soil	2	4.294	88.156	-10.479	4.29041	35.6277	2.453	33.175	128.358	2.20553	2.1515	207	708	2.45	6.7	17.4
Hamilton	8a	Volcanic Soil	2.2	4.6035	81.736	-29.505	4.58796	39.4046	4.415	34.99	129.669	1.91322	2.09739	369	924	1.53	11.3	19.3
Hamilton	8a	Volcanic Soil	2.4	4.3965	72.574	-18.837	4.38992	43.0445	6.377	36.668	118.365	1.70928	2.11147	373	955	1.59	10.9	20.2
Hamilton	8a	Volcanic Soil	2.6	4.664	100.708	-23.013	4.65201	46.7915	8.339	38.453	120.24	3.21658	2.23024	311	794	1.60	8.6	16.8
Hamilton	8a	Volcanic Soil	2.8	1.6025	79.103	-20.259	1.595	50.5348	10.3	40.234	38.3122	5.81098	2.69173	238	396	0.69	6.2	5.5

Table 6: CPT and DMT Data

				CPT DATA										DMT DATA				
Site	Pair No.	Soil Type	Depth (m)	q_c (MPa) (ave)	f_s (kPa) (ave)	u_2 (kPa) (ave)	q_t (ave)	σ_{vo} (kPa)	u_0 (kPa)	σ'_{vo} (kPa)	Q_t (ave)	F_r (Ave)	I_c (Ave)	p_o (kPa)	p_1 (kPa)	I_D	K_D	E_D (MPa)
Hamilton	8a	Volcanic Soil	3	2.1395	52.23	3.3095	2.14089	54.0452	12.26	41.783	49.8836	2.49288	2.44775	173	335	1.00	4.2	5.6
Hamilton	8a	Volcanic Soil	3.2	1.8435	31.963	-8.1305	1.84042	57.5402	14.22	43.316	41.1938	1.92792	2.44448	194	247	0.29	4.6	1.8
Hamilton	8a	Volcanic Soil	3.4	1.1015	28.2385	22.6155	1.11199	60.9572	16.19	44.771	23.4006	3.10057	2.72369	221	300	0.38	5.0	2.7
Hamilton	8a	Volcanic Soil	3.6	3.7475	42.1965	25.372	3.75769	64.382	18.15	46.234	79.6773	1.1687	2.1284	258	397	0.58	5.7	4.8
Hamilton	8a	Volcanic Soil	3.8	4.7585	60.4845	-7.921	4.75952	68.0121	20.11	47.902	98.021	1.31518	2.07729	309	726	1.44	6.7	14.5
Hamilton	8a	Volcanic Soil	4	6.147	71.099	4.5415	6.14503	71.6739	22.07	49.601	122.188	1.17539	1.98921	392	1119	1.96	8.2	25.2
Hamilton	8a	Volcanic Soil	4.2	4.3245	72.6335	-18.646	4.31284	75.39	24.03	51.356	82.7654	2.11212	2.24158	303	614	1.11	6.0	10.8
Hamilton	8a	Volcanic Soil	4.4	1.5035	50.5645	15.7275	1.50724	79.0032	26	53.007	26.8522	4.79961	2.77559	227	330	0.51	4.2	3.6
Hamilton	8a	Volcanic Soil	4.6	0.801	14.676	30.5755	0.82093	82.3457	27.96	54.387	13.5931	2.5077	2.86598	234	247	0.06	4.2	0.4
Hamilton	8a	Volcanic Soil	4.8	2.9735	27.3075	57.887	2.99742	85.5644	29.92	55.644	52.0781	1.03293	2.24993	412	953	1.41	7.6	18.8
Hamilton	8a	Volcanic Soil	5	6.2925	64.139	-17.233	6.28895	89.1778	31.88	57.295	108.049	1.06626	1.97013	625	1680	1.78	11.5	36.6
Hamilton	8a	Volcanic Soil	5.2	9.782	55.185	-10.779	9.76978	92.8839	33.84	59.039	163.623	0.59918	1.68147	713	1663	1.40	12.7	33.0
Hamilton	8a	Volcanic Soil	5.4	8.9565	45.294	6.4365	8.95991	96.5279	35.81	60.721	145.987	0.5207	1.69048	507	1408	1.91	8.5	31.3
Hamilton	8a	Volcanic Soil	5.6	5.7115	37.3055	15.709	5.7358	100.154	37.77	62.386	90.408	0.67199	1.91296	362	866	1.55	5.7	17.5
Hamilton	8a	Volcanic Soil	5.8	9.999	32.035	40.046	9.99975	103.654	39.73	63.923	154.534	0.32229	1.56404	398	1006	1.70	6.1	21.1
Hamilton	8a	Volcanic Soil	6	8.9005	64.0515	32.4165	8.92096	107.299	41.69	65.606	134.264	0.72707	1.79074	403	1108	1.95	6.0	24.4
Hamilton	8a	Volcanic Soil	6.2	12.209	48.0575	42.829	12.222	111.025	43.65	67.37	179.555	0.40384	1.54281	400	1228	2.33	5.7	28.7
Hamilton	8a	Volcanic Soil	6.4	11.8875	56.2595	34.835	11.8958	114.704	45.62	69.088	170.659	0.51755	1.60924	462	1404	2.26	6.5	32.7
Hamilton	8a	Volcanic Soil	6.6	9.382	46.4185	44.1545	9.40672	118.413	47.58	70.835	130.911	0.54987	1.69882	429	1307	2.30	5.8	30.5
Hamilton	8a	Volcanic Soil	6.8	11.4205	64.9395	49.066	11.4364	122.065	49.54	72.524	156.005	0.58536	1.66311	437	1219	2.02	5.7	27.1
Hamilton	8a	Volcanic Soil	7	7.8125	56.828	41.878	7.83484	125.804	51.5	74.302	103.728	0.73656	1.85767	689	1787	1.72	9.2	38.1
Hamilton	8a	Volcanic Soil	7.2	8.769	45.238	52.6645	8.80763	129.447	53.46	75.982	114.135	0.52241	1.74025	379	1088	2.18	4.6	24.6
Hamilton	8a	Volcanic Soil	7.4	11.598	52.8235	54.2875	11.5989	133.088	55.43	77.662	147.591	0.47456	1.61463	465	1240	1.89	5.6	26.9
Hamilton	8a	Volcanic Soil	7.6	8.906	63.3315	57.17	8.94139	136.841	57.39	79.452	110.731	0.74041	1.81959	494	1292	1.83	5.9	27.7
Hamilton	8a	Volcanic Soil	7.8	11.41	53.0285	58.5395	11.4262	140.5	59.35	81.149	139.058	0.47913	1.63487	485	1318	1.95	5.6	28.9
Hamilton	8a	Volcanic Soil	8	8.1345	38.937	57.052	8.15812	144.175	61.31	82.863	96.7103	0.47421	1.77412	430	1156	1.97	4.7	25.2
Hamilton	8a	Volcanic Soil	8.2	8.306	34.1785	50.761	8.32605	147.733	63.27	84.458	96.727	0.428	1.74006	372	915	1.76	3.9	18.8
Hamilton	8a	Volcanic Soil	8.4	9.501	50.778	55.457	9.52824	151.353	65.24	86.117	108.801	0.54345	1.74616	431	1188	2.07	4.5	26.3
Hamilton	8a	Volcanic Soil	8.6	5.4995	112.603	27.809	5.502	155.076	67.2	87.878	60.88	2.26868	2.29888	522	1396	1.92	5.5	30.3
Hamilton	8a	Volcanic Soil	8.8	3.182	51.236	102.937	3.23727	158.802	69.16	89.641	34.3122	1.70044	2.41862	434	1045	1.68	4.3	21.2
Hamilton	8a	Volcanic Soil	9	3.2255	22.116	59.952	3.24574	162.298	71.12	91.175	33.8314	0.71369	2.23638	282	694	1.95	2.4	14.3
Hamilton	8a	Volcanic Soil	9.2	1.5175	25.2855	163.561	1.6177	165.666	73.08	92.582	15.6862	2.07279	2.76232	366	643	0.95	3.3	9.6
Hamilton	8a	Volcanic Soil	9.4	4.1325	56.5695	97.036	4.13767	169.107	75.05	94.06	42.1851	1.48354	2.2922	419	731	0.91	3.8	10.8
Hamilton	8a	Volcanic Soil	9.6	1.484	84.2795	135.797	1.54674	172.806	77.01	95.797	14.3701	7.28256	3.12576	329	365	0.14	2.8	1.2
Hamilton	8a	Volcanic Soil	9.8	1.8495	33.152	214.831	1.9377	176.294	78.97	97.323	18.0671	2.0848	2.70599	315	401	0.36	2.6	3.0
Hamilton	8a	Volcanic Soil	10	0.9485	24.5385	156.065	1.01636	179.721	80.93	98.788	8.48109	3.62364	3.12522	358	398	0.14	3.0	1.4
Hamilton	8a	Volcanic Soil	10.2	1.095	23.4135	306.028	1.22854	183.019	82.89	100.12	10.4126	3.23223	3.03867	211	574	2.84	1.3	12.6
Hamilton	8a	Volcanic Soil	10.4	7.6705	30.515	132.624	7.72137	186.436	84.86	101.58	74.0242	0.46002	1.84617	613	1672	2.01	5.5	36.8
Hamilton	8a	Volcanic Soil	10.6	10.97	81.5315	112.211	11.01	190.091	86.82	103.27	104.712	0.75229	1.80524	858	2108	1.62	7.8	43.4
Hamilton	8a	Volcanic Soil	10.8	8.93	104.032	109.254	8.9893	193.942	88.78	105.16	83.6319	1.18045	2.01127	770	1733	1.41	6.8	33.4
Hamilton	8a	Volcanic Soil	11	9.792	63.072	109.012	9.83357	197.72	90.74	106.98	89.9977	0.66724	1.8361	818	2289	2.02	7.1	51.0
Hamilton	8a	Volcanic Soil	11.2	9.0225	50.774	24.347	9.03573	201.414	92.7	108.71	81.3356	0.58965	1.84511	783	1973	1.72	6.6	41.3
Hamilton	8a	Volcanic Soil	11.4	9.8205	25.548	117.413	9.86727	204.955	94.67	110.29	87.5314	0.2667	1.64265	688	1758	1.80	5.6	37.1
Hamilton	8a	Volcanic Soil	11.6	10.561	37.772	106.381	10.6104	208.536	96.63	111.91	92.954	0.36846	1.67565	492	1358	2.19	3.7	30.1
Hamilton	8a	Volcanic Soil	11.8	10.866	41.9795	125.009	10.9112	212.151	98.59	113.56	94.1545	0.39169	1.68102	743	1730	1.53	5.9	34.2
Hamilton	8a	Volcanic Soil	12	8.946	52.1945	97.189	8.98799	215.835	100.6	115.28	76.1178	0.60474	1.86197	523	1315	1.87	3.8	27.5
Hamilton	8a	Volcanic Soil	12.2	8.063	47.127	84.663	8.09659	219.478	102.5	116.96	67.3309	0.59912	1.8999	424	984	1.74	2.8	19.4
Hamilton	8a	Volcanic Soil	12.4	6.9265	37.8015	76.74	6.9558	223.101	104.5	118.62	56.7528	0.56191	1.94925	275	620	2.03	1.5	12.0
Hamilton	8a	Volcanic Soil	12.6	3.5335	30.835	39.412	3.55182	226.635	106.4	120.2	27.7077	1.33341	2.43989	371	497	0.48	2.3	4.4
Hamilton	8a	Volcanic Soil	12.8	0.708	19.418	194.561	0.79228	229.996	108.4	121.6	4.6219	3.53012	3.31274	458	571	0.32	3.0	3.9
Hamilton	8a	Volcanic Soil	13	1.132	24.9005	263.814	1.2422	233.278	110.4	122.92	8.19692	2.94163	3.07136	334	739	1.81	1.9	14.1
Hamilton	8a	Volcanic Soil	13.2	5.2105	25.1545	128.932	5.2684	236.645	112.3	124.32	40.3861	0.86978	2.22272	542	1556	2.36	3.6	35.2
Hamilton	8a	Volcanic Soil	13.4	8.4675	30.634	99.9275	8.51077	240.17	114.3	125.88	65.6723	0.37096	1.79512	594	1529	1.95	3.9	32.4
Hamilton	8a	Volcanic Soil	13.6	10.011	40.629	116.578	10.0579	243.756	116.2	127.51	76.9359	0.41384	1.75239	810	2037	1.77	5.6	42.6
Hamilton	8a	Volcanic Soil	13.8	9.344	39.7825	105.475	9.38953	247.394	118.2	129.18	70.7689	0.43631	1.79613	680	1791	1.98	4.4	38.5
Hamilton	8a	Volcanic Soil	14	9.8685	29.6265	96.111	9.90161	250.972	120.2	130.8	73.7638	0.31005	1.70621	586	1441	1.83	3.6	29.7
Hamilton	8a	Volcanic Soil	14.2	7.908	31.2475	86.5305	7.95253	254.528	122.1	132.39	58.1262	0.40769	1.85494	572	1430	1.91	3.4	29.8
Hamilton	8a	Volcanic Soil	14.4	9.5585	30.6375	113.036	9.60265	258.061	124.1	133.96	69.744	0.33239	1.73834	542	1564	2.44	3.2	35.5
Hamilton	8a	Volcanic Soil	14.6	8.418	31.0765	111.077	8.46331	261.632	126.1	135.57	60.479	0.37918	1.82121	629	1785	2.30	3.7	40.1
Hamilton	8a	Volcanic Soil	14.8	7.527	29.1755	105.022	7.57056	265.164	128	137.14	53.2632	0.40285	1.88452	512	1525	2.64	2.8	35.2
Hamilton	8a	Volcanic Soil	15	6.609	25.17	104.107	6.65824	268.644	130	138.66	46.0601	0.38522	1.93839	746	1923	1.91	4.5	40.8
Hamilton	8a	Volcanic Soil	15.2	7.9745	28.543	110.587	8.01294	272.166	131.9	140.22	55.1994	0.37345	1.85089	407	1042	2.31	2.0	22.0
Hamilton	8a	Volcanic Soil	15.4	7.5205	47.4565	113.987	7.56114	275.735	133.9	141.83	51.3491	0.66304	2.00263	845	2064	1.71	5.0	42.3
Hamilton	8a	Volcanic Soil	15.6	2.8725	65.342	108.559	2.92548	279.409	135.9	143.54	18.4514	2.65842	2.7584	544	1253	1.74	2.8	24.6
Hamilton	8a	Volcanic Soil	15.8	1.7495	23.835	235.641	1.85211	282.89	137.8	145.06	10.8172	1.66166	2.82735	496	988	1.38	2.5	17.1
Hamilton	8a	Volcanic Soil	16	1.995	35.689	207.035	2.0915	286.309	139.8	146.52	12.3096	2.15813	2.85339	503	613	0.30	2.5	3.8
Hamilton	8a	Volcanic Soil	16.2	5.8915	53.4855	94.6055	5.91407	289.849	141.8	148.09	37.9789	1.01604	2.21318	443	1539	3.64	2.0	38.0
Hamilton	8a	Volcanic Soil	16.4	2.77	54.685	165.989	2.84509	293.485	143.7	149.77	17.0169	2.61548	2.76687	482	848	1.08	2.3	12.7
Hamilton	8a	Volcanic Soil	16.6	4.1095	38.9975	99.5745	4.1521	297.045	145.7	151.37	25.4654	1.02056	2.37482	594	1750	2.58	3.0	40.1
Hamilton	8a	Volcanic Soil	16.8	3.494	44.2705	138.861	3.55229	300.609	147.6	152.97	21.2566	1.37982	2.51974	719	1721	1.75	3.7	34.8
Hamilton	8a	Volcanic Soil	17	1.9155	53.2805	150.208	1.97792	304.177	149.6	154.57	10.8336	3.45312	3.00784	703	925	0.40	3.6	7.7
Hamilton	8a	Volcanic Soil	17.2	0.8495	38.833	32.505	0.86423	307.728	151.6	156.16	3.5684	6.22182	3.59715	446	1220	2.63	1.9	26.9
Hamilton	8a	Volcanic Soil	17.4	0.8085	6.46	116.778	0.85822	310.793	153.5	157.27	3.47697	1.40513	3.25399	635	1741	2.29	3.0	38.4
Hamilton	8a	Volcanic Soil	17.6	1.877	9.717	123.124	1.92884	313.875	155.5	158.39	10.1889	0.61082	2.65679	919	2238	1.73	4.8	45.8
Hamilton	8a	Volcanic Soil	17.8	2.9665	14.5545	124.285	3.01887	317.115	157.5	159.66	16.9147	0.53858	2.40784	787	1913	1.79	3.9	39.1
Hamilton	8a	Volcanic Soil	18	3.898	17.821	125.59	3.95191	320.446	159.4	161.03	22.5388	0.49863	2.27295	812	2008	1.83	4.0	41.5
Hamilton	8a	Volcanic Soil	18.2	5.6695	23.6375	126.931	5.72305	323.856	161.4	162.48	33.2121	0.43844	2.08014	721	1616	1.60	3.4	31.0
Hamilton	8a	Volcanic Soil	18.4	7.706	40.7255	115.737	7.75422	327.386	163.3	164.05	45.26	0.54914	1.99245	909	2141	1.65	4.4	42.7
Hamilton	8a	Volcanic Soil	18.6	7.759	43.1255	135.914	7.81491	331.02	165.3	165.72	45.1466	0.57726	2.00474	913	2079	1.56	4.4	40.4
Hamilton	8a	Volcanic Soil	18.8	8.9285	37.729	145.804	8.99436	334.62	167.3	167.36	51.7148	0.44272	1.89072	746	1789	1.80	3.4	36.2
Hamilton	8a	Volcanic Soil	19	13.125	40.6615	152.375	13.186	338.233	169.2	169.01	75.98	0.31307	1.65869	1258	2896	1.50	6.3	56.8
Hamilton	8b	Volcanic Soil	0.2	1.286	51.6505	23.3225	1.29522	3.2065	0	3.2065	432.277	3.9932	2.2248	71	144	1.04	20.7	2.6
Hamilton	8b	Volcanic Soil	0.4	1.1475	89.453	0.0535	1.14854	6.81904	0	6.819	169.411	7.84902	2.5616	117	230	0.97	17.8	3.9
Hamilton	8b	Volcanic Soil	0.6	1.5895	93.925	67.268	1.61675	10.4651	0	10.465	151.273	5.91932	2.48303	151	253	0.67	15.6	3.5
Hamilton	8b	Volcanic Soil	0.8	1.7045	112.018	132.368	1.75917	14.1844	0	14.184	123.815	6.47699	2.54315	144	279	0.94	11.2	4.7
Hamilton	8b	Volcanic Soil	1	1.3485	114.006	83.7565	1.38581	17.9019	0	17.902	76.6406	8.45579	2.71711	148	356	1.40	9.3	7.2
Hamilton	8b	Volcanic Soil	1.2	2.4615	124.667	192.73	2.54202	21.6095	0	21.61	114.81	5.17251	2.47278	590	1310	1.22	30.6	25.0
Hamilton	8b	Volcanic Soil	1.4	3.025	227.943	351.76	3.17103	25.4917	0	25.492	123.647	7.32967	2.55392	852	1470	0.73	36.8	21.5
Hamilton	8b	Volcanic Soil	1.6	2.1335	138.211	769.988	2.45786	29.3832	0	29.383	82.5609	5.67917	2.55533	894	1613	0.80	33.2	25.0

Table 6: CPT and DMT Data

				CPT DATA										DMT DATA				
Site	Pair No.	Soil Type	Depth (m)	q_c (MPa) (ave)	f_s (kPa) (ave)	u_2 (kPa) (ave)	q_t (ave)	σ_{vo} (kPa)	u_0 (kPa)	σ'_{vo} (kPa)	Q_t (ave)	F_r (Ave)	I_c (Ave)	p_o (kPa)	p_1 (kPa)	I_D	K_D	E_D (MPa)
Hamilton	8b	Volcanic Soil	1.8	2.2065	114.187	826.841	2.55328	33.1193	0	33.119	75.8528	4.52779	2.51351	796	1228	0.54	25.9	15.0
Hamilton	8b	Volcanic Soil	2	2.018	130.908	959.519	2.42124	36.8888	0	36.889	64.4547	5.44588	2.60764	828	1233	0.49	24.0	14.1
Hamilton	8b	Volcanic Soil	2.2	2.1225	131.205	989.594	2.53833	40.6861	0	40.686	61.3054	5.25388	2.60394	821	1258	0.53	21.5	15.2
Hamilton	8b	Volcanic Soil	2.4	2.0155	125.06	966.86	2.42189	44.4688	0	44.469	53.4044	5.26112	2.63774	859	1382	0.61	20.5	18.1
Hamilton	8b	Volcanic Soil	2.6	2.228	107.044	1130.29	2.7025	48.2288	0	48.229	54.8659	4.06264	2.55011	906	1473	0.63	19.8	19.7
Hamilton	8b	Volcanic Soil	2.8	3.0835	121.886	1325.3	3.64004	51.9991	0	51.999	68.6709	3.49948	2.44	1083	1780	0.64	21.8	24.2
Hamilton	8b	Volcanic Soil	3	3.21	123.914	1264.78	3.74039	55.8131	0	55.813	65.9556	3.3694	2.43735	1304	2205	0.69	24.4	31.3
Hamilton	8b	Volcanic Soil	3.2	2.7065	120.075	1264.68	3.23833	59.6047	0	59.605	53.2786	3.80131	2.52926	1490	2335	0.57	26.8	29.3
Hamilton	8b	Volcanic Soil	3.4	2.555	122.046	1164.6	3.04376	63.3895	0	63.39	47.0284	4.15035	2.58737	1847	3063	0.66	32.0	42.2
Hamilton	8b	Volcanic Soil	3.6	2.315	100.776	1025.46	2.74647	67.1564	0	67.156	39.842	3.76285	2.60699	1547	2848	0.84	25.8	45.1
Hamilton	8b	Volcanic Soil	3.8	2.4595	103.541	968.275	2.86626	70.8928	0	70.893	39.3761	3.70468	2.60432	1139	1728	0.52	18.3	20.4
Hamilton	8b	Volcanic Soil	4	2.5565	108.15	945.033	2.95179	74.6408	0	74.641	38.5181	3.78624	2.61441	1105	1622	0.47	17.2	17.9
Hamilton	8b	Volcanic Soil	4.2	1.8315	78.599	898.405	2.20879	78.3769	0	78.377	27.1747	3.6762	2.71097	909	1346	0.49	13.7	15.2
Hamilton	8b	Volcanic Soil	4.4	1.2515	69.3545	427.511	1.43268	81.995	0	81.995	16.4785	5.22419	2.97261	676	1056	0.57	9.8	13.2
Hamilton	8b	Volcanic Soil	4.6	0.943	60.854	183.412	1.02028	85.5656	0	85.566	10.9262	6.53522	3.17291	604	746	0.24	8.6	4.9
Hamilton	8b	Volcanic Soil	4.8	0.9265	52.7025	248.632	1.03015	89.0836	0	89.084	10.5588	5.61243	3.14115	743	1162	0.58	10.3	14.5
Hamilton	8b	Volcanic Soil	5	0.813	45.854	235.588	0.91235	92.5716	0	92.572	8.85165	5.61707	3.20127	701	885	0.27	9.4	6.4
Hamilton	8b	Volcanic Soil	5.2	0.768	41.9355	262.571	0.87762	96.0217	0	96.022	8.12996	5.36505	3.21773	797	999	0.26	10.5	7.0
Hamilton	8b	Volcanic Soil	5.4	0.683	37.133	316.244	0.81613	99.464	0	99.464	7.19951	5.18064	3.25051	665	796	0.20	8.5	4.6
Hamilton	8b	Volcanic Soil	5.6	0.657	40.254	314.821	0.78951	102.873	0	102.87	6.66911	5.86853	3.30922	616	776	0.27	7.7	5.5
Hamilton	8b	Volcanic Soil	5.8	0.639	47.7365	312.971	0.77035	106.329	0	106.33	6.23954	7.19563	3.3865	602	711	0.19	7.3	3.8
Hamilton	8b	Volcanic Soil	6	0.755	57.7895	219.307	0.84695	109.811	0	109.81	6.70672	7.85288	3.38482	414	522	0.28	4.8	3.8
Hamilton	8b	Volcanic Soil	6.2	0.714	65.7095	258.422	0.82269	113.35	0	113.35	6.25392	9.2723	3.45438	519	615	0.20	6.0	3.3
Hamilton	8b	Volcanic Soil	6.4	0.69	67.419	277.084	0.80624	116.899	0	116.9	5.89238	9.78705	3.4893	428	498	0.18	4.8	2.4
Hamilton	8b	Volcanic Soil	6.6	0.706	65.0625	309.853	0.83612	120.442	0	120.44	5.93676	9.09546	3.46668	453	549	0.23	5.0	3.3
Hamilton	8b	Volcanic Soil	6.8	0.761	72.9565	325.98	0.89807	124.005	0.981	123.02	6.28893	9.42832	3.45717	453	548	0.23	4.9	3.3
Hamilton	8b	Volcanic Soil	7	0.8225	73.666	223.387	0.91653	127.583	2.943	124.64	6.3271	9.34427	3.45263	370	597	0.69	3.8	7.9
Hamilton	8b	Volcanic Soil	7.2	0.8135	81.224	306.862	0.94238	131.175	4.905	126.27	6.42208	10.0211	3.46696	525	616	0.19	5.5	3.2
Hamilton	8b	Volcanic Soil	7.4	0.806	83.9535	308.313	0.93547	134.783	6.867	127.92	6.25657	10.4882	3.48845	580	650	0.13	6.0	2.4
Hamilton	8b	Volcanic Soil	7.6	0.8345	84.283	338.969	0.97717	138.398	8.829	129.57	6.47052	10.0517	3.46534	577	660	0.16	5.8	2.9
Hamilton	8b	Volcanic Soil	7.8	0.8795	90.681	321.628	1.0141	142.019	10.79	131.23	6.64262	10.4022	3.46596	595	682	0.16	5.9	3.0
Hamilton	8b	Volcanic Soil	8	0.9485	96.3675	221.79	1.04153	145.667	12.75	132.91	6.73686	10.7678	3.47122	624	671	0.08	6.1	1.6
Hamilton	8b	Volcanic Soil	8.2	0.97	98.019	329.967	1.10893	149.32	14.72	134.61	7.12579	10.2158	3.4379	635	704	0.12	6.1	2.4
Hamilton	8b	Volcanic Soil	8.4	0.989	100.839	373.912	1.14585	152.987	16.68	136.31	7.28113	10.1609	3.42923	633	696	0.11	6.0	2.2
Hamilton	8b	Volcanic Soil	8.8	1.035	110.926	352.684	1.18288	160.346	20.6	139.75	7.31419	10.8474	3.44627	593	681	0.16	5.4	3.1
Hamilton	8b	Volcanic Soil	9	1.073	109.655	263.126	1.18354	164.038	22.56	141.48	7.20404	10.7714	3.44909	590	696	0.20	5.3	3.7
Hamilton	8b	Volcanic Soil	9.2	1.0335	105.18	353.173	1.18178	167.725	24.53	143.2	7.07831	10.3792	3.44459	665	754	0.15	5.9	3.1
Hamilton	8b	Volcanic Soil	9.4	1.0525	110.765	350.733	1.19987	171.414	26.49	144.93	7.09391	10.77	3.45433	669	746	0.13	5.9	2.7
Hamilton	8b	Volcanic Soil	9.6	1.0215	107.199	432.244	1.20256	175.106	28.45	146.66	7.0035	10.4375	3.44969	685	782	0.16	5.9	3.4
Hamilton	8b	Volcanic Soil	9.8	1.0095	94.409	518.817	1.22787	178.779	30.41	148.37	7.06705	9.05532	3.40608	654	828	0.30	5.5	6.0
Hamilton	8b	Volcanic Soil	10	1.126	96.945	376.513	1.28413	182.428	32.37	150.06	7.33714	8.8747	3.39227	617	864	0.45	5.1	8.6
Hamilton	8b	Volcanic Soil	10.2	1.194	114.384	580.556	1.43783	186.131	34.34	151.8	8.24233	9.1429	3.35857	591	789	0.38	4.8	6.9
Hamilton	8b	Volcanic Soil	10.4	1.24	114.563	655.521	1.5153	189.85	36.3	153.55	8.62818	8.65017	3.32774	572	728	0.31	4.5	5.4
Hamilton	8b	Volcanic Soil	10.6	1.25	109.021	742.16	1.56161	193.572	38.26	155.31	8.80556	7.96694	3.29764	436	712	0.76	3.2	9.6
Hamilton	8b	Volcanic Soil	10.8	1.2785	110.091	726.896	1.58391	197.27	40.22	157.05	8.82609	7.9401	3.2957	458	733	0.72	3.3	9.5
Hamilton	8b	Volcanic Soil	11	1.411	125.435	509.363	1.62459	201.005	42.18	158.82	8.9599	8.80879	3.3205	441	772	0.91	3.1	11.5
Hamilton	8b	Volcanic Soil	11.2	1.362	124.682	714.786	1.6626	204.757	44.15	160.61	9.07368	8.55476	3.30791	453	773	0.86	3.2	11.1
Hamilton	8b	Volcanic Soil	11.4	1.423	121.87	778.128	1.74971	208.494	46.11	162.39	9.48636	7.91096	3.27163	472	776	0.78	3.3	10.6
Hamilton	8b	Volcanic Soil	11.6	1.582	153.62	771.356	1.90619	212.272	48.07	164.2	10.3124	9.06531	3.2826	481	779	0.75	3.3	10.3
Hamilton	8b	Volcanic Soil	11.8	1.62	162.016	785.923	1.94968	216.085	50.03	166.05	10.4365	9.34722	3.28762	524	762	0.55	3.6	8.3
Hamilton	8b	Volcanic Soil	12	1.687	159.603	568.328	1.92596	219.905	51.99	167.91	10.1575	9.35832	3.29683	490	751	0.65	3.3	9.1
Hamilton	8b	Volcanic Soil	12.2	1.6235	165.43	728.835	1.92945	223.723	53.96	169.77	10.044	9.69979	3.31078	558	827	0.57	3.7	9.3
Hamilton	8b	Volcanic Soil	12.4	1.6195	169.436	719.479	1.9218	227.55	55.92	171.63	9.86831	10.0001	3.32533	653	849	0.35	4.4	6.8
Hamilton	8b	Volcanic Soil	12.6	1.627	168.071	702.902	1.92222	231.377	57.88	173.5	9.74239	9.94117	3.32777	573	870	0.62	3.7	10.3
Hamilton	8b	Volcanic Soil	12.8	1.6205	169.632	672.734	1.90552	235.204	59.84	175.36	9.52192	10.1668	3.34169	550	799	0.55	3.5	8.6
Hamilton	8b	Volcanic Soil	13	1.6595	159.945	470.023	1.85432	239.028	61.8	177.23	9.11233	9.8992	3.34853	585	779	0.40	3.7	6.7
Hamilton	8b	Volcanic Soil	13.2	1.5005	146.815	678.063	1.78525	242.828	63.77	179.06	8.61185	9.52086	3.35571	506	668	0.40	3.1	5.6
Hamilton	8b	Volcanic Soil	13.4	1.437	135.195	610.832	1.69383	246.608	65.73	180.88	7.99889	9.34107	3.37444	400	593	0.65	2.2	6.7
Hamilton	8b	Volcanic Soil	13.6	1.739	129.175	445.885	1.92751	250.367	67.69	182.68	9.17634	7.73465	3.27631	327	636	1.38	1.6	10.7
Hamilton	8b	Volcanic Soil	13.8	2.91	108.002	280.267	3.00042	254.137	69.65	184.49	14.8746	4.14308	2.93534	447	871	1.24	2.5	14.7
Hamilton	8b	Volcanic Soil	14	6.119	87.431	127.748	6.20409	257.877	71.61	186.26	31.888	1.63092	2.40777	636	1800	2.21	3.8	40.4
Hamilton	8b	Volcanic Soil	14.2	10.8695	131.998	52.819	10.8891	261.708	73.58	188.13	56.4609	1.23708	2.10815	1530	3520	1.40	10.1	69.0
Hamilton	8b	Volcanic Soil	14.4	13.18	182.428	66.651	13.2078	265.66	75.54	190.12	68.0424	1.40885	2.07859	1775	4178	1.45	11.7	83.4
Hamilton	8b	Volcanic Soil	14.6	15.182	272.468	69.661	15.2079	269.704	77.5	192.21	77.6955	1.82126	2.11297	2121	4772	1.32	13.9	92.0
Hamilton	8b	Volcanic Soil	14.8	15.861	322.833	71.7835	15.8907	273.83	79.46	194.37	80.3188	2.06762	2.14445	1223	3981	2.49	7.5	95.7
Hamilton	8b	Volcanic Soil	15	16.1605	285.446	70.8115	16.1941	277.943	81.42	196.52	80.9511	1.80031	2.0947	1981	4807	1.52	12.5	98.0
Hamilton	8b	Volcanic Soil	15.2	18.036	351.581	61.4475	18.0563	282.09	83.39	198.71	89.414	1.97771	2.09334	1997	4894	1.54	12.4	100.5
Hamilton	8b	Volcanic Soil	15.4	21.457	431.817	95.903	21.5033	286.281	85.35	200.93	105.54	2.03255	2.04957	2393	5263	1.26	14.8	99.6
Hamilton	8b	Volcanic Soil	15.6	24.358	463.341	105.892	24.3992	290.539	87.31	203.23	118.585	1.9281	1.99152	2125	5243	1.56	12.9	108.2
Hamilton	8c	Volcanic Soil	1.6	0.794	31.5	37.5	0.80312	27.6127	0	27.613	27.4105	5.08655	2.88519	975	1709	0.75	35.3	25.5
Hamilton	8c	Volcanic Soil	1.8	2.191	78.5	273	2.24063	31.1601	0	31.16	70.5951	3.52937	2.46605	802	1346	0.68	25.5	18.9
Hamilton	8c	Volcanic Soil	2	2.2945	57.5	850	2.45527	34.8166	0	34.817	69.3989	2.38466	2.35642	805	1439	0.79	22.8	22.0
Hamilton	8c	Volcanic Soil	2.2	2.0305	43	1055	2.23159	38.371	0	38.371	57.1448	1.95662	2.35868	828	1375	0.66	21.2	19.0
Hamilton	8c	Volcanic Soil	2.4	1.855	35	1039	2.05325	41.8575	0	41.857	47.974	1.73611	2.37368	837	1353	0.62	19.5	17.9
Hamilton	8c	Volcanic Soil	2.6	1.993	56	992.5	2.18073	45.3933	0	45.393	47.0049	2.61519	2.47756	747	1213	0.62	16.0	16.2
Hamilton	8c	Volcanic Soil	2.8	1.824	28.5	1047.5	2.02302	48.8992	0	48.899	40.314	1.44556	2.37091	803	1308	0.63	15.9	17.5
Hamilton	8c	Volcanic Soil	3	1.8395	30	1078	2.04432	52.3069	0	52.307	38.0317	1.50623	2.39844	838	1349	0.61	15.4	17.7
Hamilton	8c	Volcanic Soil	3.2	2.087	60.5	1078.5	2.29049	55.7864	0	55.786	39.9436	2.66579	2.51554	940	1308	0.39	16.1	12.8
Hamilton	8c	Volcanic Soil	3.4	1.937	49	1071.5	2.14965	59.409	0	59.409	35.1479	2.29886	2.5115	1085	1619	0.49	18.0	18.5
Hamilton	8c	Volcanic Soil	3.6	2.9005	80	1341	3.14799	63.032	0	63.032	48.9623	2.55359	2.43187	1103	2464	1.24	17.8	47.2
Hamilton	8c	Volcanic Soil	3.8	3.195	40	1736	3.52517	66.5835	0	66.583	51.816	1.15966	2.21271	1093	1669	0.53	17.0	20.0
Hamilton	8c	Volcanic Soil	4	3.953	81	2054	4.34057	70.1857	0	70.186	60.7129	1.88188	2.27281	1014	1682	0.66	15.3	23.2
Hamilton	8c	Volcanic Soil	4.2	3.292	74	1931.5	3.66008	73.9499	0	73.95	48.5055	2.03106	2.36581	1124	1887	0.69	16.5	26.5
Hamilton	8c	Volcanic Soil	4.4	2.6455	46	1578.5	2.94468	77.506	0	77.506	36.9936	1.65536	2.39125	928	1353	0.46	13.2	14.8
Hamilton	8c	Volcanic Soil	4.6	1.7395	43.5	895.5	1.91171	81.0732	0	81.073	22.5683	2.37574	2.65802	935	1510	0.62	12.9	20.0
Hamilton	8c	Volcanic Soil	4.8	1.797	52.5	842.5	1.95723	84.6044	0	84.604	22.1872	2.79249	2.70309	1017	1500	0.48	13.7	16.8
Hamilton	8c	Volcanic Soil	5	2.0925	50.5	992	2.27851	88.1399	1.962	86.178	25.3953	2.29774	2.60708	1134	1515	0.34	14.9	13.2
Hamilton	8c	Volcanic Soil	5.2	1.4225	29	767.5	1.57007	91.6865	3.924	87.762	16.8514	1.88594	2.68547	1238	1701	0.38	15.9	16.1
Hamilton	8c	Volcanic Soil	5.4	1.197	10	709	1.33188	94.8884	5.886	89.002	13.8999	0.82445	2.59696	1259	1661	0.33	15.8	14.0

Table 6: CPT and DMT Data

				CPT DATA										DMT DATA				
Site	Pair No.	Soil Type	Depth (m)	q_c (MPa) (ave)	f_s (kPa) (ave)	u_2 (kPa) (ave)	q_t (ave)	σ_{vo} (kPa)	u_0 (kPa)	σ'_{vo} (kPa)	Q_t (ave)	F_r (Ave)	I_c (Ave)	p_o (kPa)	p_1 (kPa)	I_D	K_D	E_D (MPa)
Hamilton	8c	Volcanic Soil	5.6	1.098	11.5	585	1.20915	98.0241	7.848	90.176	12.3102	1.04334	2.68595	1127	1512	0.35	13.8	13.4
Hamilton	8c	Volcanic Soil	5.8	0.9915	13.5	630	1.11117	101.251	9.81	91.441	11.0434	1.31944	2.76933	1088	1386	0.28	13.0	10.3
Hamilton	8c	Volcanic Soil	6	1.143	13	691.5	1.27531	104.385	11.77	92.613	12.6299	1.08569	2.68573	580	684	0.19	6.6	3.6
Hamilton	8c	Volcanic Soil	6.2	1.7775	20	1074	1.98016	107.677	13.73	93.943	19.9164	1.0813	2.51121	484	486		5.3	0.1
Hamilton	8c	Volcanic Soil	6.4	1.6375	14	1088	1.84469	111.005	15.7	95.309	18.1918	0.79576	2.47815	501	677	0.38	5.5	6.1
Hamilton	8c	Volcanic Soil	6.6	1.2795	10	826	1.43647	114.169	17.66	96.511	13.7	0.76088	2.58256	377	723	1.01	3.9	12.0
Hamilton	8c	Volcanic Soil	6.8	1.063	10	653	1.18707	117.316	19.62	97.696	10.9483	0.939	2.70867	434	921	1.22	4.5	16.9
Hamilton	8c	Volcanic Soil	7	0.926	14.5	516	1.02391	120.453	21.58	98.871	9.13306	1.61724	2.87844	541	1133	1.18	5.6	20.5
Hamilton	8c	Volcanic Soil	7.2	0.8765	10	517.5	0.97496	123.651	23.54	100.11	8.50166	1.17589	2.84955	733	925	0.28	7.5	6.7
Hamilton	8c	Volcanic Soil	7.4	0.8945	10	593	1.00734	126.776	25.51	101.27	8.69067	1.13836	2.8346	744	873	0.18	7.5	4.5
Hamilton	8c	Volcanic Soil	7.6	1.0245	10	667.5	1.15132	129.909	27.47	102.44	9.96602	0.98081	2.75213	802	1031	0.30	8.0	7.9
Hamilton	8c	Volcanic Soil	7.8	1.1215	10	706	1.25544	133.051	29.43	103.62	10.8273	0.89146	2.70104	822	906	0.11	8.0	2.9
Hamilton	8c	Volcanic Soil	8	1.0305	13.5	566	1.138	136.203	31.39	104.81	9.55484	1.35937	2.82502	691	1316	0.97	6.5	21.7
Hamilton	8c	Volcanic Soil	8.2	0.9775	10	638.5	1.09963	139.386	33.35	106.03	9.05224	1.0424	2.801	813	919	0.14	7.6	3.7
Hamilton	8c	Volcanic Soil	8.4	1.04	21.5	644	1.16209	142.581	35.32	107.26	9.50128	2.12662	2.92376	746	1006	0.37	6.8	9.0
Hamilton	8c	Volcanic Soil	8.6	1.1405	35	660	1.26596	145.956	37.28	108.68	10.2989	3.11348	2.99506	752	820	0.10	6.8	2.4
Hamilton	8c	Volcanic Soil	8.8	1.2185	49	696.5	1.35014	149.429	39.24	110.19	10.8919	4.08475	3.04188	715	782	0.10	6.3	2.3
Hamilton	8c	Volcanic Soil	9	1.23	54.5	602.5	1.34477	152.983	41.2	111.78	10.6583	4.56589	3.08023	647	655	0.01	5.6	0.3
Hamilton	8c	Volcanic Soil	9.2	1.1325	23.5	742	1.27322	156.442	43.16	113.28	9.85686	2.09472	2.90324	521	553	0.07	4.3	1.1
Hamilton	8c	Volcanic Soil	9.6	1.108	10	814.5	1.26259	162.781	47.09	115.69	9.5032	0.90933	2.75438	508	552	0.10	4.1	1.5
Hamilton	8c	Volcanic Soil	9.8	1.1335	13	829.5	1.29127	165.927	49.05	116.88	9.62412	1.15551	2.78963	395	431	0.11	3.0	1.2
Hamilton	8c	Volcanic Soil	10	1.1745	18.5	779	1.32188	169.133	51.01	118.12	9.75268	1.58838	2.84345	331	432	0.38	2.4	3.5
Hamilton	8c	Volcanic Soil	10.2	1.1795	20	771	1.32666	172.471	52.97	119.5	9.65532	1.73314	2.88178	302	553	1.08	2.1	8.7
Hamilton	8c	Volcanic Soil	10.4	1.1975	24	827.5	1.3545	175.799	54.94	120.86	9.74898	2.03498	2.91128	322	492	0.68	2.2	5.9
Hamilton	8c	Volcanic Soil	10.6	1.208	34	794	1.35922	179.171	56.9	122.27	9.647	2.88357	2.99729	324	467	0.57	2.2	5.0
Hamilton	8c	Volcanic Soil	10.8	1.2805	57	766.5	1.4258	182.65	58.86	123.79	10.0366	4.55485	3.09681	317	504	0.77	2.1	6.5
Hamilton	8c	Volcanic Soil	11	1.325	90.5	728.5	1.46358	186.276	60.82	125.45	10.1773	7.08592	3.21651	380	470	0.30	2.6	3.1
Hamilton	8c	Volcanic Soil	11.2	1.455	110	566.5	1.56263	189.961	62.78	127.18	10.7873	8.00641	3.23239	396	452	0.18	2.7	1.9
Hamilton	8c	Volcanic Soil	11.4	1.534	119.5	608	1.64925	193.695	64.75	128.95	11.284	8.21117	3.22496	369	424	0.19	2.4	1.9
Hamilton	8c	Volcanic Soil	11.6	1.453	110	704	1.587	197.42	66.71	130.71	10.627	7.91741	3.23413	162	279	1.46	0.7	4.0
Hamilton	8c	Volcanic Soil	11.8	1.471	110	718	1.60745	201.135	68.67	132.46	10.6129	7.82369	3.23119	189	312	1.17	0.9	4.3
Hamilton	8c	Volcanic Soil	12	1.49	98.5	660.5	1.61559	204.835	70.63	134.2	10.5076	6.98461	3.20179	277	473	1.03	1.5	6.8
Hamilton	8c	Volcanic Soil	12.2	1.552	97.5	779	1.69911	208.531	72.59	135.94	10.9613	6.53016	3.16944	380	1289	3.12	2.3	31.6
Hamilton	8c	Volcanic Soil	12.4	1.4075	60.5	915	1.58215	212.175	74.56	137.62	9.9522	4.41965	3.09475	837	2515	2.25	5.9	58.2
Hamilton	8c	Volcanic Soil	12.6	1.379	50	947.5	1.55893	215.713	76.52	139.2	9.64654	3.72277	3.06359	922	2573	1.99	6.4	57.3
Hamilton	8c	Volcanic Soil	12.8	1.3815	57.5	907	1.55376	219.256	78.48	140.78	9.47664	4.31111	3.10681	965	2671	1.96	6.6	59.2
Hamilton	8c	Volcanic Soil	13	1.3775	65.5	811.5	1.53138	222.833	80.44	142.39	9.18584	5.00504	3.15706	1062	2895	1.90	7.2	63.6
Hamilton	8c	Volcanic Soil	13.2	1.3105	60	802	1.46336	226.419	82.4	144.01	8.5867	4.85372	3.17264	974	2319	1.54	6.5	46.7
Hamilton	8c	Volcanic Soil	13.4	1.2015	57	738.5	1.34132	229.984	84.37	145.62	7.63007	5.12459	3.22768	953	2776	2.14	6.2	63.3
Hamilton	8c	Volcanic Soil	13.6	1.0765	41	651	1.20066	233.488	86.33	147.16	6.57059	4.25569	3.2332	1003	2591	1.76	6.5	55.1
Hamilton	8c	Volcanic Soil	13.8	1.087	50	532	1.18808	236.973	88.29	148.68	6.39489	5.24148	3.29535	1092	2695	1.62	7.0	55.6
Hamilton	8c	Volcanic Soil	14	1.1875	48.5	403	1.26427	240.484	90.25	150.23	6.81089	4.78279	3.24869	883	2283	1.80	5.4	48.6
Hamilton	8c	Volcanic Soil	14.2	1.465	40	335	1.52929	243.973	92.21	151.76	8.46453	3.1294	3.06731	1452	4027	1.91	9.2	89.3
Hamilton	8c	Volcanic Soil	14.4	2.2955	32.5	292.5	2.35344	247.433	94.18	153.26	13.7318	1.56436	2.72491	915	3285	2.94	5.4	82.2
Hamilton	8c	Volcanic Soil	14.6	4.2765	45.5	233.5	4.3208	250.949	96.14	154.81	26.263	1.14536	2.3985	720	1387	1.10	4.0	23.1
Hamilton	8c	Volcanic Soil	14.8	9.0985	83	115	9.12641	254.615	98.1	156.52	56.6225	0.92881	2.05006	1012	2573	1.74	5.9	54.2
Hamilton	8c	Volcanic Soil	15	15.1535	164.5	-44.5	15.1455	258.504	100.1	158.44	93.8991	1.09766	1.90505	666	2013	2.45	3.6	46.7
Hamilton	8c	Volcanic Soil	15.2	18.517	251.5	-73.5	18.4955	262.546	102	160.52	113.525	1.37549	1.91147	1010	3224	2.48	5.7	76.8
Hamilton	8c	Volcanic Soil	15.4	21.0075	330.5	-70	20.991	266.68	104	162.69	127.326	1.59365	1.92294	1650	3560	1.25	9.6	66.3
Hamilton	8c	Volcanic Soil	15.6	21.9775	379.5	-64	21.9662	270.866	105.9	164.92	131.501	1.74968	1.94385	2182	4963	1.35	12.8	96.5
Hamilton	8c	Volcanic Soil	15.8	22.6345	450	-60	22.6356	275.085	107.9	167.17	133.701	2.01028	1.98596	1180	3592	2.28	6.5	83.7
Hamilton	8c	Volcanic Soil	16	24.996	386.5	-49.5	24.9783	279.318	109.9	169.45	145.696	1.56802	1.87163	1038	3054	2.21	5.5	70.0
Hamilton	8c	Volcanic Soil	16.2	26.8315	400	-50	26.822	283.54	111.8	171.71	154.502	1.50743	1.8398	1191	2738	1.45	6.4	53.7
Hamilton	8c	Volcanic Soil	16.4	27.9795	407	-50	27.9677	287.771	113.8	173.98	159.047	1.46878	1.82074	921	2438	1.92	4.7	52.6
Hamilton	8c	Volcanic Soil	16.6	29.055	415.5	-47	29.0462	292.007	115.8	176.25	163.09	1.4472	1.80648	1162	2847	1.64	6.0	58.5
Hamilton	8c	Volcanic Soil	16.8	29.6795	460	-40.5	29.68	296.267	117.7	178.55	164.519	1.56499	1.83074	825	2154	1.92	4.0	46.1
Hamilton	8c	Volcanic Soil	17	30.6305	481.5	-40	30.6146	300.534	119.7	180.85	167.556	1.58728	1.82883	849	2198	1.89	4.1	46.8
Hamilton	8c	Volcanic Soil	17.2	32.0085	555.5	-49	32.0024	304.838	121.6	183.19	172.97	1.72651	1.84727	787	1960	1.80	3.7	40.7
Hamilton	8d	Volcanic Soil	1.6	0.794	31.5	37.5	0.80312	27.6127	0	27.613	27.4105	5.08655	2.88519	1055	1749	0.66	37.8	24.1
Hamilton	8d	Volcanic Soil	1.8	2.191	78.5	273	2.24063	31.1601	0	31.16	70.5951	3.52937	2.46605	956	1478	0.55	30.1	18.1
Hamilton	8d	Volcanic Soil	2	2.2945	57.5	850	2.45527	34.8166	0	34.817	69.3989	2.38466	2.35642	956	1500	0.57	26.9	18.9
Hamilton	8d	Volcanic Soil	2.2	2.0305	43	1055	2.23159	38.371	0	38.371	57.1448	1.95662	2.35868	942	1428	0.52	24.0	16.9
Hamilton	8d	Volcanic Soil	2.4	1.855	35	1039	2.05325	41.8575	0.981	40.876	49.1627	1.73611	2.36796	942	1426	0.51	21.9	16.8
Hamilton	8d	Volcanic Soil	2.6	1.993	56	992.5	2.18073	45.3933	2.943	42.45	50.2794	2.61519	2.46162	942	1545	0.64	20.2	20.9
Hamilton	8d	Volcanic Soil	2.8	1.824	28.5	1047.5	2.02302	48.8992	4.905	43.994	44.8411	1.44556	2.34526	962	1499	0.56	19.1	18.6
Hamilton	8d	Volcanic Soil	3	1.8395	30	1078	2.04432	52.3069	6.867	45.44	43.8042	1.50623	2.36381	860	1196	0.39	15.9	11.7
Hamilton	8d	Volcanic Soil	3.2	2.087	60.5	1078.5	2.29049	55.7864	8.829	46.957	47.5039	2.66579	2.47329	768	2051	1.67	13.3	44.5
Hamilton	8d	Volcanic Soil	3.4	1.937	49	1071.5	2.14965	59.409	10.79	48.618	42.9708	2.29886	2.46085	1105	1820	0.65	17.9	24.8
Hamilton	8d	Volcanic Soil	3.6	2.9005	80	1341	3.14799	63.032	12.75	50.279	61.3769	2.55359	2.37875	1255	1920	0.53	19.1	23.1
Hamilton	8d	Volcanic Soil	3.8	3.195	40	1736	3.52517	66.5835	14.72	51.868	66.5772	1.15966	2.15555	1057	1842	0.74	15.2	27.3
Hamilton	8d	Volcanic Soil	4	3.953	81	2054	4.34057	70.1857	16.68	53.509	79.6809	1.88188	2.21266	904	1653	0.83	12.4	26.0
Hamilton	8d	Volcanic Soil	4.2	3.292	74	1931.5	3.66008	73.9499	18.64	55.311	64.8491	2.03106	2.29721	847	1924	1.27	11.0	37.4
Hamilton	8d	Volcanic Soil	4.4	2.6455	46	1578.5	2.94468	77.506	20.6	56.905	50.3783	1.65536	2.31331	938	1745	0.86	11.6	28.0
Hamilton	8d	Volcanic Soil	4.6	1.7395	43.5	895.5	1.91171	81.0732	22.56	58.51	31.2764	2.37574	2.5652	804	1194	0.48	9.5	13.5
Hamilton	8d	Volcanic Soil	4.8	1.797	52.5	842.5	1.95723	84.6044	24.53	60.079	31.1562	2.79249	2.60558	548	791	0.44	6.2	8.4
Hamilton	8d	Volcanic Soil	5	2.0925	50.5	992	2.27851	88.1399	26.49	61.653	35.4865	2.29774	2.51358	285	522	0.83	3.1	8.2
Hamilton	8d	Volcanic Soil	5.2	1.4225	29	767.5	1.57007	91.6865	28.45	63.237	23.3907	1.88594	2.58528	280	490	0.75	2.9	7.3
Hamilton	8d	Volcanic Soil	5.4	1.197	10	709	1.33188	94.8884	30.41	64.477	19.1883	0.82445	2.49489	286	483	0.69	2.9	6.8
Hamilton	8d	Volcanic Soil	5.6	1.098	11.5	585	1.20915	98.0241	32.37	65.651	16.9036	1.04334	2.58234	318	531	0.67	3.1	7.4
Hamilton	8d	Volcanic Soil	5.8	0.9915	13.5	630	1.11117	101.251	34.34	66.916	15.0908	1.31944	2.66477	236	425	0.80	2.2	6.6
Hamilton	8d	Volcanic Soil	6	1.143	13	691.5	1.27531	104.385	36.3	68.088	17.1732	1.08569	2.58504	245	425	0.73	2.3	6.2
Hamilton	8d	Volcanic Soil	6.2	1.7775	20	1074	1.98016	107.677	38.26	69.418	26.946	1.0813	2.42094	218	436	1.00	1.9	7.6
Hamilton	8d	Volcanic Soil	6.4	1.6375	14	1088	1.84469	111.005	40.22	70.784	24.496	0.79576	2.38765	258	443	0.72	2.2	6.4
Hamilton	8d	Volcanic Soil	6.6	1.2795	10	826	1.43647	114.169	42.18	71.986	18.3675	0.76088	2.48757	244	458	0.88	2.1	7.4
Hamilton	8d	Volcanic Soil	6.8	1.063	10	653	1.18707	117.316	44.15	73.171	14.6177	0.939	2.61025	251	469	0.87	2.1	7.6
Hamilton	8d	Volcanic Soil	7	0.926	14.5	516	1.02391	120.453	46.11	74.346	12.1443	1.61724	2.77721	226	427	0.90	1.8	7.0
Hamilton	8d	Volcanic Soil	7.2	0.8765	10	517.5	0.97496	123.651	48.07	75.582	11.2597	1.17589	2.7483	232	441	0.92	1.8	7.3
Hamilton	8d	Volcanic Soil	7.4	0.8945	10	593	1.00734	126.776	50.03	76.745	11.4664	1.13836	2.73478	228	391	0.74	1.8	5.6
Hamilton	8d	Volcanic Soil	7.6	1.0245	10	667.5	1.15132	129.909	51.99	77.916	13.1013	0.98081	2.65596	221	396	0.83	1.7	6.1

Table 6: CPT and DMT Data

				CPT DATA										DMT DATA				
Site	Pair No.	Soil Type	Depth (m)	q_c (MPa) (ave)	f_s (kPa) (ave)	u_2 (kPa) (ave)	q_t (ave)	σ_{vo} (kPa)	u_0 (kPa)	σ'_{vo} (kPa)	Q_t (ave)	F_r (Ave)	I_c (Ave)	p_o (kPa)	p_1 (kPa)	I_D	K_D	E_D (MPa)
Hamilton	8d	Volcanic Soil	7.8	1.1215	10	706	1.25544	133.051	53.96	79.096	14.1832	0.89146	2.60743	211	423	1.06	1.6	7.4
Hamilton	8d	Volcanic Soil	8	1.0305	13.5	566	1.138	136.203	55.92	80.286	12.4727	1.35937	2.72986	264	501	0.95	1.9	8.2
Hamilton	8d	Volcanic Soil	8.2	0.9775	10	638.5	1.09963	139.386	57.88	81.507	11.7748	1.0424	2.70587	239	487	1.10	1.7	8.6
Hamilton	8d	Volcanic Soil	8.4	1.04	21.5	644	1.16209	142.581	59.84	82.74	12.3167	2.12662	2.83076	295	565	0.97	2.1	9.4
Hamilton	8d	Volcanic Soil	8.6	1.113	45.0965	610.141	1.2414	145.956	61.8	84.153	12.2933	4.19879	2.98475	267	581	1.26	1.9	10.9
Hamilton	8d	Volcanic Soil	8.8	1.035	110.926	352.684	1.18288	160.346	20.6	139.75	7.31419	10.8474	3.44627	296	570	1.00	2.0	9.5
Hamilton	8d	Volcanic Soil	9	1.073	109.655	263.126	1.18354	164.038	22.56	141.48	7.20404	10.7714	3.44909	323	572	0.83	2.2	8.6
Hamilton	8d	Volcanic Soil	9.2	1.0335	105.18	353.173	1.18178	167.725	24.53	143.2	7.07831	10.3792	3.44459	314	573	0.90	2.1	9.0
Hamilton	8d	Volcanic Soil	9.4	1.0525	110.765	350.733	1.19987	171.414	26.49	144.93	7.09391	10.77	3.45433	269	527	1.07	1.7	9.0
Hamilton	8d	Volcanic Soil	9.6	1.0215	107.199	432.244	1.20256	175.106	28.45	146.66	7.0035	10.4375	3.44969	291	553	1.00	1.9	9.1
Hamilton	8d	Volcanic Soil	9.8	1.0095	94.409	518.817	1.22787	178.779	30.41	148.37	7.06705	9.05532	3.40608	292	611	1.22	1.8	11.1
Hamilton	8d	Volcanic Soil	10	1.126	96.945	376.513	1.28413	182.428	32.37	150.06	7.33714	8.8747	3.39227	324	627	1.04	2.0	10.5
Hamilton	8d	Volcanic Soil	10.2	1.194	114.384	580.556	1.43783	186.131	34.34	151.8	8.24233	9.1429	3.35857	334	614	0.94	2.1	9.7
Hamilton	8d	Volcanic Soil	10.4	1.24	114.563	655.521	1.5153	189.85	36.3	153.55	8.62818	8.65017	3.32774	358	680	1.00	2.2	11.2
Hamilton	8d	Volcanic Soil	10.6	1.25	109.021	742.16	1.56161	193.572	38.26	155.31	8.80556	7.96694	3.29764	357	737	1.19	2.2	13.2
Hamilton	8d	Volcanic Soil	10.8	1.2785	110.091	726.896	1.58391	197.27	40.22	157.05	8.82609	7.9401	3.2957	393	785	1.11	2.4	13.6
Hamilton	8d	Volcanic Soil	11	1.411	125.435	509.363	1.62459	201.005	42.18	158.82	8.9599	8.80879	3.3205	397	746	0.98	2.4	12.1
Hamilton	8d	Volcanic Soil	11.2	1.362	124.682	714.786	1.6626	204.757	44.15	160.61	9.07368	8.55476	3.30791	350	707	1.17	2.0	12.4
Hamilton	8d	Volcanic Soil	11.4	1.423	121.87	778.128	1.74971	208.494	46.11	162.39	9.48636	7.91096	3.27163	392	745	1.02	2.3	12.2
Hamilton	8d	Volcanic Soil	11.6	1.582	153.62	771.356	1.90619	212.272	48.07	164.2	10.3124	9.06531	3.2826	402	789	1.10	2.3	13.4
Hamilton	8d	Volcanic Soil	11.8	1.62	162.016	785.923	1.94968	216.085	50.03	166.05	10.4365	9.34722	3.28762	418	747	0.89	2.4	11.4
Hamilton	8d	Volcanic Soil	12	1.687	159.603	568.328	1.92596	219.905	51.99	167.91	10.1575	9.35832	3.29683	419	787	1.00	2.3	12.8
Hamilton	8d	Volcanic Soil	12.2	1.6235	165.43	728.835	1.92945	223.723	53.96	169.77	10.044	9.69979	3.31078	409	744	0.94	2.2	11.6
Hamilton	8d	Volcanic Soil	12.4	1.6195	169.436	719.479	1.9218	227.55	55.92	171.63	9.86831	10.0001	3.32533	466	789	0.79	2.5	11.2
Hamilton	8d	Volcanic Soil	12.6	1.627	168.071	702.902	1.92222	231.377	57.88	173.5	9.74239	9.94117	3.32777	398	778	1.12	2.1	13.2
Hamilton	8d	Volcanic Soil	12.8	1.6205	169.632	672.734	1.90552	235.204	59.84	175.36	9.52192	10.1668	3.34169	466	808	0.84	2.5	11.9
Hamilton	8d	Volcanic Soil	13	1.6595	159.945	470.023	1.85432	239.028	61.8	177.23	9.11233	9.8992	3.34853	489	763	0.64	2.6	9.5
Hamilton	8d	Volcanic Soil	13.2	1.5005	146.815	678.063	1.78525	242.828	63.77	179.06	8.61185	9.52086	3.35571	448	671	0.58	2.3	7.7
Hamilton	8d	Volcanic Soil	13.4	1.437	135.195	610.832	1.69383	246.608	65.73	180.88	7.99889	9.34107	3.37444	427	669	0.67	2.1	8.4
Hamilton	8d	Volcanic Soil	13.6	1.739	129.175	445.885	1.92751	250.367	67.69	182.68	9.17634	7.73465	3.27631	398	636	0.72	1.9	8.3
Hamilton	8d	Volcanic Soil	13.8	2.91	108.002	280.267	3.00042	254.137	69.65	184.49	14.8746	4.14308	2.93534	362	585	0.76	1.7	7.7
Hamilton	8d	Volcanic Soil	14	6.119	87.431	127.748	6.20409	257.877	71.61	186.26	31.888	1.63092	2.40777	300	615	1.38	1.3	10.9
Hamilton	8d	Volcanic Soil	14.2	10.8695	131.998	52.819	10.8891	261.708	73.58	188.13	56.4609	1.23708	2.10815	375	795	1.39	1.7	14.6
Hamilton	8d	Volcanic Soil	14.4	13.18	182.428	66.651	13.2078	265.66	75.54	190.12	68.0424	1.40885	2.07859	536	1360	1.79	2.6	28.6
Hamilton	8d	Volcanic Soil	14.6	15.182	272.468	69.661	15.2079	269.704	77.5	192.21	77.6955	1.82126	2.11297	861	2045	1.51	4.4	41.1
Hamilton	8d	Volcanic Soil	14.8	15.861	322.833	71.7835	15.8907	273.83	79.46	194.37	80.3188	2.06762	2.14445	1009	2613	1.73	5.2	55.7
Hamilton	8d	Volcanic Soil	15	16.1605	285.446	70.8115	16.1941	277.943	81.42	196.52	80.9511	1.80031	2.0947	820	2492	2.26	4.1	58.0
Hamilton	8d	Volcanic Soil	15.2	18.036	351.581	61.4475	18.0563	282.09	83.39	198.71	89.414	1.97771	2.09334	982	2593	1.79	4.9	55.9
Hamilton	8d	Volcanic Soil	15.4	21.457	431.817	95.903	21.5033	286.281	85.35	200.93	105.54	2.03255	2.04957	1081	2802	1.73	5.3	59.7
Hamilton	8d	Volcanic Soil	15.6	24.358	463.341	105.892	24.3992	290.539	87.31	203.23	118.585	1.9281	1.99152	965	2487	1.74	4.7	52.8
Hamilton	8d	Volcanic Soil	15.8	5.43	96.1885	225.163	5.52483	282.89	137.8	145.06	28.3661	1.6254	2.67991	1121	2970	1.79	5.4	64.2
Hamilton	8d	Volcanic Soil	16	1.995	35.689	207.035	2.0915	286.309	139.8	146.52	12.3096	2.15813	2.85339	1191	3062	1.70	5.7	64.9
Ngaruawahia	9a	Volcanic Soil	0.2	1.502	61.5	-0.5	1.50041	3.45766	0	3.4577	469.312	4.13652	2.22852	165	242	0.46	48.6	2.7
Ngaruawahia	9a	Volcanic Soil	0.4	1.192	46.5	16.5	1.19897	7.0058	0	7.0058	168.044	4.06095	2.36986	152	398	1.61	23.3	8.5
Ngaruawahia	9a	Volcanic Soil	0.6	2.6875	56	3.5	2.68783	10.527	0	10.527	251.013	2.11419	2.08998	137	401	1.92	13.9	9.1
Ngaruawahia	9a	Volcanic Soil	0.8	4.504	61	-15	4.49882	14.1703	0	14.17	315.463	1.36916	1.89615	99	437	3.42	7.4	11.7
Ngaruawahia	9a	Volcanic Soil	1	3.4275	47	-15.5	3.41869	17.8078	0	17.808	192.699	1.39408	2.01073	181	844	3.65	10.7	23.0
Ngaruawahia	9a	Volcanic Soil	1.2	1.2945	30	-8.5	1.29975	21.3011	0	21.301	60.7379	2.39621	2.44436	250	908	2.64	12.2	22.8
Ngaruawahia	9a	Volcanic Soil	1.4	2.267	32	1.5	2.26445	24.6784	0	24.678	90.4575	1.61753	2.21198	157	778	3.94	6.5	21.5
Ngaruawahia	9a	Volcanic Soil	1.6	1.3235	27	12.5	1.33218	28.0976	0	28.098	45.6467	2.90882	2.54233	164	205	0.25	5.9	1.4
Ngaruawahia	9a	Volcanic Soil	1.8	2.6585	29	-13	2.65343	31.5041	0	31.504	84.0651	1.31514	2.1707	177	558	2.16	5.7	13.2
Ngaruawahia	9a	Volcanic Soil	2	2.5065	24	3.5	2.50417	34.9446	0	34.945	71.3885	1.15198	2.20973	169	637	2.78	4.9	16.3
Ngaruawahia	9a	Volcanic Soil	2.2	0.534	10	38.5	0.54245	38.1249	1.962	36.163	13.9069	2.14792	2.82401	181	363	1.01	5.0	6.3
Ngaruawahia	9a	Volcanic Soil	2.4	0.4195	2	-29	0.41432	41.3761	3.924	37.452	9.97796	0.41457	2.70126	117	147	0.27	3.0	1.1
Ngaruawahia	9a	Volcanic Soil	2.6	0.9125	6	-5.5	0.91312	45.0547	5.886	39.169	22.0554	0.55343	2.40648	124	266	1.20	3.1	4.9
Ngaruawahia	9a	Volcanic Soil	2.8	1.867	17.5	23.5	1.8673	48.2673	7.848	40.419	45.0082	0.97543	2.26824	185	593	2.31	4.5	14.2
Ngaruawahia	9a	Volcanic Soil	3	1.9265	12	41	1.93712	51.4924	9.81	41.682	45.0094	0.72761	2.2418	189	408	1.23	4.4	7.6
Ngaruawahia	9a	Volcanic Soil	3.2	4.3505	32	25	4.34942	54.8536	11.77	43.082	99.574	0.74486	1.94514	191	603	2.29	4.2	14.3
Ngaruawahia	9a	Volcanic Soil	3.4	1.7435	23	24	1.75423	58.3479	13.73	44.614	38.148	1.42496	2.42606	191	243	0.30	4.0	1.8
Ngaruawahia	9a	Volcanic Soil	3.6	1.962	12.5	14	1.96549	61.5278	15.7	45.832	41.3164	0.83304	2.30776	177	458	1.75	3.6	9.8
Ngaruawahia	9a	Volcanic Soil	3.8	4.978	36.5	20.5	4.97873	64.933	17.66	47.275	103.846	0.73852	1.91945	254	851	2.53	5.1	20.7
Ngaruawahia	9a	Volcanic Soil	4	4.0615	37	30	4.06853	68.498	19.62	48.878	81.8559	0.92456	2.04561	345	851	1.56	6.7	17.6
Ngaruawahia	9a	Volcanic Soil	4.2	3.1095	21.5	22	3.11285	71.9523	21.58	50.37	60.3293	0.7067	2.08254	332	891	1.80	6.2	19.4
Ngaruawahia	9a	Volcanic Soil	4.4	2.107	18	19.5	2.11251	75.3174	23.54	51.773	39.3795	0.93505	2.28367	308	772	1.63	5.5	16.1
Ngaruawahia	9a	Volcanic Soil	4.6	1.3195	9.5	11	1.31996	78.538	25.51	53.032	23.4719	0.96229	2.49451	335	955	2.00	5.8	21.5
Ngaruawahia	9a	Volcanic Soil	4.8	0.306	0	35	0.31348	81.9735	27.47	54.506	4.24982			210	534	1.78	3.3	11.3
Ngaruawahia	9a	Volcanic Soil	5	0.327	7	66	0.34087	85.7735	29.43	56.344	4.52074	4.46704		184	188	0.03	2.7	0.1
Ngaruawahia	9a	Volcanic Soil	5.2	3.305	14	51	3.31319	89.0219	31.39	57.63	55.745	0.79356	2.09816	227	262	0.18	3.4	1.2
Ngaruawahia	9a	Volcanic Soil	5.4	6.7	21.5	40	6.7076	92.36	33.35	59.006	112.002	0.32202	1.69366	216	695	2.62	3.1	16.6
Ngaruawahia	9a	Volcanic Soil	5.6	6.998	20.5	40	7.00577	95.8158	35.32	60.5	114.069	0.3036	1.67315	282	1156	3.54	4.1	30.3
Ngaruawahia	9a	Volcanic Soil	5.8	7.872	27	40	7.8831	99.303	37.28	62.025	125.484	0.34309	1.65559	396	1299	2.52	5.8	31.3
Ngaruawahia	9a	Volcanic Soil	6	7.2255	20	46	7.23057	102.763	39.24	63.523	112.168	0.28081	1.65701	303	838	2.03	4.2	18.6
Ngaruawahia	9b	Volcanic Soil	0.2	1.1475	37.5	0	1.14617	3.37407	0	3.3741	358.385	3.35551	2.2233	193	398	1.06	56.8	7.1
Ngaruawahia	9b	Volcanic Soil	0.4	0.4115	24.5	0	0.41283	6.7741	0	6.7741	63.7642	6.54364	2.74199	169	386	1.29	25.0	7.5
Ngaruawahia	9b	Volcanic Soil	0.6	0.508	22	-1.5	0.50955	9.91773	0	9.9177	46.6533	6.67928	2.84121	236	557	1.36	23.4	11.1
Ngaruawahia	9b	Volcanic Soil	0.8	2.946	77	-30	2.9433	13.3985	0	13.398	213.125	2.88972	2.18545	238	611	1.56	17.8	12.9
Ngaruawahia	9b	Volcanic Soil	1	6.0945	56.5	-18	6.08708	17.0831	0	17.083	353.91	0.93554	1.74958	144	567	2.94	8.6	14.7
Ngaruawahia	9b	Volcanic Soil	1.2	3.396	24	-1.5	3.39505	20.6685	0	20.668	167.435	0.79288	1.95177	279	545	0.95	13.8	9.2
Ngaruawahia	9b	Volcanic Soil	1.4	2.506	12.5	5.5	2.50688	23.8758	0	23.876	102.268	0.53911	1.96682	244	752	2.08	10.3	17.6
Ngaruawahia	9b	Volcanic Soil	1.6	3.343	20	10	3.34673	27.2204	0	27.22	122.187	0.60953	1.90444	274	679	1.48	10.0	14.1
Ngaruawahia	9b	Volcanic Soil	1.8	3.797	20	10	3.79707	30.5982	0	30.598	122.612	0.53465	1.85964	290	714	1.46	9.4	14.7
Ngaruawahia	9b	Volcanic Soil	2	4.567	12	10	4.56923	33.9357	0	33.936	134.033	0.27583	1.7027	215	590	1.74	6.3	13.0
Ngaruawahia	9b	Volcanic Soil	2.2	6.1745	22.5	10	6.17707	37.2656	1.962	35.304	173.784	0.37289	1.65198	268	777	1.92	7.4	17.7
Ngaruawahia	9b	Volcanic Soil	2.4	6.901	27.5	13	6.90147	40.7631	3.924	36.839	185.917	0.40441	1.64158	247	310	0.26	6.5	2.2
Ngaruawahia	9b	Volcanic Soil	2.6	6.5435	22	19	6.54828	44.2369	5.886	38.351	169.496	0.34005	1.63347	269	575	1.16	6.8	10.6
Ngaruawahia	9b	Volcanic Soil	2.8	6.4955	29.5	20	6.49897	47.7316	7.848	39.884	161.58	0.45758	1.6999	385	1138	2.00	9.4	26.1
Ngaruawahia	9b	Volcanic Soil	3	6.5255	20	20	6.53013	51.2058	9.81	41.396	156.417	0.30885	1.63262	454	1281	1.86	10.6	28.7
Ngaruawahia	9b	Volcanic Soil	3.2	6.635	20	24.5	6.63849	54.6358	11.77	42.864	153.446	0.30396	1.63024	487	1523	2.18	10.9	36.0
Ngaruawahia	9b	Volcanic Soil	3.4	7.207	20	30	7.2132	58.071	13.73	44.337	161.236	0.27975	1.59304	652	1483	1.30	14.0	28.8

Table 6: CPT and DMT Data

				CPT DATA										DMT DATA				
Site	Pair No.	Soil Type	Depth (m)	q_c (MPa) (ave)	f_s (kPa) (ave)	u_2 (kPa) (ave)	q_t (ave)	σ_{vo} (kPa)	u_0 (kPa)	σ'_{vo} (kPa)	Q_t (ave)	F_r (Ave)	I_c (Ave)	p_o (kPa)	p_1 (kPa)	I_D	K_D	E_D (MPa)
Ngaruawahia	9b	Volcanic Soil	3.6	5.4055	17	30	5.4112	61.5042	15.7	45.808	116.91	0.31505	1.72529	556	1374	1.51	11.4	28.4
Ngaruawahia	9b	Volcanic Soil	3.8	4.5035	10	30	4.51337	64.7807	17.66	47.123	94.3347	0.22575	1.74414	595	1221	1.08	11.7	21.7
Ngaruawahia	9b	Volcanic Soil	4	4.9485	10	30	4.96053	68.0313	19.62	48.411	101.1	0.20817	1.70608	438	1043	1.44	8.2	21.0
Ngaruawahia	9b	Volcanic Soil	4.2	6.561	10	36.5	6.55727	71.2834	21.58	49.701	130.311	0.15632	1.57241	443	1150	1.68	8.0	24.5
Ngaruawahia	9b	Volcanic Soil	4.4	7.504	19.5	40	7.51177	74.6367	23.54	51.093	145.487	0.26269	1.59239	454	1058	1.40	7.9	21.0
Ngaruawahia	9b	Volcanic Soil	4.6	6.435	20	40	6.44243	78.0698	25.51	52.564	120.95	0.31552	1.68368	232	433	0.97	3.7	7.0
Ngaruawahia	9b	Volcanic Soil	4.8	5.876	17.5	40	5.88343	81.5017	27.47	54.034	107.423	0.30078	1.71525	167	284	0.83	2.4	4.0
Ngaruawahia	9b	Volcanic Soil	5	5.283	10	40	5.2921	84.7969	29.43	55.367	93.9892	0.1922	1.69583	200	228	0.17	2.9	1.0
Ngaruawahia	9b	Volcanic Soil	5.2	6.623	16	42	6.62981	88.0751	31.39	56.683	115.232	0.24087	1.64549	169	230	0.44	2.3	2.1
Ngaruawahia	9b	Volcanic Soil	5.4	7.4165	20	45.5	7.42665	91.5169	33.35	58.163	126.117	0.27462	1.62762	205	290	0.50	2.8	3.0
Ngaruawahia	9b	Volcanic Soil	5.6	7.059	15.5	50	7.06383	94.8857	35.32	59.57	116.904	0.22381	1.61709	202	346	0.86	2.7	5.0
Ngaruawahia	9b	Volcanic Soil	5.8	5.9915	14	50	6.00467	98.2581	37.28	60.98	96.7896	0.23565	1.69127	172	334	1.20	2.1	5.6
Ngaruawahia	9b	Volcanic Soil	6	5.53	20	50	5.538	101.643	39.24	62.403	87.1111	0.37001	1.80109	368	1054	2.08	5.1	23.8
Ngaruawahia	9b	Volcanic Soil	6.2	4.2275	11.5	50.5	4.23826	104.998	41.2	63.796	64.8027	0.27707	1.86199	630	1771	1.94	8.9	39.6
Ngaruawahia	9b	Volcanic Soil	6.4	3.2045	17	57	3.21383	108.228	43.16	65.064	47.763	0.75243	2.10098	464	1194	1.73	6.2	25.3
Ngaruawahia	9b	Volcanic Soil	6.6	0.981	42	155.5	1.01168	111.661	45.13	66.535	13.5354	4.73264	3.01354	584	1502	1.70	7.8	31.8
Ngaruawahia	9b	Volcanic Soil	6.8	2.693	33.5	143	2.72334	115.073	47.09	67.985	38.214	1.87672	2.4483	316	790	1.76	3.8	16.4
Ngaruawahia	9b	Volcanic Soil	7	5.49	56.5	70	5.49983	118.656	49.05	69.606	77.2058	1.05054	2.05373	298	458	0.64	3.4	5.5
Ngaruawahia	9b	Volcanic Soil	7.2	4.2625	52.5	81	4.27562	122.315	51.01	71.303	58.3725	1.51856	2.24521	467	1459	2.39	5.6	34.4
Ngaruawahia	9b	Volcanic Soil	7.4	2.957	31.5	120	2.98307	125.83	52.97	72.856	39.0613	1.90206	2.41476	934	2289	1.54	11.6	47.0
Ngaruawahia	9b	Volcanic Soil	7.6	6.255	20	47	6.26343	129.271	54.94	74.335	82.4573	0.3273	1.77027	956	2313	1.50	11.6	47.1
Ngaruawahia	9b	Volcanic Soil	7.8	6.8435	24	66	6.85604	132.702	56.9	75.804	88.6123	0.35434	1.75358	863	2001	1.41	10.1	39.5
Ngaruawahia	9b	Volcanic Soil	8	7.4035	30	70	7.41797	136.226	58.86	77.366	94.0852	0.41234	1.75702	703	1563	1.33	7.9	29.8
Ngaruawahia	9b	Volcanic Soil	8.2	8.6835	32	70	8.6958	139.75	60.82	78.928	108.293	0.37101	1.68115	602	1443	1.55	6.5	29.2
Ngaruawahia	9b	Volcanic Soil	8.4	9.4345	40	70	9.44413	143.359	62.78	80.575	115.417	0.43448	1.68699	388	503	0.36	3.8	4.0
Ngaruawahia	9b	Volcanic Soil	8.6	6.2805	32.5	72.5	6.29661	146.947	64.75	82.201	74.8221	0.52877	1.88442	429	783	0.97	4.2	12.3
Ngaruawahia	9b	Volcanic Soil	8.8	6.496	26	80	6.5197	150.425	66.71	83.717	75.9551	0.41421	1.8315	767	2027	1.80	7.9	43.7
Ngaruawahia	9b	Volcanic Soil	9	9.744	46	80	9.7527	154.001	68.67	85.331	112.405	0.47826	1.70685	1142	2628	1.38	11.9	51.6
Ngaruawahia	9b	Volcanic Soil	9.2	9.7935	38.5	80	9.80787	157.66	70.63	87.028	110.889	0.39702	1.66943	1092	2352	1.23	11.1	43.7
Ngaruawahia	9b	Volcanic Soil	9.4	11.7085	34.5	80	11.7174	161.225	72.59	88.631	130.17	0.30665	1.56027	899	2129	1.49	8.8	42.7
Ngaruawahia	9b	Volcanic Soil	9.6	14.0115	43	89.5	14.0348	164.866	74.56	90.31	153.44	0.31016	1.49015	709	1756	1.65	6.6	36.3
Ngaruawahia	9b	Volcanic Soil	9.8	15.4525	63.5	90	15.4708	168.582	76.52	92.064	166.198	0.42039	1.52152	558	1305	1.55	4.9	25.9
Ngaruawahia	9b	Volcanic Soil	10	13.762	70	90	13.7779	172.36	78.48	93.88	144.905	0.51659	1.61864	538	1291	1.64	4.6	26.1
Ngaruawahia	9b	Volcanic Soil	10.2	11.401	46	92	11.4185	176.093	80.44	95.651	117.53	0.40818	1.63556	686	1850	1.92	6.0	40.4
Ngaruawahia	9b	Volcanic Soil	10.4	9.875	44	90	9.88997	179.717	82.4	97.313	99.7144	0.45243	1.71682	731	1881	1.77	6.3	39.9
Ngaruawahia	9b	Volcanic Soil	10.6	6.1745	34.5	100	6.1938	183.36	84.37	98.994	60.7746	0.56622	1.9629	963	2479	1.73	8.4	52.6
Ngaruawahia	9b	Volcanic Soil	10.8	4.779	17.5	100	4.80067	186.783	86.33	100.45	45.8946	0.39262	1.98021	960	2339	1.58	8.2	47.8
Ngaruawahia	9b	Volcanic Soil	11	6.5665	20	100	6.58467	190.168	88.29	101.88	62.7184	0.31568	1.81861	969	1807	0.95	8.1	29.1
Ngaruawahia	9b	Volcanic Soil	11.2	7.6535	23	100	7.66367	193.61	90.25	103.36	72.2592	0.31143	1.75418	851	2280	1.88	6.9	49.6
Ngaruawahia	9b	Volcanic Soil	11.4	6.5555	23.5	100	6.5895	197.106	92.21	104.89	60.9218	0.3679	1.85032	641	1731	1.99	4.9	37.8
Ngaruawahia	9b	Volcanic Soil	11.6	9.732	27.5	101	9.74386	200.572	94.18	106.4	89.616	0.28778	1.65496	943	2470	1.80	7.4	53.0
Ngaruawahia	9b	Volcanic Soil	11.8	10.189	34	110	10.2111	204.133	96.14	107.99	92.6253	0.34035	1.66586	894	2117	1.53	6.8	42.4
Ngaruawahia	9b	Volcanic Soil	12	9.8685	32.5	110	9.8854	207.733	98.1	109.63	88.2489	0.3361	1.68028	508	1257	1.82	3.5	26.0
Ngaruawahia	9b	Volcanic Soil	12.2	8.685	22	110	8.7164	211.254	100.1	111.19	76.4451	0.26149	1.69038	841	2064	1.65	6.2	42.4
Ngaruawahia	9b	Volcanic Soil	12.4	12.4985	36	111.5	12.5132	214.772	102	112.75	109.014	0.29129	1.56392	812	1985	1.65	5.8	40.7
Ngaruawahia	9b	Volcanic Soil	12.6	12.727	51.5	120	12.7695	218.426	104	114.44	109.609	0.40913	1.63003	619	1486	1.69	4.2	30.1
Ngaruawahia	9b	Volcanic Soil	12.8	15.35	45.5	120	15.3528	222.136	105.9	116.19	130.209	0.30374	1.49594	410	723	1.03	2.4	10.9
Ngaruawahia	9b	Volcanic Soil	13	13.2805	49	120	13.2978	225.825	107.9	117.92	110.855	0.37771	1.60504	546	669	0.28	3.4	4.3
Ngaruawahia	9b	Volcanic Soil	13.2	8.6665	28	120	8.6963	229.42	109.9	119.55	70.8029	0.32987	1.74938	645	747	0.19	4.2	3.5
Ngaruawahia	9b	Volcanic Soil	13.4	10.64	37	121	10.6628	232.974	111.8	121.14	86.021	0.35352	1.68686	664	899	0.43	4.2	8.2
Ngaruawahia	9b	Volcanic Soil	13.6	12.647	53.5	130	12.6707	236.654	113.8	122.86	101.179	0.43007	1.66023	563	688	0.28	3.4	4.3
Ngaruawahia	9b	Volcanic Soil	13.8	12.57	60.5	130	12.6015	240.37	115.8	124.61	99.1461	0.49094	1.6972	663	784	0.22	4.1	4.2
Ngaruawahia	9b	Volcanic Soil	14	14.1685	72.5	130	14.1842	244.137	117.7	126.42	110.235	0.52052	1.66893	720	879	0.26	4.5	5.5
Ngaruawahia	9b	Volcanic Soil	14.2	13.813	65	132	13.8472	247.912	119.7	128.23	106.02	0.4777	1.65977	774	977	0.31	4.8	7.0
Ngaruawahia	9b	Volcanic Soil	14.4	14.1715	80	132.5	14.1878	251.688	121.6	130.04	107.149	0.57563	1.70077	738	913	0.28	4.5	6.1
Ngaruawahia	9b	Volcanic Soil	14.6	11.695	61	140	11.7194	255.473	123.6	131.87	86.9307	0.52998	1.75694	540	732	0.46	3.0	6.7
Ngaruawahia	9b	Volcanic Soil	14.8	8.2015	38	140	8.22943	259.146	125.6	133.58	59.6793	0.4706	1.8767	465	608	0.42	2.4	5.0
Ngaruawahia	9b	Volcanic Soil	15	6.348	20	140	6.3756	262.721	127.5	135.19	45.3581	0.23711	1.84824	709	1991	2.21	4.1	44.5
Ngaruawahia	9c	Volcanic Soil	0.2	1.414	21	0	1.413	3.38336	0	3.3834	442.56	1.49548	1.9817	155	359	1.31	45.7	7.1
Ngaruawahia	9c	Volcanic Soil	0.4	0.7705	10	0	0.77133	6.56743	0	6.5674	120.095	1.34674	2.22201	136	242	0.78	20.2	3.7
Ngaruawahia	9c	Volcanic Soil	0.6	0.541	10	0	0.54083	9.65673	0	9.6567	55.2642	1.88758	2.45274	143	223	0.56	14.5	2.8
Ngaruawahia	9c	Volcanic Soil	0.8	0.508	10	0	0.5085	12.7319	0	12.732	38.8237	2.02088	2.54422	145	220	0.51	11.2	2.6
Ngaruawahia	9c	Volcanic Soil	1	0.71	10	0	0.70983	15.8185	0	15.818	43.603	1.45228	2.43194	160	254	0.59	9.9	3.3
Ngaruawahia	9c	Volcanic Soil	1.2	0.9815	10	0	0.9815	18.9291	0	18.929	50.4037	1.06111	2.31579	150	258	0.72	7.8	3.8
Ngaruawahia	9c	Volcanic Soil	1.4	1.22	10	0	1.2195	22.0688	0	22.069	54.2378	0.83805	2.23822	168	342	1.04	7.5	6.0
Ngaruawahia	9c	Volcanic Soil	1.6	1.035	10	0	1.036	25.2034	0	25.203	40.0038	0.99042	2.35095	226	518	1.29	8.8	10.1
Ngaruawahia	9c	Volcanic Soil	1.8	1.3395	10	0	1.3395	28.3416	0	28.342	46.084	0.76607	2.24839	405	782	0.93	13.9	13.1
Ngaruawahia	9c	Volcanic Soil	2	1.6495	10	0	1.64817	31.5012	0	31.501	51.6392	0.62088	2.16517	459	931	1.03	14.0	16.4
Ngaruawahia	9c	Volcanic Soil	2.2	1.3785	10	3.5	1.38	34.6602	1.962	32.698	41.1139	0.74349	2.26748	304	681	1.25	8.8	13.1
Ngaruawahia	9c	Volcanic Soil	2.4	1.4575	10	10	1.45973	37.8117	3.924	33.888	41.8949	0.70686	2.2489	338	659	0.96	9.3	11.1
Ngaruawahia	9c	Volcanic Soil	2.6	1.7375	10	10	1.74057	40.9763	5.886	35.09	48.3831	0.59789	2.16784	354	760	1.17	9.3	14.1
Ngaruawahia	9c	Volcanic Soil	2.8	2.773	38.5	10	2.7736	44.2659	7.848	36.418	74.9199	1.59955	2.20749	373	747	1.02	9.4	13.0
Ngaruawahia	9c	Volcanic Soil	3	4.4755	92	3.5	4.47613	47.884	9.81	38.074	115.773	2.22864	2.20004	376	760	1.05	9.0	13.3
Ngaruawahia	9c	Volcanic Soil	3.2	4.139	92.5	0	4.13833	51.6983	11.77	39.926	102.572	2.23222	2.22991	371	814	1.23	8.5	15.4
Ngaruawahia	9c	Volcanic Soil	3.4	2.511	58	21.5	2.51542	55.3245	13.73	41.591	59.1258	2.38245	2.39104	386	760	1.00	8.5	13.0
Ngaruawahia	9c	Volcanic Soil	3.6	3.037	70	22.5	3.04161	58.9609	15.7	43.265	68.7999	2.39114	2.34466	311	712	1.36	6.5	13.9
Ngaruawahia	9c	Volcanic Soil	3.8	3.464	56	15	3.46652	62.6066	17.66	44.949	75.6664	1.64602	2.21674	366	721	1.02	7.5	12.3
Ngaruawahia	9c	Volcanic Soil	4	3.416	50	23	3.42054	66.2039	19.62	46.584	71.9597	1.49174	2.20459	359	720	1.06	7.0	12.5
Ngaruawahia	9c	Volcanic Soil	4.2	3.349	41	30	3.35307	69.7738	21.58	48.192	68.0737	1.25111	2.17486	393	752	0.97	7.4	12.5
Ngaruawahia	9c	Volcanic Soil	4.4	3.034	46.5	40.5	3.04316	73.319	23.54	49.775	59.605	1.56891	2.26831	374	709	0.96	6.8	11.6
Ngaruawahia	9c	Volcanic Soil	4.6	3.659	38	31	3.66522	76.879	25.51	51.373	69.7554	1.06958	2.12197	328	721	1.30	5.7	13.6
Ngaruawahia	9c	Volcanic Soil	4.8	4.204	39.5	21.5	4.20809	80.4154	27.47	52.947	77.879	0.95754	2.05882	347	722	1.17	5.9	13.0
Ngaruawahia	9c	Volcanic Soil	5	4.7585	41	21.5	4.76392	83.9762	29.43	54.546	85.7041	0.87621	2.00351	353	748	1.22	5.8	13.7
Ngaruawahia	9c	Volcanic Soil	5.2	6.2095	61.5	30	6.2194	87.5895	31.39	56.197	108.92	0.99874	1.95603	360	713	1.07	5.7	12.2
Ngaruawahia	9c	Volcanic Soil	5.4	9.1285	121.5	40.5	9.13066	91.3551	33.35	58.001	155.663	1.35426	1.91511	405	813	1.10	6.3	14.2
Ngaruawahia	9c	Volcanic Soil	5.6	11.6285	190.5	38	11.6351	95.315	35.32	59.999	191.946	1.71732	1.92366	427	943	1.31	6.4	17.9
Ngaruawahia	9c	Volcanic Soil	5.8	13.548	166.5	37.5	13.556	99.2818	37.28	62.004	216.84	1.23662	1.79423	1189	2933	1.51	18.4	60.5
Ngaruawahia	9c	Volcanic Soil	6	14.5505	185.5	44	14.558	103.272	39.24	64.032	225.485	1.28469	1.79129	969	2311	1.44	14.4	46.6
Ngaruawahia	9c	Volcanic Soil	6.2	16.4575	226.5	38.5	16.465	107.304	41.2	66.102	247.211	1.38321	1.78519	1112	2699	1.48	16.1	55.1

Table 6: CPT and DMT Data

				CPT DATA										DMT DATA				
Site	Pair No.	Soil Type	Depth (m)	q_c (MPa) (ave)	f_s (kPa) (ave)	u_2 (kPa) (ave)	q_t (ave)	σ_{vo} (kPa)	u_0 (kPa)	σ'_{vo} (kPa)	Q_t (ave)	F_r (Ave)	I_c (Ave)	p_o (kPa)	p_1 (kPa)	I_D	K_D	E_D (MPa)
Ngaruawahia	9c	Volcanic Soil	6.4	17.793	272.5	51	17.8064	111.385	43.16	68.221	259.117	1.53869	1.80294	1168	2480	1.17	16.4	45.5
Ngaruawahia	9c	Volcanic Soil	6.6	19.7625	316	52.5	19.7698	115.512	45.13	70.386	278.987	1.60754	1.79396	1134	2664	1.40	15.4	53.1
Ngaruawahia	9c	Volcanic Soil	6.8	19.7395	372.5	40	19.7428	119.688	47.09	72.6	270.12	1.89894	1.8557	1197	2776	1.37	15.8	54.8
Ngaruawahia	9c	Volcanic Soil	7	18.459	354	49	18.4728	123.877	49.05	74.827	245.062	1.92909	1.88217	1361	2956	1.22	17.5	55.3
Ngaruawahia	9c	Volcanic Soil	7.2	20.2985	383.5	56	20.3085	128.05	51.01	77.038	261.73	1.8996	1.85766	1429	3288	1.35	17.8	64.5
Ngaruawahia	9c	Volcanic Soil	7.4	19.876	407	57.5	19.8859	132.26	52.97	79.286	249.023	2.06065	1.89516	1563	3532	1.30	19.0	68.3
Ngaruawahia	9c	Volcanic Soil	7.6	18.771	272.5	27.5	18.7769	136.429	54.94	81.493	228.623	1.46025	1.79562	1654	3601	1.22	19.6	67.6
Ngaruawahia	9c	Volcanic Soil	7.8	18.927	257.5	-4.5	18.924	140.52	56.9	83.622	224.498	1.37114	1.78003	1723	3563	1.10	19.9	63.8
Ngaruawahia	9c	Volcanic Soil	8	19.4205	261.5	-17	19.4203	144.623	58.86	85.763	224.562	1.35838	1.77393	1779	3757	1.15	20.0	68.6
Ngaruawahia	9c	Volcanic Soil	8.2	21.021	310	-30	21.0146	148.744	60.82	87.922	237.149	1.4842	1.78489	1863	4369	1.39	20.5	87.0
Ngaruawahia	9c	Volcanic Soil	8.4	20.5515	375.5	-30	20.5431	152.927	62.78	90.143	226.129	1.84308	1.86859	331	1116	2.93	3.0	27.3
Ngaruawahia	9c	Volcanic Soil	8.6	18.2945	287.5	-25	18.2949	157.09	64.75	92.344	196.311	1.58543	1.85178	164	260	0.96	1.1	3.3
Ngaruawahia	9c	Volcanic Soil	8.8	19.4135	351	-30	19.4016	161.213	66.71	94.505	203.471	1.8254	1.88466	851	2391	1.96	8.4	53.5
Ngaruawahia	9c	Volcanic Soil	9	18.937	352.5	-43	18.9348	165.403	68.67	96.733	193.915	1.87934	1.90805	252	775	2.85	1.9	18.1
Ngaruawahia	9c	Volcanic Soil	9.2	19.8375	365.5	-57	19.825	169.578	70.63	98.946	198.537	1.8596	1.89633	187	336	1.28	1.2	5.2
Ngaruawahia	9c	Volcanic Soil	9.4	20.443	417.5	-54	20.4321	173.773	72.59	101.18	200.109	2.06054	1.92703	662	2259	2.71	6.0	55.4
Ngaruawahia	9c	Volcanic Soil	9.6	19.44	376.5	-45	19.4296	177.985	74.56	103.43	186.075	1.95509	1.92635	1851	4386	1.43	17.8	88.0
Ngaruawahia	9c	Volcanic Soil	9.8	18.6295	393	-31.5	18.6285	182.171	76.52	105.65	174.484	2.13235	1.97162	2125	4588	1.20	20.1	85.5
Ngaruawahia	9c	Volcanic Soil	10	20.0445	469	-26	20.0359	186.392	78.48	107.91	183.865	2.36196	1.99096	2274	5191	1.33	21.1	101.2
Ngaruawahia	9c	Volcanic Soil	10.2	19.5115	472.5	-20	19.5094	190.634	80.44	110.19	175.229	2.44589	2.01423	2135	4991	1.39	19.3	99.1
Ngaruawahia	9c	Volcanic Soil	10.4	19.6665	478.5	-12	19.6626	194.878	82.4	112.47	173.001	2.45711	2.01749	2622	6153	1.39	23.4	122.5
Ngaruawahia	9d	Volcanic Soil	0.4	3.458	56	-21.5	3.45041	7.0239	0	7.0239	487.433	1.65026	1.91195	155	479	2.10	22.7	11.3
Ngaruawahia	9d	Volcanic Soil	0.6	3.099	38.5	-4.5	3.09881	10.6103	0	10.61	293.359	1.25405	1.92648	175	441	1.51	17.0	9.2
Ngaruawahia	9d	Volcanic Soil	0.8	2.2215	37.5	-10	2.21843	14.1199	0	14.12	159.021	1.96955	2.15886	110	429	2.91	8.0	11.1
Ngaruawahia	9d	Volcanic Soil	1	1.182	26	6	1.18597	17.5427	0	17.543	65.7482	2.49074	2.40619	183	639	2.49	10.7	15.8
Ngaruawahia	9d	Volcanic Soil	1.2	1.379	29	26.5	1.38254	20.9292	0	20.929	65.7174	2.11888	2.38836	175	527	2.01	8.5	12.2
Ngaruawahia	9d	Volcanic Soil	1.4	1.214	15	42	1.22348	24.1463	0	24.146	49.315	1.22264	2.33053	155	1700	9.94	6.4	53.6
Ngaruawahia	9d	Volcanic Soil	1.6	1.9175	23	271.5	1.96712	27.4797	0	27.48	70.2505	1.19133	2.20723	454	1376	2.03	16.2	32.0
Ngaruawahia	9d	Volcanic Soil	1.8	2.079	20	820.5	2.2342	30.8382	0	30.838	71.1902	0.9132	2.13709	645	859	0.33	20.2	7.4
Ngaruawahia	9d	Volcanic Soil	2	1.6495	12.5	1082.5	1.85604	34.1443	0	34.144	53.3452	0.67719	2.15834	848	2270	1.68	23.9	49.3
Ngaruawahia	9d	Volcanic Soil	2.2	1.7235	10	1046.5	1.92221	37.3174	0	37.317	50.3665	0.53211	2.12725	819	2030	1.48	20.9	42.0
Ngaruawahia	9d	Volcanic Soil	2.4	1.8845	10	977.5	2.07015	40.5012	0	40.501	50.1051	0.49481	2.10831	568	904	0.59	13.2	11.7
Ngaruawahia	9d	Volcanic Soil	2.6	1.938	33	549	2.04181	43.8096	0	43.81	45.4861	1.64255	2.36976	469	1465	2.13	10.0	34.6
Ngaruawahia	9d	Volcanic Soil	2.8	1.8625	46.5	208.5	1.90258	47.2394	0	47.239	39.1318	2.43973	2.50246	545	1003	0.84	10.8	15.9
Ngaruawahia	9d	Volcanic Soil	3	2.3145	98.5	112	2.33599	50.8754	0	50.875	44.9871	4.34955	2.62529	630	1303	1.07	11.6	23.4
Ngaruawahia	9d	Volcanic Soil	3.2	2.9085	99.5	11.5	2.90851	54.6228	1.962	52.661	54.1868	3.54573	2.51226	624	1053	0.69	11.1	14.9
Ngaruawahia	9d	Volcanic Soil	3.4	2.406	74.5	10	2.4099	58.3411	3.924	54.417	43.2252	3.14698	2.54382	431	904	1.11	7.4	16.4
Ngaruawahia	9d	Volcanic Soil	3.6	1.884	58.5	22.5	1.88808	61.9436	5.886	56.058	32.5522	3.21297	2.63113	370	1027	1.81	6.2	22.8
Ngaruawahia	9d	Volcanic Soil	3.8	1.8335	60	41	1.84149	65.5198	7.848	57.672	30.7769	3.37958	2.66224	358	766	1.17	5.7	14.2
Ngaruawahia	9d	Volcanic Soil	4	1.7765	60	56.5	1.78757	69.105	9.81	59.295	28.9639	3.49287	2.6887	325	759	1.37	5.1	15.0
Ngaruawahia	9d	Volcanic Soil	4.2	1.9345	52.5	71	1.94766	72.6819	11.77	60.91	30.7652	2.81321	2.61072	326	751	1.35	4.9	14.8
Ngaruawahia	9d	Volcanic Soil	4.4	1.8385	50	83	1.85427	76.2283	13.73	62.494	28.4333	2.81228	2.63538	363	778	1.19	5.3	14.4
Ngaruawahia	9d	Volcanic Soil	4.6	1.945	44.5	75	1.95925	79.7716	15.7	64.076	29.3104	2.37979	2.57958	335	711	1.18	4.8	13.0
Ngaruawahia	9d	Volcanic Soil	4.8	2.2665	40	68	2.27959	83.2747	17.66	65.617	33.4413	1.83265	2.47217	395	860	1.23	5.5	16.1
Ngaruawahia	9d	Volcanic Soil	5	2.45	40	79	2.46518	86.7866	19.62	67.167	35.3749	1.6886	2.43183	327	646	1.04	4.4	11.1
Ngaruawahia	9d	Volcanic Soil	5.2	2.8865	31.5	85	2.90295	90.2832	21.58	68.701	40.9117	1.12149	2.28289	311	611	1.04	4.0	10.4
Ngaruawahia	9d	Volcanic Soil	5.4	3.213	40	85.5	3.22911	93.7854	23.54	70.241	44.6031	1.27709	2.28289	303	585	1.01	3.8	9.8
Ngaruawahia	9d	Volcanic Soil	5.6	3.5315	36	68	3.54409	97.3246	25.51	71.819	47.9577	1.05245	2.20762	341	664	1.03	4.2	11.2
Ngaruawahia	9d	Volcanic Soil	5.8	4.108	37.5	51.5	4.11779	100.831	27.47	73.363	54.7099	0.9318	2.13399	465	835	0.84	5.8	12.8
Ngaruawahia	9d	Volcanic Soil	6	4.988	54	60	5.00076	104.411	29.43	74.981	65.2128	1.10036	2.11445	393	792	1.10	4.7	13.8
Ngaruawahia	9d	Volcanic Soil	6.2	10.391	147.5	53	10.401	108.161	31.39	76.769	133.726	1.41452	1.95938	439	887	1.10	5.1	15.6
Ngaruawahia	9d	Volcanic Soil	6.4	14.0645	203	10	14.0614	112.165	33.35	78.811	176.919	1.45639	1.87289	435	897	1.15	5.0	16.0
Ngaruawahia	9d	Volcanic Soil	6.6	11.474	170	23.5	11.482	116.167	35.32	80.851	140.545	1.49658	1.94575	617	1053	0.75	7.1	15.1
Ngaruawahia	9d	Volcanic Soil	6.8	11.719	172.5	40	11.7287	120.127	37.28	82.849	139.986	1.48862	1.94251	422	863	1.15	4.6	15.3
Ngaruawahia	9d	Volcanic Soil	7	12.5155	205	41	12.5321	124.12	39.24	84.88	146.101	1.65497	1.95953	373	973	1.79	3.9	20.8
Ngaruawahia	9d	Volcanic Soil	7.2	15.4205	266	50	15.4178	128.166	41.2	86.964	175.648	1.73601	1.92043	498	1061	1.23	5.2	19.5
Ngaruawahia	9d	Volcanic Soil	7.4	16.9095	323	58.5	16.9296	132.287	43.16	89.123	188.275	1.92605	1.93366	407	973	1.56	4.1	19.6
Ngaruawahia	9d	Volcanic Soil	7.6	18.991	378.5	60	18.9944	136.457	45.13	91.331	206.443	2.01825	1.92052	578	1393	1.53	5.9	28.3
Ngaruawahia	9d	Volcanic Soil	7.8	16.7185	310	23	16.7224	140.624	47.09	93.536	177.218	1.87172	1.93514	678	1418	1.17	6.8	25.7
Ngaruawahia	9d	Volcanic Soil	8	15.9765	335	30	15.9839	144.759	49.05	95.709	165.4	2.11384	1.99234	424	1039	1.64	4.0	21.4
Ngaruawahia	9d	Volcanic Soil	8.2	16.668	350	36.5	16.6771	148.915	51.01	97.903	168.713	2.11849	1.98554	458	1000	1.33	4.3	18.8
Ngaruawahia	9d	Volcanic Soil	8.4	16.4245	337	43.5	16.4394	153.079	52.97	100.1	162.697	2.07702	1.98769	370	728	1.13	3.3	12.4
Ngaruawahia	9d	Volcanic Soil	8.6	17.9425	281.5	45.5	17.9503	157.195	54.94	102.26	173.806	1.58943	1.87713	637	1386	1.29	5.9	26.0
Ngaruawahia	9d	Volcanic Soil	8.8	24.2205	514.5	50	24.2248	161.383	56.9	104.49	230.138	2.13166	1.8975	895	2056	1.39	8.3	40.3
Ngaruawahia	9d	Volcanic Soil	9	23.142	652	56	23.1296	165.695	58.86	106.84	215.113	3.03107	2.03675	848	2301	1.84	7.7	50.4
Ngaruawahia	9d	Volcanic Soil	9.2	5.7005	316.5	45	5.73172	169.886	60.82	109.06	50.9662	6.30083	2.67982	1059	2380	1.32	9.6	45.8
Ngaruawahia	9d	Volcanic Soil	9.4	7.147	181.5	12	7.13764	173.892	62.78	111.11	62.7423	2.70259	2.3583	1365	3018	1.27	12.2	57.3
Ngaruawahia	9d	Volcanic Soil	9.6	1.54	49.5	-6	1.55153	177.633	64.75	112.89	12.1715	3.62398	2.93202	1366	3224	1.43	12.0	64.5
Ngaruawahia	9d	Volcanic Soil	9.8	1.9855	32	0.5	1.98143	180.998	66.71	114.29	15.7486	1.79279	2.69876	1655	3550	1.19	14.3	65.8
Ngaruawahia	9d	Volcanic Soil	10	2.271	107.5	10	2.27357	184.559	68.67	115.89	18.0065	5.06115	2.93083	1252	3321	1.75	10.5	71.8
Ngaruawahia	9d	Volcanic Soil	10.2	3.3285	190.5	10	3.33907	188.398	70.63	117.77	26.7534	6.29262	2.86397	1791	3925	1.24	14.9	74.0
Ngaruawahia	9d	Volcanic Soil	10.4	5.856	128	-26.5	5.83847	192.296	72.59	119.7	47.1234	2.49734	2.3789	1775	4097	1.36	14.5	80.6
Ngaruawahia	9d	Volcanic Soil	10.6	6.6635	90	-7	6.66517	196.078	74.56	121.52	53.1981	1.39647	2.19802	1762	3960	1.30	14.1	76.3
Ngaruawahia	9d	Volcanic Soil	10.8	6.563	97	-6	6.56706	199.855	76.52	123.34	51.6033	1.55352	2.23343	246	409	0.96	1.4	5.6
Ngaruawahia	9d	Volcanic Soil	11	9.243	97.5	-10	9.22427	203.651	78.48	125.17	72.0115	1.07506	2.01574	204	454	1.99	1.0	8.7
Ngaruawahia	9d	Volcanic Soil	11.2	11.1375	407.5	12	11.1641	207.587	80.44	127.14	85.9674	3.82068	2.36174	951	2983	2.33	7.0	70.5
Ngaruawahia	9d	Volcanic Soil	11.4	12.016	586	33	12.0159	211.864	82.4	129.46	91.398	6.25791	2.52325	1589	3686	1.39	11.9	72.8
Ngaruawahia	9d	Volcanic Soil	11.6	13.968	553	50.5	13.9911	216.057	84.37	131.69	104.362	4.5255	2.36101	2070	4623	1.29	15.4	88.6
Ngaruawahia	9d	Volcanic Soil	11.8	27.2085	634	44.5	27.1275	220.357	86.33	134.03	200.776	2.41371	1.95827	2446	5435	1.27	18.0	103.7
Ngaruawahia	9d	Volcanic Soil	12	5.1505	203.5	72.5	5.23267	224.54	88.29	136.25	36.8227	3.68654	2.62858	1673	4470	1.77	11.9	97.1
Ngaruawahia	9d	Volcanic Soil	12.2	3.501	88.5	123.5	3.53127	228.198	90.25	137.95	23.9129	2.55064	2.65114	2006	5033	1.58	14.1	105.0
Ngaruawahia	9d	Volcanic Soil	12.4	7.3005	333	127.5	7.31883	232.126	92.21	139.91	50.612	4.73564	2.57983	470	1110	1.70	2.7	22.2
Ngaruawahia	9d	Volcanic Soil	12.6	10.6035	227.5	50	10.6137	236.188	94.18	142.01	73.0143	2.25365	2.21744	202	328	1.17	0.8	4.4
Ngaruawahia	9d	Volcanic Soil	12.8	11.7875	218.5	-15	11.7842	240.217	96.14	144.08	80.1011	1.89153	2.13622	1399	3841	1.87	9.3	84.7
Ngaruawahia	9d	Volcanic Soil	13	11.3485	200	-38	11.3408	244.224	98.1	146.12	75.9153	1.80254	2.13768	1446	4164	2.02	9.4	94.3
Ngaruawahia	9d	Volcanic Soil	13.2	12.106	200	-42.5	12.0988	248.228	100.1	148.17	79.947	1.68869	2.09897	1596	3998	1.61	10.3	83.4
Ngaruawahia	9d	Volcanic Soil	13.4	13.051	216	-40	13.0506	252.242	102	150.22	85.1571	1.68605	2.07681	1752	4333	1.56	11.2	89.6
Ngaruawahia	9d	Volcanic Soil	13.6	14.0185	244.5	-29.5	14.0022	256.297	104	152.31	90.2545	1.8032	2.0776	1664	4373	1.74	10.5	94.0
Ngaruawahia	9d	Volcanic Soil	13.8	9.748	275.5	-28.5	9.73942	260.351	105.9	154.4	61.3731	2.94772	2.36028	1777	4396	1.57	11.0	90.9

Table 6: CPT and DMT Data

				CPT DATA										DMT DATA				
Site	Pair No.	Soil Type	Depth (m)	q_c (MPa) (ave)	f_s (kPa) (ave)	u_2 (kPa) (ave)	q_t (ave)	σ_{vo} (kPa)	u_0 (kPa)	σ'_{vo} (kPa)	Q_t (ave)	F_r (Ave)	I_c (Ave)	p_o (kPa)	p_1 (kPa)	I_D	K_D	E_D (MPa)
Ngaruawahia	9d	Volcanic Soil	14	8.2355	343	-19	8.23339	264.45	107.9	156.54	50.8992	4.32643	2.54597	2137	4684	1.26	13.2	88.4
Ngaruawahia	9d	Volcanic Soil	14.2	4.8735	105	-7	4.87634	268.433	109.9	158.56	29.0689	2.14358	2.48985	1993	5402	1.81	12.1	118.3
Ngaruawahia	9d	Volcanic Soil	14.4	6.546	178.5	1.5	6.57278	272.028	111.8	160.19	39.245	2.35466	2.46237	3122	6768	1.21	19.1	126.5
New Lynn	10a	Alluvium	1.4	1.47	630	140	1.4785	28.7476	0	28.748	50.4303	42.7659	3.35442	419	648	0.55	17.1	7.9
New Lynn	10a	Alluvium	1.6	1.41	600	170	1.38817	32.8342	0	32.834	41.278	42.7939	3.40128	331	491	0.48	11.8	5.5
New Lynn	10a	Alluvium	1.8	1.24	540	210	1.34403	36.8962	0.981	35.915	36.3951	40.2916	3.40969	288	403	0.40	9.4	4.0
New Lynn	10a	Alluvium	2	1.27	440	210	1.24673	40.9278	2.943	37.985	31.7444	39.2545	3.43399	270	374	0.39	8.4	3.6
New Lynn	10a	Alluvium	2.2	1.12	440	160	1.13627	44.923	4.905	40.018	27.2713	38.1792	3.46245	227	335	0.49	6.7	3.8
New Lynn	10a	Alluvium	2.4	0.92	370	150	0.9585	48.886	6.867	42.019	21.6477	42.1424	3.55653	257	327	0.28	7.2	2.4
New Lynn	10a	Alluvium	2.6	0.75	340	140	0.82993	52.8103	8.829	43.981	17.6694	43.7511	3.62298	292	361	0.24	7.9	2.4
New Lynn	10a	Alluvium	2.8	0.74	310	130	0.73803	56.6993	10.79	45.908	14.8412	44.5205	3.67585	293	362	0.25	7.6	2.4
New Lynn	10a	Alluvium	3	0.65	260	120	0.6974	60.5364	12.75	47.783	13.3281	38.7315	3.6586	292	354	0.22	7.3	2.1
New Lynn	10a	Alluvium	3.2	0.63	170	130	0.6447	64.3075	14.72	49.593	11.7032	32.7365	3.63985	280	347	0.25	6.7	2.3
New Lynn	10a	Alluvium	3.4	0.58	140	140	0.59327	67.9789	16.68	51.302	10.2392	24.1138	3.58079	288	363	0.27	6.7	2.6
New Lynn	10a	Alluvium	3.6	0.49	70	150	0.54517	71.5565	18.64	52.918	8.94997	18.2992	3.53606	274	339	0.26	6.1	2.3
New Lynn	10a	Alluvium	3.8	0.48	50	160	0.5131	75.0449	20.6	54.444	8.046	13.6969	3.4828	285	344	0.22	6.1	2.0
New Lynn	10a	Alluvium	4	0.48	60	160	0.53437	78.5363	22.56	55.973	8.1437	13.1628	3.46727	284	343	0.22	5.9	2.0
New Lynn	10a	Alluvium	4.2	0.55	70	170	0.55103	82.0544	24.53	57.529	8.15199	14.2153	3.48957	288	348	0.23	5.8	2.1
New Lynn	10a	Alluvium	4.4	0.53	70	160	0.585	85.6092	26.49	59.122	8.44675	15.352	3.50115	285	345	0.23	5.5	2.1
New Lynn	10a	Alluvium	4.6	0.58	90	170	0.5823	89.1315	28.45	60.683	8.12703	13.518	3.47574	296	345	0.18	5.6	1.7
New Lynn	10a	Alluvium	4.8	0.54	40	180	0.5842	92.572	30.41	62.161	7.90894	9.49227	3.38275	296	351	0.21	5.4	1.9
New Lynn	10a	Alluvium	5	0.53	10	190	0.57817	95.9763	32.37	63.603	7.58122	8.29548	3.35918	310	367	0.20	5.5	2.0
New Lynn	10a	Alluvium	5.2	0.56	70	180	0.58753	99.4001	34.34	65.065	7.50222	8.87736	3.38149	323	383	0.21	5.6	2.1
New Lynn	10a	Alluvium	5.4	0.57	50	170	0.62087	102.916	36.3	66.619	7.77488	12.2277	3.46073	350	451	0.32	6.0	3.5
New Lynn	10a	Alluvium	5.6	0.63	70	190	0.8634	106.597	38.26	68.338	11.0744	15.4157	3.41792	343	412	0.23	5.6	2.4
New Lynn	10a	Alluvium	5.8	1.28	230	220	0.99973	110.308	40.22	70.087	12.6903	14.2414	3.35175	391	503	0.32	6.3	3.9
New Lynn	10a	Alluvium	6	0.96	80	270	1.17177	114.032	42.18	71.849	14.7217	11.9753	3.25292	405	507	0.28	6.4	3.5
New Lynn	10a	Alluvium	6.2	1.11	70	380	1.41313	117.782	44.15	73.637	17.5912	10.2932	3.15176	367	495	0.40	5.5	4.4
New Lynn	10a	Alluvium	6.4	1.93	250	610	1.68133	121.653	46.11	75.546	20.6455	13.678	3.19306	386	552	0.49	5.7	5.8
New Lynn	10a	Alluvium	6.6	1.7	320	610	7.89233	125.969	48.07	77.9	99.6963	12.4898	2.74803	353	492	0.45	5.0	4.8
New Lynn	10a	Alluvium	6.8	19.8	2340	80	12.1462	130.286	50.03	80.255	149.723	14.5917	2.7164	375	678	0.94	5.2	10.5
New Lynn	10a	Alluvium	7	14.8	2600	40	12.3804	134.602	51.99	82.609	148.238	15.2161	2.73369	457	695	0.59	6.3	8.3
New Lynn	10a	Alluvium	7.2	2.49	650	150	6.33417	138.918	53.96	84.963	72.9167	18.2936	2.95716	553	893	0.68	7.6	11.8
New Lynn	10a	Alluvium	7.4	1.57	150	560	1.9598	142.911	55.92	86.994	20.8853	18.8968	3.29471	608	879	0.49	8.2	9.4
New Lynn	10a	Alluvium	7.6	1.58	230	550	1.63813	146.737	57.88	88.858	16.7841	11.8457	3.2095	671	1105	0.71	8.9	15.0
New Lynn	10a	Alluvium	7.8	1.43	150	650	1.70433	150.602	59.84	90.761	17.119	13.3013	3.23973	669	947	0.46	8.7	9.7
New Lynn	10a	Alluvium	8	1.78	240	500	1.9405	154.511	61.8	92.708	19.2647	13.4379	3.20779	659	910	0.42	8.3	8.7
New Lynn	10a	Alluvium	8.2	2.26	330	700	2.10507	158.454	63.77	94.689	20.5581	13.8702	3.19878	806	1170	0.49	10.1	12.6
New Lynn	10a	Alluvium	8.4	1.88	240	880	2.08107	162.395	65.73	96.668	19.848	14.0722	3.21371	811	1176	0.49	9.9	12.7
New Lynn	10a	Alluvium	8.6	1.67	240	700	1.77077	166.274	67.69	98.585	16.2752	13.5038	3.25965	899	1200	0.36	10.8	10.5
New Lynn	10a	Alluvium	8.8	1.35	170	590	1.62193	170.146	69.65	100.5	14.4464	14.9241	3.32685	903	1197	0.35	10.6	10.2
New Lynn	10a	Alluvium	9	1.5	240	530	1.53957	174.014	71.61	102.4	13.3353	15.8666	3.37013	904	1279	0.45	10.4	13.0
New Lynn	10a	Alluvium	9.2	1.44	240	610	1.544	177.882	73.58	104.31	13.097	15.86	3.37545	920	1240	0.38	10.3	11.1
New Lynn	10a	Alluvium	9.4	1.35	170	660	1.50493	181.714	75.54	106.18	12.4623	14.107	3.3544	980	1386	0.45	10.8	14.1
New Lynn	10a	Alluvium	9.6	1.36	150	650	1.51747	185.53	77.5	108.03	12.3292	13.0136	3.33307	845	1285	0.57	9.0	15.3
New Lynn	10a	Alluvium	9.8	1.47	200	650	1.60207	189.341	79.46	109.88	12.857	11.7975	3.29028	942	1374	0.50	9.9	15.0
New Lynn	10a	Alluvium	10	1.6	150	680	1.5589	193.297	81.42	111.87	12.2066	23.1888	3.51629	919	1383	0.55	9.4	16.1
New Lynn	10a	Alluvium	10.2	1.24	600	600	1.5505	197.25	83.39	113.87	11.8846	23.1541	3.52369	908	1460	0.67	9.1	19.2
New Lynn	10a	Alluvium	10.4	1.46	190	570	1.51827	201.214	85.35	115.87	11.3669	25.056	3.562	955	1350	0.45	9.4	13.7
New Lynn	10a	Alluvium	10.6	1.49	200	750	1.70917	205.03	87.31	117.72	12.7772	11.0806	3.27333	1006	1491	0.53	9.7	16.8
New Lynn	10a	Alluvium	10.8	1.75	110	930	1.9698	208.865	89.27	119.59	14.7242	9.84326	3.19328	1133	1548	0.40	10.8	14.4
New Lynn	10a	Alluvium	11	2.24	210	580	2.0363	212.68	91.23	121.45	15.0157	8.59097	3.1464	1303	1879	0.48	12.3	20.0
New Lynn	10a	Alluvium	11.2	1.68	150	800	1.96933	216.529	93.2	123.33	14.2119	10.4594	3.22265	1508	2133	0.44	14.2	21.7
New Lynn	10a	Alluvium	11.4	1.57	190	820	1.82627	220.35	95.16	125.19	12.8276	10.3783	3.25248	1491	1876	0.28	13.7	13.4
New Lynn	10a	Alluvium	11.6	1.75	160	900	2.00577	224.216	97.12	127.1	14.0173	11.0391	3.24326	1374	1671	0.23	12.3	10.3
New Lynn	10a	Alluvium	11.8	2.19	240	950	2.2283	228.179	99.08	129.1	15.493	14.4991	3.29675	1261	1854	0.51	11.0	20.6
New Lynn	10a	Alluvium	12	2.23	470	860	2.26627	232.152	101	131.11	15.5147	14.7484	3.30168	1266	1849	0.50	10.9	20.2
New Lynn	10a	Alluvium	12.2	1.9	190	710	2.2047	236.139	103	133.13	14.7863	16.4249	3.34997	1259	2049	0.68	10.6	27.4
New Lynn	10a	Alluvium	12.4	2.03	310	820	2.16677	240.121	105	135.15	14.2552	16.4362	3.36112	1198	1552	0.32	9.9	12.3
New Lynn	10a	Alluvium	12.6	2.12	450	840	2.3488	244.142	106.9	137.21	15.3386	17.4217	3.35777	1174	1721	0.51	9.5	19.0
New Lynn	10a	Alluvium	12.8	2.41	340	900	2.3326	248.144	108.9	139.25	14.9689	16.1513	3.34101	1112	1716	0.60	8.8	21.0
New Lynn	10a	Alluvium	13	1.97	220	880	2.21467	252.06	110.9	141.21	13.8988	12.0588	3.27277	1070	1583	0.54	8.2	17.8
New Lynn	10a	Alluvium	13.2	1.77	150	820	2.38737	255.982	112.8	143.17	14.8874	11.1039	3.22636	908	1437	0.67	6.7	18.4
New Lynn	10a	Alluvium	13.4	2.93	340	890	2.901	260.013	114.8	145.24	18.1841	13.5051	3.2265	873	1424	0.73	6.3	19.1
New Lynn	10a	Alluvium	13.6	3.49	580	990	3.65803	264.068	116.7	147.33	23.0366	10.8035	3.08552	914	1781	1.09	6.5	30.1
New Lynn	10a	Alluvium	13.8	4.1	180	510	4.95947	268.193	118.7	149.49	31.3815	9.52122	2.95436	1218	2474	1.14	8.9	43.6
New Lynn	10a	Alluvium	14	6.84	580	860	6.21963	272.411	120.7	151.75	39.1915	10.4811	2.92264	1092	1822	0.75	7.7	25.3
New Lynn	10a	Alluvium	14.2	7.09	1110	1940	7.58353	276.727	122.6	154.1	47.4153	14.1877	2.974	883	2171	1.70	6.0	44.7
New Lynn	10a	Alluvium	14.4	7.92	1420	1940	9.32273	281.044	124.6	156.46	57.7904	14.341	2.92675	1276	2921	1.43	8.9	57.1
New Lynn	10a	Alluvium	14.6	12.05	1360	900	10.3431	285.36	126.5	158.81	63.3315	19.4212	3.01246	1833	4568	1.60	13.0	94.9
New Lynn	10a	Alluvium	14.8	10.4	3080	630	11.0868	289.676	128.5	161.17	66.994	23.2161	3.06413	1696	4424	1.74	11.7	94.7
New Lynn	10a	Alluvium	15	10.96	2950	19400	13.2706	293.993	130.5	163.52	79.3578	23.0672	3.02292	2160	5135	1.47	14.9	103.2

APPENDIX E: RESULTS OF GRNN ANALYSIS

Table 7: Results of GRNN Analysis

		Inputs (Smooting factor adjustment)										Outputs					Correlations		Percentage within:				
Run	Description	qc (ave)	fs (ave)	u (ave)	qt (ave)	ó,v	u0	ó',vo	Qt (ave)	Fr (Ave)	Ic (Ave)	Po	P1	Id	Kd	Ed	Set	Corr. Coeff r	<5%	5%-10%	10%-20%	20%-30%	>30%
1	ALL DATA-ID	2.64706	1.11765	2.74118	0.94118	2.84706	3.00000	0.29412	1.49412	1.68235	0.37647			Output			Combined	0.7004	15.650	12.083	20.829	13.119	38.320
																	training	0.7260	16.236	12.644	21.983	12.644	36.494
																	test	0.5993	13.295	9.827	16.185	15.029	45.665
2	ALL DATA-KD	1.54118	2.14118	1.05882	0.69412	2.49412	2.58824	1.37647	1.65882	0.57647	1.17647				Output		Combined	0.9198	49.022	14.845	14.845	6.789	14.499
																	training	0.9552	58.046	14.943	13.075	5.029	8.908
																	test	0.8262	12.717	14.451	21.965	13.873	36.994
3	ALL DATA-ED	0.18824	1.58824	1.23529	0.15294	2.75294	2.72941	0.77647	1.07059	2.97647	1.50588					Output	Combined	0.9113	20.598	13.809	23.475	12.198	29.919
																	training	0.9460	23.132	14.799	23.851	11.782	26.437
																	test	0.7952	10.405	9.827	21.965	13.873	43.931
4	ALL DATA-P0	1.55294	2.41176	2.82353	0.02353	1.77647	2.98824	0.80000	2.81176	1.03529	1.87059	Output					Combined	0.9271	30.495	19.678	20.829	11.392	17.606
																	training	0.9487	34.195	19.684	20.690	10.201	15.230
																	test	0.8529	15.607	19.653	21.387	16.185	27.168
5	ALL DATA-P1	0.11765	2.01176	1.09412	0.00000	2.89412	2.97647	1.64706	2.23529	1.32941	2.45882		Output				Combined	0.9337	37.745	18.297	17.722	8.055	18.182
																	training	0.9597	43.103	19.253	16.523	6.466	14.655
																	test	0.8414	16.185	14.451	22.543	14.451	32.370
6	ALL DATA-P0	0.38824	1.96471	0.28235								Output					Combined	0.7522	8.055	7.940	18.642	14.960	50.403
7	ALL DATA-P1	0.37647	2.47059	0.36471									Output				Combined	0.8026	11.738	9.666	17.722	12.083	48.792
8	ALL DATA-ID	0.76471	0.75294	2.60000										Output			Combined	0.6924	15.190	11.623	18.987	13.003	41.197
9	ALL DATA-KD	2.64706	2.85882	0.90588											Output		Combined	0.7163	20.253	11.047	14.384	11.392	42.923
10	ALL DATA-ED	0.43529	1.72941	0.29412												Output	Combined	0.8231	12.313	8.400	12.888	13.234	53.165
11	ALL DATA-P0		2.92941	2.84706	1.14118	3.00000	1.58824					Output					Combined	0.9077	23.936	16.456	22.325	13.464	23.820
12	ALL DATA-P1		2.98824	1.74118	0.70588	2.84706	2.20000						Output				Combined	0.9126	23.705	14.730	21.174	13.003	27.388
13	ALL DATA-ID		1.44060	2.98824	1.52941	0.07059	0.68235							Output			Combined	0.7220	18.642	11.623	17.952	14.154	37.629
14	ALL DATA-KD		2.02353	2.23529	0.96471	2.82353	0.72941								Output		Combined	0.9068	55.351	11.277	11.277	7.135	14.960
15	ALL DATA-ED		2.85882	2.40000	1.55294	3.00000	2.47059									Output	Combined	0.9013	15.535	13.003	21.289	13.809	36.364
16	ALL DATA-P0								0.56471	2.76471	2.88235	Output					Combined	0.4460	5.178	5.639	12.428	11.853	64.902
17	ALL DATA-P1								2.08235	2.85882	3.00000		Output				Combined	0.6014	9.321	7.250	11.853	9.896	61.680
18	ALL DATA-ID								1.55294	1.68235	1.31765			Output			Combined	0.5170	8.516	8.400	16.110	13.003	53.970
19	ALL DATA-KD								2.83529	1.49412	1.17647				Output		Combined	0.8068	13.119	9.781	16.110	15.420	45.570
20	ALL DATA-ED								1.61176	1.54118	1.96471					Output	Combined	0.7107	7.480	7.250	12.428	10.357	62.486
21	ALL DATA-KD		2.01176			3.00000	1.75294								Output		Combined	0.8208	33.602	13.349	14.499	11.392	27.158
22	ALL DATA-KD		1.69412	2.05882		3.00000									Output		Combined	0.8688	36.249	13.579	15.880	9.781	24.511
23	ALL DATA-P0		2.10588	2.03529			2.95294		2.60000			Output					Combined	0.9126	21.519	15.765	21.519	14.730	26.467
24	ALL DATA-P1		2.01176			2.09412	2.90588		2.97647		1.76471		Output				Combined	0.9191	24.741	17.031	20.483	12.083	25.662
25	SELECT-P0	0.47059	2.41176	3.00000	0.78824	1.27059	2.37647	0.74118	2.96471	1.49412	2.51765	Output					Combined	0.9853	65.141	12.324	13.028	3.521	5.986
																	training	0.9952	73.684	11.842	9.211	2.632	2.632
																	test	0.9752	30.357	14.286	28.571	7.143	19.643
26	SELECT-P1	0.02353	1.52941	1.45882	0.68235	2.68235	2.18824	2.42353	0.52941	1.87059	0.16471		Output				Combined	0.9909	67.254	10.915	9.859	5.282	6.690
																	training	0.9945	78.070	9.649	7.456	3.070	1.754
																	test	0.9772	23.214	16.071	19.643	14.286	26.786
27	SELECT-ID	1.60000	1.40000	1.54118	0.22353	0.62354	2.84706	0.18824	0.71765	0.15294	2.48235			Output			Combined	0.9251	22.535	17.958	27.465	10.916	21.127
																	training	0.9328	22.807	20.175	26.754	11.404	18.860
																	test	0.8737	21.429	8.929	30.357	8.929	30.357
28	SELECT-KD	1.64706	1.72941	1.71765	0.32941	2.89412	2.36471	0.22353	1.68235	2.97647	0.81176				Output		Combined	0.9862	81.338	5.986	4.930	3.169	4.577
																	training	0.9996	95.614	2.632	0.877	0.000	0.877
																	test	0.9264	23.214	19.643	21.429	16.071	19.643
29	SELECT-ED	1.50588	1.70588	2.87059	0.18824	1.31765	1.67059	0.98824	2.17647	0.14118	1.02353					Output	Combined	0.9903	59.507	11.620	10.915	4.930	13.028
																	training	0.9976	71.491	10.965	8.333	3.947	5.263
																	test	0.9383	10.714	14.286	21.429	8.929	44.643
30	SELECT-P0	0.95294	0.45882	2.90588		0.50588	2.38824					Output					Combined	0.9906	79.225	8.099	8.099	2.817	1.761
																	training	0.9993	92.544	4.386	1.316	0.877	0.877
																	test	0.9867	25.000	23.214	35.714	10.714	5.357
31	SELECT-P1	1.34118	0.22353	2.94118		0.42353	0.63529						Output				Combined	0.8605	10.211	11.620	14.085	19.014	45.070
32	SELECT-ID	3.00000	1.60000	1.50588		2.68235	1.96471							Output			Combined	0.9288	21.479	21.479	22.887	10.563	23.592
33	SELECT-KD	0.09412	0.41176	1.07059		2.89412	1.48235								Output		Combined	0.9339	57.746	9.859	13.732	7.746	10.915
34	SELECTED	1.63529	0.34118	2.48235		0.05882	0.71765									Output	Combined	0.7814	6.338	8.099	19.366	13.380	52.817
35	SELECT-P0							0.72941	0.28235	3.00000	2.16471	Output					Combined	0.8859	78.873	7.042	5.282	3.873	4.930
																	training	0.9989	92.982	3.509	2.630	0.877	0.000
																	test	0.5993	21.429	21.429	16.071	16.071	25.000
36	SELECT-P1							0.67059	0.47059	2.22353	2.62353		Output				Combined	0.9937	80.986	3.873	6.690	2.465	5.986
																	training	0.9996	96.053	2.632	1.316	0.000	0.000
																	test	0.9703	19.643	8.929	28.571	12.500	30.357
37	SELECT-ID							0.08235	0.14118	0.10588	2.00000			Output			Combined	0.8855	15.141	13.732	23.592	14.789	32.746
38	SELECT-KD							0.50588	2.29412	0.74118	2.65882				Output		Combined	0.9410	42.958	13.732	20.423	10.915	11.972
39	SELECT-ED							0.81176	1.08235	2.97647	0.58824					Output	Combined	0.8172	10.211	7.042	19.718	11.620	51.408
40	SELECT-P0									2.02353	0.15294	Output					Combined	0.3739	5.282	5.282	15.141	16.197	58.099
41	SELECT-P0			2.92941						0.21176	0.25882	Output					Combined	0.8276	10.211	6.690	21.479	17.958	43.662
42	SELECT-P0			0.84706					3.00000	0.03529		Output					Combined	0.9235	10.915	13.380	18.310	15.845	41.549
43	SELECT-P0			0.48235					2.80000		0.10588	Output					Combined	0.9439	13.732	13.028	19.366	17.958	35.915
44	SELECT-P0			0.38824					2.67059			Output					Combined	0.9433	17.254	10.211	19.014	16.197	37.324
45	SELECT-P0								2.47059	2.17647	2.14118	Output					Combined	0.8395	39.437	11.620	14.789	10.563	23.592
46	SELECT-P0								2.67059		2.22353	Output					Combined	0.8293	35.563	10.915	15.141	13.732	24.648
47	SELECT-P0								0.30588	2.67059		Ouput					Combined	0.5507	7.746	7.042	16.197	14.085	54.930
48	SELECT-P0			0.50588			2.04706					Output					Combined	0.8912	11.972	11.972	17.606	15.493	42.958
49	SELECT-P0		0.37647	1.50588	0.14118							Output					Combined	0.9131	26.056	14.437	22.887	16.197	20.423
50	SELECT-P0			2.92941	1.02353							Output					Combined	0.8657	11.620	8.421	15.845	20.070	44.014
51	SELECT-P0	0.28235	0.96471	1.10588								Output					Combined	0.8797	11.268	13.732	19.014	16.197	39.789
52	SELECT-P0			2.95294	1.24706		3.00000					Output					Combined	0.9558	41.197	13.380	14.437	11.268	19.710
53	SELECT-P0		2.01176	2.03529								Output					Combined	0.9260	69.718	9.155	9.859	2.113	9.155
																	training	0.9460	23.132	14.799	23.851	11.782	26.437
																	test	0.7952	10.405	9.827	21.965	13.873	43.931
54	SELECT-P0		1.52941	1.52941			2.55294					Output					Combined	0.9727	58.099	7.394	14.437	9.507	10.563
																	training	0.9775	67.105	6.579	9.649	8.333	8.333
																	test	0.9735	21.429	10.714	33.929	14.286	19.643
55	SELECT-P0			0.38824					2.67059			Output					Combined	0.9433	17.254	10.211	19.014	16.197	37.324
56	SELECT-P0			1.98824							1.09412	Output					Combined	0.8576	11.268	12.324	15.845	12.324	48.239
57	SELECT-P0							2.67059		2.82353	1.02353	Output					Combined	0.8721	47.183	17.254	17.958	7.042	10.563
58	SELECT-P0			2.75294				0.36471		0.52941		Output					Combined	0.8568	22.535	14.085	21.831	13.028	28.521
59	SELECT-P1									2.97647	0.37647		Output				Combined	0.5291	7.746	5.986	13.380	15.845	57.042
60	SELECT-P1					2.34118	2.07059			2.15294			Output				Combined	0.9536	29.930	14.789	21.127	13.028	21.127
61	SELECT-P1									2.97647	0.37647		Output				Combined	0.5291	7.746	5.986	13.380	15.845	57.042
62	SELECT-P1								2.76471		2.35294		Output				Combined	0.9594	41.901	9.859	12.676	11.268	24.296
63	SELECT-P1							2.49412	2.62353		2.31765		Output				Combined	0.9910	66.197	8.803	12.676	4.577	7.746
																	training	0.9983	78.509	9.211	9.649	1.316	1.316
																	test	0.9615	16.071	7.143	25.000	17.857	33.929
64	SELECT-P1							2.75294		2.82353	0.64706		Output				Combined	0.9764	35.563	21.479	21.479	9.859	11.620
65	SELECT-P1				1.97647			1.97647			2.98824		Output				Combined	0.9926	81.338	3.521	5.634	2.113	7.394
																	training	0.9996	96.053	2.193	1.754	0.000	0.000
																	test	0.9648	21.429	8.929	21.429	10.714	37.500
66	SELECT-KD						1.51765				2.67059			Output			Combined	0.6757	12.676	11.268	20.423	14.085	41.549
67	SELECT-KD								2.72941		0.95294				Output		Combined	0.9204	37.324	13.732	19.014	10.915	19.014
																	training	0.9667	39.912	14.912	17.544	9.649	17.982
																	test	0.6351	26.786	8.929	25.000	16.071	23.214
68	SELECT-KD							0.64706	2.09412		2.21176				Output		Combined	0.9371	42.606	13.732	21.831	10.563	11.268
69	SELECT-KD					1.91765				2.24706					Output		Combined	0.7111	12.324	11.268	14.437	14.085	47.887
70	SELECT-KD							0.55294	0.81176		0.36471					Output	Combined	0.8299	9.859	8.803	20.423	11.972	48.944
																	training	0.8261	9.211	10.088	20.614	11.404	48.684
																	test	0.9356	12.500	3.571	19.643	14.286	50.000
71	SELECT-ED			1.48235					0.81176		2.35294					Output	Combined	0.9752	21.127	17.254	18.662	11.620	31.338
																	training	0.9824	23.246	19.298	18.421	13.596	25.439
																	test	0.9332	12.500	8.929	19.643	3.571	55.357
72	SELECT-ED								1.98824		2.70588					Output	Combined	0.9105	13.732	14.437	11.620	12.676	47.535
73	SELECT-ED							0.75294	0.87059	2.57647						Output	Combined	0.8228	9.859	8.099	17.958	14.789	49.296
74	SELECT-ED								2.62353	2.23529						Output	Combined	0.8486	12.324	7.746	12.324	11.268	56.338
75	SELECT-ED	0.61176	0.61176	1.75294			0.91765		2.45882							Output	Combined	0.8625	9.859	11.972	15.141	13.732	49.296
76	SELECT-ED				0.30588	0.17647					2.38824					Output	Combined	0.8957	9.507	8.451	16.901	18.310	46.831
53V	VALIDATE-P0											Output					Validation	0.3330	30.447	5.726	9.497	6.983	47.346
65V	VALIDATE-P1												Output				Validation	0.6829	33.644	4.654	9.574	5.053	47.074
67V	VALIDATE-KD														Output		Validation	0.6379	16.686	8.631	13.809	11.277	49.597
70V	VALIDATE-ED															Output	Validation	0.5909	5.639	6.789	14.614	10.012	62.946
27V	VALIDATE-ID													Output			Validation	0.5761	11.392	9.896	17.031	10.242	51.435
30V	VALIDATE-P0											Output					Validation	0.7313	40.193	6.270	10.129	9.968	33.441
36V	VALIDATE-P1												Output				Validation	0.6482	34.417	5.149	8.943	6.640	44.851
28V	VALIDATE-KD														Output		Validation	0.8377	42.024	6.003	6.346	5.832	39.794
29V	VALIDATE-ED															Output	Validation	0.4552	21.926	4.756	8.121	6.381	58.817

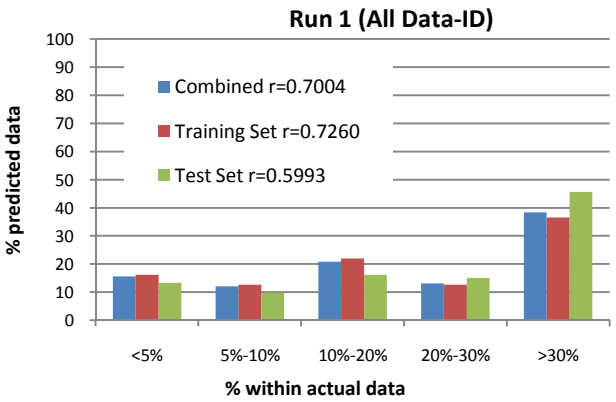
Run 1 (All Data-ID)
Combined r=0.7004
Training Set r=0.7260
Test Set r=0.5993
% predicted data
% within actual data
<5%
5%-10%
10%-20%
20%-30%
>30%


Run 2 (All Data-KD)
Combined r=0.9198
Training Set r=0.9552
Test Set r=0.8262
% predicted data
% within actual data
<5%
5%-10%
10%-20%
20%-30%
>30%

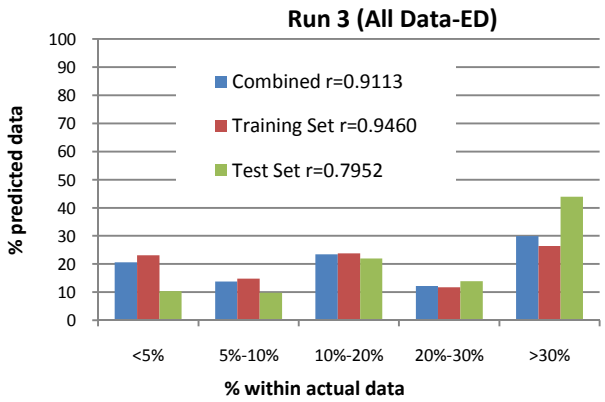
Run 3 (All Data-ED)
Combined r=0.9113
Training Set r=0.9460
Test Set r=0.7952
% predicted data
% within actual data
<5%
5%-10%
10%-20%
20%-30%
>30%

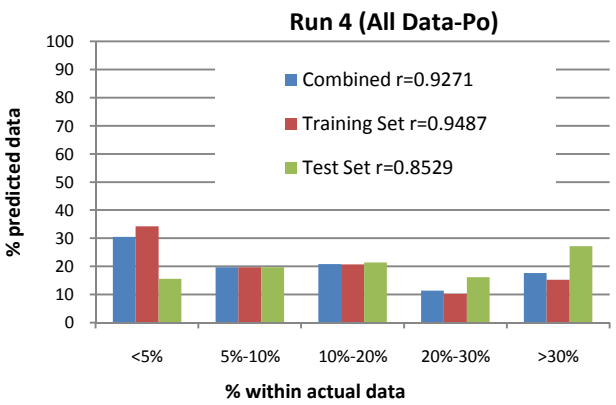
Run 4 (All Data-Po)
Combined r=0.9271
Training Set r=0.9487
Test Set r=0.8529
% predicted data
% within actual data
<5%
5%-10%
10%-20%
20%-30%
>30%

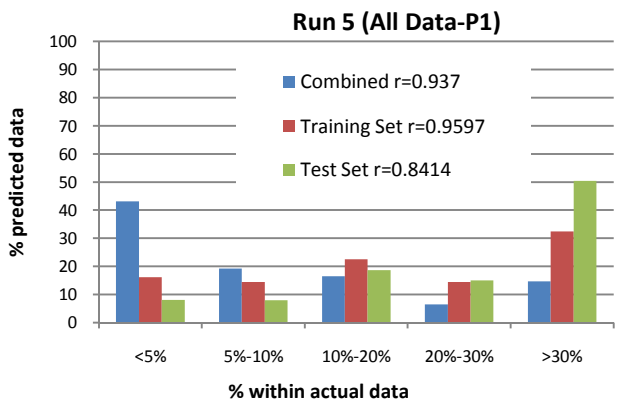
Run 5 (All Data-P1)
Combined r=0.937
Training Set r=0.9597
Test Set r=0.8414
% predicted data
% within actual data
<5%
5%-10%
10%-20%
20%-30%
>30%

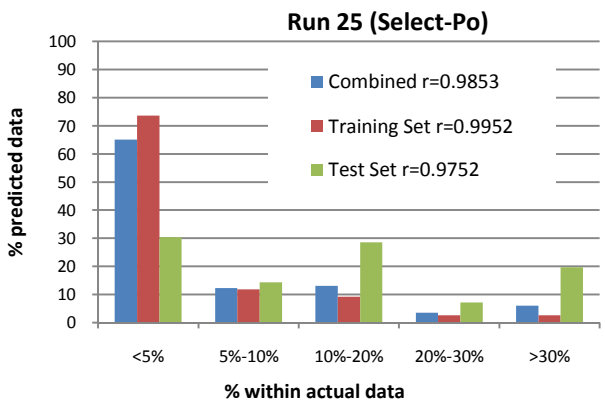
Run 25 (Select-Po)
Combined r=0.9853
Training Set r=0.9952
Test Set r=0.9752
% predicted data
% within actual data
<5%
5%-10%
10%-20%
20%-30%
>30%

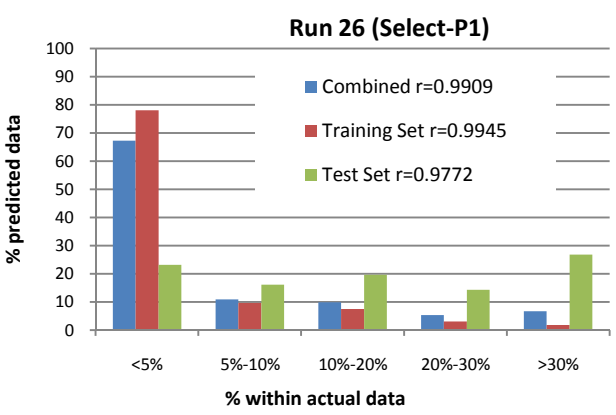
Run 26 (Select-P1)
Combined r=0.9909
Training Set r=0.9945
Test Set r=0.9772
% predicted data
% within actual data
<5%
5%-10%
10%-20%
20%-30%
>30%


Run 27 (Select-ID)
Combined r=0.9251
Training Set r=0.9328
Test Set r=0.8737
% predicted data
% within actual data
<5%
5%-10%
10%-20%
20%-30%
>30%

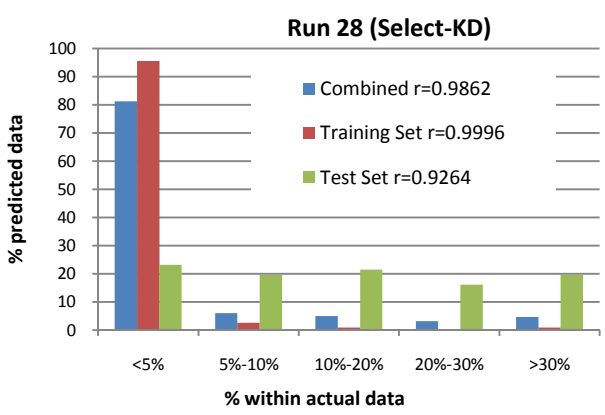
Run 28 (Select-KD)
Combined r=0.9862
Training Set r=0.9996
Test Set r=0.9264
% predicted data
% within actual data
<5%
5%-10%
10%-20%
20%-30%
>30%

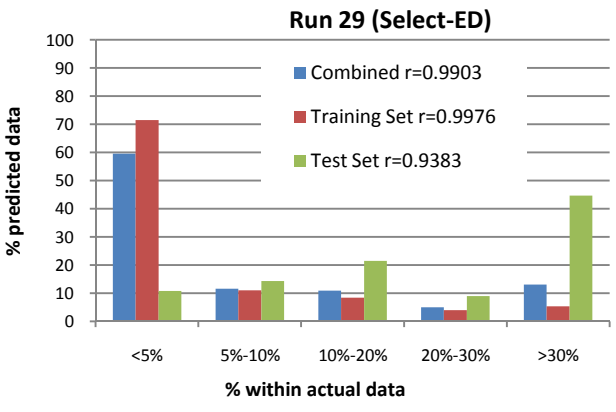
Run 29 (Select-ED)
Combined r=0.9903
Training Set r=0.9976
Test Set r=0.9383
% predicted data
% within actual data
<5%
5%-10%
10%-20%
20%-30%
>30%

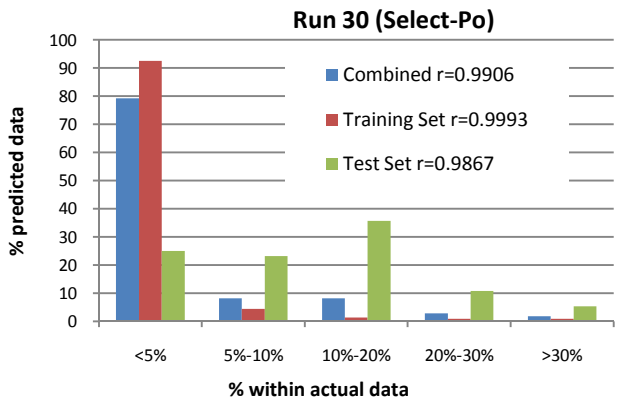
Run 30 (Select-Po)
Combined r=0.9906
Training Set r=0.9993
Test Set r=0.9867
% predicted data
% within actual data
<5%
5%-10%
10%-20%
20%-30%
>30%

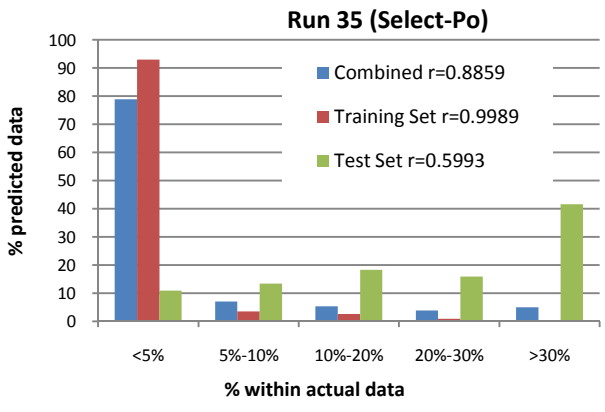
Run 35 (Select-Po)
Combined r=0.8859
Training Set r=0.9989
Test Set r=0.5993
% predicted data
% within actual data
<5%
5%-10%
10%-20%
20%-30%
>30%

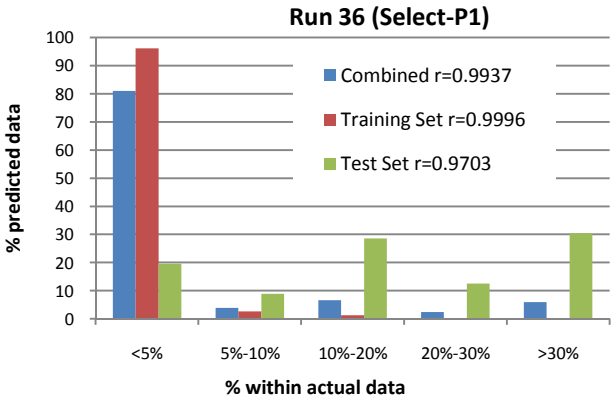
Run 36 (Select-P1)
Combined r=0.9937
Training Set r=0.9996
Test Set r=0.9703
% predicted data
% within actual data
<5%
5%-10%
10%-20%
20%-30%
>30%

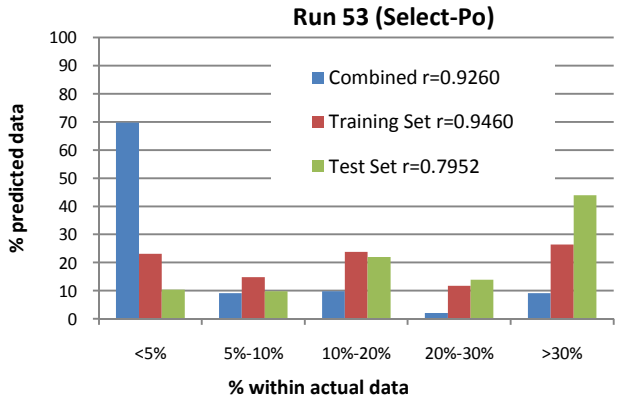
Run 53 (Select-Po)
Combined r=0.9260
Training Set r=0.9460
Test Set r=0.7952
% predicted data
% within actual data
<5%
5%-10%
10%-20%
20%-30%
>30%

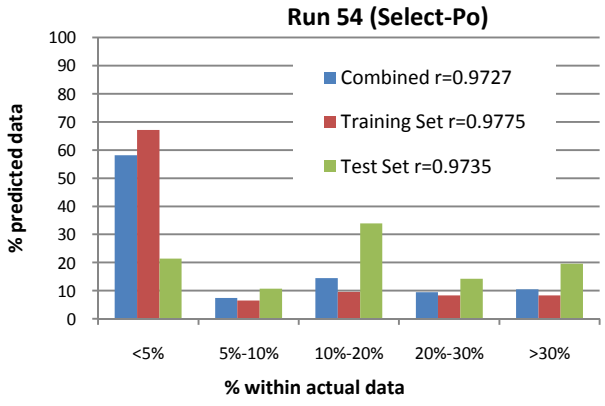
Run 54 (Select-Po)
Combined r=0.9727
Training Set r=0.9775
Test Set r=0.9735
% predicted data
% within actual data
<5%
5%-10%
10%-20%
20%-30%
>30%

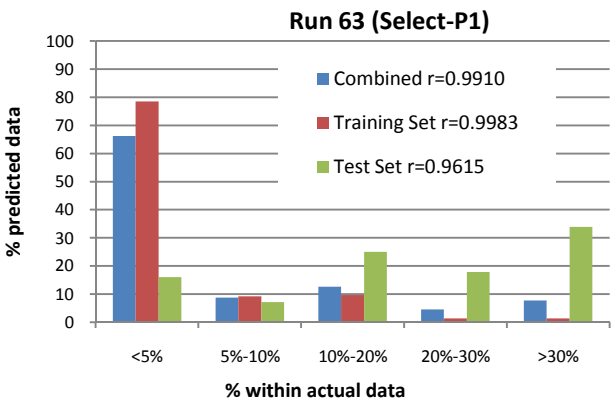
Run 63 (Select-P1)
Combined r=0.9910
Training Set r=0.9983
Test Set r=0.9615
% predicted data
% within actual data
<5%
5%-10%
10%-20%
20%-30%
>30%

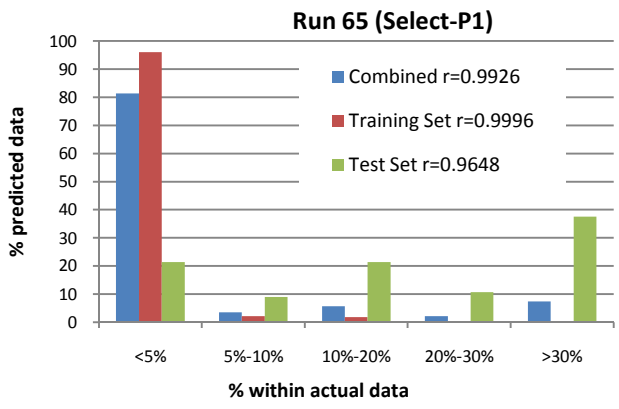
Run 65 (Select-P1)
Combined r=0.9926
Training Set r=0.9996
Test Set r=0.9648
% predicted data
% within actual data
<5%
5%-10%
10%-20%
20%-30%
>30%

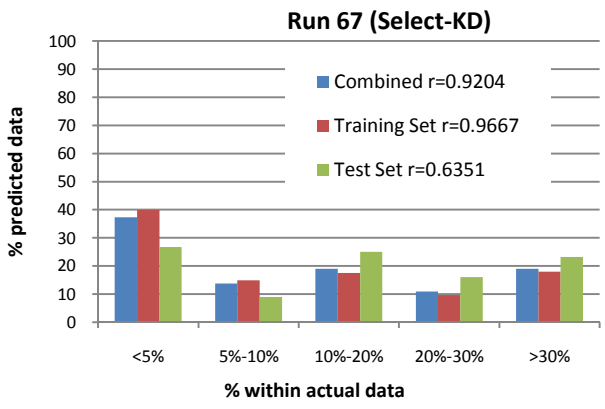
Run 67 (Select-KD)
Combined r=0.9204
Training Set r=0.9667
Test Set r=0.6351
% predicted data
% within actual data
<5%
5%-10%
10%-20%
20%-30%
>30%

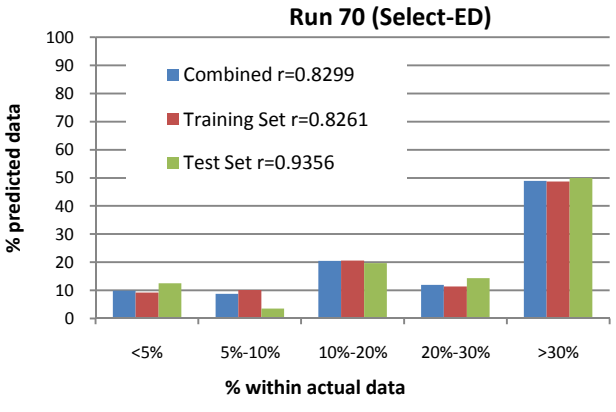
Run 70 (Select-ED)
Combined r=0.8299
Training Set r=0.8261
Test Set r=0.9356
% predicted data
% within actual data
<5%
5%-10%
10%-20%
20%-30%
>30%

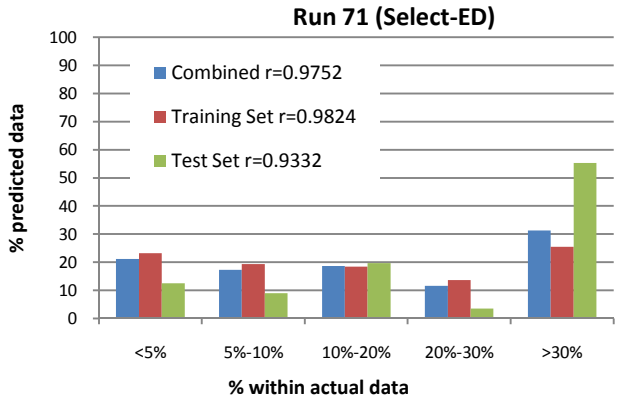
Run 71 (Select-ED)
Combined r=0.9752
Training Set r=0.9824
Test Set r=0.9332
% predicted data
% within actual data
<5%
5%-10%
10%-20%
20%-30%
>30%

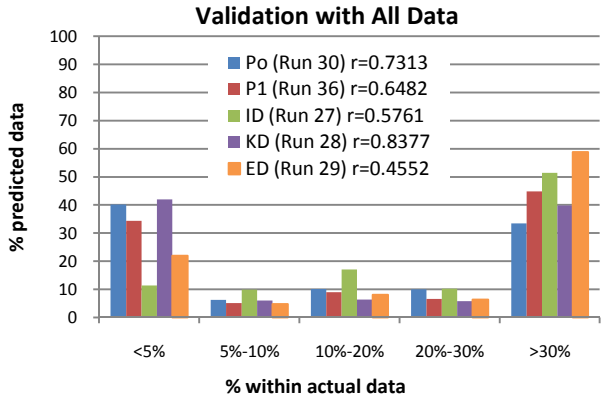
Validation with All Data
Po (Run 30) r=0.7313
P1 (Run 36) r=0.6482
ID (Run 27) r=0.5761
KD (Run 28) r=0.8377
ED (Run 29) r=0.4552
% predicted data
% within actual data
<5%
5%-10%
10%-20%
20%-30%
>30%

LIST OF REFERENCES

Aas, G., Lacasse, S., Lunne, T. & Hoeg, K. (1986) "Use of In-Situ Tests for Foundation Design on Clay", Use of In-Situ Tests in Geotechnical Engineering, GSP No. 6, ASCE, New York, p. 1-30

Abu-Kiefa, M.A. (1998) "General Regression Nerual Networks for Driven Piles in Cohesionless Soils" J. Geotech.& Geoenv. Eng. ASCE, 124(12), p. 1177-1185

Abuel-Naga, H.M (2001) "Calibration of Dynamic Cone Results in Cohensionless Soils usinf Articial Neural Network" MSC Thesis, Faculty of Eng, Cairo Unives.

Admadi, M.M. & Robertson, P.K. (2005) "Thin Layer Effects on the CPT qc measurement" Canadian Geotechnical Journal, 42(5): p. 1302-1317

AGI (1991) "Geotechnical Characterisation of Fucino Clay". Proc. 10th ECSMFE, Firenze, Vol. 1, p. 27-40

Anderson, J.B., Townsend, F.C. & Rahelison, L. (2007) "Load Testing and Settlement of Shallow Foundation", Jnl. Geotech. Geoenviron, Eng., 13(12), p. 1494-1502

Andrus, R.D. & Stokoe, K.H. (2000) "Liquefaction Resistance of Soils from Shear Wave Velocity", Jnl. GGE, ASCE, 126(11), p. 1015-1025

ASTM. (2007) "Standard Test Method for Permorming the Flat Dilatometer" ASTM Standard D6635-01, ASTM International, West Conshohocken, Pa.

ASTM. (2007) "Standard Test Method for Electronic Friction Cone and Piezocone Penetration Testing of Soils" ASTM Standard D5778-07. ASTM International, West Conshohocken, Pa.

Aversa, S (1997) "Experimental Aspects and Modelling in Design of Retaining Walls and Excavations"., Proc. 4th Nat. Conf. of the Geotechn. Ational Research Council Group, Perugia, Vol. II, p. 121-207

Aykin, K., Akcakal, O. & Dunrgunoglu, H.T. (2010) "Comparison of Soil Modelling Using CPT and DMT – a Case Study", Proc. 2nd Int. Conf. on Cone Penetration Testing, Huntington Beach, CA., Vol. 2, p. 487-494

Baldi, G., Bellotti, R., Ghionna, V., Jamiolkowski, M., Marchetti, S. & Pasqualini, E. (1986) "Flat Dilatometer Tests in Calibration Chambers", Use of In-Situ Tests in Geotechnical Engineering, GSP No. 6, ASCE, New Yor, p. 431-446

Baldi, G., Bellotti, R., Ghionna, V., Jamiolkowski, M. & LoPresti, D..F. (1989) "Modulus of sands from CPT's and DMT's". Proc. 12th Int. Conf. on Soil Mechanics and Foundation Engineering, Rio de Janeiro, Vol. 1, p. 1-6

Baligh, M.M.(1975) "Theory of Deep Site Static Cone Penetration Resistance", Research Report R 75-76, No. 517, Massachusetts Institute of Technology, Cambridge, Mass., USA

Baligh, M.M. & Scott, R.F. (1975) "Quasi Static Deep Penetration in Clays", *ASCE Jnl GE*, Vol. 101, No. GT11: 1119-1133

Baligh, M.M. (1985) "The strain path method," Journal of Geotechnical Engineering, ASCE, Vol. 111, pp. 1108-1136

Begemann, H.K.S. Ph. (1953) “Improved Method of Determining Reistance to Adhesion by Sounding through a Loose Sleeve placed behind he Cone”, Proc. 3rd Int. Conf. on Soil Mechanics and Foundation Engineering, Zurich, Vol. 1, p. 213-217

Bellotti, R., Ghionna, V., Jamiokowski, M., Lancellotta, R & Manfredini, G. (196) “Deformation Characteristics of Cohesionless Soils from In-Situ Tests”, Use of In-Situ Tests In Geotechnical Engineering, GSP No. 6, ASCE, New York, p. 47-73

Bellotti, R., Ghionna, V>, Jamiokowski, M. & Bobertson, P.K. (1989) “Design Parameters of Cohensionless Soils from In-Situ ests”, Transportation Research Record, 1235, Washington, D.C., p. 150-155

Bellotti, R., Fretti, C., Jamiokowski, M & Tanizawa, F. (1994) “Flat Dilatometer Tests in Toyoura Sand”, Proc. 13th Int. Conf. on Soil Mechanics and Foundation Engineering, New Delhi, Vol. 4, p. 1779-1782

Benoit, J. & Lutenegger, A.J. (1993) “Determining Lateral Stress in Soft Clays”, Predictive Soil Mechanics, Thomas Telford, London, p. 135-155

Bihs, A., Long, M., Marchetti, D. & Ward, D. (2010) “Interpretation of CPTU and SDMT in Organic, Irish Soils”, Proc. 2nd Int. Conf. on Cone Penetration Testing, Huntington Beach, CA., Vol. 2, p. 257-264

Blechman, D. & Feferbaum, S. (1997) “Flat Dilatometer Testing in Israel”, Proc. 14th Int. Conf. on Soil Mechanics and Foundation Engineering, New Delhi, Vol. 1, p. 581-584

Boghrat, A. (1987) “Dilatomeer Testing in Highly Overconsolidated Soils”, Journal of Geotechnical Engineering, Vol.113, No. 5, p. 516-517

Bogossian, F., Muxfeldt, A.S. and Dutra, A.M., (1989) “Some Results of Flat Dilatometer Tests in Brazilian Soils”, Proceedings, 12th International Conference on Soil Mechanics and Foundation Engineering, Rio de Janeiro, Vol. 1, p. 187-190.

Borden, R.H., (1991) “Boundary Displacement Induced by DMT Penetration”,. Calibration Chamber Testing, Elsevier, New York, p. 101-118.

Borden, R.H., Aziz, C.N., Lowder, W.M. and Khosla, N.P. (1985) “Evaluation of Pavement Subgrade Characteristics from the DMT”, Transportation Research Record, No. 1022, Washington, D.C., p. 120-127.

Borden, R.H., Raymond, E.S. and Lowder, W.M., (1986) “Compressibility of Compacted Fills Evaluated by the Dilatometer”, Transportation Research Record, No. 1089, Washington, D.C., p. 1-10.

Burghignoli, A., Cavalera, L., Chieppa, V., Jamiolkowski, M., Mancususo, C., Marchetti, S., Pane, V., Paoliani, P., Silvestri, F &Vittori, E. (1991) “Geotechnical Characterisation of Fucino Clay”, Proc. 10th ECSMFE, Florence, Vol. 1, p. 27-40

Campanella, R.G., Gillespie, D. & Robertson, P.K. (1982) “Pore Water Pressure during Cone Penetration Testing”, Proc. 2nd European Symposium on Penetration Testing, ESOPT-II, Amsterdam, p. 507-512

Campanella, R.G. & Robertson, P.K. (1983) “Flat Plate Dilatometer Testing; Research and Development at UBC”, Proc. First International Conference on the Flat Dilatometer, Edmonton, Mobile Augers, Inc., Alberta, p. 69-112.

Campanella, R., Robertson, P., Gillespie, D. and Grieg, J. (1985) “Recent Developments in In-Situ Testing of Soils”, Proceedings, 11th International Conference on Soil Mechanics and Foundation Engineering, Vol. 2, San Francisco, p. 849-854.

Campanella, R.G. and Robertson, P.K. (1991) “Use and Interpretation of a Research Dilatometer”, Canadian Geotechnical Journal, Vol. 28, No. 1, pp. 113-126.

Chan, A.C.Y. and Morgenstern, N.R. (1986) “Measurement of Lateral Stresses in a Lacustrine Clay Deposit” Proceedings, 39th Canadian Geotechnical Conference, Ottawa, pp. 285-290.

Chang, M.F. (1986) “The Flat Dilatometer Test and its Application to Two Singapore Clays”,. Proc. 4th Int. Geotechnical Seminar on Field Instrumentation and In-Situ Measurements, Singapore, p. 85-101.

Chang, M.F. (1987) “The Flat Dilatometer Test and its Role in Site Investigation”, Proceedings, 9th Southeast Asian Geotechnical Conference, Vol. 1, Bangkok, p.3-93 to 3-108.

Chang, M.F. (1991a). "Interpretation of Overconsolidation Ratio from In-Situ Tests in Recent Clay Deposits in Singapore and Malaysia," Canadian Geotechnical Journal, Vol. 28, No. 2, p. 210-225.

Chang, M.F. (1991b) “Flat Dilatometer Tests in Recent Clay Deposits of Singapore”, Proceedings, 8th Asian Regional Conference on Soil Mechanics and Foundation Engineering, Vol. 1, Bangkok, p. 23-28.

Chang, M.F., Choa, V., Cao, L.F., and Win, B.M. (1997) “Overconsolidation ratio of a seabed clay from in-situ tests”, Proceedings, 14th International Conference on Soil Mechanics and Foundation Engineering, Vol. 1, New Delhi, published by Balkema, Rotterdam & Oxford-IBH, India, 453-456.

Clarke, B.G., and Wroth, C.P., (1988). "Comparison Between Results from Flat Dilatometer and Self Boring Pressuremeter," Penetration Testing in the UK, Thomas Telford, London, p. 141-144.

Clough, G.W. and Goeke, P.M. (1986) “In Situ Testing for Lock and Dam 26 Cellular Cofferdam”,. Use of In Situ Tests for Geotechnical Engineering, (GSP 6), ASCE, New York, pp. 131-145.

Coutinho, R.Q. and Oliverira, J. (1997) “Geotechnical characterization of a Recife soft clay”, Proceedings, 14th International Conference on Soil Mechanics and Foundation Engineering, Vol. 1, New Delhi, published by Oxford-IBH, India, p 69-72.

Cruz, N., Viana de Fonseca, A., Coelho, P., and Lemos, J.L. (1997) “Evaluation of geotechnical parameters by DMT in Portuguese soils”, Proceedings, 14th International Conference on Soil Mechanics and Foundation Engineering, Vol. 1, New Delhi, published by Oxford-IBH, India, 77-80.

Davidson, J.L. and Boghrat, A., (1983) “Flat Dilatometer Testing in Florida, U.S.A”, Proceedings, Symposium International on In-Situ Testing, Vol. 2, Paris, France, p. 251-255.

de Ruiter, J. (1971) “Electric Penetrometer for Site Investigations”, Jnl. of the Soil Mechanics and Foundation Division, ASCE, 97, SM2, p. 457-472

Fabius, M., (1984) “Experience with the Dilatometer in Routine Geotechnical Design”, Proceedings, 37th Canadian Geotechnical Conference, Toronto, 10 pages.

Failmezger, R.A., Rom, D & Ziegler, S.B. (1999) “Behavioral Charactoristics of Residual Soils. SPT? – A Better Approach to Site Characterisation of Resdual Soils using other In-Situ Tests”, ASCE Geot, Special Pub. No. 92, Edelen, Bill, ed., ASCE, Reston, VA, p. 158-175

Finno, R. J. (1993) “Analytical Interpretation of Dilatometer Penetration through Saturated Cohesive Soils” Geotechnique 43, No. 2, p. 241-254

Gabr, M.A. and Borden, R.H., (1988) “Analysis of Load Deflection Response of Laterally Loaded Piers using Dilatometer Tests”, Penetration Testing 1988, (Proc., ISOPT-1, Orlando), Vol. 1, Balkema, Rotterdam, p. 513-520.

Gabr, M., Lunne, T., Mokkelbost, K.H. and Powell, J.J.M. (1991) “Dilatometer Soil Parameters for Analysis of Piles in Clay”, Proceedings, 10th European Conference on Soil Mechanics and Foundation Engineering, Vol. 1, Firenze, Italy, p. 403-406.

Greig, J.W., Campanella, R.G. and Robertson, P.K. (1988) “Comparison of Field Vane Results with other In Situ Test Results”,. Vane Shear Strength Testing in Soils: Field and Laboratory Studies, STP 1014, ASTM, Philadelphia, p. 247-263.

Goh, A.T.C. (1994) “Seismic Liquifaction Potential assessed by Neural Networks” J. Geotech. & Geoenv. Eng ASCE, 120(9), p.293-297

Goh, A.T.C. (1995) “Modelling Soil Correlations using Neural Networks” J. Computing in Civil Eng, ASCE 9(4), p.275-278

Goldberg, D.E. (1989) “Gnetic Algorithms in Search Optimization and Machine Learning”, Reading, MA, Addison-Wesley

Hamouche, K.K., Leroueil, S., Roy, M. and Lutenegger, A.J. (1995) “In-Situ Evaluation of Ko in Eastern Canada Clays”,. Canadian Geotechnical Journal, Vol. 32, No. 4, pp. 677-688.

Hepton, P. (1988) “Shear Wave Velocity Measurements during Penetration Testing”, Penetration Testing in the U.K., Thomas Telford, London, p. 275-278

Hryciw, R.D., (1990) “Small-Strain Shear Modulus of Soil by Dilatometer”, Journal of Geotechnical Engineering, Vol. 116, No. 11, p. 1700-1716.

Hryciw, R.D. and Woods, R.D., (1988) “DMT-Cross Hole Shear Correlations”,. Penetration Testing 1988, (Proc., ISOPT-1, Orlando), Vol. 1, Balkema, Rotterdam, p. 527-532.

Huang, A-B. and Haefele, K.C. (1990) “Lateral Earth Pressure Measurements in a Marine Clay”, Transportation Research Record 1278, National Academy Press, Washington, D.C., p. 156-163.

Hughes, J.M.O. & Robertson, P.K. (1985) “Full Displacement Pressuremeter Testingin Sand”, Canadian Geot. Jnl, Vol. 22, No.3, Aug., p. 298-307

Iwasaki, K., Tsuchiya, H., Sakai, Y. & Yamamoto, Y. (1991) “Applicability of the Marchetti Dilatometer Test to Soft Ground in Japan”, Geo-Coast ’91, Yokohama, Vol. 1, p. 29-32

ISSMFE (1989) Appendix A: “International Refernce Tst Procedure for Cone Penetration Test (CPT)”, Repoprt of the ISSMFE Technical Committee on Penetraion Testing of Soils – TC16, with Reference to Test Procedures, Swedish Geotechnical Institute, Linkoping, Information, 7, p. 6-16

Jamiolkowski, M., Ghionna, V.N., Lancellotta, R. and Pasqualini, E. (1988) “New Correlations of Penetration Tests for Design Practice”, Penetration Testing 1988, (Proc., ISOPT-1, Orlando), Vol. 1, Balkema, Rotterdam, p. 263-296.

Janbu, N. & Seneset, K. (1974) “Effective Stress Interpretation of In-Situ Static Penetration Testing”, Proc. of the European Symp. On Penetration Testing, ESOPT, Stockholm, Vol. 2.2, p. 181-193

Kalteziotis, N.A., Pachakis, M.D. and Zervogiannis, H.S. (1991) “Applications of the Flat Dilatometer Tests in Cohesive Soils”, Proceedings, 10th European Conference on Soil Mechanics and Foundation Engineering, Vol. 1, Firenze, p. 125-128.

Kamei, T. & Iwasaki, K. (1995) “Evaluation of Undrained Shear Strength of Cohesive Soils using a Flat Dilatometer”, Soils and Foundations, Vol. 35, No. 2, p. 111-116

Kates (Martin), G.L. (1996) “Development and implementation of a seismic flat dilatometer test for small- and high-strain soil properties”, MS Thesis, Civil & Environmental Engineering, Georgia Institute of Technology, Atlanta, 173 p.

Keaveny, J. and Mitchell, J.K. (1986) “Strength of Fine-Grained Soils Using the Piezocone”, Use of In-Situ Tests in Geotechnical Engineering (GSP 6), ASCE, New York, 668-685.

Kim Y.T. (1991) “Evaluation of Engineering Properties of Clays Through Flat Dilatometer Tests”, MS Thesis, Dept. of Civil Engineering, Korea Advanced Institute of Science and Technology, Korea. 56 p.

Kim, S.I., Jeong, S.S., and Lee, S.R. (1997) “Characterization of in-situ properties of Korean marine clays using CPTU and DMT”, Proceedings, 14th International Conference on Soil Mechanics and Foundation Engineering, Vol. 1, New Delhi, published by Oxford-IBH, India, 519-522.

Konrad, J.M. (1988) “Interpretation of Flat Plate Dilatometer tests in Sands in Terms of the State Parameter”, Geotechnique, Volume 38, No. 2, pp. 263-277.

Kulhawy, F.H. and Mayne, P.W. (1990) “Manual on Estimating Soil Properties for Foundation Design”, Report EL-6800, Electric Power Research Institute, Palo Alto, 306 p.

Lacasse, S (1986) “In Situ Site Investigation Techniques and Interpretation for Offshore Practice”, Norwegian Geotechnical Inst. Report 400, p. 19-28

Lacasse, S. and Lunne, T. (1983) “Dilatometer Tests in Soft Marine Clays”,. Report No. 146, Norwegian Geotechnical Institute, Oslo, p. 1-8.

Lacasse, S. and Lunne, T. (1986) “Dilatometer Tests in Sand,. Use of In-Situ Tests in Geotechnical Engineering”, (GSP 6), ASCE, New York, p. 686-699.

Lacasse, S. & Lunne, T. (1988) “Calibration of Dilatometer Correlations”, Penetration Testing 1988, (Proc. ISOPT-1, Orlando, USA), Vol. 1, Balkema, Rotterdam, p. 539-548

Ladd, C.C., Foot, R., Ishihara, K., Poulos, H.G. & Schlosser, F (1977) “Stress-Deformation and Strength Characteristics”, Proc. 9th Int. Conf. on Soil Mechanics and Foundation Engineering, Vol. 2, State-of-the-Art-Paper, Tokyo, Japan, p. 421-494

Larsson, R. and Eskilson, S., (1989) “Dilatometerforsok i organisk jord”, Swedish Geotechnical Institute Report No. 258, Linkoping, p. 1-78.

Lawter, R.S. and Borden, R.H., (1990) “Determination of Horizontal Stress in Normally Consolidated Sands Using the DMT”, Transportation Research Record, No. 1278, Washington, D.C., pp. 135-140.

Lehane, B., Xiangtao, X. & Fahey, M. (2004) “Relationship between Dilatomter Test Parameters and In-Situ Sand Stiffness”, Proc. 9tgh Ausralia New Zeland Conf. on Geomechanics, Auckland, p.832-839

Leonards, G.A. and Frost, J.D. (1988) “Settlement of Shallow Foundations on Granular Soils”, Journal of Geotechnical Engineering, Vol. 114, No. 7, p. 791-809.

Lunne, T., Christophersen, H.P. & Tjelta, T.I. (1985) “Engineering Use of Piezocone Data in North Sea Clays”, Proc. 11th Int. Conf. on Soil Mechanics and Foundation Engineering, San Francisco, Vol. 2, p. 907-912

Lunne, T., Powell, M., Hauge, E.A., Mokkelbost, K.H. and Uglow, I.M. (1990) "Correlation for Dilatometer Readings with Lateral Stress in Clays", Transportation Research Record, No. 1278, Washington, D.C., pp. 183-193.

Lunne. T., Lacasse, S. And Rad, N.S. (1992) "General Report: SPT, CPT, Pressuremeter Testing and Recent Developments in In-Situ Testing", Proc. 12th Int. Conf. on Soil Mechanics and Foundation Engineering, Rio de Janeiro, Vol. 4, p. 2339-2403

Lunne, T., Robertson, P.K. & Powell, J.J.M. (1997) "Cone Penetration Testing in Geotechnical Practice", Routledge, New York

Lutenegger, A.J., (1988). "Current Status of the Marchetti Dilatometer Test," Penetration Testing 1988, (Proc., ISOPT 1, Orlando), Vol. 1, Balkema, Rotterdam, pp. 137-155.

Lutenegger, A.J., (1990). .Determination of In-Situ Lateral Stresses in a Dense Glacial Till, Transportation Research Record, No. 1278, National Academy Press, Washington, D.C., pp. 194-182.

Lutenegger, A.J. and Timian, D.A. (1986) "Flat-Plate Penetrometer Tests in Marine Clays", Proceedings, 39th Canadian Geotechnical Conference, Ottawa, p. 301-309.

Lutenegger, A.J. and Kabir, M.G. (1988) "Dilatometer C-Reading to Help Determine Stratigraphy", Penetration Testing 1988, (Proc., ISOPT-1, Orlando), Vol. 1, Balkema, Rotterdam, p. 549-554.

Marchetti, S. (1975) "A new In Situ Test for the Measurement of Horizontal Soil Deformability", Proc. Conf. On "In Situ Measurement of Soil Properties", ASCE, Spec. Conf., Raleigh. 2. 255-259

Marchetti, S. (1979) "The In-Situ Determination of an "Extended" Overconsolidation Ratio", Proc. 7th European Conf. on Soil Mechanics and Foundation Engineering, Brighton, England, Vol. 2, p. 239-244

Marchetti, S. (1980) "In Situ Tests by Flat Dilatometer". Journal of the Geotechn. Engineering Division, ASCE, Vol. 106, No. GT3, Proc. Paper 15290, p. 299-321

Marchetti, S & Crapps, D.K. (1981) "Flat Dilatometer Manual" Internal Report of G.P.E. Inc.

Marchetti, S., (1982) "Detection of Liquefiable Sand Layers by means of Quasi-Static Penetration Tests", Proceedings, 2nd European Symposium on Penetration Testing, Amsterdam, Vol. 2, Balkema, Rotterdam, p. 689-695.

Marchetti, S., (1985) "On the Field Determination of K_0 in Sand", Proceedings, 11th International Conference on Soil Mechanics and Foundation Engineering, San Francisco, Vol. 5, p. 2667-2672.

Marchetti , S., Totani, G. and Campanella, R.G. (1986) "DMT -σ_{hc} Method for Piles Driven in Clay", Use of In Situ Tests in Geotechnical Engineering, (GSP 6), ASCE, New York, p. 765-779.

Marchetti, S. and Totani, G. (1989) "c_h Evaluations from DMTA Dissipation Curves", Proceedings, 12th International Conf. on Soil Mechanics and Foundation Engineering, Vol. 1, Rio de Janeiro, p. 281-286.

Marchetti, S., Totani, G., Calabrese, M. and Monaco, P. (1991). "p-y Curves from DMT Data for Piles Driven in Clay", Proceedings, 4th International Conference for Deep Foundation Institute, Vol. 1, Balkema, Rotterdam, pp. 263-272.

Marchetti, S., Totani, G. and Calabrese, M., (1993). Internal report, Istituo di Idraulica, Facolta di Ingegneria, L.Aquila, Italy, 10 pages..

Marchetti, S. (1997) "The Flat Dilatometer: Design Applications", Proc. 3rd Int. Geotech. Eng. Conf., Keynote Lecture, Cairo University, p. 421-448

Marchetti, S., Monaco, P., Totani, G. & Marchetti, D. (2008) "In-Situ Tests by Seismic Dilatometer (SDMT)", ASCE Geotechnical Special Publication Honouring Dr. John H. Schmertmann, From Research to Practice in Geotechnical Engineering, GSP, No. 170, Geo-Institute Meeting, New Orleans, March 9-12, 2008

Marchetti, S., Monaco, P., Calabrese, M. & Totani, G. (2006) "Comparison of Moduli Determined by DMT and Backfigured from Local Strain Measurements under a 40m Diamater Test Load in Venice Area", Proc. 2nd Int. Conf. on the Flat Dilatometer, Washington D.C., Insitu Soil, Virginia, p. 220-231

Marchetti, S. (2010) "Sensitivity of CPT and DMT to Stress History and Aging in Sands for Liquifaction Assessment", Proc. 2nd Int. Conf. on Cone Penetration Testing, Huntington Beach, CA., Vol. 3, p. 395-403

Martin, G.K. & Mayne, P.W. (1997) "Seismic Flat Dilatometer Tests in Connecticut Valley Varved Clay", ASTM Geotech. Testing J., 20(3), p. 357-361

Martin, G.K. & Mayne, P.W. (1998) "Seismic Flat Dilatometer in Piedmont Residual Soils" Proc. 1st Int. Conf. On Site Characterization ISC'98, Atlanta, 2, p. 837-843

Masood, T. and Kibria, M. (1994) "Estimation of In-Situ Lateral Stresses by Full Displacement Methods", Proceedings, 13th International Conference on Soil Mechanics and Foundation Engineering, Vol. 2, New Delhi, p. 689-694.

Mayne, P.W. (1987) "Determining Preconsolidation Stress and Penetration Pore Pressures from DMT Contact Pressures", Geotechnical Testing Journal, Vol. 10, No. 3, p. 146-150.

Mayne, P.W. and Frost, D.D. (1988) "Dilatometer Experience in Washington, D.C., and Vicinity", Transportation Research Record, No. 1169, National Academy Press, Washington, D.C., p. 16-23.

Mayne, P.W. and Stewart, H.E. (1988) "Pore Pressure Behavior of Ko-Consolidated Clays", Journal of Geotechnical Engineering 114 (11), p. 1340-1346.

Mayne, P.W. and Bachus, R.C. (1989) "Penetration Pore Pressure in Clay by CPTU, DMT, and SBP", Proceedings, 12th International Conference on Soil Mechanics and Foundation Engineering, Vol. 1, Rio de Janeiro, p.291-294.

Mayne, P.W. and Kulhawy, F.H. (1990) "Direct and Indirect Determinations of In-Situ Ko in Clays", Transportation Research Record, No. 1278, National Academy Press, Washington, D.C., p. 141-149.

Mayne, P.W. (1995) "Profiling Yield Stresses in Clays by In Situ Tests", Transportation Research Record, No. 1479, National Academy Press, Washington, D.C., p. 43-50.

Mayne, P.W. & Martin, G.K. (1998) "Commentary on Marchetti Flat Dilatometer Correlations in Soils", ASTM Geotechnical Journal, Vol.21, No. 3, p. 222-239

Mayne, P.W. (2001) "Stress-Strain-Strength-Floe Parameters from Enhanced In-Situ Tests", Proc. Int. Conf. on In-Situ Measurement of Soil Properties and Case Histories, Bali, p. 27-47

Mayne, P.W. & Liao, T. (2004) "CPT-DMT Interrealtionships in Piedmont Residuum", Proc. 2nd Int. Conf. on Geophysical and Geotechnical Site Characterization, ISC-2, Porto, p. 345-350

Mayne, P.W. (2006) "Interrelationships of DMT and CPT readings inSoft Clays", Proc. 2nd Int. Conf. on the Flat Dilatometer, Washington D.C. p. 231-236

Mayne, P.W. & McGillivray (2008) "Improved Shear Wave Measurements using Autoseis Sources" Deformational Characteristics of Geomaterials, Vol. 2 (Proc. 4th ISDCG, Atlanta), Millpress/IOS Press, Amsterdam: 853-860.

Mayne, P.W., Scheider, J.A. and Martin, G.K. (1999) "Small and Large Strain Soil Properties from Seismic Flat Dilatometer Tests", Proc. 2nd Int. Symp. On Pre-failure Deformation Characteristics of Geomaterials, Torino, 1, p. 419-427

McNulty, G. & Harney, M.D. (2010) "Comparison of CPT- and DMT- Correlted Effective Friction Angle in Clayey and Silty Sands", Proc. 2nd Int. Conf. on Cone Penetration Testing, Huntington Beach, CA., Vol. 2, p. 551-558

McGillivray, A. & Mayne, P.W. (2004) "Seismic Piezocone and Seismic Flat Dilatometer Tests at Treporti", Proc. 4th Int. Conf. on Site Characterisation ISC'2, Porto, Vol. 2, p. 1695-1700

Mello Vieira, M.V.C., Danziger, F., Almeida, M., and Lopes, P. (1997) "Dilatometer tests at Sarapui soft clay site," Proceedings, 14th International Conference on Soil Mechanics and Foundation Engineering, Vol. 1, New Delhi, published by Oxford-IBH, India, 161-162

Meng, J., Hajduk, E.L., Casey, T.J. & Wright, W.B. (2006) "Observations from IN-Situ Testing within a Clacareous Soil", Proc. 2nd Int. Conf. on the Flat Dilatometer, Washington D.C. In-Situ Soil, Virginia, p. 237-243

Meigh, A.C. (1987) "Cone Penetration Testing: Methods and Interpretation" CIRIA, Butterworths

Mlynarek, Z., Gogolik, S. & Marchetti, D (2006) "Suitability of the sDMT Method to Assess Geotechnical Parameters of Post-Flotation Sediments", Proc. 2nd Int. Conf. on the Flat Dilatometer, Washington D.C., p. 148-153

Mlynarek, Z., Wierzbicki, K. & Stefaniak, K. (2010) "CPTU, DMT, SDMT Results for Organic and Fluvial Soils", Proc. 2nd Int. Conf. on Cone Penetration Testing, Huntington Beach, CA., Vol. 2, p. 455-462

Monaco, P., Marchetti, S., Totani, G & Calabrese, M (2005) "Sand Liquefiability Assessment by Flat Dilatometer Test (DMT)", Proc. XVI ICSMGE, Osaka, Vol. 4, p. 2693-2697

Monaco, P., Marchetti, S & Totani, G. (2007) "The Flat Dilatometer Test (DMT): Design Applications and Recent Developments" Proc. 10th Australia New Zealand Conf. On Geomechanics, Brisbane, p. 516-521

Motan, E.S. and Gabr, M.A. (1984) "A Flat-Dilatometer Study of Lateral Soil Response", Analysis and Design of Pile Foundations, ASCE, New York, p. 232-248.

Motan, E.S. and Khan, A.Q. (1988) "In-Situ Shear Modulus of Sands by a Flat-Plate Penetrometer: A Laboratory Study", Geotechnical Testing Journal, Vol. 11, No. 4, p. 257-262.

Nash, D.F.Y., Powell, J.J.M. & Lloyd, I.M. (1992) "Initial Investigations of the Soft Clay Test Site at Bothkennar", Geotechnique, 42, No. 2, p. 163-181

Penna, A. (2006) "Some Recent Experience Obtained with DMT in Brazilian Soils", Porc. 2nd Int. Conf. on the Flat Dilatomete, Washington, D.C., In-Situ Soil, Virginia, p. 170-177

Pool, R.G. (1994) "Rational Framework for Interpreting Overconsolidation Ratio, Undrained Strength Ratio, and Lateral Stress Coefficient from Flat Dilatometer Tests in Clay", MS Thesis, School of Civil and Environmental Engineering, Georgia Institute of Technology, Atlanta, Georgia, 262 p.

Powell, J.J.M. and Uglow, I.M. (1986) "Dilatometer Testing in Stiff Overconsolidated Clays", Proceedings, 39th Canadian Geotechnical Conference, Ottawa, p. 317-326.

Powell, J.J.M. and Uglow, I.M. (1988a) "Marchetti Dilatometer Testing in U.K. Soils", Penetration Testing 1988 (Proc., ISOPT-1, Orlando), Vol. 1, Balkema, Rotterdam, 555-562.

Powell, J.J.M. & Uglow, I.M. (1988) "The Interpretation of the Marchetti Dilatometer Test in UK Soils" Proc. Inst. Civil Engineers, Penetration Testing in the UK, Univ. of Birmingham, Paper 34, p. 269-273

Rankka, K. (1990) "Measuring & Predicting Lateral Earth Pressures in Slopes in Soft Clays in Sweden", Transportation Research Record, No. 1278, National Academy Press, Washington, D.C., p. 172-181.

Reyna, F. and Chameau, J.L. (1991) "Dilatometer Based Liquefaction Potential of Sites in the Imperial Valley", Proceedings, Second Intl. Conference on Recent Advances in Geotechnical Earthquake Engineering and Soil Dynamics, St. Louis, Vol. 1, p. 385-392.

Robertson, P.K. and Campanella, R.G., (1986) "Estimating Liquefaction Potential of Sands Using the Flat Plate Dilatometer", Geotechnical Testing Journal, Vol. 9, No. 1, p. 38-40

Robertson, P.K., Campanella, R.G., Gillespie, D. and Greig, J. (1986) "Use of piezometer cone data", Use of In-Situ Tests in Geotechnical Engineering (GSP 6), ASCE, Reston, VA: p. 1263-1280

Robertson, P.K., Campanella, R.G., Gillespie, D. and By, T. (1988) "Excess Pore Pressure and the Flat Dilatometer Test", Penetration Testing 1988, (Proc., ISOPT-1, Orlando), Vol. 1, Balkema, Rotterdam, p. 567-576

Robertson, P.K., Davies, M.P. and Campanella, R.G. (1989) "Design of Laterally Loaded Driven Piles using the Flat Dilatometer", Geotechnical Testing Journal, Vol. 12, No. 1, p. 30-38

Robertson, P.K. (1990) "Soil Classification using the Cone Penetration Test", Can. Geotech. Jnl., 27(1), p. 151-158

Robertson, P.K. (2009a) "Interpretation of cone penetration tests – a unified approach". Canadian Geotechnical Journal, 2009, 46: p. 1337-1355

Robertson, P.K. (2009b) "CPT-DMT Correlations", Jnl. Of Geotechnical and Geoenvironmental Engineering, ASCE, Vol. 135, No. 11

Robertson, P.K. & Cabal, K.L. (2010) "Guide to Penetration Testing for Geotechnical Engineering", Gregg Drilling & Testing Inc., 4th Ed., July 2010

Roque, R., Janbu, N. and Senneset, K. (1988) "Basic Interpretation Procedures of Flat Dilatometer Tests", Penetration Testing 1988, (Proc., ISOPT-1, Orlando), Vol. 1, Balkema, Rotterdam, p. 577-587.

Sanglerat, G (1972) "The Penetrometer and Soil Exploration", Elsevier, Amsterdam, 464 p.

Saye, S.R. and Lutenegger, A.J. (1988) "Site Assessment and Settlement Evaluation of Firm Alluvial Silts and Clays with the Marchetti Flat Dilatometer", Penetration Testing 1988, (Proc., ISOPT-1, Orlando), Vol. 1, Balkema, Rotterdam, p. 589-596.

Schmertmann, J.H. (1981). "Discussion, .In Situ Test by Flat Dilatometer", Journal of Geotechnical Engineering, ASCE, Vol. 107, No. 6, p. 831-832.

Schmertmann, J.H. (1982) "A Method for Determining the Friction Angle in Sands from the Marchetti Dilatometer Test (DMT)", Proceedings, 2nd European Symposium on Penetration Testing, Vol. 2, Amsterdam, p. 853-861.

Schmertmann, J.H. (1983) "Revised Procedure for Calculating Ko and OCR from DMTs with I_D<1.2 and which Incorporate the Penetration Force Measurement to Permit Calculating the

Plane Strain Friction Angle", DMT-Workshop, Gainesville, GPE, Inc., 4509 NW 23rd Avenue, Suite 19, Gainesville, FL 32601.

Schmertmann, J.H. (1986a) "Suggested Method for Performing the Flat Dilatometer Test", Geotechnical Testing Journal, Vol. 9, No. 2, p. 93-101.

Schmertmann, J.H. (1986b) "Dilatometer to Compute Foundation Settlements", Use of In Situ Tests in Geotechnical Engineering, (GSP 6), ASCE, New York, p. 303-321.

Schmertmann, J.H. (1986c) "Some Developments in Dilatometer Testing and Analysis", Proceedings, Innovations in Geotechnical Engineering, Pennsylvania Department of Transportation, Harrisburg, 14 p.

Schmertmann, J.H. (1988a). DMT Digest No. 10, GPE, Inc., 4509 NW 23rd Avenue, Suite 19, Gainesville, FL 32601, 28 p.

Schmertmann, J.H. (1988b) "Guidelines for Using the CPT, CPTU, and Marchetti DMT for Geotechnical Design", Report No. FHWA-PA-024+84-24, Vol. III (of IV), DMT Test Methods and Data Reduction, Pennsylvania Dept. of Transportation and Federal Highway Administration, Washington, D.C., prepared by Schmertmann & Crapps, Gainesville, Florida, 183 p.

Schmertmann, J.H. (1989). DMT Digest No. 11, GPE, Inc., 4509 NW 23rd Avenue, Suite 19, Gainesville, FL 32601, 18 p.

Schmertmann, J.H. (1991). DMT Digest No. 12, GPE, Inc., 4509 NW 23rd Avenue, Suite 19, Gainesville, FL 32601, 22 p.

Schneider, J.A., Randolph, M.F., Mayne, P.W. & Ramsey, N. (2008) "Influence of Partial Consolidation during Penetration on Normalised Soil Classifuication by Piezocone", Proc. 3rd Int. Conf. on Site Characterization, Geotechnical and Geophysical Site Characterisation, A.B. Huang and P.W. Mayne, eds., Taylor and Francis, London, p. 1159-1165

Senneset, K., Janbu, N. & Svano, G. (1982) "Strength and Deformation Parameters from Cone Penetration Tests", Proc. 2nd European Sym. On Penetration Testing, ESOPT, Amsterdam, Vol. 2, p. 863-870

Senneset, K., Sandven, R & Janbu, N. (1989) "The Evaluation of Soil Parameters from Piezocone Tests" Transport Research Record, No. 1235, p. 24-37

Shahin, M.A., Jaksa, M.B. and Maier, H.R> (2001) "Artificial Neural Network Applications in Geotechnical Engineering" Australian Geomechanics (March 2001)

Skiles, D.L. and Townsend, F.C. (1994) "Predicting Shallow Foundation Settlement in Sands from DMT", Vertical and Horizontal Deformations of Foundations and Embankments, (GSP No. 40), Vol. 1, ASCE, New York, p. 132-142.

Smith, M.G. and Houlsby, G.T. (1995). "Interpretation of the Marchetti Dilatometer in Clay," Proceedings, 11th European Conference on Soil Mechanics and Foundation Engineering, Vol. 1, Copenhagen, p. 1.247-1.253.

Specht, D.F. (1991) "A General Regression Neural Network", IEE Trans Neural Networks, 2(6): p. 568-576

Su, P.C., Chen, Y.C., Sun, C.Y. and Wang, G.S. (1993). "The Flat Dilatometer Tests in Clay," Proceedings, 11th Southeast Asian Geotechnical Conference, Singapore, p. 205-210.

Sully, J.P. and Campanella, R.G. (1989) "Correlation of Maximum Shear Modulus with DMT Test Results in Sand", Proceedings, 12th International Conference on Soil Mechanics and Foundation Engineering, Vol. 1, Rio de Janeiro, p. 339-343.

Sully, J.P. and Campanella, R.G. (1990) "Measurement of Lateral Stress in Cohesive Soils by Full-Displacement In-Situ Test Methods", Transportation Research Record 1278, National Academy Press, Washington, D.C., p. 164-171.

Tanaka, H., Tanaka, M., Iguchi, H. and Nishida, K. (1994) "Shear Modulus of Soft Clay Measured by Various Kinds of Tests", Proceedings, International Symposium on Pre-Failure Deformation Characteristics of Geomaterials, Vol. 1, Sapporo, Balkema Publishers, Rotterdam, p. 235-240.

TC16 (2001) – Marchetti S., Monaco P., Totani G. & Calabrese M. "The Flat Dilatometer Test (DMT) in Soil Investigations" A Report by the ISSMGE Technical Committee TC16. Proc. In Situ 2001, Int. Conf on In-Situ Measurement of Soil Properties, Bali, Indonesia

Teh, C.I. (1987) "An Analytical Study of the Cone Penetration Test", PhD Thesis, Oxford University

Terzaghi, K. (1943) "Theoretical Soil Mechanics", John Wile and Sons, New York, 550 p

Totani, G., Marchetti, S., Calabrese, M. and Monaco, P. (1994) "Field Studies of an Instrumented Full-Scale Pile Driven in Clay", Proceedings, 13th International Conference on Soil Mechanics and Foundation Engineering, Vol. 2, New Delhi, p. 695-698.

Totani, G., Calabrese, M., Marchetti, S. and Monaco, P. (1997) "Use of in-situ DMT for ground characterization in the stability analysis of slopes", Proceedings, 14th International Conference on Soil Mechanics and Foundation Engineering, Vol. 1, New Delhi, published by Oxford-IBH, India, p. 607-610.

Totani, G., Marchetti, S., Monaco, P. & Calabrese, M. (2001) "Use of the Flat Dilatometer Test (DMT) in Geotechnical Design, In-Situ 2001, Int. Conf. on In-Situ Measurement of Soil Properties, Bali, Indonesia

Vermeiden, J. (1948) "Improved Sounding Apparatus as Developed in Holland since 1936". Proc. 2nd Int. Conf. on Soil Mechanics and Foundation Engineering, Rotterdam, Vol. 1, p. 280-287

Whittle, A.J. and Aubeny, C.P. (1993) "The Effects of Installation Disturbance on Interpretation of In Situ Tests in Clay", Predictive Soil Mechanics, Thomas Telford, London, p. 743-767.

Wong, J.T.F., Wong, M.F & Kassim, K. (1993) "Comarison between ilatmeter and Other In-Situ and Laboratory Tests in Mayalsian Alluvial Clay", Proc. of 11th Southeast Asian Geotechnical Conference, Singapore

Yu, H.S., Carter, J.P. & Booker, J.R. (1993) "Analysis of the Dilatometer Test in Undrained Clay" Predictive Soil Mechanics, Thomas Telford, London, p. 783-795

Yu, H.S. (2004) "James K. Mitchell Lecture. In Situ Testing: from Mechanics to Interpretation" Proc. ISC-@ on Geotechnical and Geophysical Site Characterization, Viana de Fonseca & Mayne (eds.), Millpress, Rotterdam, ISBN 90 5966 009 9